

Generation of Novel Polymers and Surfactants from Renewable Resources

Joseph Kolawole Ogunjobi

Doctor of Philosophy

University of York
Chemistry

May 2016

Abstract

This research study aimed at using renewable resources from biomass to generate novel polymers and surfactants for applications in Home and Personal Care products. Esterification, transesterification, epoxidation and ring opening reactions were applied with the instrumentality of clean synthetic techniques to deliver over sixty nonionic surfactants with main hydrophilic head containing 9-34 units of ethylene oxide (EO) and hydrophobic tail containing C19-28 hydrocarbons from oleate derivatives, epoxidised linseed oil and sophorolipid. The surfactants were fully characterised with nuclear magnetic resonance spectroscopy, super-critical fluid chromatography, differential scanning calorimetry, electrospray ionisation-mass spectrometry and infrared spectroscopy. Surfactants properties were assessed based on physicochemical measurements and hydrophilic-lipophilic balance. The synthesised polymeric surfactants have great potential applications ranging from oil-in water emulsification, wetting and spreading, detergency and to solubilisation purposes, and can be incorporated into Home and Personal Care products.

Alongside the above study, attempts were made to convert 2,5-furan dicarboxylic acid to diethyl terephthalate as a step to making 100% bio-based poly(ethylene terephthalate), and vital plastic packaging for Home and Personal Care formulations. The bio-based aromatic monomer was synthesised *via* Diels-Alder addition of diester of the furan to ethene under a solventless system catalysed by inexpensive heterogeneous Lewis acid catalysts. DET yield up to 59% was obtained, this being a substantial improvement compared to yields for the same or similar reaction of FDCA and its esters reported elsewhere. The synthetic route herein described was compared with other published biomass routes to bio-based PET using green chemistry metric toolkits, and ours stands as the preferred biomass route based on this comprehensive assessment.

Table of Contents

Abstract	3
Table of Contents.....	5
List of Figures	13
List of Tables	25
Acknowledgements	27
Declaration.....	29

CHAPTER ONE

1.0 Introduction.....	33
1.1 Aim and objectives.....	33
1.2 Clean synthesis.....	35
1.2.1 Heterogeneous catalysis.....	36
1.2.2 Green chemistry metrics.....	40
1.2.3 Critical elements.....	43
1.2.4 Clean technologies.....	44
1.3 Platform molecules.....	46
1.4 Bio-derived monomers- specifically aromatic monomers.....	49
1.5 Surfactants.....	52
1.5.1 Introduction to surfactants	52
1.5.2 Classification of surfactants	53
1.5.3 Surfactant interaction.....	56
1.5.4 Renewable surfactants.....	58
1.6 Conclusions.....	62

CHAPTER TWO

2.0	Synthesis of alkyl oleates <i>via</i> transesterification	67
2.1	Introduction.....	67
2.2	Synthesis of methyl oleate	68
2.3	Synthesis of alkyl oleates.....	70
2.4	Effect of catalyst type on transesterification	74
2.5	Investigating KF and Al ₂ O ₃ as catalysts and concentration effect of KF/Al ₂ O ₃ on transesterification.....	80
2.6	Investigating optimum loading of KF on Al ₂ O ₃ support for transesterification.....	82
2.7	Effect of activation and treatment on MgO catalyst.....	83
2.8	Reuse of transesterification catalysts.....	84
2.9	Conclusions	87

CHAPTER THREE

3.0	Synthesis of alkyl oleate epoxide.....	91
3.1	Introduction.....	91
3.2	Synthesis of alkyl oleate epoxides.....	92
3.3	Epoxidation with preformed phosphotungstic acid (PTA) catalyst	95
3.4	Epoxidation with in situ generated phosphotungstic acid (PTA).....	97
3.5	Characterisation of synthesised surfactants	98
3.6	Studies on factors affecting epoxidation	104
3.6.1	Effect of acetic acid on epoxidation with PTA	104
3.6.2	Effect of solvent nature on epoxidation with PTA.....	105
3.6.3	The need for a PTC in PTA-catalysed epoxidation reaction.....	107

3.6.4	Effect of PTA nature and source on epoxidation	107
3.7	Investigation into the formation of aldehyde and ketone during epoxidation of oleates	110
3.8	Epoxidation with heterogeneous catalyst.....	117
3.9	Ultrasound-Assisted epoxidation (UAE) of alkyl oleate with supported and unsupported PTA catalysts.....	120
3.10	Synthesis of lactonic sophorolipid epoxide	122
3.11	Conclusions.....	127

CHAPTER FOUR

4.0	Ring opening of epoxides with PEGs and carbohydrates.....	131
4.1	Introduction	131
4.2	Ring opening of epoxides.....	132
4.3	Model reactions	133
4.4	Synthesis of oleate-based surfactants.....	153
4.4.1	Alkyl oleate surfactants based on PEG 400.....	154
4.4.2	Alkyl oleate surfactants based on MePEG 400	155
4.4.3	Alkyl oleate surfactants based on MePEG 750	156
4.4.4	Alkyl oleate surfactants based on PEG 1000.....	158
4.4.5	Alkyl oleate surfactants based on PEG 1500.....	159
4.5	Epoxide ring opening with other heterogeneous catalysts	160
4.6	Characterisation of synthesised surfactants	161
4.6.1	NMR spectroscopy.....	162
4.6.2	FT-IR spectroscopy measurement	166
4.6.3	ESI mass spectrometry measurement.....	167

4.6.4	Supercritical fluid chromatography (SFC) measurement.....	169
4.6.5	Differential scanning calorimetry (DSC) measurement	170
4.6.6	CHN elemental analysis.....	171
4.6.7	ICP mass spectrometry measurement	172
4.7	Microwave-Assisted epoxide ring opening reaction.....	172
4.8	One-Pot synthesis of surfactant	172
4.9	Reuse of catalyst for PEGylation reaction	173
4.10	Synthesised surfactants as phase transfer catalyst.....	173
4.11	Ring opening of epoxides with carbohydrates.....	174
4.11.1	Ring opening of alkyl oleate epoxides with fructose	174
4.11.2	Ring opening of alkyl oleate epoxide with Inulin.....	1775
4.11.3	Ring opening of alkyl oleate epoxide with D-sorbitol	177
4.12	Synthesis and characterisation of sophorolipid-based surfactants.....	178
4.13	Synthesis and characterisation of linseed oil-based surfactants	182
4.14	Conclusions	185

CHAPTER FIVE

5.0	Assessment of surfactants properties.....	189
5.1	Introduction.....	189
5.2	Physicochemical measurements.....	189
5.2.1	Dynamic surface tension of synthesised surfactants.....	189
5.2.2	Equilibrium surface tension of synthesised surfactants	194
5.2.3	Emulsion formation	198
5.2.4	Surfactant self-assembly.....	201

5.3 Hydrophilic-Lipophilic Balance (HLB): Potential application of synthesised surfactants	203
5.4 Conclusions.....	212

CHAPTER SIX

6.0 Towards a 100% bio-derived poly(ethylene terephthalate)	217
6.1 Introduction	217
6.2 Synthesis of 2,5-furan dicarboxylic acid diethyl ester (FDEE).....	219
6.3 Synthesis of diethyl terephthalate (DET) via Diels-Alder addition of ethene to FDEE.....	220
6.3.1 DA reactions and mechanism.....	220
6.3.2 DA of 2,5-furandicarboxylic acid dimethyl ester (FDME) to ethene 224	
6.3.3 DA addition of FDEE to pressurised ethene catalysed by aluminium montmorillonite (Al-mont) clay.....	224
6.3.4 DA addition of FDEE to pressurised ethene catalysed by other heterogeneous Lewis acids	229
6.3.5 Acidity effect on ethene oligomerisation.....	234
6.4 Large scale synthesis of DET	235
6.4.1 Product mass recovery and isolation.....	236
6.4.2 Reuse of catalyst.....	237
6.4.3 Characterisation of isolated products.....	238
6.5 Comparison of routes to bio-PET.....	241
6.6 Conclusions.....	248

CHAPTER SEVEN

7.0	Concluding remarks and future work.....	253
7.1	Outcomes of this work.....	258
7.1.1	Conferences	258
7.1.2	Presentations	259
7.1.3	Publications	259
7.1.4	Awards.....	259

CHAPTER EIGHT

8.0	Experimental.....	263
8.1	Material and reagents	263
8.2	Analytical instruments and equipment.....	263
8.2.1	Gas chromatography (GC).....	263
8.2.2	GC-MS, SFC, IR and NMR.....	264
8.2.3	ICP-MS and CHN.....	264
8.2.4	TGA, DSC and porosimetry.....	264
8.2.5	Ultrasound and microwave	266
8.2.6	Tensiometry and dynamics of surfactants	266
8.3	Catalyst preparation.....	266
8.3.1	Potassium fluoride on alumina (KF/Al ₂ O ₃).....	266
8.3.2	Treated magnesium oxide catalyst.....	266
8.3.3	Activated MgO catalyst.....	267
8.3.4	Fe-K30 montmorillonite catalyst	267
8.3.5	Al-montmorillonite catalyst	267

8.3.6	Acid free Al-montmorillonite catalyst.....	268
8.3.7	Fe-montmorillonite catalyst.....	268
8.3.8	Al-Y zeolite catalyst.....	268
8.3.9	Mesoporous silica catalyst support	269
8.3.10	Amino-propyl functionalised mesoporous silica catalyst support.	269
8.3.11	Phosphotungstic acid impregnated on mesoporous silica support	269
8.3.12	Phosphotungstic acid immobilized on amino propyl functionalised mesoporous silica support.....	269
8.4	Synthesis of methyl oleate.....	270
8.5	Synthesis of alkyl oleates via transesterification of methyl oleate.....	271
8.6	Syntheses of alkyl oleate epoxides (octadecanoic acid-9, 10-epoxy alkyl esters).....	278
8.6.1	Syntheses of alkyl oleate epoxides <i>via in situ</i> phosphotungstic acid	278
8.6.2	Syntheses of alkyl oleate epoxides <i>via</i> phosphotungstic acid...	278
8.7	Synthesis of lactonic sophorolipid epoxide	285
8.8	Epoxidation with PTA-SBA-15-NH ₂	286
8.9	Ultrasound-Assisted Epoxidation (UAE).....	286
8.9.1	UAE epoxidation with phosphotungstic acid (PTA).....	286
8.9.2	UAE epoxidation with PTA-SBA-15-NH ₂	286
8.10	Ring opening of alkyl oleate, lactonic sophorolipid and linseed oil epoxides.....	287
8.10.1	Model reactions	287

8.10.2 Synthesis of alkyl oleate-based surfactant via PEGylation.....	291
8.10.3 Synthesis of lactonic sophorolipid-based surfactant <i>via</i> PEGylation.....	311
8.10.4 Synthesis of linseed oil-based surfactant <i>via</i> PEGylation	314
8.11 Microwave-Assisted PEGylation: ring opening of epoxide.....	318
8.12 One-pot PEGylation of methyl oleate	318
8.13. Reuse of iron-exchanged montmorillonite catalyst for PEGylation reaction.....	318
8.14 Surfactant properties testing.....	319
8.14.1 Dynamic surface tension measurement	319
8.14.2 Equilibrium surface tension measurement.....	319
8.15 Synthesis of 2,5-furandicarboxylic diethyl ester (FDEE).....	320
8.16 Synthesis of acid- free 2, 5-furandicarboxylic diethyl ester (FDEE).....	320
8.17 Pre-adsorption of FDEE onto catalyst	321
8.18 Synthesis of diethyl terephthalate (DET).....	321
8.19 Effect of acidity on side reactions products from DET synthesis.....	322
8.20 Effect of Al-pillared montmorillonite on side reaction products from DET synthesis	323
8.21 Reuse of aluminium-pillared montmorillonite for DET synthesis	323
8.22 Measurement of titanium in aluminium-pillared montmorillonite.....	323
8.23 Measurement of residual metal catalyst in surfactant.....	324
8.24 Measurement of residual metal catalyst in oleate	324
8.25 Measurement of residual metal catalyst in oleate epoxide	324
Abbreviations.....	327
References.....	333

List of Figures

CHAPTER ONE

Figure 1- 1 The wheel driving Green Chemistry through the years

Figure 1- 2 A typical catalytic reaction is a cycle starting from coming together of reactants on the catalyst to product formation and desorption of the product to form a free catalyst ready for another cycle.

Figure 1- 3 Examples of forms of hydroxyl groups in silica

Figure 1- 4 Periodic table highlighting critical elements

Figure 1- 5 Relationship between renewable resources and clean technologies with respect to clean synthesis.

Figure 1- 6 Heat distribution in conventional and microwave systems.

Figure 1- 7 Platform molecules are processed to generate a number of bio-based chemicals

Figure 1- 8 Examples of platform molecules derived from lignin

Figure 1- 9 Some investigated routes to bio-based TA from glucose and xylose.

Figure 1- 10 Schematic illustration of a typical surfactant.

Figure 1- 11 Applications of surfactants around 2006

Figure 1- 12 Examples of anionic surfactants

Figure 1- 13 Examples of cationic surfactants

Figure 1- 14 Common examples of non-ionic surfactants

Figure 1- 15 Common examples of zwitterionic surfactants

Figure 1- 16 Schematic representation of surface activity and micelle formation. (a) air-water interface; (b) oil-water interface; (c) adsorption onto nonpolar solids; (d) soap films; (e) bilayers; (f) micelles. Redrawn from literature source

Figure 1- 17 Bio-based surfactants are made from renewable hydrophilic end (head) e.g. sucrose, citric acid, glycerol, glucose, and renewable hydrophobic end (tail) e.g. sterol, triglycerides and cardanol

Figure 1- 18 World production of soyabean, sunflower and canola/rapeseed oils from 2001 to 2014

Figure 1- 19 Common transformations of triglycerides in the manufacture of surfactants

Figure 1- 20 Surfactants based on renewable hydrophiles

CHAPTER TWO

Figure 2- 1 Generation of bio-based non-ionic surfactant from oleic acid

Figure 2- 2 Mechanism of acid-catalysed esterification of carboxylic acid with alcohol

Figure 2- 3 Proton NMR spectrum of synthesised methyl oleate

Figure 2- 4 Carbon 13 and DEPT NMR spectra of synthesised methyl oleate

Figure 2- 5 Mechanisms of transesterification reaction catalysed by (a) a base and (b) an acid

Figure 2- 6 FT-IR spectra of synthesised oleates showing contrast in band intensity and pattern

Figure 2- 7 Proton NMR spectra of alkyl oleates showing variation between the branched chain oleates (last three signals) and the straight chain oleates (first 5 signals)

Figure 2- 8 GC chromatogram of synthesised 1-octyl oleate showing epoxide and diols as side products

Figure 2- 9 Formation of aldehydes, keto esters, epoxides and diols observed in higher alkyl oleates during transesterification of methyl oleate leading to reduced selectivity

Figure 2- 10 Structures of alkyl oleates synthesised from methyl oleate via transesterification with alcohol

Figure 2- 11 Transesterification products showing (a) formation of waxy oleates (b) different shades of amber coloured KF/Al₂O₃ and MgO-T600 catalysed oleates (c) residues from filtered waxy oleates (d) different shades of amber coloured Ti(O-i-Pr)₄ catalyst

Figure 2- 12 Methyl oleate dimer: an example of a dimer

Figure 2- 13 Effectiveness of KF, Al₂O₃ and KF/Al₂O₃ as catalysts for transesterification reaction.

Figure 2- 14 Effect of KF/Al₂O₃ concentration on transesterification of methyl oleate with 1-butanol.

Figure 2- 15 Effect of KF loading on alumina support tested for transesterification reaction.

Figure 2- 16 Preparation of hydroxylated MgO (MgOT600) and activated MgO (MgO600) catalysts

Figure 2-17 Reuse of KF/Al₂O₃ catalyst in transesterification of methyl oleate with ethanol using acetone and cyclohexane as wash solvents.

Figure 2-18 Reuse of MgO-T600 catalyst in transesterification of methyl oleate with 1-octanol.

CHAPTER THREE

Figure 3- 1 Generation of bio-based non-ionic surfactant from oleic acid

Figure 3- 2 Mechanism of epoxidation reaction between an olefin and peracetic acid

Figure 3- 3 Keggin structure of phosphotungstic acid, H₃PW₁₂O₄₀

Figure 3- 4 Mechanism for a phase transfer co-catalyst aided epoxidation with PTA

Figure 3- 5 Methyl trialkyl (C8-C10) ammonium chloride

Figure 3- 6 Side reaction products from epoxidation of fatty acid alkyl esters, R = alkyl group of varying length and functionality

Figure 3- 7 Generation of peroxyoxycarboxylic acid from the reaction of acetonitrile and hydrogen peroxide to favour epoxide formation

Figure 3- 8 Proton NMR spectra of methyl oleate and epoxidised methyl oleate showing (i) signal shifts and reduced integral value as a result of addition of oxygen heteroatom into the chain; (ii) disappearance of C=C protons and appearance of epoxy protons

Figure 3- 9 Carbon DEPT NMR spectra of methyl oleate and epoxidised methyl oleate showing disappearance of olefinic carbons and appearance of epoxy carbons

Figure 3- 10 FT-IR spectra of methyl oleate (bottom) and epoxidised methyl oleate (top) showing disappearance of =C-H vibration and appearance of epoxy bands

Figure 3- 11 Variation of colour shades with (a) alkyl oleate epoxides at production, (b) frozen alkyl oleate epoxides days after production, (c) alkyl oleate juxtaposed with corresponding epoxides at production, (d) alkyl oleates juxtaposed with corresponding epoxides days after production

Figure 3- 12 Effect of acetic acid-doped epoxidation reaction on conversion and yield in the presence of PTA.

Figure 3- 13 Effect of nature of solvents on epoxidation with hydrogen peroxide in the presence of PTA with respect to conversion and yield.

Figure 3- 14 Influence of the nature and source of PTA catalyst on methyl oleate conversion and epoxide yield.

Figure 3- 15 ATR-FTIR spectra of hydrated and dehydrated PTAs and their sources

Figure 3- 16 Formation of aldehydes and ketones from unsaturated fatty esters (a) two-step oxidation of double bond and diol to carboxylic acid and acid ester (b) mechanism of the first step of the reaction leading to formation of diols.

Figure 3- 17 Profile of side reaction products from epoxidation of methyl oleate in acetonitrile solvent (system A) over 24 hours of reaction

Figure 3- 18 Profile of side reaction products from epoxidation of methyl oleate in system B over 24 hours of reaction

Figure 3- 19 Profile of side reaction products from epoxidation of methyl oleate in tert-butanol solvent (system C) over 24 hours of reaction

Figure 3- 20 Routes to formation of side products from epoxidation of methyl oleate

Figure 3- 21 Proton and Carbon 13 NMR spectra of System A at 6 h of reaction

Figure 3- 22 Synthesis of functionalized mesoporous silica supported phosphotungstic acid

Figure 3- 23 Effectiveness of supported PTA catalyst for epoxidation under different conditions.

Figure 3- 24 Ultrasound assisted epoxidation reaction set up

Figure 3- 25 Effectiveness of PTA and PTA-SBA-15-NH₂ catalysts for UAE of methyl oleate.

Figure 3- 26 Additional side reaction products formed with UAE of methyl oleate

Figure 3- 27 Forms of occurrences of sophorolipids

Figure 3- 28 Synthesis of lactonic sophorolipid epoxide

Figure 3- 29 Proton NMR spectra of lactonic sophorolipid (LSL) and epoxidised lactonic sophorolipid (ELSL). AV 700 MHz Bruker spectrometer, CDCl₃ solvent.

Figure 3- 30 FT-IR spectra of lactonic sophorolipid (top) and epoxidised lactonic sophorolipid (bottom).

Figure 3- 31 ESI mass spectra of LSL and epoxidised LSL (ELSL)

CHAPTER FOUR

Figure 4- 1 Synthesis of non-ionic surfactants starting from oleic acid

Figure 4- 2 Mechanism of epoxide ring-opening reaction in (a) acidic condition (b) basic condition

Figure 4- 3 Ring-opening reaction of CHexO with TEG

Figure 4- 4 FT-IR spectra of cyclohexene oxide, triethylene glycol and cyclohexene oxide ring-opened with triethylene glycol in the presence of Yb(TFA)₃ catalyst

Figure 4- 5 Proton NMR spectra of cyclohexene oxide, triethylene glycol and cyclohexene oxide ring-opened with triethylene glycol in the presence of Yb(TFA)₃ catalyst.

Figure 4- 6 ¹³C and DEPT NMR spectra (top) of cyclohexene oxide, triethylene glycol and cyclohexene oxide ring-opened with triethylene glycol in the presence of Yb(TFA)₃ catalyst. HSQC NMR spectrum of the product (bottom).

Figure 4- 7 Ring-opening reaction of CHexO with EG

Figure 4- 8 Chromatogram of resulting crude products of cyclohexene oxide ring-opened with ethylene glycol.

Figure 4- 9 FT-IR spectra of cyclohexene oxide, ethylene glycol and cyclohexene oxide ring-opened with ethylene glycol in the presence of Yb(TFA)₃ catalyst.

Figure 4- 10 Proton NMR spectra of cyclohexene oxide and cyclohexene oxide ring-opened with ethylene glycol in the presence of Si-BF₃ and Yb(TFA)₃ catalysts.

Figure 4- 11 ¹³C and DEPT NMR spectra (top) of cyclohexene oxide and cyclohexene oxide ring-opened with ethylene glycol in the presence of Yb(TFA)₃ catalyst. HSQC NMR spectrum of the product (below).

Figure 4- 12 Ring-opening reaction of CHexO with MeEG

Figure 4- 13 GC-FID chromatogram of crude product from reaction between cyclohexene oxide and 2-methoxy ethanol catalysed by Yb(TFA)₃.

Figure 4- 14 Formation of oligomers during ring opening reaction between cyclohexene oxide and 2-methoxy ethanol catalysed by an acid.

Figure 4- 15 Proton NMR spectra of cyclohexene oxide, 2-methoxy ethanol and ring-opened epoxide catalysed by Si-BF₃ and Yb(TFA)₃.

Figure 4- 16 ¹³C and DEPT NMR spectra (top) of cyclohexene oxide, 2-methoxy ethanol and ring-opened epoxide in the presence of Yb(TFA)₃ catalyst. HSQC NMR spectrum of the product (below).

Figure 4- 17 Ring-opening reaction of CHexO with PEG 400

Figure 4- 18 GC-FID chromatogram of cyclohexene oxide ring-opened with poly (ethylene) glycol 400 catalysed by Yb(TFA)₃.

Figure 4- 19 ¹H (top) and carbon DEPT (below) NMR spectra of cyclohexene oxide ring-opened with poly (ethylene) glycol 400 catalysed by Yb(TFA)₃

Figure 4- 20 Ring-opening of methyl oleate epoxide with TEG

Figure 4- 21 GC-FID chromatogram of ring-opened epoxidised methyl oleate catalysed by Yb(TFA)₃.

Figure 4- 22 FT-IR spectra of triethylene glycol, epoxidised methyl oleate and ring-opened epoxidised methyl oleate catalysed by Yb(TFA)₃

Figure 4- 23 ¹H NMR spectra of triethylene glycol, epoxidised methyl oleate and ring-opened epoxidised methyl oleate catalysed by Yb(TFA)₃

Figure 4- 24 Carbon DEPT NMR spectra of epoxidised methyl oleate and ring-opened epoxidised methyl oleate catalysed by Yb(TFA)₃. HSQC of ring-opened epoxidised methyl oleate (below).

Figure 4- 25 Ring-opening reaction of epoxidised methyl oleate with MeEG

Figure 4- 26 GC-FID chromatogram of ring-opened epoxidised methyl oleate catalysed by Fe(TFA)₃.

Figure 4- 27 ¹H NMR spectrum of MeEG ring-opened epoxidised methyl oleate

Figure 4- 28 Two possible positions for OH and PEGs on ring-opened methyl oleate epoxide

Figure 4- 29 Occurrence of transesterification reaction during ring opening of epoxidised methyl oleate with 2-methoxy ethanol.

Figure 4- 30 ¹³C (top) and HSQC (below) NMR spectra of epoxidised methyl oleate ring-opened with 2-methoxy ethanol

Figure 4- 31 HMBC NMR spectrum of epoxidised methyl oleate ring-opened with 2-methoxy ethanol

Figure 4- 32 Formation of oligomers during ring opening reaction of epoxidised methyl oleate with 2-methoxy ethanol

Figure 4- 33 Ring-opening of alkyl oleate epoxides (including branched isomers) with PEGs of varying chain length

Figure 4- 34 Alkyl oleate based surfactants from PEG 400

Figure 4- 35 Alkyl oleate based surfactants from MePEG 400

Figure 4- 36 Alkyl oleate based surfactants from MePEG 750

Figure 4- 37 Alkyl oleate based surfactants from PEG 1000

Figure 4- 38 Alkyl oleate based surfactants from PEG 1500

Figure 4- 39 Alkyl oleate-based surfactants synthesised via Si-BF₃ catalysis (A), Fe-mont catalysis (B) and FeCl₃ catalysis (C)

Figure 4- 40 ¹H (top), carbon DEPT-135 (middle) and HMBC (bottom) NMR spectra of formation of surfactant from ring-opened epoxidised methyl oleate.

Figure 4- 41 Carbon DEPT-135 NMR spectrum of epoxidised 2-propyl oleate ring-opened with PEG 1500

Figure 4- 42 Oligomerisation occurrence during ring opening reaction of epoxidised 2-propyl oleate with PEG 1500.

Figure 4- 43 Mechanism for transesterification of 2-propyl oleate epoxide with PEG 1500 in the presence of a Lewis acid.

Figure 4- 44 IR spectra of transformation of oleate to epoxide and then to PEGylated surfactant.

Figure 4- 45 ESI spectra of alkyl oleate surfactants based on PEG 400. (A) PEMO 400 surfactant with a trace impurity of Adogen 464 residue from epoxidation process. (B) PEOO 400 surfactant made from purified 1-octyl oleate epoxide.

Figure 4- 46 SFC chromatograms showing separation of methyl oleate, PEG 400, PEMO 400 and iso-mixture of PEMO 400 and PEG 400.

Figure 4- 47 MDSC melt profile of PEMO 400 surfactant

Figure 4- 48 Ring-opening of methyl oleate epoxide with fructose

Figure 4- 49 Ring-opening reaction of methyl oleate epoxide with inulin

Figure 4- 50 DSC melt profiles of modified inulin (green), inulin (red) and a mixture of modified inulin and epoxidised methyl oleate (blue).

Figure 4- 51 SEM images of modified inulin and inulin at a magnification of 10000

Figure 4- 52 Ring-opening reaction of methyl oleate epoxide with D-sorbitol

Figure 4- 53 ^1H NMR spectra of D-sorbitol (top) and product from ring-opening reaction with epoxidised methyl oleate in 3 hours of reaction time.

Figure 4- 54 Ring-opening reaction of ELSL with PEGs

Figure 4- 55 Five surfactants prepared from ELSL.

Figure 4- 56 FT-IR spectra of LSL, ELSL and PEGylated surfactants based on ELSL

Figure 4- 57 ^1H NMR spectra of ELSL (top) and PELSL 400 surfactant (bottom).

Figure 4- 58 Ring-opening reaction of epoxidised linseed oil with PEGs

Figure 4- 59 Surfactants based on ELO are viscous to hard solid materials

Figure 4- 60 ^1H NMR spectra of ELO (top) and PELO 400 (bottom)

CHAPTER FIVE

Figure 5- 1 Dynamic surface tension of unpurified PEMO 400, MPEMO 400, PEEO 400 and PEEO 1500 surfactants

Figure 5- 2 Dynamic surface tension of unpurified PE2BO 400, PE2B 1500, PEOO 400 and PEOO 1500 surfactants

Figure 5- 3 Dynamic surface tension of unpurified PELO 400, PELO 1500, PE2OO 400 and PE2OO 1500 surfactants

Figure 5- 4 Surface tension versus the logarithm of surfactant concentration for unpurified PEMO 400 (1 mg/ ml) and PEEO 400 (1 mg/ml) surfactants at $\sim 26^\circ\text{C}$

Figure 5- 5 Surface tension versus the logarithm of surfactant concentration for purified PEMO 400 (1 mg/ ml) and PEEO 400 (1 mg/ml) surfactants at $\sim 26^\circ\text{C}$.

Figure 5- 6 Packing of surfactant molecules at the surface relates to the structure and geometry of the surfactant. Critical packing parameter (CPP) relates the volume of the hydrophobic group, v ; area of the hydrophilic group, a ; and the length of the surfactant, l as $\text{CPP} = v/(al)$

Figure 5- 7 Emulsions after 20 days (a) formed from toluene (50 v%) and water (50 v%) were grouped into (b) very stable emulsion, (c) stable emulsion, (d) slightly stable emulsion and (e) unstable emulsion

Figure 5- 8 Formation of micelles from the aggregation of surfactant molecules in the bulk solution after CMC is attained

Figure 5- 9 Prediction of structures of self-assembled surfactants in aqueous solutions based on critical packing parameters

Figure 5- 10 Predicting aggregate shape in surfactants based on CPP in variation with PEG length and alkyl chain length

Figure 5- 11 Hydrophilic and hydrophobic groups in PEMO 400 surfactant

Figure 5- 12 Hydrophilic and hydrophobic groups in MPEMO 400 surfactant

Figure 5- 13 HLB values and average molecular weight obtained for alkyl oleate surfactants based on PEG 400

Figure 5- 14 HLB values and average molecular weight obtained for alkyl oleate surfactants based on MePEG 400

Figure 5- 15 HLB values and average molecular weight obtained for alkyl oleate surfactants based on MePEG 750

Figure 5- 16 HLB values and average molecular weight obtained for alkyl oleate surfactants based on PEG 1000

Figure 5- 17 HLB values and average molecular weight obtained for alkyl oleate surfactants based on PEG 1500

Figure 5- 18 Hydrophilic groups in sophorolipid-based surfactants

Figure 5- 19 HLB values and average molecular weight obtained for sophorolipid-based surfactants

CHAPTER SIX

Figure 6- 1 Synthesis of PET from transesterification of dialkyl terephthalate with EG

Figure 6- 2 Example applications of PET in packaging and textiles

Figure 6- 3 Synthetic route to 100% bio-derived PET via transesterification of bio-based EG with bio-based DET

Figure 6- 4 Synthesis of FDCA from HMF a degradation product of cellulose

Figure 6- 5 DA reaction is intrinsically atom economic with addition of a four-carbon compound to a two-carbon compound to form a six-carbon molecule

Figure 6- 6 Orbital correlation diagram showing the difference between a normal electron demand involving an electron-rich diene and electron-poor dienophile

(left) and an inverse electron demand involving an electron-poor diene and an electron-rich dienophile (right) DA reaction

Figure 6- 7 Orbital diagrams illustrating the formation of (a) endo and exo adducts in DA reaction involving asymmetric dienophile and ringed diene; (b) a single product in DA reaction in which the dienophile is symmetrical

Figure 6- 8 Cause of peaks of 198 and 212 g/mol from FDME and ethene Diels-Alder addition

Figure 6- 9 Auto aromatization of DA oxo-adduct to DET in the presence of an acid

Figure 6- 10 GC-FID of Diels-Alder addition of FDEE and ethene with Al-mont at 60 bar and 200 °C for 48hours (Table 1 entry 5). The protruded baseline (highlighted in pink) is an indication of the presence of alkanes and alkene

Figure 6- 11 Compounds formed as a result of ethene oligomerization reaction

Figure 6- 12 Side reaction products from decarboxylation, transesterification with ethanol and hydrolysis of FDEE and DET during DA to ethene

Figure 6- 13 ¹H NMR spectrum, with suggested assignments, of the oil collected from the oligomerisation of pressurised ethene in the presence of Al-mont catalyst. Data collected by Farmer

Figure 6-14 ¹³C NMR spectrum, with suggested assignments, of the oil collected from the oligomerisation of pressurised ethene in the presence of Al-mont catalyst. Data collected by Farmer

Figure 6- 15 Substitution of interlayer gap cations of metal exchanged montmorillonite clay with polyoxocations of inorganic metals widens the basal gap between clay sheets and results in formation of pillared montmorillonite clay upon calcination

Figure 6-16 GC-FID Chromatogram (top) from DET synthesis using Al-pillared montmorillonite catalyst under a 60 bar fill pressure of ethene, 250 °C, 24 hour (Table 2 entry 12); (bottom) ethanol wash of ethene oligomerisation test sample with Al-pillared montmorillonite catalyst

Figure 6- 17 Isolated DET crystallizes as soon as it cools down

Figure 6- 18 Conversion, yield and selectivity of three reuse cycles of Al-pillared montmorillonite for scaled-up Diels-Alder addition of FDEE and ethene. Temperature (250 °C), filling pressure (60 bar), time (24 hr), 50% catalyst loading and pre-adsorbed system

Figure 6- 19 GC-FID chromatograms of isolated DET and recovered FDEE

Figure 6- 20 GC-EI-MS chromatograms of DET (a) before isolation (b) after isolation with spectrum showing fragmentation pattern

Figure 6- 21 FT-IR spectra showing transformation from FDCA to FDEE and then to isolated DET which is compared with a standard DET

Figure 6- 22 ¹H NMR of isolated DET with trace impurity

Figure 6- 23 Transformations from cellulose to bio-based DET *via* Diels-Alder addition of DMF to ethene

Figure 6- 24 Transformations from cellulose to bio-based DET *via* Diels-Alder addition of DMF to acrolein

Figure 6- 25 Transformations from cellulose to bio-based DET *via* Diels-Alder addition of HMF oxidation derivatives to ethene

Figure 6- 26 Transformations from glucose to bio-based DET isobutanol- Gevo process

Figure 6- 27 Transformations from glucose to bio-based DET *via* “absolute ethene” process

Figure 6- 28 Transformations from hemicellulose (xylose) to bio-based DET *via* “absolute furfural” process

Figure 6- 29 Transformations from cellulose to bio-based DET *via* Diels-Alder addition of FDEE to ethene

CHAPTER SEVEN

Figure 7- 1 Transformation from rapeseed oil to non-ionic surfactants *via* esterification of oleic acid to methyl oleate, transesterification to alkyl oleate and epoxidation to alkyl oleate epoxides and ring opening with PEGs

List of Tables

CHAPTER ONE

Table 1- 1 Fatty acid distribution in selected vegetable oils and fats

CHAPTER TWO

Table 2- 1 Comparative effectiveness of $\text{Ti}(\text{O}-i\text{-Pr})_4$, MgO-T600 and $\text{KF/Al}_2\text{O}_3$ catalysts for alkyl oleate synthesis

Table 2-2 Effectiveness of MgO-T600 and $\text{KF/Al}_2\text{O}_3$ catalysts for transesterification between different chain lengths of oleates

CHAPTER THREE

Table 3- 1 Effectiveness of PTA for large scale synthesis of alkyl oleate epoxides

Table 3- 2 Effectiveness of PTA formed in situ for synthesis of alkyl oleate epoxides

Table 3- 3 Epoxide proton and carbon NMR chemical shifts variation within various chain lengths of alkyl oleate epoxides

Table 3- 4 Composition of side reaction products from some fatty acid ester epoxides

Table 3- 5 Composition of systems used to investigate formation of aldehydes and ketones in epoxidation reaction

CHAPTER FOUR

Table 4- 1 Effectiveness of different Lewis acids screened for ring opening catalysis

Table 4- 2 Synthesised surfactants based on PEG 400

Table 4- 3 Synthesised surfactants based on MePEG 400

Table 4- 4 Synthesised surfactants based on MePEG 750

Table 4- 5 Synthesised surfactants based on PEG 1000

Table 4- 6 Synthesised surfactants based on PEG 1500

Table 4- 7 CHN elemental composition of epoxide and surfactants after treatment with an ion exchange resin

Table 4- 8 Synthesised surfactants on lactonic sophorolipid

Table 4- 9 CHN composition of ELSL and synthesised sophorolipid-based surfactants

Table 4- 10 Synthesised surfactants based on epoxidised linseed oil

CHAPTER FIVE

Table 5- 1 Emulsion ranking based on variation between hydrophobic chain length and PEG chain length as (1) very stable emulsion (2) stable emulsion (3) slightly stable emulsion (4) unstable emulsion

Table 5-2 HLB ranges and applications

Table 5- 3 Group numbers for different functionalities according to ECL method

CHAPTER SIX

Table 6- 1 Yield, Conversion and Selectivity of DA addition of FDEE to ethene using aluminium montmorillonite catalyst under varying reaction conditions with 50% (entries 1-5) and 60% (entries 6 and 7) catalyst loadings

Table 6- 2 Yield, Conversion and Selectivity of DA addition of FDEE to ethene catalysed by different heterogeneous Lewis acid catalysts under varying reaction conditions with 50% (entries 1-10) and 60% (entries 11-17) catalyst loadings

Table 6- 3 Variation of DET yield and selectivity with acidity content in FDEE-Al-mont mixture under different reaction conditions

Table 6- 4 Conversion, yield, selectivity and mass recovery under a scale-up DET synthesis with a preadsorbed system in 24 hours

Table 6- 5 Cumulative Metrics Result for synthesis of 5 mol bio-derived DET from glucose/pentose

Acknowledgements

I sincerely appreciate my supervisors, Professor James H. Clark and Doctor Thomas J. Farmer, for giving me the opportunity to work in this interesting area of chemistry, for their excellent, painstaking and thoughtful supervision, suggestions and discussions throughout the study. Special appreciation to Doctor Con R. McElroy for being part of the supervisory team; your efforts and contributions throughout the study are well commended. I am also grateful to Doctor Tony Wild (Wild Fund), Unilever PLC (United Kingdom) and TETFund (Nigeria) for providing funds for this research.

The following people were very supportive during my study: Doctors Duncan Macquarrie, Avtar Matharu, Vitaly Budarin, Peter Shuttleworth, Heather Fish and Karl Heaton; members of the Green Chemistry Centre of Excellence (GCCE) and Biorenewable Development Centre (BDC) especially Paul Elliot, Alison Edmonds, Sophie Palmer, Katie Brooke, Christine Vis and Andrea Garcia for their technical and administrative supports. Thanks to Professor David Thornthwaite, Doctors Ian Tucker and Antoine Charbonnier, and Sean Ruane of Unilever for a successful placement at the Unilever R&D, Port Sunlight, Liverpool, UK.

Special thanks to Oluwatayo "Ifemi" for believing in my abilities and supporting me always, and to Itunu "Boboe" who also in a little while has been a great motivation to me. I would not have come this far without your understanding and sacrifices. I love you both.

My ultimate thanks goes to God Almighty the giver of true wisdom who has endowed me with grace and good health to achieve this feat at this stage of my life.

"Better is the end of a thing than the beginning thereof..."-Eccl. 7:8a

Declaration

I declare that this thesis is a presentation of original work and I am the sole author. This work has not previously been presented for an award at this, or any other, University. All sources are acknowledged as references.

Introduction

Chapter 1

1.0 Introduction

1.1 Aim and objectives

There are increasing legislations worldwide imposed on the chemical industry to minimize and if possible eliminate wastes as well as control chemical use in order to protect human health and the environment. Many organisations and agencies spread across the globe have been born out of this movement to champion, set the curriculum and implement legislations to which the chemical industry must comply. Some of these agencies at the forefront of implementing legislations include the US Environmental Protection Agency (EPA) and European Chemicals Agency (ECHA). One of the legislations implemented by ECHA in 2007 is the REACH (Registration, Evaluation, Authorisation and restriction of Chemicals) legislation which mandates industries to have their chemicals tested, use more benign alternatives where applicable and provide detailed information about toxicology and environmental impact of chemicals and products consumed.^{1,2} The aftermath of this is that both the chemical industry and consumers have been affected greatly. Consumers are now more informed of the need for their safety and the environment and mount pressure on the chemical industry to gravitate towards “green production”. Coincidentally, there are awoken interests in the industry to reduce waste, use renewable resources, review production processes and invent new sustainable technologies which consequently has spurred competitive and collaborative researches between industries and academia, e.g. CHEM 21 project which is a collaboration between the EU and leading pharmaceutical companies.³ This creates a ground for the green chemistry philosophy to thrive and become implemented globally.

Every section of the chemical industry has particular challenges to address in order to gain a sense of “green” acceptance in the environment. For surfactant and polymer industries there are major needs to reduce CO₂ emissions arising from the production and use of surfactants and polymers, as well as to employ renewable and more biodegradable chemicals. Currently surfactants are chiefly produced from

petrochemical feedstock. A report has shown that about 75% of the organic carbons found in common surfactants come from petrochemical feedstock.⁴ With growing concerns over depleting crude oil reserve and fluctuating cost,⁵ the surfactant industry is putting more effort on using oleochemical feedstock as alternative resources.^{6, 7} The use of renewable feedstock will not only replace petrochemical derived surfactants but also reduce the release of CO₂ (that could have resulted from their production and use) into the environment.

Yet another challenge that the surfactant industry has been faced with, and will still be a matter of consideration in any synthesis plan, is the biodegradability of surfactants after use by the consumer. Alkyl benzene sulphonates (ABSs) produced in the 1950s were not biodegradable because of their branched chemical structures, and their replacement with linear alkyl benzene sulphonates (LABSs), which are poorly biodegradable anaerobically,^{8,9} gave only a form of relief, but did not resolve the issue entirely. Ethylene oxide and propylene oxide are now being incorporated between the head and the tail group of surfactants to make them highly biodegradable in the environment.⁹ Even with this, the fact that these have petrochemical origins is still a major drawback in a sustainability sense.

The polymer industry is being faced with similar challenges although there are known bio-based polymers such as polyhydroxybutyrate (PHB), soy based plastics, cellulose esters, polylactic acid (PLA), starch based bioplastics, poly (trimethylene terephthalate), polyethylene furanoate (PEF) and biopolyethylene already developed. Nevertheless, they have gained limited applications because of inferior properties when compared with those from petroleum feedstock.¹⁰

Some of the possible directions suggested to address the current challenges include: the utility of degradable or renewable raw materials, such as vegetable oil that is universal in the seeds, nuts, and fruits of the plants, for the synthesis;¹¹⁻¹³ the introduction of degradable functionality, for instance, amido or ester group, to the

final products;^{13, 14} and decrease of the dosage by using long-chain surfactants with high surface activity and low critical micelle concentration (CMC).¹⁵

This study seeks to develop novel bio-derived surfactants based on oils sourced from different plant materials and seeds, and on naturally occurring biomolecules to:

- i. deliver a range of biomass-derived surfactants that will replace those produced from fossil fuel resources currently being used in the industry (e.g. alkylbenzene sulphonates);
- ii. develop new sustainable synthetic approaches to a range of target compounds *via* the use of bio-platform molecules and green chemistry techniques; and
- iii. incorporate new bio-derived surfactants into Home and Personal Care formulations.

Additionally, it is planned to develop a bio-based monomer (DET) from cellulose-derived platform molecule towards the delivery of a 100% bio-based polyethylene terephthalate (PET).

1.2 Clean synthesis

Clean synthesis is a term that has no rigid definition but its contents are described within the United Nations Environmental Programme as:

The continuous application of an integrated preventative environmental strategy to processes and products to reduce risks to humans and the environment. For production processes, cleaner production includes conserving raw materials, and reducing the quality and toxicity of all emissions and wastes before they leave a process.

Clean synthesis can be achieved through the use of alternative synthesis routes that eliminates toxic solvents and feedstock; better and more effective catalyst; methods

with reduced synthetic steps; energy efficient process and by avoiding waste generation.¹⁶ These objectives are in line with the principles driving green chemistry for nearly three decades now. The principles are summarised in Figure 1-1.^{17, 18}

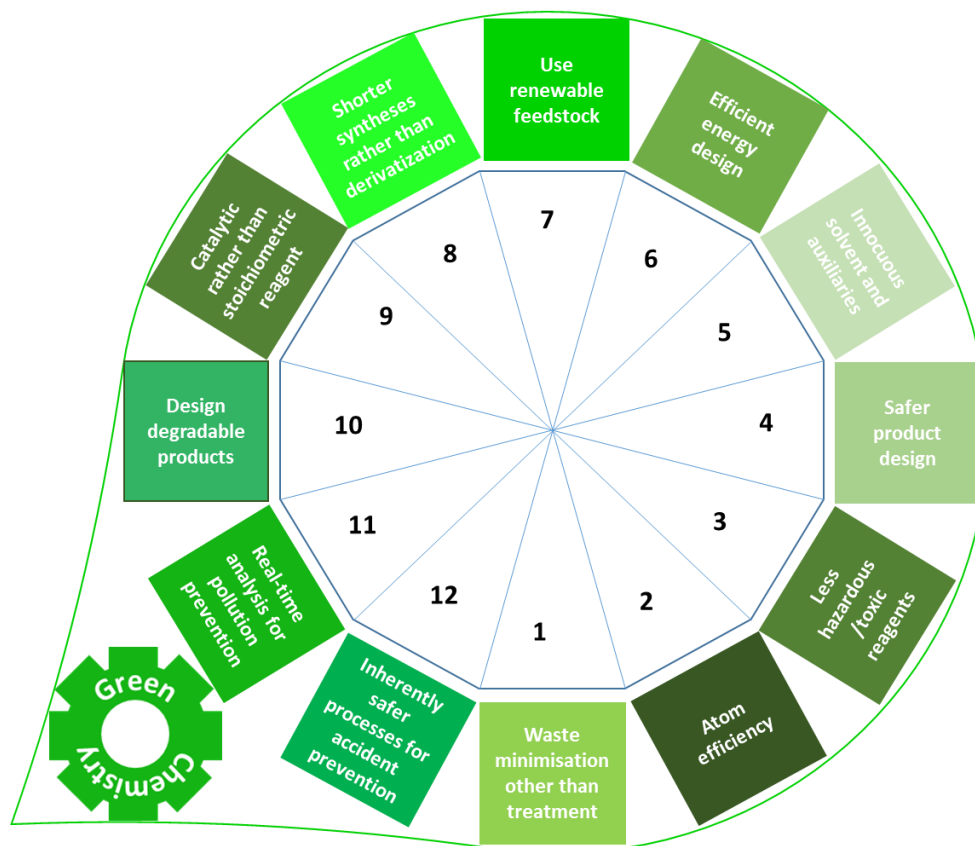


Figure 1- 1 The wheel driving Green Chemistry through the years.

1.2.1 Heterogeneous catalysis

What makes the fine chemicals and pharmaceutical industries environmental-pollution culprits is their use of stoichiometric inorganic reagents for synthesis which generate significant quantities of inorganic wastes especially from oxidations and reductions, sulfonations, nitrations, halogenations and diazotizations processes. A viable solution is catalysis. A catalyst is a chemical species capable of enhancing the rate at which a chemical reaction occurs. A catalyst participates in a reaction but is unaltered after forming the product. A typical overall catalytic

process can be seen as a cycle. For example, in Figure 1-2 reactants R_A and R_B come together to form product P_C in the presence of a catalyst. Prior to forming P_C , R_A and R_B first bonded to the catalyst to form R_A - R_B -catalyst complex, in which they reacted to form P_C -catalyst complex. The product formed then detaches from the P_C -catalyst complex as P_C leaving the catalyst available for another contact.

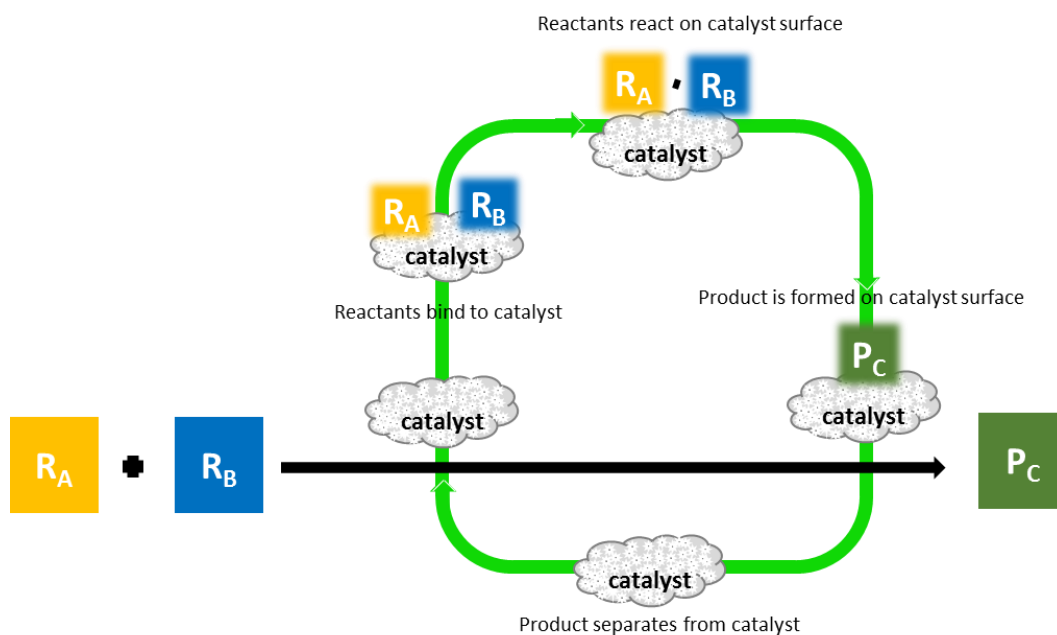


Figure 1- 2 A typical catalytic reaction is a cycle starting from coming together of reactants on the catalyst to product formation and desorption of the product to form a free catalyst ready for another cycle.

From reaction kinetics, it is apparent that a catalyst actually offers a complex alternative reaction route that is energetically favourable and requires a smaller activation energy compared to an un-catalysed reaction. It does not however affect the equilibrium constant of the overall reaction, which is instead determined by the energy difference of the starting materials and the products.

Over the years heterogeneous catalysis, in which solids are typically used to catalyse a reaction in a gaseous or liquid medium, has witnessed tremendous interests with respect to clean synthesis. Employing heterogeneous catalysis means that the catalyst can easily be separated from reaction product mixtures, there is flexibility in regenerating the catalyst and less expensive and environment-friendly reaction processes are possible.¹⁹⁻²¹ Solid acid catalysts are ideal for flow processes as there

is essentially an in situ separation of reagents and catalyst and also mixing/diffusional issues that can arise when using heterogeneous catalysts are often assisted by flow as the reaction media is pushed through the pores.

1.2.1.1 Catalyst supports

To make a heterogeneous catalyst from a homogeneous catalyst, a support is usually required. Supports are capable of improving heat dissipation, increasing poison resistance and stabilising metal catalysts which ordinarily are prone to sintering.²² Support materials can either be organic or inorganic in nature but must satisfy the criteria of being thermally stable, chemically inert relative to the catalyst and, normally have a high surface area greater than 100 m²/g.^{23, 24} Alumina, silica and carbon are the most commonly used support materials. Pores are important for increasing surface area and therefore increasing the number of catalytic sites per gram of catalyst, but pores also cause issues with diffusion. Smaller pores typically give higher surface areas but if they are too small the diffusion limits can hinder rates of reactions especially when large molecules are involved. Pores can also lead to positive and negative effects with regards to selectivity, for example oligomerisation can be reduced by using smaller pores as it is harder for larger molecules to form. Based on pore sizes a heterogeneous catalyst could be categorised into microporous (<2 nm), mesoporous (2-50 nm) and macroporous (>50 nm).

Alumina exists in numerous structures but the most commonly used for support is γ -Al₂O₃ as it possesses high surface areas up to 300 m²/g, mesopore size between 5 nm to 15 nm, high thermal stability and can be transformed into mechanically stable extrudates and pellets.²³ α -Al₂O₃ is employed in reactions where high temperature is required. Alumina generally has been widely applied as supports in many reactions such as dehydrogenations,²⁵⁻²⁹ epoxidations,³⁰⁻³⁴ steam reformings,³⁵⁻³⁸ transesterifications,³⁹⁻⁴⁴ and polymerisations.^{45, 46}

Silica is a flexible inorganic support whose properties can be easily tuned and tailored for a desired application. It is not as thermally stable as alumina and is typically used in processes where temperature requirement is not more than 300 °C due to the fact that it is liable to form volatile hydroxides when in contact with steam at elevated temperatures.²³ Reactions in which silica is applied include hydrations,⁴⁷ and hydrogenations,⁴⁸⁻⁵⁰ polymerisations,^{51, 52} and oxidations⁵³⁻⁵⁵ among many others.

Carbon is used as a catalyst support mainly for noble metal-catalysis and liquid phase reactions. Carbon has micropores >1 nm and a high surface area of up to 1500 m²/g and it is easy to recover the expensive noble metal from a spent carbon. It is usually applied as a support in hydrogenation reactions.⁵⁶⁻⁵⁹

Other supports used include titanium oxide, magnesium oxide, zirconia, zinc oxide, and aluminosilicates (such as zeolites and clays). All these have their peculiar properties for particular applications.

1.2.1.2 Preparation of supported catalyst

Homogeneous catalysts can be made heterogeneous by incorporation of supports. For instance, the homogeneous boron trifluoride can be made heterogeneous on a silica support.⁶⁰ Any of the following methods could be used to make a heterogeneous catalyst: impregnation, grafting, immobilization, ion-exchange or equilibrium adsorption, deposition-precipitation, chemical vapour deposition (CVD) and anchoring. Immobilization is the most preferred of all these methods especially when it involves asymmetric catalysis because the properties of the homogeneous catalyst are retained with additional benefits of ease of recovery and reusability of the catalyst.⁶¹ The supported catalyst is expected to be more stable, selective and of course recoverable than its homogeneous counterpart without loss of activity. To reuse an immobilized catalyst, both the support and the catalytic sites must be stable enough to maintain the catalytic activity during the recycling

process.⁶¹ The properties of a catalyst support can be tailored to a specific application. In silica, the available hydroxyl groups on the silica surface provide reactive sites for functionalization and tunable surface properties (Figure 1-3).^{23, 62-}

67

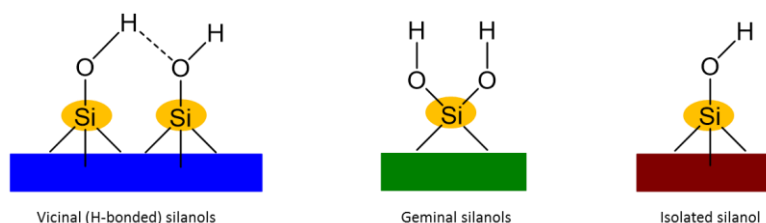


Figure 1- 3 Examples of forms of hydroxyl groups in silica

1.2.2 Green chemistry metrics

As the word “greenness” proliferates around the world pressured with the need for environmental safety and sustainability, it became obvious to unify metrics by which the greenness of a chemical process could be assessed and compared to others. Traditionally, the efficiency of a chemical process is evaluated by yield, conversion and selectivity. These tools, however, in today’s resource and waste-conscious globe are not adequate and comprehensive enough to compare different chemical routes with respect to waste generated.^{68, 69} From the view point of green chemistry, more tools are required in addition to these to quantitatively evaluate the greenness of a reaction. Some of the tools that are being used today include atom economy (AE) and E-factor, reaction mass efficiency (RME), and process mass intensity (PMI) among others.⁶⁹ One of the most recent advancements on metrics development was reported by McElroy *et al.*⁷⁰ In this report, three additional tools: optimum efficiency (OE), renewable percentage (RP) and waste percentage (WP) were proposed to further expand quantitative and qualitative assessment of the greenness of a reaction. The so-called metrics toolkit was developed in collaboration with the pharmaceutical industry, a sector of the chemical industry known for producing large quantities of waste per kg of product.

AE also known as atom utilization (AU),⁷¹⁻⁷³ estimates the amount of waste that a process generates. Percentage AE is calculated as:^{20, 72, 74, 75}

$$\text{AE} = \frac{\text{Molecular mass of desired product}}{\text{Sum of molecular masses of all reactants}} \times 100$$

It is a useful quantitative tool in comparing efficiencies of different reaction routes even right at the reaction planning stage. A well balanced equation is required in order to arrive at an accurate AE. AE assumes a 100% yield and the higher the value the less the amount of waste generated in a chemical reaction. A number of reactions in chemistry such as additions (e.g. Diels-Alder) and rearrangement (such as Beckmann) reactions are inherently atom-economic with a theoretical 100% AE while some such as elimination, substitution, Grignard and Wittig reactions are not.²⁰ In planning and designing clean synthesis these atom-economic reactions should be given priority before opting for alternatives. Notwithstanding, a number of factors have to be considered when selecting a reaction pathway:⁶⁸

- i. Hazardous nature of starting materials
- ii. Reaction yields
- iii. Ease of product isolation and purification
- iv. Solvent requirements
- v. Nature of waste materials
- vi. Equipment requirements, cost and availability
- vii. Reaction times
- viii. Energy requirements
- ix. Cost and availability of raw materials

RME as a metric is expressed as:⁷⁰

$$\text{RME} = \frac{\text{mass of product isolated}}{\text{total mass of reactants}} \times 100$$

It gives information on the actual practical efficiency of AE which is only theoretical.

OE combines AE and RME and is expressed as:⁷⁰

$$OE = \frac{\text{mass of product isolated}}{\text{total mass of reactants}} \times \frac{\text{Sum of molecular masses of all reactants}}{\text{Molecular mass of desired product}} \times 100$$

$$OE = \frac{\text{RME}}{\text{AE}} \times 100$$

This new metric provides a ground to draw a-bit-fair comparison between reactions routes whether or not they are inherently atom-economic.

The E-factor is another useful tool to evaluate the potential environmental impact of a process, and is expressed as:⁷⁶

$$\text{E-factor} = \frac{\text{mass of waste generated}}{\text{mass of desired product}}$$

E-factor gives an idea of the actual amount of waste formed in the process and usually includes everything except the desired product. It is a holistic tool in that it encompasses the chemicals used from the start of a reaction to the end (including work-up stage). Actually, it seeks to also include the fuel used in running equipment although this is a tricky measurement in most cases to actually make. However, in order to have a reasonable E-factor, water is not included in the calculation.⁷⁷ E-factor is usually applicable to industrial processes where kilograms of chemicals are used and assumes an ideal chemical process should have a E-factor of 0, thus the lower the value the better.

PMI is another important mass-based metric and is expressed as:⁷⁰

$$\text{PMI} = \frac{\text{total mass in a process or process step}}{\text{mass of product}}$$

This means it takes into consideration all the chemicals used up to work-up stage. However, it can be calculated in stages for reactants-reagents-catalysts, solvents, and work-up chemicals.

In order to make the best of green metrics to evaluate chemical processes, cumulative metrics (i.e. adding up the metric for each step) should be done for multi-step processes to capture their overall greenness.

1.2.3 Critical elements

The availability and abundance of elements used in a chemical process will soon contribute significantly to the evaluation of its greenness. In terms of availability, some important chemical elements are largely concentrated in one region (country, continent or geo-political zone) than the other. For instance, China controls about 95% of the world's rare earth metals.⁷⁸ There are possibilities that the supply of these elements to other countries or regions may soon be affected by political influences. Additionally, some elements are likely to become depleted from their primary sources within a short time if current rate of consumption persists. According to the EU, an element that is of high economic value and has a risk of becoming depleted with continuous use or restricted in supply due to geo-political reasons may be considered "critical".⁷⁹ As shown in Figure 1-4 most of periods 4, 5, 6 and rare earth elements which are largely applied in today's catalysis fall within this definition of "critical".

1		Remaining years until depletion of known reserves (based on current rate of extraction)																2					
H 1.00794																		He 4.002602					
3	4																	5	6	7	8	9	10
Li 6.941	Be 9.012182																	B 10.811	C 12.0107	N 14.00674	O 15.9994	F 18.99840	Ne 20.1797
11	12																	13	14	15	16	17	18
Na 22.98977	Mg 24.3050																	Al 26.98153	Si 28.0855	P 30.97376	S 32.066	Cl 35.4527	Ar 39.948
19	20	21	22	23	24	25	26	27	28	29	30	31	32	33	34	35	36						
K 39.0983	Ca 40.078	Sc 44.95591	Ti 47.867	V 50.9415	Cr 51.9961	Mn 54.93804	Fe 55.845	Co 58.93320	Ni 58.6934	Cu 63.546	Zn 65.39	Ga 69.723	Ge 72.61	As 74.92160	Se 78.96	Br 79.904	Kr 83.80						
37	38	39	40	41	42	43	44	45	46	47	48	49	50	51	52	53	54						
Rb 85.4678	Sr 87.62	Y 88.906	Zr 91.224	Nb 92.90635	Mo 95.94	Tc [98]	Ru 101.07	Rh 102.9055	Pd 106.42	Ag 107.8682	Cd 112.411	In 114.818	Sn 118.710	Sb 121.760	Te 127.60	I 126.9044	Xe 131.29						
55	56	57	58	59	60	61	62	63	64	65	66	67	68	69	70	71	72						
Cs 132.9054	Ba 137.327	La* 138.9055	Hf 178.49	Ta 180.9479	W 183.84	Re 186.207	Os 190.23	Ir 192.227	Pt 195.078	Au 196.9665	Hg 200.59	Tl 204.3833	Pb 207.2	Bi 208.9804	Po [209]	At [210]	Rn [222]						
87	88	89	90	91	92	93	94	95	96	97	98	99	100	101	102	103	104						
Fr [223]	Ra 226.025	Ac‡ [227]	Rf [257]	Db [260]	Sg [263]	Bh [267]	Hs [265]	Mt [266]	Ds [271]	Rg [272]	Uub [285]	Uut [284]	Uuq [289]	Uup [288]	Lv [292]	Uus [291]	Uuo [292]						
Lanthanides*		58	59	60	61	62	63	64	65	66	67	68	69	70	71								
		Ce 140.9077	Pr 144.24	Nd 145	Pm [145]	Sm 150.36	Eu 151.964	Gd 157.25	Tb 158.9253	Dy 162.50	Ho 164.9303	Er 167.26	Tm 168.9342	Yb 173.04	Lu 174.967								
Actinides‡		90	91	92	93	94	95	96	97	98	99	100	101	102	103								
		Th 232.0381	Pa 231.0389	U 238.0289	Np [237]	Pu [244]	Am [243]	Cm [247]	Bk [247]	Cf [251]	Es [252]	Fm [257]	Md [258]	No [259]	Lr [262]								

Figure 1- 4 Periodic table highlighting critical elements.⁸⁰

Green metrics have now also been extended to consider element criticality in its evaluation of the greenness of a chemical process.⁷⁰ It is therefore important to design chemical reactions in such a way that less amount of critical elements are used if at all there are no alternatives.

1.2.4 Clean technologies

A chemical process is a combination of various components which in addition to reagents and catalysts include equipment operations and other ancillaries such as energy. The use of renewable resources will not automatically label a process as green unless accompanied with clean technologies. Using a non-clean technology with renewable resources will likely deliver a partially green process (Figure 1-5). These have to be taken into consideration alongside “greenness” consciousness. Processes that use low-energy input yet with advantageous reaction efficiencies are often termed clean technologies and include sonochemistry (ultrasound), microwave, photochemistry, electrochemistry, supercritical fluid technique, superheated water technique etc.^{20, 68} Many of these technologies are recent advances while others have only found interest in the last decade.

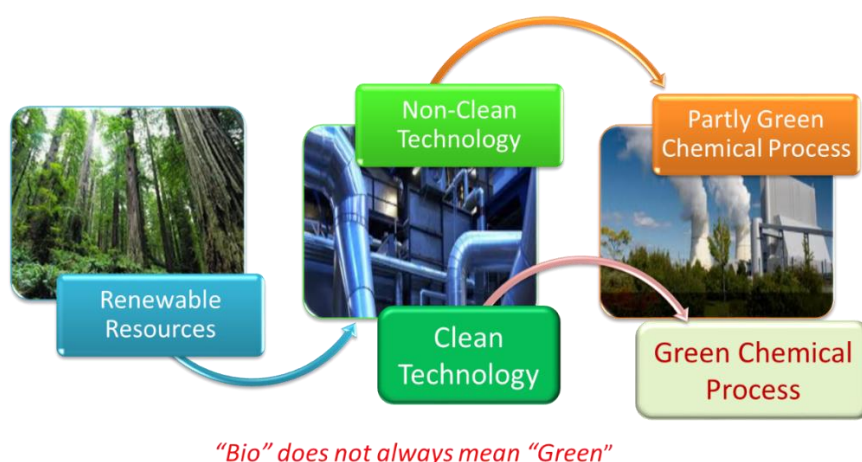


Figure 1- 5 Relationship between renewable resources and clean technologies with respect to clean synthesis.

Ultrasound is a benign technique for energising systems that has been known for decades. It has been applied to enhance mechanical effects in heterogeneous

catalysis and is strikingly known to effect other reactions through a still-debated process called cavitation to yield new products not observed in conventional processes.^{68, 81, 82}

Microwave technology is considered environmentally friendly simply because it is energy efficient and cost effective.⁸³ The main driving force for this technique is the fact that heat distribution in microwave is homogeneous or volumetric (that is, from inside to outside) while conventional heat distribution is by external radiation (that is, from outside to inside) as shown in Figure 1-6. Homogeneous heating means that sample molecules have direct contact with microwave energy and does not allow localised heating of reaction wall thus preventing side reaction. The consequences are: high heating rates, less reaction time, improved yield and selectivity.¹⁹ Microwave technology has been applied in many organic reactions, extractions and pyrolysis.^{46, 84, 85}

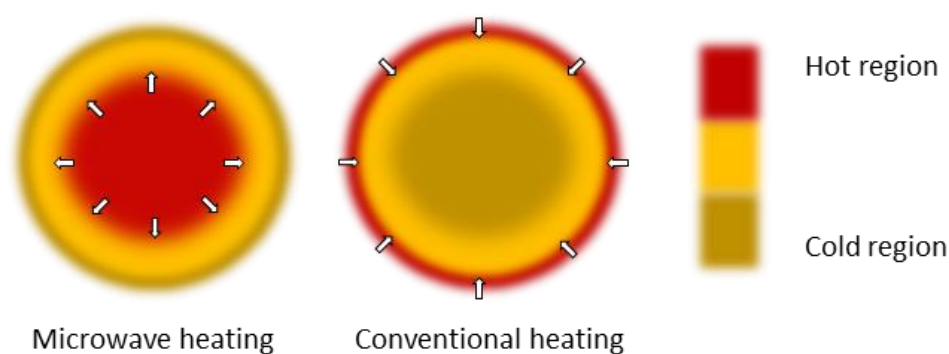


Figure 1- 6 Heat distribution in conventional and microwave systems.

Electrochemistry as a process is considered a green technology because it involves mild chemical conditions and inexpensive electrons, is typically a water-based process and energy efficient, offers high process selectivity, atom-economic and capable of giving reaction products impossible in conventional processes.^{20, 68}

1.3 Platform molecules

The word “platform” has been used differently by many authors to mean renewable or green feedstock. A unified definition for platform molecules has been proposed as:⁸⁶

A bio-based (or bio-derived) platform molecule is a chemical compound whose constituent elements originate wholly from biomass (material of biological origin, excluding fossil carbon sources), and that can be utilised as a building block for the production other chemicals.

As building blocks, platform molecules possess multiple functionalities through which they can be transformed into other useful chemicals. Platform molecule feedstocks can be sourced from carbohydrates (saccharides), lignins, proteins and extractives (triglycerides, terpenes, waxes). A number of platform molecules that have capacity to provide bio-derived chemicals for the chemical industry have been identified and reported.⁸⁷ A 2004 report from the US Department of Energy listed the top twelve of these chemicals as: 1,4-diacids (succinic, fumaric and malic), 2,5-furandicarboxylic acid (FDCA), 3-hydroxy propionic acid, aspartic acid, glucaric acid, glutamic acid, itaconic acid, levulinic acid, 3-hydroxybutyrolactone, glycerol, sorbitol, and xylitol or arabinitol. Figure 1-7 shows various bio-based chemicals that can be derived from these platform molecules *via* selective reduction, oxidation, hydrogenation, condensation, dehydration, direct polymerisation etc. In fact, it is possible that a platform molecule is capable of producing another platform molecule, e.g. 5-hydroxymethylfurfural (HMF) can be catalytically oxidized to succinic and fumaric acids alongside other acids.⁸⁸

Some of these platform molecules are already engaged commercially to produce bio-based chemicals. An Italian based company, Bio-on, is set to produce the world's first 100% poly hydroxyalkanoates (PHAs) bio-plastic from glycerol at the rate of 5000 tons per year.⁸⁹ Demand for glycerol in cosmetics, pharmaceuticals, food, polymer

industries is still growing and estimation projected global production of crude glycerol to reach around 4 billion gallons this year.⁹⁰

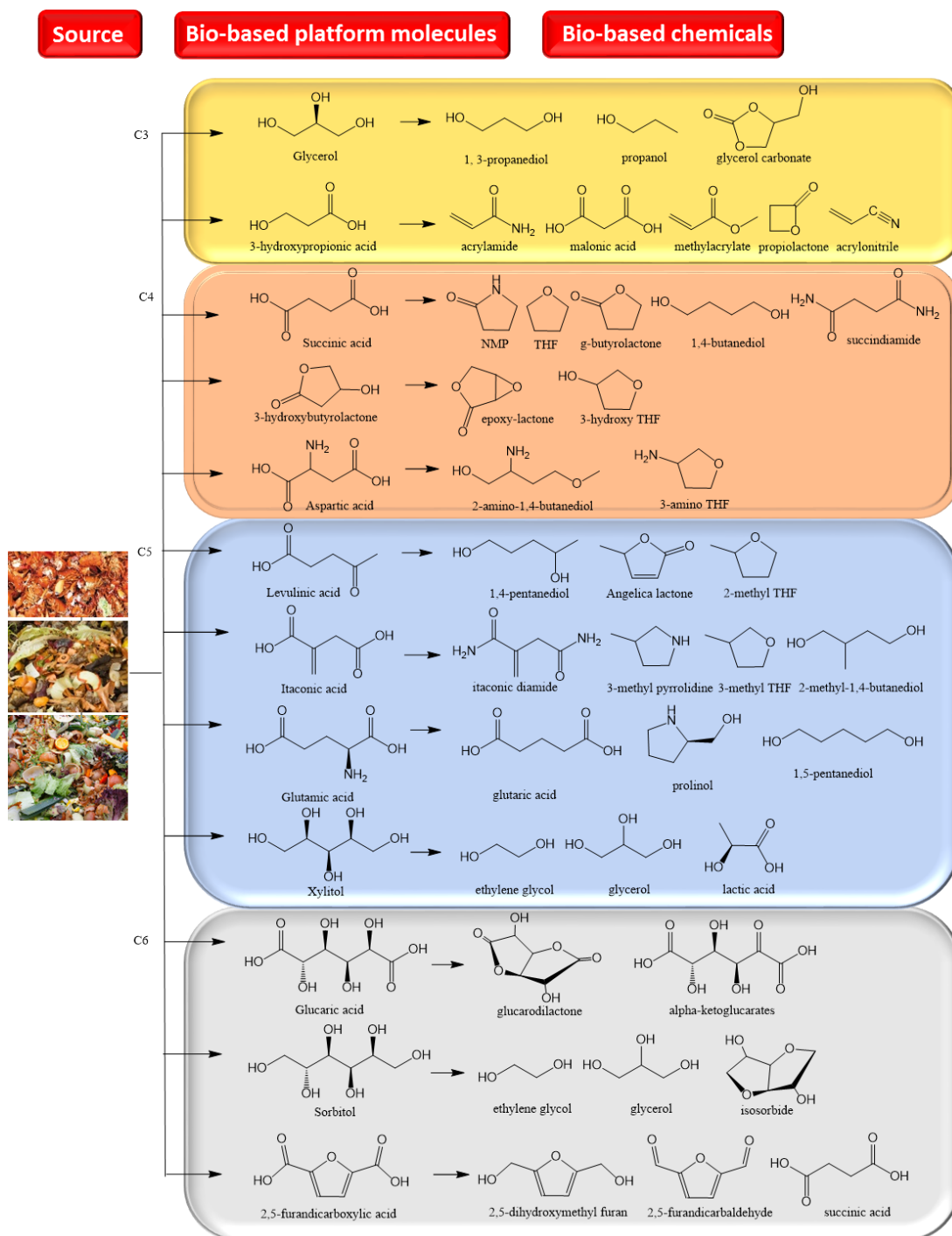


Figure 1- 7 Platform molecules are processed to generate a number of bio-based chemicals

Furfural from which other valuable platform molecules such as FDCA and levulinic acid can be produced is currently standing at over 0.2 Mt. annual production.⁹¹ FDCA as a platform molecule is seen to have capacity for increasing potentials in the

chemical industry especially for bio-based polyesters.⁹²⁻⁹⁶ Presently it has been developed to produce a 100% bio-based poly ethylenefuroate (PEF) that is claimed to be a potential PET replacement.⁹⁷ PEF bottles, according to a recent report by Avantium, the inventing company, will be used to serve drinks at the 2020 Olympics.⁹⁸

Large contribution to bio-based chemical production could come from cellulose because of its abundance.⁹⁹ Unfortunately at the moment most of these chemicals still come from starch and sugar because of the many challenges with utilizing recalcitrant cellulosic biomass. In using cellulose there is need for harsh hydrolytic conditions in order to release glucose from the matrix and this usually produces side products such as fructose, HMF, levulinic acid and levoglucosan.¹⁰⁰ Also, enzymatic transformation of the biomass mainly produces oligomers though taking place under mild conditions.¹⁰¹ Thermochemical treatment of cellulosic biomass is capable of delivering some of these platform molecules though in low yields and requires separation from complex mixtures.¹⁰²⁻¹⁰⁵

Inulin, chitin and fucoidan can serve as alternative non-food saccharide feedstocks for platform molecules. These biomasses are processed *via* hydrolysis, pyrolysis or other means to deliver bio-based chemicals rich in oxygen, nitrogen and sulphur functionalities.¹⁰⁶⁻¹⁰⁹ Other sources such as lignin and triglyceride are discussed under different sections of this chapter.

As much as there are pressures to use renewable feedstocks for chemical production, much care is being taken not to use materials that compete with food production. As such wastes like agricultural and industrial wastes are being targeted for this purpose. The functionalities possessed by these molecules mean that the chemical industry could save a lot on oxidations and aminations processes etc. Therefore reactions must be designed in such a way that functionalities are not first removed then later re-introduced, a concept that we consider in greater depth in chapter 6 of this thesis.

1.4 Bio-derived monomers- specifically aromatic monomers

The majority of the world's aromatic feedstocks come from petroleum sources; and most of the easily transformable platform molecules like glucose, fructose do not primarily yield aromatics without additional difficult modifications. Lignin remains the largest potential source for bio-derived aromatics. The structure of lignin is complex and very difficult to transform to other useful bio-based chemicals because of resistance to biological and degradation treatments.¹¹⁰ However, pyrolysis and depolymerisation of the complex molecule have proven to yield some encouraging results.^{102, 103, 111-114} Figure 1-8 shows some aromatics that can be obtained from the pyrolysis, hydrolysis and hydrogenolysis of lignin.

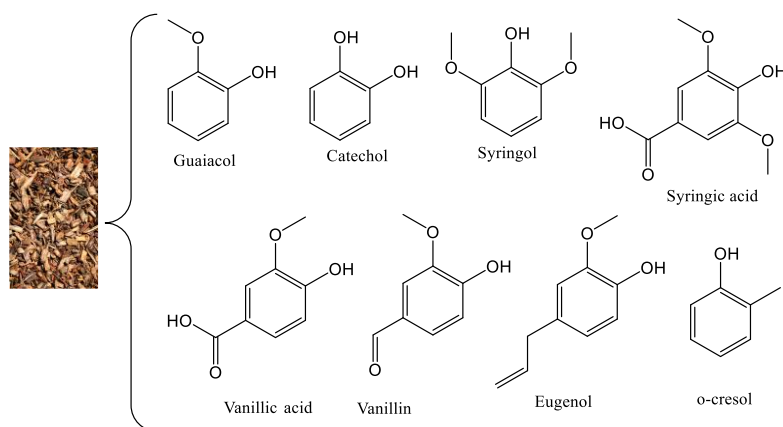


Figure 1- 8 Examples of platform molecules derived from lignin

Despite the potentials of these processes, there remain the challenges of structural complexity and variability in lignin, need for isolation and purification of processed lignin, severe conditions for lignin degradation, complex mixture of products and low yield among others.^{86, 112} These challenges make it non-economical when compared to petrochemical alternatives.

One of the areas where bio-based aromatics are highly sought after is in the production of 100% bio-based PET. Interestingly, ethylene glycol (EG), which accounts for 30% PET composition, can now be obtained from bio-derived ethylene and also from platform molecules such as sorbitol and xylitol *via* hydrogenolysis as discussed in section 1.3.^{115,87} In fact, there is an established route for biomass-

derived EG from sugar-based feedstock which is presently commercialised in products like the Coca Cola company plant bottle (30% bio-based).¹¹⁶ *Para*-Xylene is a fossil-derived base chemical serving as the source of both the aromatic and 1,4-substitution for TA which accounts for the remaining 70% PET composition to make a 100% bio-based PET.¹¹⁷ Phthalic acid (PA) and isophthalic acid (IPA) obtained from oxidation of *ortho* and *meta*-xylenes can also be used for this purpose. In fact, it is actually much easier to obtain 1,2- and 1,3-substitution on aromatics from bio-platform molecules and biomass. For example, *meta*-xylene is the favoured isomer of xylene readily obtainable from lignin depolymerisation.¹¹⁸ The major issue with poly (ethylene phthalate) and poly (ethylene isophthalate), however, is that the crystalline regions are less well ordered, and the substitution of the aromatic backbone must remain 1,4- (i.e. *para*).¹¹⁹ Many researchers have subsequently focussed efforts and reported on the production of bio-derived *para*-xylene.

2, 5-dimethyl furan (DMF) from HMF has been converted to *para*-xylene *via* Diels-Alder addition to acrolein,¹²⁰ or ethene under different reaction conditions.¹²¹⁻¹²⁴ Rather than DMF, oxidation derivatives of HMF have been added to ethene *via* Diels-Alder reaction over a series of Lewis acid catalysts possessing weak Brønsted acids.^{125, 126} Interestingly, synthesis of *para*-xylene from ethene as the sole starting material has been demonstrated.¹²⁷ The synthesis proceeded *via* trimerisation of ethene to hexene, conversion of hexene to hexadienes over an iridium complex catalyst, Diels-Alder addition of hexadiene to ethene and then catalytic dehydrogenation of the product 3, 6-dimethyl cyclohexene. Fermentation of sugar to isobutanol followed by dehydration to isobutene, which upon dimerization, dehydrocyclization and oxidation of product has also been reported to give a bio-derived TA.¹²⁸ Another route is the Virent process that converts sugar beets to a mixture of intermediates which are further processed to give BioFormPX (*para*-xylene) as one of the products.^{117, 129-131} This route forms the basis for the Coca Cola's recent exhibition of the world's first 100% bio-based PET.^{28, 29} A non-cellulosic route to bio-derived TA *via* terpenes such as limonene which involved

isomerisation to *para*-cymene with subsequent oxidation to TA was also reported.¹³² Another route which uses furfural as the sole starting molecule has been reported.¹³³ This “absolute furfural” route proceeded *via* oxidation of furfural to both fumaric acid and maleic acid which were subsequently dehydrated to maleic anhydride. Diels-Alder addition of furan (obtainable from decarbonylation of furfural)¹³⁴ to maleic anhydride gives an exo-Diels-Alder adduct which was subsequently converted to anhydride and phthalate salt and finally to TA. Analysis of the obtained TA with accelerator mass spectroscopy showed it had a 100% bio-based carbon content.¹³³ Figure 1-9 summarises some of the routes investigated.

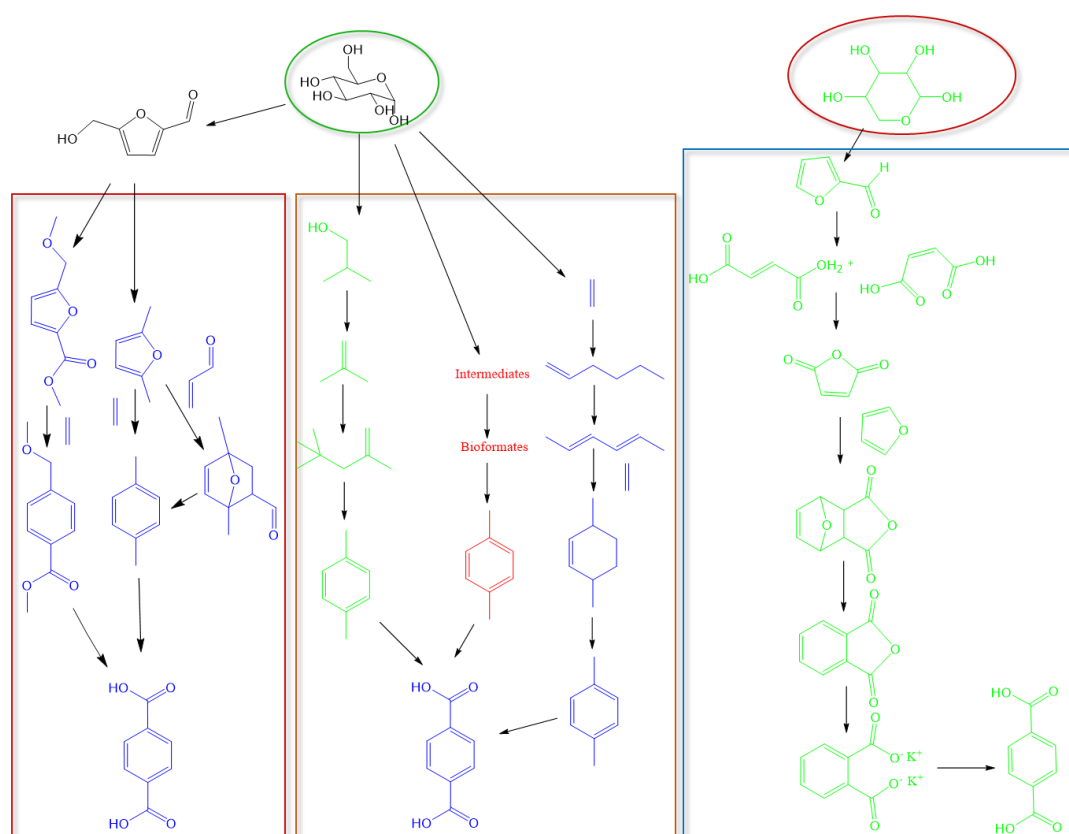


Figure 1- 9 Some investigated routes to bio-based TA from glucose and xylose.

While some of the routes look very promising, the issue with most of them is that the starting biomass has to be reduced first with most of the oxygen molecules partially or completely removed and thereafter reoxidised to form TA. This lowers considerably the AE of the overall pathway. Also, they continue to require the harsh oxidation steps previously employed in TA synthesis. For the limonene route, only

around 70,000 tons limonene is annually produced globally,¹³⁵ which means it is never going to meet up with the demand for TA required to produce PET. Therefore, cellulose *via* HMF remains a most promising route to source bio-based TA.

1.5 Surfactants

1.5.1 Introduction to surfactants

Surface active agents (surfactants) are amphiphilic molecules that typically possess both hydrophilic head(s) and hydrophobic tail(s) in the same molecule and with opposing ends they modify the surface of an interface (Figure 1-10). They are one of the most indispensable chemicals used in the chemical industry probably because they provide the foundation for most of the chemical formulations we see today.¹³⁶ Surfactants are widely used as catalysts in organic synthesis,¹³⁷ in drug delivery as carrier vehicles,¹³⁸ as templates in the synthesis of nanoparticles,¹³⁹ as solubilizing, wetting, emulsifying agents; in detergency, spreading, biocidal, anti-static and corrosion inhibition, foaming, defoaming and lubricity among others in the industries.

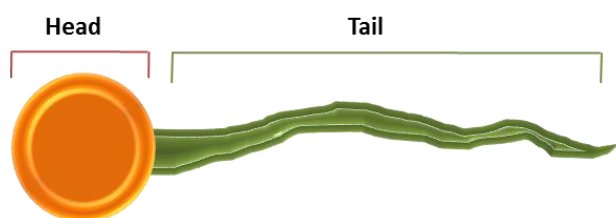


Figure 1- 10 Schematic illustration of a typical surfactant.

The production of surfactants has continued to grow over many decades and detergency takes the largest share in surfactant applications. About half of the surfactants produced around 2006 were applied in detergent formulations (Figure 1-11).¹⁴⁰ The global surfactants market is projected to reach 22.8 Mt, by volume and \$40.3 billion net value by 2019.¹⁴¹

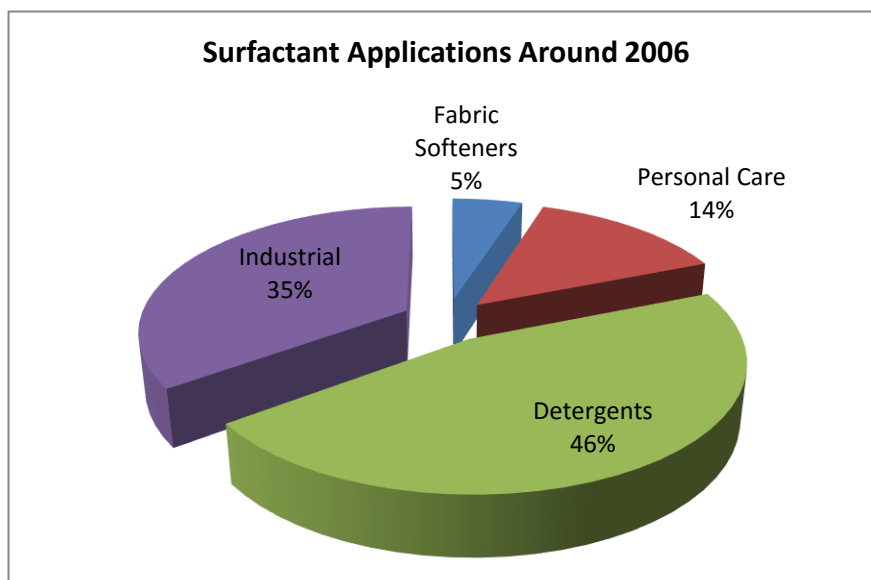


Figure 1- 11 Applications of surfactants around 2006.¹⁴⁰

1.5.2 Classification of surfactants

Surfactants are primarily classified into cationic, anionic, nonionic and zwitterionic based on the charge of their polar head group. The discussions below are based on a recent description on surface chemistry of surfactants and polymers,¹⁴² and other sources.¹⁴³

1.5.2.1 Anionic surfactants

Anionic surfactants are those containing polar head groups such as sulphates, sulphonates, carbonates and phosphates. Various counterions including calcium, potassium, sodium, ammonium, and alkyl amines are used in the synthesis of anionic surfactants for different purposes. Amine salts are used to impart both oil and water solubility while sodium and potassium give water solubility in the product.¹⁴² Anionic surfactants are easy and in-expensive to manufacture and remains the largest class (~70%) of surfactants. They are used mostly in detergent formulations. These surfactants are however sensitive to hard water and have

limited compatibility with cationic surfactants.¹⁴² A few common examples are shown in Figure 1-12.

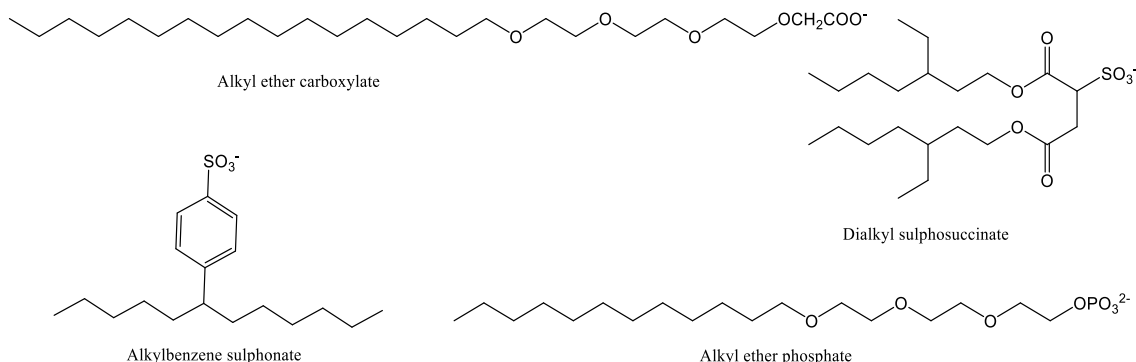


Figure 1- 12 Examples of anionic surfactants

1.5.2.2 Cationic surfactants

Cationic surfactants are largely based on nitrogen atom which carries a positive charge. Common products are the amine and quaternary ammonium surfactants. They are compatible with nonionic and zwitterionic surfactants but limited compatibility with anionic surfactants. Cationic surfactants show poor detergency and are more expensive than both anionics and nonionics.¹⁴² They are mainly used for adsorption purposes because of their strong interaction with the interface but also applied in anticorrosion, anticaking, antistatic, dispersing agents, conditioners and as fabric softeners. Examples are shown in Figure 1-13.

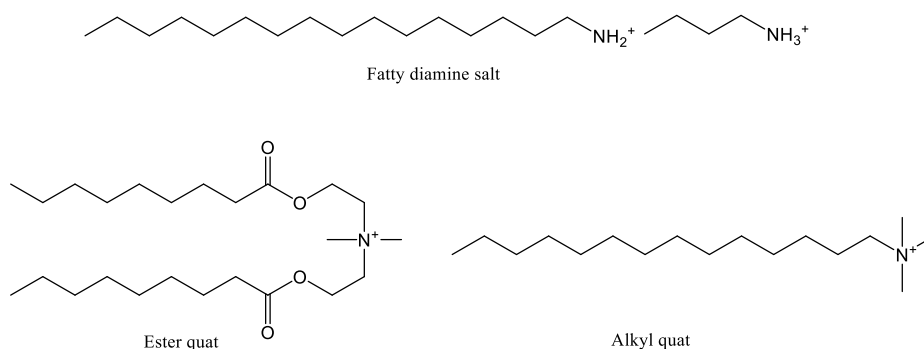


Figure 1- 13 Examples of cationic surfactants

1.5.2.3 Nonionic surfactants

These surfactants carry no formal charge on them and are commonly synthesised from the reaction of fatty alcohols, fatty acids, fatty amines and alkylphenols with polyethers or polyhydroxyls *via* ethoxylation.¹⁴² Nonionic surfactants are the second largest class of surfactants, compatible with all other types of surfactants and their physicochemical properties are not significantly affected in the presence of electrolytes. Figure 1-14 shows a few examples of this class of surfactants.

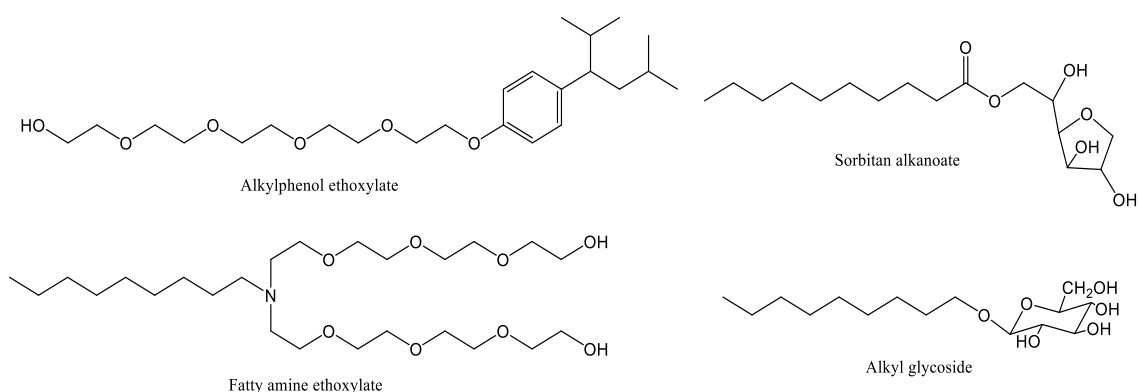


Figure 1- 14 Common examples of non-ionic surfactants

One uniqueness of nonionic surfactants is that they become more hydrophobic (less soluble) as temperature increases. They are soluble in hard water and organic solvents, including hydrocarbons and are used as antifoam agent, in dishwashing detergents, and as emulsifying agents. Figure 1-14 shows a few examples of this class of surfactants.

1.5.2.4 Zwitterionic surfactants

Zwitterionic surfactants are those in which the hydrophilic end carries two opposite charges (positive and negative). The positive charge is usually ammonium but the negative charge varies (commonly carboxylates). These surfactants are compatible with all other types of surfactants and have proven to be dermatologically useful in personal care products and shampoos as they exhibit less skin and eye irritations than other types of surfactants.^{142, 143} As they possess no net charge, zwitterionic surfactants function well in formulations containing electrolytes.¹⁴² They possess

high stability in acids and bases. A good example is the betaines that retain their surface activity in spite of high pH. Examples of this class of surfactants are shown in Figure 1-15.

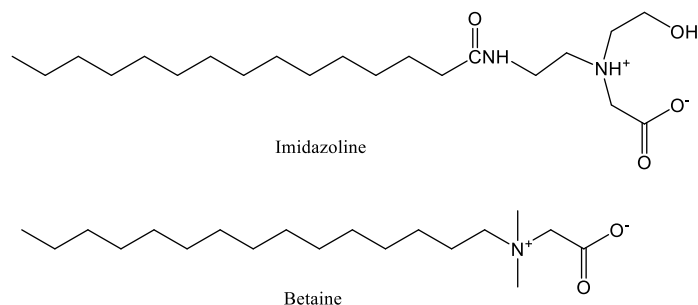


Figure 1- 15 Common examples of zwitterionic surfactants

1.5.3 Surfactant interaction

As discussed earlier, the presence of hydrophilic (polar) and hydrophobic (non-polar) groups in surfactants is responsible for their interaction at an interface and hence all the interesting properties exhibited by surfactants. Generally, there are two forces: electrostatic force (hydrogen bonding, dipolar interaction, ionic bonding) and hydrophobic interaction (van der Waal), responsible for surfactant interaction with their surroundings.^{142, 144} The polar head of the surfactant interacts with the polar part of the system such as water or ions while the non-polar end of the surfactant interacts with the non-polar part of the system. The interaction actually depends on the type of interface present. Figure 1-16 (top) shows a schematic depiction of five possible scenarios. In an air-water interface, the surfactant head is buried in the solution while the tail is withdrawn (that is associated in solution and adsorbed at interface) whereas in an oil-water interface the head and the tail are directed to the polar and non-polar phases respectively (associated at both ends). In a single non-polar phase, only the tail is adsorbed on the solid while the head is directed away from it. For a soap film, which is air-water-air interface, the surfactant heads are buried in the solution but repelled from each

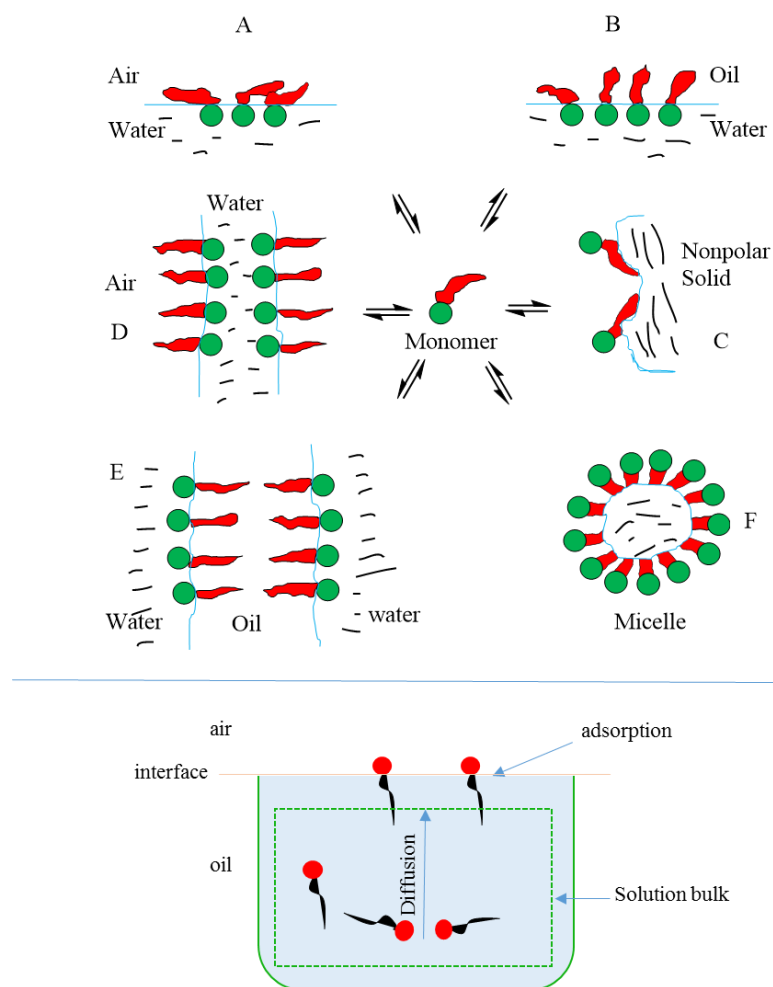


Figure 1- 16 Schematic representation of (top) surface activity and micelle formation. (a) air-water interface; (b) oil-water interface; (c) adsorption onto nonpolar solids; (d) soap films; (e) bilayers; (f) micelles. Redrawn from literature source.¹⁴⁴, (Bottom) diffusion of surfactant molecules from the bulk solution to the surface and their adsorption at the surface.

other while the tails are withdrawn on both sides. In a water-oil-water system, the tails are buried in the oil but repelled from each other while the heads are withdrawn into the aqueous phases. The two main phenomena that occur in the interaction of surfactants are diffusion and adsorption.¹⁴² A surfactant molecule upon dissolution in a phase will diffuse through the bulk solution, and self-assemble at the surface based on its structure and the system (Figure 1-16 bottom). This interaction produces adsorption of surfactants at the surface and as their concentration increases at the surface they aggregate to form a small closed structure called a micelle (Figure 1-16 top). Micelles can be of various sizes and

shapes depending on the concentration and structure of surfactant; pH, ionic strength and temperature among other factors.

1.5.4 Renewable surfactants

There are renewed and growing interests in the synthesis of renewable (bio-based) and importantly biodegradable surfactants owing to environmental pressures. In making such surfactants, their two ends namely: hydrophilic ends (hydrophiles) and hydrophobic ends (hydrophobes) have been reconstructed. The hydrophobes have been selected from sources like vegetable oils and other natural hydrophobic molecules like cardanol and, anacardic acid from cashew nuts shell liquid (CNSL) while amino acids and polyols such as sugar, sorbitol, cellulose and other carbohydrates have been sourced as hydrophiles (Figure 1-17). Recent developments in the use of these renewable hydrophiles and hydrophobes in the production of renewable surfactants are reviewed by Foley *et al.*⁶

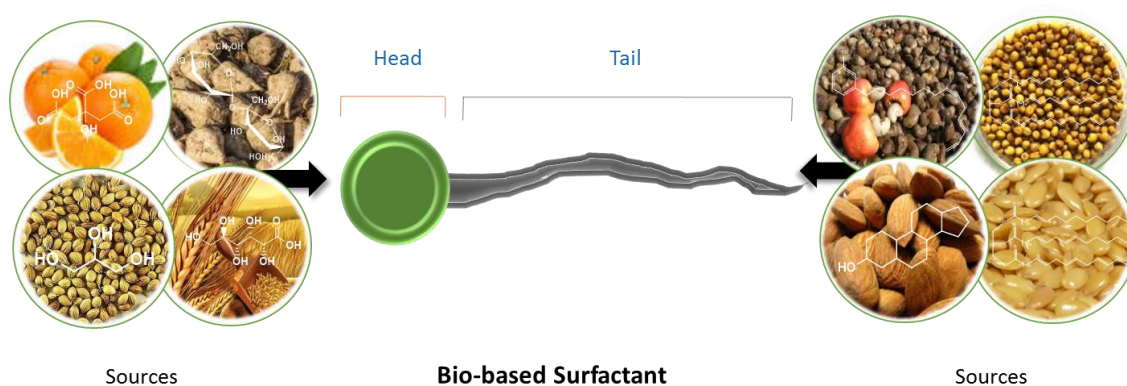


Figure 1- 17 Bio-based surfactants are made from renewable hydrophilic end (head) e.g. sucrose, citric acid, glycerol, glucose, and renewable hydrophobic end (tail) e.g. sterol, triglycerides and cardanol.

1.5.4.1 Renewable hydrophobes

Vegetable oils have inherent properties as potential replacements for petroleum feedstock for the manufacture bio-based surfactants, and indeed have been used

extensively for the synthesis of common surfactants such as sodium lauryl sulfate. They are readily available, biodegradable, possess variety of functionalities and have low toxicity. Vegetable oils are composed of triglycerides which contain different fatty chains in the same molecule. Triglycerides are sometimes referred to as *triglyceride platform* while the individual fatty acids in them are called platform molecules.¹⁴⁵

Common vegetable oil sources include rapeseed, sunflower, linseed, soyabean and palm. The type of fatty acid obtained in a particular vegetable depends on the composition of the oil. World vegetable oil production from soyabean, rapeseed and sunflower has increased drastically from around 73.3 Mt in 2001 to 143.8 Mt in 2014 (Figure1-18). The current global vegetable oil and fat production is around 187 Mt and global vegetable oil production is expected to increase by over 30% by 2020 though increasing interest in biodiesel production could be largely responsible for this.¹⁴⁶

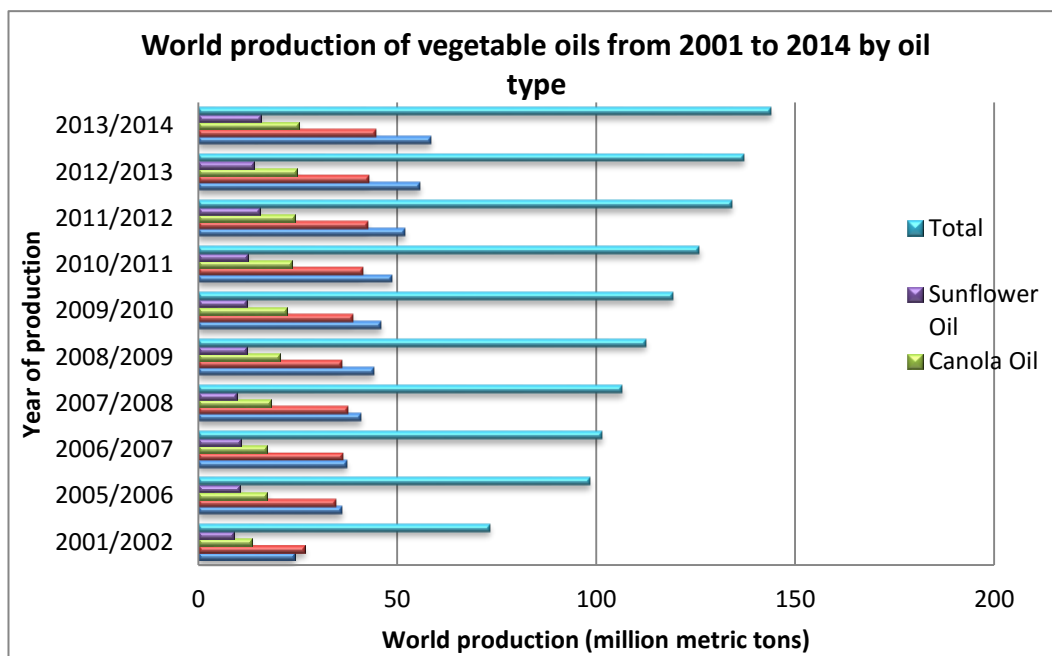


Figure 1- 18 World production of soyabean, sunflower and canola/rapeseed oils from 2001 to 2014.¹⁴⁷

As discussed earlier, triglycerides fatty acids possess diverse chain length of interesting properties. Table 1-1 shows the distribution of the fatty acid in most

known vegetable oil. Lauric acid, C12, is largely present in palm kernel and coconut while palmitic acid, C16, is largely present in palm oil. Stearic acid, C18:0, is always in low amount compared to the unsaturated acid C18:1 and C18:2 in most of the vegetable oils.

Interesting functionalities in triglycerides are the double bonds and the carboxylic acid group which can be transformed into different derivatives allowing for a spectrum of possible bio-derived substrates. The use of triglycerides in chemical development has traditionally involved reactions with the carboxylic acid group with about 10% of the modification involving the alkyl chain or the double bond.¹⁴⁸ Currently, interests are now in the exploitation of the alkyl group and the double bond functionalities in developing highly branched and bulky hydrophobes from oils.^{6, 12}

Table 1- 1 Fatty acid distribution in selected vegetable oils and fats

Source	Saturated acids					Unsaturated acids				
	<12	12	14	16	18:0	18:1	18:2	18:3	>20	
Palm ^{149, 150}			5	36	4	39	11	0-1		
Palm kernel ¹⁵⁰	7	45	18	9	3	15	2			
Coconut ¹⁵⁰	15	48	16	9	2	7	2			
Low erucic rapeseed (Canola) ^{150, 151}				4	2	61	21	10	1	
High erucic rapeseed ¹⁵⁰				3	1	16	14	10	56	
Normal Linseed ¹⁵⁰				6	3	17	14	60		
Conventional sunflower ^{150, 152}				6	5	19	60	0-1		
Low linolenic linseed ¹⁵²				6	3	15	73	3		
High oleic sunflower ¹⁵²				7		83	10			
Conventional soyabean ¹⁵⁰				11	4	23	53	8		

Figure 1-19 shows some of the chemical transformations employed to produce surfactants from vegetable oil. Hydrogenation of triglyceride using nickel catalyst at temperature of 110-190 °C and under pressure removes the unsaturations.¹⁵³ Transesterification of the saturated triglyceride with methanol yields fatty acid methyl ester (FAME) which can subsequently be sulphonated or reduced to fatty alcohols. The saturated triglyceride can also be hydrolysed to fatty acid and then reduced to fatty alcohol but this method is not always preferred because the reduction catalyst and glycerol are degraded and requires too high a temperature to be energy effective.¹⁵⁴ Direct epoxidation of the triglyceride for subsequent ring-opening is another possible transformation.

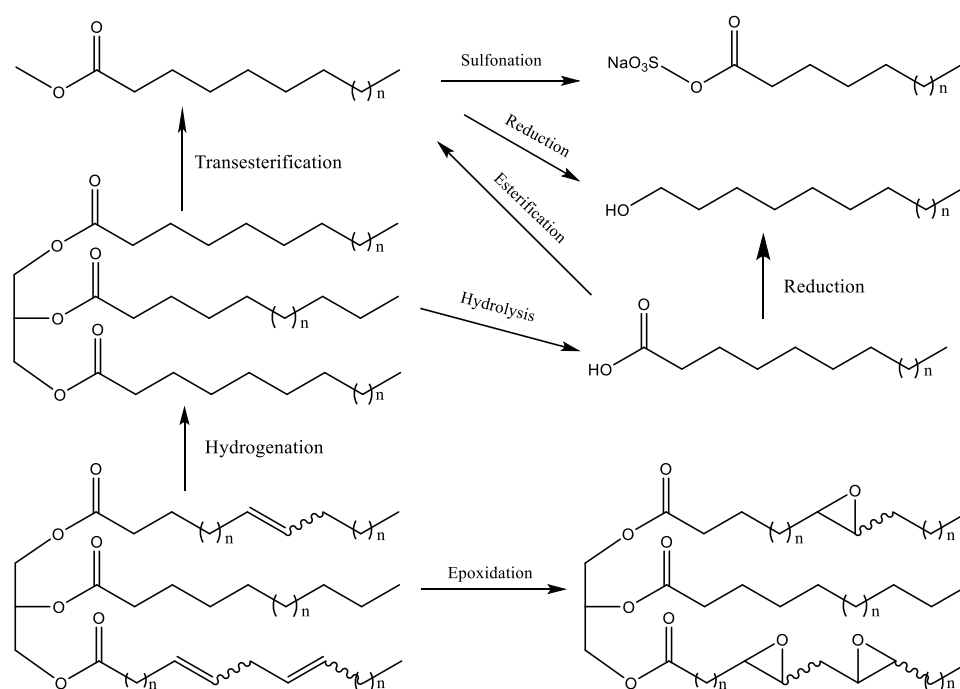


Figure 1- 19 Common transformations of triglycerides in the manufacture of surfactants

1.5.4.2 Renewable hydrophiles

Polyols are among the most suitable candidates for use as renewable hydrophiles because they are easily biodegradable aerobically and anaerobically; possess low toxicity and high solubility in water. Glycerol (from triglyceride hydrolysis), sucrose (from sugar cane and sugar beets), glucose (starchy crops such as potato, maize) and

sorbitan (from glucose *via* sorbitol) are examples of bio-derived polyols that have all been used in surfactant synthesis. Alternatively organic acids such as lactic acid, citric acid, gluconic acid, ascorbic acid can also be used as hydrophiles.⁶ These molecules are available in large quantity up to 150 Mt/a for sucrose.¹⁵⁵ With the availability of bio-based ethylene glycol, poly (ethylene glycol) could be a ready candidate for this purpose as well. Examples of surfactants based on some of the hydrophiles are shown in Figure 1-20. Prominent among these examples are the alkyl polyglucosides (APGs) which have been around for several decades. Current worldwide production of APGs is approximately 85000 tonnes/ annum,¹⁵⁵ and are applied in personal care products, detergents, agrochemicals, hard surface cleaners and industrial cleaners. Major global suppliers of APGs include Cognis, BASF, SEPPIC, AkzoNobel and Dai-Ichi Kogyo Seiyaku.

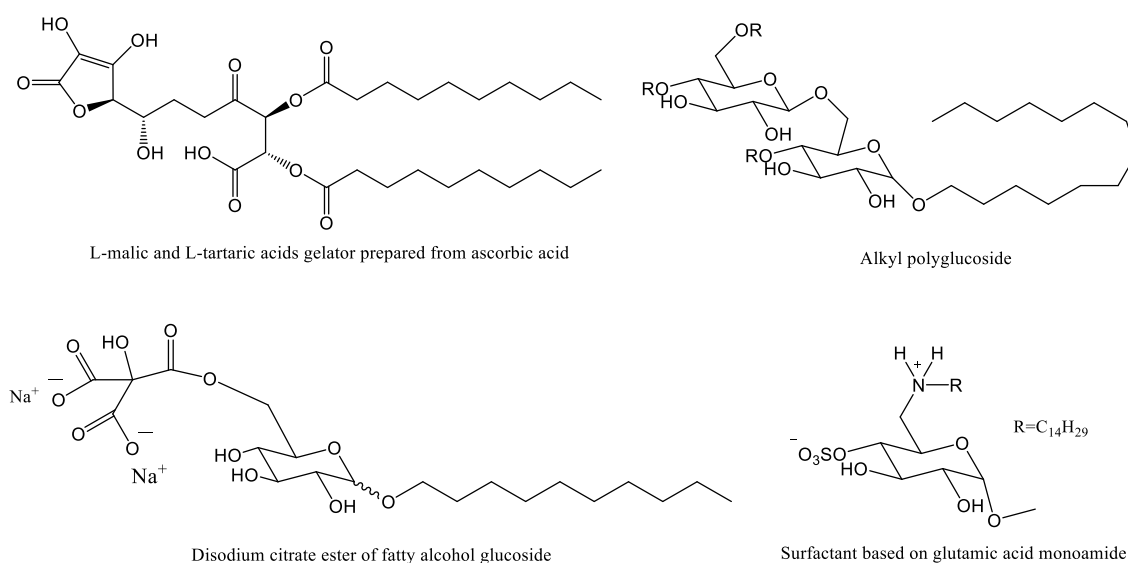


Figure 1- 20 Surfactants based on renewable hydrophiles.¹⁵⁶⁻¹⁵⁹

1.6 Conclusions

Increasing strict environmental legislations and fluctuating costs of crude oil are major drivers for the use of renewable resources and production of biodegradable products. The surfactant and polymer industries are probably more concerned than other industries in making their ubiquitous products bio-based and biodegradable.

Green chemistry is at the centre of this development and is giving direction to the chemical industry by outlining 12 principles to follow. Clean synthetic technologies and use of renewable resources will deliver a green chemical process which must be evaluated with green metrics tools. Over the years polyols and amino acids are major renewable hydrophilic heads while fatty acids from vegetable oil are the major hydrophobic tails used in making bio-based surfactants. Surfactants are very useful in our day-to-day activities and should therefore be safe and not bio-accumulate in the environment. The goal of this project is to demonstrate that renewable platform molecules can be converted to novel surfactants and polymers *via* the application of clean synthesis, and that the chosen routes can be compared, where possible, using metrics.

Synthesis of Alkyl Oleates *via* Transesterification

Chapter 2

2.0 Synthesis of alkyl oleates *via* transesterification

2.1 Introduction

Oleic acid (*cis*-9-octadecenoic acid) is possibly the most abundant monoene fatty acid in vegetable oils.¹⁵⁰ It is highly abundant in olive oil, almond, low erucic rapeseed (canola) and sunflower,¹⁵⁰⁻¹⁵² and can be obtained from hydrolysis of the triglyceride. Oleic acid and its ester derivatives have found much application in home and personal care product industries as hydrophobic ends of surfactants. They are said to be more biodegradable than conventional hydrophobes,^{160, 161} thus they are being used as replacements for petroleum-derived hydrophobes in surfactants. They are also incorporated to make the hydrophobic end of surfactants long and bulky enough to lower critical micelle concentration (CMC) and decrease surfactant dosage used by consumers.^{15, 162} This study intended to use oleic acid-derived alkyl esters as bio-derived hydrophobes for generation of series of non-ionic surfactants. In the industry, the best route to obtain fatty acid alkyl esters is *via* transesterification of triglycerides. Therefore, oleic acid was esterified to methyl oleate which was subsequently transesterified into various oleate analogues. The synthesis of the surfactants is a 4-step process involving esterification of oleic acid, generation of alkyl oleates *via* transesterification of methyl oleate, epoxidation of alkyl oleate and ring opening of the epoxide. The first two steps are covered in this chapter as shown in Figure 2-1.

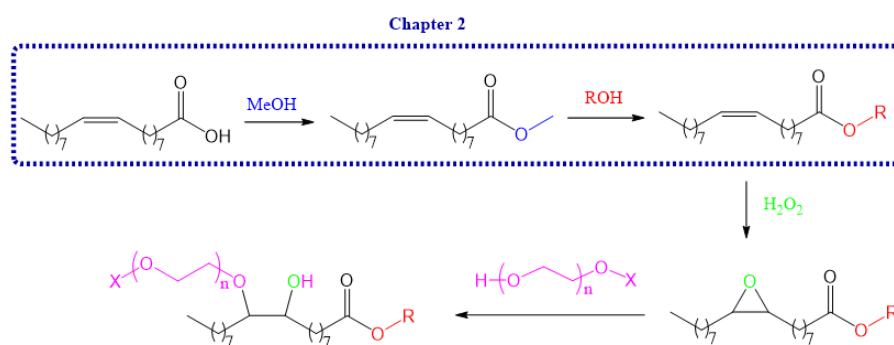


Figure 2- 1 Generation of bio-based non-ionic surfactant from oleic acid

2.2 Synthesis of methyl oleate

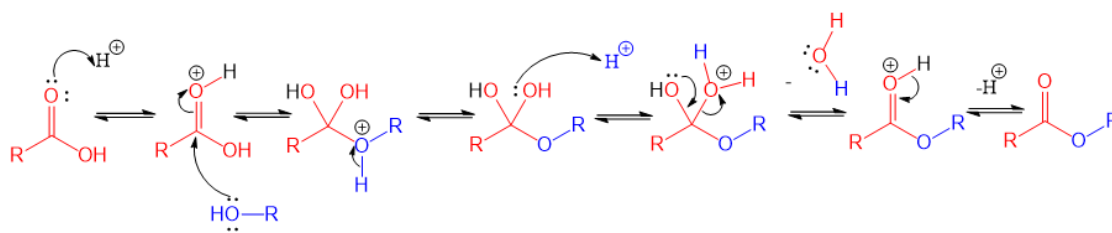


Figure 2-2 Mechanism of acid-catalysed esterification of carboxylic acid with alcohol

Carboxylic groups can be made electrophilic by protonation of the carbonyl oxygen by an acid. To activate a carbonyl group ready enough for esterification with any nucleophilic alcohol, a strong acid, is needed to protonate the carbonyl oxygen which consequently makes the carbonyl carbon more electrophilic to be attacked by even a weak nucleophile as shown in Figure 2-2.¹⁶³ Sulphuric acid-catalysed esterification of oleic acid with methanol in molar ratio 1:10 afforded an amber colour oil with oleic acid conversion of 99.7% and selectivity reaching to 100% in 18 hours of reaction.

The purity of oleic acid used for synthesis was $\geq 90\%$. Commercially available oleic acid usually come with a purity as low as 60-90% because of various minor impurities inherently present in the source oil.¹⁶⁴ The presence of these impurities reduce the qualities of the oil and are responsible for its colour, odour and instability.¹⁶⁵⁻¹⁶⁷ Considering the end product of this research study, that is surfactant, the area of its application, personal and home care and the number of reaction steps involved in the synthesis, it is essential that the oleic acid used be free of impurities to a large extent. The impurities can be removed by a number of methods including a combination of adsorption and distillation techniques.^{164, 168-170}

A $\geq 90\%$ purity oleic acid was purchased and used for this study. However, as is typical of natural fats and oils, minor impurities in the 90% purity oleic acid as analysed by GC-MS include stearic acid, hexadecanoic acid, heptadecanoic acid, 14-methyl-hexadecanoic acid, 16-methyl-heptadecanoic acid and 17-methyl-

octadecanoic acid in descending order of abundance. Their presence at such low concentration, notwithstanding, does not present much concern as they do not possess a reactive bond (C=C). Thus, they remain unaffected in the modification steps involved in the generation of the proposed surfactant although they were equally esterified and transesterified alongside the oleate. The synthetic procedure employed was reproducible enough to obtain up to 900 g high purity (99.7%) methyl oleate ready for transesterification into different alkyl oleates.

The synthesised methyl oleate was characterised by FT-IR spectroscopy, GC-MS, ESI-MS and 1D and 2D NMR spectroscopy. IR spectrum showed the diagnostic bands expected for methyl oleate and are in agreement with the literature:¹⁷¹ 3004 cm^{-1} for =C-H stretch, 2924 cm^{-1} for asymmetric CH_2 stretch, 2854 cm^{-1} for symmetric CH_2 stretch, 1742 cm^{-1} for C=O stretch, 1459 cm^{-1} for asymmetric CH_3 bend, 1363 cm^{-1} for symmetric CH_3 bend, and the three band 1244 cm^{-1} , 1196 cm^{-1} and 1170 cm^{-1} for C-O- stretch.

^1H NMR spectrum showed seven signals (Figure 2-3) namely: the end chain methyl proton (0.83 ppm, triplet), methylene protons (1.24 ppm, broad overlapping peaks), methylene proton alpha to olefinic carbon (1.57 ppm, quartet), methylene proton beta to the carbonyl carbon (1.95 ppm, quintet), methylene proton alpha to carbonyl carbon (2.25 ppm, triplet), methyl proton on the ester group (3.61 ppm, single) and olefinic proton (5.29 ppm, sextet).

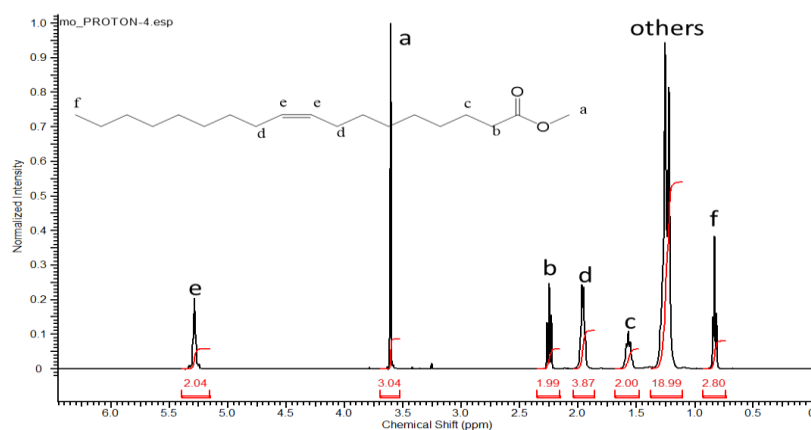


Figure 2- 3 Proton NMR spectrum of synthesised methyl oleate

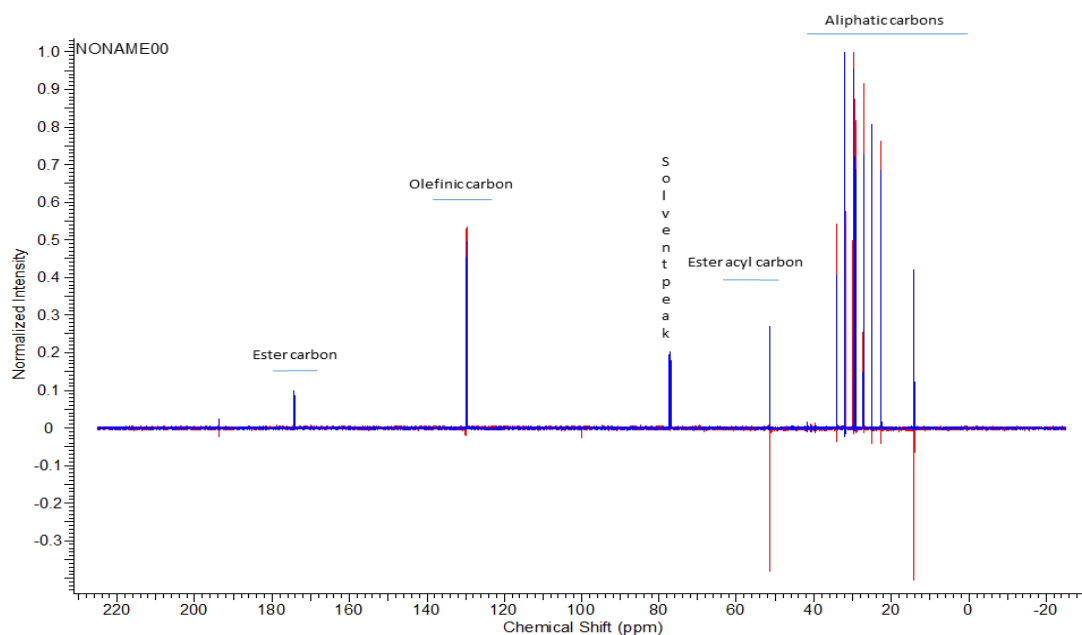


Figure 2- 4 Carbon 13 and DEPT NMR spectra of synthesised methyl oleate

From the ^{13}C NMR spectrum four distinct spectra regions are obvious which are the ester carbon (173.98 ppm), the olefinic carbon (129.73 and 129.97 ppm), the ester acyl carbon (51.37 ppm) and the aliphatic carbons (14.12 -34.09 ppm) as shown in the Figure 2-4. The assignment is in agreement with the literature.^{150, 172, 173}

2.3 Synthesis of alkyl oleates

Transesterification mechanism is well known whether catalysed by an acid or a base. A base-catalysed transesterification is usually preferred because it takes fewer reaction steps and consequently time as mechanistically shown in Figure 2-5. The need to use heterogeneous catalysts is well in line with green chemistry principles as they are easy to separate from reaction product mixture, flexible to regenerate, less expensive and environment-friendly.¹⁹⁻²¹ Oleate analogues were synthesised from methyl oleate *via* transesterification with ethanol, 1-propanol, 2-propanol, 1-butanol, 2-butanol, 1-octanol, 2-octanol and 1-decanol. Three different catalysts: titanium tetra isopropoxide ($\text{Ti}(\text{O-}i\text{-Pr})_4$), potassium fluoride on alumina support ($\text{KF}/\text{Al}_2\text{O}_3$) and magnesium oxide (MgO-T600), were used to affect transesterification.

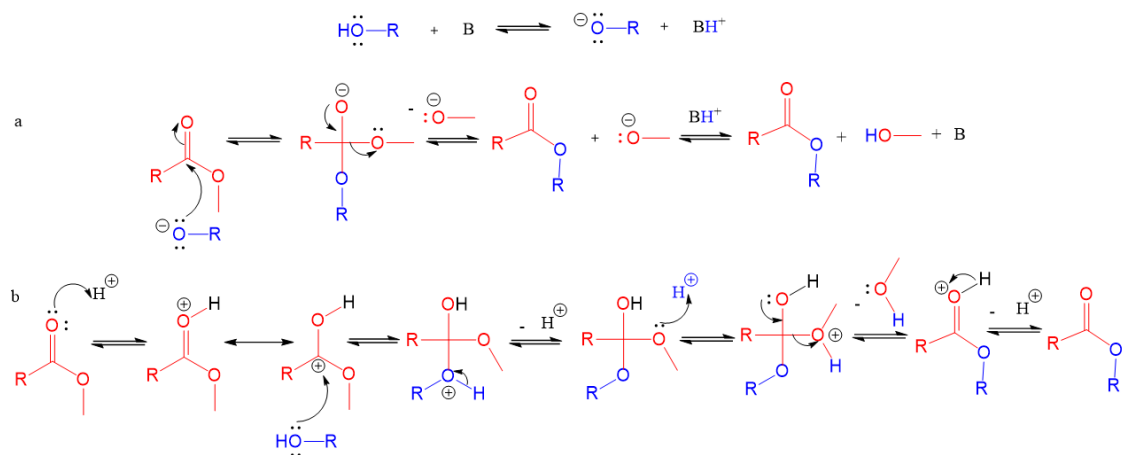


Figure 2- 5 Mechanisms of transesterification reaction catalysed by (a) a base and (b) an acid

$\text{Ti}(\text{O}-i\text{-Pr})_4$ is known to effectively catalyse esterification and transesterification reactions.¹⁷⁴⁻¹⁷⁷ $\text{KF}/\text{Al}_2\text{O}_3$ and MgO are known to catalyse transesterification reactions.^{39-41, 178-181} The catalysts are inexpensive and are based on very abundant metals. Alumina supported-potassium fluoride has been applied to affect many organic reactions including Michael additions,^{46, 182, 183} epoxidations,^{184, 185} Knoevenagel reactions,¹⁸⁶ *N*-alkylation of amides,¹⁸⁷ and Suzuki couplings.¹⁸⁸ The versatility has been attributed to its high basicity which makes it a good replacement for many heterogeneous base catalysts in organic syntheses.¹⁸⁹ Alumina is used as a support because it has a high surface area and readily available.¹⁹⁰

A molar ratio of 1:6 (methyl oleate to alcohol) was used for the synthesis and refluxing was done for typically 24 hours. All alcohols used were first dried in Celite® before being applied for transesterification to avert possible hydrolysis of oleates formed. Initial reflux set up for transesterification was fitted with a Liebig condenser but there was no visible product formation after 48 hours (confirmed with GC-MS), even with increasing temperature and catalyst concentration. A Dean-Stark trap was, therefore, applied to remove methanol from the system, thereby shifting equilibrium toward the product side, thus favouring formation of alkyl oleate according to Le Chatelier's principle of chemical equilibrium. Under reflux condition there was a need to replenish the alcohol in the flask by addition of alcohol at 1 hour

interval for at least the first 3 hours into the reaction which also supposedly forced the reaction in favour of the product.

Alkyl oleates were recovered from reaction product mixture using different methods depending on the transesterification catalyst used. With $\text{KF}/\text{Al}_2\text{O}_3$, the resulting product was suction filtered to recover catalyst and a rotary evaporator used to remove the solvent to yield an amber oil. Filtration using sintered funnel (size 4 μ) did not satisfactorily hold MgO-T600 catalyst and using a finer sintered funnel resulted in the catalyst blocking the pores of the filter. Therefore, the resulting product was allowed to cool down and centrifuged on a Thermo Scientific Megafuge 40R centrifuge at 3500 rpm at 20 °C for 20 minutes. The supernatant (oleate and solvent) was transferred into a round bottomed flask and a rotary evaporator used to recover the product. For synthesis involving $\text{Ti}(\text{O-}i\text{-Pr})_4$ catalyst, water was added to reaction product to break the catalyst into titanium (IV) oxide and isopropanol, the mixture was thereafter transferred into a separating funnel and shaken with dichloromethane (DCM). While it was preferred to avoid the use of DCM, it was the most suitable among the solvents (ethyl acetate, diethyl ether, 2-methyl tetra hydrofuran) to extract the organics from the mixture. The organic phase was collected, dried over anhydrous magnesium sulphate, filtered and solvent removed *in vacuo* to yield an amber oil.

Alkyl oleates were characterised with FT-IR spectroscopy, GC-MS, ESI-MS and 1D and 2D NMR spectroscopy. Infra-red spectra of the oleates (Figure 2-6) showed expected diagnostic bands. The three intense bands characteristic of esters due to $\text{C}=\text{O}$, $\text{C}-\text{C}=\text{O}$ and $\text{C}-\text{C}-\text{O}$ stretching vibrations were observed at ~ 1700 , ~ 1200 and $\sim 1100\text{ cm}^{-1}$ respectively.¹⁹¹ Some interesting changes in spectral bands and intensity were noted in their spectra. The $\text{C}-\text{O}$ stretch vibration was observed as a three-peak band 1244, 1196 and 1170 cm^{-1} in methyl oleate (Figure 2-6) according to the literature.^{192, 193} However, only two peaks (the first and the last) of this $\text{C}-\text{O}$ band were observed in the rest of the oleates. This could be due to increasing carbon

atom attached to the ester carbon in the compounds which masked the missing band.

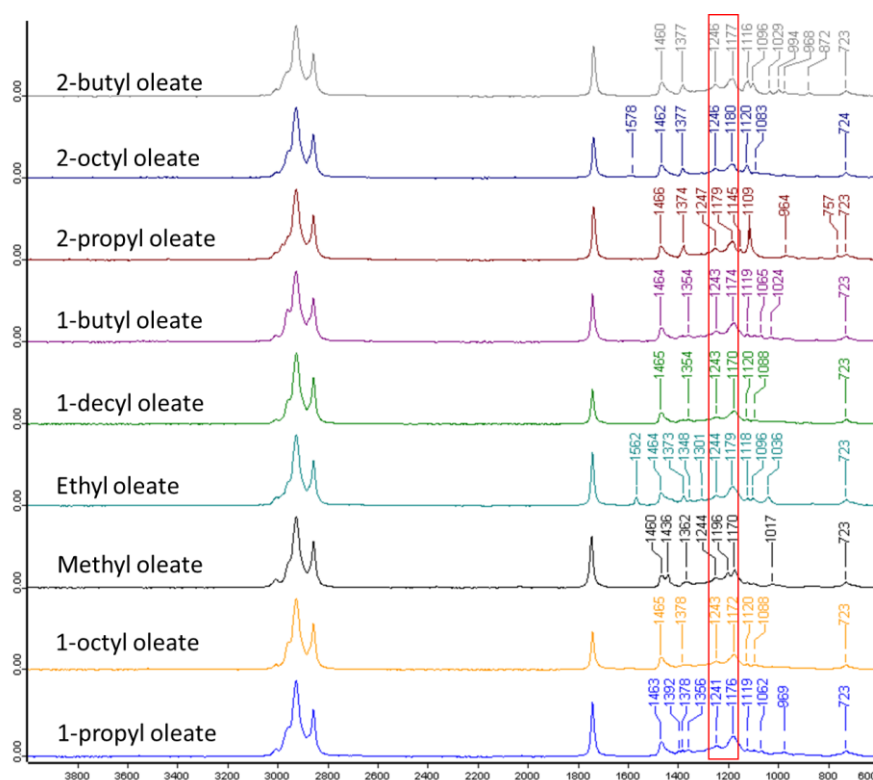


Figure 2- 6 FT-IR spectra of synthesised oleates showing contrast in band intensity and pattern.

It may be of interest to confirm if the three-peak band only show in ester carbon having a terminal methyl group. The bands 723 and 724 cm^{-1} in all the spectra are due to methylene rocking. All aliphatics possessing more than four unbranched carbon atoms show these bands at such distinct positions.^{193, 194} Another difference noticed across the spectra is that the band depicting C=C stretch was observed between 1562 and 1588 cm^{-1} in ethyl oleate, 1-propyl oleate, 2-octyl oleate and 1-octyl oleate lower than values (1680-1600 cm^{-1}) often quoted in the literature though Sinclair *et al.* quoted a range of 1580-1650 cm^{-1} for some unsaturated fatty acids and esters.^{171, 194, 195} However, it was observed between 1658 and 1678 cm^{-1} in methyl oleate and 2-propyl oleate. Some of these bands belonging to C=C stretch are weak and are not visible in Figure 2-6 due to compression of the spectra. Additionally, it was observed that the ester C-O stretch band intensity reduced as carbon number increased in oleates.

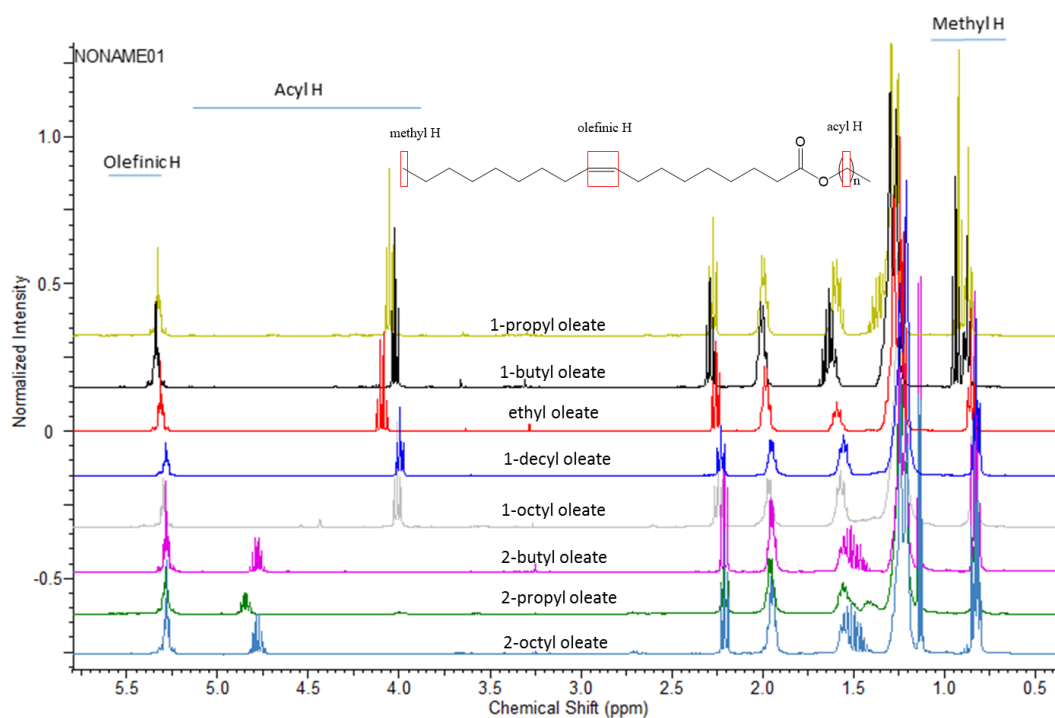


Figure 2- 7 Proton NMR spectra of alkyl oleates showing variation between the branched chain oleates (last three signals) and the straight chain oleates (first 5 signals).

Proton and carbon 13 NMR spectra of the oleates are similar in number of signals (7 or 8) and identical in chemical shifts to that of methyl oleate for proton NMR. Variation was only observed, as expected, for the alkyl carbon proton connected to the ester group. Nevertheless the variation, all the branched oleates have similar proton NMR signals and same for the straight oleates as shown in Figure 2-7. Details of NMR assignment and analytical data are included in the experimental section.

2.4 Effect of catalyst type on transesterification

Results showing how synthesised oleates compared between reaction catalysts are shown in Table 2-1. Green metrics toolkit developed at the Green Chemistry Centre of Excellence, York was used to evaluate the greenness of the reaction.⁷⁰ Conversion of methyl oleate, yield and selectivity was generally very high each reaching 100% in most of the reactions under different conditions (entries 1-10). In the syntheses of 1-octyl oleate, 2-octyl oleate and 1-decyl oleate, however, selectivity reduced to between 88% and 98% (entries 11-15) with 100% methyl oleate conversion as there was formation of side products.

Table 2- 1 Comparative effectiveness of Ti(O-*i*-Pr)₄, MgO-T600 and KF/Al₂O₃ catalysts for alkyl oleate synthesis.

Entry	Oleate	Catalyst	Temp. (°C)	Time (Hr)	*Conversion/Yield /Selectivity. (%)	AE
1	Ethyl oleate	KF/Al ₂ O ₃	80	30	99/99/100	91
2	Ethyl oleate	Ti (O- <i>i</i> -Pr) ₄	90	10	99/99/100	91
3	1-propyl oleate	KF/Al ₂ O ₃	102	30	99/99/100	91
4	1-propyl oleate	Ti (O- <i>i</i> -Pr) ₄	110	10	99/99/100	91
5	2-propyl oleate	KF/Al ₂ O ₃	88	36	98/98/100	91
6	2-propyl oleate	Ti (O- <i>i</i> -Pr) ₄	100	24	100/100/100	91
7	1-butyl oleate	KF/Al ₂ O ₃	122	24	100/100/100	91
8	1-butyl oleate	Ti (O- <i>i</i> -Pr) ₄	120	10	96/96/100	91
9	2-butyl oleate	KF/Al ₂ O ₃	105	30	100/100/100	91
10	2-butyl oleate	Ti (O- <i>i</i> -Pr) ₄	110	10	98/98/100	91
11	1-octyl oleate	MgO-T600	200	24	100/95/95	93
12	1-octyl oleate	Ti (O- <i>i</i> -Pr) ₄	200	13	100/88/88	93
13	2-octyl oleate	MgO-T600	190	39	100/98/98	93
14	2-octyl oleate	Ti (O- <i>i</i> -Pr) ₄	180	17	100/97/97	93
15	1-decyl oleate	MgO-T600	200	24	100/98/98	93

* Calculated by GC

GC-FID (Figure 2-8) and GC-MS data showed the presence of corresponding epoxides and diols in the both crude and final product. In some cases, aldehydes and keto esters were formed alongside the epoxides and diols (Figure 2-9). The compounds, however, could not be detected by NMR spectroscopy and FT-IR spectroscopy; possibly because of their low concentration.

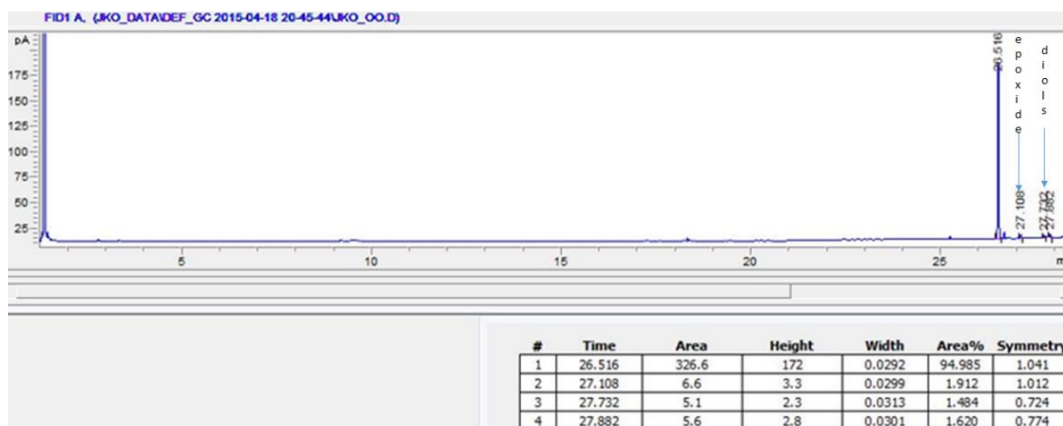


Figure 2- 8 GC chromatogram of synthesised 1-octyl oleate showing epoxide and diols as side products (Table 2-1 entry 11).

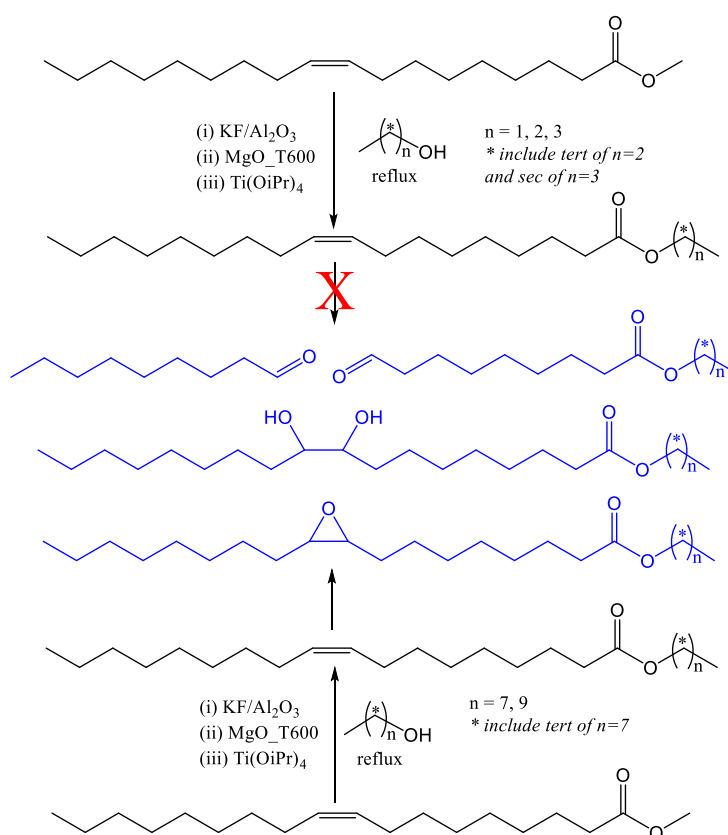


Figure 2- 9 Formation of aldehydes, keto esters, epoxides and diols observed in higher alkyl oleates during transesterification of methyl oleate leading to reduced selectivity.

It was noted that these side products were not observed in lower oleates but only in the higher ones (1-octyl oleate, 2-octyl oleate and 1-decyl oleate) over the three catalysts used for transesterification (Figure 2-9). The major difference in their synthesis is the reflux temperature (180-200 °C) and subsequent removal of excess alcohol from reaction product *via* a high vacuum distillation pump. In as much as

these compounds were formed in the presence of the three catalysts, it can be concluded that air oxidation of the oleate at elevated temperature was responsible for the formation of the side products. Interestingly, there have been studies that reported formation of these products amongst others from catalytic air oxidation of unsaturated fatty esters.¹⁹⁶⁻¹⁹⁸ and detailed discussions are made on this in chapter 3.

Atom economy (AE) for each synthesis is generally very high- all above 90%, indicating that transesterification of fatty acid methyl ester (FAME) utilises nearly all the reactants. Thus this can be described as a green process that minimises waste generation.

Transesterification was observed to progress faster in reactions involving $\text{Ti}(\text{O-}i\text{-Pr})_4$ catalyst possibly as the catalyst was in an homogeneous state with the reactants. Methyl oleate conversion up to 100% was obtained in about 13 hours. Most of the reactions were stopped after 10 hours and worked up. The effectiveness of solid aluminium triisopropoxide ($\text{Al}(\text{O-}i\text{-Pr})_3$) and $\text{Ti}(\text{O-}i\text{-Pr})_4$ for transesterification of oleates was investigated. GC-FID results showed that conversion and yield was higher in $\text{Ti}(\text{O-}i\text{-Pr})_4$ (99/99) when compared with $\text{Al}(\text{O-}i\text{-Pr})_3$ (87/87) in 24 hours. The result is therefore in agreement with the literature which placed Ti-alkoxyl catalyst above many other metal-alkoxyl catalysts including Al-alkoxyl catalyst in activity.^{176, 199} Attempts were made to recover titanium (IV) oxide from $\text{Ti}(\text{O-}i\text{-Pr})_4$ catalyst suspension but further purifications and tests were not carried out.

The heterogeneous catalysts, $\text{KF}/\text{Al}_2\text{O}_3$ and MgO-T600 , as expected took longer reaction time (between 24 hours and 39 hours) to compare effectively as the homogeneous catalyst (Table 2-1). Initial efforts showed that $\text{KF}/\text{Al}_2\text{O}_3$, being a more hydrophilic catalyst, was more effective for transesterification with more hydrophilic alcohols (ethanol, 1-propanol, 2-propanol, 1-butanol and 2-butanol) than less hydrophilic alcohols (1-octanol and 2-octanol) as evidenced by longer

reaction time in the latter (Table 2-2: entries 1-2). However, subsequent attempts negated the observation as the catalyst later demonstrated similar high activity across the spectrum of oleates studied (Table 2-2 entries 3-4 compared against Table 2-1). Use of different batches of KF/Al₂O₃ catalyst could be responsible for this divergent observation. On the other hand, MgO-T600, a more hydrophobic catalyst, was observed as being more effective for transesterification with longer chain alcohols (1-octanol, 2-octanol and 1-decanol) considered in this work as its activity demonstrated in Table 2-2 entries 5-6.

Table 2-2 Effectiveness of MgO-T600 and KF/Al₂O₃ catalysts for transesterification between different chain lengths of oleates.

Entry	Oleate	Catalyst	Temp. (°C)	Time (Hr)	*Conversion/Yield /Selectivity. (%)	AE
1	2-octyl oleate [‡]	KF/Al ₂ O ₃	120	46	0/0/0	-
2	2-octyl oleate ^{†‡}	KF/Al ₂ O ₃	175	93	60/59/98	93
3	1-octyl oleate	MgO-T600	200	24	100/95/95	93
4	1-octyl oleate	KF/Al ₂ O ₃	200	24	100/97/97	93
5	Ethyl oleate	KF/Al ₂ O ₃	80	30	99/99/100	91
6	Ethyl oleate	MgO-T600	80	30	11/11/100	91

* Calculated by GC, [‡]Methyl oleate from ~68% oleic acid was used for synthesis in this case, [†]Reaction solution turned dark red

The synthesised oleates (structures shown in Figure 2-10) were of different shades of amber colour depending on the type of catalyst and transesterification temperature applied (Figures 2-11b and d). A wax crystal appearance was observed in some oleates, specifically ethyl oleate, 1-propyl oleate and 1-butyl oleate (not as significant as in the first two), which partly disappeared when heated and reformed at room temperature as shown in Figure 2-11a. The resulting product was therefore heated, re-filtered and the residue tested with GC-MS and NMR spectroscopy (Figure 2-11c).

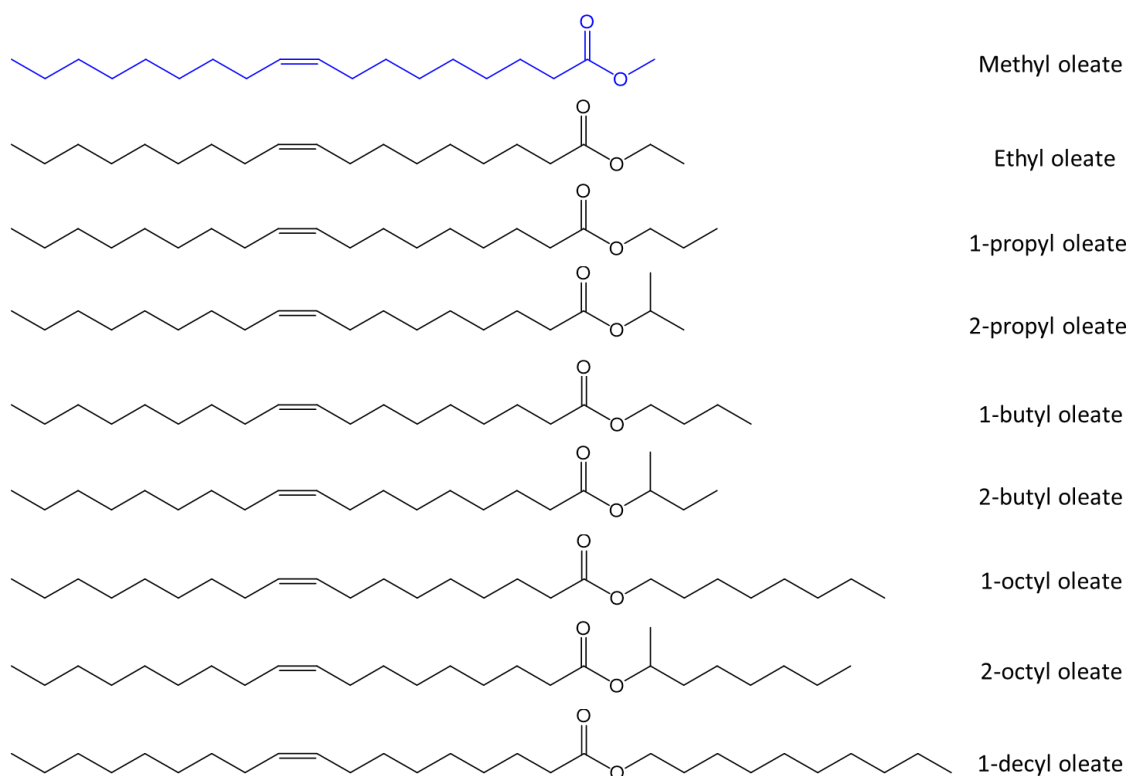


Figure 2- 10 Structures of alkyl oleates synthesised from methyl oleate via transesterification with alcohol



Figure 2- 11 Transesterification products showing (a) formation of waxy oleates (b) different shades of amber coloured KF/Al_2O_3 and $MgO-T600$ catalysed oleates (c) residues from filtered waxy oleates (d) different shades of amber coloured $Ti(O-i-Pr)_4$ catalysed oleates

Interestingly, analysis of the residues by GC-MS and proton NMR spectroscopy confirmed them to be oleates though efforts were not made to verify with other analytical techniques if there were traces of oleate dimers (Figure 2-12) in the residue. This observation indicates that such oleates have cloud points (temperatures at which they begin to form wax or crystal upon cooling) around room temperature. Crystal formation is common with FAAE and has been reported to occur at lower temperatures as alcohol chain length increases in alkyl fatty esters.^{200, 201} However, such waxy appearance was not observed or significant in corresponding oleates from $\text{Ti}(\text{O-}i\text{-Pr})_4$ catalysis though they were a bit cloudy as shown in Figure 2-11d.

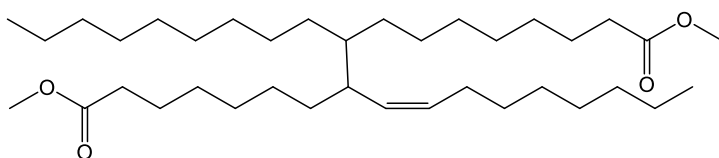


Figure 2- 12 Methyl oleate dimer: an example of a dimer

2.5 Investigating KF and Al_2O_3 as catalysts and concentration effect of $\text{KF}/\text{Al}_2\text{O}_3$ on transesterification

The catalytic effect of KF, the support and optimum concentration of $\text{KF}/\text{Al}_2\text{O}_3$ for transesterification reaction was also investigated. KF when applied as a catalyst without a support gave a methyl oleate conversion of 3% (Figure 2-13) while Al_2O_3 gave a conversion of 1%. A combination of these catalysts ($\text{KF}/\text{Al}_2\text{O}_3$), however, proved very effective for transesterification with a methyl oleate conversion of 91%. This corroborates reports which demonstrated that $\text{KF}/\text{Al}_2\text{O}_3$ is a more reactive basic catalyst than non-supported KF.^{202, 203} It has also been demonstrated that there is a salt support interaction existing between alumina and potassium including the formation of oxide sites at the surface of $\text{KF}/\text{Al}_2\text{O}_3$ during a transesterification reaction which could account for the high activity and basicity.^{178, 204} The alumina used in this study is the neutral form.

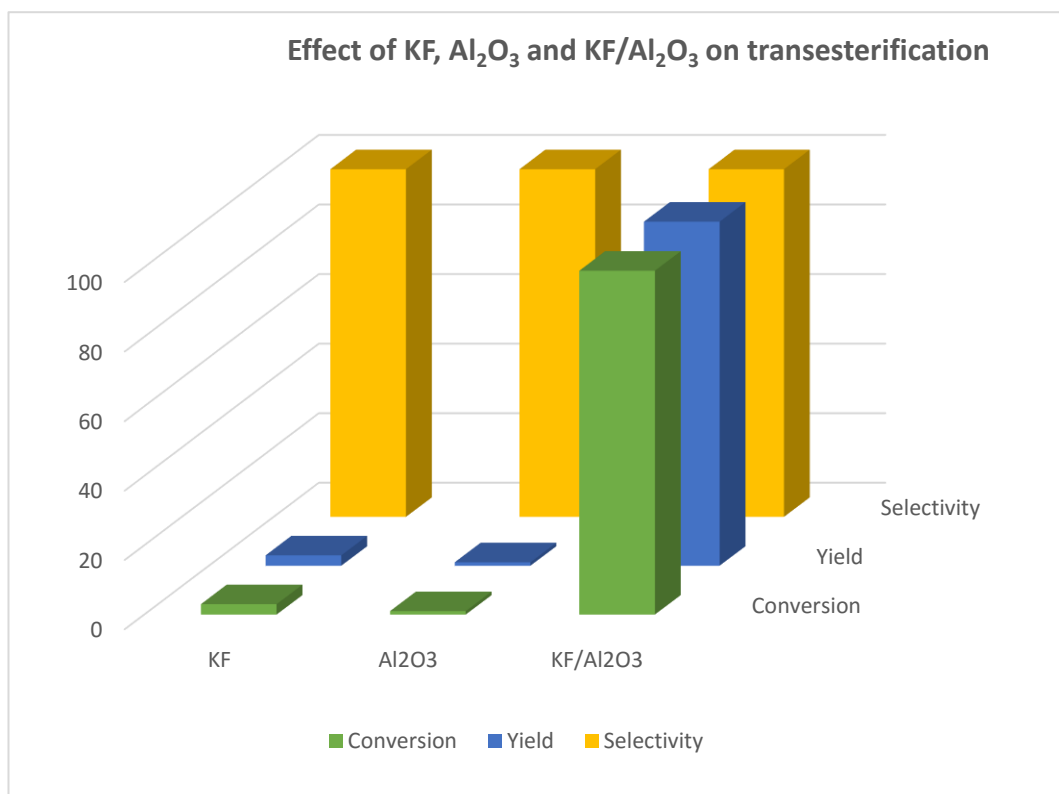


Figure 2- 13 Effectiveness of KF, Al₂O₃ and KF/Al₂O₃ as catalysts for transesterification reaction. Reaction conditions:- ethanol-methyl oleate molar ratio =10, 80 °C, 28 hrs, 10.0% w/w catalyst with respect to methyl oleate

Effect of catalyst concentration on transesterification was investigated with 2.5, 5.0, 7.5 and 10.0% w/w catalyst with respect to methyl oleate for the synthesis of 1-butyl oleate. Figure 2-14 shows a progressive activity with increasing KF/Al₂O₃ concentration from 24% to 73% conversion. It was noted that at a catalyst concentration of 10%, conversion was only 73% when molar ratio of 1-butanol: methyl oleate was 10 whereas conversion was 100% at molar ratio of 6 under similar reaction conditions in Table 2-1 entry 7. This is probably because, although excess alcohol is necessary for reaction, a little more excess alcohol in transesterification releases more alkoxide ions into the system which might lead to a reverse reaction, less contact with catalyst and consequently reduced methyl oleate conversion. A reduction in conversion and yield after exceeding optimum alcohol/oil molar ratio for transesterification has been reported.¹⁷⁸ It must be stated that catalyst concentration was not investigated beyond 10% w/w because of the mindedness to minimise the amount of catalyst that goes into the system.

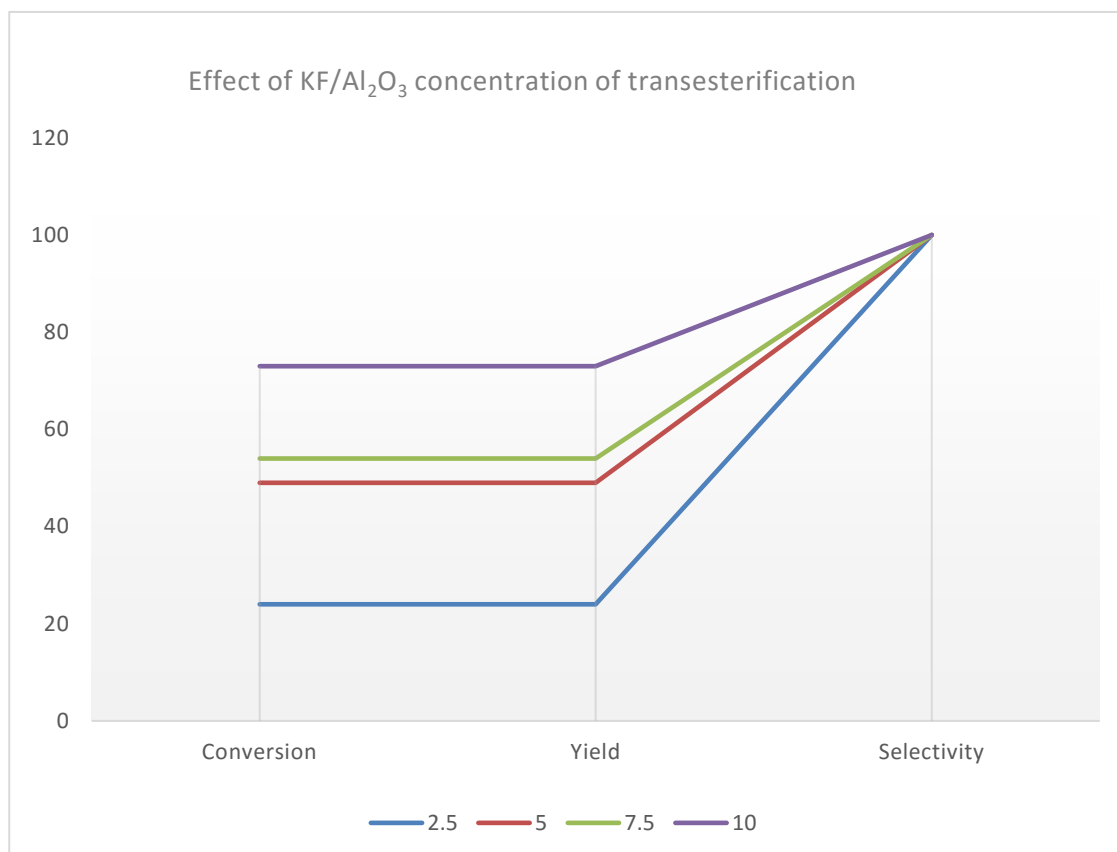


Figure 2- 14 Effect of KF/Al₂O₃ concentration on transesterification of methyl oleate with 1-butanol. Reaction conditions:- 1-butanol:methyl oleate molar ratio =10, 122 °C, 24 hrs, 2.5, 5.0, 7.5 and 10.0% w/w catalyst with respect to methyl oleate

2.6 Investigating optimum loading of KF on Al₂O₃ support for transesterification

It was of interest to investigate the KF loading on Al₂O₃ that would give the optimum conversion for the synthesis of FAAEs being studied. Five different loadings of KF per gramme of Al₂O₃ (1.0, 2.5, 5.0, 7.5 and 10.0 mmol) were prepared and tested against methyl oleate and ethanol. Figure 2-15 showed how methyl oleate conversion increased with increasing KF concentration on the catalyst surface. There was a dramatic ten-fold conversion increase as KF concentration impregnated on alumina support increased from 1 mmol to 2.5 mmol. At a 5.0 mmol KF concentration, KF/Al₂O₃ was three times more active and another 2.5 mmol addition on the support gave a peak conversion of 71% after which a further KF addition was not so effective as conversion reduced to 56%. The last two steps of addition (7.5 mmol and 10.0 mmol) were repeated to confirm the observation.

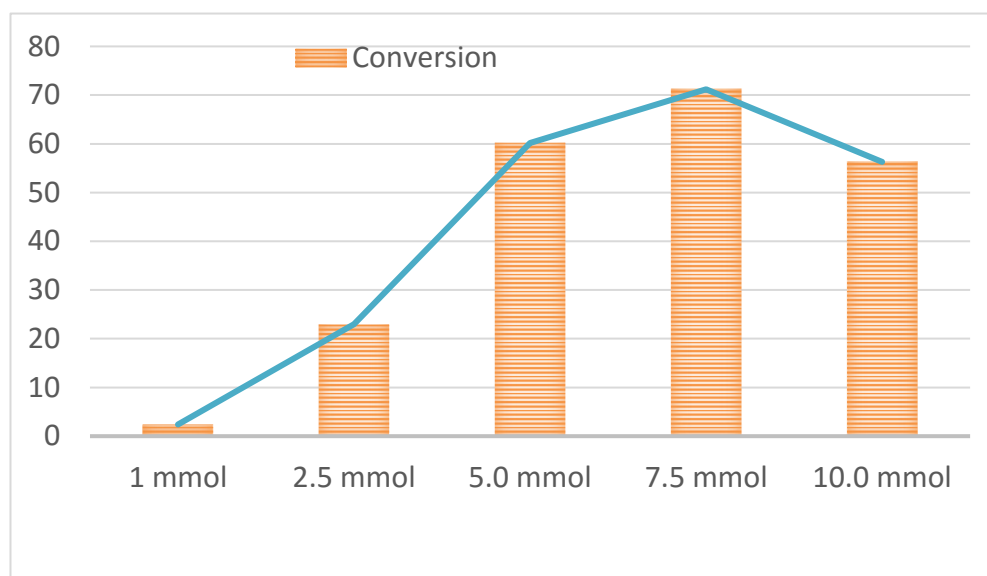


Figure 2- 15 Effect of KF loading on alumina support tested for transesterification reaction. Reaction conditions:- ethanol-methyl oleate molar ratio =10, 80 °C, 28 hrs, 10.0% w/w catalyst with respect to methyl oleate

This trend observed and the decline in conversion could possibly mean that as KF concentration increases with increasing activity, KF spreads on the support surface to form a monolayer surface until a point is exceeded at which KF begins to form another layer on top of each other giving rise to a multilayer surface. The implication is that the first layer which, actually, is in contact with the support and is responsible for catalytic activity is not directly available for interaction with alcohol for transesterification reaction. Some authors have reported a reduction of activity upon exceeding a certain level of KF concentration on the support.²⁰⁵⁻²⁰⁷

2.7 Effect of activation and treatment on MgO catalyst

Effect of activation and treatment of MgO was considered on transesterification. Activated magnesium oxide (MgO600) and treated magnesium oxide (MgOT600) shown in Figure 2-16 were prepared (chapter 8 sections 8.3.2-8.3.3) and their activity tested. Surface characterisation of the two catalysts was performed on a Tristar porosimeter. MgO-T600 was significantly different from MgO600 in surface properties. The former was found to be mesoporous (average pore diameter of 33.66 nm) while the latter was macroporous (average pore diameter of 55.01 nm).

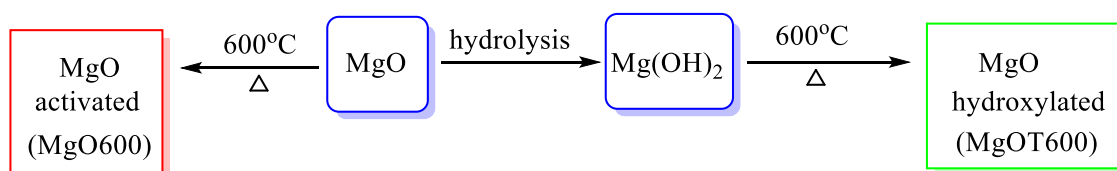


Figure 2- 16 Preparation of hydroxylated MgO (MgOT600) and activated MgO (MgO600) catalysts

The increased porosity observed in MgO-T600 could be attributed to the treatment during its preparation. As expected, it should be more effective as a catalyst than MgO-600 because of increased porosity. However, transesterification results showed that there was not much difference in activity between the two catalysts. While they both gave a conversion of 100%, the activated catalyst gave higher yield (92%) than the treated catalyst (89%) for 1-octyl oleate synthesis in 23 hours. The treated catalyst which was prepared by first converting MgO to its hydroxide and then decomposed to MgO upon calcination at 600 °C was not better than MgO600. Whereas it was intended that the intercalated ions of MgO will improve its basicity, hence increased activity,²⁰⁸ the calcination temperature applied was probably too high to have driven off OH groups from it which impacted on the basic sites to give same performance with the activated catalyst (MgO600).

It has been shown that MgO catalyst alone is active enough for transesterification reaction and addition of a support, say Al₂O₃ does not improve the catalytic performances.²⁰⁹ Therefore, efforts were not made to impregnate MgO on a support for transesterification reaction.

2.8 Reuse of transesterification catalysts

Reuse of transesterification catalysts was investigated with the synthesis of ethyl oleate (for KF/Al₂O₃) and 1-octyl oleate (for MgO-T600). Four KF/Al₂O₃ reuse cycles was performed by thoroughly washing catalyst with acetone and without activation recirculated for synthesis. Results in Figure 2-17 showed a conversion of 72% after

24 hours in the first cycle which markedly reduced to 29% in the second cycle. Conversion was 16% and 7% in the third and fourth cycles respectively.

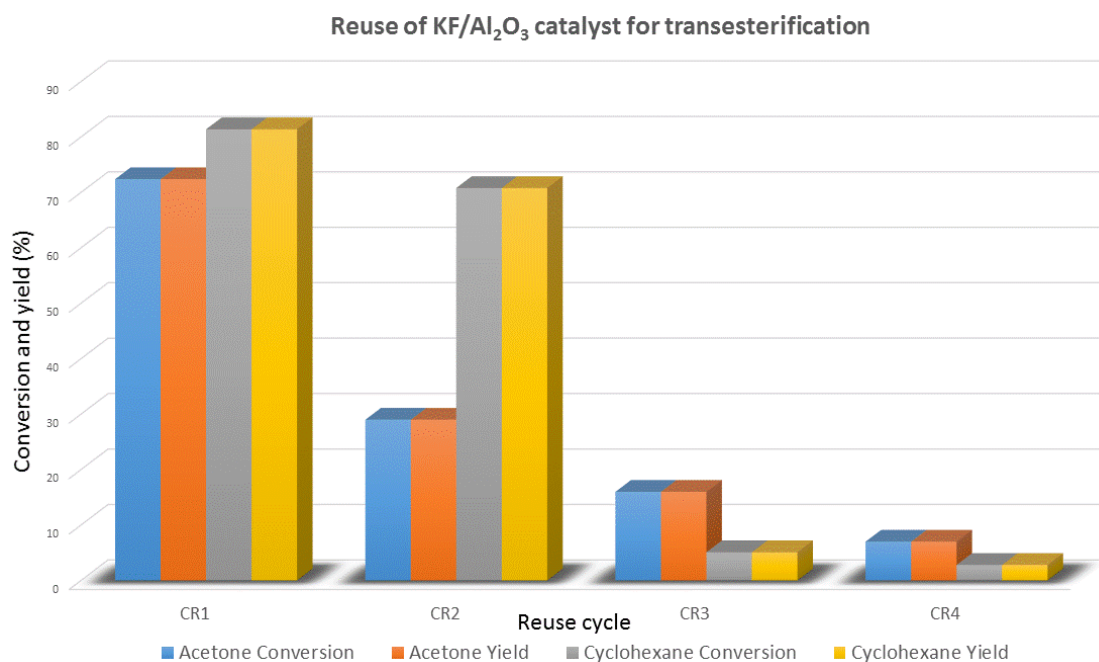


Figure 2-17 Reuse of $\text{KF}/\text{Al}_2\text{O}_3$ catalyst in transesterification of methyl oleate with ethanol using acetone and cyclohexane as wash solvents. Reaction conditions- ethanol: methyl oleate molar ratio = 6, 80 °C, 24 hrs, 10% w/w catalyst with respect to methyl oleate.

The trend of reduction observed was such that conversion was halved in all the cycles. The marked rapid reduction in catalytic activity especially in the second reuse could be due to the fact that acetone is too polar a solvent to effectively wash the catalyst free from the oil (ethyl oleate) thus leaving some still trapped within the catalyst pore sites or surface. When using a combination of hydrocarbon solvent (cyclohexane) and acetone, that is, cyclohexane wash followed by acetone, another reduction trend in conversion was observed. Conversion was 71% in the second cycle, after which it dropped markedly to 5% and 3% in the third and fourth cycles respectively. Undoubtedly, the sharp reduction in conversion observed in the third and fourth cycles signalled catalyst leaching into the solution. While there was some leaching when washing only with acetone it was much pronounced when using cyclohexane. It appeared that in the former, the oil trapped within the catalyst pore sites slowed down the rate of catalyst leaching but in the latter the catalyst pore sites are much more vulnerable to leach into solution. Leaching of $\text{KF}/\text{Al}_2\text{O}_3$ catalyst into

solution during reuse for transesterification has been studied.^{40,178} In the study, EDS and ICP-OES analyses of reused catalyst showed a depletion in K content of the catalyst which consequently lowered its availability for interaction to form Al-O-K that is purportedly responsible for the catalyst's basicity.

Cyclohexane was used as a wash solvent followed by acetone when MgO-T600 catalyst was reused for transesterification. Surprisingly, it was observed that catalytic activity was intact with the conversion and the yield almost unchanged throughout the four recycles (Figure 2-18). This shows that the MgO-T600 is very stable even upon continuous use at such high temperature and active without a prior reactivation before recycling. This stability could be traced to the treatment performed on the catalyst. In fact, the stability of treated MgO has been related to its calcination temperature.²⁰⁸

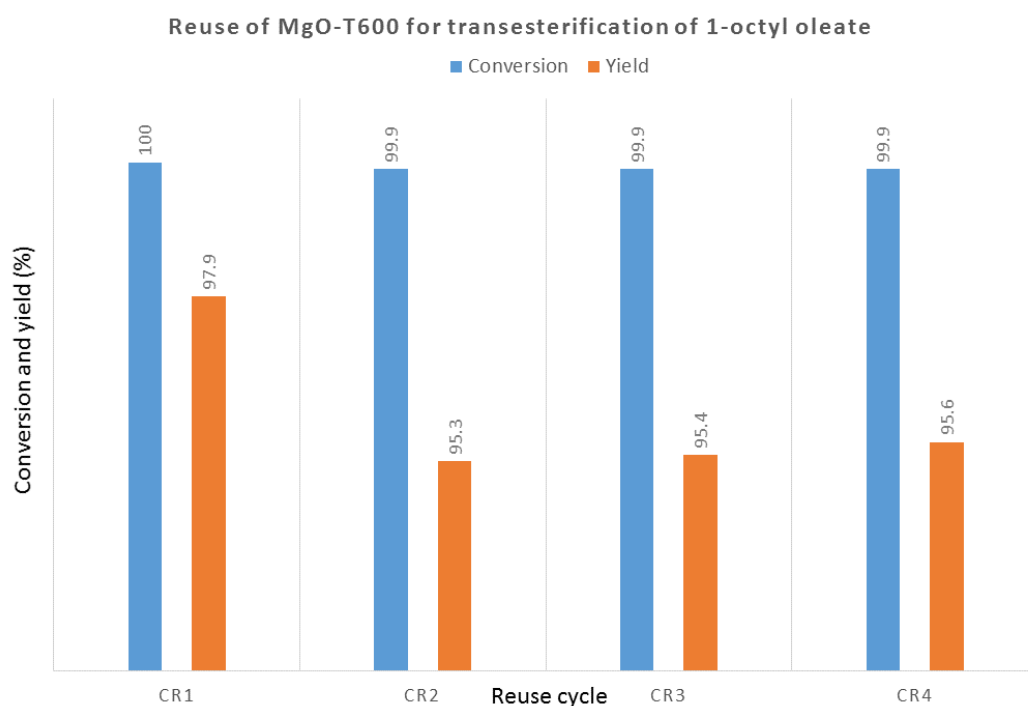


Figure 2-18 Reuse of MgO-T600 catalyst in transesterification of methyl oleate with 1-octanol. Reaction conditions- 1-octanol: methyl oleate molar ratio = 10, 200 °C, 24 hrs, 10% w/w catalyst with respect to methyl oleate.

2.9 Conclusions

Starting from oleic acid, which is predominantly sourced from rapeseed oil triglyceride hydrolysis, methyl oleate was synthesised to serve as a building block for transesterification to eight other oleates analogues (ethyl-, 1-propyl-, 2-propyl-, 1-butyl-, 2-butyl-, 1-octyl-, 2-octyl- and 1-decyl-) in good yields. As expected, transesterifications with secondary alcohols progressed much slower than with primary alcohols. Higher reaction temperature, despite increasing alcohol chain length, resulted in increased rates of reaction and consequently a shorter reaction time. $\text{Ti}(\text{O-}i\text{-Pr})_4$, $\text{KF}/\text{Al}_2\text{O}_3$ and MgO-T600 were found to be very active catalyst for transesterification reaction. $\text{KF}/\text{Al}_2\text{O}_3$ was effective for all the chain length of alcohols considered whereas MgO was found to be more effective with higher alcohols. Unlike KF that was not active without a support, MgO was found active enough to catalyse a transesterification reaction. Optimum KF loading on Al_2O_3 for transesterification reactions was found to be 7.5 mmol/g. While there was a leaching suspected in the reuse of $\text{KF}/\text{Al}_2\text{O}_3$, MgO was very stable throughout recycle regime. The choice of wash solvent has impact on the effectiveness of the catalyst in their subsequent reuse.

Synthesis of Alkyl Oleate Epoxides

Chapter 3

3.0 Synthesis of alkyl oleate epoxide

3.1 Introduction

Epoxides are versatile reactive organic compounds whose activity or stability is controlled by their basicity and the strain in the oxirane ring.²¹⁰⁻²¹² They are used as intermediates to make various organic compounds and industrial chemicals. Epoxidation is one of the means of valorising and functionalising unsaturated fatty esters. Researchers have reported many processes on the epoxidation of unsaturated fatty acids, which utilise many oxidants including chlorohydrin and organic peroxides and peracids,²¹³⁻²¹⁷ but there has always been a need to curtail side reaction products and use of toxic reagents and oxidants. The challenges include hydrolysis of the ester group, low yield resulting from acid-catalysed ring opening side reactions, separation of acidic by products and corrosion of reaction vessels.²¹⁸ Hydrogen peroxide is a relatively environmentally benign oxidant that has a high content of active oxygen, decomposes to give water as the only by-product and it is not expensive.^{216, 219} This increased content of active oxygen means the use of hydrogen peroxide makes an epoxidation process more atom economic than is the case for other oxidants such as mCPBA.

In this chapter, the synthesised alkyl oleates in chapter 2 were modified *via* oxidation with hydrogen peroxide in the presence of homogeneous and heterogeneous catalysts (Figure 3-1). Apart from these oleates commercially available bio-surfactant, lactonic sophorolipid, was also modified *via* epoxidation to generate a novel epoxide. As lactonic sophorolipids demonstrate medicinal activity in addition to their surfactancy,^{220, 221} we hope the modified derivative will possess interestingly different properties from the parent sophorolipid.

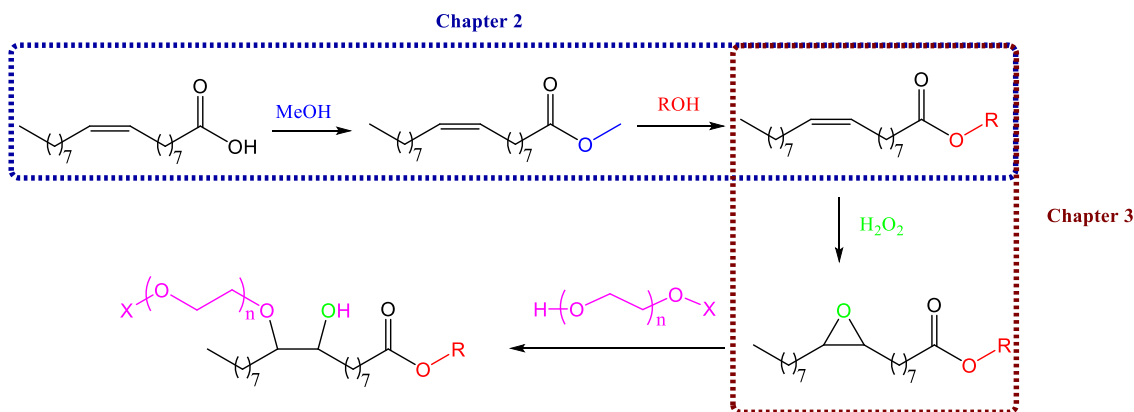


Figure 3- 1 Generation of bio-based non-ionic surfactant from oleic acid

3.2 Synthesis of alkyl oleate epoxides

Epoxidation is an example of a concerted reaction whereby all the changes occur in one simultaneous step. The mechanism when using a peracid as shown in Figure 3-2 involves nucleophilic attack from the double bond olefin on the electrophilic oxygen on peracetic acid, followed by breaking of the O-O bond and making a new C=O bond, breaking the original C=O to make a new O-H bond and finally breaking the original O-H bond to form a C-O bond to give an epoxide and acetic acid. The mechanism as shown is believed to proceed *via* a transition state such as that shown on Figure 3-2.²²² It has been experimentally shown that epoxidation is a stereospecific *syn*-addition reaction.^{223, 224}

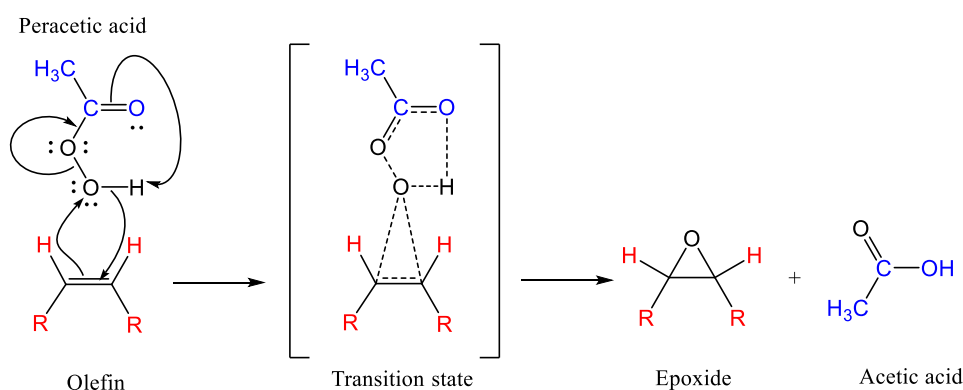


Figure 3-2 Mechanism of epoxidation reaction between an olefin and peracetic acid.

Epoxidation of the methyl oleate, ethyl oleate, 1-propyl oleate, 2-propyl oleate, 1-butyl oleate, 2-butyl oleate, 1-octyl oleate, 2-octyl oleate and 1-decyl oleate was

affected by oxidation with hydrogen peroxide *via* catalysis with phosphotungstic acid (PTA) and supported PTA. Phosphotungstic acid is a crystalline polyoxometalate (also called heteropolyacid) whose reactivity has been widely reviewed and is available commercially.²²⁵⁻²³⁰ PTA has a formula $H_3PW_{12}O_{40}$ where phosphorus (P) is the heteroatom and tungsten (W) is the addenda atom in its highest oxidation state.^{231, 232} The soccer ball-shaped structure as described by Keggin is shown in Figure 3-3.²³³ Polyoxometalates (POMs) are widely employed in oxidation reactions because they are environmentally benign and are stable at high temperature up to 450 °C in the presence of molecular oxygen.^{219, 225, 231, 234}

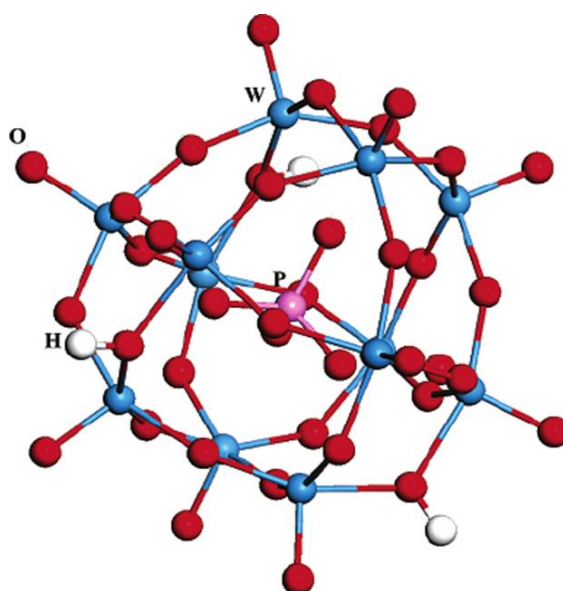


Figure 3- 3 Keggin structure of phosphotungstic acid, $H_3PW_{12}O_{40}$.²³⁵

The versatility of POMs, especially those containing tungsten (W) and molybdenum (Mo) has led to the development of variants of Keggin structures.^{236, 237} Acidity of POMs has been reported to impart greatly upon their effectiveness for epoxidation,²³⁸ and PTA has been the most preferred. The acid strength of PTA has been studied by calorimetry and reported.²³⁸⁻²⁴⁰ ¹³C NMR spectroscopy studies showed that the acid strength of protons of $H_3PW_{12}O_{40}$ in concentrated acetic acid solution was higher than sulfuric acid and perchloric acid.²⁴¹

Typically, epoxidation reaction time was 3 hours and catalyst concentration of 6 wt% relative to alkyl oleate was applied in all reactions. As fatty acid esters are

hydrophobic and PTA is hydrophilic, a biphasic system resulted. Transfer of reactants to the active sites of catalyst was slow. As a result, a phase transfer co-catalyst (PTC) was added to the solution to form an emulsion in order to aid the transfer of the oil to the catalyst active sites. Quaternary ammonium salts (QNSs) are typically used as PTCs for these reactions. The effectiveness of a quaternary ammonium salt as a PTC depends on the size of its carbon number. It has been shown that those possessing large carbon numbers demonstrate higher catalytic reactivity than those with less carbon number.²⁴²

A mechanism for a PTC-aided epoxidation involving PTA and hydrogen peroxide has been proposed as shown in Figure 3-4.²⁴² The reaction between PTA, hydrogen peroxide and PTC denoted as Q generates an active intermediate catalyst, $[Q_3PW_{12}(O)_nO_{40}]$, which subsequently acts as the new catalyst. Effects of acetic acid, solvent nature and the need for a phase transfer catalyst on epoxidation were considered. It was also of interest to investigate the influence of PTA nature and source on epoxidation.

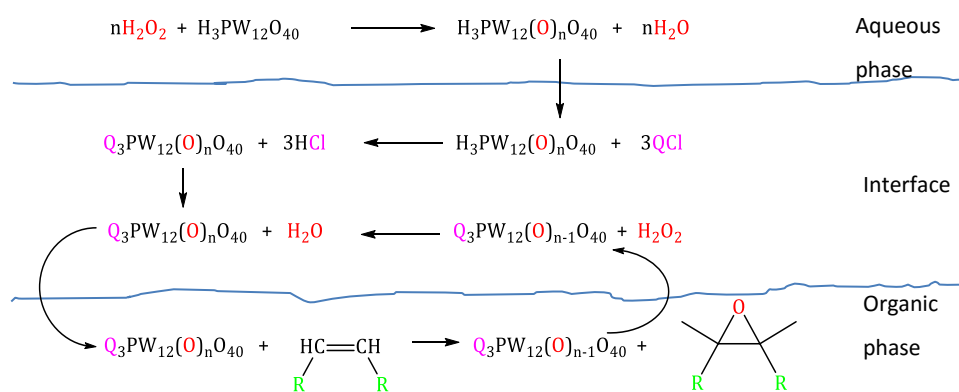


Figure 3- 4 Mechanism for a phase transfer co-catalyst aided epoxidation with PTA

Adogen 464 was chosen because it has a larger carbon number than other available QNSs. Adogen 464 is methyl trialkyl (C8-C10) ammonium chloride shown in Figure 3-5. Typically 3 wt% Adogen 464 concentration relative to oleate was used for epoxidation reaction.

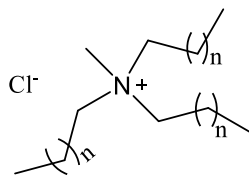


Figure 3- 5 Methyl trialkyl (C8-C10) ammonium chloride

Two methods were used to synthesise the epoxide as described in chapter 8 section 8.6. The first method involved the preparation of phosphotungstic acid *in situ* by reacting tungsten powder, hydrogen peroxide and ortho phosphoric acid. The second method involved the use of a preformed commercial phosphotungstic acid, and both methods used Adogen 464 as the PTC. For both epoxidation methods, the reaction mixture was vigorously agitated to create a vortex in the solution and as such aided mass transfer of oleates to the catalyst active sites.

3.3 Epoxidation with preformed phosphotungstic acid (PTA) catalyst

Conversion, yield and selectivity were calculated using metrics toolkit developed by McElroy *et al.*⁷⁰ Table 3-1 shows alkyl oleate conversion up to 100%, yield up to 93% and selectivity up to 95% for synthesis. Side reactions are commonly observed with FAAE epoxidation.^{213, 214, 243} As such the following side products were detected alongside the desired epoxides: nonanal, 9-oxo-alkyl ester nonanoic acid, cis-9,10-epoxy octadecanoic acid, and diol shown in Figure 3-6. The concentration of the side reaction products varied from one alkyl oleate epoxide to another. For example entry 1 gave 6.5% nonanal and 6.7% 9-oxo-methyl ester nonanoic acid, ~6% epoxy acid and ~7% diols while entry 4 gave 0.4% nonanal and 0.4% 9-oxo-isopropyl ester nonanoic acid, 0.7% epoxy acid and 3.8% diols. Details about their formation is discussed in section 3.7. Reaction time was varied for some epoxides. It was noted that those oleates in which crystals were formed (Table 3-1 entries 1, 2, 3, 5 and 8) as mentioned in chapter 2 section 2.4 took longer reaction time to reach a comparable level of conversion with those in which there were no crystals (entries 4, 6, 7 and 9). This could be due to reduced molecular collision of reactants resulting from increased viscosity and reduced mobility of the oleate molecules.

Table 3- 1 Effectiveness of PTA for large scale synthesis of alkyl oleate epoxides

Entry	Oleate epoxide	Time (Hr)	*Conversion/Yield /Selectivity. (%)	AE
1	Epoxidised methyl oleate	3.5	99/73/73	95
2	Epoxidised ethyl oleate	5.5	98/93/95	95
3	Epoxidised 1-propyl oleate	5.5	95/88/92	95
4	Epoxidised 2-propyl oleate	3.0	100/93/93	95
5	Epoxidised 1-butyl oleate	6.0	95/79/83	95
6	Epoxidised 2-butyl oleate	3.0	99/81/82	95
7	Epoxidised 1-octyl oleate	3.0	99/83/84	96
8	Epoxidised 2-octyl oleate	3.5	95/77/81	96
9	Epoxidised 1-decyl oleate	3.0	99/90/90	96

* Calculated by GC. Reaction conditions: temp.= 50 °C, catalyst=6 wt% relative to oleate, Adogen 464 =3 wt% relative to oleate, typically 100 mmol alkyl oleate reacted.

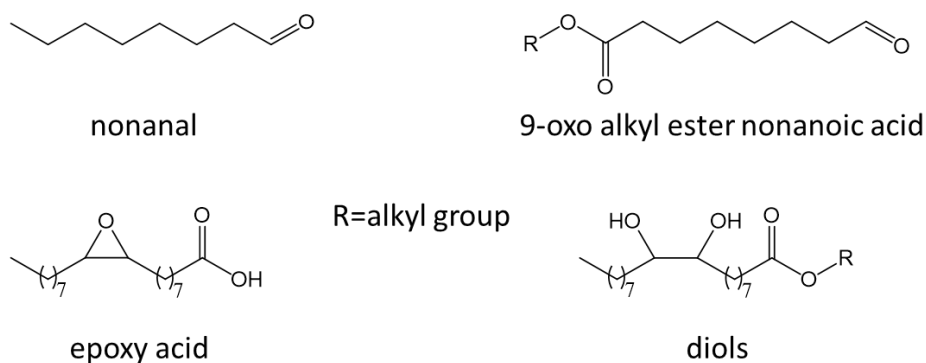


Figure 3- 6 Side reaction products from epoxidation of fatty acid alkyl esters, R = alkyl group of varying length and functionality

Atom economy of the epoxidation process was very high (entries 1-9) and thus demonstrated how atom efficient the process is when using hydrogen peroxide as the oxidant. Between the two epoxidation methods, the one that used preformed PTA catalyst was the preferred process as it gave the least side reaction products.

3.4 Epoxidation with *in situ* generated phosphotungstic acid (PTA)

Phosphotungstic acid was generated *in situ* when using tungsten catalyst and ortho phosphoric acid as described in chapter 8 section 8.6.1. Results obtained using this method are shown in Table 3-2. The method closely compares with the first method which uses a preformed PTA for epoxidation (Table 3-1). Reaction time was typically 4 hours with about 61 mmol alkyl oleate reacted at 50 °C. Under a normal condition, that is, with water added as a solvent, roughly 100% conversion and 70-90% yield (entries 1-8) was obtained with some side reaction products as earlier described (Figure 3-6). With a 5-hour reaction time epoxide yield was 90% though at a much lower scale, 5.5 mmol, of methyl oleate (entry 9).

Table 3- 2 Effectiveness of PTA formed *in situ* for synthesis of alkyl oleate epoxides

Entry	Oleate epoxide	Time (Hr)	*Conversion/Yield /Selectivity. (%)
1	Epoxidised methyl oleate	4	100/71/71
2	Epoxidised ethyl oleate	4	99/92/93
3	Epoxidised 1-propyl oleate	4	99/93/94
4	Epoxidised 2-propyl oleate	4	100/93/93
5	Epoxidised 1-butyl oleate	4	95/79/83
6	Epoxidised 2-butyl oleate	4	99/95/96
7	Epoxidised 1-octyl oleate	4	97/86/89
8	Epoxidised 2-octyl oleate	4	98/79/81
9	Epoxidised methyl oleate	5	100/90/90
10	Epoxidised methyl oleate	5	99/1.4/1.4

* Calculated by GC. Reaction conditions for entries 1-8: temp.= 50 °C, W catalyst=2.6 wt% relative to oleate, Adogen 464 =2.6 wt% relative to oleate, H₃PO₄ =2.2 wt% relative to oleate, total H₂O₂ =16 mL, total H₂O=28 mL, typically 61 mmol alkyl oleate reacted. Reaction conditions for entries 9-10: temp.= 50 °C, W catalyst=2.6 wt% relative to oleate, Adogen 464 =2.6 wt% relative to oleate, H₃PO₄ =2.2 wt% relative to oleate, total H₂O₂ =1.4 mL, typically 5.5 mmol alkyl oleate reacted, total H₂O=3.8 mL (entry 9), total CH₃CN=3.8 mL (entry 10).

When acetonitrile was used as a solvent, it was expected that its presence would enhance the formation of epoxide by producing peroxyacetic acid with hydrogen peroxide as mechanistically shown in Figure 3-7. However, it appeared rather too oxidising to form a stable epoxide. Conversion was 99% with 1.4% selectivity to epoxide (entry 10). There was rapid conversion to diols, 35%; nonanal, 15%; and the oxo-product, 15% alongside as major by products. Further details about effect of solvents on epoxidation are discussed in section 3.6.2.

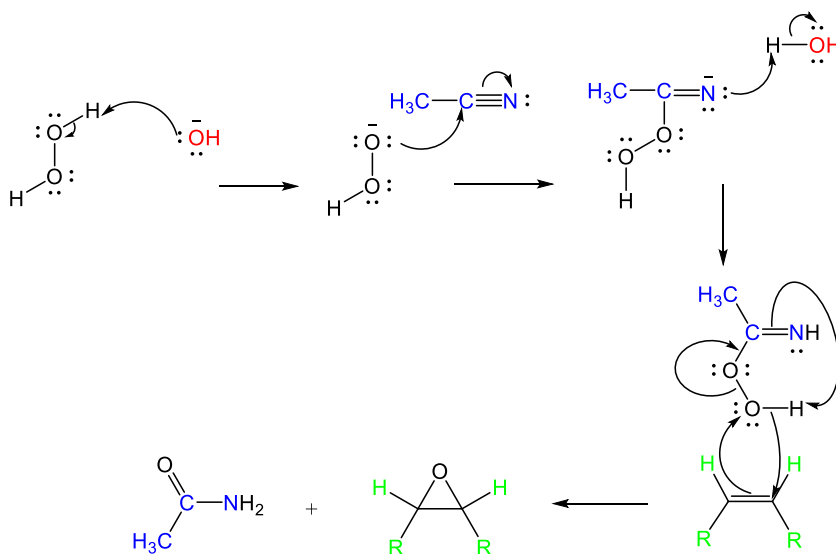


Figure 3- 7 Generation of peroxyacetic acid from the reaction of acetonitrile and hydrogen peroxide to favour epoxide formation

3.5 Characterisation of synthesised surfactants

Synthesised epoxides were characterised with FT-IR spectroscopy, GC-FID, GC-MS, ESI-MS, CHN analyser and NMR spectroscopy. Reactions were monitored with ^1H NMR spectroscopy as it showed the disappearance of the olefinic protons **f** at ~ 5.29 ppm and the appearance of epoxide protons **g** between 2.7-2.8 ppm (Figure 3-8). Incorporation of oxygen heteroatom in between the olefinic carbons caused their protons to resonate upfield (2.7-2.8 ppm) and the alpha carbon protons **e** to now appear more upfield at ~ 1.34 ppm unlike in the unsaturated oil where it resonated at ~ 1.95 ppm (Figure 3-8). This is because oxygen is a less electron withdrawing group than double bond being replaced thus leaving the protons to resonate at a

much lesser frequency. It was noted that the epoxide peak **g** is broad and has a lower integral compared to other signal with the same proton number, for example **d**. Three possibilities exist for this observation.²⁴⁴ This could be as a result of extended relaxation (time delay) between pulse reading and start of digitization of free induction decay (FID) which generates a broad signal. In the frequency domain a broad signal corresponds to a rapidly decaying signal amplitude in the time domain. Therefore, such a broad signal will have a lower integral value than expected. Another reason could be due to partial exchange of the heteroatom proton with deuterons ²Hs in the solvent. Third, baseline corrections of the spectrum may wipe out the edge of broad resonances thus subtracting intensity from the peak.

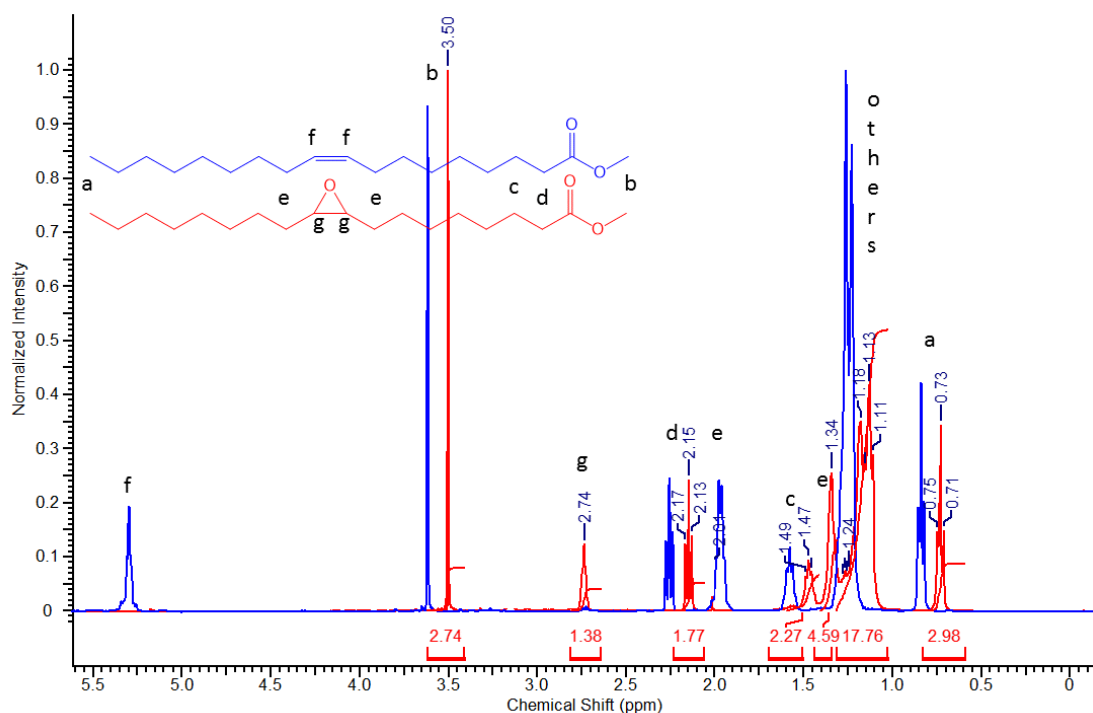


Figure 3- 8 Proton NMR spectra of methyl oleate and epoxidised methyl oleate showing (i) signal shifts and reduced integral value as a result of addition of oxygen heteroatom into the chain; (ii) disappearance of C=C protons and appearance of epoxy protons

¹³C and DEPT NMR spectra of synthesised epoxides showed the appearance of epoxy carbons around 57 ppm and disappearance of the olefinic carbon peak at ~130 ppm (Figure 3-9). Precise carbon and proton NMR spectra assignment was achieved by combination of COSY, HSQC and DEPT carbon.

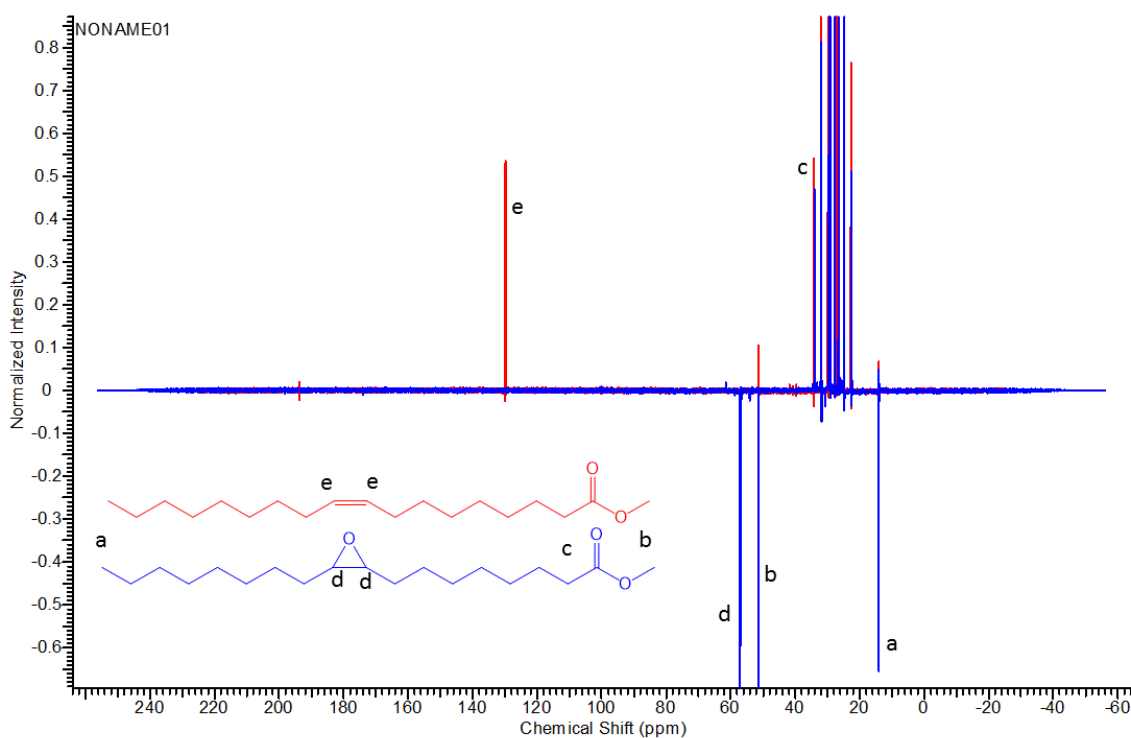
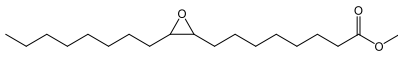
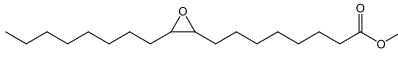
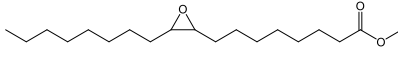
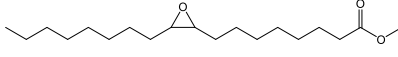
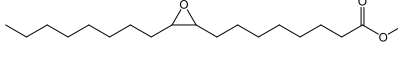
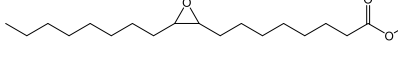
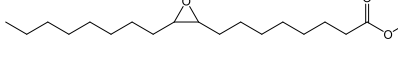
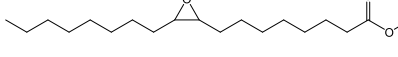
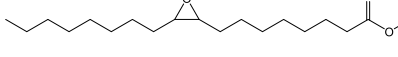


Figure 3- 9 Carbon DEPT NMR spectra of methyl oleate and epoxidised methyl oleate showing disappearance of olefinic carbons and appearance of epoxy carbons

A trend was observed in the epoxide chemical shift as we moved from primary chain to secondary chain and as the chain length of the alkyl oleate increased. Table 3-3 showed chemical shifts of both epoxy protons and carbons resonating increasingly downfield (higher frequency) as we moved from C19-C21 (entries 1, 2 and 3) but resonated increasingly upfield (lower frequency) as we moved from C22-C26 (entries 5, 7). However, the C28 chain was observed to resonate at a much higher frequency, 2.82 ppm; 57.16-57.20 ppm (entry 9). Across epoxides with the same chain length, that is isomers, all epoxy protons and carbons of the primary isomers resonated at higher frequencies compared to their corresponding secondary epoxides (entries 3 and 4; 5 and 6) except in the C26 epoxides where the primary isomer epoxy protons and carbons resonated at a lower frequency relative to the secondary epoxide (entries 7 and 8). While it is clear how the alkyl group attached to the ester of the oleate contributes to chemical shifts among the attached chain but is not clear how it affect the chemical shifts of the epoxy proton and carbon.

Table 3- 3 Epoxide proton and carbon NMR chemical shifts variation within various chain lengths of alkyl oleate epoxides

Entry	Oleate Epoxide	Proton Chemical Shift (ppm)	Carbon Chemical Shift (ppm)
1		2.74	57.02-57.06
2		2.82	57.16-57.21
3		2.85	57.24-57.29
4		2.80	57.13-57.16
5		2.84	57.22-57.27
6		2.70	56.90-56.94
7		2.63	56.72-56.78
8		2.84	57.20-57.24
9		2.82	57.16-57.20

IR spectra (Figure 3-10) equally showed the disappearance of the 3004 cm^{-1} band belonging to the olefinic C-H stretch and appearance of vibrations belonging to epoxy band between 953 and 979 cm^{-1} (asymmetric deformation) and between 822 and 837 cm^{-1} (symmetric ring deformation). The epoxy bands are in line with values reported in the literature.^{212, 245} However, the epoxy ring stretch “breathing” expected around 1280-1230 cm^{-1} did not show in the spectra.¹⁹⁵ Additionally, IR spectra did not show any band belonging to OH group (3425 cm^{-1}) which indicated that the level of ring opening to form diol was not significant. There was no absorption peak at ~1600 cm^{-1} representative of quaternary ionic nitrogen centre

which confirms there is no Adogen 464 left over in the product or may be in very low concentration,²⁴⁶⁻²⁴⁸ although CHN elemental analysis detected trace nitrogen in the sample (chapter 8 section 8.6.2). Further details are discussed in chapter 4.

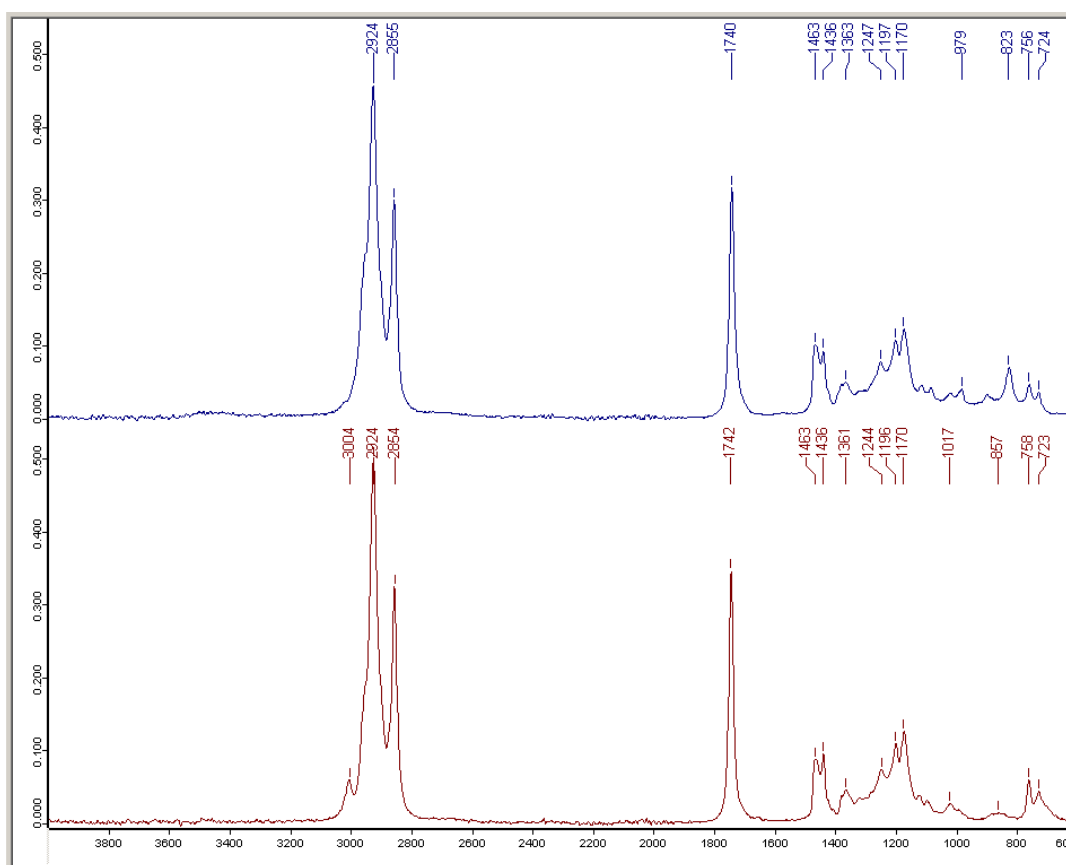


Figure 3- 10 FT-IR spectra of methyl oleate (bottom) and epoxidised methyl oleate (top) showing disappearance of =C-H vibration and appearance of epoxy bands

ESI-mass spectrometry was employed to determine accurate masses for all the epoxides synthesised as recorded in chapter 8.

Figure 3-11 shows the appearance of a range of alkyl oleate epoxides and their corresponding oleates. As the FAAEs were transformed to corresponding epoxides, there was a change in colour from deep to light amber noticed in the compounds formed (Figure 3-11c and d). This was probably due to bleaching of the oleates by hydrogen peroxide. It was also noted that some epoxides turned dark in colour a few days after being synthesised. Figure 3-11 a shows epoxides on the day of production while Figure 3-11 b shows methyl oleate epoxide, 2-propyl oleate epoxide and 2-butyl oleate epoxide turning darker in colour after synthesis.



Figure 3- 11 Variation of colour shades with (a) alkyl oleate epoxides at production, (b) frozen alkyl oleate epoxides days after production, (c) alkyl oleate juxtaposed with corresponding epoxides at production, (d) alkyl oleates juxtaposed with corresponding epoxides days after production

It was observed that when the epoxides were stored in a freezer to ameliorate their discoloration, some epoxides, specifically, ethyl oleate epoxide, 1-octyl oleate epoxide and 1-decyl oleate epoxide crystallized as shown in Figure 3-11 **b**. The reason for this discoloration was not so obvious and was never previously mentioned for unsaturated fatty ester epoxides in any literature. However, it could possibly be as a result of residual acidity from the PTA catalyst employed in the epoxidation process. Inductively coupled plasma mass spectrometry (ICP-MS) analysis of methyl oleate epoxide showed it contained trace amount of W (0.6 wt%). Residual PTA could initiate or promote oxidation of side reaction products, especially the ketone and aldehyde, in the epoxide. Ketones and aldehydes are known to impart colour while undergoing oxidation.^{150, 249-251} However, while this assertion could be true for methyl oleate epoxide and 2-butyl oleate epoxide with significant amount of these products (Table 3-4 entries 1 and 4), it might not be

substantive enough a reason to justify the case in 2-propyl oleate epoxide which also showed discoloration even with much less side products (entry 2; Figure 3-11a, b and d) whereas 2-octyl oleate epoxide with roughly same amount of ketone and aldehyde did not exhibit discoloration (entry 5; Figure 3-11a and b). More so, 1-butyl oleate epoxide did not exhibit discoloration with significant presence of ketone and aldehyde on storage (entry 3; Figure 3-11a and b). Unfortunately, a check on methyl oleate epoxide with proton NMR spectroscopy did not reveal any ongoing oxidation or the presence of these side products upon storage.

Table 3- 4 Composition of side reaction products from some fatty acid ester epoxides

Entry	Oleate Epoxide	Total side product (%)	Aldehyde (%)	Ketone (%)	Epoxy acid (%)	Diols (%)	Others*
1	Methyl oleate epoxide	26	6.5	6.7	6	7	-
2	2-propyl oleate epoxide	7	0.4	0.4	0.7	3.8	1.7
3	1-butyl oleate epoxide	16	3.9	5.9	4.3	1.9	-
4	2-butyl oleate epoxide	18	3.2	3.6	7.2	2.2	2
5	2-octyl oleate epoxide	22	0.5	0.6	3.5	9	4

*Some of these compounds could not be identified with GC-MS.

3.6 Studies on factors affecting epoxidation

3.6.1 Effect of acetic acid on epoxidation with PTA

Acetic acid upon reaction with hydrogen peroxide will generate a peracid which could promote an epoxidation reaction. To investigate the effect of acetic acid, two experiments were set up in which one was doped with acetic acid and the other as a control. Results monitored by GC-FID (Figure 3-12) showed that conversion rate was faster in the acetic acid-doped system reaching 88% in 1 hour and 99% in 2 hours while the undoped system reached 74% and 90% in 1 hour and 2 hours

respectively. However, while epoxide yield increased rapidly with increasing conversion in the undoped system, the epoxide being formed in the doped system was gradually converted to side products, thus the yield decreased with increasing methyl oleate conversion. It was observed that epoxide yield decrease from 73% to 8% after 6 hours of reaction. As observed in earlier reactions, both systems generated side reaction products of epoxy acid, diols, ketones and aldehydes. The presence of both acetic acid and acetonitrile will concomitantly lead to the formation of peracids which probably made the system too oxidising for a stable epoxide formation, hence the declining epoxide yield rate in the doped system. There have been studies that reported favourable conversion of FAAEs with acetic acid under different reaction conditions but also with attendant low selectivity due to side products formation.^{212, 214, 252}

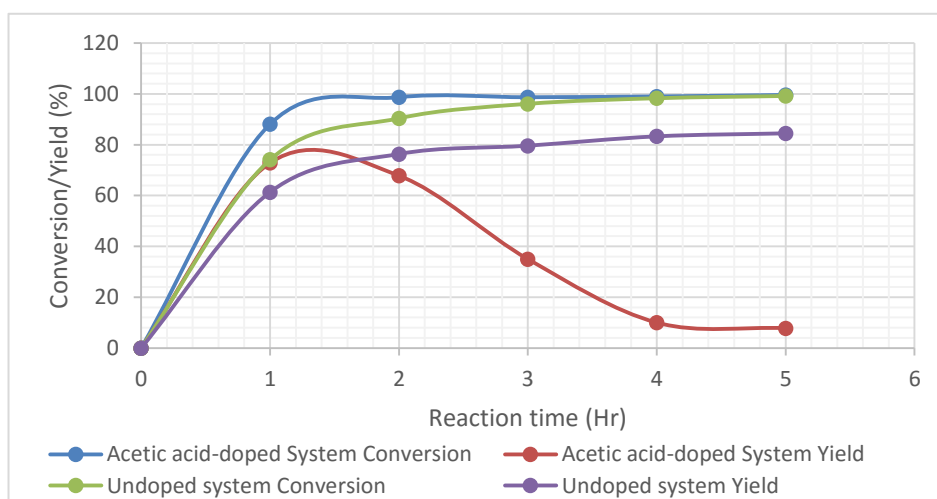


Figure 3- 12 Effect of acetic acid-doped epoxidation reaction on conversion and yield in the presence of PTA. In the acetic acid-doped system, epoxide yield decreased with increasing methyl oleate conversion as the epoxide so formed is gradually converted to side products while the epoxide yield in the undoped system increased with increasing conversion. Reaction conditions: temp.= 50 °C, catalyst=10 wt% relative to oleate, Adogen 464 =6 wt% relative to oleate, 6 mmol alkyl oleate reacted, 1 mL H₂O₂, 1 mL CH₃CN, 2 drops of CH₃COOH.

3.6.2 Effect of solvent nature on epoxidation with PTA

Five systems were considered for this investigation; three contained dichloromethane, acetonitrile and tert-butanol each as solvent, another contained “as-is hydrogen peroxide” with additional water and the last system contained “as-

is hydrogen peroxide” only i.e.- “solventless”. Halogenated solvents are very toxic and undesirable for handling and in the environment but are effective solvents with hydrogen peroxide for minimizing side reactions in epoxidation reactions.^{236, 253} Their immiscibility with water may make them hinder hydrolysis of epoxides in solution.

Results in Figure 3-13 showed that dichloromethane and acetonitrile solvents competed to both give roughly 80% epoxide yield. Contrary to expectation the magnitude of side reaction products formation in the DCM system was not significantly different from the acetonitrile system. Tert-butanol-solvent system only gave 20% conversion and 10% epoxide yield after 3 hours of reaction. There was not so much difference observed between when additional water was added to the solution and when hydrogen peroxide was used “as is”. It was surprising that both systems gave the highest selectivity to epoxide (90%) among the systems despite their potential to hydrolyse the epoxide formed. It is, however, preferable to consider the system with additional water to enhance the transfer of oleate into the aqueous phase, and that reducing the concentration of H₂O₂ in water is desirable on safety grounds.

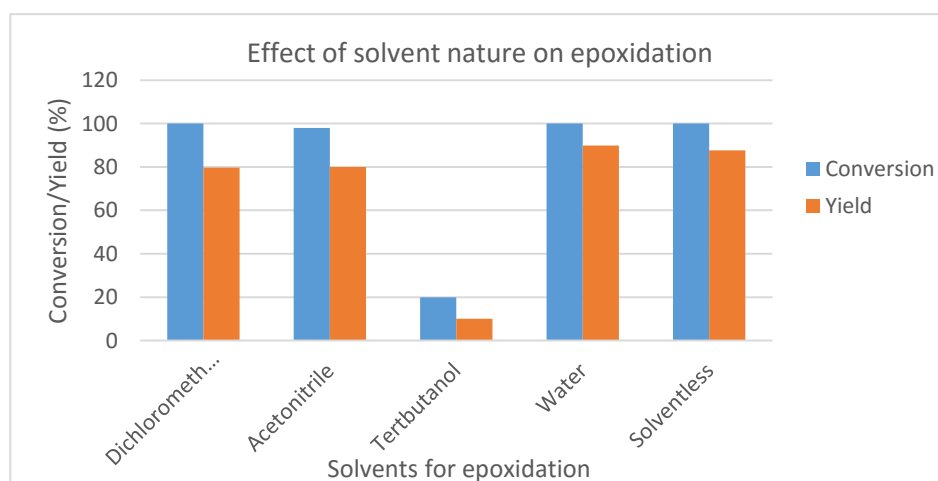


Figure 3- 13 Effect of nature of solvents on epoxidation with hydrogen peroxide in the presence of PTA with respect to conversion and yield. Reaction conditions: temp.= 50 °C, time =3 hours, 6 wt% catalyst relative to oleate, Adogen 464 =6 wt% relative to oleate, 1 mmol alkyl oleate reacted, 1 mL H₂O₂, 1 mL H₂O, 1 mL CH₃CN, 1 mL CH₂Cl₂ and 1 mL CH₃C(CH₃)₂OH

3.6.3 The need for a PTC in PTA-catalysed epoxidation reaction

It was also of interest to investigate the need for a phase transfer catalyst (PTC) in the system by setting up two experiments from which PTC was completely excluded. The first, system **A**, contained 2 mmol methyl oleate, 2 mL H₂O₂, 2 mL CH₃CN and four drops of CH₃COOH while the second, system **B**, contained 2 mmol methyl oleate, 2 mL H₂O₂, 2 mL CH₃CN and 6 wt% PTA relative to oleate. GC-FID showed 3% methyl oleate conversion and 99% selectivity to epoxide after 6 hours in system **A** and 3.8% conversion and 59% selectivity to epoxide after 6 hours in system **B**. Interestingly, while methyl oleate conversion in the absence of Adogen 464 was very low in both systems, it was noticed that 0.7% epoxy acid and 0.8% diols side products were formed in the **B** system. It appears that the peracid generated by both acetonitrile and acetic acid in system **A** was not as strongly oxidising as the one formed by acetonitrile alone in the presence of PTA in system **B**. Low methyl oleate conversion with these systems, therefore, suggests that a PTC is needed to enhance conversion although a combination of acetonitrile and acetic acid could be effective enough to give a platform with high selectivity to epoxide at prolonged reaction time when PTA is excluded.

3.6.4 Effect of PTA nature and source on epoxidation

Crystalline “wet” PTA was purchased from Sigma-Aldrich chemicals and a few grams from this was oven-dried at 105 °C for 16 hours. PTA was also purchased from Acros organics (which was in a powdery form) and used “as is”. Comparing results between the Sigma PTAs, both demonstrated similar effectiveness for epoxidation. The dried PTA gave 100% methyl oleate conversion and 87% epoxide yield while the “as is” PTA gave 93% oleate conversion and 85% epoxide yield as shown in Figure 3-14. PTA from Acros organics performed fairly better than the Sigma catalyst with 90% epoxide yield. This experiment was repeated two times. The reasons for the differences in conversion and yield are not so obvious. It was of

interest to investigate this seemingly insignificant difference in performance with infrared spectroscopy.

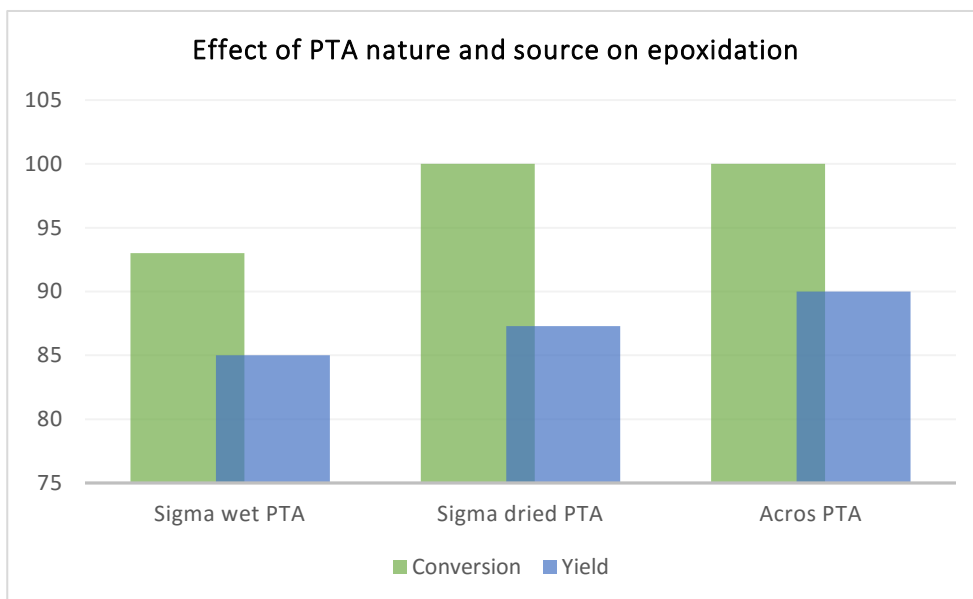


Figure 3- 14 Influence of the nature and source of PTA catalyst on methyl oleate conversion and epoxide yield. Reaction conditions: temp.= 50 °C, time =3 hours, catalyst=6 wt% relative to oleate, Adogen 464 =6 wt% relative to oleate, 1 mmol alkyl oleate reacted, 1 mL H₂O₂ and 1 mL H₂O.

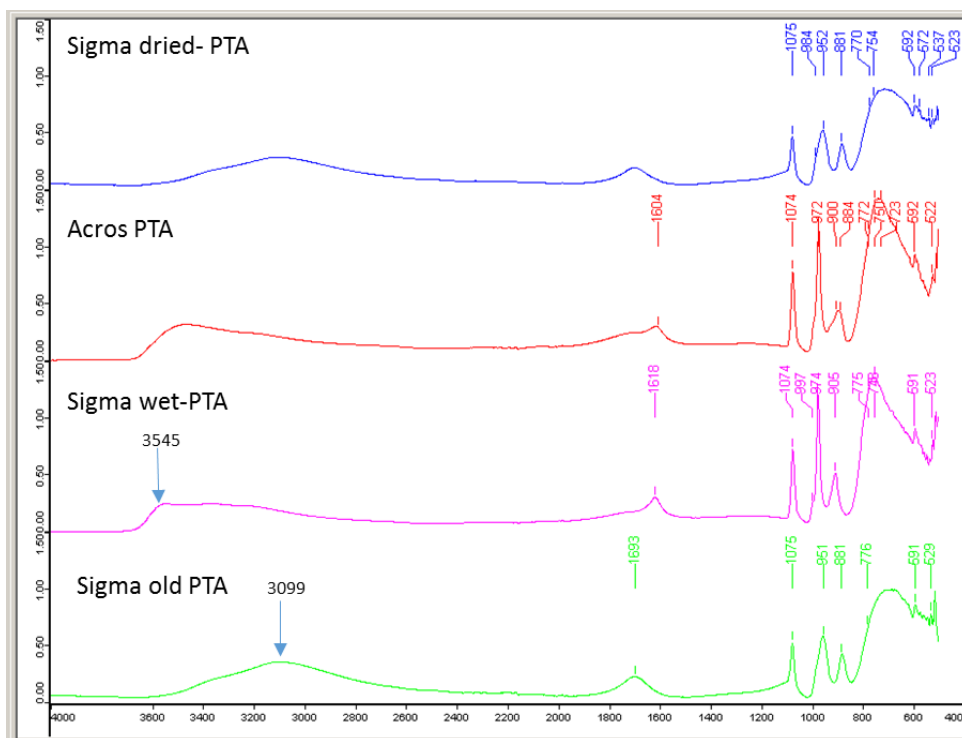


Figure 3- 15 ATR-FTIR spectra of hydrated and dehydrated PTAs and their sources

ATR-FTIR spectroscopic analysis of the PTAs was performed and the catalysts were compared along with another “old” Sigma PTA catalyst purchased and used at the

initial stage of this study. All the PTAs were hydrates, containing $x\text{H}_2\text{O}$ (water of crystallisation) at purchase. Two regions were noted in the all the spectra (Figure 3-15). The assignment of bands for Keggin structure agrees with the literature.^{232, 254, 255} The region $1075\text{-}522\text{ cm}^{-1}$ represents absorptions associated with metal-oxygen skeletal modes of the Keggin unit: $1075\text{-}1074\text{ cm}^{-1}$ (a. P-O stretch), $997\text{-}951\text{ cm}^{-1}$ (W=O stretch), $905\text{-}881$ and $770\text{-}723\text{ cm}^{-1}$ (W-O-W stretch). The region at $3545\text{-}1604\text{ cm}^{-1}$ connotes absorptions associated with OH stretching (ν) and bending (δ) modes of acidic hydroxyls and of water molecules present in the catalyst.²⁵⁴ The dried and the old Sigma PTAs are much alike in their spectra. The spectra of the Acros and Sigma “wet” PTAs resemble that of a fully hydrated PTA showing a broad asymmetric absorption centered at 3490 and 3545 cm^{-1} respectively that is associated with both neutral and protonated water species ($\nu(\text{OH})$ modes) and another band at 1604 and 1618 cm^{-1} ($\delta(\text{OH})$ modes) respectively. Surprisingly the Acros PTA looked different in appearance from the “wet” Sigma catalyst. The former was an off-white powdery solid in appearance and its better catalytic performance than the latter does not justify why they have identical spectra. The shift from 3545 to 3099 cm^{-1} and from 1618 to 1693 cm^{-1} in the water band region ($\nu(\text{OH})$ modes) and ($\delta(\text{OH})$ modes) respectively is due to dehydration of PTA as confirmed by other author.²⁵⁴ A shift from 974 to 951 cm^{-1} with reduced absorption intensity belonging to W=O vibration band was also noted. It should be recalled that the Acros PTA has a spectrum that is identical with that of a fully hydrated PTA but its appearance defied this fact. It could therefore mean that the catalyst possessed some level of dehydration, and the dried and old Sigma PTAs are more dehydrated catalysts. It is also possible that the powdered catalyst has a higher surface area and are more capable of transferring to the organic phase, staying suspended there. As earlier mentioned PTA acidity strength affects its epoxidation performance. The Acros catalyst had the best performance as discussed earlier. It is not as dehydrated as the dried and old Sigma PTAs and not as hydrated as the “wet” catalyst. Therefore, this could mean that there is a level of water of crystallisation required to enhance the

acid strength of the catalyst. More measurements will be needed to accurately justify this conclusion.

3.7 Investigation into the formation of aldehyde and ketone during epoxidation of oleates

So far formation of aldehydes and ketones in varying concentration among other side reaction products has continuously characterised our epoxidation process. Their formation is much more pronounced with acetonitrile used as a reaction solvent. There exists in the literature significant evidence for the formation of oxidation products of aldehydes and ketones from unsaturated fatty acid in the presence of hydrogen peroxide and an acid as shown in Figure 3-16a.^{196, 256-260} These are typically two-step reactions leading to this formation.

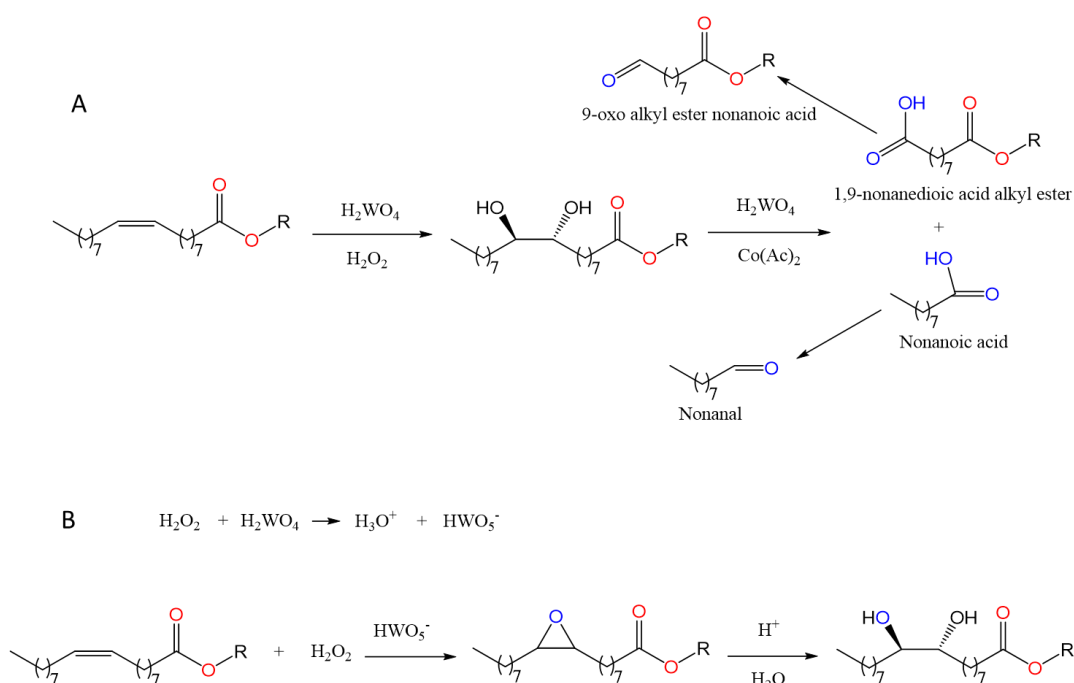


Figure 3- 16 Formation of aldehydes and ketones from unsaturated fatty esters (a) two-step oxidation of double bond and diol to carboxylic acid and acid ester (b) mechanism of the first step of the reaction leading to formation of diols.

The first step involves oxidation of the double bond in the presence of tungstic acid and hydrogen peroxide to form diols. The second step occurs under mild pressure and involves oxidative cleavage of the carbon-carbon bond of the diols with

hydrogen peroxide,²⁵⁹ or molecular oxygen in the presence of the residual tungstic acid from the first step.²⁵⁶ With molecular oxygen used, a cobalt carboxylate catalyst is required in addition to tungstic acid.²⁵⁹

The mechanism of the first step has been studied and reported.^{196, 258, 259, 261, 262} An epoxide is first formed as an intermediate product from the unsaturated fatty acid ester facilitated by HWO_5^- which is subsequently hydrolysed in the presence of the strong acid H^+ as shown in Figure 3-16b. The mechanism for oxidative cleavage of the diols has not been so studied extensively but there are two proposals in the literature. The first argued that direct cleavage of the diol carbon-carbon forms an aldehyde as an intermediate with subsequent oxidation to an acid. The second argument involves the oxidation of one OH group to an alpha-hydroxyketone and successive oxidation to acid. The former proposal can only proceed *via* a radical mechanism and the latter is generally preferred by authors.^{256, 263} Another study considered preparation of polycarboxylic acids from cyclic olefins by oxidative cleavage with hydrogen peroxide.²⁶² According to this report in which 1,2,3,6-tetrahydrophthalic acid anhydride was one of the compounds investigated, it was concluded that oxidation of olefin to epoxide then to diol and subsequently to polyacids in the presence of PTA is the only feasible way to oxidation cleavage of cyclic olefin to produce such compounds.

However, aldehydes and ketones have been observed (sometimes simultaneously) alongside their corresponding acids in this study. This means the first argument is more likely to be true in this case. To investigate this, three systems of reactions with different chemical compositions were considered as shown in Table 3-5. All reactions were carried out at 50 °C and monitored with GC and NMR spectroscopy by collecting samples at 5 and 30 minutes and 1, 2, 3, 6 and 24 hours of reaction. Collected samples were dried over anhydrous magnesium sulphate and ran through a column of neutral alumina before characterisation. In system A, there was

formation of diol and epoxy acid, nonanal and 9-oxo nonanoic acid methyl ester 30 minutes into the reaction.

Table 3- 5 Composition of systems used to investigate formation of aldehydes and ketones in epoxidation reaction

<i>System</i>	<i>Composition</i>	<i>Amount</i>
A	Methyl oleate	4.1 mmol
	Hydrogen peroxide	4 mL
	Phosphotungstic acid	6 wt % relative to oleate
	Adogen 464	6 wt% relative to oleate
	Acetonitrile	4 mL
B	Methyl oleate	4.1 mmol
	Hydrogen peroxide	4 mL
	Phosphotungstic acid	6 wt% relative to oleate
	Adogen 464	6 wt% relative to oleate
C	Methyl oleate	4.1 mmol
	Hydrogen peroxide	4 mL
	Phosphotungstic acid	6 wt% relative to oleate
	Adogen 464	6 wt% relative to oleate
	Tert-butanol	4 mL

Epoxide yield increased and peaked (78%) at 1 hour reaction time before a rapid decrease began as shown in Figure 3-17. The decrease in epoxide yield from 2 hours onward was complemented by an increasing yield of nonanal, nonanoic acid, 9-oxo nonanoic acid methyl ester, nonanedioic acid methyl ester, diol, epoxy acid and 10-oxo octadecanoic acid methyl ester. A further increase in yield was observed for nonanal (15.4%), nonanoic acid (3.4%), 9-oxo nonanoic acid methyl ester (14.9%), nonanedioic acid mono methyl ester (4.5%), 1.9% 10-oxo octadecanoic acid methyl ester and 26.8% epoxide after 24 hours (Figure 3-17).

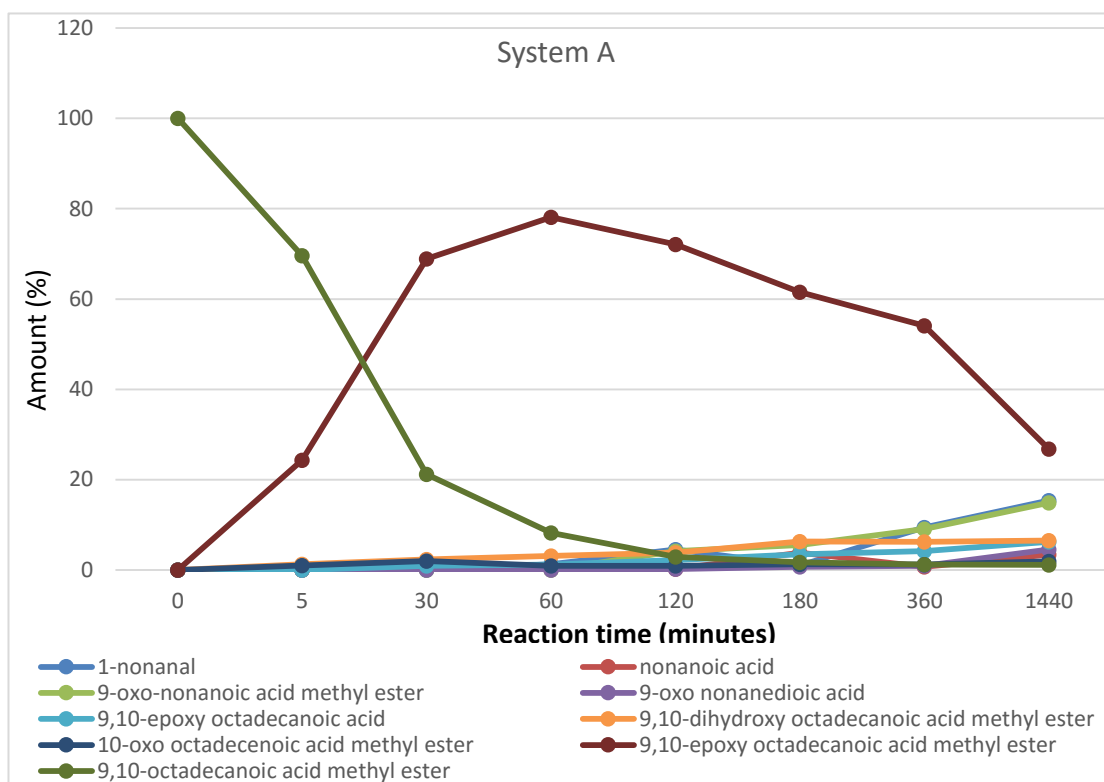


Figure 3- 17 Profile of side reaction products from epoxidation of methyl oleate in acetonitrile solvent (system A) over 24 hours of reaction

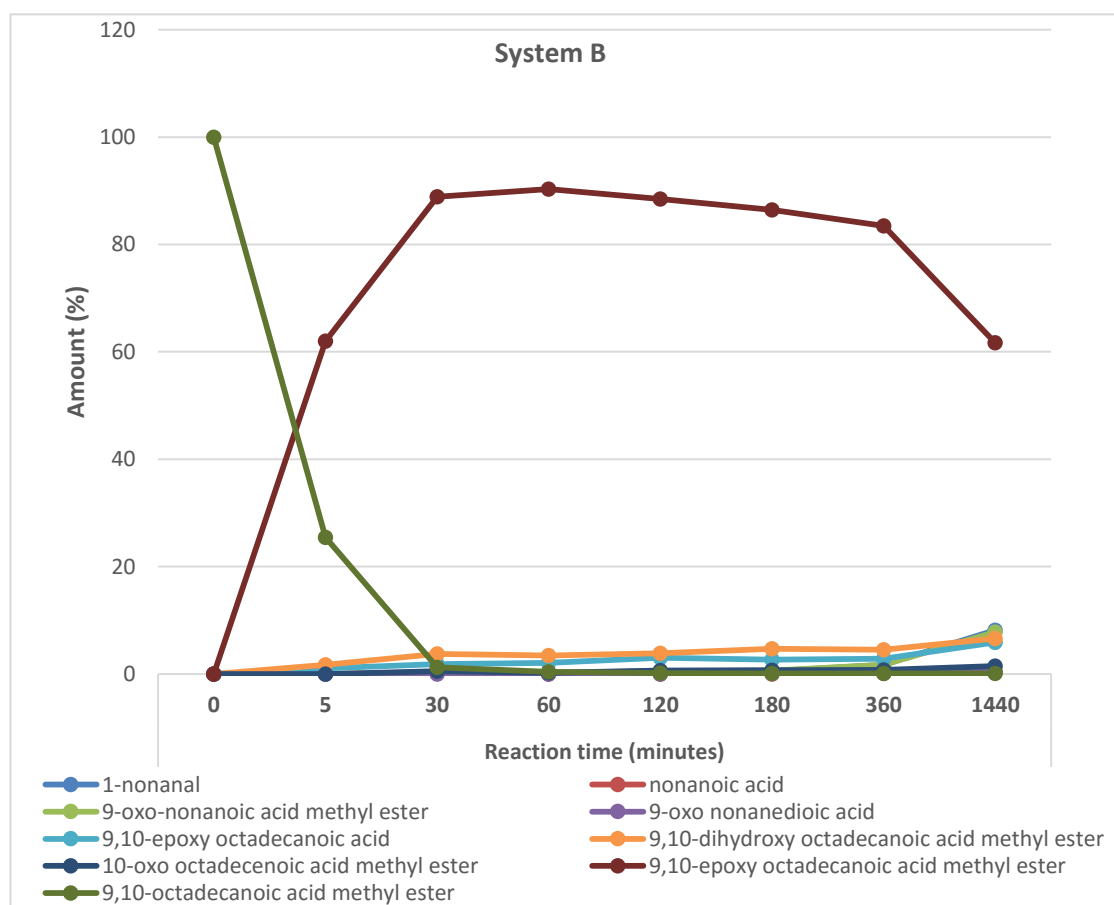


Figure 3- 18 Profile of side reaction products from epoxidation of methyl oleate in system B over 24 hours of reaction

Epoxide yields in system B (Figure 3-18) were 62% and 89% in 5 minutes and 30 minutes of reaction respectively and peaked (90%) at 1 hour before it began to drop. There was an increase in the yield of nonanal, nonanoic acid, 9-oxo nonanoic acid methyl ester, nonanedioic acid methyl ester, diol and epoxy acid as the yield of epoxide decreased. After 24 hours, there was 61.7% epoxide left while 8.1% nonanal, 0.4% nonanoic acid, 7.8% 9-oxo nonanoic acid methyl ester, 0.4% nonanedioic acid monomethyl ester, 6.6% diol, 5.9% epoxy acid and 1.5% 10-oxo octadecanoic acid methyl ester have been formed.

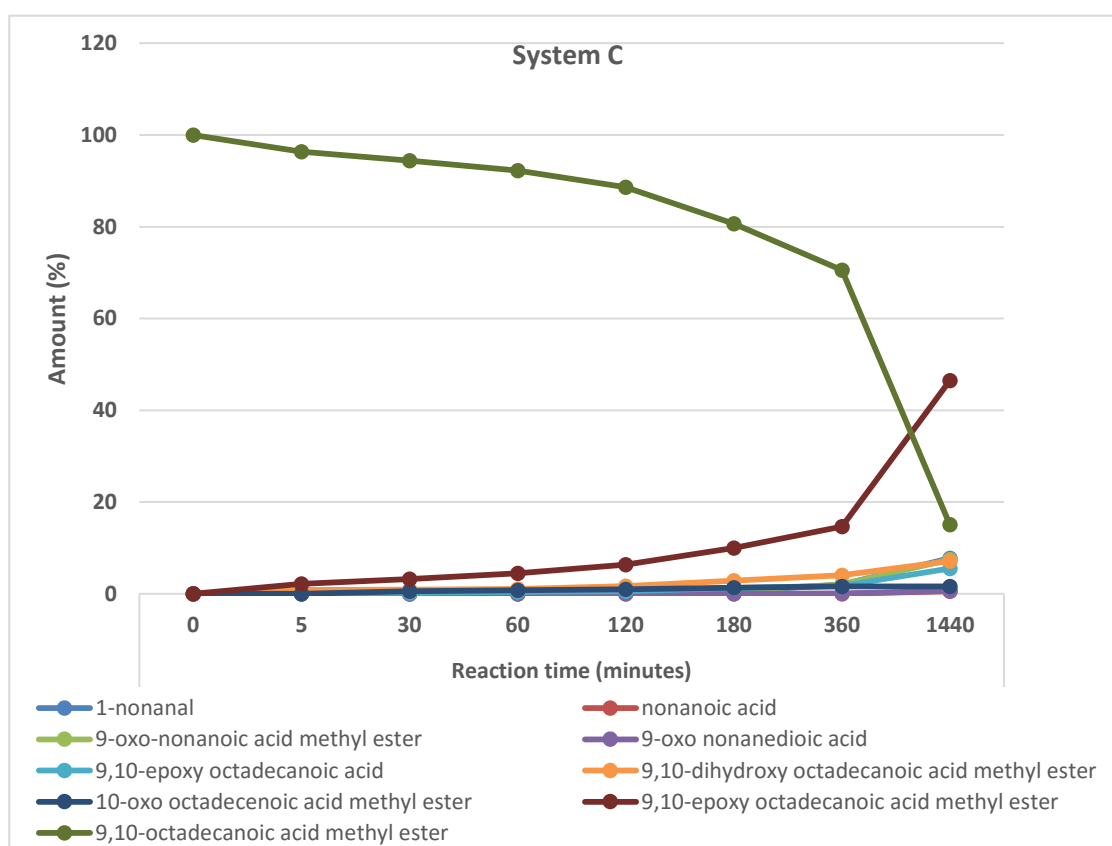


Figure 3- 19 Profile of side reaction products from epoxidation of methyl oleate in tert-butanol solvent (system C) over 24 hours of reaction

In system C epoxide yield increased from 2.1% to 46.5% between 5 minutes and 24 hours of reaction without the formation of nonanal and 9-oxo nonanoic acid monomethyl ester within the first 1 hour of reaction (Figure 3-19). Unlike in the first two systems where epoxide yield increased at the on-set of reaction and thereafter dropped, epoxide yield in system C increased all through the reaction time. At the

end of reaction, 7.8% nonanal, 0.6% nonanoic acid, 7.6% 9-oxo nonanoic acid methyl ester, 0.7% nonanedioic acid monomethyl ester, 7.1% diol, 5.5% epoxy acid and 1.6% 10-oxo octadecanoic acid methyl ester have been formed. System B is preferred to A as epoxide yield is higher with lesser concentration of side products.

It was obvious from the result that in all the three systems concentration of side products increased with decreasing epoxide yield and increasing reaction time showing that the epoxide was being gradually converted to the side products observed. Interestingly, in all the systems the concentration or amount of nonanal (including nonanoic acid) relative to 9-oxo nonanoic acid monomethyl ester (including the acid) remained similar throughout the reaction time. Nonanal was seen to undergo oxidation to nonanoic acid while 9-oxo nonanoic acid monomethyl ester oxidised to nonanedioic acid monomethyl ester with prolonged reaction time. This suggests that 9-oxo nonanoic acid monomethyl ester and nonanal were being formed from the same source. Considering the fact that number of carbon atoms in the two compounds sum up to 19, it suggests they were formed from a ruptured or cleaved double bond or epoxy ring. This is in line with the literature described earlier. Figure 3-20 shows the possible routes to some of the side products generated in all the systems.

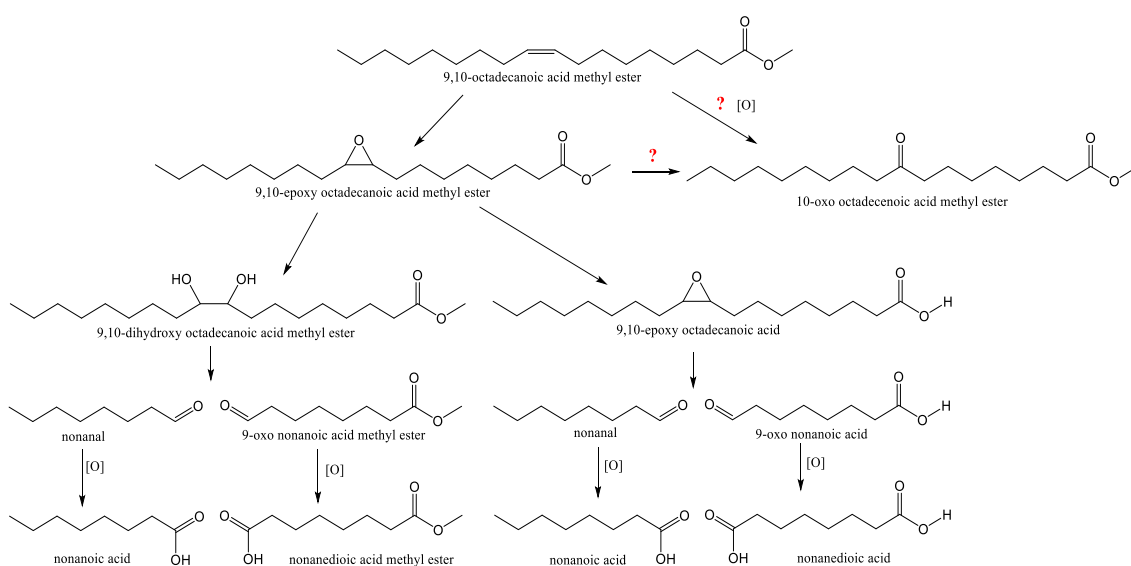


Figure 3-20 Routes to formation of side products from epoxidation of methyl oleate

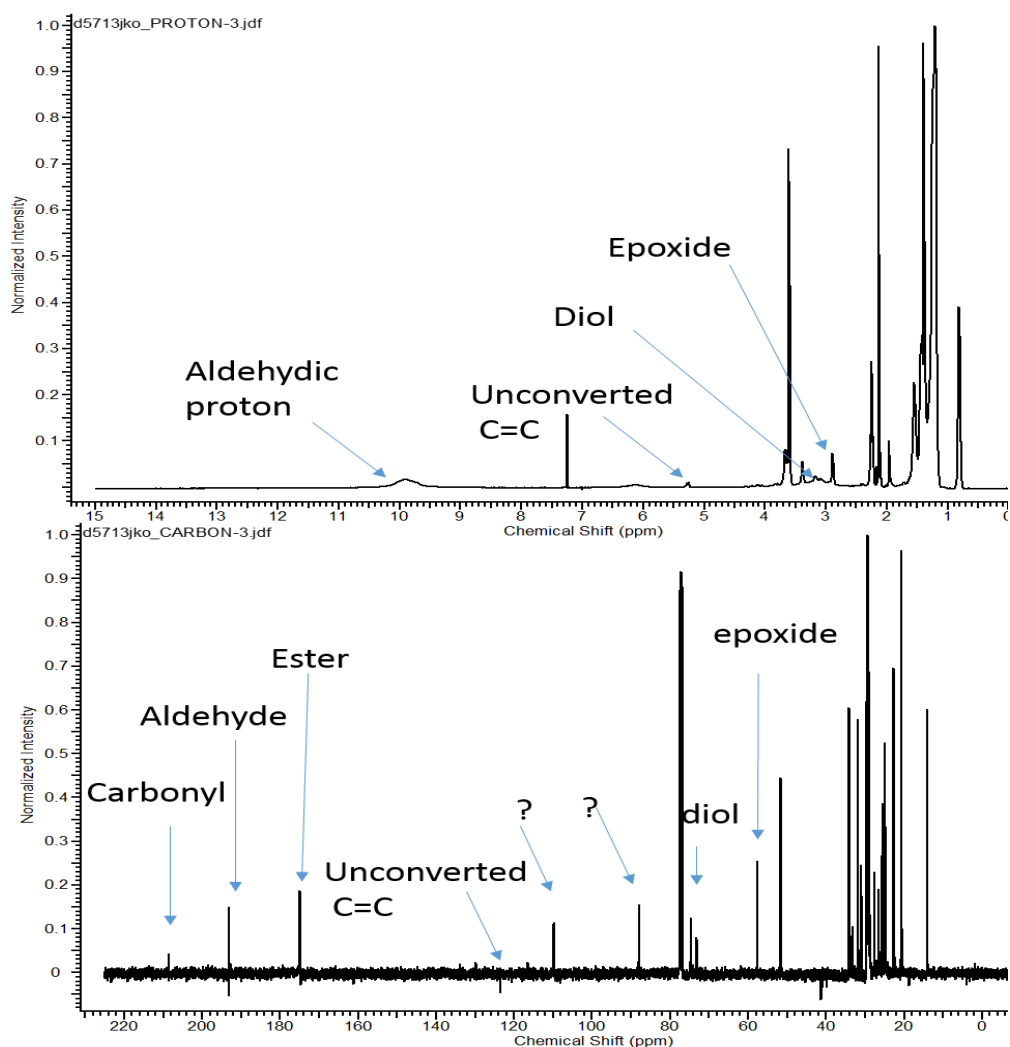


Figure 3- 21 Proton and Carbon 13 NMR spectra of System A at 6 h of reaction

The formation of the diol and epoxy acid were expectedly from hydrolysis of epoxy bond and ester group by the water and acid in the system. Proton (wide) and carbon 13 DEPT NMR spectroscopy confirmed the presence of these side products as shown in Figure 3-21.

A trace amount of 10-oxo octadecanoic acid monomethyl ester was observed in all the systems. While it is known that an olefin can be converted to a ketone *via* a modified Wacker-Tsuji oxidation process,²⁶⁴ it was not obvious how the compound was formed under this condition and if it contributed to the formation of nonanal and 9-oxo nonanoic acid monomethyl ester. Surprisingly, there was no trace of nonanedioic acid and 9-oxo nonanoic acid observed in the GC spectrum. Following supporting literatures on the result obtained above, it can be concluded that methyl

epoxide was undergoing hydrolysis to form diols which later oxidised to alkanones and alkanals and corresponding acid.

3.8 Epoxidation with heterogeneous catalyst

PTA is highly soluble in polar solvents and noted for a low surface area usually less than 10 m²/g.²²⁵ This limits its use for catalysis in hydrophobic systems and recovery is usually problematic in its homogeneous forms. A number of supports have been employed to develop heterogeneous catalysts based on PTA for different reactions.²⁶⁵⁻²⁷² Silica has been found to be a good support that most retains the acidity and stability of PTA when used.²⁷³ Of all the techniques including impregnation and sol-gel technique used to adsorb PTA on supports, immobilization is the preferred. Unlike in other methods in which there could be significant leaching problem, in immobilization method PTA is chemically bonded to the support *via* functionalization which makes it less vulnerable to leaching.²⁷⁴ Functionalization of catalyst supports allows for more stability, varied and improved properties of the support surface such as hydrophobicity.²⁷⁴ Mesoporous silicas are types of ordered silica materials that have high surface area for improved catalytic activity, but with pores of a large enough size to reduce diffusional limitations of larger molecules such as triglycerides or fatty esters. SBA-15 is a commonly used type of mesoporous silica with surface area of 600–1,000 m²/g in which the tuneable tubular pores are hexagonally arrayed.²⁷⁵ SBA-15s are non-toxic, biocompatible and thermally stable.^{62, 276} Many mesoporous silica supported PTA catalysts have been used for epoxidation of olefins but there is no report where unsaturated fatty acids are involved. Figure 3-22 shows the processes involved in the synthesis of heterogeneous catalysts used for epoxidation in this study.

Mesoporous silica (SBA-15) was synthesised as described in chapter 8 section 8.3.9 using Pluronic 123 triblock copolymer surfactant as a template and characterised according to the literature.²⁷⁷⁻²⁸⁰

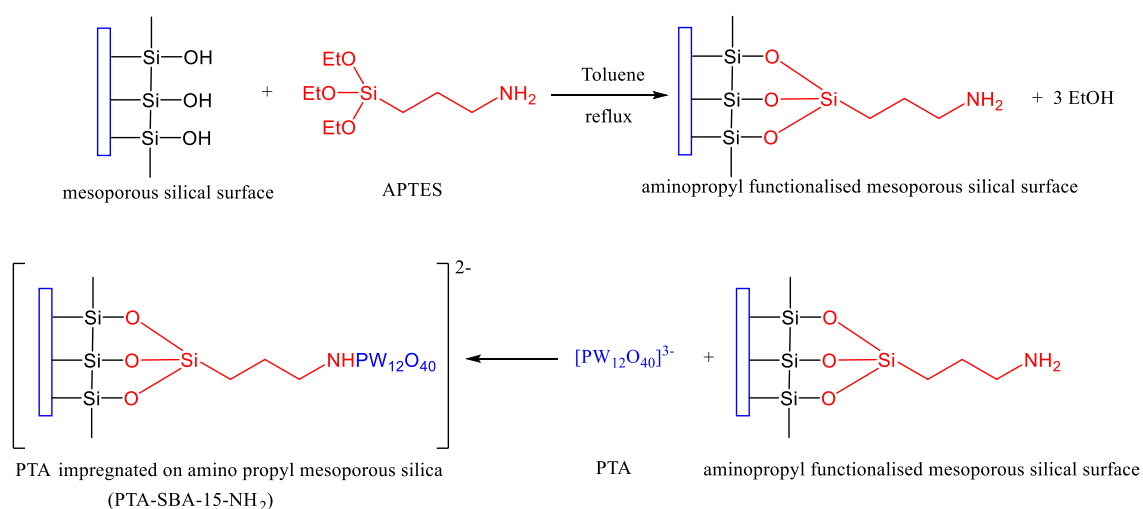


Figure 3- 22 Synthesis of functionalized mesoporous silica supported phosphotungstic acid

Functionalization of SBA-15 was achieved by surface reaction with 3-aminopropyl triethoxy silane, APTES, (chapter 8 section 8.3.10) to make the mesoporous support more hydrophobic by exchanging some available hydroxyl group with amino group thus reducing their availability for bonding with water. Incorporation of amino propyl functionality will also improve sorption properties and PTA attachment within the support. PTA was immobilized on the functionalized silica and designated PTA-SBA-15-NH₂ as described in chapter 8 section 8.3.12. Another catalyst (PTA-SBA-15) was made by impregnating PTA directly on a non-functionalized silica support (chapter 8 section 8.3.11). Both catalysts alongside their supports were characterised by FT-IR spectroscopy.

PTA immobilized on amino propyl functionalised mesoporous silica was investigated as a catalyst for epoxidation reaction under different conditions at 60 °C. Figure 3-23 shows that the maximum yield of epoxide was 41% with 55% methyl oleate conversion under system A after 27 hours. To both systems B and C 1 mL H₂O₂ was added every hour of the reaction. In system B the highest concentration of nonanal (32.2%) was formed. Systems C and D used dichloromethane as a solvent. Prolonged reaction time did not alter oleate conversion for these systems but D gave much less concentration of side products.

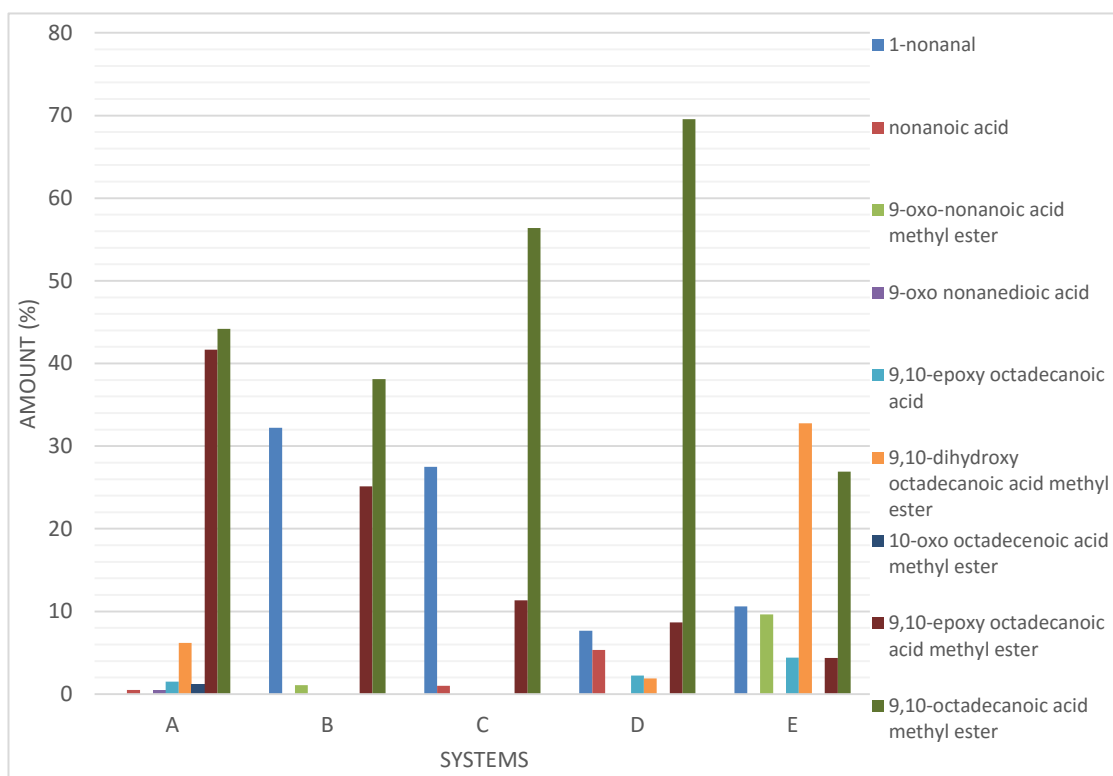


Figure 3- 23 Effectiveness of supported PTA catalyst for epoxidation under different conditions. Reaction conditions @ 60 °C (A) 2 mmol methyl oleate; catalyst= 10 wt% relative to oleate; 0.17 g H₂O₂; 1.23 g CH₃CN; time= 27 hours, (B) 2 mmol methyl oleate; catalyst= 20 wt% relative to oleate; 2 mL H₂O₂; time= 3hours, (C) 2 mmol methyl oleate; catalyst= 20 wt% relative to oleate; 2 mL H₂O₂; 2 mL DCM; time= 3 hours, (D) 2 mmol methyl oleate; catalyst= 20 wt% relative to oleate; 2 mL H₂O₂; 2 mL DCM; time= 24 hours, (E) 2 mmol methyl oleate; catalyst= 20 wt% relative to oleate; 2 mL H₂O₂; 2 mL t-butanol; time= 48 hours

However, excess H₂O₂ concentration in C gave about three times the amount of nonanal formed in D while leaving no diol or epoxy acid un-oxidised. The use of *t*-butanol as solvent for reaction (system E) only yielded 4.4% epoxide, 32.8% diols, 10.6% nonanal and 9.6% 9-oxo nonanoic acid monomethyl ester with 26.9% methyl oleate still unconverted under 48 hours. Interestingly formation of the same side reaction products as found for the unsupported catalyst systems was also observed in the supported systems though not in the same concentration or magnitude.

Generally, the heterogeneous catalysts were found to be ineffective for higher oleates even with prolonged reaction time and increased catalyst concentration. The catalysts were also tested on cyclohexene, a lower molecular weight olefin. Here, both supported phosphotungstic acid catalysts gave high conversion with this alkene. PTA-SBA-15 catalyst gave a conversion of 93% while PTA-SBA-15-NH₂

catalyst gave 98% conversion under 18 hours of reaction. It was expected that the functionalised mesoporous silica supported catalyst gave a higher conversion compared to the non-functionalised catalyst because of the reasons earlier stated. Karimi *et al* ²³⁶ already reported PTA-SBA-15 catalyst to give conversion of 90% with cyclooctene under 12 hours and 77% cyclohexene conversion with hexamethyl phosphoramidate-phosphotungstic acid on mesoporous silica support hybrid catalyst under the same time. With the pore size of PTA-SBA-15-NH₂ measured as ~6.0 nm on the porosimeter, our observed in-effectiveness of the catalysts for epoxidation of alkyl oleates considered could be attributed to slow diffusion rate of oleate molecules into the pores of the catalyst as a result of their bulkiness compared to the catalyst pore size.

Many other heterogeneous catalysts have been developed to affect epoxidation.²⁸¹⁻²⁸⁵ In fact alumina has been reported to catalyse epoxidation of methyl oleate with a conversion of 95% and selectivity greater than 97%,²⁸⁶ but long reaction time (24 hours) and high temperature requirement (80 °C) leaves a concern about this process in terms of energy consumption when compared with other available alternatives. An attempt was made to use alumina for epoxidation but the method described in the literature was not reproducible though a balance of hydrogen peroxide strength and other parameters have to be considered to obtain high conversion and selectivity.²⁸⁷

3.9 Ultrasound-Assisted epoxidation (UAE) of alkyl oleate with supported and unsupported PTA catalysts

The application of ultrasound has been recognised as a clean and environmentally benign technology which has capacity to promote miscibility of phases, yields and selectivity and easy product recovery.²⁸⁸⁻²⁹¹ Ultrasonic-assisted epoxidation (UAE) was attempted to circumvent the challenge of hydrophilic nature of PTA catalyst which made it to stay more in the aqueous phase during the reaction regime, causing a very slow reaction rate. The UAE set up is as shown in Figure 3-24 and initial works

showed significant formation of diols, aldehydes and low molecular acids side products of oleates.

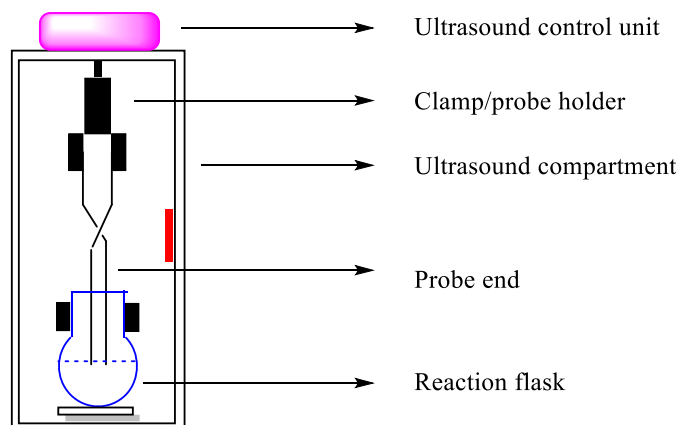


Figure 3- 24 Ultrasound assisted epoxidation reaction set up

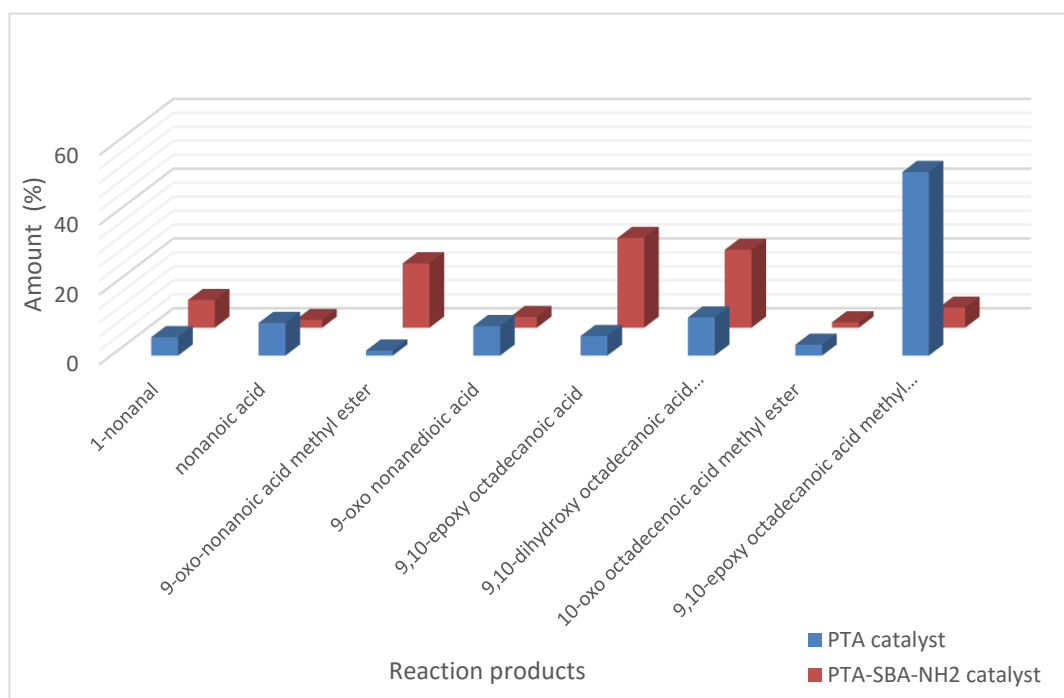


Figure 3- 25 Effectiveness of PTA and PTA-SBA-15-NH₂ catalysts for UAE of methyl

oleate. Reaction conditions @ 100% amplitude, 130 W, 20 kHz, catalyst= 20 wt% relative to oleate (i) for PTA catalyst: 2 mmol methyl oleate; 2mL H₂O₂; time= 1 hour, (ii) for PTA-SBA-15-NH₂ catalyst: 2 mmol methyl oleate; 3 mL H₂O₂ with additional 2 mL every hour; time= 5 hours.

Homogeneous PTA catalyst gave a methyl oleate conversion of 99.8% and 52.6% epoxide in 1 hour while supported catalysts 99.1% conversion and 5.7% epoxide yield in 5 hours (Figure 3-25). Addition of excess hydrogen peroxide led to increased concentration of side products in the supported catalyst system.

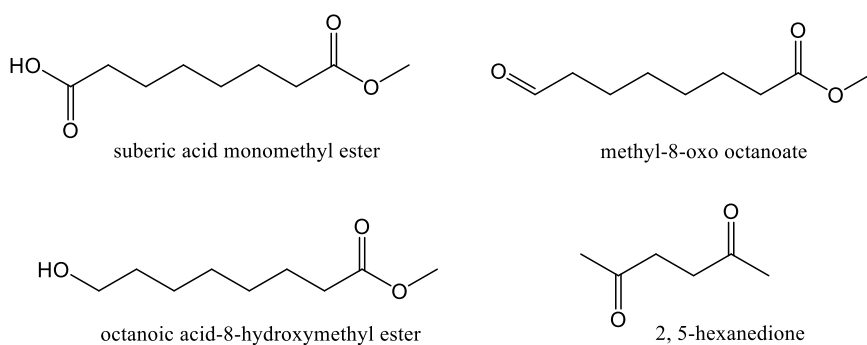


Figure 3- 26 Additional side reaction products formed with UAE of methyl oleate which were not observed in conventional epoxidation process

Other side products (Figure 3-26) formed under UAE reaction include 2, 5-hexanedione, suberic acid monomethyl ester, methyl-8-oxo-octanoate and octanoic acid -8-hydroxymethyl ester although these were only suggestions from NIST library but could not be confirmed by NMR spectroscopy.

One observation from this study is that ultrasound can be seen to enhance the ring-opening of epoxides. Advantageously, a one-step epoxidation-PEGylation system can be considered for surfactant synthesis with UAE. An attempt on this is discussed in the subsequent chapter.

3.10 Synthesis of lactonic sophorolipid epoxide

Sophorolipids (SLs) are a class of glycolipid bio-surfactants first reported in 1961.²⁹² They are synthesised by non-pathogenic yeasts such as called *Candida gropengiesseri*,²⁹³ *Candida apicola*,²⁹⁴ but the most effective organism for the synthesis of SLs has been *Starmerella bombocla*.²⁹⁵ SLs consist of two molecules of glucose (sophorose) which are connected by a glycosidic bond to a hydroxyl fatty acid. The carboxylic end of the fatty acid could either bond to the sophorose at the 4''-hydroxyl position to form a lactone or be left free (Figure 3-27). The commonly attached fatty acid group on the sophorose include palmitic, stearic, oleic, linoleic and alpha-linolenic acids. The sophorose group at times contain acetyl groups either at the 6' or 6'' hydroxyl positions (mono-acetylated) or at both positions (di-acetylated).²⁹⁶ The surfactants have attracted commercial and academic interests

for their applications in detergency, bioremediation, enhanced oil recovery, medicine, home and personal care products and antimicrobial agents.²⁹⁷⁻³⁰¹ They are readily biodegradable, less toxic and have low cytotoxicity compared to conventional surfactants.^{302, 303}

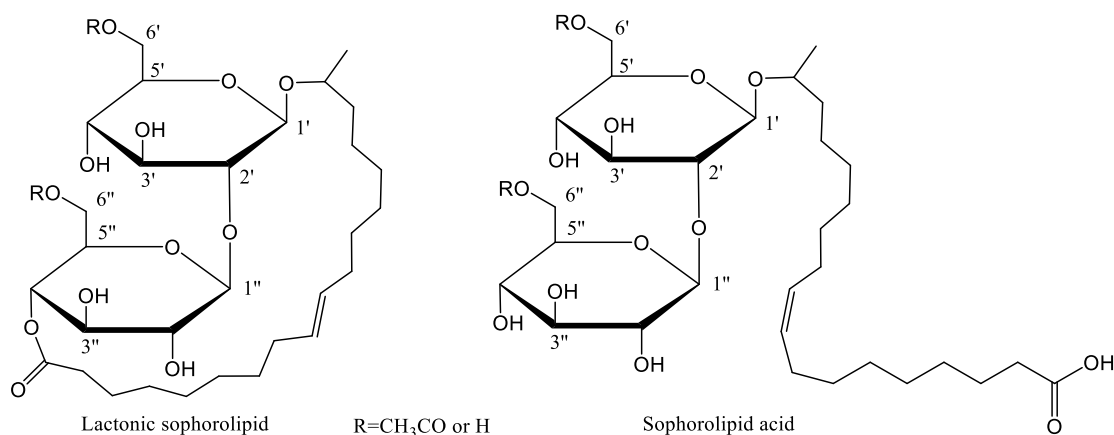


Figure 3- 27 Forms of occurrences of sophorolipids

Modification of SLs is essential to improve properties and enhance the spectrum of their applications.³⁰⁴ A challenge with SLs, in particular the lactonic form (LSL), is poor water solubility as a result of the hydrophobic nature of the ester groups. Alkaline and acid hydrolysis of LSL gives hydroxyl fatty acid and cleaves the ester groups to improve solubility.³⁰⁵ Ozonolysis of double bond of the fatty acid chain with a free carboxyl end gives a surfactant with improved properties. A recent review by Delbeke *et al*³⁰⁴ also considered several modifications reported on the sophorose and fatty acid moieties of SLs. Some of these modifications include acetylation of all the hydroxyl groups on the sophorose, oxidation of the fatty acid group to form oxo-ester and dioc acids,^{292, 294} polymer-derived sophorolipids,³⁰⁶⁻³⁰⁸ among others. Surprisingly, there has not been any study that engaged the fatty acid double bond in LSL to form an epoxide through which further modifications can be made.

Several attempts were made to epoxidize the double bond using PTA catalyst as applied for alkyl oleates under series of reaction conditions but conversion was low. However, success was recorded with PTA catalyst prepared *in situ* as shown in

Figure 3-28 and described in chapter 8 section 8.7 under 3 hours with complete conversion and good yield (99.2%) recovered.

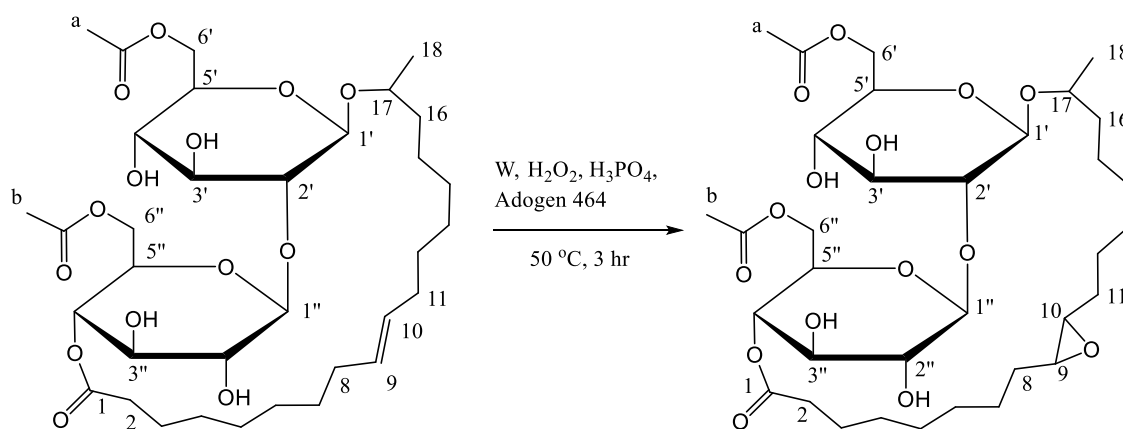


Figure 3- 28 Synthesis of lactonic sophorolipid epoxide

The product, epoxidised lactonic sophorolipid (ELSL), that transformed from a white powder to a puffy sticky white crystal was characterised by FT-IR spectroscopy, ESI-MS, NMR spectroscopy and CHN elemental analysis.

In Figure 3-29, proton NMR spectra obtained for ELSL and LSL showed a full conversion of LSL with a complete disappearance of double bond C9-C10 at 5.33 ppm and appearance of epoxy protons C9-C10 at 2.93 ppm. This was complimented by carbon 13 and DEPT NMR spectra which showed disappearance of C9-C10 at 129.84-130.07 ppm and appearance of C9-C10 epoxy carbon at 57.67-57.91 ppm. The methyl end of the fatty acid C18 was not observed in the LSL but showed at the expected position in the epoxide. The C8 and C11 protons shifted upfield after epoxidation. Fortunately, HSQC and HMBC confirmed that the glycosidic bonds at C17 bonded to C1', C4'' bonded to C1 and between C1'' and C2'' were not cleaved despite the acidic solution. The ELSL spectrum also does not show any peak representative of aldehyde or a carboxylic acid which corroborate the fact that the lactone was not ring-opening. The acetyl groups (a, b) on the sophorose were not hydrolysed but remained intact. Full assignment of NMR spectroscopy is described in chapter 8 section 8.7 which agree with the literature.³⁰⁸ Some impurities were

observed on the proton and carbon 13 NMR spectra for LSL despite the claim by manufacturer to have 99% purity.

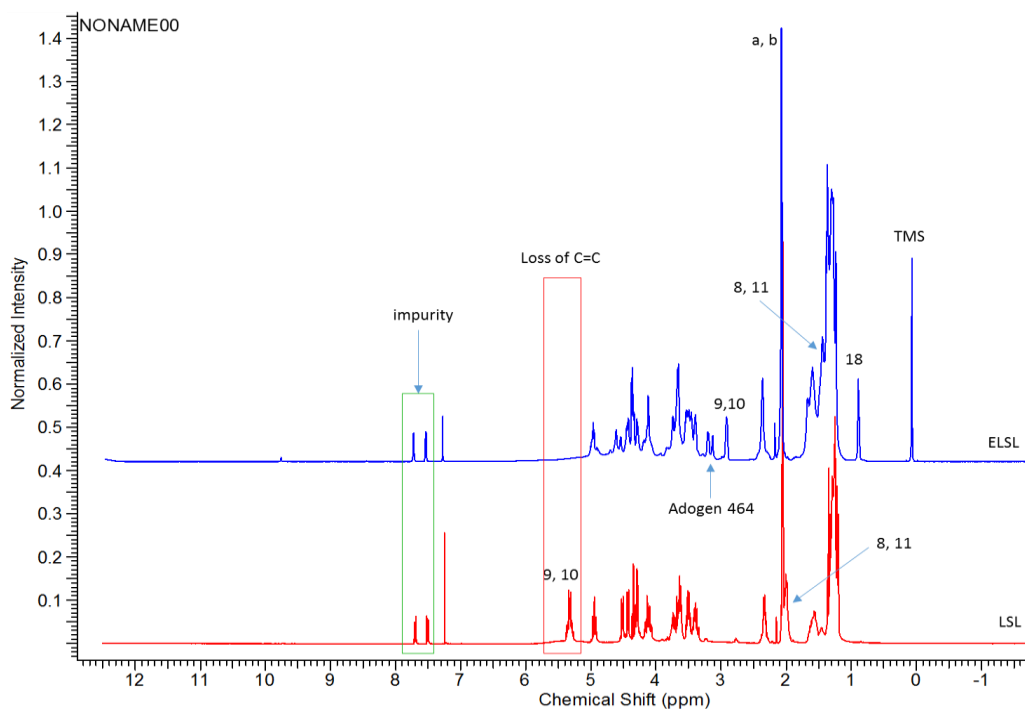


Figure 3- 29 Proton NMR spectra of lactonic sophorolipid (LSL) and epoxidised lactonic sophorolipid (ELSL). AV 700 MHz Bruker spectrometer, CDCl₃ solvent.

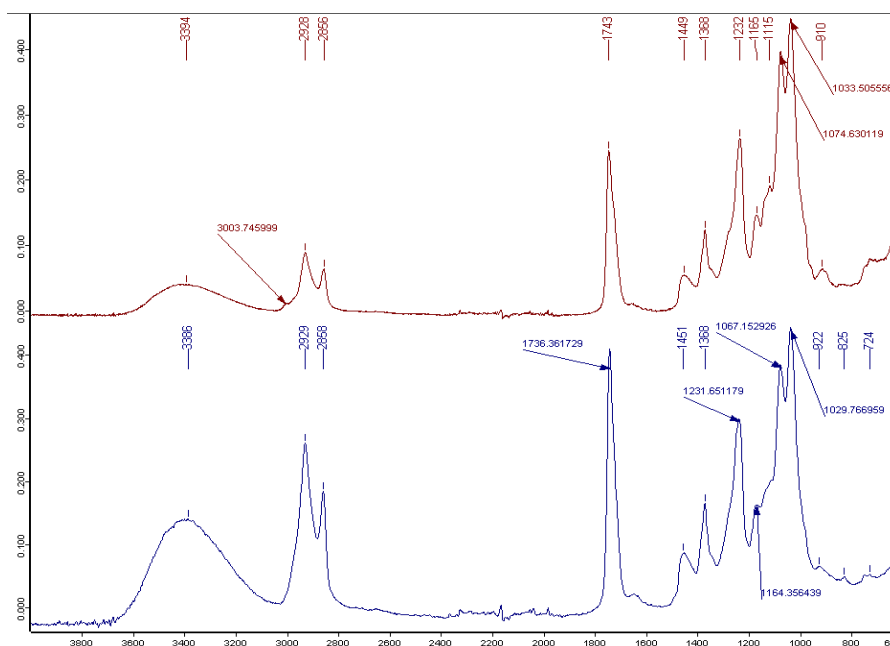


Figure 3- 30 FT-IR spectra of lactonic sophorolipid (top) and epoxidised lactonic sophorolipid (bottom).

IR spectra of both ELSL and LSL are shown in Figure 3-30 with olefinic C-H stretching vibration disappearing at 3003 cm^{-1} and the epoxy symmetric deformation vibration appearing at 825 cm^{-1} . The presence of 1740 cm^{-1} for C=O stretching and 1236 cm^{-1} for C-O stretching vibration corroborate NMR spectroscopy that the acetyl groups are still intact.

CHN analysis recorded %C (56.040 found, 57.940 calc.), %H (7.826 found, 8.010 calc.), %N (0.105 found). The trace nitrogen detected is possibly from residual Adogen 464 used for epoxidation procedure. ESI-MS accurate mass was measured for LSL as 711.3559 (MNa^+ , $\text{C}_{34}\text{H}_{56}\text{NaO}_{14}$) and ELSL as 727.3499 (MNa^+ , 727.3511 calculated for $\text{C}_{34}\text{H}_{56}\text{NaO}_{15}$). Obviously, the difference of 16 between their m/z values confirms the addition of oxygen atom across the double bond of LSL. Residual Adogen 464 was also detected in the ESI spectrum of ELSL as shown in Figure 3-31.

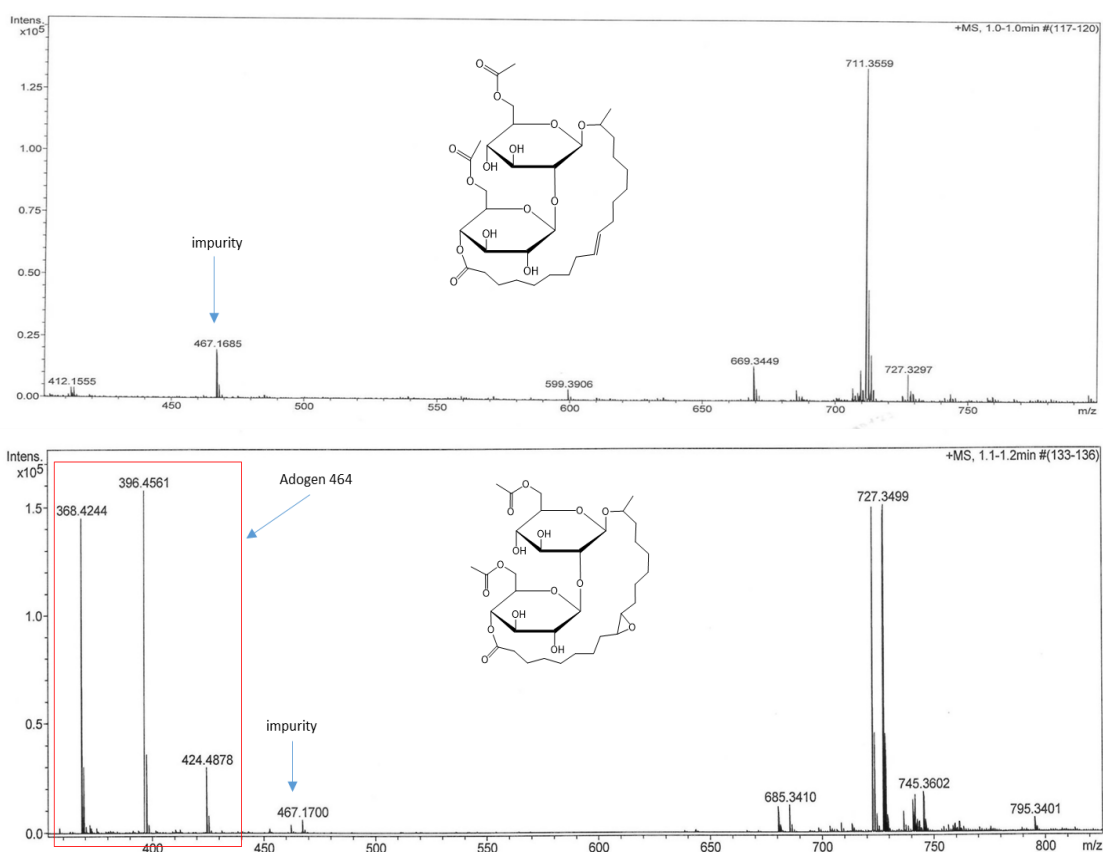


Figure 3- 31 ESI mass spectra of LSL and epoxidised LSL (ELSL)

3.11 Conclusions

Alkyl oleate epoxides *viz* methyl, ethyl, 1-propyl, 2-propyl, 1-butyl, 2-butyl, 1-octyl, 2-octyl and 1-decyl oleate epoxides have been synthesised in good yield (>70%) and large quantities (~20 g each) supported with comprehensive characterisation. It was observed in our study that epoxide yield reduced with increasing moles of oleate used for reaction. Doping a PTA catalysed epoxidation reaction with acetic acid enhanced conversion at short reaction time and the highest yield was observed within 90 minutes of reaction. The clean synthetic methods of heterogeneous catalysis and ultrasound were applied to epoxidation of alkyl oleate. Generally, conversion was slow with the heterogeneous supported PTA even at prolonged reaction time. Side reaction products such as aldehydes, ketones, epoxy acids, diols, were formed in varying concentration and observed in most of the reactions. The concentration of these side products depend on the nature of solvent used and the reaction time. UAE reactions gave high methyl oleate conversion but attended with low selectivity to epoxide due to the formation of side products. With respect to how the side products are formed, it can be concluded that alkyl oleate epoxide was undergoing hydrolysis to form diols which later got oxidised to aldehydes and ketones and corresponding acids as the case may be. A novel lactonic sophorolipid epoxide has been successfully synthesised in good yield and characterised.

Ring-opening of Epoxides with PEGs and Carbohydrates

Chapter 4

4.0 Ring opening of epoxides with PEGs and carbohydrates

4.1 Introduction

Epoxides are very reactive because of their ring strain, thus can be easily modified to make other useful organic chemicals. A ring opening reaction is one of the processes of utilizing the very reactive epoxy ring by a nucleophilic attack to deliver β -substituted alcohols.³⁰⁹⁻³¹⁴ Epoxy fatty acid esters can be ring-opened or modified to produce new materials with useful properties having wide applications.³¹⁵⁻³²¹ With particular interest in home and personal care products, fatty acid esters, which usually act as hydrophobes, are modified with hydrophiles such as alcohols, poly(ethyleneglycol) (PEG), or carbohydrates *via* ethoxylation to generate non-ionic surfactants. In this chapter, epoxidised alkyl oleates synthesised in chapter 3 are ring-opened with PEGs of different chain lengths (Figure 4-1), carbohydrates and other hydrophiles from renewable sources to deliver surfactants. Also discussed in the chapter are novel non-ionic surfactants derived from epoxidised lactonic sophorolipid and epoxidised linseed oil.

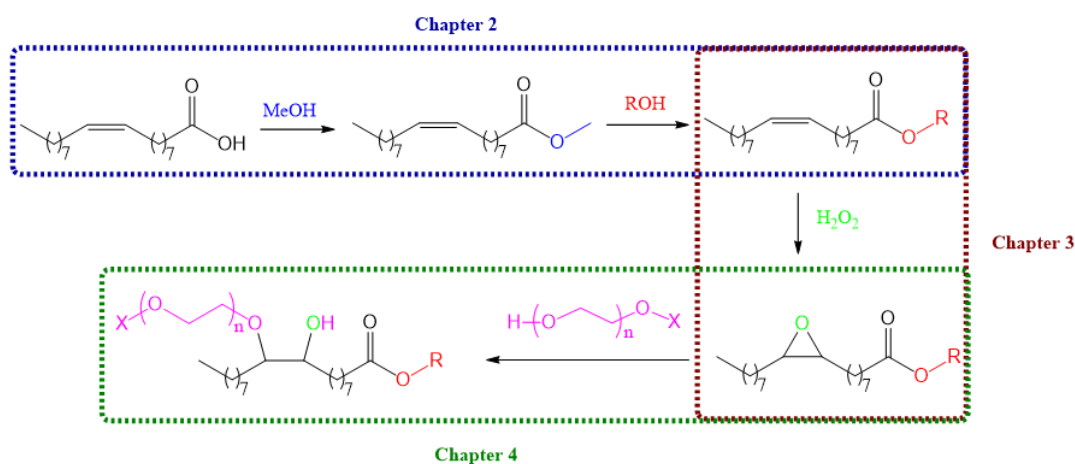


Figure 4- 1 Synthesis of non-ionic surfactants starting from oleic acid

4.2 Ring opening of epoxides

Epoxides can be ring-opened in the presence of an acid or a base. Under an acidic condition involving weak nucleophiles like water and alcohol, the oxygen on the epoxide is first protonated followed by a nucleophilic attack on the most substituted carbon on the epoxide. The attached nucleophile is thereafter deprotonated to give a neutral product with an inverted stereochemistry (Figure 4-2a). Under basic conditions, the nucleophile attacks the least substituted carbon position which causes the epoxy ring to break open. The resulting alkoxide is thereafter protonated by the reaction solvent to deliver a neutral alcohol (Figure 4-2b). In this case also the stereochemistry is inverted.

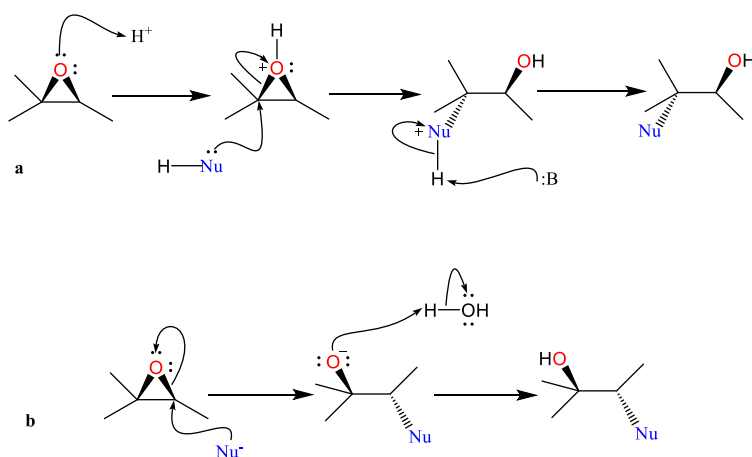


Figure 4- 2 Mechanism of epoxide ring-opening reaction in (a) acidic condition (b) basic condition

It is intended to ring open the synthesised epoxides with monomethylated PEGs, uncapped PEGs, inulin, fructose, D-sorbitol and isosorbide. These are weak nucleophiles and as a result, Lewis acid catalysts were required for these reactions. A wide range of homogeneous and heterogeneous metal and non-metal Lewis acid catalysts were employed: ytterbium (III) triflate, $Yb(TFA)_3$; indium (III) triflate, $In(TFA)_3$; iron (III) triflate, $Fe(TFA)_3$; scandium (III) triflate, $Sc(TFA)_3$; silica-supported boron trifluoride, $Si-BF_3$; boron trifluoride diethyl etherate, BF_3-Et_2O ; sulphuric acid, H_2SO_4 ; iron (III) chloride, $FeCl_3$; iron exchanged montmorillonite clay, Fe-mont; aluminium exchanged montmorillonite clay, Al-mont; and aluminium

exchanged zeolite clay, Al-zeolite. While $\text{BF}_3\text{-Et}_2\text{O}$ has been widely employed for epoxide ring opening reactions,³²²⁻³³⁴ other are less well known for this type of reaction.³³⁵⁻³⁴² The metal-exchanged montmorillonite catalysts were prepared as described in chapter 8 sections 8.3.4 - 8.3.8. All other catalysts were purchased. Initial attempts included screening of these catalysts at different reaction conditions. After several efforts, Si- BF_3 and FeCl_3 emerged the most suitable and selective catalysts under the reaction conditions considered. The only problem with FeCl_3 was that the resulting product was dark brown in colour which might have effect on its end-application in HPC formulations.

4.3 Model reactions

Initial studies on this work by Dr Con R. McElroy (GCCE, University of York, 2012) screened some of the catalysts discussed above for ring-opening epoxidised methyl oleate with 1-butanol under different reaction conditions. In order to accurately characterise resulting surfactants owing to their high molecular masses, model reactions with low molecular weight compounds of same functionalities as PEGs were investigated and products characterised with GC-FID, GC-MS, IR spectroscopy and proton and decoupled NMR spectroscopy. The reactions (only a few discussed) involved ring-opening cyclohexene oxide and methyl oleate epoxide with ethylene glycol, triethylene glycol, poly (ethylene glycol) and 2-methoxy ethanol.

4.3.1 Cyclohexene oxide (CHexO) ring-opened with triethylene glycol (TEG)

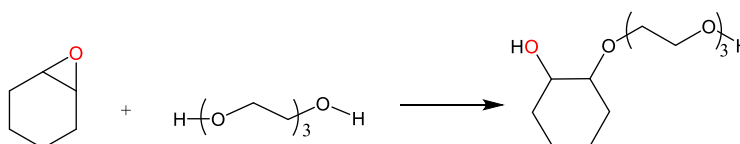


Figure 4- 3 Ring-opening reaction of CHexO with TEG

Reaction between TEG and CHexO (Figure 4-3) was as described in chapter 8 section 8.10.1.1. GC-MS showed evidence of formation of diol, aldehyde and oligomers. This was confirmed by IR and NMR spectra. IR spectrum of the final product (Figure 4-4) showed the disappearance of the epoxy bands at 966 cm^{-1} (a. stretch) and 780 cm^{-1} (s. stretch), reduction in the intensity of hydroxyl band and the presence of C-O-C

ether stretch at 1083 cm^{-1} . The band at 1727 cm^{-1} is due to residual solvent (ethyl acetate). Proton (Figure 4-5), COSY and HSQC NMR spectra of the product in its chair conformation in comparison with those of TEG and CHexO revealed that the four equatorial protons (3, 4, 5, 6 H_{eq}) are now resonating at the same position while their two equivalent axial protons (H_{ax}) are now separated farther.

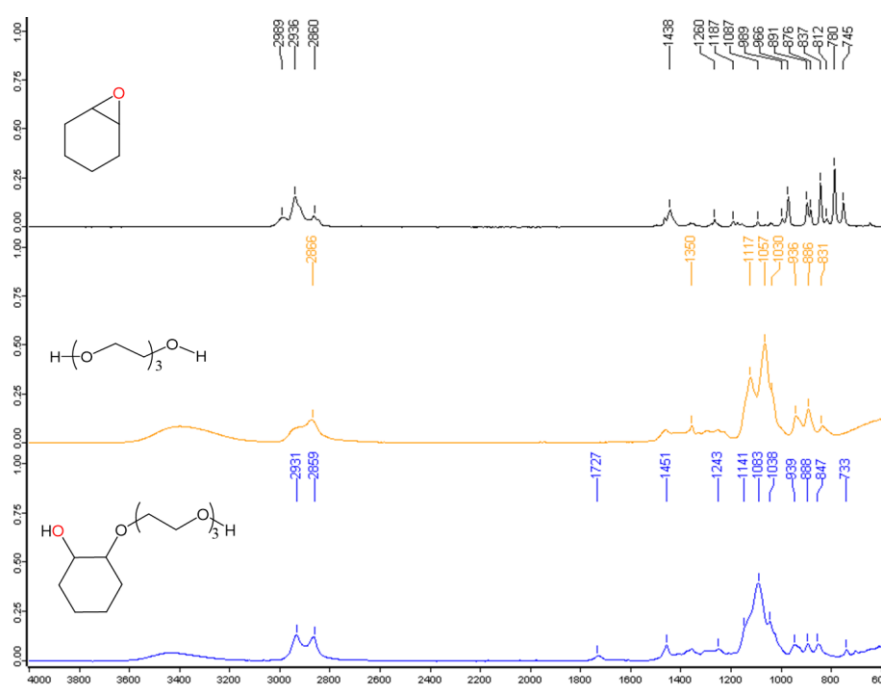


Figure 4- 4 FT-IR spectra of cyclohexene oxide, triethylene glycol and cyclohexene oxide ring-opened with triethylene glycol in the presence of $Yb(TFA)_3$ catalyst

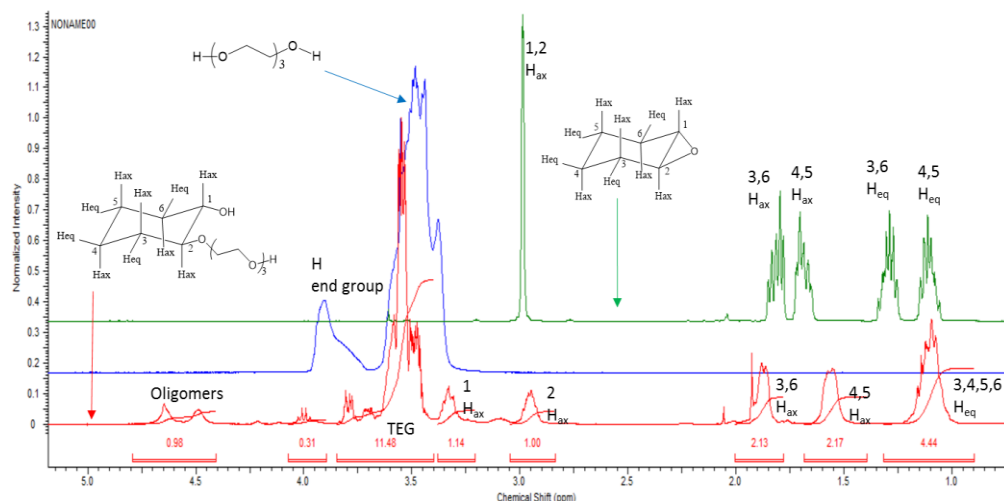


Figure 4- 5 Proton NMR spectra of cyclohexene oxide, triethylene glycol and cyclohexene oxide ring-opened with triethylene glycol in the presence of $Yb(TFA)_3$ catalyst. Reaction condition: 15 mmol TEG, 5 mmol CHexO, 0.5 wt.% catalyst relative to TEG, time=20 hours, temp.=100 °C.

^1H NMR spectra also showed formation of two new peaks at 3.01 ppm and 3.39 ppm. The 3.01 ppm peak with an integration value of 1 occupied the same position as the epoxy protons in CHexO. There were also indications of oligomers and diols being formed. ^{13}C and DEPT NMR spectra (Figure 4-6) however confirmed total conversion of the epoxide as the epoxy carbon at 51.99 ppm in CHexO completely disappeared. Two new peaks, which DEPT showed to be primary or tertiary carbons, were observed at 73.96 ppm and 85.24 ppm and HSQC NMR spectra confirmed them as the hydroxyl carbon (C1) and ether linkage carbon (C2) respectively (Figure 4-6) of the ring-opened epoxide. It was noted that when Si-BF_3 catalyst was used instead of $\text{Yb}(\text{TFA})_3$ oligomers were not observed but diols were present. Full IR and NMR spectroscopy assignment is available in chapter 8 section 8.10.1.1.

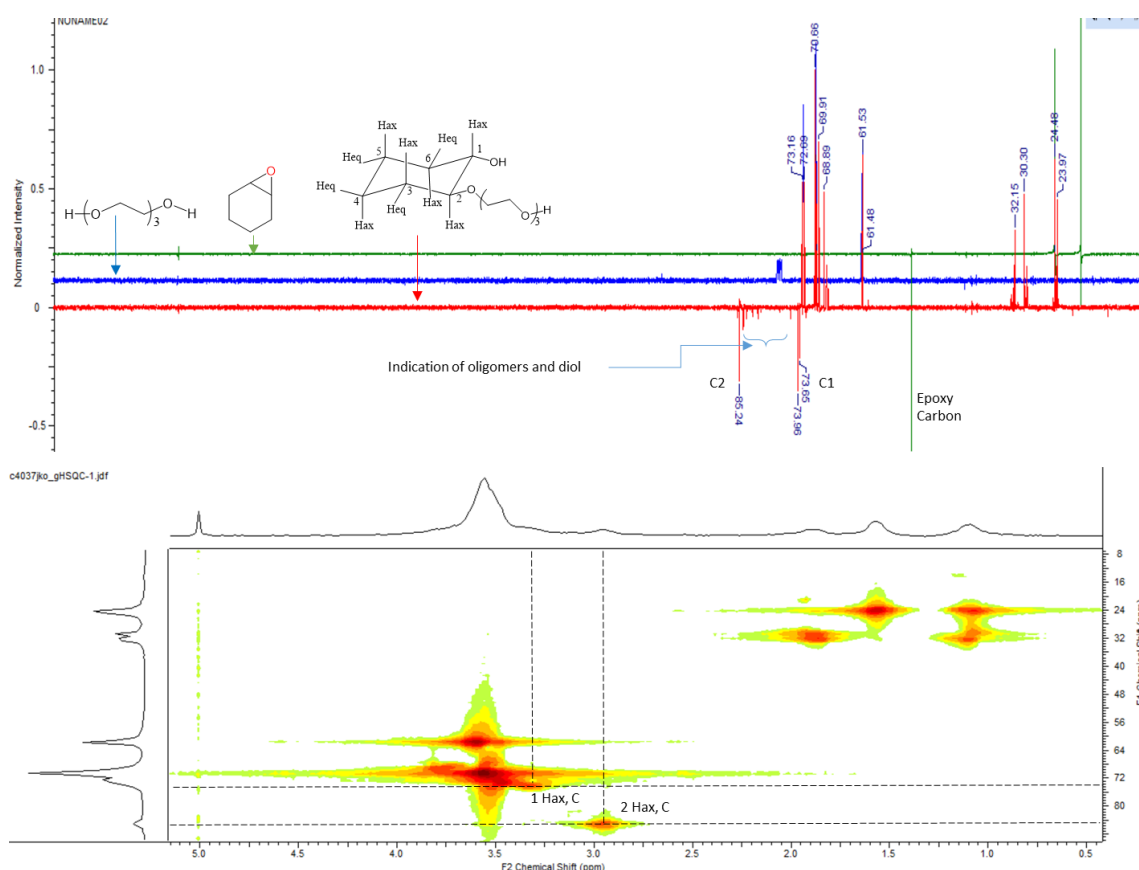


Figure 4- 6 ^{13}C and DEPT NMR spectra (top) of cyclohexene oxide, triethylene glycol and cyclohexene oxide ring-opened with triethylene glycol in the presence of $\text{Yb}(\text{TFA})_3$ catalyst. HSQC NMR spectrum of the product (bottom).

4.3.2 Cyclohexene oxide (CHexO) ring-opened with ethylene glycol (EG)

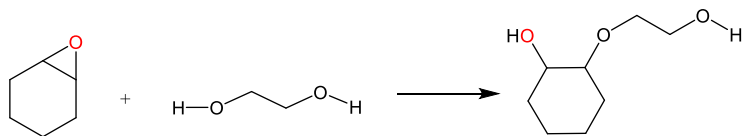


Figure 4- 7 Ring-opening reaction of CHexO with EG

TEG was replaced with a simpler glycol, EG, (Figure 4-7) and synthesis carried out as described in chapter 8 section 8.10.1.2. GC-FID chromatogram (Figure 4-8) showed a 100% conversion of CHexO to yield 77.8% product, 17.8% dimer, 0.6% diol and 2.2% unknown. GC-MS analysis confirmed these compounds as 2-hydroxyethoxy-cyclohexan-2-ol, that is the ring-opened epoxide (molecular mass=160 g/mol), 1, 2-cyclohexadiol (molecular mass=116 g/mol) and dimer of 2-hydroxy ethoxy-cyclohexan-2-ol (molecular mass=258 g/mol). As formation of diol is only possible with an acid in the presence of water, a likely source of water was the solid acid catalyst in a closed reaction vessel. FT-IR spectroscopy (Figure 4-9) confirmed the success of the reaction by the disappearance of the epoxy bands at 966 cm⁻¹ (a. stretch) and 780 cm⁻¹ (s. stretch), reduction in the intensity of hydroxyl band and the presence of C-O-C ether stretch at 1070 and 1036 cm⁻¹.

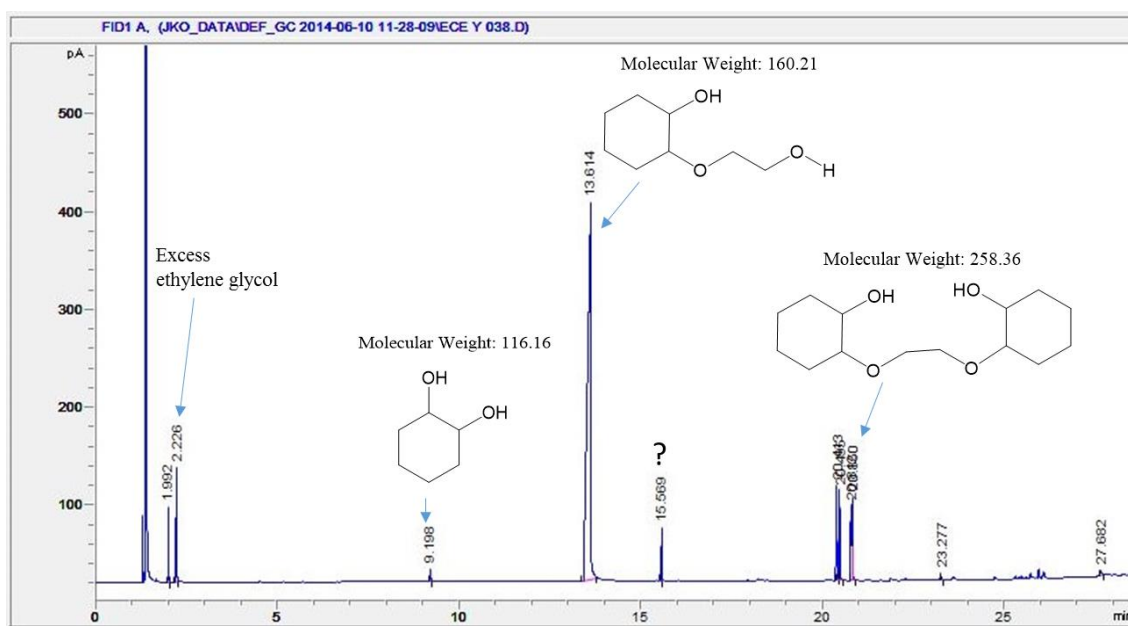


Figure 4- 8 Chromatogram of resulting crude products of cyclohexene oxide ring-opened with ethylene glycol. Reaction condition: 30 mmol EG, 5 mmol CHexO, catalyst=0.5 wt.% relative to EG, time=20 hours, temp.=100 °C, work-up solvent=2-methyl THF.

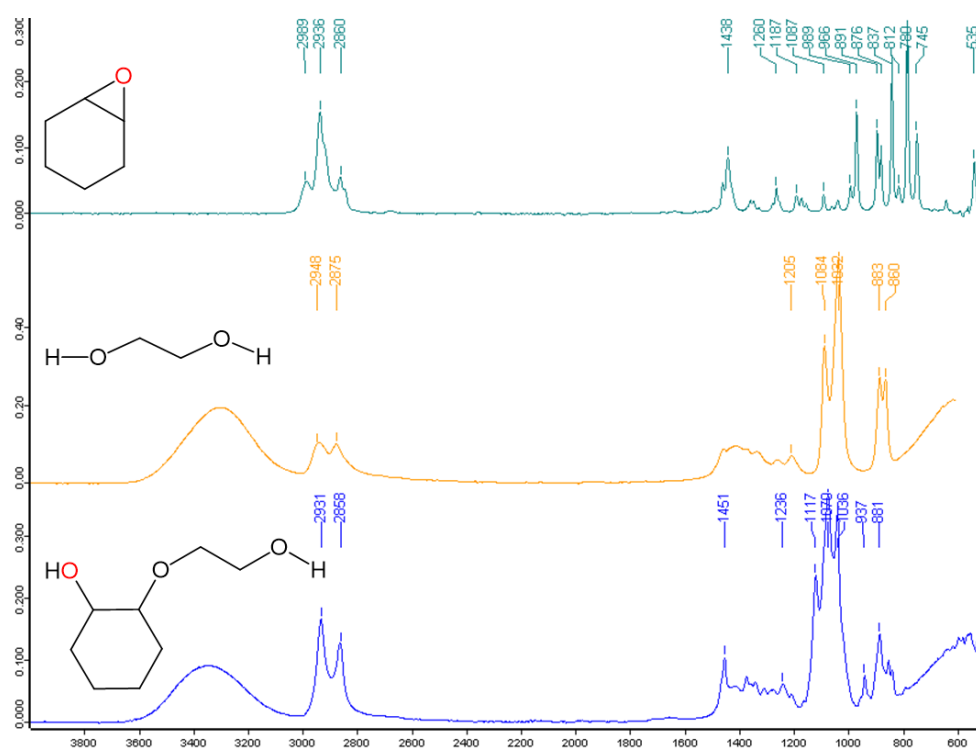


Figure 4- 9 FT-IR spectra of cyclohexene oxide, ethylene glycol and cyclohexene oxide ring-opened with ethylene glycol in the presence of Yb(TFA)₃ catalyst.

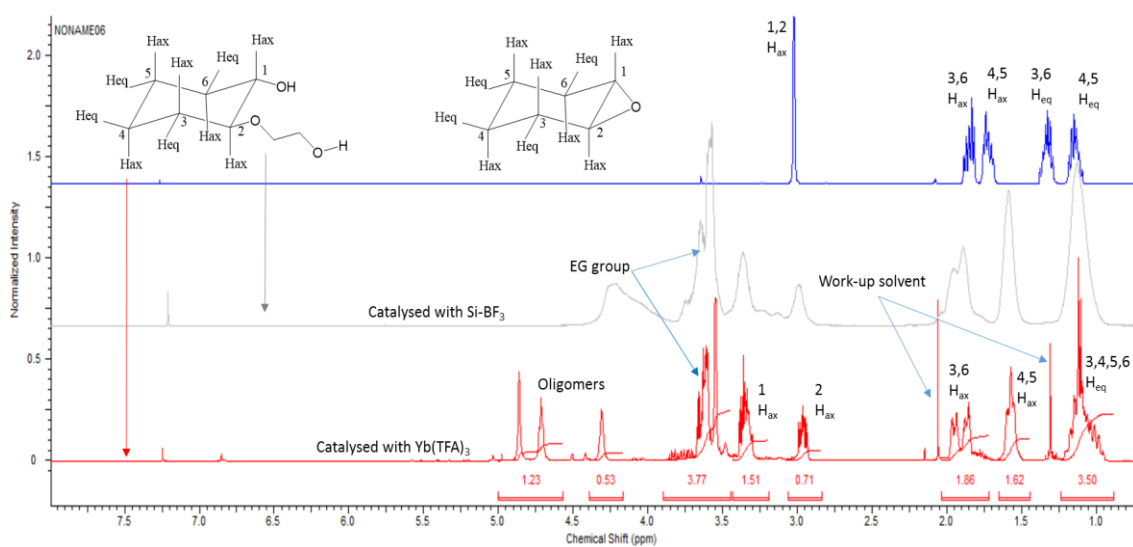


Figure 4- 10 Proton NMR spectra of cyclohexene oxide and cyclohexene oxide ring-opened with ethylene glycol in the presence of Si-BF₃ and Yb(TFA)₃ catalysts.

Proton, COSY and HSQC NMR spectra (Figure 4-10) of a Yb(TFA)₃ catalysed ring-opening reaction showed the four equatorial protons (3, 4, 5, 6 H_{eq}) at 1.17 ppm and their two equivalent axial protons (H_{ax}) at 1.62 ppm and 1.99 ppm, and disappearance of the epoxy protons peak at 2.92 ppm. There now appeared another

two peaks at 3.03 ppm and 3.37 ppm near the position of the disappeared epoxy protons peak which both have an integration value of ~1. There were also additional peaks between 4.31 ppm and 4.86 ppm signalling formation of oligomers. Proton NMR spectrum of product resulting from a silica-supported BF_3 catalysed ring-opening reaction showed a clean baseline downfield after EG peak in which there appeared to be no formation of oligomers. ^{13}C , DEPT and HSQC NMR spectra (Figure 4-11) further showed that CHexO conversion was 100% as the epoxy carbon peak at 51.99 ppm completely disappeared in the crude product spectrum. The carbon to which the hydroxyl group of the ring-opened epoxide was attached was resonating at 73.77 ppm while the carbon, C2, bearing the ether linkage resonated at 84.17 ppm. Full IR and NMR spectroscopy assignment is described in chapter 8 section 8.10.1.2.

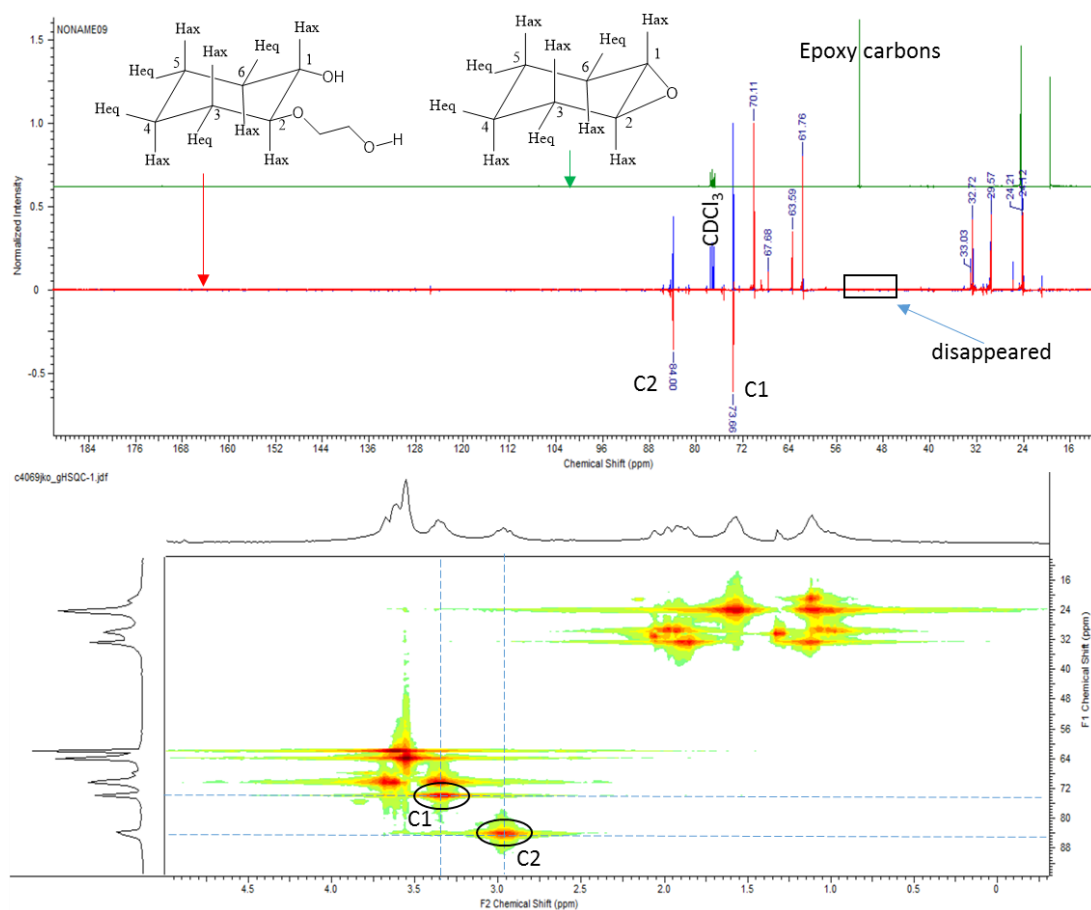


Figure 4- 11 ^{13}C and DEPT NMR spectra (top) of cyclohexene oxide and cyclohexene oxide ring-opened with ethylene glycol in the presence of $\text{Yb}(\text{TFA})_3$ catalyst. HSQC NMR spectrum of the product (below).

4.3.3 Cyclohexene oxide (CHexO) ring-opened with 2-methoxy ethanol (MeEG)

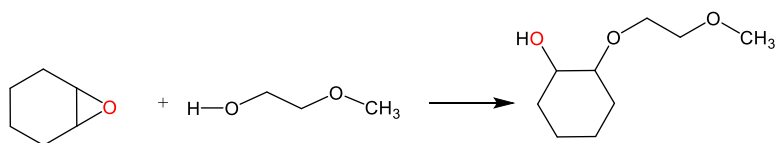


Figure 4- 12 Ring-opening reaction of CHexO with MeEG

In order to reduce or eliminate oligomerisation observed in the above reactions, MeEG was used in place of EG and TEG (Figure 4-12) and synthesis carried out as stated in chapter 8 section 8.10.1.3. GC-FID chromatogram showed a total conversion of CHexO as observed above with EG and TEG. Five major peaks were shown representing formation of 1.1% diol, 33.2% product and 39.6% dimer, 14.2% trimer and ~4.0% tetramer of the product (Figure 4-13). While oligomerisation was anticipated when using EG and TEG, it was not expected to occur significantly with MeEG. In the previous syntheses, the hydroxyl end of EG or TEG on the ring-opened epoxide attacks the epoxide to form oligomers but with MeEG the ring-opened epoxide attacks CHexO with its free hydroxyl group to form oligomers as shown in Figure 4-14.

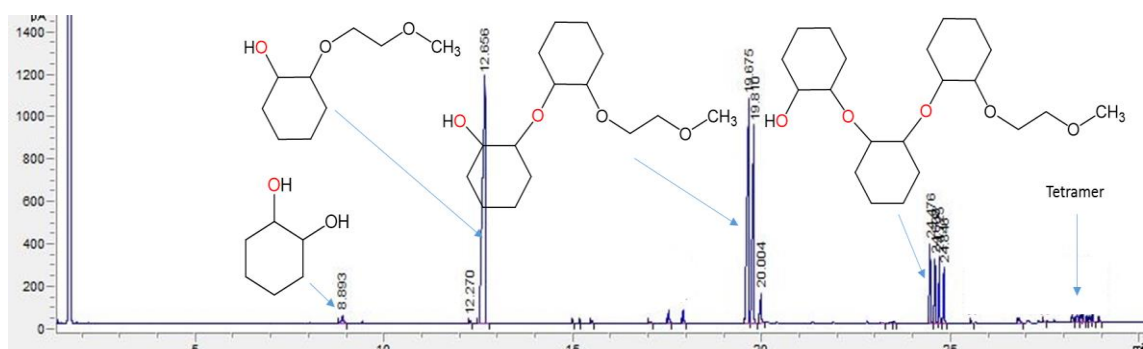


Figure 4- 13 GC-FID chromatogram of crude product from reaction between cyclohexene oxide and 2-methoxy ethanol catalysed by Yb(TFA)₃. Reaction condition: 4 mmol MeEG, 4 mmol CHexO, catalyst=0.5 wt.% relative to MeEG, time=6 hours, temp.=60 °C

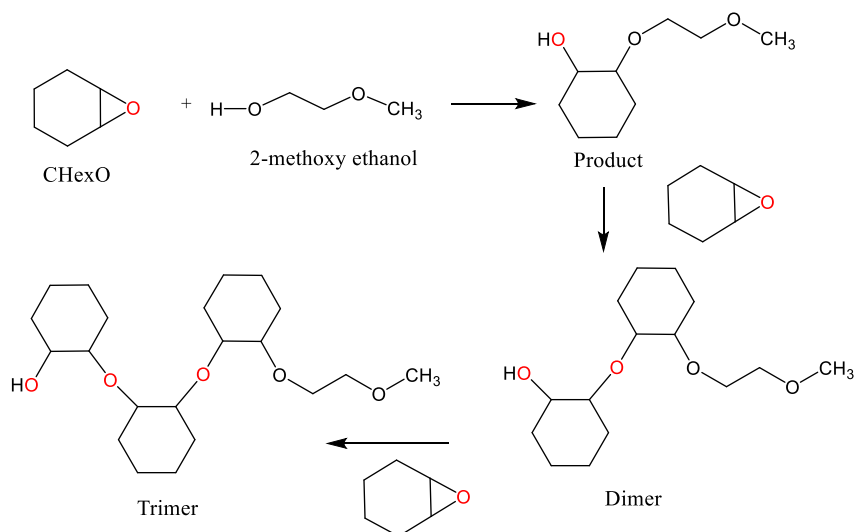


Figure 4- 14 Formation of oligomers during ring opening reaction between cyclohexene oxide and 2-methoxy ethanol catalysed by an acid.

Comparative proton NMR spectra of reactants and product (Figure 4-15) showed the success of the ring-opening reaction. 2 H_{ax} and 1 H_{ax} protons (each having an integration value of ~1) were observed at 2.94 ppm and 3.34 ppm respectively at the chemical shift which are approximate positions being occupied by the methoxy proton on the nucleophilic MeEG and the epoxy proton on CHexO. ¹³C, DEPT and HSQC NMR spectra (Figure 4-16) showed that these new peaks are actually not from the starting materials. As observed with EG and TEG nucleophiles, the hydroxyl α-proton and ether α-proton on the product were around 73.88 ppm and 84.87 ppm respectively. The spectra also confirmed a 100% conversion of CHexO by the total loss of the epoxy proton in the product spectra. There was also a level of oligomerisation observed in both proton spectra when using Yb(TFA)₃ and Si-BF₃ but ¹³C NMR revealed it was more pronounced with the former catalyst. More so, the spectra also showed more peaks between 73 ppm and 86 ppm than were observed in previous syntheses with EG and TEG which confirms GC-FID chromatogram that showed formation of dimers, trimers and tetramers.

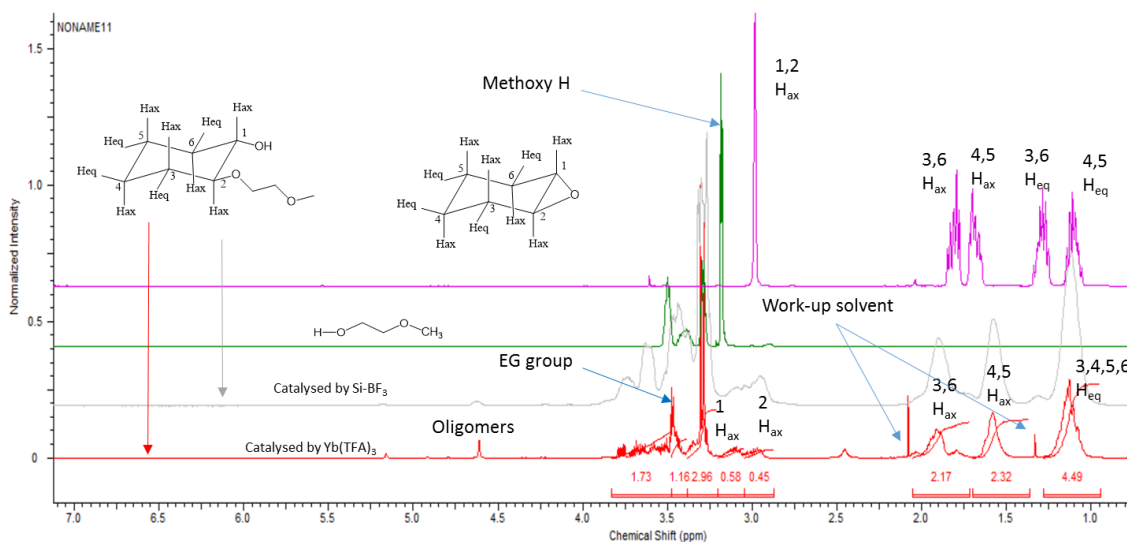


Figure 4- 15 Proton NMR spectra of cyclohexene oxide, 2-methoxy ethanol and ring-opened epoxide catalysed by Si-BF_3 and $\text{Yb}(\text{TFA})_3$.

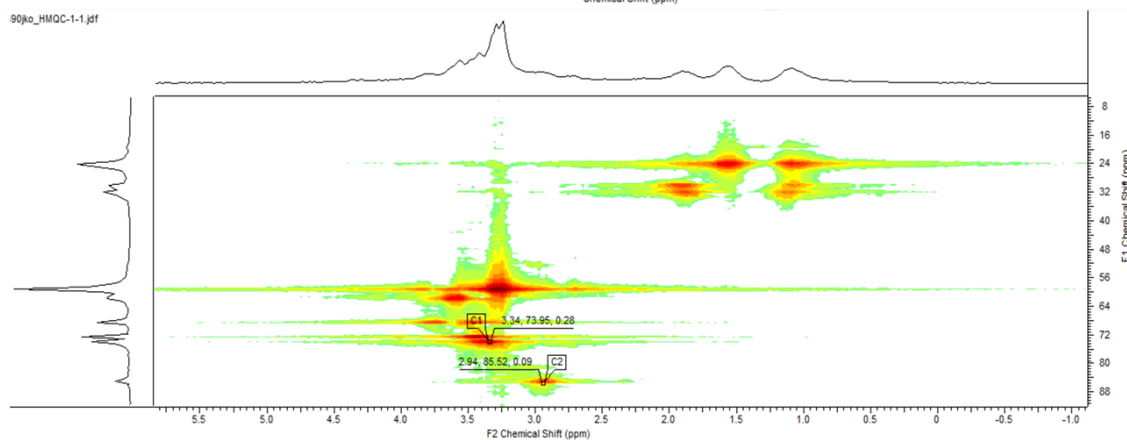
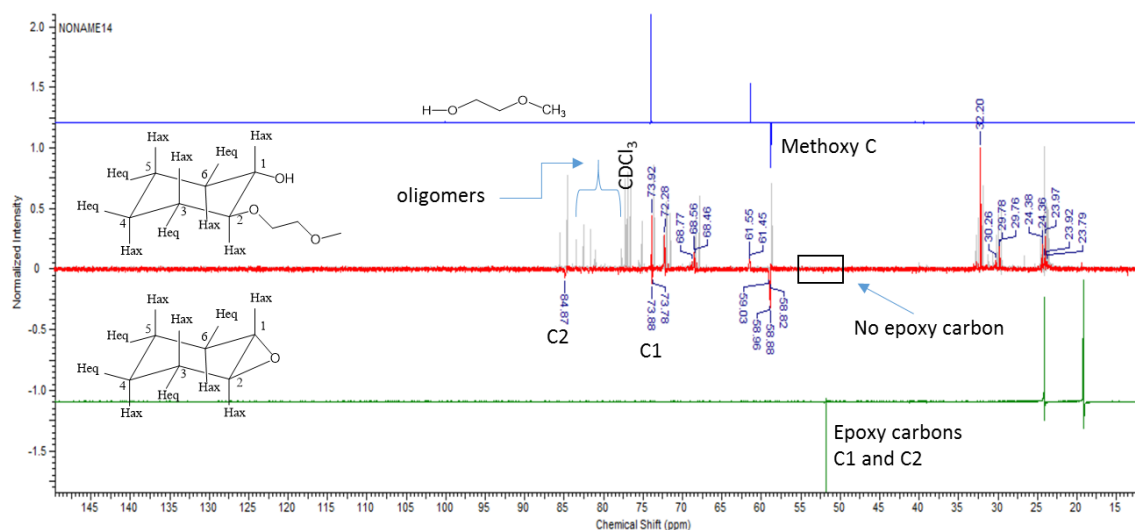


Figure 4- 16 ^{13}C and DEPT NMR spectra (top) of cyclohexene oxide, 2-methoxy ethanol and ring-opened epoxide in the presence of $\text{Yb}(\text{TFA})_3$ catalyst. HSQC NMR spectrum of the product (below).

^1H NMR spectrum showed 2 peaks for 2 H_{ax} and 1 H_{ax} protons both having an integration value of ~ 1 . Other peaks shown are the 3, 6 H_{ax} , 4, 5 H_{ax} , 3, 4, 5, 6 H_{eq} protons similar to what was observed in TEG, EG and MeEG. The PEG protons resonated around 3.5 ppm with an integration value of ~ 29 . Ideally there should be ~ 36 protons present in the repeating chain of PEG400 when $n=9$, so with 29 protons obtained it means the removal method for excess nucleophile was more effective for PEG400 than EG and TEG or that the chain for the PEG sample is smaller on average than specified on the bottle. Additionally, the two carbons of interest C2 and C1 were at 84.44 ppm 73.62 ppm respectively while the PEG carbons resonated at 61.37 ppm, 68.40 ppm, 70.17 ppm, 70.42-70.80 ppm and 72.58-72.62 ppm on the carbon DEPT NMR spectrum (Figure 4-19). HSQC and HMBC NMR spectra were also collected to arrive at these results and full assignment is presented in chapter 8 section 8.10.1.7.

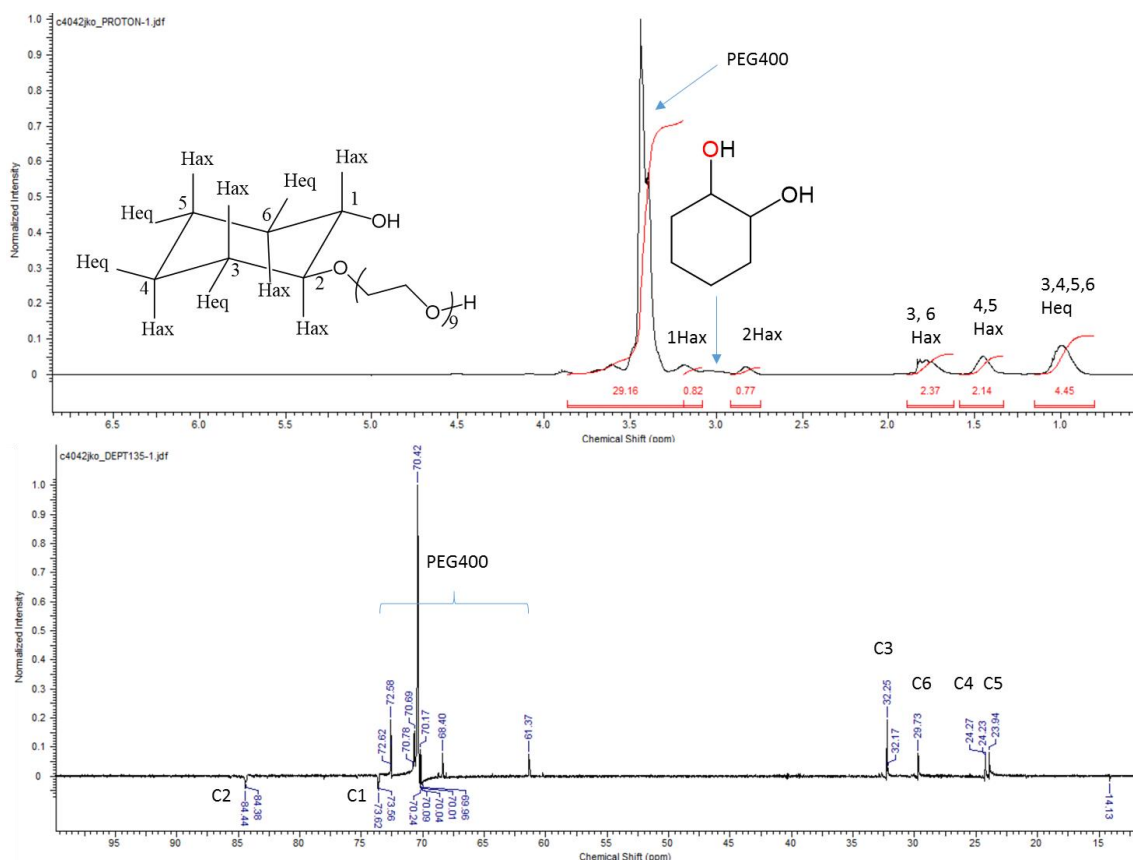


Figure 4- 19 ^1H (top) and carbon DEPT (below) NMR spectra of cyclohexene oxide ring-opened with poly (ethylene) glycol 400 catalysed by $\text{Yb}(\text{TFA})_3$

4.3.5 Methyl oleate epoxide ring-opened with triethylene glycol (TEG)

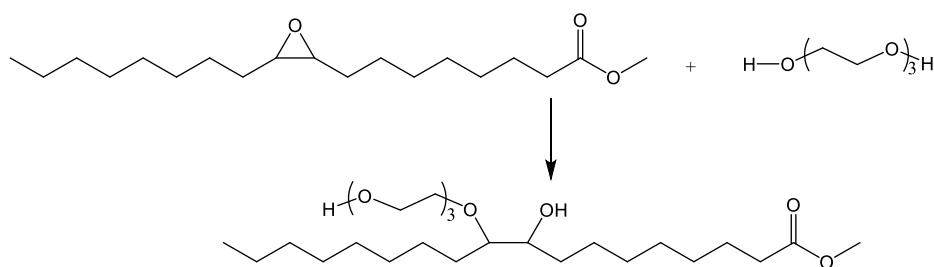


Figure 4- 20 Ring-opening of methyl oleate epoxide with TEG

CHexO was replaced with one of our previously investigated epoxides, epoxidised methyl oleate (EMO), and ring-opened with TEG (Figure 4-20) as stated in the experimental chapter (chapter 8 section 8.10.1.4). From a 100% EMO conversion, ~80% product having a molecular mass of 464 g/mol was obtained. The chromatogram (Figure 4-21) also showed excess TEG, an unknown compound suggested as butylated hydroxyl toluene (BHT) by GC-MS NIST library, saturated fatty esters residual in the epoxide and diol. Interestingly there appeared no trace of oligomers in the chromatogram after 35 minutes. IR spectrum showed bands expected in the product: a strong stretch band for C-O-C ether linkage centred at 1100 cm^{-1} , reduced OH band intensity with the disappearance of the epoxy band (817 cm^{-1} symmetrical stretch) from the epoxide as shown in Figure 4-22.

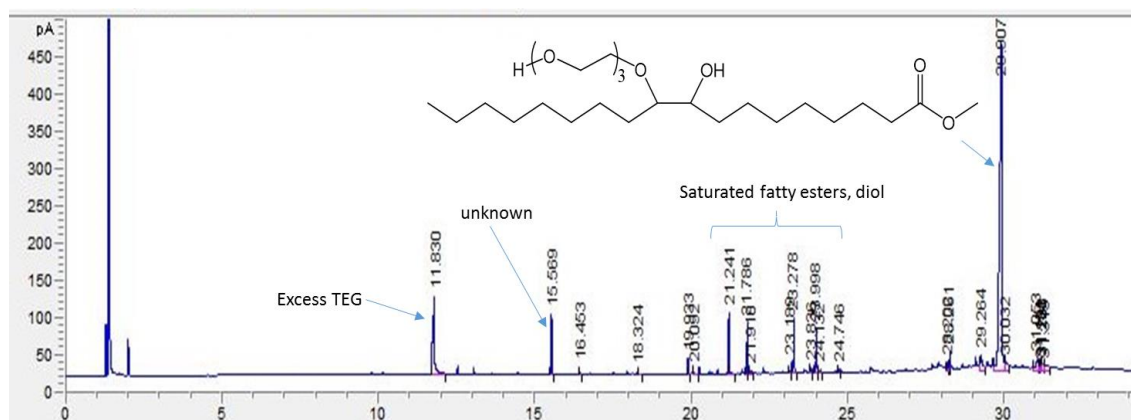


Figure 4- 21 GC-FID chromatogram of ring-opened epoxidised methyl oleate catalysed by $\text{Yb}(\text{TFA})_3$. Reaction condition: 15 mmol TEG, 1 mmol EMO, catalyst=0.5 wt.% relative to TEG, time=20 hours, temp.=100 °C

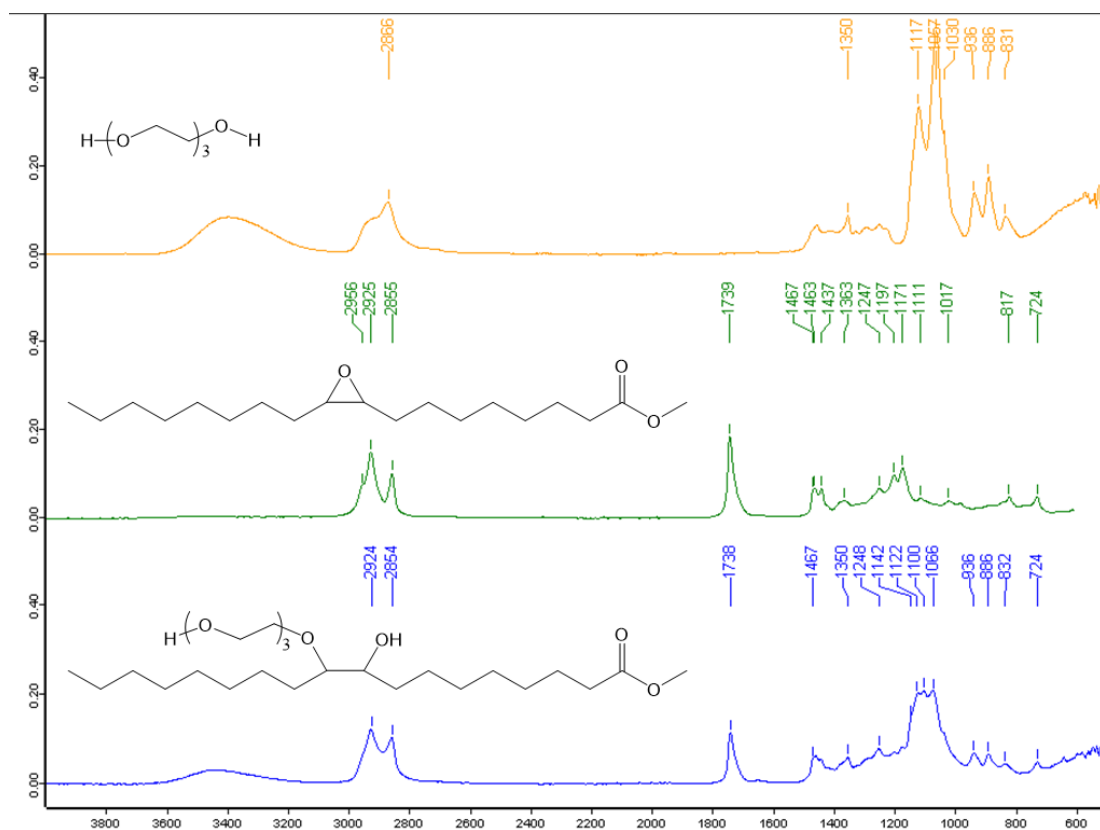


Figure 4- 22 FT-IR spectra of triethylene glycol, epoxidised methyl oleate and ring-opened epoxidised methyl oleate catalysed by $\text{Yb}(\text{TFA})_3$.

^1H NMR spectra of reactants and product (Figure 4-23) showed total conversion of EMO as the peaks **c** and **d** for epoxy protons at 2.74 ppm from the epoxide disappeared in the product spectrum to reappear now as α -protons of the hydroxyl group **d** at 3.42 ppm and ether group **c** at 3.06 ppm of the ring-opened epoxide. Additionally the epoxy ring β -protons **b** lost its distinct position and moved up-field in the product spectrum. All other peaks in the epoxide retained their relative positions on the chemical shift after ring opening. Overlapping peaks **h** and **e** in the product spectrum showed an integration value of $\sim 21\text{H}$. Peak **h**, the epoxide ester methyl protons, is 3 H while peak **e** the TEG chain proton is $\sim 18\text{H}$ instead of 13 H expected. This suggests there is still excess TEG left unremoved. As earlier discovered and stated unreacted TEG and EG were not as effectively removed as PEGs because of decreasing hydrophilicity with decreasing repeating ethoxyl chain.

Carbon DEPT NMR spectra of EMO and product confirmed the total conversion of the epoxide with the loss of epoxy carbons **c** and **d** (57.02 ppm, 57.06 ppm) in the product spectrum (Figure 4-24). The new α -carbons for hydroxyl group **d** (73.91 ppm) and ether group **c** (85.27 ppm) of the ring-opened epoxide were confirmed with support from HSQC and HMBC spectra. The loss or displacement of the β -epoxy carbon peaks **b** on the product spectrum was noted which corroborates the observation from the proton NMR spectra. Full NMR assignment is provided in the experimental chapter 8 section 8.10.1.4.

4.3.6 Methyl oleate epoxide ring-opened with 2-methoxy ethanol (MeEG)

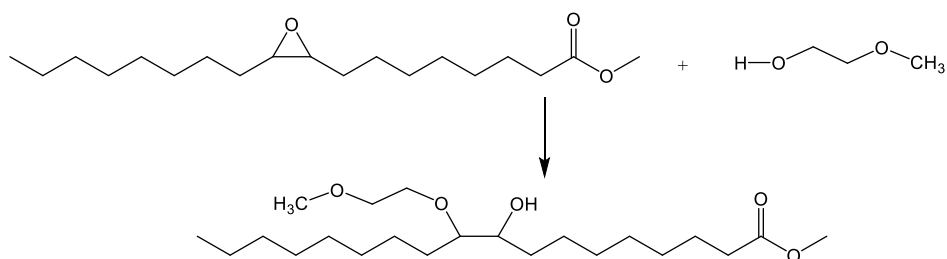


Figure 4- 25 Ring-opening reaction of epoxidised methyl oleate with MeEG

A simpler nucleophile, MeEG, was used instead of TEG to ring-open EMO (Figure 4-25) as described in chapter 8 section 8.10.1.6. Result from GC-FID showed a 100% epoxide conversion with around 78% product yield, 12% diol, 10% compounds eluted after the product (assumed to be oligomers), and then residual saturated fatty ester (Figure 4-26).

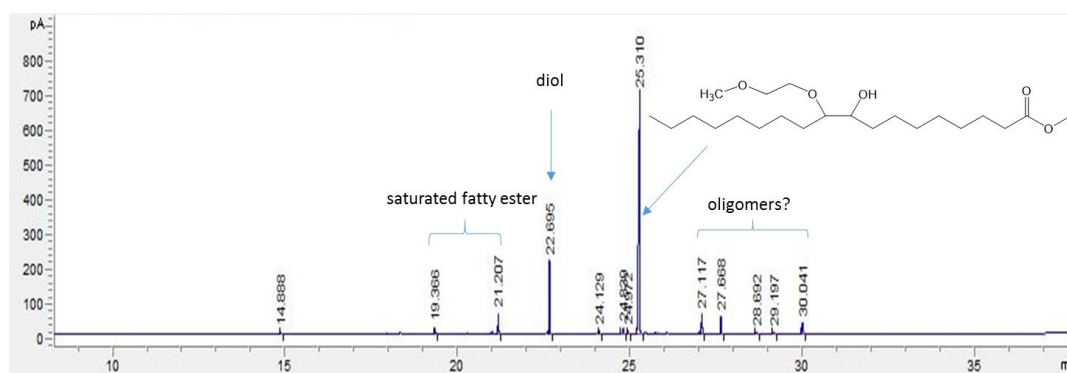


Figure 4- 26 GC-FID chromatogram of ring-opened epoxidised methyl oleate catalysed by $Fe(TFA)_3$. Reaction condition: 4 mmol MeEG, 1 mmol EMO, 0.6 wt.% $Fe(TFA)_3$ relative to MeEG, time=5 hours, temp.=100 °C

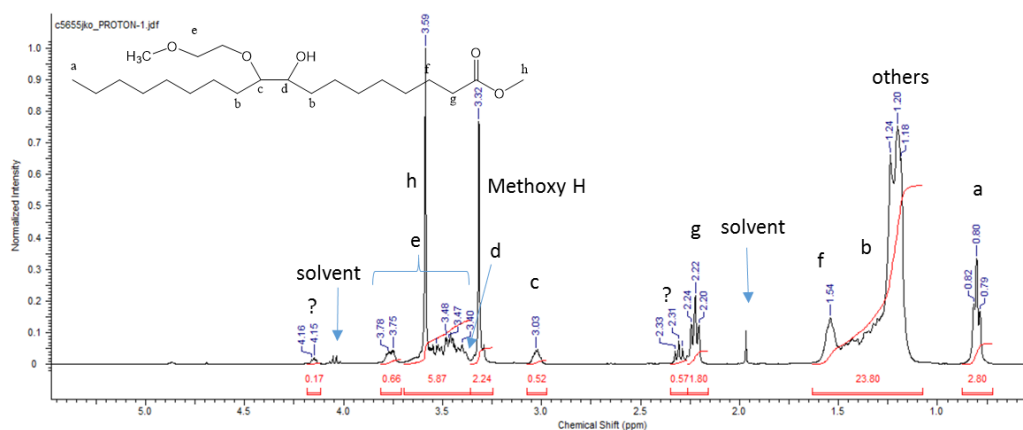


Figure 4- 27 ^1H NMR spectrum of MeEG ring-opened epoxidised methyl oleate

^1H NMR spectrum showed expected diagnostic peaks for the product. The hydroxyl α -proton **d** of the ring-opened epoxide overlapped with the MeEG protons as shown in Figure 4-27. EMO conversion was assumed complete as there was no peak traced to the epoxide in the product spectrum. The disappearance/loss of peaks **b** or their shifting upfield also evidenced the synthesis was successful. Solvents peaks (ethyl acetate) were also noted in the final product despite a prolonged drying on rotary evaporator at 60 °C (atmospheric pressure). There were also 2 unknown peaks observed; one at 2.31 ppm close to **g** and the other at 4.15 ppm. The unknown peaks are not residual fatty acids identified in the GC chromatogram (Figure 4-26) as their α -carbon to the ester group should resonate close enough to be the same as those on the ring-opened epoxide. Although there are two possible positions (9, 10) for both the OH and MeEG groups to alternate on the epoxide as shown in Figure 4-28, this change may not likely cause significant shifts in the position of **g** to give the unknown peak at 2.31 ppm. It was, however, suspected the catalyst could be aiding transesterification of the epoxide ester end with the hydroxyl end of MeEG as shown in Figure 4-29.

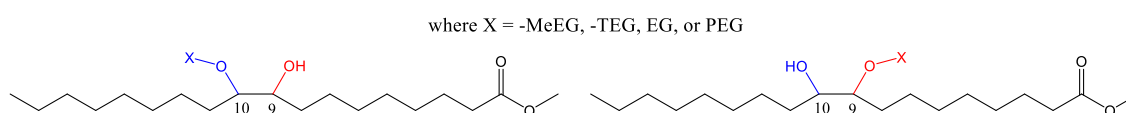


Figure 4- 28 Two possible positions for OH and PEGs on ring-opened methyl oleate epoxide

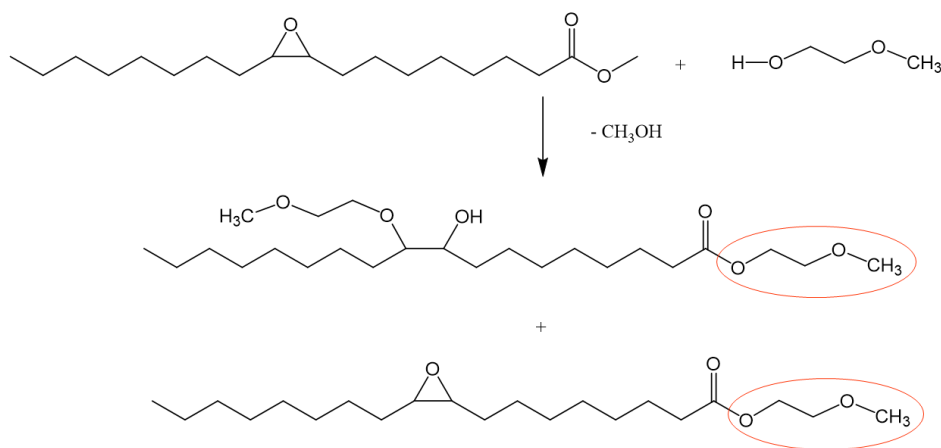


Figure 4- 29 Occurrence of transesterification reaction during ring opening of epoxidised methyl oleate with 2-methoxy ethanol.

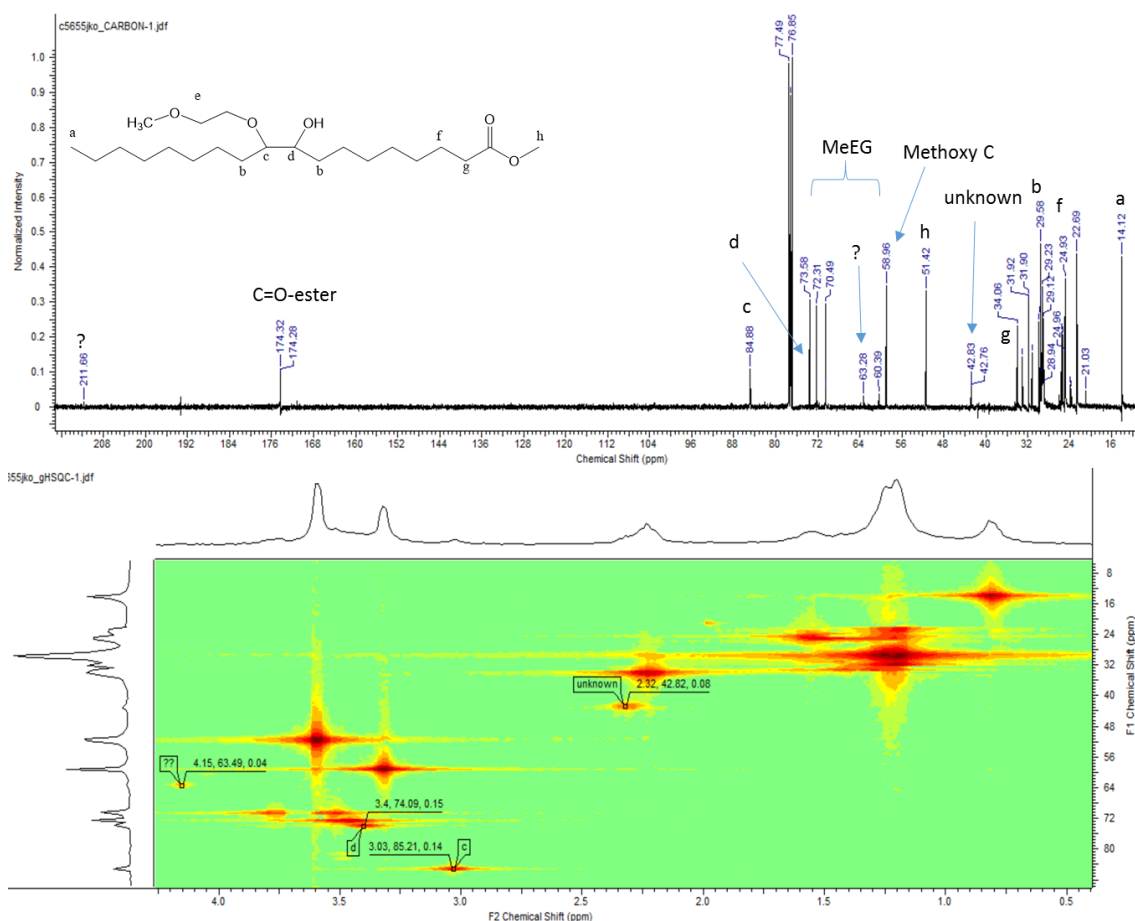


Figure 4- 30 ¹³C (top) and HSQC (below) NMR spectra of epoxidised methyl oleate ring-opened with 2-methoxy ethanol

¹³C NMR spectrum (Figure 4-30 top) showed that the α -carbons to the hydroxyl end and ether end of the ring-opened epoxide are 73.58 ppm and 84.86 ppm respectively. Three unknown peaks 42.83 ppm, 63.28 ppm and 211.66 ppm were

noted in the carbon spectrum. HSQC NMR spectra (Figure 4-30 bottom) was collected to correlate these carbons with protons and the results identified the proton at 2.31 ppm as the 42.83 ppm carbon while the 4.15 ppm signal was correlated to the 63.28 ppm carbon. Heteronuclear multiple bond correlation (HMBC) NMR was collected to correlate how these peaks link with others in the spectrum. The spectrum (Figure 4-31) showed that peaks **f**, **g**, **h** are connected to the ester carbon, peaks **f** and **g** connected to neighbouring carbons two to three bonds away while peak the methoxyl carbon showed correlation with MeEG methylene carbon. The unknown peak is not directly correlated to nuclei in the product but is connected to the carbons resonating at around 29.65 ppm and 211.66 ppm.

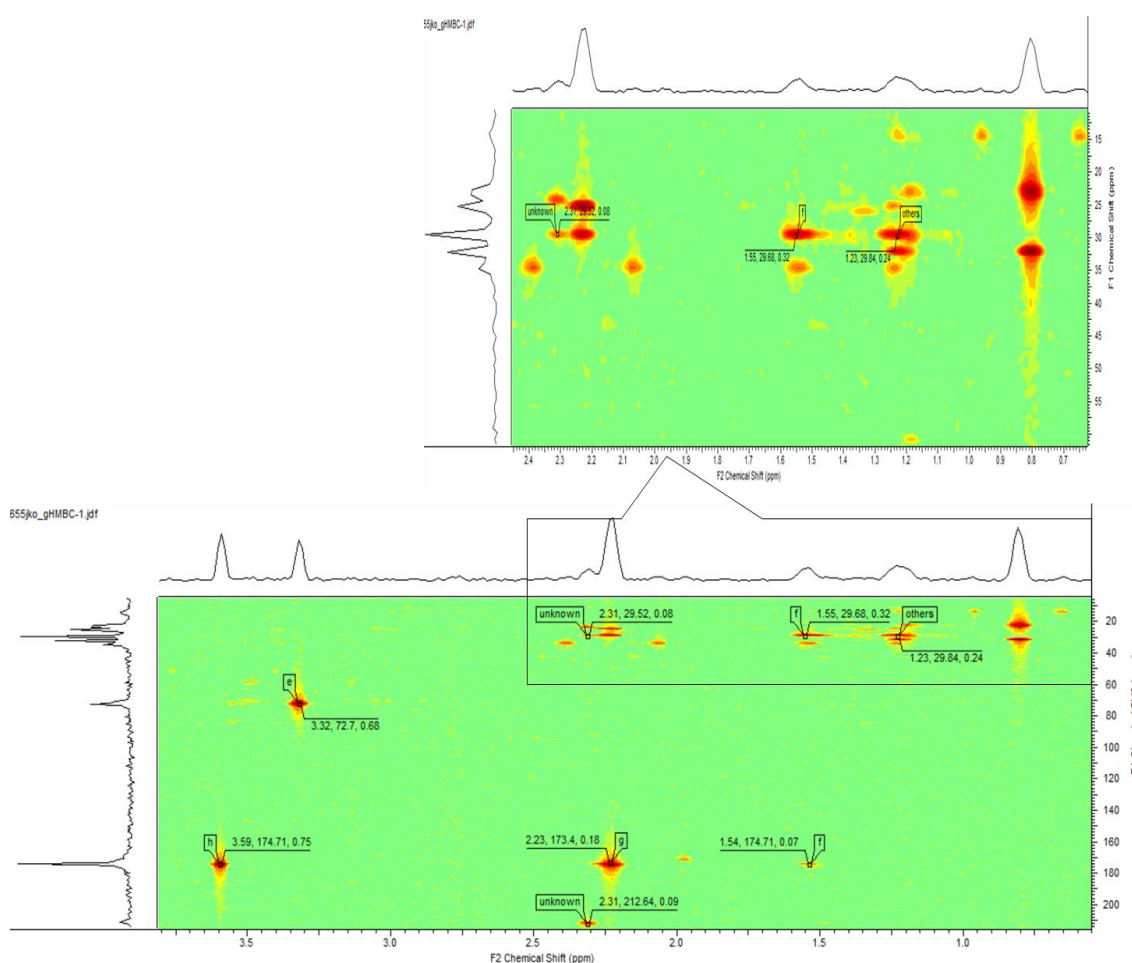


Figure 4- 31 HMBC NMR spectrum of epoxidised methyl oleate ring-opened with 2-methoxy ethanol

The 29.65 ppm carbons are expected to have the resemblance of those of the ring-opened epoxide while the 211.66 ppm is a ketone. As HMBC did not show any correlation between MeEG methylene carbon and the ester carbon at 174 ppm as seen for **f**, **g**, and **h**, it is obvious the epoxide ester methyl end has not been transesterified with MeEG. Interestingly, the GC quantity of saturated fatty acid esters in the resulting surfactant is too low to have become so significant in the NMR spectrum. Additionally, the fatty acid esters are saturated and should be less reactive under the reaction condition in view. Another possibility that could be responsible for these peaks is oligomerisation which was suspected on the GC chromatogram. Unfortunately, formation of oligomers (Figure 4-32) should not have significant effect on the position of **g** on the NMR chemical shift, and if it does peak **f** is expected to shift as well.

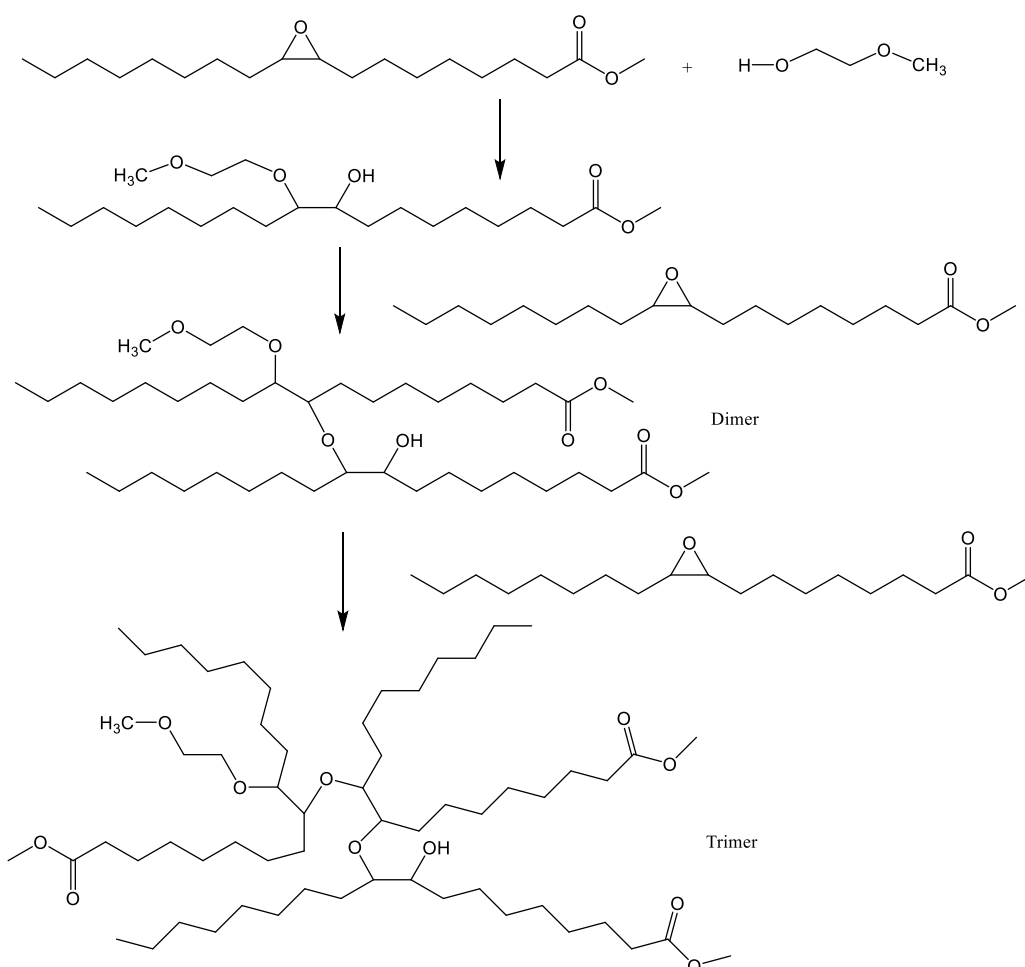


Figure 4- 32 Formation of oligomers during ring opening reaction of epoxidised methyl oleate with 2-methoxy ethanol

IR spectrum showed bands expected in the product as observed in other model reactions. Electrospray ionisation mass spectrometry (ESI-MS) was used to determine accurate mass of the resulting product as MNa^+ : 411.3081 m/z found and 411.3100 m/z calculated for $C_{22}H_{44}NaO_5$.

The formation of additional peak close to **g** discussed above was most pronounced when using In and Fe triflates followed by sulphuric acid and then Yb triflate. Screening results are summarised in Table 4-1 with activity order for triflates as: Yb>Fe>In>Sc. It was observed that $FeCl_3$ is more active than its corresponding triflate catalyst.

Table 4- 1 Effectiveness of different Lewis acids screened for ring opening catalysis

<i>Catalyst</i>	<i>Form</i>	<i>Effectiveness*</i>	<i>Remark</i>
<i>BF₃-Et₂O</i>	Homogeneous	1	Side reaction products, limited reaction temperature, catalyst recovery difficult
<i>Silica-BF₃</i>	Heterogeneous	1	Less side reaction products, catalyst recovery easy, large quantity needed, high temperature possible
<i>H₂SO₄</i>	Homogeneous	2	Formed side reaction products, high temperature possible, catalyst recovery difficult
<i>FeCl₃</i>	Heterogeneous	1	Formed side reaction products, high temperature possible, catalyst recovery difficult, discoloration of product
<i>Yb(TFA)₃</i>	Heterogeneous	1	Formed less side reaction products, high temperature possible, catalyst recovery easy
<i>Fe(TFA)₃</i>	Heterogeneous	2	Formed side reaction products, high temperature possible, catalyst recovery easy
<i>In(TFA)₃</i>	Heterogeneous	2	Formed significant side reaction products, high temperature possible, catalyst recovery easy
<i>Sc(TFA)₃-polymer</i>	Heterogeneous	4	Not effective
<i>Al-mont</i>	Heterogeneous	1	Formed side reaction products, high temperature required, catalyst recovery easy, large amount required
<i>Fe-mont</i>	Heterogeneous	1	Formed side reaction products, high temperature required, catalyst recovery easy, large amount required
<i>Al-zeolite</i>	Heterogeneous	3	Formed side reaction products, high temperature required, catalyst recovery easy, large amount required

* 1=>70% conversion: very effective; 2=50-70% conversion: effective; 3=<50% conversion: less effective;

4=no conversion: ineffective

4.4 Synthesis of oleate-based surfactants

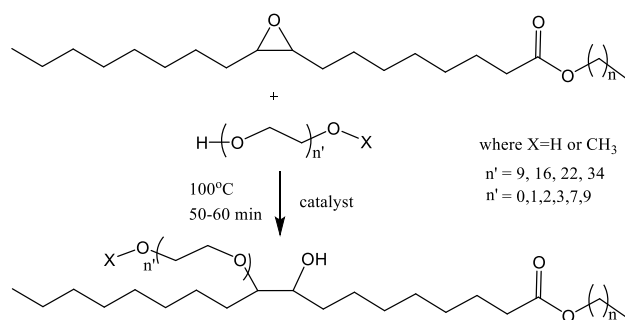


Figure 4- 33 Ring-opening of alkyl oleate epoxides (including branched isomers) with PEGs of varying chain length

Epoxides of methyl, ethyl, 1-propyl, 2-propyl, 1-butyl, 2-butyl, 1-octyl, 2-octyl and 1-decyl oleates were ring-opened with poly (ethylene glycol) 400 (PEG 400), poly (ethylene glycol) 1000 (PEG 1000), poly (ethylene glycol) 1500 (PEG 1500), methoxy poly (ethylene glycol) 400 (MePEG 400) and methoxy poly (ethylene glycol) 750 (MePEG 750) as shown in Figure 4-33. PEGs are interesting petroleum-derived polyether having the general structural backbone $-\text{[CH}_2\text{CH}_2\text{O]}_n-$. They are polymers with molecular weight less than 50, 000 and when higher than this they are classified as poly(ethylene oxides) (PEOs).³⁴⁴ PEGs are soluble in water and a number of organic solvents including toluene, acetone, ethanol and dichloromethane depending on their molecular weight. They are non-toxic, easily retrieved from human body systems and are readily available in various functionalities.³⁴⁵ These properties make them useful materials in home and personal care products, foods, pharmaceuticals, drug delivery, tissue engineering scaffolds among many others.^{344,346} PEGs with molecular weight less than 1,000 are viscous and colourless liquids, while higher molecular weight PEGs are waxy white solids.

The synthesis of the surfactants was typically performed by heating PEGs or MePEGs to 80°C , the catalyst added followed by a dropwise addition of epoxide over 5 to 10 minutes depending on the amount of epoxide added as described in chapter 8 section 8.10.2. Most of the ring opening reactions were catalysed by Si-BF_3 catalyst

and typical reaction time was 50 minutes. Initial attempts involved 1 wt% and 2 wt% amount of Si-BF₃ relative to PEG or MePEG but there was no conversion after 2 hours of reaction, thus 5 wt% Si-BF₃ was used for synthesis. Completion of reaction was usually marked with a change in reaction mixture colour from amber to golden amber or brown. Excess PEG was removed by transferring filtrate (resulting solution from which catalyst has been removed) into a separating funnel and water added and solution shaken to form an emulsion which was broken up with the addition of brine. The organic phase was collected and dried over anhydrous MgSO₄ and product recovered on the rotary evaporator. However, excess MePEG could not be removed as it was discovered that the same amount injected for separation was recovered for all attempts. Therefore, synthesis involving MePEG and other higher PEG chains were subsequently carried out using an equimolar amount of epoxide and PEG. A study by Hedman *et al.*³³² previously reported the use of BF₃-Et₂O catalyst to ring-open epoxidised methyl oleate sourced from tall oil. The epoxide was added dropwise for 30 minutes and the reaction left for a further 30 minutes. Attempts were made to adopt this procedure for our synthesis. However, it was not reproducible even with increased reaction time and catalyst concentration.

4.4.1 Alkyl oleate surfactants based on PEG 400

These non-ionic surfactants made from methyl, ethyl, 1-propyl, 2-propyl, 1-butyl, 2-butyl, 1-octyl, 2-octyl and 1-decyl oleate epoxides were viscous and golden amber like in colour (Figure 4-34 and Table 4-2). Complete recovery of the final product from the flask used on the rotary evaporator was difficult because of increased viscosity. However, with excess PEG removed, about 77% of the product mass was recovered. The average molecular weight of these polymeric surfactants range from 726 g/mol to 852 g/mol.



Figure 4- 34 Alkyl oleate based surfactants from PEG 400

Table 4- 2 Synthesised surfactants based on PEG 400

<i>Entry</i>	<i>Surfactant code</i>	<i>Surfactant description</i>
1	PEMO400	Epoxidised methyl oleate ring-opened with PEG 400
2	PEEO400	Epoxidised ethyl oleate ring-opened with PEG 400
3	PEPO400	Epoxidised 1-propyl oleate ring-opened with PEG 400
4	PE2PO400	Epoxidised 2-propyl oleate ring-opened with PEG 400
5	PEBO400	Epoxidised 1-butyl oleate ring-opened with PEG 400
6	PE2BO400	Epoxidised 2-butyl oleate ring-opened with PEG 400
7	PEOO400	Epoxidised 1-octyl oleate ring-opened with PEG 400
8	PE2OO400	Epoxidised 2-octyl oleate ring-opened with PEG 400
9	PEDO400	Epoxidised 1-decyl oleate ring-opened with PEG 400
10	PEPOFC400	Epoxidised 1-propyl oleate ring-opened with PEG 400 by FeCl ₃

4.4.2 Alkyl oleate surfactants based on MePEG 400

Surfactants made from ring-opening methyl, ethyl, 1-propyl, 2-propyl, 1-butyl, 2-butyl, 1-octyl, 2-octyl and 1-decyl oleate epoxides with MePEG 400 were less viscous and of different shades of amber colour when compared with those of PEG 400 (Figure 4-35 and Table 4-3). Recovery of the product from the flask on the rotary evaporator was less difficult because the MePEG is not as viscous as PEG 400.

Typically, about 97% product mass was recovered and the average molecular weight of these polymeric surfactants range from 739 g/mol to 865 g/mol.



Figure 4- 35 Alkyl oleate based surfactants from MePEG 400

Table 4- 3 Synthesised surfactants based on MePEG 400

Entry	Surfactant code	Surfactant description
1	MPEMO400	Epoxidised methyl oleate ring opened with MePEG 400
2	MPEEO400	Epoxidised ethyl oleate ring opened with MePEG 400
3	MPEPO400	Epoxidised 1-propyl oleate ring opened with MePEG 400
4	MPE2PO400	Epoxidised 2-propyl oleate ring opened with MePEG 400
5	MPEBO400	Epoxidised 1-butyl oleate ring opened with MePEG 400
6	MPE2BO400	Epoxidised 2-butyl oleate ring opened with MePEG 400
7	MPEOO400	Epoxidised 1-octyl oleate ring opened with MePEG 400
8	MPE2OO400	Epoxidised 2-octyl oleate ring opened with MePEG 400
9	MPEDO400	Epoxidised 1-decyl oleate ring opened with MePEG 400

4.4.3 Alkyl oleate surfactants based on MePEG 750

These surfactants are viscous and golden amber in colour (Figure 4-36, Table 4-4). They are gel-like and cannot be transferred into another vial by pouring at room temperature. Complete recovery of the product was difficult because of increased

viscosity after solvent removal. However, over 90% of the product mass was recovered after solvent was removed. The average molecular weight of these polymeric surfactants range from 1049 g/mol to 1175 g/mol.

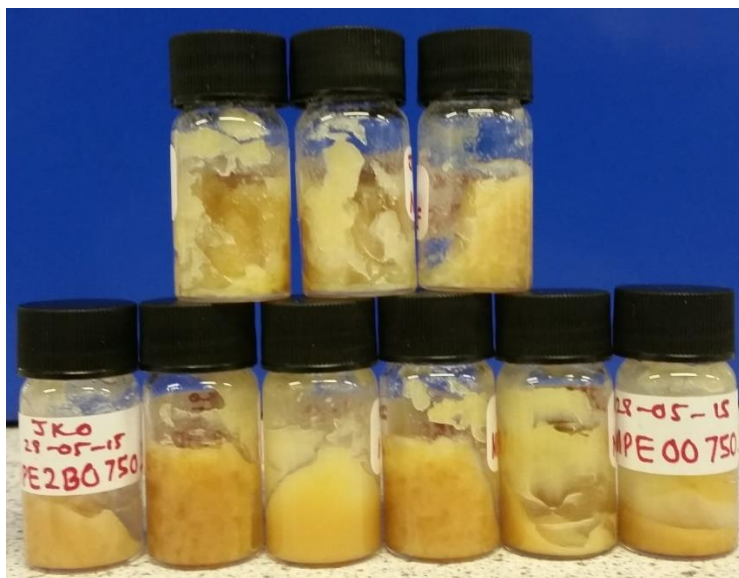


Figure 4- 36 Alkyl oleate based surfactants from MePEG 750

Table 4- 4 Synthesised surfactants based on MePEG 750

<i>Entry</i>	<i>Surfactant code</i>	<i>Surfactant description</i>
1	MPEM0750	Epoxidised methyl oleate ring opened with MePEG 750
2	MPEEO750	Epoxidised ethyl oleate ring opened with MePEG 750
3	MPEPO750	Epoxidised 1-propyl oleate ring opened with MePEG 750
4	MPE2PO750	Epoxidised 2-propyl oleate ring opened with MePEG 750
5	MPEBO750	Epoxidised 1-butyl oleate ring opened with MePEG 750
6	MPE2BO750	Epoxidised 2-butyl oleate ring opened with MePEG 750
7	MPEO0750	Epoxidised 1-octyl oleate ring opened with MePEG 750
8	MPE2O0750	Epoxidised 2-octyl oleate ring opened with MePEG 750
9	MPEDO750	Epoxidised 1-decyl oleate ring opened with MePEG 750

4.4.4 Alkyl oleate surfactants based on PEG 1000

Non-ionic surfactants based on PEG 1000 are very viscous when hot but crystallize into hard-to-cut-through materials at room temperature (Figure 4-37; Table 4-5). It was difficult to recover all the product from evaporating flask because of increased viscosity after removal of work-up solvent but about 95% product mass was recovered for each of the surfactants. The average molecular weight of these polymeric surfactants range from 1298 g/mol to 1424 g/mol.

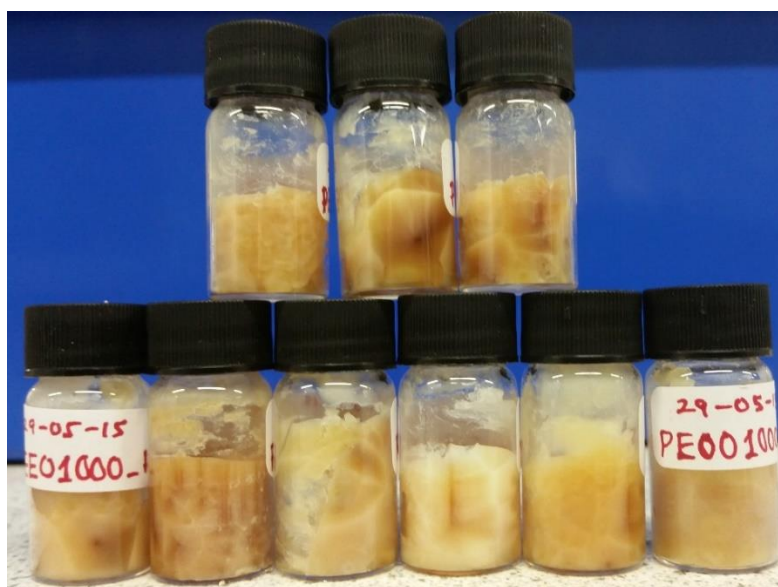


Figure 4- 37 Alkyl oleate based surfactants from PEG 1000

Table 4- 5 Synthesised surfactants based on PEG 1000

<i>Entry</i>	<i>Surfactant code</i>	<i>Surfactant description</i>
1	PEMO1000	Epoxidised methyl oleate ring opened with PEG 1000
2	PEEO1000	Epoxidised ethyl oleate ring opened with PEG 1000
3	PEPO1000	Epoxidised 1-propyl oleate ring opened with PEG 1000
4	PE2PO1000	Epoxidised 2-propyl oleate ring opened with PEG 1000
5	PEBO1000	Epoxidised 1-butyl oleate ring opened with PEG 1000
6	PE2BO1000	Epoxidised 2-butyl oleate ring opened with PEG 1000

Table 4- 5 Synthesised surfactants based on PEG 1000 cont'd

<i>Entry</i>	<i>Surfactant code</i>	<i>Surfactant description</i>
7	PEO01000	Epoxidised 1-octyl oleate ring opened with PEG 1000
8	PE2001000	Epoxidised 2-octyl oleate ring opened with PEG 1000
9	PEDO1000	Epoxidised 1-decyl oleate ring opened with PEG 1000

4.4.5 Alkyl oleate surfactants based on PEG 1500

PEG 1500 from which these non-ionic surfactants were formed was a waxy, flaky white solid. Resulting surfactants are crystalline golden amber hard-to-cut-through materials at room temperature (Figure 4-38 and Table 4-6). As expected they are harder than those from PEG 1000 and product mass recovery was about 93%. The average molecular weight of these polymeric surfactants range from 1826 g/mol to 1952 g/mol.



Figure 4- 38 Alkyl oleate based surfactants from PEG 1500

Table 4- 6 Synthesised surfactants based on PEG 1500

<i>Entry</i>	<i>Surfactant code</i>	<i>Surfactant description</i>
1	PEMO1500	Epoxidised methyl oleate ring opened with PEG 1500
2	PEEO1500	Epoxidised ethyl oleate ring opened with PEG 1500
3	PEPO1500	Epoxidised 1-propyl oleate ring opened with PEG 1500
4	PE2PO1500	Epoxidised 2-propyl oleate ring opened with PEG 1500
5	PEBO1500	Epoxidised 1-butyl oleate ring opened with PEG 1500
6	PE2BO1500	Epoxidised 2-butyl oleate ring opened with PEG 1500
7	PEOO1500	Epoxidised 1-octyl oleate ring opened with PEG 1500
8	PE2OO1500	Epoxidised 2-octyl oleate ring opened with PEG 1000
9	PEDO1500	Epoxidised 1-decyl oleate ring opened with PEG 1500

4.5 Epoxide ring opening with other heterogeneous catalysts

As earlier mentioned the use of heterogeneous catalysts is at the heart of green chemistry because of the many advantages they offer. Silica-supported boron trifluoride despite its high selectivity is a toxic catalyst although assumed less toxic than its non-supported form. Efforts were made to improve on the effectiveness of other heterogeneous catalysts especially the metal-exchanged montmorillonite clay catalysts. The triflates were not considered because ytterbium is a rare earth metal, toxic, expensive and catalysis takes a long time of reaction while $\text{Fe}(\text{TFA})_3$ is not very selective toward the product although takes less reaction time. FeCl_3 catalyst proved very effective but gave a dark brown coloration to the surfactants (Figure 4-39). With the application of these surfactants in view, the catalyst may therefore not be a good choice.

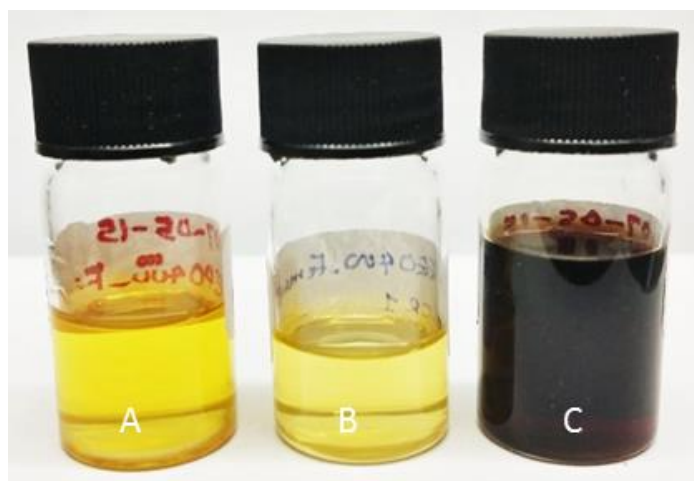


Figure 4- 3961 Alkyl oleate-based surfactants synthesised via Si-BF_3 catalysis (A), Fe-mont catalysis (B) and FeCl_3 catalysis (C)

Four metal-exchanged montmorillonite (mont) clay catalysts: aluminium (III) exchanged mont.; iron (III) exchanged mont from FeCl_3 , designated as Fe-mont (Cl^-); iron (III) exchanged mont. from $\text{Fe}(\text{NO}_3)_3$, designated as Fe-mont (NO_3^-) and iron (III) exchanged K30-mont were prepared as described in chapter 8 sections 8.3.4-8.3.7. Mont catalysts from both sources of Fe^{3+} have been prepared to see what difference it makes in their catalysis. Different catalyst concentrations were initially applied but 20 wt% catalyst concentration gave the best conversion in 2 hours. Interestingly, 20 wt% each of Al-mont, Fe-mont (NO_3^-) and Fe-mont (Cl^-) catalysts relative to PEG was found as effective as 5 wt% Si-BF_3 catalyst in 2 hours of reaction. However, Fe-K30-mont was not effective at these conditions as a large portion of the epoxide was converted to diol. Exchanging Fe in FeCl_3 into montmorillonite clay will avert the need for bleaching of resulting surfactants that might be required if used for synthesis. Metal-exchanged mont catalyst generates surfactants with a pale amber colour (Figure 4-39) which will easily blend with most cosmetic formulations.

4.6 Characterisation of synthesised surfactants

Synthesised surfactants from alkyl oleate epoxides could not be quantitatively characterised on the GC because of their high molecular weight and non-volatile nature. Interestingly, model reactions of methyl oleate epoxide with TEG and PEG

400 using Si-BF₃ catalyst already gave a minimum yield of 75% for surfactants. Nonetheless, they were characterised with 1D and 2D NMR spectroscopy, FT-IR spectroscopy, differential scanning calorimetry (DSC), supercritical fluid chromatography (SFC), ESI mass spectrometry, CHN elemental analysis and inductively coupled plasma mass spectrometry (ICP-MS). In order to avoid structural complexity associated with higher alkyl oleate-PEG based surfactants, methyl oleate-PEG 400 surfactant was used as an example for most of the characterisations discussed below.

4.6.1 NMR spectroscopy

¹H, HSQC, DEPT-135 and HMBC NMR spectra of model reactions (especially those involving EMO and TEG, EMO and MeEG, CHexO and PEG) helped in identifying corresponding chemical shift values of α -protons and carbons to which the hydroxyl end and PEG ether group end of the ring-opened epoxide were attached. The same NMR positions were obtained in the syntheses of the remaining PEGylated surfactants. Using methyl oleate epoxide as an example, ring opening was accompanied by disappearance and/or displacement of the epoxy β -protons **b** at 1.34 ppm and epoxy protons and carbons at 2.74 ppm and 57.02-57.06 ppm, and the appearance α -proton **d** (3.27 ppm) and carbon **d** (73.17 ppm) attached to the hydroxyl end, and another α -proton **c** (2.89 ppm) and carbon **c** (84.37 ppm) attached to the PEG or MePEG ether end group (Figure 4-40). Apart from the diagnostic peaks, all other peaks remained intact in or very near their prior chemical shift relative to the epoxide after ring opening. In some cases, the peak of the α -proton to which hydroxyl end of the ring-opened epoxide is attached overlapped with the peaks of PEG or MePEG methylene chain group but are conspicuously identified in the carbon DEPT-135 spectrum.

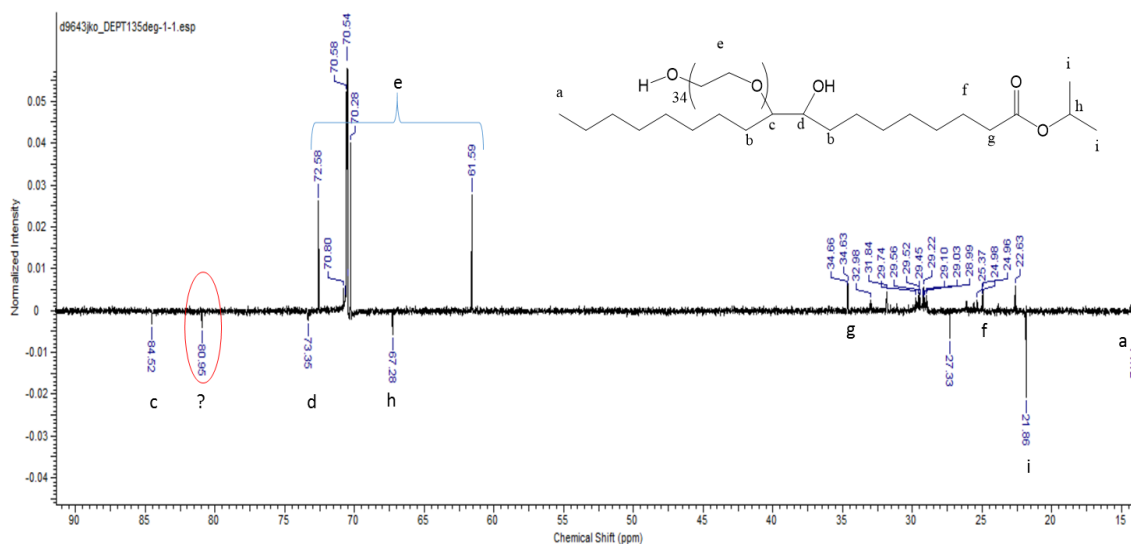


Figure 4- 41 Carbon DEPT-135 NMR spectrum of epoxidised 2-propyl oleate ring-opened with PEG 1500

Suspected side reactions are oligomerisation and transesterification of the ester end of the epoxide with the PEG. As earlier stated oligomerisation side reaction is less likely to occur under conditions involving large alkyl oleate epoxide molecules and PEG 1000 or 1500. It is envisaged that resulting polymers are too bulky (steric hindrance) to favour such a side reaction as shown in Figure 4-42. HMBC NMR spectrum of the resulting surfactant, similar to what is shown in Figure 4-40, did not correlate the PEG carbon chains **e** to either the ester carbonyl carbon at 174 ppm or **f** and **g** carbon peaks. In the presence of an acid the electrophilic carbon on the epoxide could be attacked by the nucleophilic PEG 1500 to eject 2-propanol from the epoxide as shown in Figure 4-43. Obviously the unknown peak is not due to transesterification of the ester end of the epoxide. As discovered in the model reactions, the peak could be due to diols formed during the ring-opening reaction. Full NMR assignments for all surfactants synthesised are provided in the experimental chapter 8 section 8.10.2.

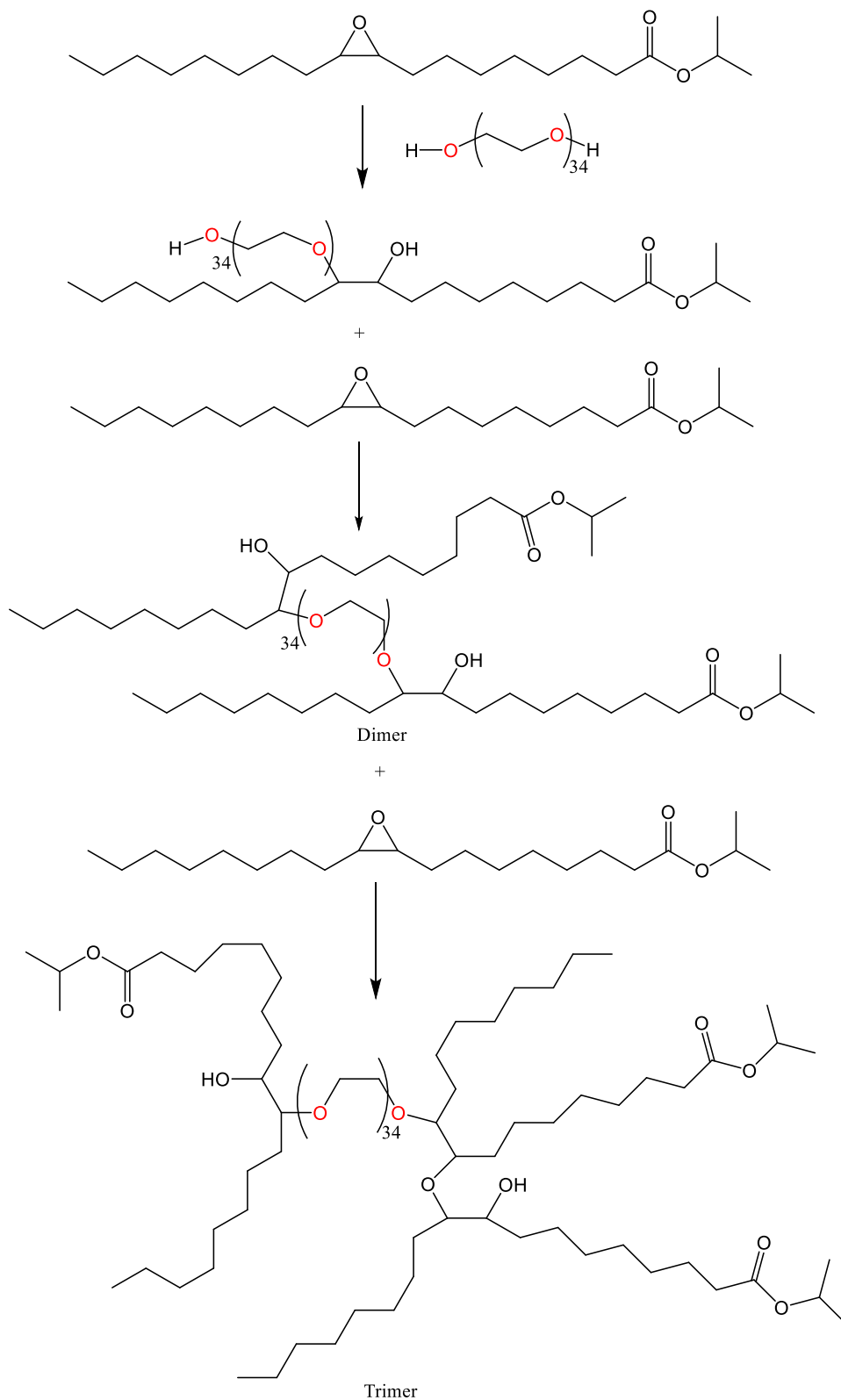


Figure 4- 42 Oligomerisation occurrence during ring opening reaction of epoxidised 2-propyl oleate with PEG 1500.

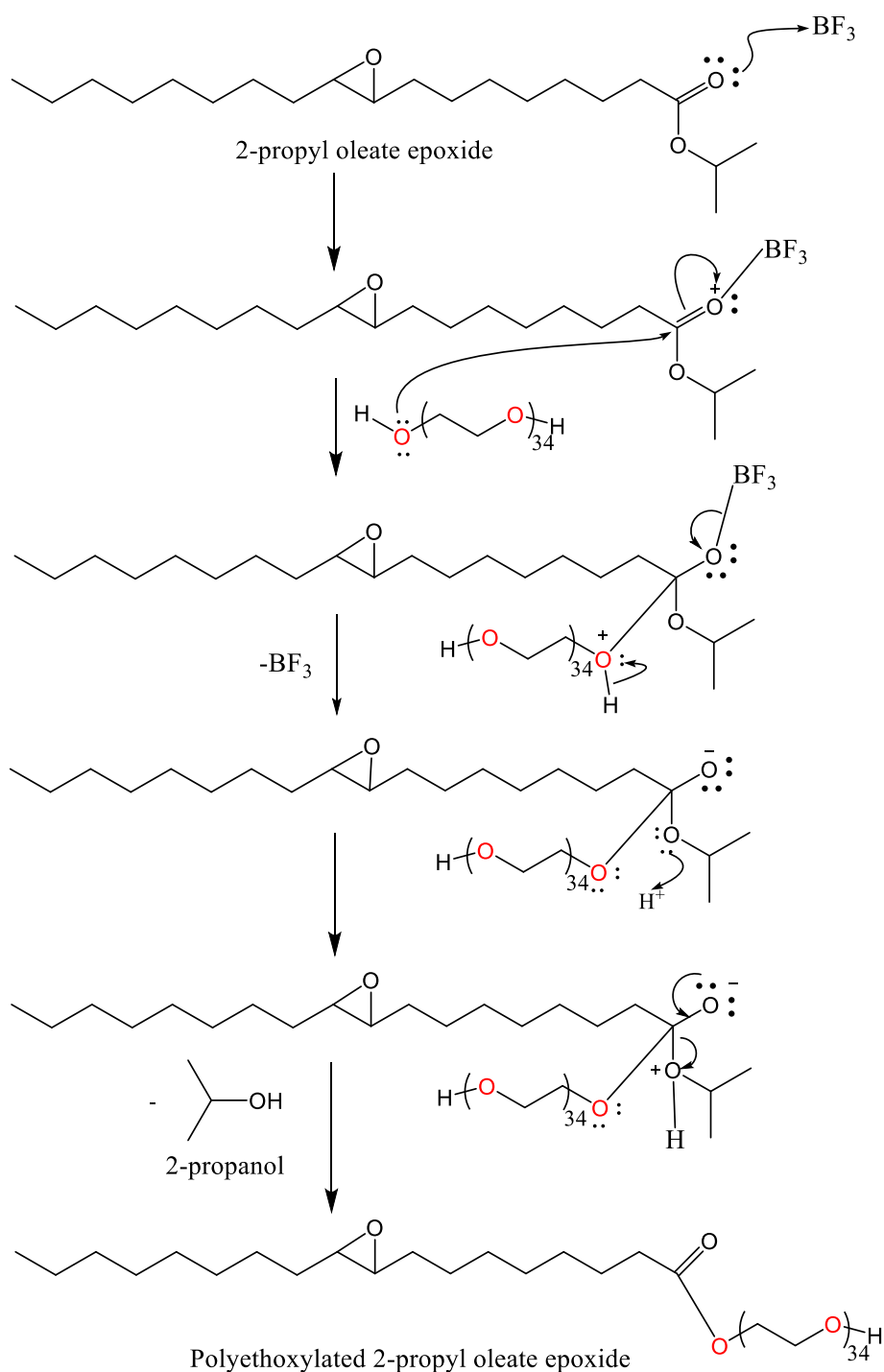


Figure 4- 43 Mechanism for transesterification of 2-propyl oleate epoxide with PEG 1500 in the presence of a Lewis acid.

4.6.2 FT-IR spectroscopy measurement

FT-IR spectra show in Figure 4-44 the transformations from a representative oleate (methyl oleate) to epoxide and then to PEGylated surfactant. The disappearance of the $=\text{C}-\text{H}$ stretch vibration at 3005 cm^{-1} of the double bond in oleate and the appearance of epoxy symmetric stretch vibration between 817 cm^{-1} and 825 cm^{-1}

marked the formation of alkyl oleate epoxides in all syntheses. The formation of surfactant was accompanied by disappearance of the epoxy symmetric stretch vibration, increased absorbance intensity of methylene C-H stretch vibrations relative to that of methyl C-H stretch, a strong stretch band for C-O-C ether linkage centred at 1100 cm^{-1} as well as reduction in OH band intensity at around 3500 cm^{-1} . This indicated that epoxide ring opening took place to form ether linkages and hydroxyl-terminated polymer. Full FT-IR spectroscopic assignments are given for all surfactants in the experimental chapter.

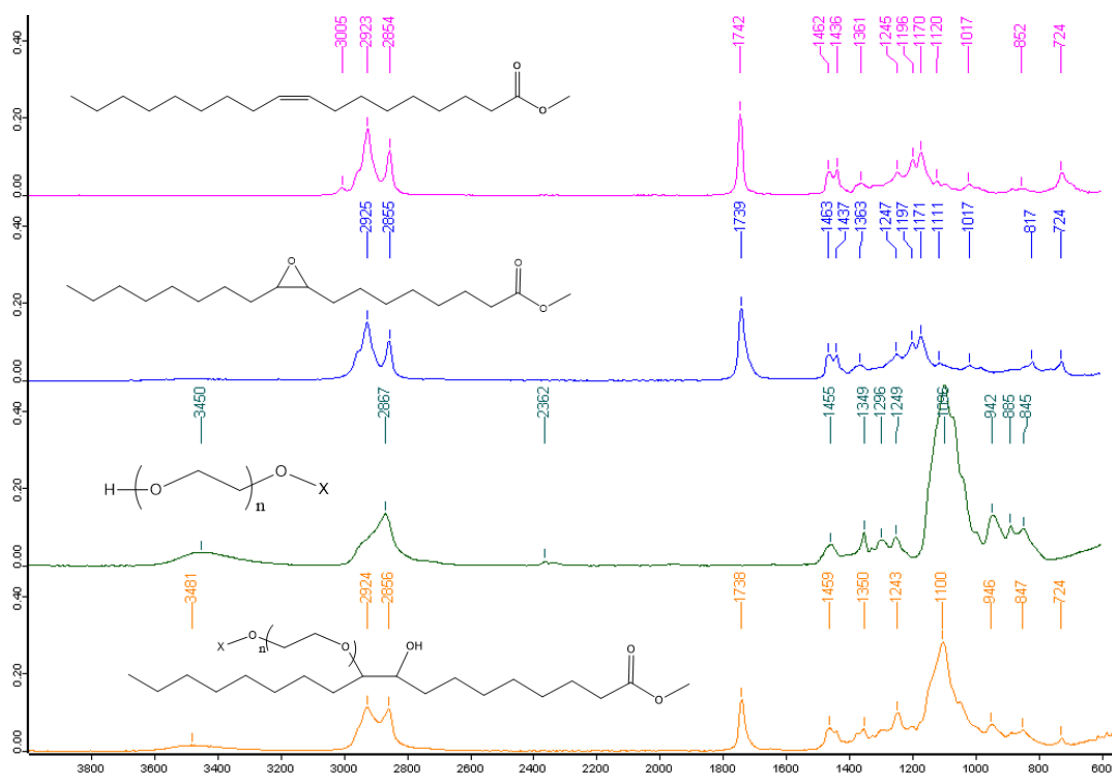


Figure 4- 44 IR spectra of transformation of oleate to epoxide and then to PEGylated surfactant.

4.6.3 ESI mass spectrometry measurement

Electrospray ionization mass spectrometry is a soft ionisation method known for determining the molecular mass of large molecules without causing significant fragmentation.^{347, 348} ESI, when coupled with a suitable mass analyser, is highly sensitive and accurate enough for quantitative and qualitative measurements.³⁴⁷ Accurate mass determination was done for PEMO 400 and PEOO 400 in the

microTOF mode and ESI spectra showed the mass/charge ions binomially distributed across the chain length of the surfactants (Figure 4-45). With an average molecular weight of 400 gmol⁻¹ and EO number 9 for PEG the PEMO 400 and PEOO 400 have molecular weights of 726 and 824 gmol⁻¹ respectively.

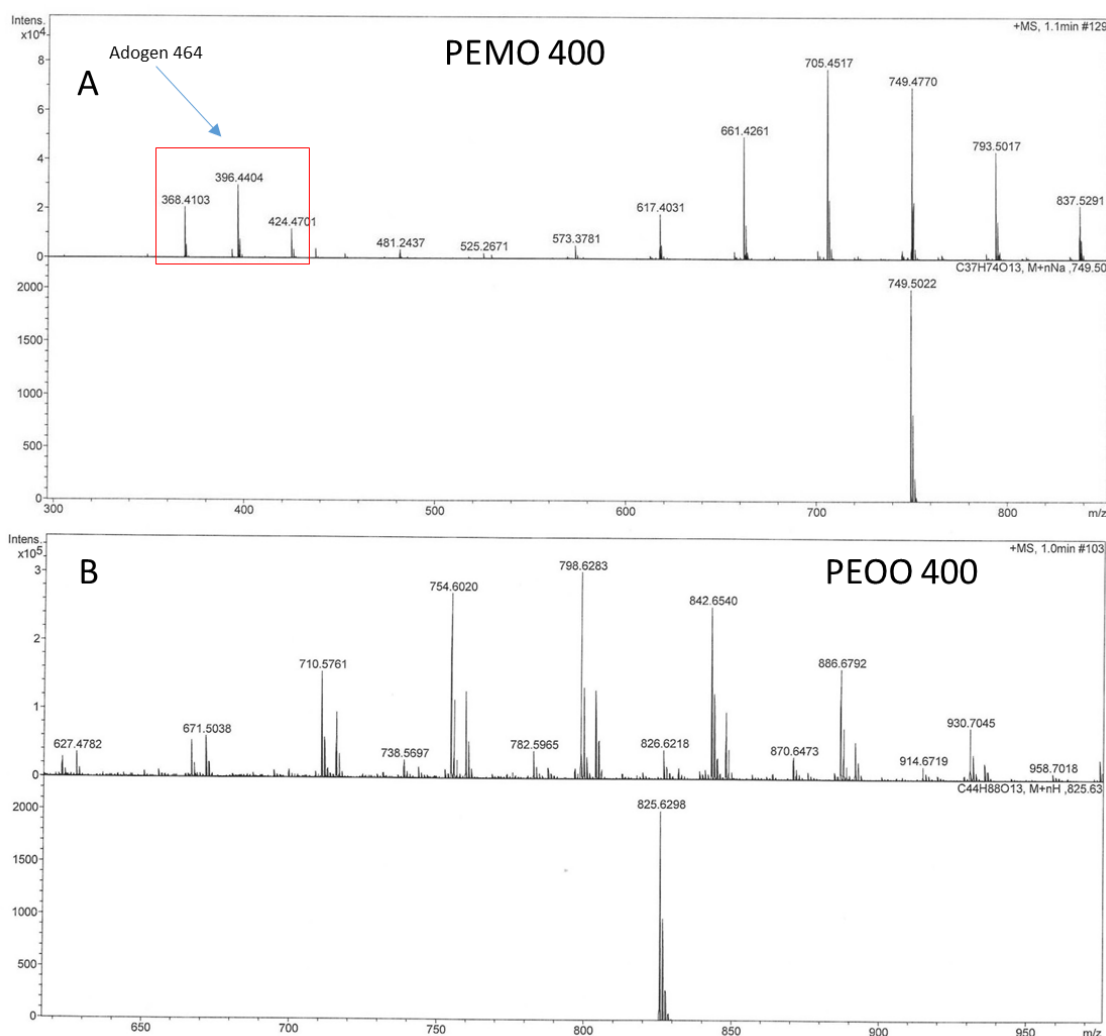


Figure 4- 45 ESI spectra of alkyl oleate surfactants based on PEG 400. (A) PEMO 400 surfactant with a trace impurity of Adogen 464 residue from epoxidation process. (B) PEOO 400 surfactant made from purified 1-octyl oleate epoxide.

Interestingly there were no molecular mass ions corresponding to PEG400 (423, i.e., 400+ 23 from Na), methyl oleate epoxide (335, i.e., 312 + 23 from Na) and 1-octyl oleate epoxide (433, i.e., 410 + 23 from Na) indicating total conversion of epoxide and the effectiveness of the removal method of excess PEG. Surprisingly, there was still a trace of Adogen 464 used as a PTC in epoxidation reaction left in the PEMO

400 surfactant. This was not observed in PEOO 400 because 1-octyl oleate epoxide was purified *via* column chromatography before the ring opening reaction. However, after a few runs on the ESI the instrument soon became contaminated and sensitivity dropped after being cleaned, hence, analysis of other surfactants was suspended.

4.6.4 Supercritical fluid chromatography (SFC) measurement

Synthesised surfactants were characterised on the SFC to separate any impurity. The starting materials methyl oleate and PEG400, PEMO 400 surfactant and isomix of PEG400 and PEMO 400 were separated on a 4.6 Acclaim surfactant and Luna columns using THF or methanol as co-solvents under different preset conditions. Methyl oleate was used instead of its epoxide so as to avoid any chance of the epoxide opening up on the expensive column and destroy it. Fortunately, under 15 minutes of 5% isocratic elution with THF co-solvent on 4.6 Acclaim surfactant column there was a fairly distinct separation for the surfactant.

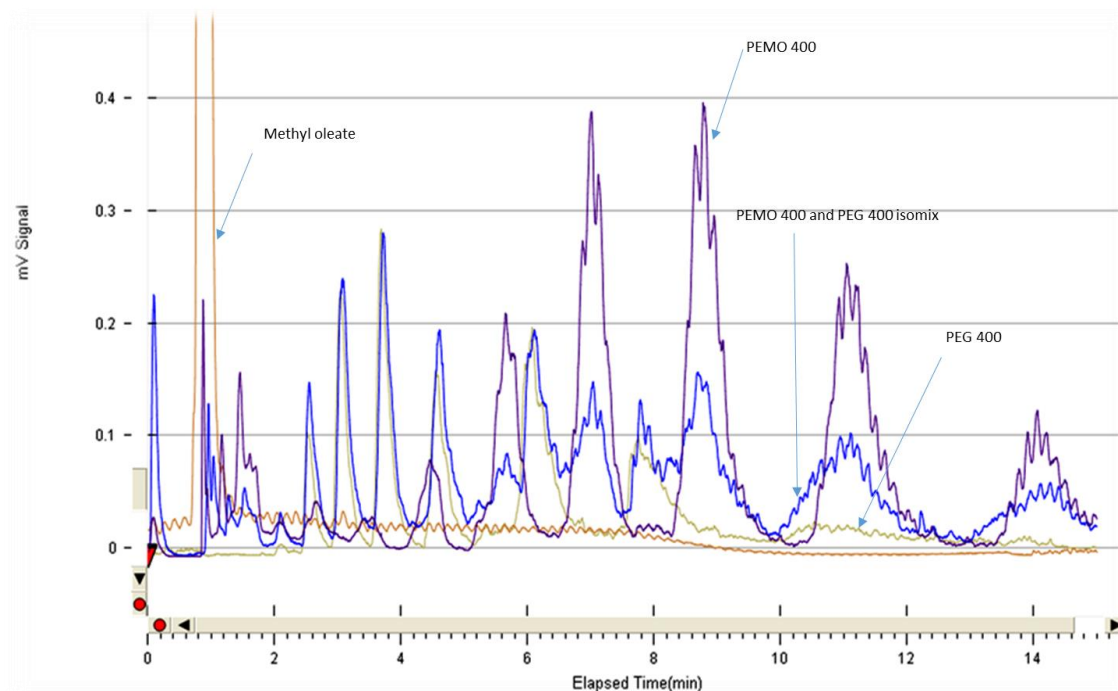


Figure 4- 46 SFC chromatograms showing separation of methyl oleate, PEG 400, PEMO 400 and iso-mixture of PEMO 400 and PEG 400.

Figure 4-46 shows clearly that the so-called surfactant, PEMO 400, is not a mixture of the epoxide and PEG 400 and that there was no residual PEG left in the surfactant although a better chromatogram resolution will be preferred to ascertain the presence of any impurity.

4.6.5 Differential scanning calorimetry (DSC) measurement

DSC can be employed to study phase behaviours of surfactants in solutions.^{349, 350} In order to further characterise these polymeric non-ionic surfactants, their melt profiles were determined. Modulated differential scanning calorimetry (MDSC) showed a distinct difference in the melt profiles of the starting materials (EMO and PEG 400 separately), surfactant (PEMO B040- one of the first samples made which likely contained impurity) and mixture of these compounds (EMO plus PEG 400). The surfactant melt profile shown in Figure 4-47 suggested the product went through a glass transition temperature, T_g , (-73 °C) that showed enthalpic relaxation. Afterwards the system gained enough mobility for cold crystallisation and then a very broad melt.

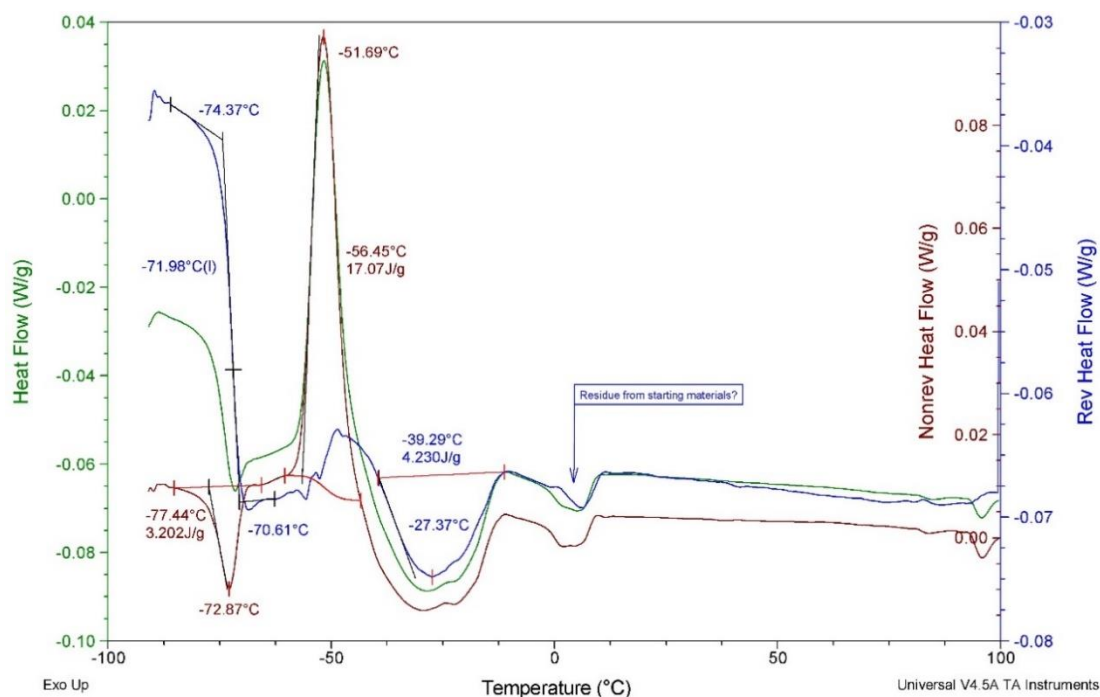


Figure 4- 47 MDSC melt profile of PEMO 400 surfactant

The peaks around 0 °C to 10 °C could be from the starting materials or residual Adogen 464. However, studies from the literature have observed that although the phase transition temperature of a surfactant is predominantly determined by the alkyl chain length, the chain length of PEG has an inverse effect on transition temperature.³⁵⁰

4.6.6 CHN elemental analysis

It became obvious that some of the synthesised surfactants contained residual Adogen 464, thus the surfactant-ethyl acetate mixture was passed through a narrow column packed with Amberlyst 15 ion exchange resin to remove the cationic surface-active impurity as described in chapter 8 section 8.10.2. CHN elemental analyses were performed to evaluate the effectiveness of this approach in removing the impurity. Results are presented in Table 4-7 and attested that some epoxides, 2-butyl oleate epoxide for example, contained a trace amount of nitrogen (0.15%, entry 3). The amount is equivalent to about 10% Adogen 464 not removed from the epoxide after work-up. However, nitrogen was not detected (ND) in any of the surfactants after purification with Amberlyst 15 resin which implies that Adogen 464 impurity had been successfully removed.

Table 4- 7 CHN elemental composition of epoxide and surfactants after treatment with an ion exchange resin.

Entry	Surfactant code	Percentage found before ring-opening			Percentage found after ring-opening and treatment		
		C	H	N	C	H	N
1	PEMO 400				60.673	10.089	ND
2	MPEMO 750				57.262	9.637	ND
3	PE2BO 400	70.712	11.329	0.148	63.418	10.395	ND
4	PEMO 1500				55.236	8.782	ND

4.6.7 ICP mass spectrometry measurement

Determination of residual metal catalysts in surfactants was achieved using ICP-MS. Results for PEEO 400 surfactant made *via* Fe-mont catalysis showed that it contained 0.002 wt% aluminium (Al), 0.009 wt% potassium (K), 0.011 wt% iron (Fe) and 0.06 wt% tungsten (W). Al and K have come from KF/Al₂O₃ transesterification catalyst while W has come from phosphotungstic acid used to catalyse epoxidation process. Fe has come from Fe-mont catalyst used for ring-opening reaction. It is obvious there has been a catalyst leach at every stage of synthesis although the presence of these metals may not impair surfactant end-application performances as their overall concentrations are low.

4.7 Microwave-Assisted epoxide ring opening reaction

In order to circumvent the use of large amount of heterogeneous catalyst which was 20 wt% relative to PEG, microwave technology was applied to ring-opening reaction using Al-mont catalyst under preset conditions. At 200 °C and 0.5 - 1.0 wt% catalyst relative to PEG, there was no conversion in 5 hours of reaction but when temperature was raised to 220 °C the epoxide was largely converted to ketone and aldehyde as observed in chapter 3.

4.8 One-Pot synthesis of surfactant

Following results obtained from UAE reactions in which a great amount of diol was generated as discussed in chapter 3, a one-pot PEGylation reaction was attempted. Epoxidation process was mimicked with or without Adogen 464 and the reaction performed in an ultrasound device as described in chapter 8 section 8.12. When not using Adogen 464, there was no conversion in 3 hours of reaction but when used, methyl oleate was completely converted to corresponding epoxide, ketone, aldehyde and diol without being ring-opened by PEG 400 present in the solution. Consequently, PTA catalyst was replaced with Si-BF₃ and the process repeated in

the presence of Adogen 464 but ^1H NMR spectra showed there was no obvious difference in the performance of the two catalysts.

4.9 Reuse of catalyst for PEGylation reaction

Attempts were made to reuse Si-BF₃ and Fe-mont catalysts to ring-open alkyl oleate epoxides. Disappointingly both catalysts could not convert the epoxides to the product beyond their first cycles though the catalysts were recirculated directly as recovered without prior activation in an oven. Prolonged reaction time did not improve performance either but a small quantity of the epoxides was converted to diols. Leaching was suspected for the sudden loss of activity by these catalysts and ICP mass spectrometry was used to investigate the level of Fe before and after ring opening reaction. Interestingly, results revealed that Fe-mont catalyst contained 5.59% Fe before use and 3.81% Fe after use. The remaining Fe content should still be capable of significantly affecting a further ring-opening reaction in the reuse experiment. Obviously, factors such as blocking of catalyst pore sites other than catalyst leaching were responsible for the non-effectiveness of this catalyst for reuse.

4.10 Synthesised surfactants as phase transfer catalyst

In order to ensure cost reduction in production of the surfactants attempts were made to use synthesised surfactants from epoxidised methyl oleate in place of Adogen 464 (the phase transfer catalyst) in the epoxidation process. Surfactants of methyl oleate based on PEGs 400 and 1000 were used but there was no success with this even with prolonged reaction times. The surfactants, being non-ionic in nature, are probably not suitable for this transfer and perhaps have reduced interaction with the very polar phosphotungstic acid. Potentially our non-ionic surfactants could be made ionic by sulphonating the terminal hydroxyl group on the PEG chain or the -OH generated following the ring-opening of the epoxide.

4.11 Ring opening of epoxides with carbohydrates

PEGs, though innocuous and environmentally safe, are currently derived from non-renewable petroleum feedstocks. Therefore, it is expedient to explore other possible hydrophilic compounds from renewable sources to replace them. Carbohydrates are a class of natural polymers that are often highly hydrophilic, degradable, abundant and very cheap having hydroxyl functionalities similar to PEGs through which attachments can be made with alkyl oleate epoxides.

4.11.1 Ring opening of alkyl oleate epoxides with fructose

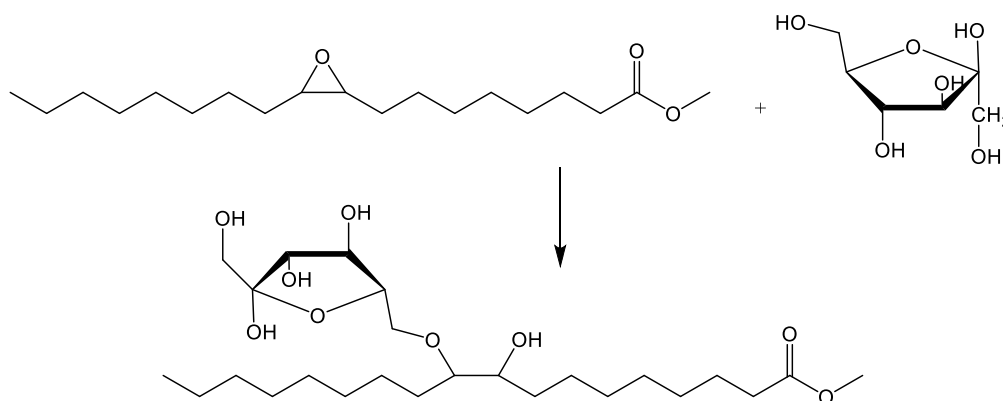


Figure 4- 48 Ring-opening of methyl oleate epoxide with fructose

An attempt was made with fructose to ring-open alkyl oleate epoxide using BF_3 at $125\text{ }^\circ\text{C}$ for 2 hours (Figure 4-48). The product obtained resembled toffee and analysis with supercritical fluid chromatography (SFC) and FT-IR revealed it as a mixture of the epoxide and caramelised fructose. To further enhance the reactivity of fructose, it was dissolved in ethanol-water mixture (3:2) and dried on lyophiliser in an attempt to increase the surface area, but this was not successful as water molecules were entrapped in the fructose forming a gel. Considering the volatility of BF_3 and reaction temperature above, a more stable Lewis acid catalyst, Fe-mont, was used at $60\text{ }^\circ\text{C}$ for 2.5 hours but SFC and FT-IR spectroscopy confirmed the synthesis was unsuccessful. The main challenge has been the non-solubility of fructose in the reaction media. A method described by Rogge *et al.*,³⁵¹ was adopted with modifications in which fructose was dissolved in N-methyl-2-pyrrolidone and

reacted with alkyl oleate epoxide as temperature was raised to 60 °C in the presence of triethylamine (TEA) under nitrogen for 18 hours. However, SFC and FT-IR analyses showed that the desired surfactant was again not being formed.

4.11.2 Ring opening of alkyl oleate epoxides with inulin

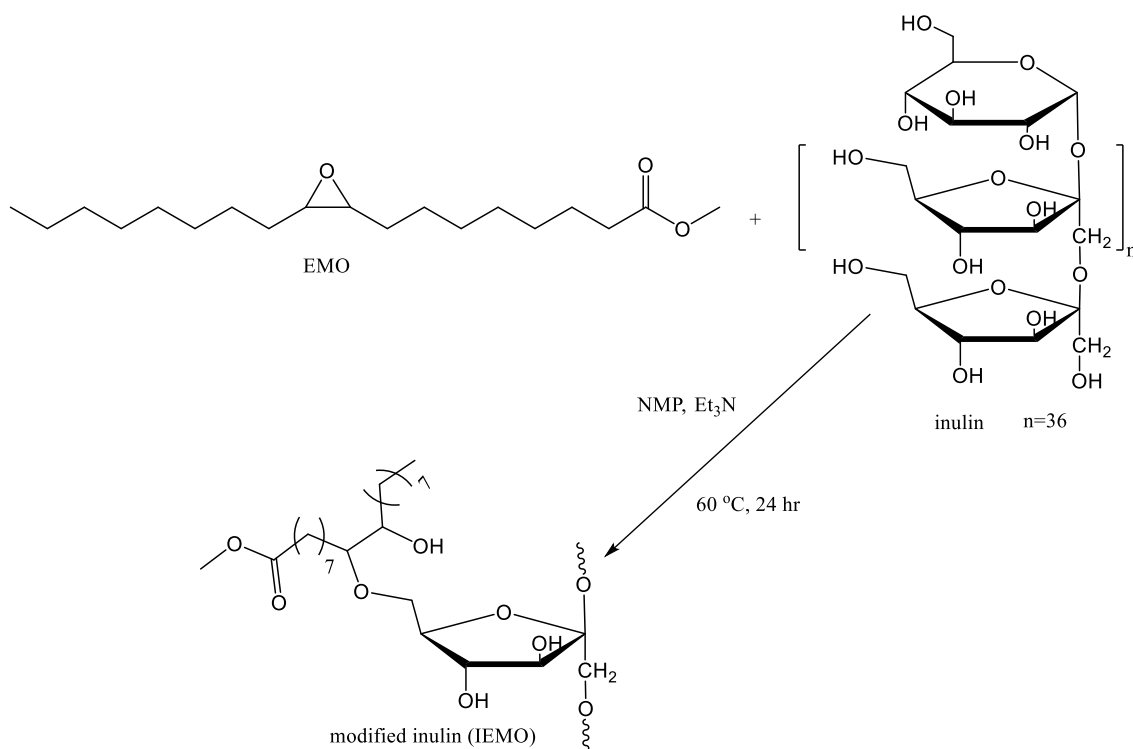


Figure 4- 49 Ring-opening reaction of methyl oleate epoxide with inulin

Encouraged by some successful works reported on inulin-based surfactants,³⁵¹⁻³⁵³ methyl oleate epoxide was reacted with inulin (Figure 4-49) as described above for fructose for 24 hours. The product crystallised in vigorously stirred dichloromethane and was further purified with acetone wash. Owing to limited solubility in methanol, SFC could not be used to analyse the product. DSC analysis showed three distinct melt cycles for modified inulin (IEMO_1), inulin and mixture of modified inulin and epoxidised methyl oleate (IEMO_1_EMO) as shown in Figure 4-50. Scanning electron microscopy (SEM) images (Figure 4-51) showed that the resulting inulin (IEMO) has a more porous and loose surface than the starting material. However, these differences could not be confirmed with ¹H and ¹³C NMR spectra (though spectra showed the epoxide had completely disappeared).

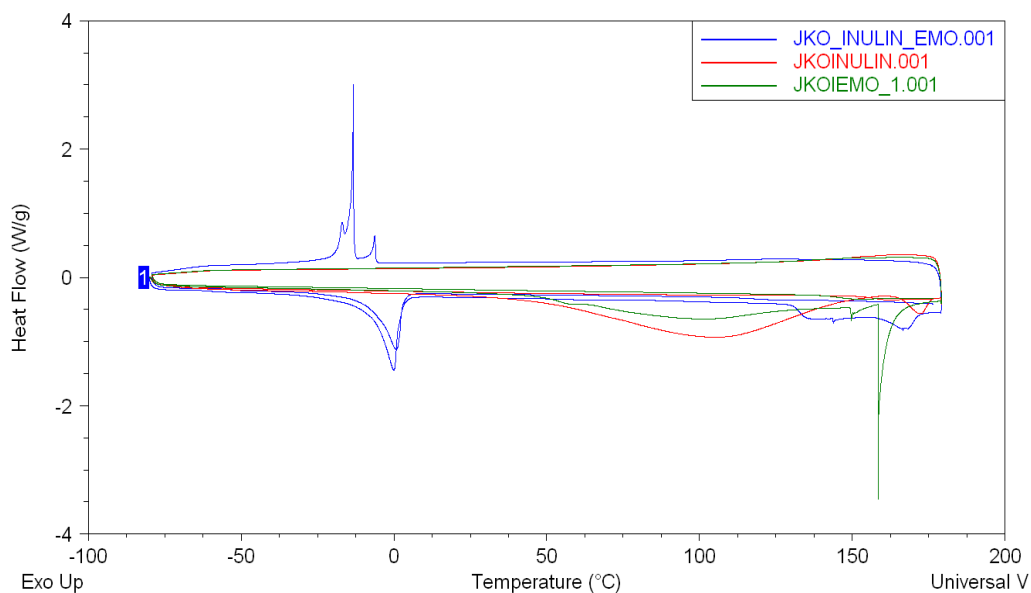


Figure 4- 50 DSC melt profiles of modified inulin (green), inulin (red) and a mixture of modified inulin and epoxidised methyl oleate (blue).

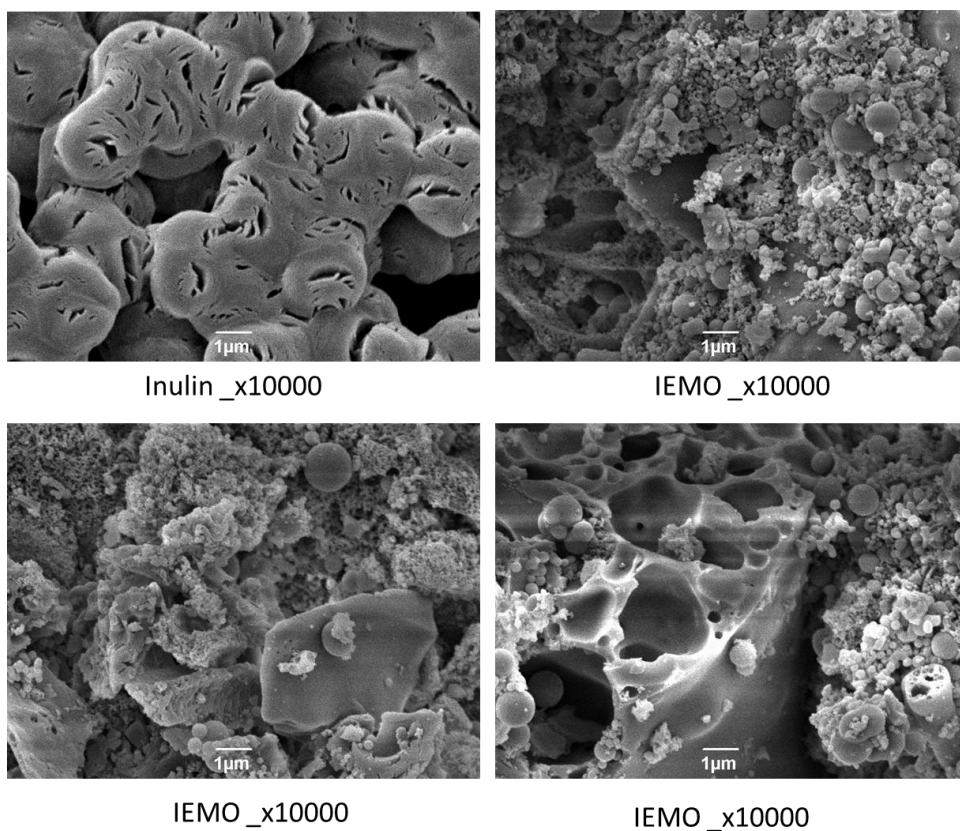


Figure 4- 51 images of modified inulin and inulin at a magnification of 10000

4.11.3 Ring opening of alkyl oleate epoxide with D-sorbitol

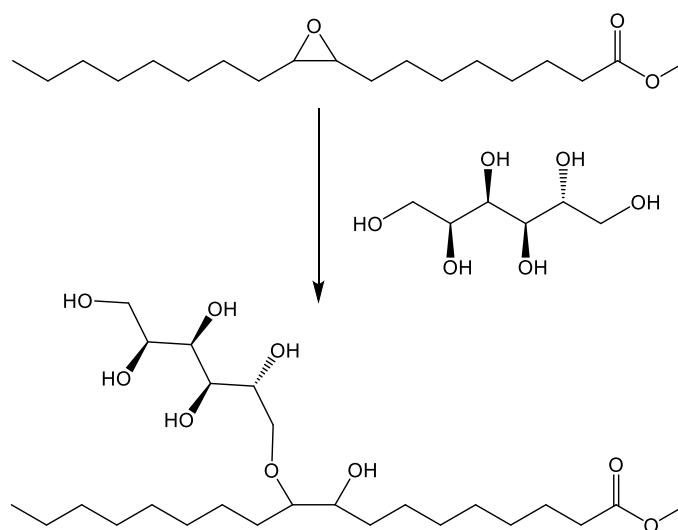


Figure 4- 52 Ring-opening reaction of methyl oleate epoxide with D-sorbitol

D-sorbitol, the reduced form of glucose, was used instead of fructose and inulin to ring-open methyl oleate epoxide (Figure 4-52) as described in chapter 8 section 8.10.5.3. From ^1H and proton-decoupled ^{13}C NMR spectra (Figure 4-53- proton only) it was not clear what products have been formed but it revealed that the epoxide has been largely converted in 3 hours of reaction as the epoxy proton and carbon disappeared and intensity of peak **E**, the β -protons to the epoxy group, greatly reduced. The sorbitol protons retained their chemical shifts though the hydroxyl protons have merged as a single broad peak centred at 4.38 ppm with an integration value of 6. Some unknown peaks were observed at 2.67 ppm and 2.00 ppm and 2D NMR spectra did not correlate them with any known peaks. The two diagnostic peaks for a successfully ring-opened alkyl oleate epoxide at ~ 73 ppm and ~ 84 ppm were observed on the carbon spectrum (though weak intensity) in addition to another two peaks at ~ 77 ppm and 100 ppm. This suggests that some epoxide was converted to surfactant though largely to side reaction products. The 100 ppm and 77 ppm peaks are likely due to formation of diol in the system. After 4 hours of reaction, a ketone carbon peak was observed at ~ 214 ppm (it was assumed ketone as an aldehydic proton was not observed in the ^1H spectrum) while the hydroxyl protons on D-sorbitol disappeared from their position. This suggests the epoxide

had been transformed primarily into diol which subsequently oxidised to ketone. However, more studies are required to be certain of what products are being formed in this reaction.

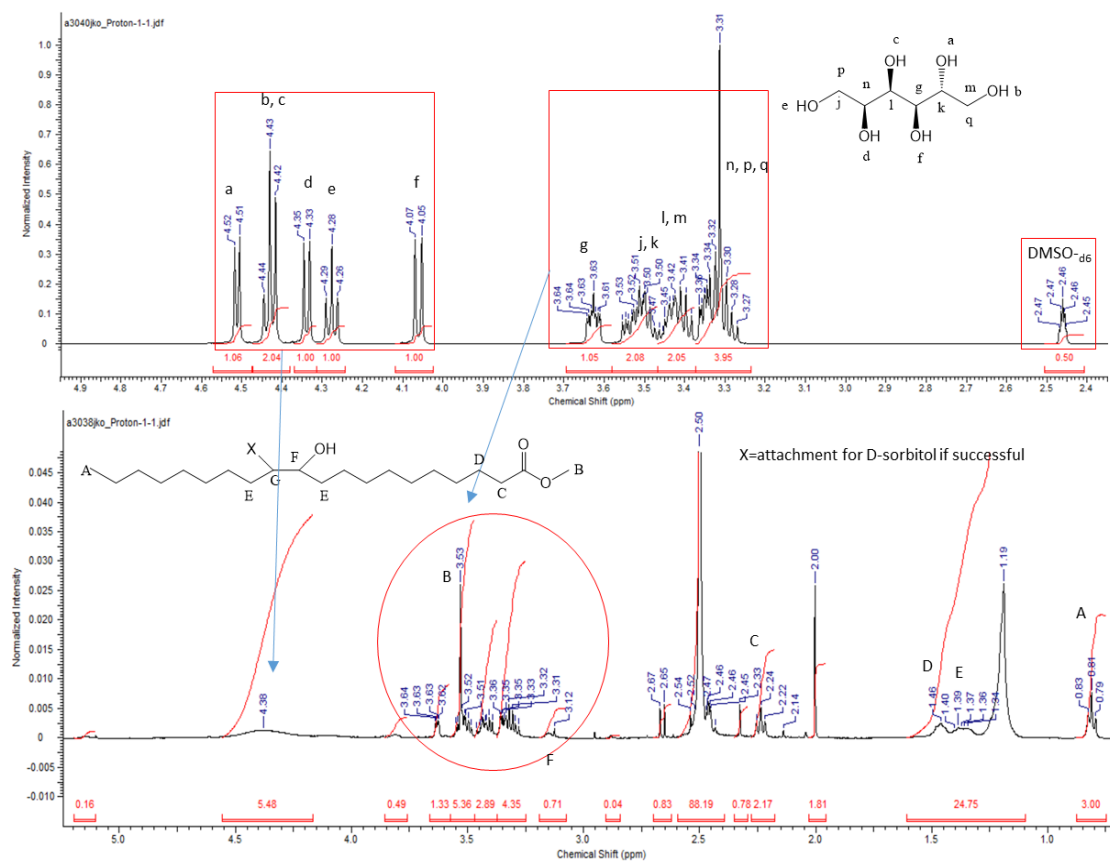


Figure 4- 53 ¹H NMR spectra of D-sorbitol (top) and product from ring-opening reaction with epoxidised methyl oleate in 3 hours of reaction time.

4.12 Synthesis and characterisation of sophorolipid-based surfactants

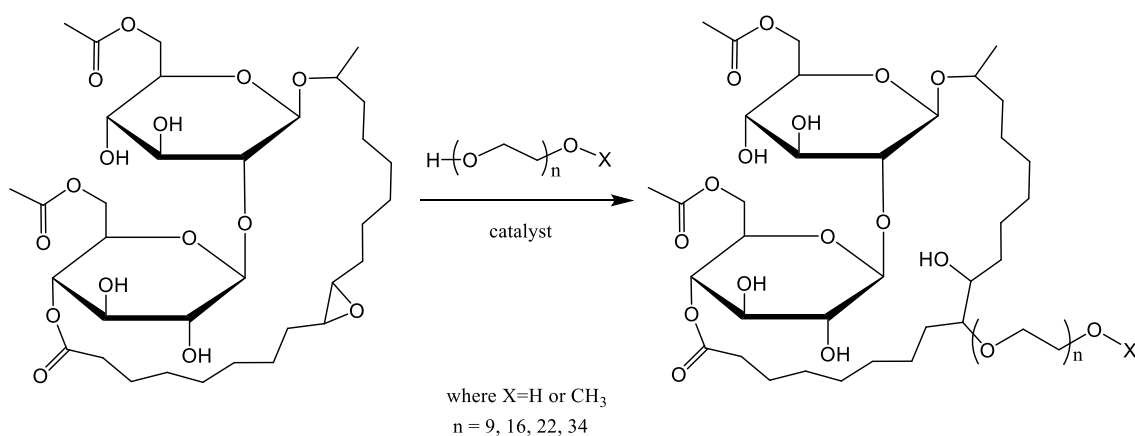


Figure 4- 54 Ring-opening reaction of ELSL with PEGs

Following the synthesis of a novel ELSL in chapter 3, the epoxide was dissolved in ethyl acetate to allow for dropwise addition to heated PEGs (Figure 4-54) as described in chapter 8 section 8.10.3. Resulting surfactants are off-white to amber colour in appearance (Figure 4-55 and Table 4-8). Those based on PEG 400 to MePEG 750 are viscous liquid while those with PEGs 1000 and 1500 attached are hard-to-cut-through solids.

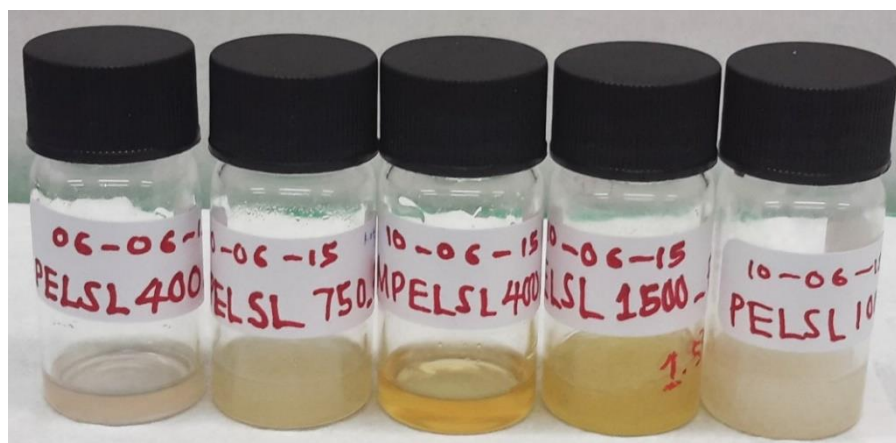


Figure 4- 55 Five surfactants prepared from ELSL.

Table 4- 8 Synthesised surfactants on lactonic sophorolipid

<i>Entry</i>	<i>Surfactant code</i>	<i>Surfactant description</i>
1	PELSL400	Epoxidised lactonic sophorolipid ring opened with PEG 400
2	MPELSL400	Epoxidised lactonic sophorolipid ring opened with MePEG 400
3	MPELSL750	Epoxidised lactonic sophorolipid ring opened with MePEG 750
4	PELSL1000	Epoxidised lactonic sophorolipid ring opened with PEG 1000
5	PELSL1500	Epoxidised lactonic sophorolipid ring opened with PEG 1500
6	ELSL	Epoxidised lactonic sophorolipid

IR spectra of the surfactants are presented in Figure 4-56 and show transformation from the original sophorolipid, LSL, to the epoxide, ELSL, and then to individual PEGylated surfactant. It was obvious that the epoxy symmetric deformation at 818

cm⁻¹ disappeared in all the surfactants. The methylene symmetric stretch vibration increased in intensity while the asymmetric reduced in intensity as the number of ethylene oxide units in the PEG increased. It was observed that the C-O-C ether stretching vibration centre shifted from 1095 cm⁻¹ to 1109 cm⁻¹ with increasing EO repeating unit in PEG. As there was no band observed at 1725-1700 cm⁻¹ belonging to carboxylic C=O stretch vibration, and the ester C=O stretch vibration at 1741 cm⁻¹ remained intact in all surfactants, it was deduced that the acetyl ends were not hydrolysed or the lactone C=O cleaved.

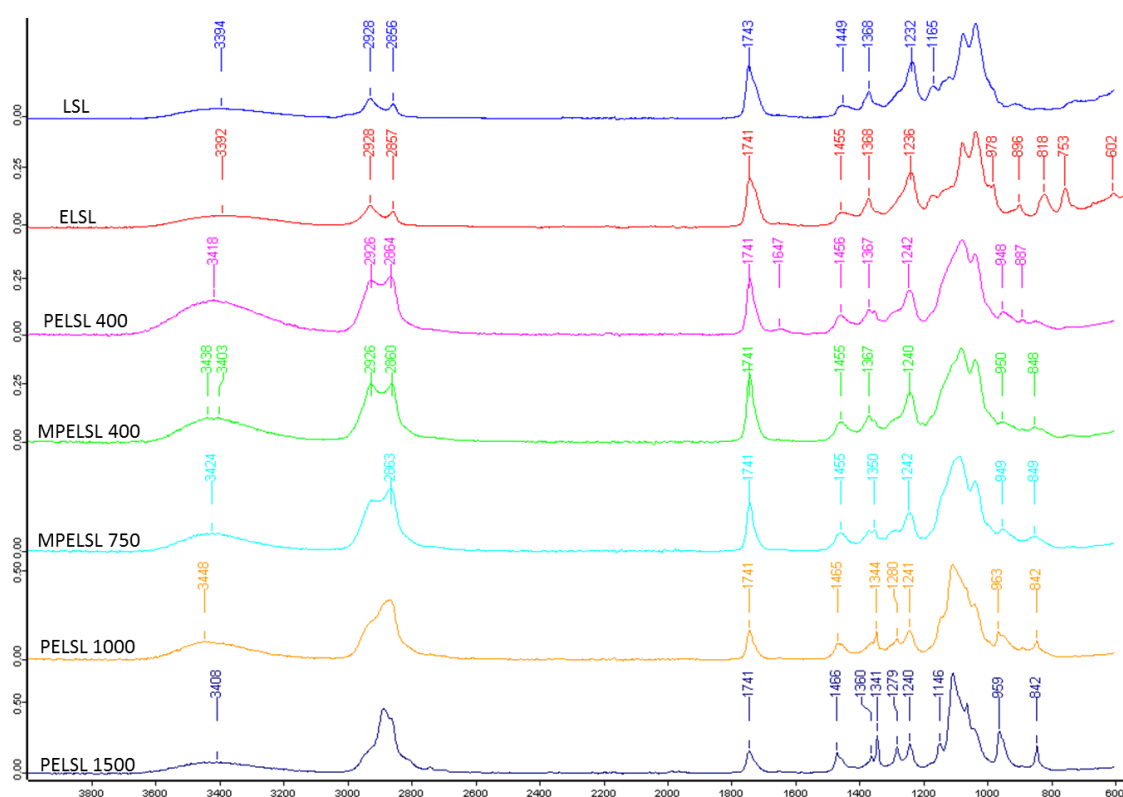


Figure 4- 56 FT-IR spectra of LSL, ELSL and PEGylated surfactants based on ELSL.

Surfactants were also characterised on a Bruker Avance-AV 700 MHz spectrometer. Comparison between 1Ds and 2Ds NMR spectra of ELSL and PELSL 400 (Figure 4-57- proton only) showed that the surfactant was successfully formed. The epoxy protons peak 9, 10 disappeared while the β-epoxy protons peak 8, 11 shifted or levelled with other methylene protons in the fatty acid group to form surfactant. While the proton peak 9 to which the PEG is attached was conspicuous resonating at 3.22 ppm, the proton peak 10 that bears the hydroxyl end overlapped with the

protons of the surfactant sophorose group. ^{13}C and DEPT-135 spectra did not show the corresponding positions of these peaks (9 and 10) but HSQC showed correlate the 3.22 ppm proton with the 83.75 ppm carbon. These chemical shift positions are identical to what was observed in the oleate based surfactants. Interestingly, COSY and HMBC showed that positions 17 and 1', 1'' and 2', and 1 and 4'' are still bonded after synthesis. All other peaks significantly retained their chemical shift positions after ring opening reaction.

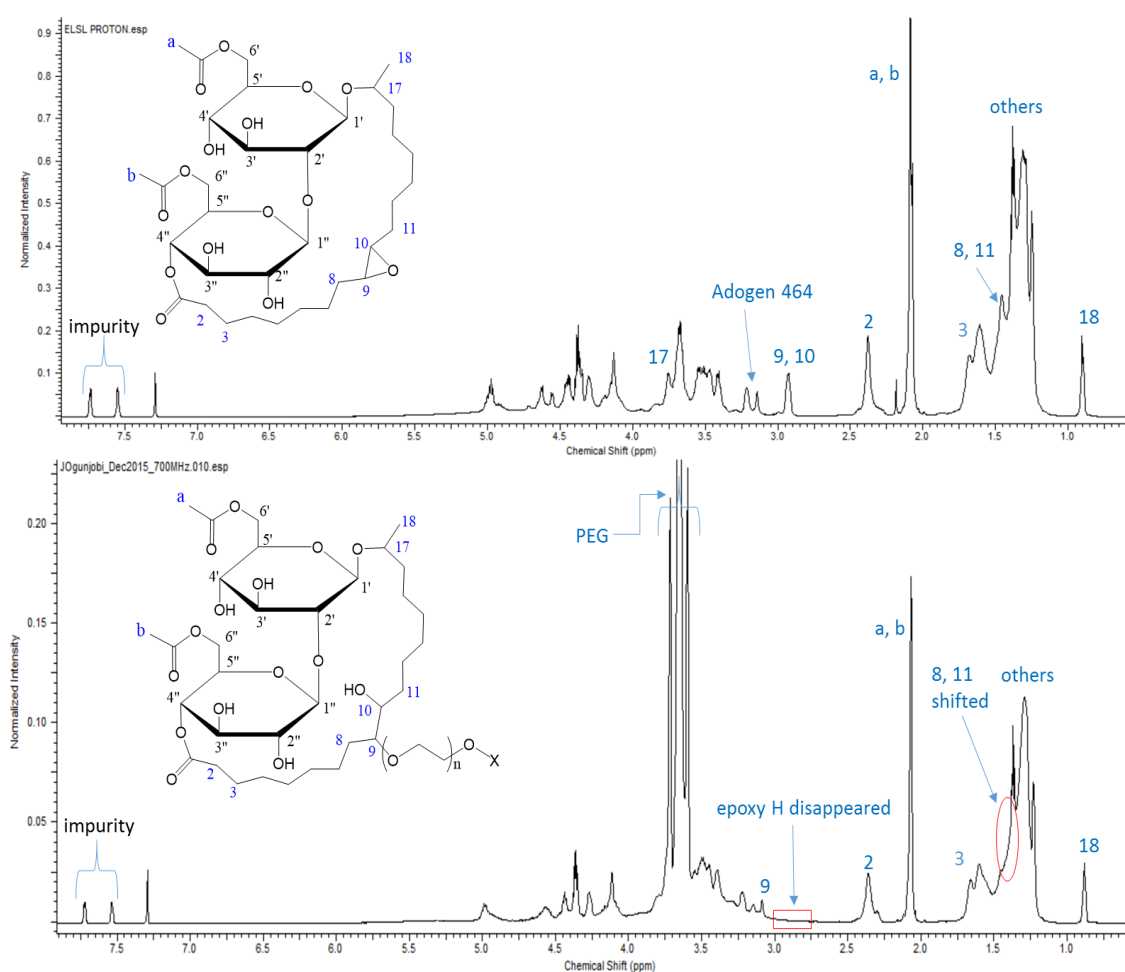


Figure 4-57 ^1H NMR spectra of ELSL (top) and PELSL 400 surfactant (bottom).

As nitrogen, purportedly from residual Adogen 464, was detected in ELSL, CHN analysis of resulting surfactants was performed after ring-opening reaction. Results presented in Table 4-9 showed that nitrogen was not detected (ND) in all the surfactants except PELSL 1500 which contained 0.048% trace nitrogen after synthesis.

Table 4- 9 CHN composition of ELSL and synthesised sophorolipid-based surfactants

Entry	Surfactant code	Percentage found before ring-opening			Percentage found after ring-opening		
		C	H	N	C	H	N
1	ELSL	56.040	7.826	0.105			
2	PELSL 400	56.040	7.826	0.105	53.249	8.610	ND
3	MPELSL 400	56.040	7.826	0.105	55.155	8.515	ND
4	MPELSL 750	56.040	7.826	0.105	54.852	8.581	ND
5	PELSL 1000	56.040	7.826	0.105	53.724	8.702	ND
6	PELSL 1500	56.040	7.826	0.105	54.393	8.269	0.048

4.13 Synthesis and characterisation of linseed oil-based surfactants

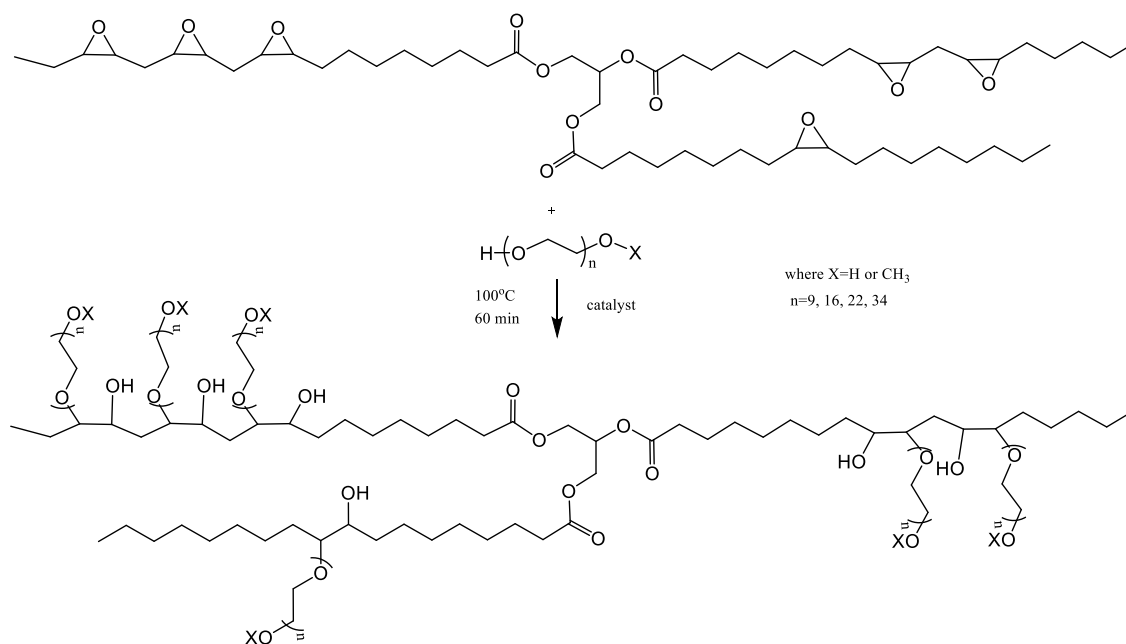


Figure 4- 58 Ring-opening reaction of epoxidised linseed oil with PEGs

Surfactants based on epoxidised linseed oil (ELO) were synthesised with molar ratio 6 of PEG or MePEG to epoxide (Figure 4-58). The viscous epoxide was thinned with toluene and added in drops to the melted PEG or MePEG –along with a catalyst as

described in chapter 8 section 8.10.4. Resulting surfactants generated listed in Table 4-10 were viscous to solid dark brown materials (Figure 4-59).

Table 4- 10 Synthesised surfactants based on epoxidised linseed oil

<i>Entry</i>	<i>Surfactant code</i>	<i>Surfactant description</i>
1	PELO400	Epoxidised linseed oil ring opened with PEG 400
2	MPELO400	Epoxidised linseed oil ring opened with MePEG 400
3	MPELO750	Epoxidised linseed oil ring opened with MePEG 750
4	PELO1000	Epoxidised linseed oil ring opened with PEG 1000
5	PELO1500	Epoxidised linseed oil ring opened with PEG 1500

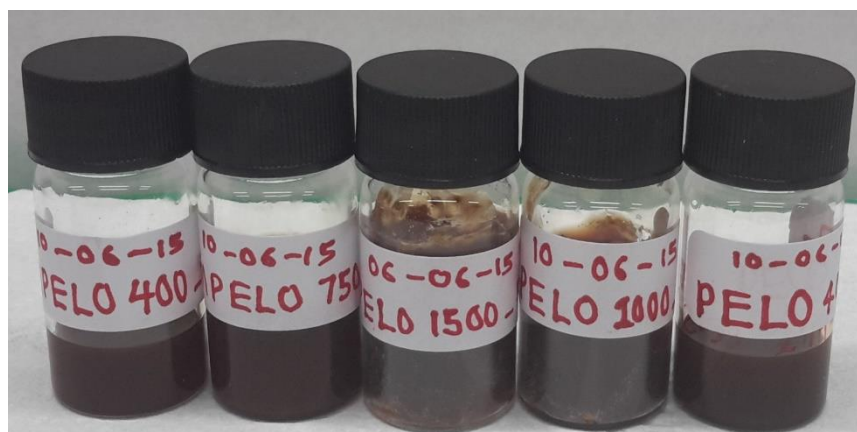


Figure 4- 59 Surfactants based on ELO are viscous to hard solid materials

FT-IR spectroscopy was used to study the transformation from ELO to surfactants. Formation of PEGylated surfactants was marked with the disappearance of epoxy symmetric deformation at 822 cm^{-1} in all syntheses. The methylene C-H symmetric stretch vibrations became dominant as PEG chain length increased while a strong stretch band for C-O-C ether linkage centre was observed between 1102 and 1110 cm^{-1} . The OH band which reduced in intensity with increasing PEG chain length was centred at around 3454 cm^{-1} . Full FT-IR spectroscopic assignments are given for all surfactants in the experimental chapter.

^1H NMR spectrum for ELO (Figure 4-60 top) showed the epoxy proton peaks 3'', 4'', 6'', 7'', 7'', 9'', 9'', 10, 10' and 10'' are resonating between 2.5 ppm and 3.5 ppm with an integration value of 12. These peaks together with the epoxy β -proton peaks disappeared in PELO 400 spectrum (Figure 4-60 bottom).

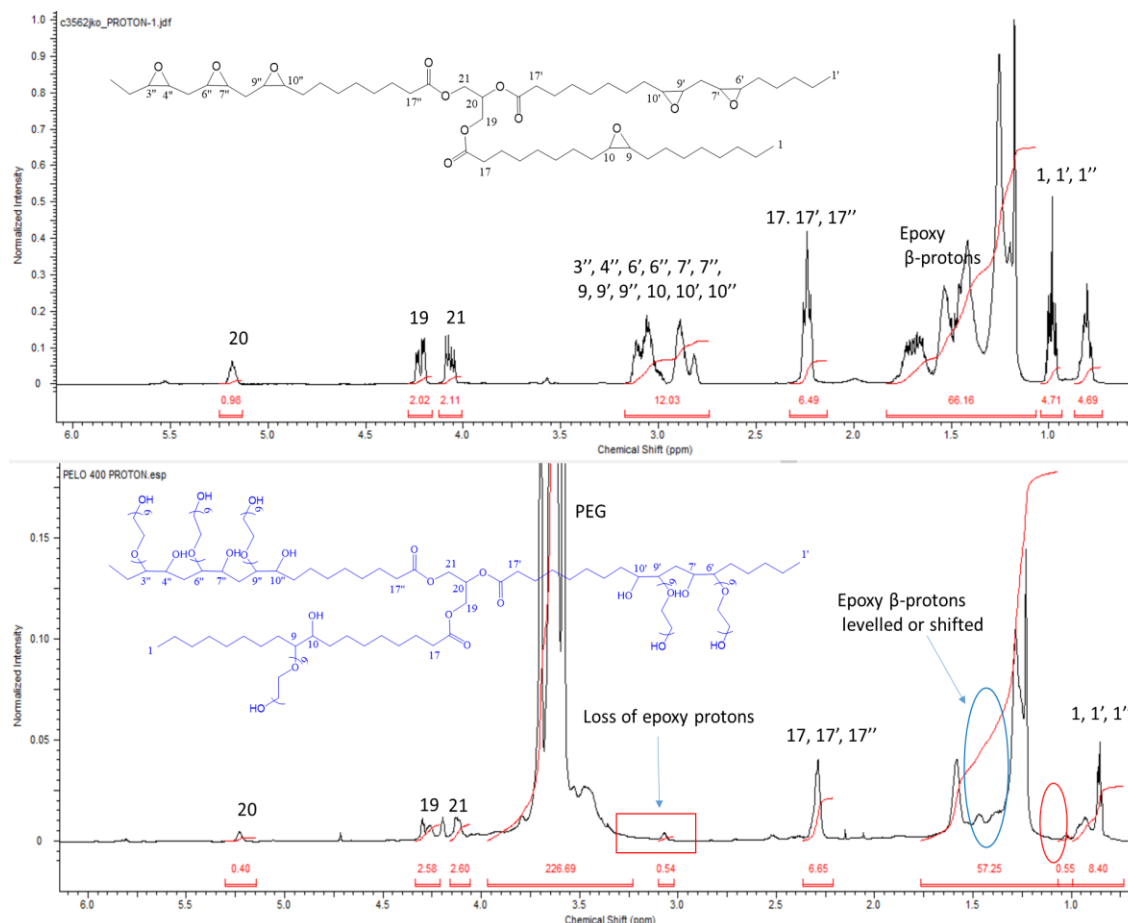


Figure 4- 60 ^1H NMR spectra of ELO (top) and PELO 400 (bottom).

The methyl peak 1'' belonging to the fatty acid group that carried three epoxy groups also shifted upfield after ring opening the ELO. The proton and carbon peaks to which PEGs are attached were assigned to 3.07-3.09 ppm (though with an integration value of 1) and 84.55 ppm positions using ^{13}C and HSQC. Those peaks bearing the hydroxyl end overlapped with the PEG methylene protons but ^{13}C showed 73.40 ppm for this. All other peaks significantly retained their chemical shift positions after ring opening reaction.

Triglycerides ring-opened with PEGs containing a polymerisable group at the other end has been reported to have found applications as bio-based binders in composites.³⁵⁴

4.14 Conclusions

Over fifty non-ionic surfactants have been prepared from alkyl oleate epoxides, lactonic sophorolipids epoxide and epoxidised linseed oil *via* ring-opening reaction with PEGs of varying chain lengths. In order to accurately characterise these surfactants owing to their high molecular masses, model reactions with cyclohexene oxide, methyl oleate oxide, ethylene glycol, 2-methoxy ethanol, triethylene glycol and poly (ethylene glycol) 400 were carried out. Heterogeneous catalysts were screened for use in epoxide ring-opening reactions and silica-supported boron trifluoride, Fe-montmorillonite, and Al-montmorillonite were found to be the most effective and selective. These catalysts have not been reported before for ring-opening of fatty acid epoxides. Results from model reactions gave ~80% surfactant yield with attendant side reaction products. The surfactants so formed took the physical form of the PEG attached to them. Characterisation of surfactants was performed using IR spectroscopy, SFC, NMR spectroscopy, DSC, ESI mass spectrometry, CHN elemental analysis and ICP mass spectrometry. Treatment of surfactants with Amberlyst 15 resin removed residual Adogen 464 impurity from epoxidation step but they contained trace amount of residual catalyst metals used in transesterification, epoxidation and ring opening processes. Some of the side reaction products remains categorically unidentified. Epoxides were also ring-opened with fructose, inulin and D-sorbitol but not to much success. Other attempts made, which include one-pot surfactant synthesis, use of microwave technique in PEGylation, use of synthesised surfactants as a phase transfer catalyst in epoxidation reaction and reuse of catalysts for PEGylation were not successful.

Assessment of Surfactants Properties

Chapter 5

5.0 Assessment of surfactants properties

5.1 Introduction

Surfactants have properties that make them applicable in different fields of endeavour. In this chapter the properties of synthesised surfactants were assessed. Over sixty different surfactant samples were sent to Unilever R&D, Port Sunlight, Liverpool, UK for physicochemical assessments. However, owing to time and logistics limits, results for these have not been fully generated and compiled at the time of writing this chapter. Preliminary measurements, predominately dynamics studies, were carried out in 2015 on a few surfactant samples the result of which was inconclusive as there was evidence of surface-active impurities in the samples. After removal of impurities, two surfactant samples were reassessed prior to sending the remaining samples to Unilever. Therefore the discussion in this chapter will be based on measurements taken before and after purification. A few concepts that could help predict potential applications for surfactants will also be discussed.

5.2 Physicochemical measurements

5.2.1 Dynamic surface tension of synthesised surfactants

The measurement of surface tension is called tensiometry. Surface tension is a key parameter in studying the properties of surface active compounds. Surface tension results from an imbalance of attractive forces between molecules at the surface of a liquid and those in the bulk of the liquid. It is this surface tension that makes liquid form droplets on a surface. Water is a liquid with one of the highest surface tensions (72 mN/m) and is usually used as a standard for tensiometry. In some applications in which the solution changes frequently with time, which is in motion, surface tension is measured as a dynamic surface tension. Dynamic surface tension is the change in surface tension before equilibrium conditions are attained, but is required information when considering detergency formulations where long equilibration times are common.

Dynamic surface tension was studied with a maximum bubble pressure tensiometer which allowed us to have an idea of the dependency of surface tension on time and allowed measurement to be taken for a maximum of 100 seconds. Results for some of the surfactants are shown in Figures 5-1, 5-2 and 5-3. Obviously the synthesised surfactants demonstrated surface activity with good dynamics. PEMO400 (hydroxyl end-group to PEG chain) lowered surface tension of water to 32 Nm/m and appeared to have reached equilibrium in 76 seconds while MPEMO400 (methoxy end-group to PEG chain) lowered surface tension to 33 mN/m and appeared to have reached equilibrium in 54 seconds. While PEEO 400 (short PEG chain) surfactant lowered surface tension to 32 mN/m and appeared to have reached equilibrium in 52 seconds PEEO 1500 (long PEG chain) only lowered it to 42 mN/m in 35 seconds and would still take a lot more time to reach equilibrium as shown in Figure 5-1. The same trend was noticed in surfactants based on epoxidised linseed oil which bear on average six separate PEG chains. Two phenomena are involved in dynamic surface tension: diffusion through the bulk solution and adsorption of surfactant molecule at the interface. The latter is the rate determining step for polymeric surfactants (such as those containing PEG hydrophile units).¹⁴² As they diffuse to the surface and attain equilibrium, they lower the surface tension at the surface, and consequently the solution surface tension is reduced. Generally, it was observed that the diffusion rate of the surfactant molecules through the bulk solution to the interface reduces as alkyl chain length and EO number increase in the surfactants. As a result PEMO 400, MPEMO 400 and PEEO 400 surfactants attained equilibrium faster (under 100 s) than PEEO 1500 and others. Interestingly, the slow diffusion of these high molecular weight surfactants is otherwise advantageous in the sense that once equilibrium is attained such surfactants will be very stable at the interface. Trace impurities in surfactants are supposedly responsible for the jumps in curves noticed for PEEO400, PEOO400 and some other surfactants.

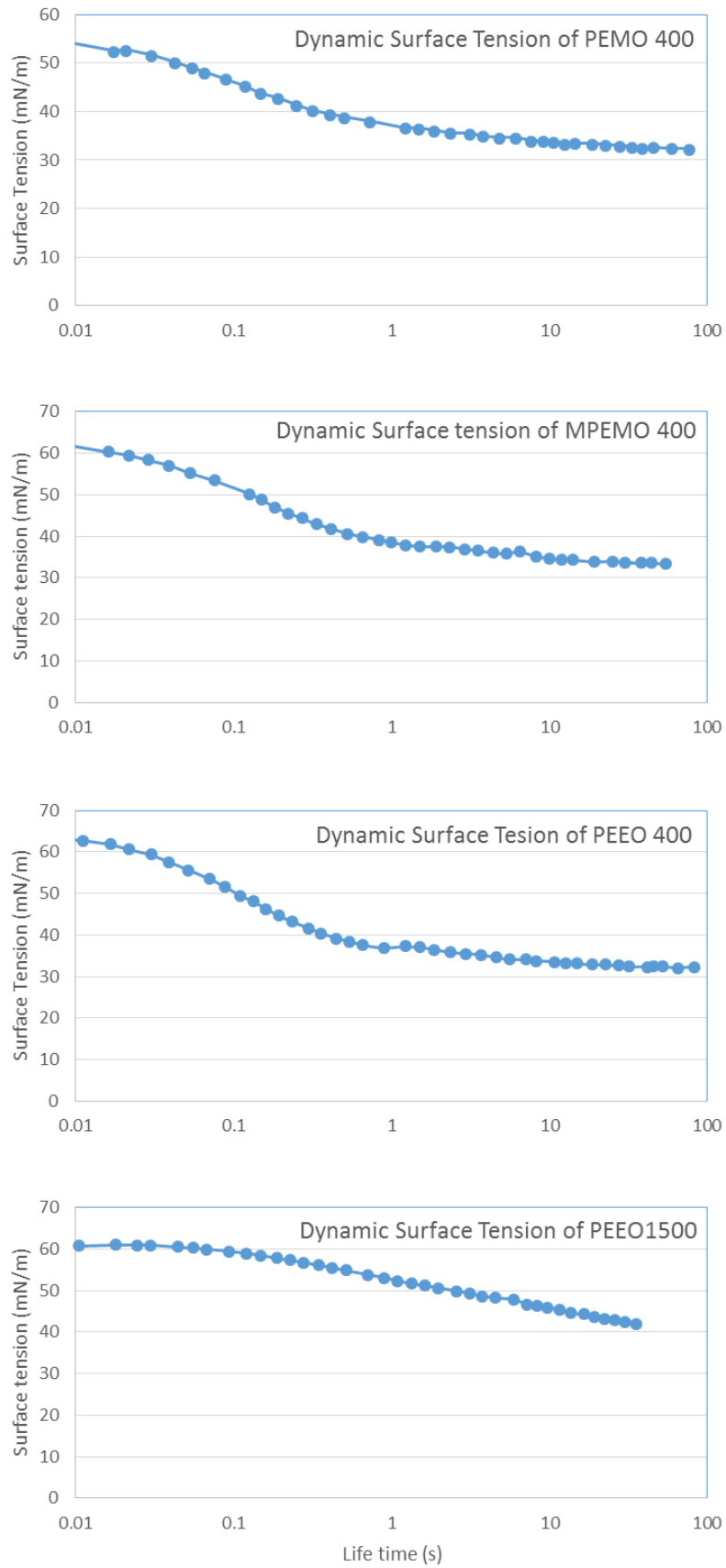


Figure 5- 1 Dynamic surface tension of unpurified PEMO 400, MPEMO 400, PEE0 400 and PEE0 1500 surfactants

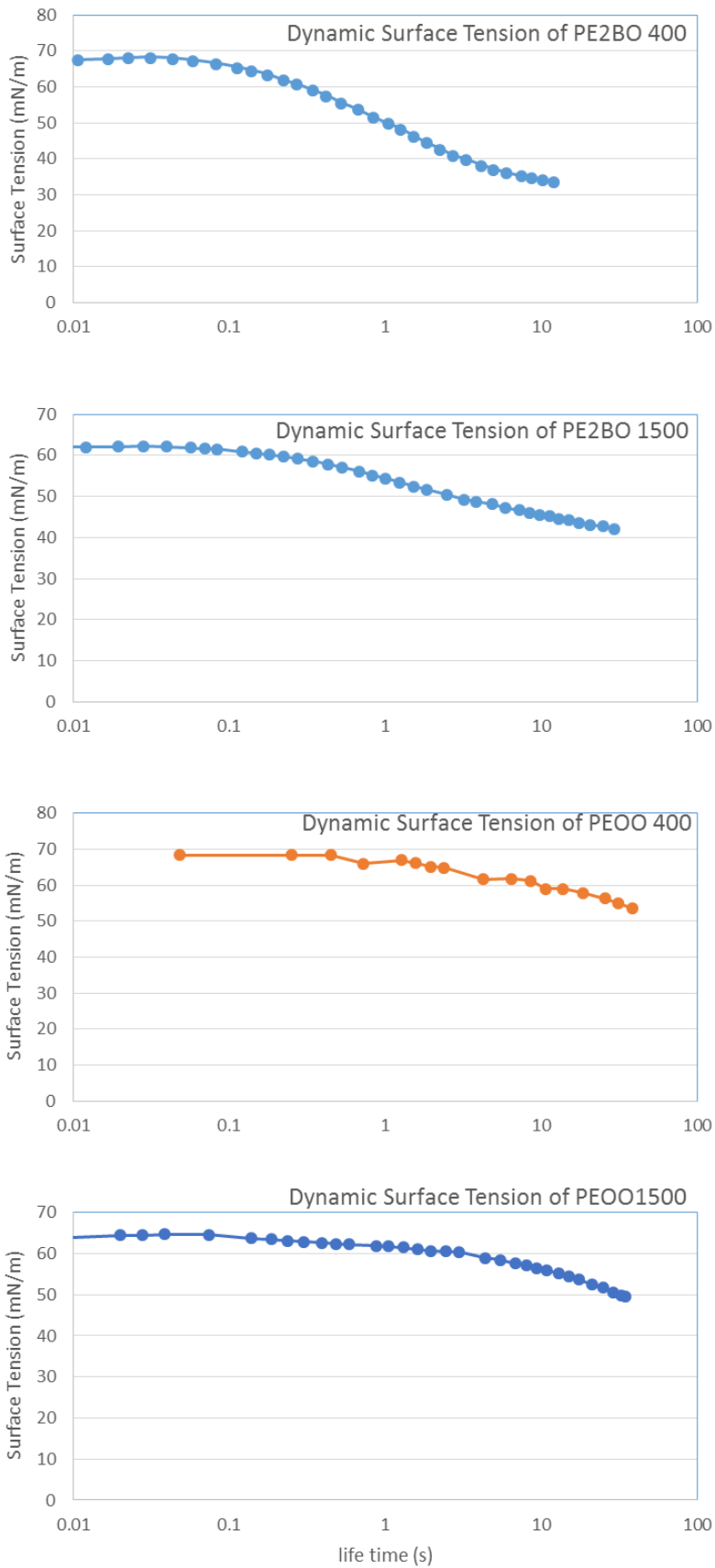


Figure 5-2 Dynamic surface tension of unpurified PE2BO 400, PE2B 1500, PEOO 400 and PEOO 1500 surfactants

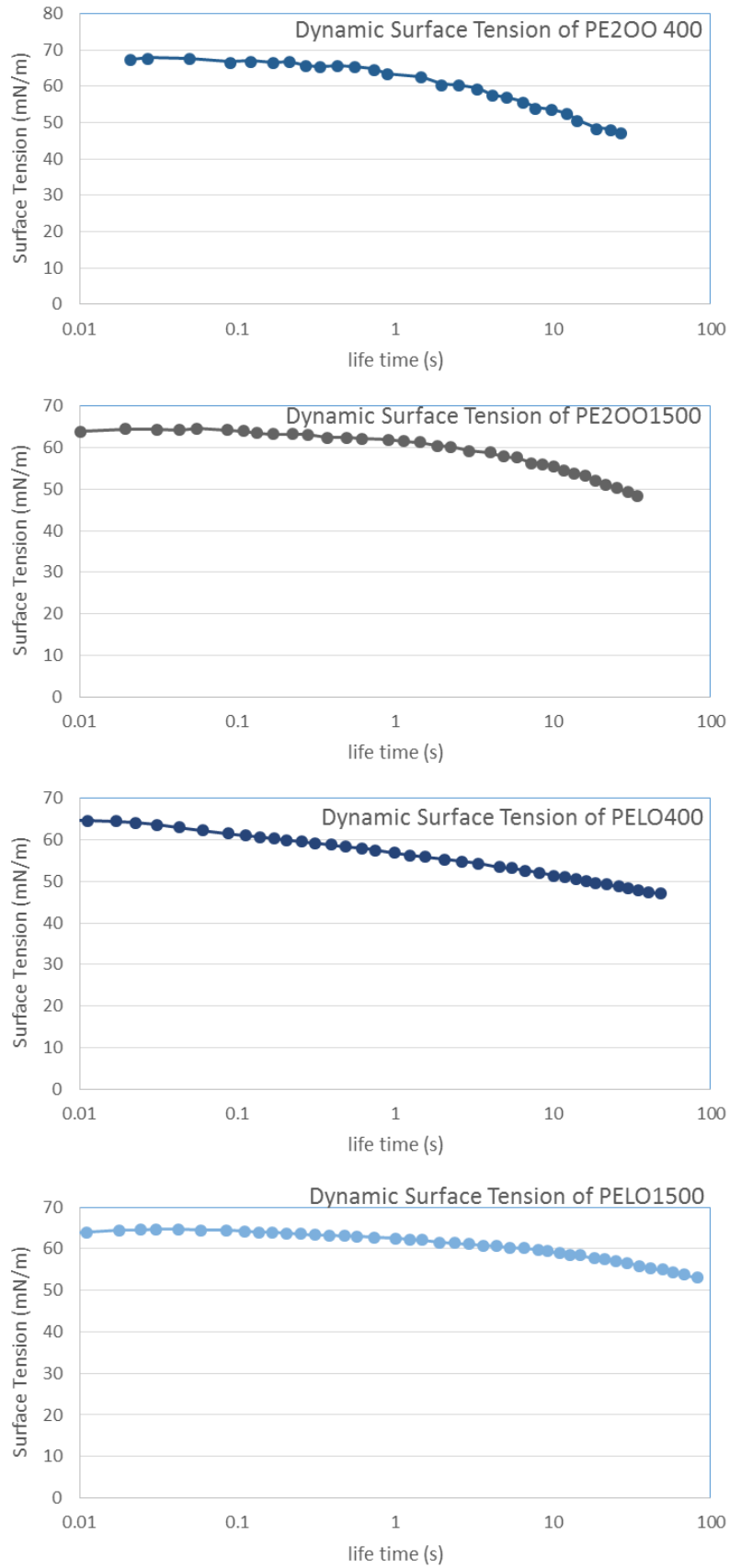


Figure 5- 3 Dynamic surface tension of unpurified PELO 400, PELO 1500, PE2OO 400 and PE2OO 1500 surfactants

5.2.2 Equilibrium surface tension of synthesised surfactants

Measurements of equilibrium surface tension on a Kruss K100 tensiometer showed the variation between the surface tension and change in surfactant concentration. A surfactant solution of 1 mg/ml was prepared and diluted by the instrument while changes in surface tension were measured. Dilution was not extended to a concentration low enough to reach the surface tension of water (72 mN/m) for all measurements. Results are shown in Figure 5-4 and 5-5. For most of the unpurified surfactants, CMC and other related parameters (efficiency and effectiveness) could not be determined as the surfactant could not reach equilibrium, although surface tension did lower to around 32 mN/m for most samples. The efficiency of a surfactant is the concentration needed to attain a certain surface tension reduction usually 20 mN/m and is designated as C_{20} .¹⁴² The effectiveness of a surfactant is linked to the surface tension reduction at CMC, that is, the difference between the surface tension of water and surface tension at CMC. A sharp decrease in surface tension with increase in surfactant concentration shows that the surfactant is effective whereas a minimum slow decrease in surface tension with increasing concentration shows that the surfactant is efficient. The effectiveness of a surfactant is related to its detergency, which is, cleaning capacity. Detergency increases with surfactant concentration up to the CMC.

CMC values obtained for PEEO 400 was approximately 0.1 mg/ml respectively while that of PEMO 400 was inconclusive as a result of jumps in the curve producing two possibilities as shown in Figure 5-4. Surface active impurity either in the surfactants or arising from the instrument (on the Wilhelmy plate, in the beaker) was supposedly responsible for the jumps in the surface tension versus concentration curves. Residual Adogen 464 (the phase transfer catalyst from the epoxidation steps), saturated alkyl oleates and PEGs are the suspected surface active impurities in the original surfactants. Hydrophobic impurities in a surfactant sample normally cause a minimum in the curve. Since such curves were not observed it suggests the

impurities were not the saturated esters. Their significantly low concentration in the synthesised epoxide is another obvious reason for this. The presence of hydrophilic impurities like PEG, glucose and other sugars does not significantly affect the physicochemical behaviours of a surfactant.¹⁴² The purification process and subsequent analysis of the surfactants is discussed in chapter 4.

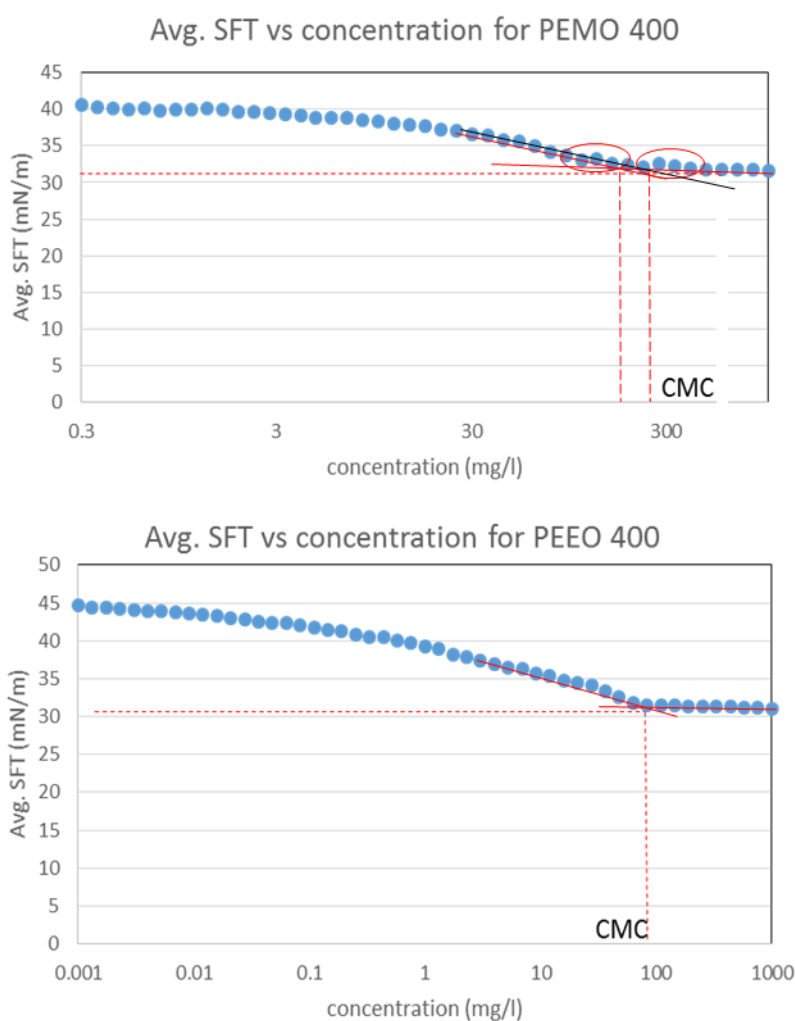


Figure 5- 4 Surface tension versus the logarithm of surfactant concentration for unpurified PEMO 400 (1 mg/ml) and PEEO 400 (1 mg/ml) surfactants at ~26 °C.

Results for the purified samples are shown in Figure 5-5 and compared with those of unpurified surfactants (Figure 5-4). The surface tension vs concentration curves for both purified and unpurified PEEO 400 surfactants showed that surface tension at 0.001 mg/l concentration was higher in the former (58 mN/m) than in the latter (45 mN/m) as a result of the removal of the surface active impurities. The same trend was observed in the purified and unpurified PEMO 400 surfactants curves in

which surface tension increased from around 40 mN/m to over 46 mN/m at 0.3 mg/l concentration after removing the impurities.

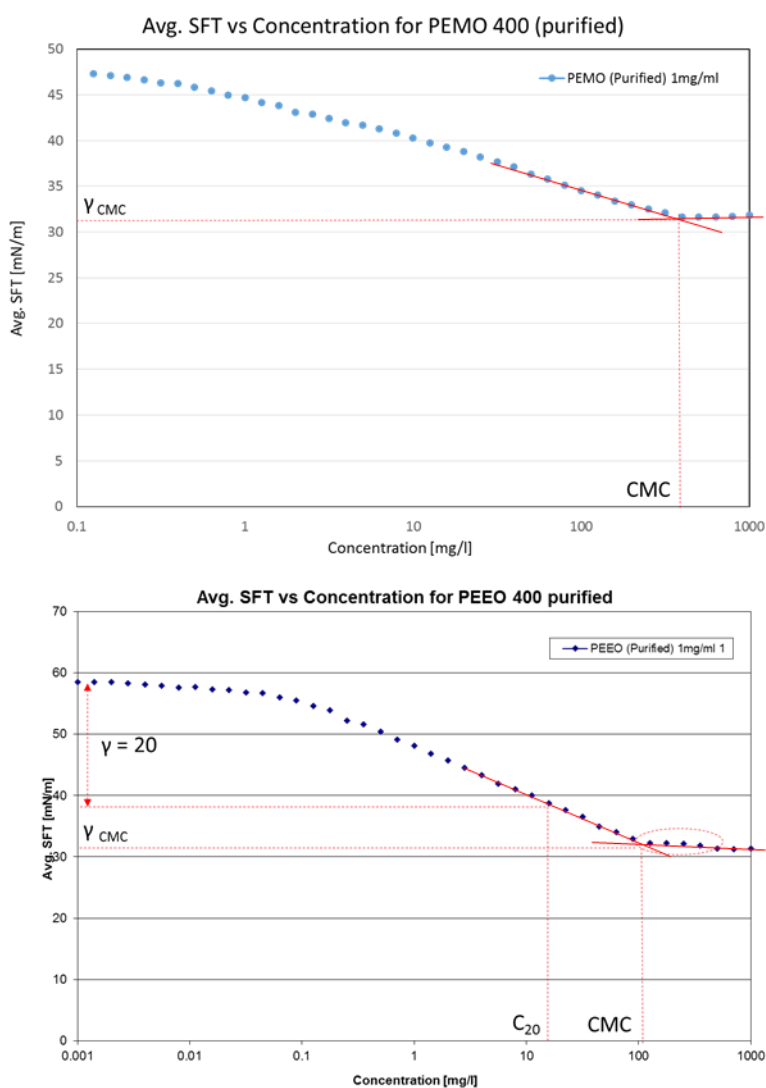


Figure 5- 5 Surface tension versus the logarithm of surfactant concentration for purified PEMO 400 (1 mg/ ml) and PEE0 400 (1 mg/ml) surfactants at ~26 °C. The circled area indicates a jump in the curve due to Wilhelmy plate.

CMC for both purified PEMO 400 and PEE0 400 were ~0.7 mg/ml and ~0.1 mg/ml respectively; close to what was recorded for the unpurified samples. With both having the same hydrophilic head group, CMC is eight times lower in PEE0 400 with an addition of one CH₂ to the hydrophobic tail. This observed factor of seven reduction is far more than a factor of about three that Traube's rule states on adding one CH₂ group to nonionics.^{142, 355, 356} Structural difference in surfactant types could be the likely reason for this observation. Most surfactants with EO either have this

group attached to the alcohol or ester end, whereas our surfactants have hydrophobic group further attached to the ester end. However, it is not obvious how this is linked with surface tension and CMC reduction. With a lower CMC, PEEO 400 is a better surfactant than PEO 400 depending on their area of application. Both PEEO 400 and PEO 400 surfactants have an effectiveness of ~ 40.5 mN/m when extended to the surface tension of water (Figure 5-5). Efficiency could not be evaluated for PEO 400 (unless if concentration is extended) but PEEO 400 recorded an efficiency of 0.018 mg/ml, that is, the concentration required to reduce solution surface tension by 20 mN/m. This value is similar to what is obtainable in commercial non-ionic surfactants.³⁵⁷

CMC is both sensitive to alkyl chain length and EO number in polymeric surfactants. However, it is more sensitive to an increase in alkyl chain length than an increase in EO number.¹⁴² It therefore means, for other surfactants where measurements were not taken, CMC could still be speculated based on the values obtained for PEO 400 and PEEO 400 where EO number is 9. CMC values will vary significantly for all surfactants having the same EO number, for example when EO number is 9, but a change in CMC that is not of this magnitude will be expected for those having the same alkyl chain length as we move from 9 to 16 and from 22 to 34.

Another major factor worth discussing with respect to a surfactant's behaviour at a surface is the critical packing parameter (CPP) or surfactant number which is the volume of surfactant hydrophobe divided by the product of the area of the hydrophilic group and the extended length of the surfactant hydrophobe as depicted in Figure 5-6. It implies that as the EO number increases the area occupied per hydrophilic group increases and consequently the CPP decreases. Studies have shown that surfactants with shorter EO chains pack better at the surface (liquid-air interface) with effectiveness increasing as EO number decreases,³⁵⁸ and for nonionics CPP increases with increasing temperature.³⁵⁹ This means at higher

temperature, EO chains compress and pack well at the surface and are able to accommodate more surfactant molecules resulting in higher effectiveness.

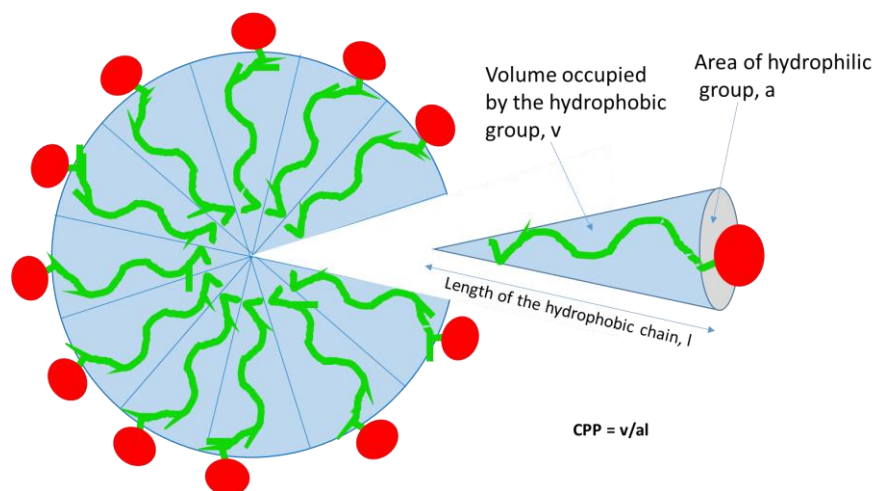


Figure 5- 6 Packing of surfactant molecules at the surface relates to the structure and geometry of the surfactant. Critical packing parameter (CPP) relates the volume of the hydrophobic group, v ; area of the hydrophilic group, a ; and the length of the surfactant, l as $CPP = v/al$.³⁶⁰

5.2.3 Emulsion formation

An emulsion is formed from two immiscible liquids in which one is being dispersed as a multitude of small particles or droplets in the other. The liquid which forms small particles in the other is called the dispersed phase while the surrounding liquid in which the other is preferentially dispersed is called the continuous phase. An emulsion can be of two types: oil-in-water (O/W) and water-in-oil (W/O). Examples of these are commonplace including margarines (W/O), paints (O/W) and milk (O/W). The disperse phase will in a short time separate from the continuous phase resulting in two immiscible liquid layers again. High emulsion stability under a variety of conditions is a requirement in such products as these. Good practise in formulation is to therefore stabilize the emulsion with a surfactant (an emulsifier).

The first set of surfactants synthesised from ~76% purity oleic acid were tested for emulsion formation by shaking 25 mg surfactant in 0.5 mL toluene and 0.5 mL

distilled water. This formulation, that is 50% each of water and oil, is noted to be of higher standard compared to the technical emulsion (25-50% dispersed phase).¹⁴² Emulsions formed were assessed 20 days (Figure 5-7a) after they were prepared and grouped into four categories on the basis of their visual stability namely: very stable, stable, slightly stable and unstable emulsions. The very stable emulsions were those that remained very milky and had no visible sign of phasing out (Figure 5-7b). The stable emulsions were milky but had a slight, non-conspicuous trace of phasing out at the bottom (Figure 5-7c). The slightly stable emulsions were also milky but had a distinct appearance of phasing out (Figure 5-7d). In the unstable emulsions, there was a pronounced separation into slightly clear and milky phases (Figure 5-7e).

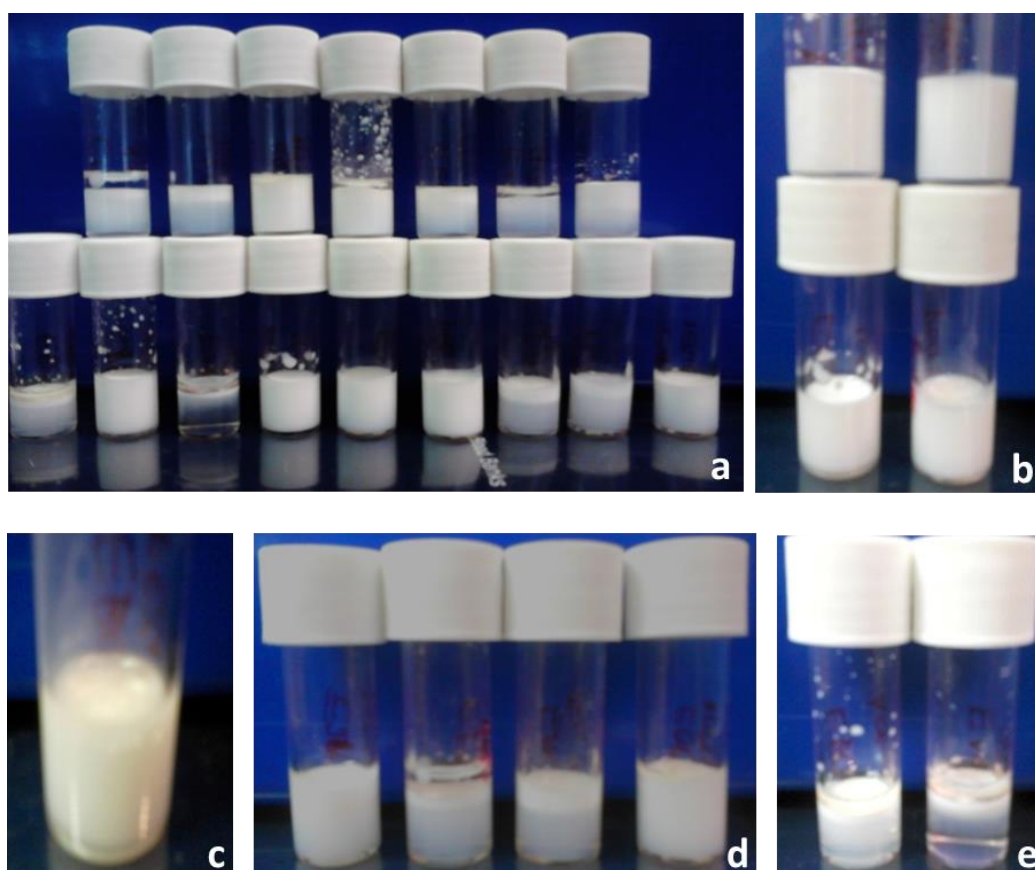


Figure 5- 7 Emulsions after 20 days (a) formed from toluene (50 v%) and water (50 v%) were grouped into (b) very stable emulsion, (c) stable emulsion, (d) slightly stable emulsion and (e) unstable emulsion

Table 5-1 shows the variation of ranking of the emulsion stability of surfactants with hydrophobic carbon chain and PEG chain length. The trend of emulsion stability observed with increasing hydrophobic or hydrophilic length was however not consistent. Actually, as hydrophobicity increases a surfactant molecule adsorbs more strongly at the surface resulting in higher stability. Increasing hydrophobicity and hydrophilicity simultaneously will lead to solidification of the surfactant which causes insolubility.¹⁴² With the composition of our emulsion (50% dispersed phase), an O/W or a W/O emulsion could be formed depending on temperature and surfactant structural geometry. The packing of surfactant at the interface is also important in determining their emulsion stability. The higher the value of CPP the more space occupied by the surfactant tail on the oil phase. Such surfactants will give a W/O emulsion. Surfactants with higher EO number will occupy more space in water and will preferentially result in an O/W emulsion. This is in a way related to Bancroft's rule which states that the phase in which the surfactant is most stable will be the continuous phase.³⁶¹

From Table 5-1, it was observed across the row for C-19, C-20, C-21' and C-22' that stability increased with increasing EO number because as PEG chain increases across a fixed hydrophobic group there will be increased solubility and partitioning in water. Down the table at a fixed EO number, it was expected that stability will increase as a result of increasing hydrophobicity. It was however noted that the trend was not consistent for some of the surfactants across the row and down the table. This could be due to observational error during ranking or linked to the previously described impurities in the surfactants.

Table 5- 1 Emulsion ranking based on variation between hydrophobic chain length and PEG chain length as (1) very stable emulsion (2) stable emulsion (3) slightly stable emulsion (4) unstable emulsion

Alkyl oleate	Hydrophobic chain length	PEG type		
		400	1000	1500
Methyl oleate	C-19	4	3	3
Ethyl oleate	C-20	3	2	2
1-propyl oleate	C-21	4	1	3
2-propyl oleate	C-21'	3	1	1
1-butyl oleate	C-22	3	3	4
2-butyl oleate	C-22'	3	1	1
1-octyl oleate	C-26	3	1	4
2-octyl oleate	C-26'	3	4	4

5.2.4 Surfactant self-assembly

At concentrations above the CMC, the surfactant molecules begin to self-associate in solution to form aggregates of various dimensions. This property of a surfactant is called self-assembly. The first of these aggregates to be formed in a solution are generally of spherical shape and are called micelles (Figure 5-8). The shape and size of aggregate formed depends on the structure and concentration of surfactants and temperature among others. At higher surfactant concentration micelles will change from spherical to rod-like or thread-like shape. Micellar growth in nonionics varies strongly with EO chain length. Growth is much more pronounced in surfactants with shorter EO chain length than those with higher EO number. Increasing temperature in nonionics leads to higher micellar growth to such an extent that the solution become cloudy. The temperature at which this occurs is called the cloud point. The size of a micelle can be determined by passing light through such cloudy solution.

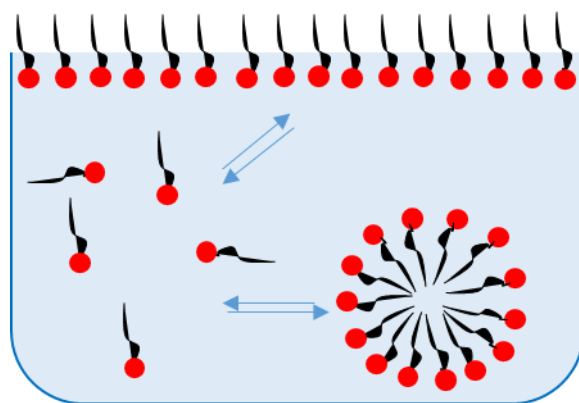


Figure 5- 8 Formation of micelles from the aggregation of surfactant molecules in the bulk solution after CMC is attained.

Dynamic light scattering (DLS) study of purified PEMO 400 and PEEO 400 surfactants showed that the former was micellar above 0.5 mg/ml, with aggregates around 1-10 nm in diameter while the latter did not seem to show any aggregates under DLS.

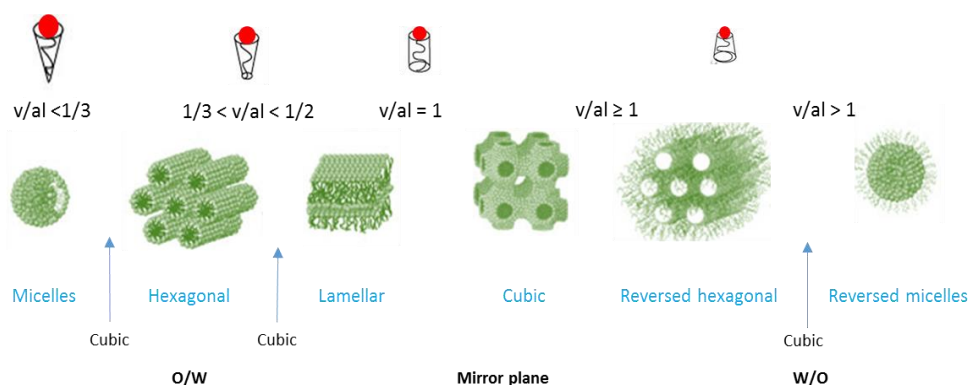


Figure 5- 9 Prediction of structures of self-assembled surfactants in aqueous solutions based on critical packing parameters.^{142, 362}

Using CPP, micellar shapes can be predicted for the synthesised surfactants based on their structure and geometry as shown in Figure 5-9. Surfactants with higher EO number will have higher area per group and consequently are more likely to form spherical micelles while those with lower EO number will more likely form lamellae. The implication is that surfactants with PEG 1500 and 1000 are more likely to form spherical or cylindrical micelles than those with PEG 400 and 750 of similar size with their hydrophobic length while surfactants with PEG 400 having C-26 and C-28 hydrophobic length will more likely favour bilayer or lamellae micelles than those

of C-19 as shown in Figure 5-10. The CPP of a surfactant is related to its detergency; and surfactants demonstrate their best detergency at CPP values close to 1.³⁶³

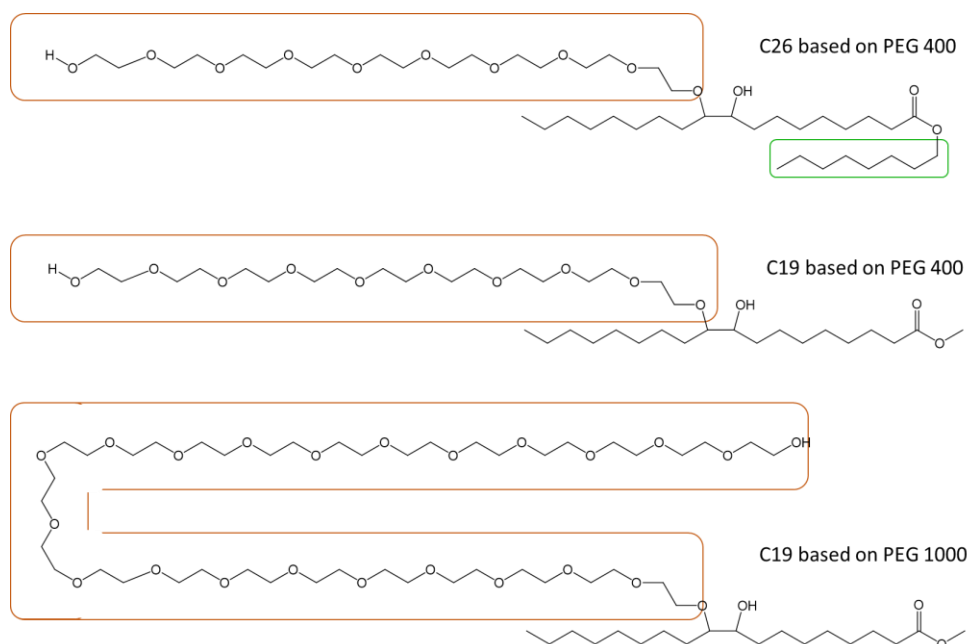


Figure 5- 10 Predicting aggregate shape in surfactants based on CPP in variation with PEG length and alkyl chain length.

5.3 Hydrophilic-Lipophilic Balance (HLB): Potential application of synthesised surfactants

The amphiphilic nature of a surfactant can also be expressed in terms of hydrophilic-lipophilic balance (HLB) in addition to grouping them on the basis of their ionization in solution as discussed in chapter 1. The HLB concept, initiated by Griffin,³⁶⁴ is a very important tool that expresses the partitioning tendency of the hydrophilic and lipophilic ends of surfactants in an O/W or a W/O emulsion. This partitioning is believed to affect the physicochemical behaviours of these surface active agents and therefore can be applied to predict the potential application for a surfactant. Table 5-2 shows HLB values and their likely areas of applications. From this table it is obvious that water soluble surfactants have an HLB value higher than 13 and those with poor or zero dispersion in water have HBL values less than 6.

Table 5-2 HLB ranges and applications ^{365, 366}

<i>HLB range</i>	<i>Application</i>
3.5-6	Water in oil emulsifier
7-9	Wetting agent
8-15	Oil in water emulsifier
13-15	Detergent
15-18	Solubilizer

Since proposed in 1949, the HLB concept has been modified by many authors in order to develop a reproducible method that is consistent with experimental data.³⁶⁷⁻³⁷⁰ For instance, the original method by Griffin could not be applied correctly for non-ionic surfactants containing propylene oxide, butylene oxide, nitrogen or sulphur which exhibit special characteristics and whose HLB values must be experimentally determined.^{368, 371, 372} Among the new methods introduced, Davies' method has been the most preferred as group numbers were assigned to individual lipophilic and hydrophilic regions in a surfactant.³⁶⁸ However, for most non-ionic surfactants containing polyethylene oxide (EO) chain as the main hydrophilic group, HLB values obtained using Davies' method did not perfectly agree with experimental data.³⁷³ Improving on his method to address the flaws, Guo *et al* introduced an effective chain length (ECL) method which uses a contributive effect of the same group in a continuous chain rather than treating them as an individual group.³⁷⁴ HLB values obtained for non-ionic surfactants using this method are more precise and have less average errors in comparison with experimental data. According to Guo *et al*, for surfactants having polyethylene oxide (EO) groups, HLB is expressed as:

$$\text{HLB} = 7 + (\text{GN}_{\text{EO}} \times \text{N}_{\text{EO eff}}) + (\text{GN}_{\text{CH}_2} \times \text{N}_{\text{CH}_2 \text{ eff}}) + \Sigma (\text{other hydrophilic groups}) \\ + \Sigma (\text{other lipophilic groups})$$

$$N_{EO \text{ eff}} = 13.45 \ln(N_{EO}) - 0.16 N_{EO} + 1.26$$

$$N_{CH_2 \text{ eff}} = 0.965 N_{CH_2} - 0.178$$

Where GN_{EO} is the group number of EO, $N_{EO \text{ eff}}$ is effective number of EO units; and N_{EO} is number of EO units in the surfactant while

GN_{CH_2} is the group number of CH_2 , $N_{CH_2 \text{ eff}}$ is effective number of CH_2 units; and N_{CH_2} is the number of CH_2 units in the surfactant.

The group numbers assigned to each of these moieties are shown in Table 5-3 according to Guo *et al.*³⁷⁴ Based on these group numbers, HLB values were obtained for the surfactants synthesised in chapter 4.

In all HLB calculations involving surfactants with uncapped PEGs, for instance, PEMO 400 surfactant, five groups were identified: -OH, -CH₂CH₂O- (EO), -CH₂CH₂OH (PEG end group), -CH₂, and -COO groups (Figure 5-11). The methyl group attached to the ester is also treated as a lipophilic group and added to the CH₂ group.

Table 5- 3 Group numbers for different functionalities according to ECL method

<i>Hydrophilic end</i>	<i>Group number</i>	<i>Lipophilic end</i>	<i>Group number</i>
Ester (free)	2.316	-CH ₂ -	-0.475
-OH (free)	2.255	-CH ₃	-0.475
-CH ₂ CH ₂ OH	0.479	-CH-	-0.475
-CH ₂ CH ₂ O-	0.33	=CH-	-0.475
Ester (sorbitan)	11.062	sorbitan ring	-20.565
-OH (sorbitan)	5.148		
-CH ₂ OH	0.724		

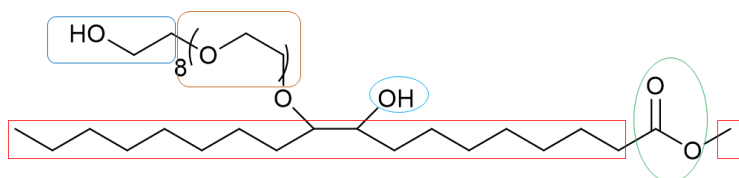


Figure 5- 11 Hydrophilic and hydrophobic groups in PEO 400 surfactant

For PEO 400 surfactant HLB calculation we have:

$$GN_{EO} = 0.33; GN_{CH_2} = -0.475; GN_{COO} = 2.316; GN_{OH} = 2.255; GN_{EOH} = 0.479,$$

$$N_{EO} = 8, N_{CH_2} = 18$$

$$N_{EO\text{ eff}} = 13.45 \ln(N_{EO}) - 0.16 N_{EO} + 1.26$$

$$= 13.45 \ln(8) - (0.16 \times 8) + 1.26$$

$$= 27.948$$

$$N_{CH_2\text{ eff}} = 0.965 N_{CH_2} - 0.178$$

$$= 0.965 \times 18 - 0.178$$

$$= 17.192$$

$$HLB = 7 + (GN_{EO} \times N_{EO\text{ eff}}) + (GN_{CH_2} \times N_{CH_2\text{ eff}}) + \Sigma (\text{other hydrophilic groups}) \\ + \Sigma (\text{other lipophilic groups})$$

$$= 7 + (GN_{EO} \times N_{EO\text{ eff}}) + (GN_{CH_2} \times N_{CH_2\text{ eff}}) + GN_{COO} + GN_{OH} + GN_{EOH}$$

$$= 7 + (0.33 \times 27.948) + (-0.475 \times 17.192) + 2.316 + 2.255 + 0.479$$

$$= 13.11$$

In all HLB calculations involving surfactants with capped PEGs, that is, MePEG 400 and MePEG 750, five groups were also identified: -OH, -CH₂CH₂O- (EO), -CH₃ (PEG end group), -CH₂, and -COO groups as shown in Figure 5-12. The methyl group attached to the ester group is also treated as a lipophilic group and added to the CH₂ group whereas the -CH₃ attached to MePEG was treated separately since the hydrophilicity of EO may affect its contribution differently from those of the fatty acid esters.

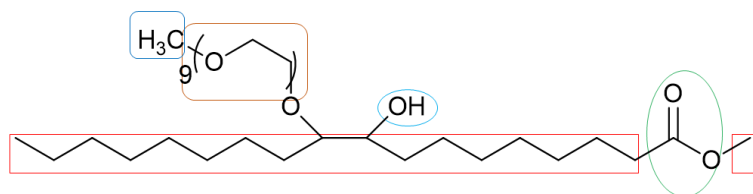


Figure 5- 12 Hydrophilic and hydrophobic groups in MPEMO 400 surfactant

For MPEMO 400 surfactant HLB value was derived as follows:

$$GN_{EO} = 0.33; GN_{CH_2} = -0.475; GN_{COO} = 2.316; GN_{OH} = 2.255; GN_{CH_3} = -0.475,$$

$$N_{EO} = 9, N_{CH_2} = 18$$

$$N_{EO\text{ eff}} = 13.45 \ln(N_{EO}) - 0.16 N_{EO} + 1.26$$

$$= 13.45 \ln(9) - (0.16 \times 9) + 1.26$$

$$= 29.3727$$

$$N_{CH_2\text{ eff}} = 0.965 N_{CH_2} - 0.178$$

$$= 0.965 \times 18 - 0.178$$

$$= 17.192$$

$$HLB = 7 + (GN_{EO} \times N_{EO\text{ eff}}) + (GN_{CH_2} \times N_{CH_2\text{ eff}}) + \Sigma (\text{other hydrophilic groups}) \\ + \Sigma (\text{other lipophilic groups})$$

$$= 7 + (GN_{EO} \times N_{EO\text{ eff}}) + (GN_{CH_2} \times N_{CH_2\text{ eff}}) + GN_{COO} + GN_{OH} + GN_{CH_3}$$

$$= 7 + (0.33 \times 29.3727) + (-0.475 \times 17.192) + 2.316 + 2.255 - 0.475$$

$$= 12.62$$

HLB was calculated for other alkyl oleate based surfactants as done for PEO 400 and MPEMO 400 surfactants above using ECL method and results are presented in Figure 5-13 to 5-17. Results show that HLB values decrease with increasing alkyl group in the fatty chain but increase with increasing EO number in the hydrophilic head. Based on the HLB values in Figures 5-13 to 5-15 in comparison with the HLB range in Table 5-2, surfactants with PEG 400, MePEG 400 and MePEG 750 (EO number 9 and 16) will likely find applications as either oil-in water emulsifiers or

detergents. Surfactants with higher EO number (PEG 1000) spread between three potential applications. From PEO 1000 to PE2BO 1000 with HLB values between 16.70 and 15.33 potential application will be as solubilizing agents while PEO 1000, PE2OO 1000 and PEDO 1000 surfactants have potentials as either oil-in water emulsifiers or detergents (Figure 5-16). Surfactants with PEG 1500 attached also have three potential applications. The methyl-, ethyl-, 1-propyl-, 2-propyl-, 1-butyl- and 2-butyl-oleate PEGylated surfactants will most likely find application as solubilizing agents while the 1-octyl-, 2-octyl- and 1-decyl-oleate PEGylated surfactants have potentials as oil-in water emulsifiers and detergents (Figure 5-17).

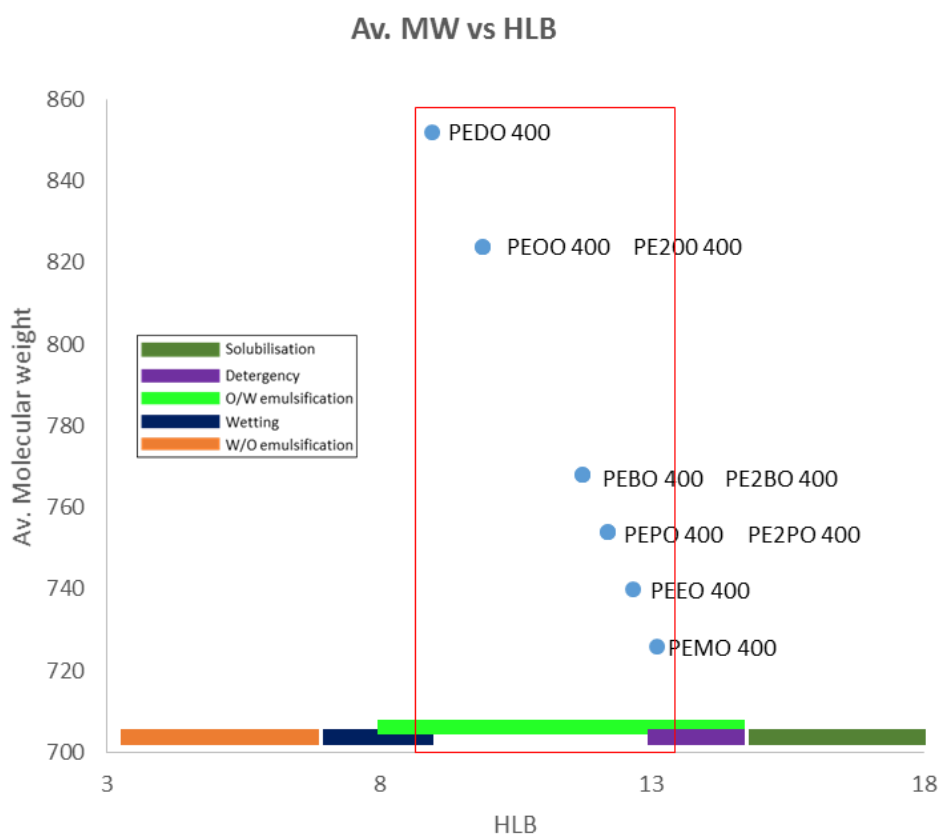


Figure 5- 13 HLB values and average molecular weight obtained for alkyl oleate surfactants based on PEG 400

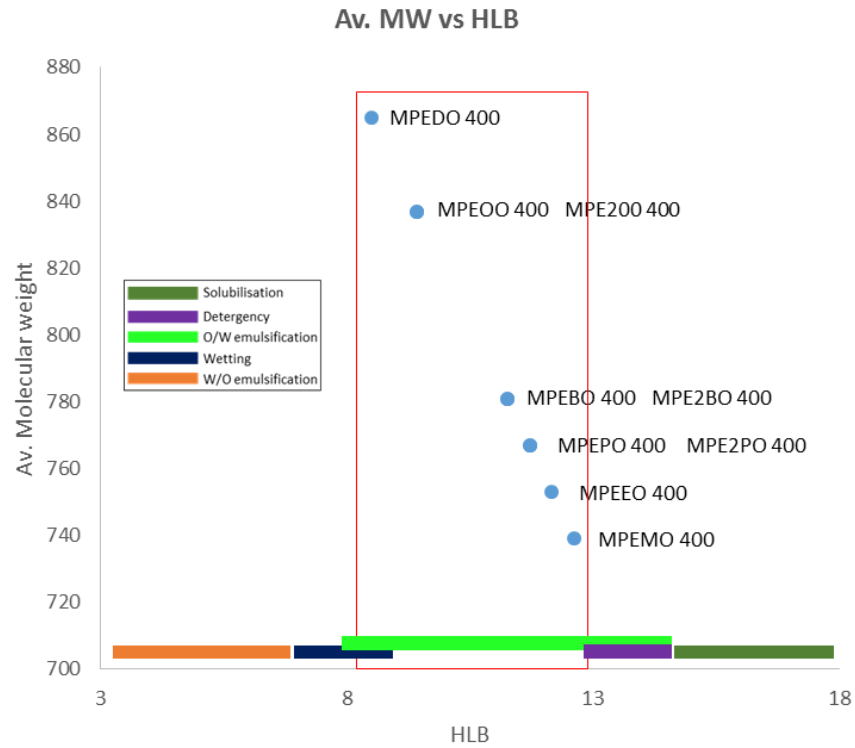


Figure 5- 14 HLB values and average molecular weight obtained for alkyl oleate surfactants based on MePEG 400

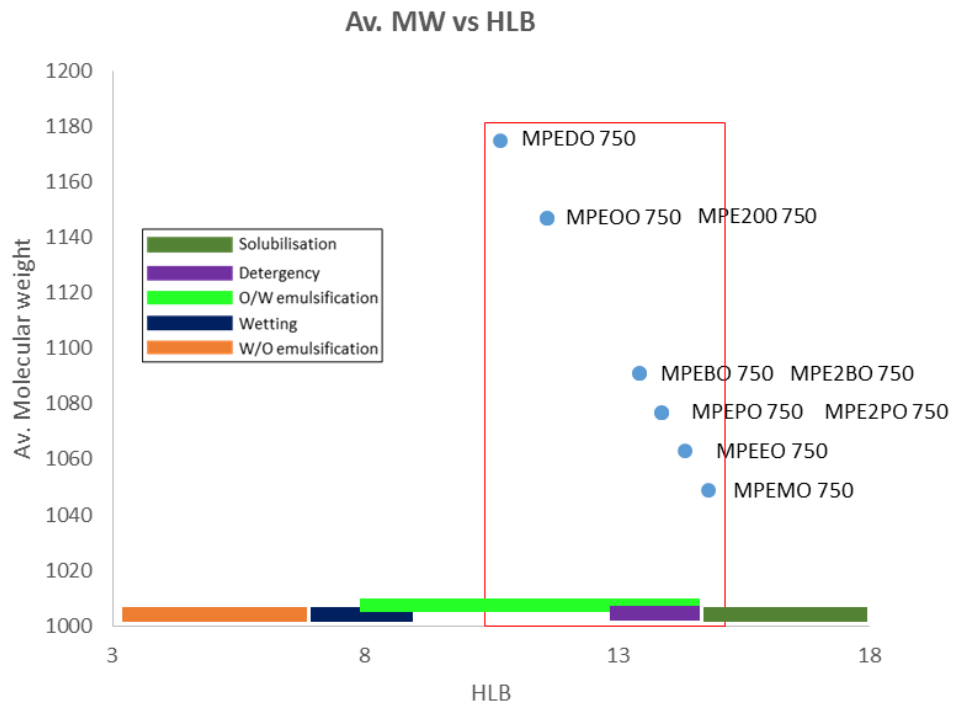


Figure 5- 15 HLB values and average molecular weight obtained for alkyl oleate surfactants based on MePEG 750

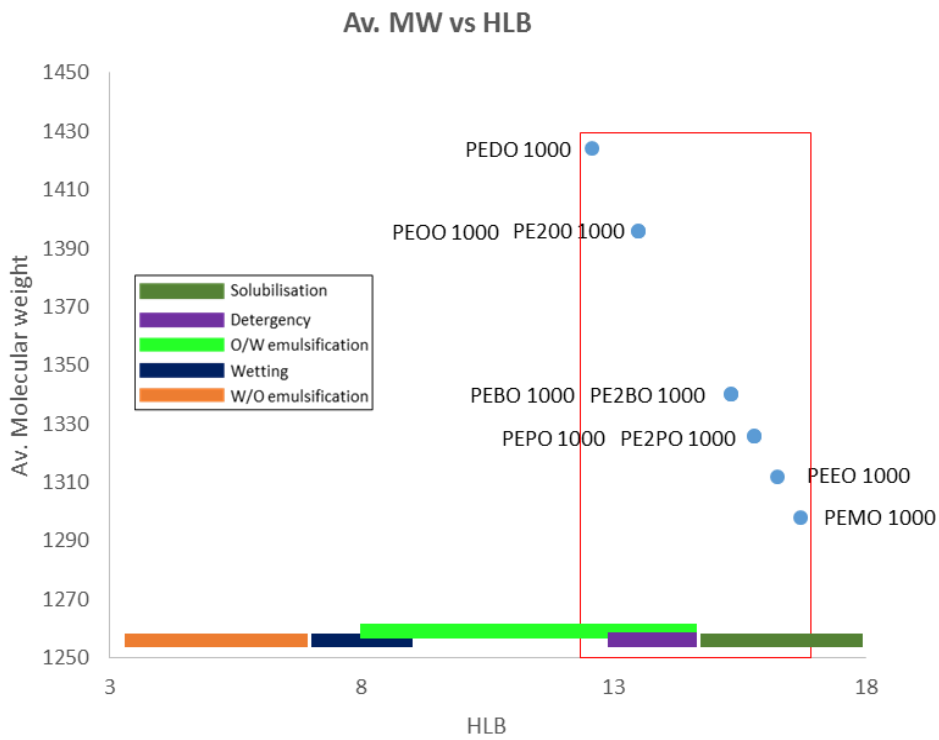


Figure 5- 16 HLB values and average molecular weight obtained for alkyl oleate surfactants based on PEG 1000

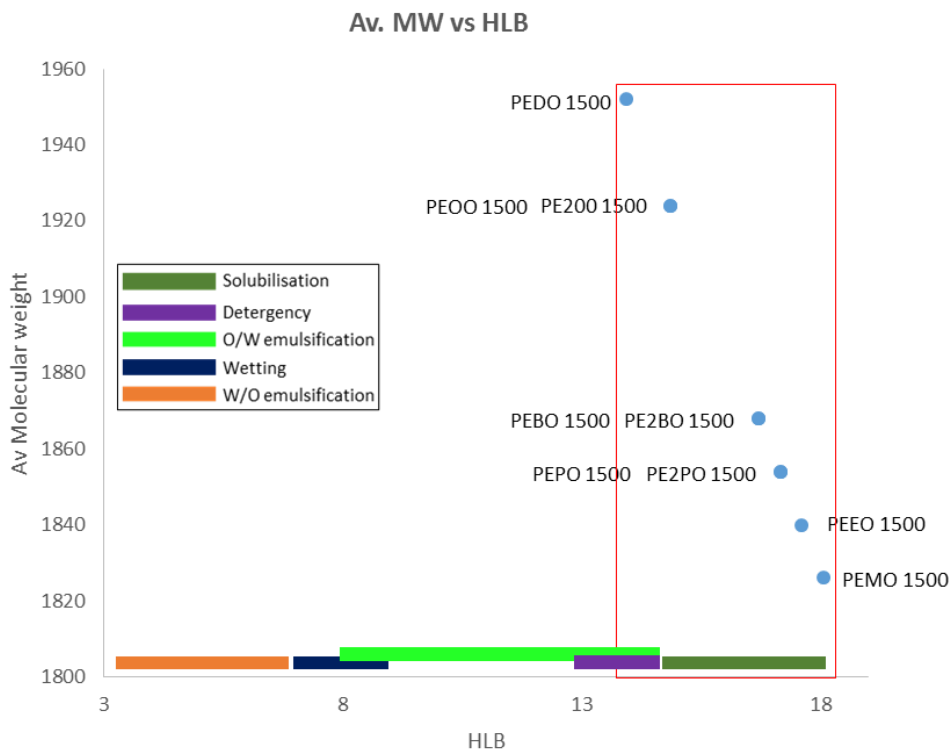


Figure 5- 17 HLB values and average molecular weight obtained for alkyl oleate surfactants based on PEG 1500

Although HLB values obtained for isomeric surfactants of the same EO chain length, for example, 1-propyl oleate and 2-propyl oleate based surfactants, showed no obvious difference, their arrangement and interaction at the interface will likely be different, and it is believed CPP values will be different for these surfactants.

As Davies and ECL method have not assigned a group number to the glucose ring, HLB for sophorolipid based surfactants was obtained using Griffin's equation.

$$\text{HLB} = \frac{\text{Molecular weight of hydrophilic group}}{\text{Molecular weight of surfactant}} \times 20$$

The hydrophilic groups in a typical sophorolipid-based surfactant are as shown in Figure 5-18. The ether on the glycosidic bond and those in the sophorose can act as sites for hydration by water molecules just as it does in the PEG and as such included in the hydrophilic group.

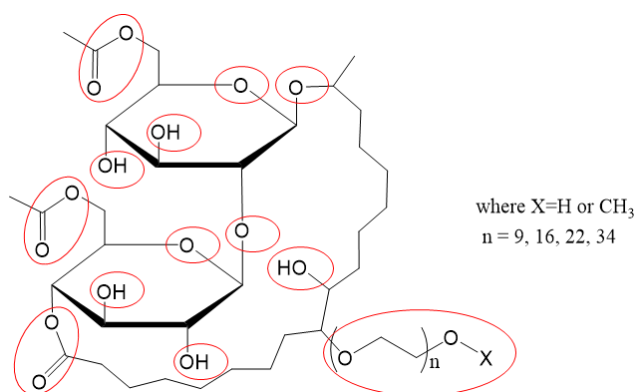


Figure 5- 18 Hydrophilic groups in sophorolipid-based surfactants

For PELSL 400, HLB was calculated as:

$$\begin{aligned} \text{HLB} &= \frac{\text{Mass of PEG 400} + \text{mass of OHs} + \text{mass of ether groups} + \text{mass of ester groups}}{\text{Molecular weight of surfactant}} \times 20 \\ &= \frac{414 + 85 + 132 + 64}{1135} \times 20 \\ &= \frac{695}{1135} \times 20 \\ &= 12.25 \end{aligned}$$

HLB was calculated for other sophorolipid-based surfactants in the same way. For HLB calculation involving surfactants with capped PEGs, the methyl group at the PEG end was included in the hydrophobic group. Results presented in Figure 5-19 show that the non-PEGylated epoxidised lactonic sophorolipid could serve as a wetting agent while PELSL 400, MPELSL 400, MPELSL 750 and PELSL 1000 could have application as oil-in water emulsifiers. MPELSL 750 and PELSL 1000 could also be used in detergency while PELSL 1500 could be applied as solubilising agents.

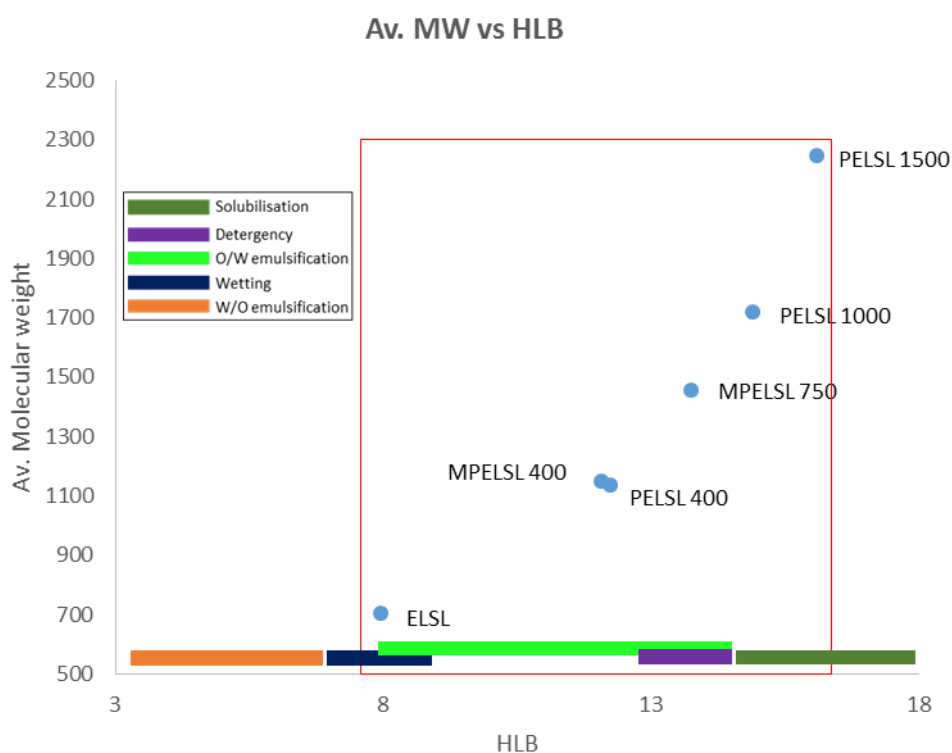


Figure 5- 19 HLB values and average molecular weight obtained for sophorolipid-based surfactants

5.4 Conclusions

Attempts were made to assess some of the physicochemical behaviours of synthesised surfactants at Unilever PLC, Liverpool, UK. Although results of measurements were not available at the time of completing this chapter, preliminary studies covering tensiometry, micelle size determination and emulsion formation were earlier investigated on some of the samples. Additionally, concepts

such as HLB and CPP were also used to assess the surfactants and predict their potential applications. Dynamic surface tension studies revealed that the lower molecular weight surfactants were more spontaneous in reaching equilibrium than the higher molecular weight surfactants. Although diffusion-limited (as a result of their high molecular weight), the latter will adsorb more strongly at the interface on attaining equilibrium. Equilibrium surface tension measurements showed the surfactants have low CMCs (0.1-0.7 mg/ml) and are efficient and effective. DLS study showed one of the surfactants as micellar aggregates above CMC. The surfactants formed emulsions of varying stability depending on their molecular weight and chemical structure. These initial results do clearly demonstrate that the synthesised surfactants have suitable properties for use in formulations, and that structure variation has altered these properties accordingly. Based on theoretical HLB results the family of synthesised surfactants will potentially find applications as oil-in water emulsifiers, detergents, solubilisers and wetting agents, their final use being heavily dependent on the structure (size of alkyl group on ester and length of PEG chain).

Towards a 100% Bio-derived Poly(ethylene terephthalate)

Chapter 6

6.0 Towards a 100% bio-derived poly(ethylene terephthalate)

6.1 Introduction

As discussed in chapter 1, the polymer industry is being faced with challenges of product biodegradability and use of petrochemical feedstock. Much efforts are being made to manufacture more polymers based on renewable resources. Importantly, polyethylene terephthalate (PET) is one polymer product attracting significant attention in academia and industry to be made completely bio-based. In fact many packaging industries are competing to make the first 100% bio-based PET.^{116, 129} PET is a plastic derived from the esterification of terephthalic acid (TA), or transesterification of dialkyl terephthalate, with ethylene glycol (EG) shown in Figure 6-1.

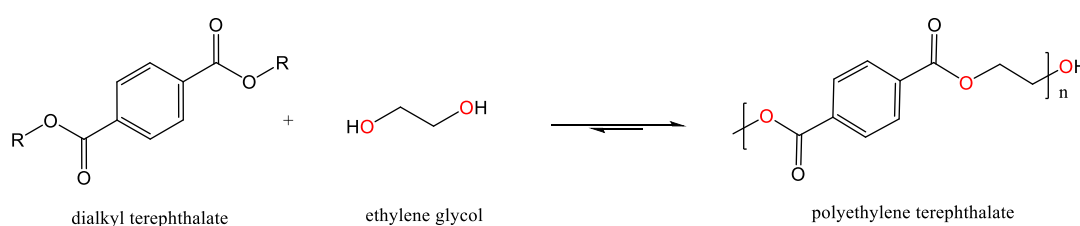


Figure 6- 1 Synthesis of PET from transesterification of dialkyl terephthalate with EG

PET has several characteristics that make it ideal for use in packaging applications, which include durability, high resistance to oxygen and water,³⁷⁵ low weight to filling volume,³⁷⁶ low permeability to gas and non-toxicity to human among others.^{377, 378} It is also widely used for fabrics in the textile industry (Figure 6-2). Current global PET production is well in excess of 80 million tonnes per annum, with fibre, films, sheets and packaging included.^{379,131} Advantageously, it is easy to recycle PET either *via* melting and reforming or *via* depolymerisation (hydrolysis, alcoholysis or glycolysis) to reform the constituent monomer units.^{376, 377, 380-384} Recycling of PET does not result in the total loss of mechanical properties, so can therefore be reused many times reducing gas emissions and saving energy.^{380, 385}

More than the ease of its recycling a sustainable process for the production of PET from biomass is also desirable. Cellulose is the most abundant constituent of biomass with ca. 220 million tonnes cellulose waste produced annually alone in the Europe,⁹⁹ and therefore is the most attractive feedstock for the synthesis of bio-PET.

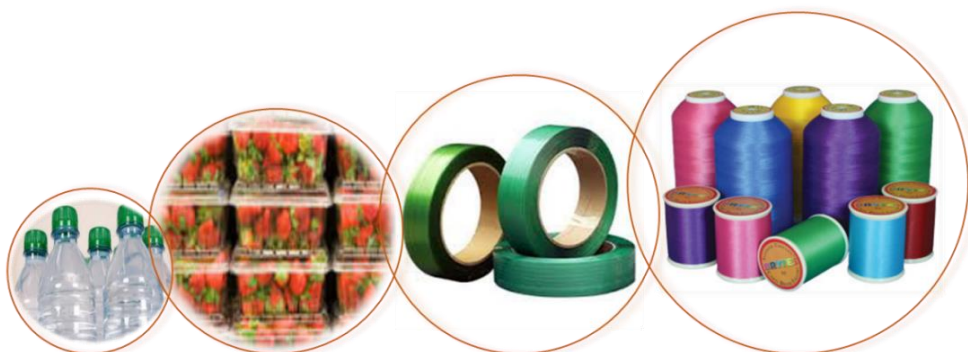


Figure 6- 2 Example applications of PET in packaging and textiles

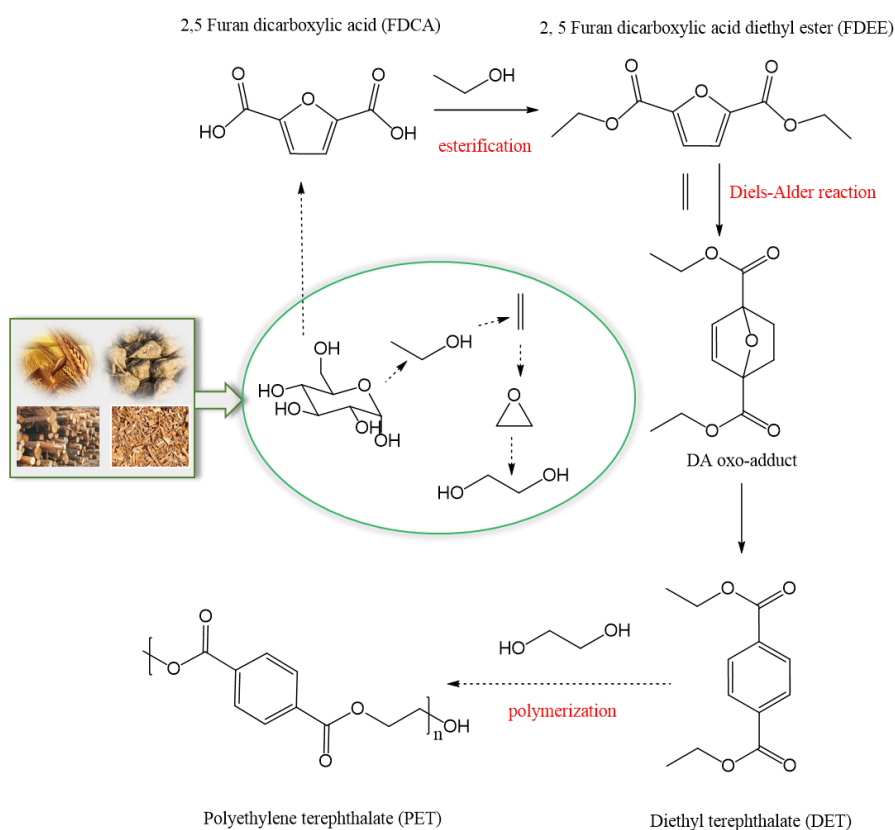


Figure 6- 3 Synthetic route to 100% bio-derived PET via transesterification of bio-based EG with bio-based DET.

In chapter 1 section 1.4 some of the main routes to bio-based PET reported in the literature were discussed, most of which involved Diels-Alder addition reactions. Here in chapter 6 we report the synthesis of diethyl terephthalate (DET) from renewable resources (2, 5-furan dicarboxylic acid, FDCA) as a bio-based monomer for production of 100% bio-derived PET. The synthetic route followed is shown in Figure 6-3. Factors affecting DET yield optimisation were considered and a comparison of main routes to bio-PET through cellulose and hemicellulose based on green metrics are also reported below.

6.2 Synthesis of 2,5-furan dicarboxylic acid diethyl ester (FDEE)

2,5-furan dicarboxylic acid diethyl ester (FDEE) was synthesised by esterification of FDCA with excess ethanol catalysed by inexpensive mineral acid, H₂SO₄, as described in chapter 8 section 8.16. FDCA can be obtained from oxidation of 5-hydroxymethyl furfural (HMF) which is a product from the hydrothermal treatment of cellulose (Figure 6-4).^{386,387} Traditional fossil-derived TA is obtained from partial oxidation of *p*-xylene in acetic acid at high temperature and pressure (air, 200 °C, 20 atm) with a series of oxidizing homogeneous catalyst such as manganese, bromine and cobalt metal salts.³⁸⁸⁻³⁹⁰ Using FDEE for DET production averts the need for this expensive oxidation process and harsh chemistry involved in the conversion of *p*-xylene to TA and delivers a greener process in terms of AE as discussed later in this chapter. The ethanol for esterification reaction can be obtained from glucose fermentation to deliver a completely bio-based FDCA³⁹¹ as demonstrated in Figure 6-3.

FDEE was characterised by IR spectroscopy, GC-MS, GC-FID and NMR spectroscopy. The purity of FDEE obtained from GC-FID was >98%. Spectroscopic measurements for IR and NMR are discussed in chapter 8 section 8.15.

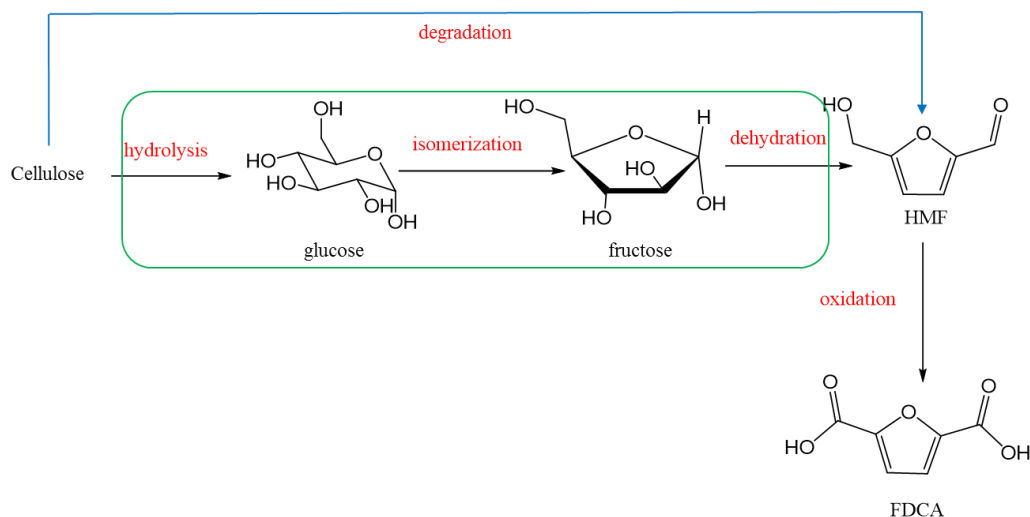


Figure 6- 4 Synthesis of FDCA from HMF a degradation product of cellulose.

6.3 Synthesis of diethyl terephthalate (DET) via Diels-Alder addition of ethene to FDEE

DET synthesis described in chapter 8 section 8.18 was *via* Diels-Alder (DA) addition of ethene to FDEE using heterogeneous Lewis acid catalysts as shown with unbroken arrows in Figure 6-3. Structures drawn with broken arrows were not synthesised in the study.

6.3.1 DA reactions and mechanism

DA reactions are inherently atom economic because they are concerted reactions in which typically a six-membered ring is formed through addition of four- π molecule (diene) to a two- π molecule (dienophile) with all ending up in the product as shown in Figure 6-5.

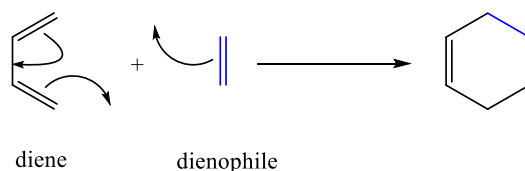


Figure 6- 5 DA reaction is intrinsically atom economic with addition of a four-carbon compound to a two-carbon compound to form a six-carbon molecule.

The presence of substituents on the diene and dienophile affects reactivity or promotion in DA reactions. When an electron-donating group (EDG) is introduced to the diene and an electron-withdrawing group (EWG) on the dienophile, a normal electron demand DA results. In contrast, the introduction of EWG on the diene and EDG on the dienophile will result in an inverse electron demand DA. This effect on DA reaction can be particularly understood from Frontier Molecular Orbital (FMO) theory which states that a reaction between two compounds is controlled by the efficiency of the interaction between the molecular orbitals of the combining components.³⁹²⁻³⁹⁴ It assumes an interaction between the electrons in the highest occupied molecular orbital (HOMO) of one of the components and the electrons in the lowest unoccupied molecular orbital (LUMO) strongly determines reactivity. For a normal electron demand DA, the diene HOMO will interact with the dienophile LUMO while it is reversed in an inverse electron demand DA as shown in Figure 6-6. The energy gap between diene HOMO and dienophile LUMO can be reduced (to facilitate the reaction) by either introducing EDG to the diene to raise HOMO or adding EWG to the dienophile to lower LUMO in the normal electron demand DA. However in the inverse electron demand DA energy gap can be reduced by adding EWG to the diene to lower LUMO or EDG to the dienophile to raise HOMO.

DA reactions have been largely catalysed by Lewis acids as they affect reaction rate, regioselectivity and stereoselectivity by interaction with either the diene, dienophile or their substituents.³⁹⁵ Using FDEE (electron-poor due to the presence of oxygen and ester groups) and ethene (electron-rich) the inverse electron demand DA is observed. Applying a Lewis acid generates an interaction with these functional groups by pulling away electrons from them. This further lowers the LUMO of the diene and brings it closer to the dienophile HOMO, thus increasing reaction rate.

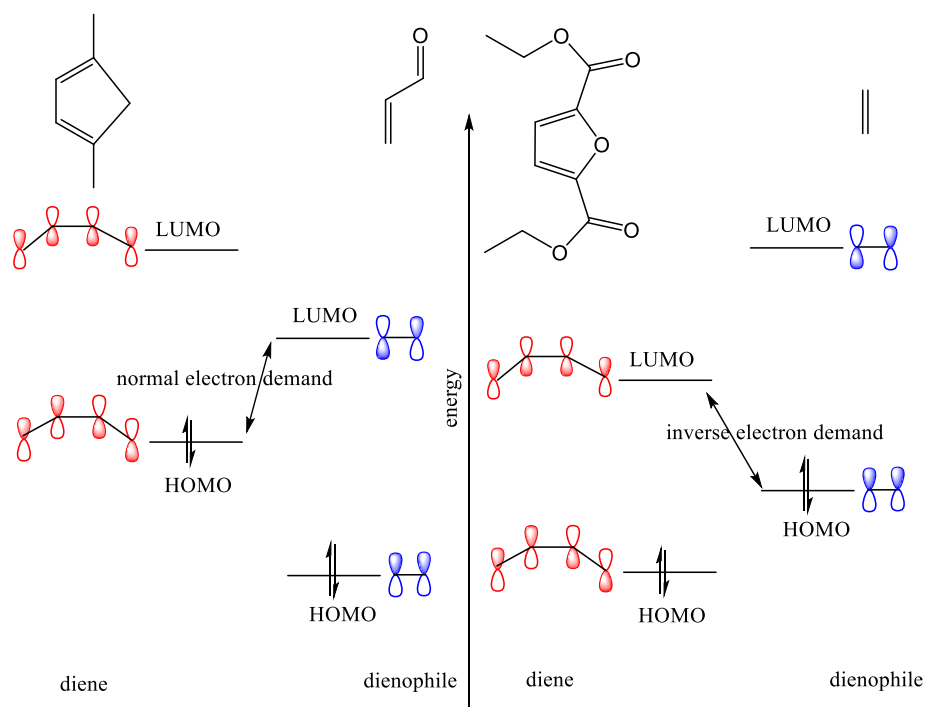


Figure 6- 6 Orbital correlation diagram showing the difference between a normal electron demand involving an electron-rich diene and electron-poor dienophile (left) and an inverse electron demand involving an electron-poor diene and an electron-rich dienophile (right) DA reaction.

Depending on the stereochemistry of DA reaction endo-adduct or exo-adduct or mixture can be formed as illustrated in Figure 6-7a. For DA reactions involving electron-poor dienophile having a carbonyl group, C=O, shown in Figure 6-6, the endo adduct is the preferred product because it is more kinetically favoured than the exo isomer. This is because a secondary orbital interaction exists between the electron-poor C=O of the dienophile and a new transient π bond at the back of the diene which lowers the energy of the transition state, which having a carbonyl group.^{396, 397} For a dienophile carrying more than one substituents, the favoured arrangement is that in which the more bulky group on the dienophile is under the ring.^{398, 399} Some authors have attributed this preference also to steric effects between the substituents on the diene and dienophile especially in DA reactions involving mono-olefin dienophiles where the secondary orbital interaction fails,⁴⁰⁰⁻⁴⁰² and nature of reaction solvents used.⁴⁰³⁻⁴⁰⁶ Although formation of the exo adduct

is generally uncommon, use of Lewis acid catalysts has been reported to favour formation of endo product over the exo isomer.⁴⁰⁷⁻⁴⁰⁹

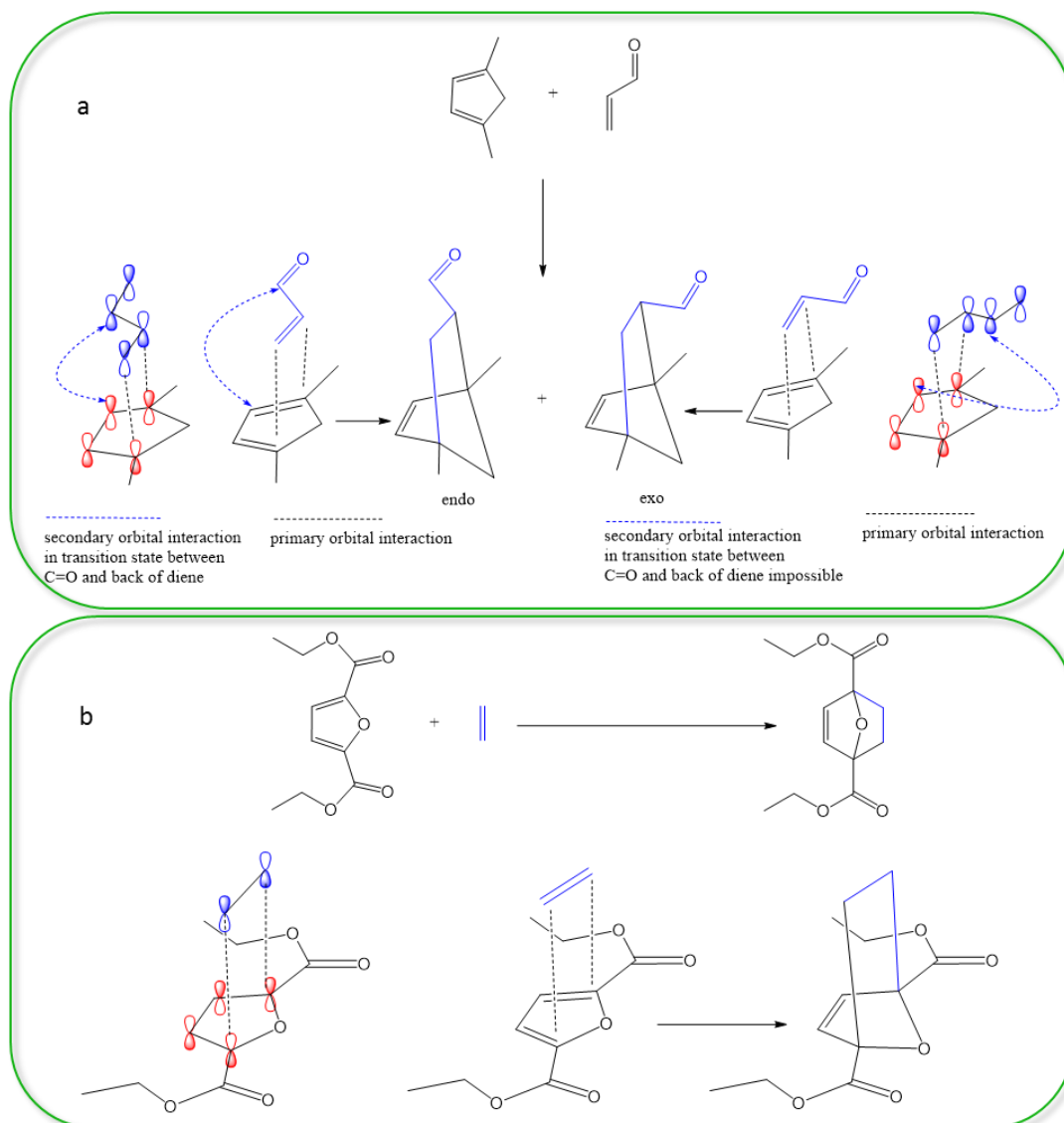


Figure 6- 7 Orbital diagrams illustrating the formation of (a) endo and exo adducts in DA reaction involving asymmetric dienophile and ringed diene; (b) a single product in DA reaction in which the dienophile is symmetrical.

In our case the dienophile, ethene, is symmetrical and only one product is expected (Figure 6-7b), although there are possibilities for the formation of the hetero-Diels-Alder reaction product *via* reaction of the carbonyl group and one of the double bonds on the diene with the dienophile.^{410, 411}

6.3.2 DA of 2, 5-furandicarboxylic acid dimethyl ester (FDME) to ethene

Initial studies, performed by Dr Thomas Farmer (GCCE, University of York, 2012) prior to this study, focused on Diels-Alder addition of 2, 5-furandicarboxylic acid dimethyl ester (FDME) to ethene in a 16 mL stainless steel high-pressure reactor. From this reaction, there was evidence of ethene hydration to ethanol, followed by transesterification of FDME to FDEE along with a compound with a molecular mass 198 g/mol in the reaction product (Figure 6-8). The 198 mass matches a single ester hydrolysis of the DA oxo-adduct or 2-ethyl-5-methyl furan dicarboxylate, but the observation of FDEE suggests that mechanism causing the appearance of this peak is the transesterification of the methyl ester with ethanol formed by hydration of ethene. The detection of methyl ethyl terephthalate (0.3%) along with dimethyl terephthalate (0.6%) alongside the product further supported this claim. NMR spectroscopy analysis of the crude mixture also showed the presence of methyl-ethyl furoate, as opposed to a hydrolysed oxo-adduct. It was also discovered that FDEE (and other FDCA diesters) sublimed at conditions initially investigated.

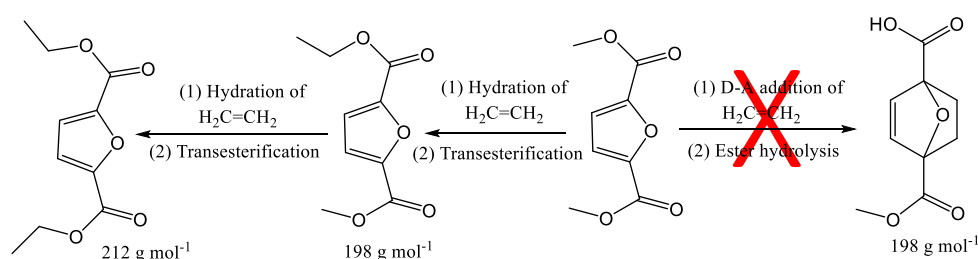


Figure 6- 8 Cause of peaks of 198 and 212 g/mol from FDME and ethene Diels-Alder addition

6.3.3 DA addition of FDEE to pressurised ethene catalysed by aluminium montmorillonite (Al-mont) clay

In order to avoid the complications brought about by ethene hydration and subsequent transesterification of the starting material, FDME was replaced with FDEE in this study. With FDEE ethene hydration and subsequent transesterification

while still occurring ceases to be a problem with regard to product selectivity. DA addition of FDEE to pressurised ethene in the presence of Al-mont catalyst and elevated temperature gave the oxo-adduct which auto-aromatised *via* dehydration, forming the desired DET. To minimise sublimation below the critical point of ethene (9.5 °C and 50.7 bar),⁴¹² FDEE was first pre-adsorbed onto the Al-mont catalyst. At reaction conditions of 60 bar and 150-250 °C, 28-61% DET yield was obtained in 48 hours as shown in Table 6-1 entries 3-7 and at a higher fill pressure of ethane (80 bar), conversion and yield reached 48% and 36% respectively in 48 hours but with reduced selectivity (75%) entries 1-2.

Table 6- 1 Yield, Conversion and Selectivity of DA addition of FDEE to ethene using aluminium montmorillonite catalyst under varying reaction conditions with 50% (entries 1-5) and 60% (entries 6 and 7) catalyst loadings

Entry	Temp. (°C)	P _f /P _r (bar)	Time (h)	Conversion (%)*,∞	Yield (%)	Selectivity (%)
1	150	80/230	24	18	17	94
2	150	80/150	48	48	36	75
3	150	60/140	48	34	34	100
4	200	60/130	24	56	37	66
5	200	60/140	48	66	44	66
6	200	60/160	48	96	61	63
7	250	60/230	48	65	28	43

P_f = filling pressure, P_r = reaction pressure, ∞Ethene oligomerisation products ignored for entries 4-7, *determined by GC peak area.

It was noticed that selectivity reached 100% at 150 °C but with a low yield (34%), whereas selectivity dropped to 75% on increasing ethene pressure (concentration) to 80 bar though with increased FDEE conversion at the same temperature and time (entries 2 and 3). Raising reaction temperature increased FDEE conversion, though selectivity significantly dropped (i.e. comparing entry 3 to entry 5).

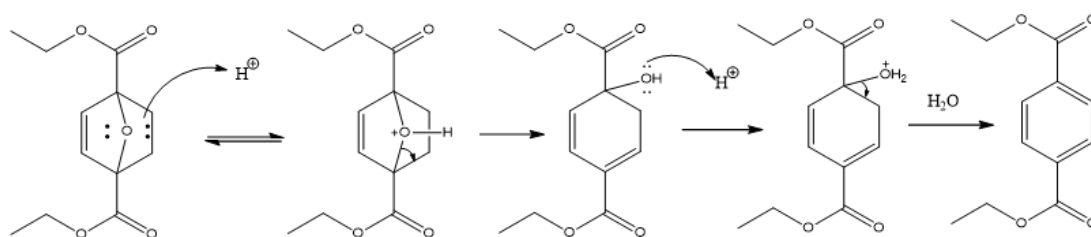


Figure 6- 9 Auto aromatization of DA oxo-adduct to DET in the presence of an acid.

As discussed earlier previous works by Farmer showed that under the conditions investigated some of the ethene will be hydrated to ethanol, as confirmed above in reactions involving FDME. In this instance the primary source of water for the hydration is assumed to be from the dehydration of the oxo-adduct (Figure 6-9). GC-FID chromatogram of entry 5 sample (Figure 6-10) showed a very broad peak on the baseline of the chromatogram which indicates the presence of low molecular weight alkanes: 2, 4-dimethyl heptane, 2, 5-dimethyl heptane; alkenes: 2, 4-dimethyl heptene; polyalkylated aromatics with diverse chain lengths and structures (Figure 6-11). These hydrocarbon compounds were formed *via* oligomerisation of ethene, most likely through formation of carbocations, and subsequent hydrogenation (forming alkanes), dehydrogenations (forming aromatics) and hydrations (forming alcohols).^{413, 414}

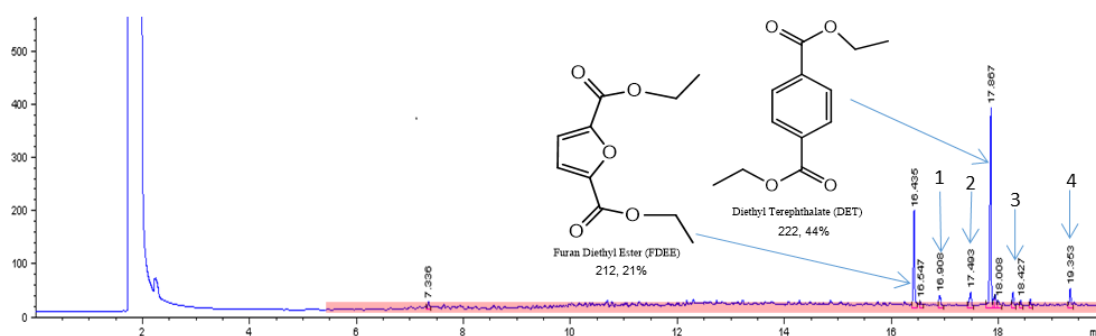


Figure 6- 10 GC-FID of Diels-Alder addition of FDEE and ethene with Al-mont at 60 bar and 200 °C for 48hours (Table 6-1 entry 5). The protruded baseline (highlighted in pink) is an indication of the presence of alkanes and alkene

GC-FI-MS and GC-EI-MS of reaction products showed that peaks 1 and 2 (Figure 6-10) are compounds having mass 204 g/mol and 218 g/mol (poly alkylated

aromatics shown in Figure 6-11) with fragmentation patterns readily confirming that they were not formed from the furan. Peaks 3 and 4 relate to compounds that have possibly been formed *via* transesterification reactions of FDEE and DET with newly formed alcohols derived from ethene to give furan dibutyl ester –mass: 268 g/mol and butyl ethyl terephthalate–mass: 250 g/mol (Figure 6-12).

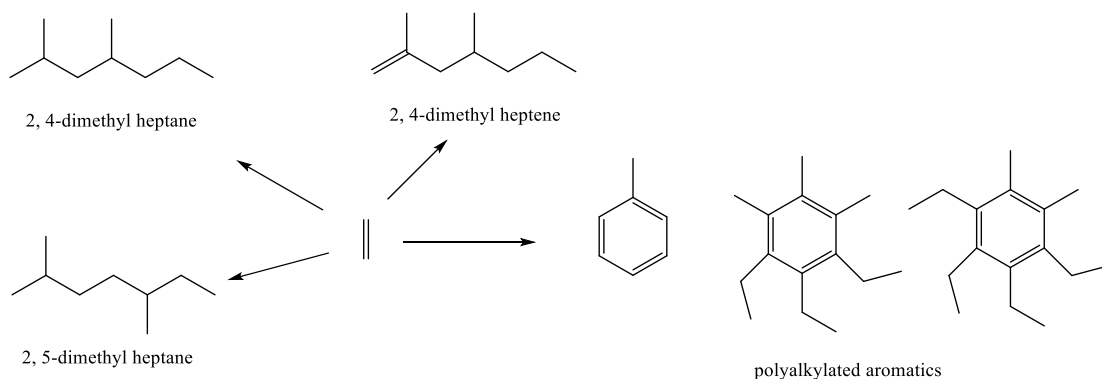


Figure 6- 11 Compounds formed as a result of ethene oligomerization reaction.

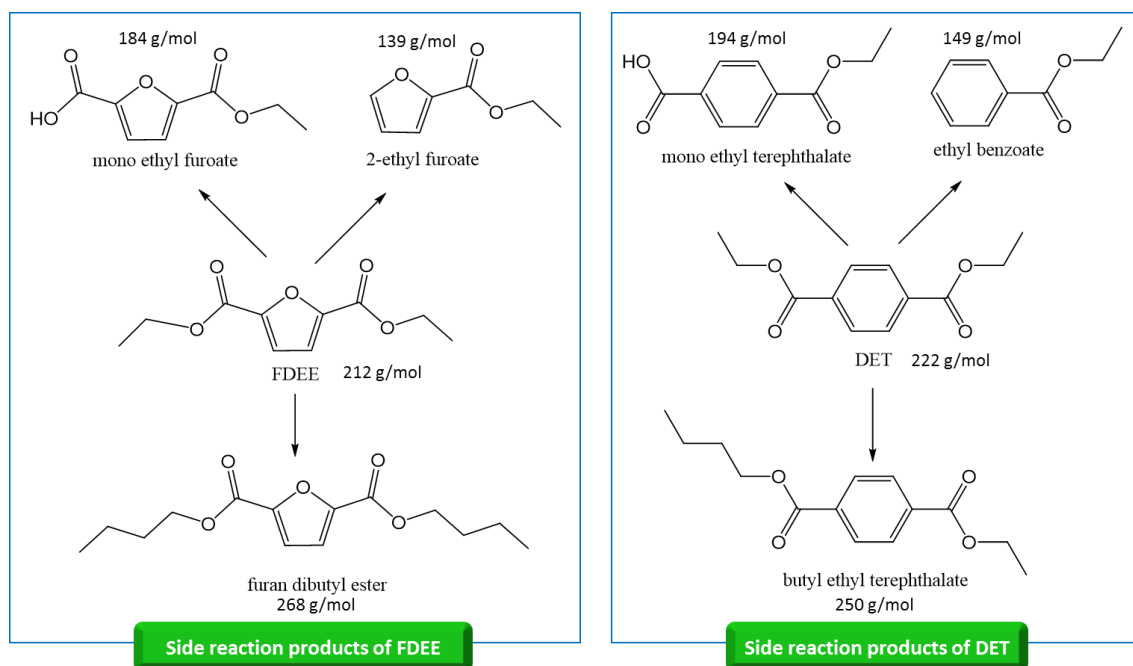


Figure 6- 12 Side reaction products from decarboxylation, transesterification with ethanol and hydrolysis of FDEE and DET during DA to ethene.

Other side reaction products observed at different times in varying amount depending on reaction conditions apart from butyl ethyl terephthalate and furan dibutyl ester, include 2-ethyl furoate, ethyl benzoate, mono ethyl terephthalate, mono ethyl furoate (Figure 6-12).

Broadly from Table 6-1 entries 1-7, results showed that increasing catalyst loading resulted in alkane, alkene and poly-alkene oligomerisation becoming more pronounced. Ethene was, therefore, pressurised and heated in the presence of the Al-mont catalyst without FDEE in order to further confirm the formation of ethene oligomers and aromatics, and result showed the presence of all the non-furan species discussed above. Farmer already confirmed the presence of these compounds with ^1H and ^{13}C NMR spectroscopic analysis (Figures 6-13 and 6-14 respectively). The carbon spectrum clearly revealed the aromatics carbons but almost no aromatic protons in the proton spectrum, thus indicating that all the aromatic species formed were hex-substituted (polyalkylated).

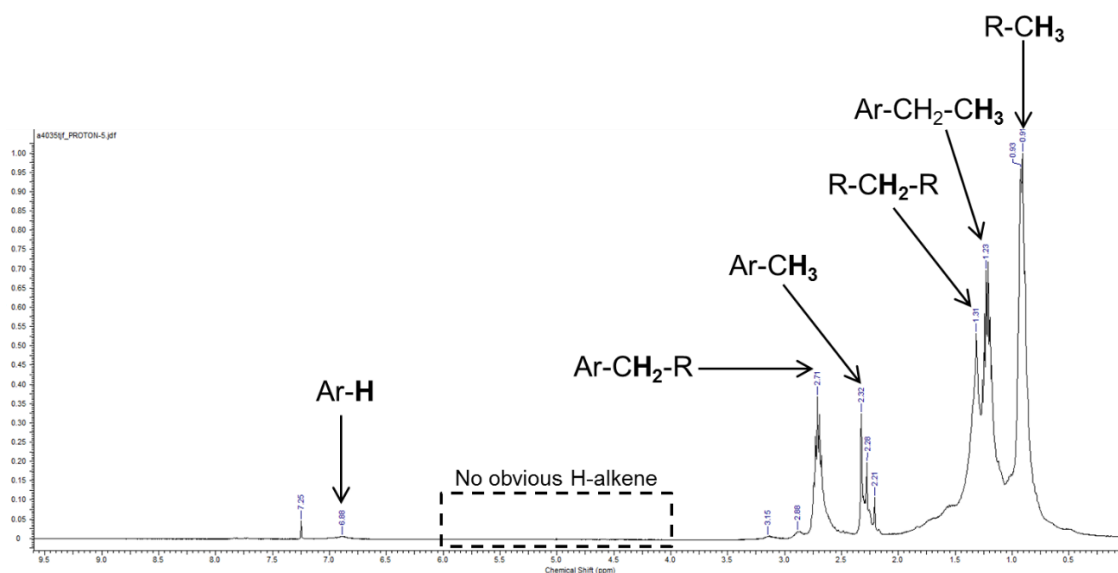


Figure 6- 13 ^1H NMR spectrum, with suggested assignments, of the oil collected from the oligomerisation of pressurised ethene in the presence of Al-mont catalyst. Data collected by Farmer.

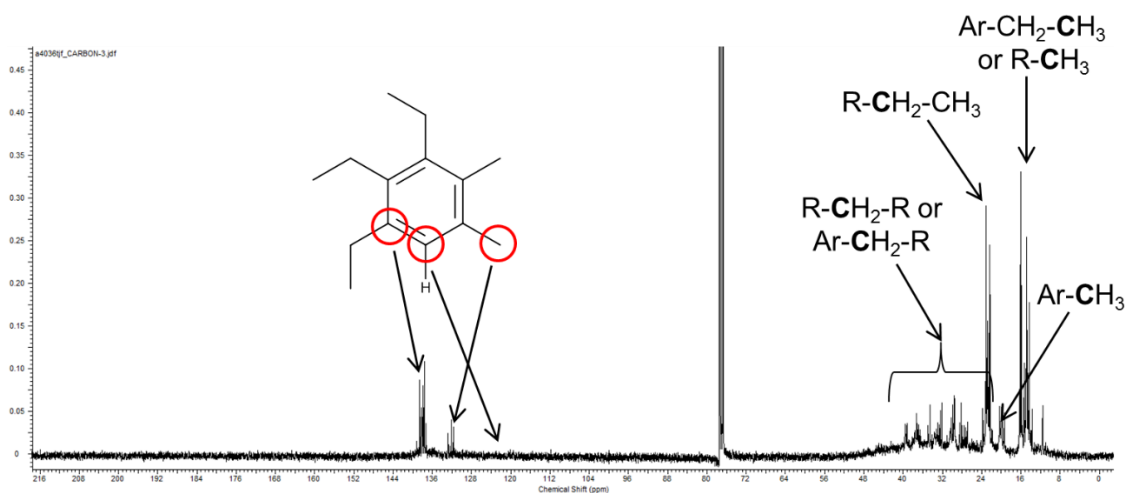


Figure 6- 14 ^{13}C NMR spectrum, with suggested assignments, of the oil collected from the oligomerisation of pressurised ethene in the presence of Al-mont catalyst. Data collected by Farmer.

6.3.4 DA addition of FDEE to pressurised ethene catalysed by other heterogeneous Lewis acids

Aluminium pillared montmorillonite clay (Al-P-MC), titanium silicate (TS1), titanium oxide (T1) and Al-Y-zeolite were also screened for the DA reaction. In montmorillonites two-dimensional layers of oxoanions are separated by hydrated cations. At the centre of each layer of oxoanions is an octahedral (O) sheet of Al surrounded by two tetrahedral (T) sheets of Si. In montmorillonites natural form Al^{3+} in the octahedral sheet are occasionally substituted by Fe^{2+} or Mg^{2+} , resulting in a negative layer charge across the surface of the sheet. This negative charge can be compensated by hydrated cations such as Na^+ , Mg^{2+} and K^+ adsorbed in the interlayer (basal) space as shown in Figure 6-15. In Al-P-MC, some of the interlayered cations of montmorillonites have been substituted with bulky inorganic polyoxocations such as $[\text{AlO}_4\text{Al}_{12}(\text{OH})_{24}(\text{H}_2\text{O})_{12}]^{7+}$, thus increasing the basal spacing of the clay sheets (Figure 6-15).^{415,416} The resulting pillared clays after calcination at high temperature (500 °C) are microporous in structure and the presence of acid sites on the interlayers and on the pillars would possibly make them better Lewis acid catalysts over standard Al-mont.⁴¹⁷ Al-P-MC can potentially contain traces of titanium dioxide,⁴¹⁸ therefore titanium containing catalysts were

also investigated to ensure that these sites in the pillared clay were not responsible for any catalytic activity.

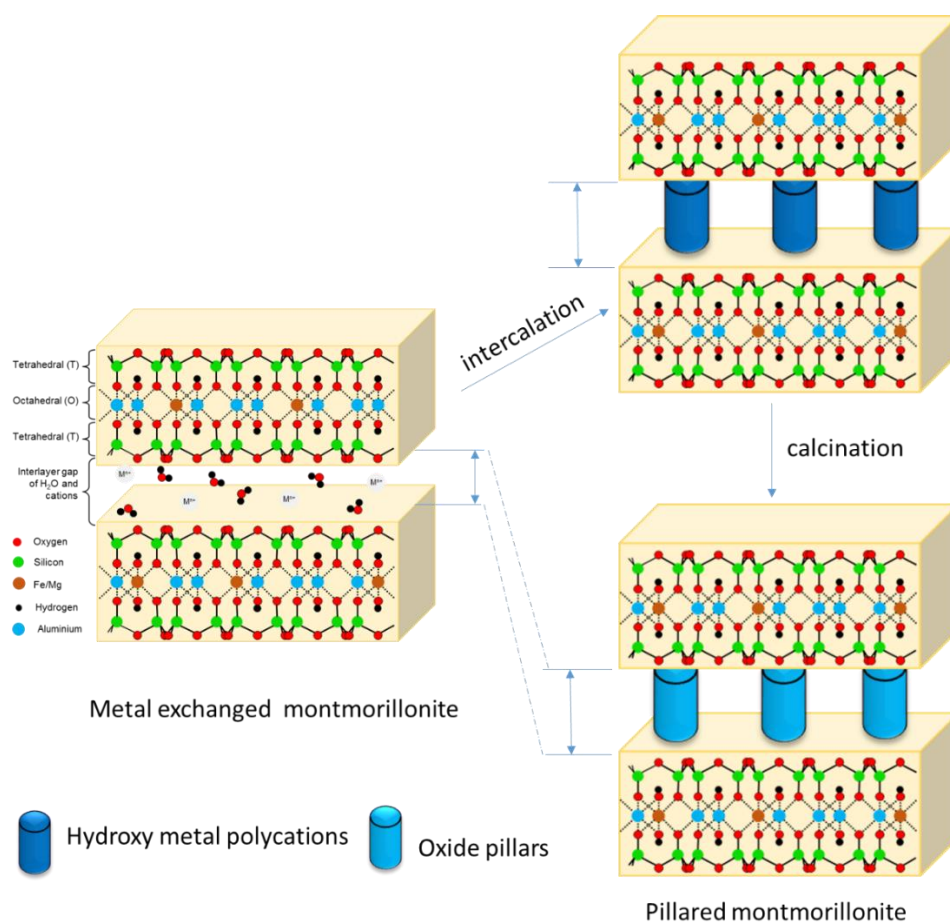


Figure 6- 15 Substitution of interlayer gap cations of metal exchanged montmorillonite clay with polyoxocations of inorganic metals widens the basal gap between clay sheets and results in formation of pillared montmorillonite clay upon calcination

Effectiveness of Al-P-MC, Al-Y-Z, TS1 and T1 in terms of yield, conversion and selectivity under varying reaction conditions are presented in Table 6-2 entries 1-10 and entries 11-17 for 50% and 60% catalyst loadings respectively. There was no conversion of FDEE to DET at 200 °C and 60 bars fill pressure in 24 hours whether or not it was pre-adsorbed on to the Al-Y-Zeolite catalyst (entries 1-2). However at elevated temperature (250 °C) approximately 6% FDEE conversion and 6% DET yield was obtained in 24 hours for the un-pre-adsorbed system (entry 3).

Table 6- 2 Yield, Conversion and Selectivity of DA addition of FDEE to ethene catalysed by different heterogeneous Lewis acid catalysts under varying reaction conditions with 50% (entries 1-10) and 60% (entries 11-17) catalyst loadings

Entry	Catalyst	Temp. (°C)	P _f /P _r (bar)	Time (h)	Conversion (%)*	Yield (%)	Selectivity (%)	Remark
1	Al-Y-Z	200	60/130	24	0	0	0	U
2		200	60/130	24	0	0	0	P
3		250	60/140	24	6	6	100	U
4	Al-P-MC	150	60/120	48	0	0	0	P
5		200	60/160	48	19	17	88	P
6		200	70/160	48	8	5	63	P
7		250	60/150	6	23	20	87	P
8		250	60/230	48	68	50	74	P
9		250	70/170	48	51	48	94	P
10	TS1	250	60/190	24	32	17	52	P
11	Al-P-MC	200	60/160	48	18	17	97	P
12		250	60/250	24	66	59	88	P
13		250	60/250	48	81	51	63	P
14	TS1	250	60/170	24	31	20	65	U
15		250	60/170	24	33	14	42	P
16	T1	250	60/140	24	92	15	16	U
17		250	60/150	24	95	23	24	P
18	‡	250	60/110	24	9	5	61	U

P_f = filling pressure, P_r = reaction pressure, Al-Y-Z=Al-Y-Zeolite, Al-P-MC=Al-pillared montmorillonite clay, TS1=Titanium silicate, T1=Titanium dioxide, ‡ =T1 catalyst loading was 25%, *determined by GC peak area, P=furan preadsorbed onto catalyst system,

U=unpreadsorbed system

Initial attempt with Al-P-MC catalyst gave no conversion for FDEE under a low temperature (150 °C) with prolonged reaction time (entry 4). Increase in conversion up to 68% and yield (50%) was recorded by raising the reaction temperature to 250 °C for pre-adsorbed systems (entries 4-9). With 60% Al-P-MC loading, the same trend of increased conversion and yield was observed with increasing temperature (entries 11 and 13). However, yield and selectivity decreased when reaction time was prolonged as a result of greater side reaction (entries 12 and 13). Side reaction products in this case were 2-ethyl furoate, ethyl benzoate, mono ethyl terephthalate, mono ethyl furoate and toluene.

At both catalyst loadings, TSI gave roughly 30% FDEE conversion and 14-20% DET yield in the pre-adsorbed and un-pre-adsorbed systems (entries 10, 14 and 15). Interestingly T1 catalyst at 60% loading greatly favoured FDEE conversion up to 95% but DET yield and selectivity was considerably lower due to increased concentration of decarboxylated FDEE and DET (entries 16-17). Reducing T1 loading to 25% improved selectivity to 61% but markedly reduced conversion to 9% (entry 18). The catalytic activity demonstrated by T1 could mean it is responsible for or contributed to the catalytic activity of Al-P-MC. Probing into this with ICP-MS measurement of the Al-P-MC used (chapter 8 section 8.22), it was discovered that Al-P-MC only contained 0.062% titanium. This low concentration of titanium in the catalyst suggests titanium sites were not responsible for the catalytic activity of Al-P-MC.

Generally, Al-P-MC performed better at higher temperature than higher pressure. At higher pressures there is more ethene in the system and therefore a greater chance of saturating the catalyst with ethene, not allowing enough furan to the active sites, and this would also increase ethene oligomerisation. The oxo-adduct was rarely observed at this temperature and it appears that high temperature causes its rapid dehydration and subsequent conversion to DET as shown in Figure 6-9. This is

potentially the driving force for the increased yields of the DA and could explain why DET yield is highest at 250 °C. Another thing that is potentially responsible for or favouring aromatisation of oxo-adduct is the hydration of ethene to ethanol which removes water from the system and therefore pulls the oxo-adduct towards aromatisation. Surprisingly, contrary to the presence of oligomers with Al-mont catalyst, there was little or no oligomerisation noticed with the pillared clay system as observed from GC chromatograms (Figure 6-16 top). A confirmation of this was achieved by charging the reactor with Al-P-MC and ethene and reacted under the same conditions used for investigating the presence of oligomers with Al-mont above (section 6.3.3). GC chromatogram of ethanol wash of resulting product appeared clean indicating the absence of any compound no matter how volatile (Figure 6-16 bottom).

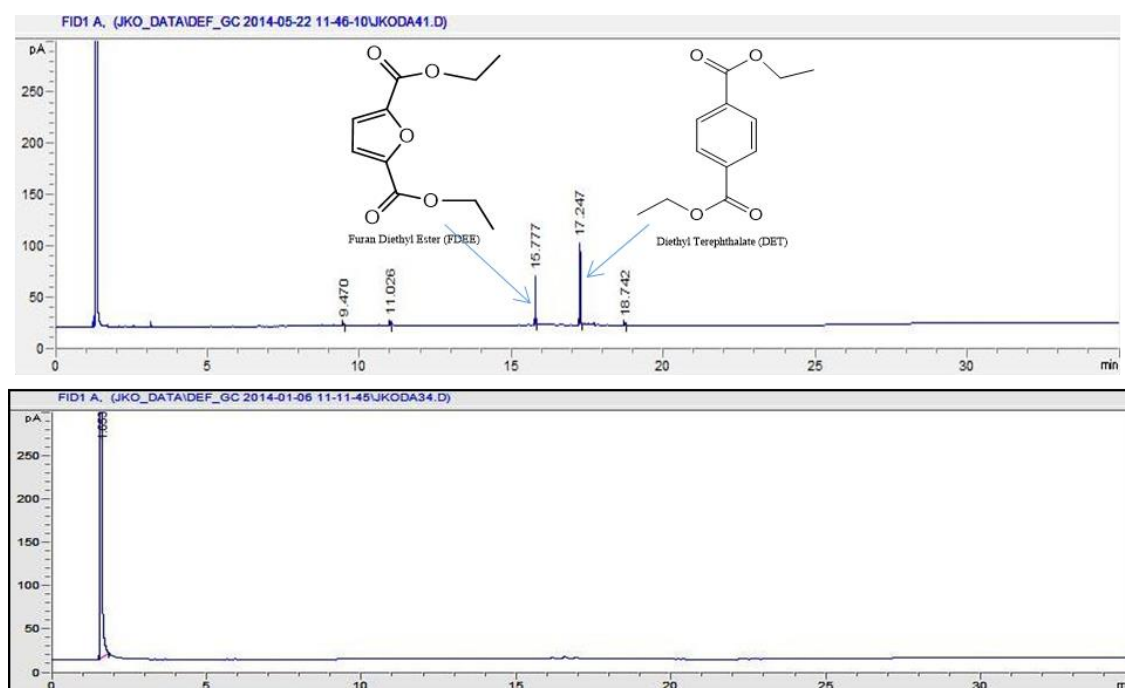


Figure 6-16 GC-FID Chromatogram (top) from DET synthesis using Al-pillared montmorillonite catalyst under a 60 bar fill pressure of ethene, 250 °C, 24 hour (Table 2 entry 12); (bottom) ethanol wash of ethene oligomerisation test sample with Al-pillared montmorillonite catalyst

6.3.5 Acidity effect on ethene oligomerisation

It was suspected that acidity in the system could be having some influence on ethene oligomerisation. Likely sources of acid in the system were residual H_2SO_4 catalyst in the esterification of FDEE and the nitrate from which the catalyst was prepared. Effect of acidity of ethene oligomerisation was studied by setting up a control and a furan diester-catalyst mixture doped with concentrated H_2SO_4 at the pre-adsorption stage. This mixture was reacted with pressurised ethene at 60 bar and 200 °C for 72 hours. The Al-mont catalyst loading used for this investigation was 60%. Comparing the results of both systems there was not much difference with respect to ethene oligomerisation. However, it appeared that DET yield was higher in the un-doped system. Difference in reaction pressure of the two systems (145 bar for un-doped, 115 bar for doped) using two identical but separate 16 mL reactors despite the same fill pressure could be a possibility for this observation. Therefore, a new batch of FDEE was synthesised which was purified by a water/2-methyl tetrahydrofuran (MTHF) separation and subsequently with 5% sodium bicarbonate and brine solution. The FDEE was assumed to be acid-free or to some extent contain less acid because of this purification. A new Al-mont catalyst was also prepared which was also assumed to be acid-free (chapter 8 section 8.3.6). The new batch of FDEE was pre-adsorbed separately on both Al-mont catalysts and then pressurised with ethene. In all experiments the reactor was always purged with nitrogen and ethene each three times at least before finally filling with ethene for the reaction. Reaction product mixtures, including the clay catalyst, were always washed from the reactor with ethanol sonicated for 20 minutes (to assist desorption from the catalyst surface), filtered and the filtrate taken for GC analyses.

Results shows that both systems with new FDEE- Al-mont and new FDEE-acid free Al-mont have similar DET yields (Table 6-3). The FDEE-old Al-mont system gave higher selectivity than the acid-free Al-mont after 32 hours of reaction (entries 1-2)

while after 24 hours both systems have very slightly differing selectivity (entries 3-4). The trend of acidity effect is not particularly obvious but it was noticed that ethene oligomerisation was not evident in the reactions ran for 24 hours whereas it occurred in those ran for 32 hours. It appears prolonged reaction time contributed to the formation of ethene oligomers.

Table 6- 3 Variation of DET yield and selectivity with acidity content in FDEE-Al-mont mixture under different reaction conditions

Entry	Catalyst loading (%)	Temp. (°C)	P _f /P _r (bar)	Time (h)	Conversion (%) [*]	Yield (%)	Selectivity (%) [§]	Remark
1	50	200	60/160	32	55	48	87	F/AM
2	50	200	60/130	32	46	35	76	F/AFAM
3	50	200	60/160	24	60	54	90	F/AM
4	50	200	60/150	24	72	68	94	F/AFAM

P_f = filling pressure, P_r = reaction pressure, [§]All values calculated by ignoring ethene oligomerisation products, ^{*}determined by GC peak area, F=FDEE, AM= Al-mont catalyst, AFAM= Acid-free Al-mont catalyst

6.4 Large scale synthesis of DET

DET synthesis was scaled-up for Al-P-MC catalysed reaction in a 50 mL pressure reactor using typically 5 g of FDEE. The results were similar, but not identical to those carried out in the 16 mL reactor, the highest yield being 50% with reduced selectivity (Table 6-4 entries 1-4). Difference in batch of FDEE and amount of pressurised ethene used for synthesis could be responsible for this result. In the 16 mL reactor using 60 bar of pressurised ethene at room temperature 82 moles of ethene was present per mole of FDEE while in the 50 mL reactor only 5 moles of ethene was present per mole of FDEE. This mole ratio difference was enough to cause a marked drop in yield between the two scales. Thus for the 50 mL scale selectivity reduced. Proportional scale-up requiring 0.625 g FDEE-Al-P-MC mixture was performed and DET yield went up to 55% with improved selectivity (entry 5).

Table 6- 4 Conversion, yield, selectivity and mass recovery under a scale-up DET synthesis with a preadsorbed system in 24 hours

<i>Entry</i>	<i>Catalyst loading (%)</i>	<i>Temp. (°C)</i>	<i>P_f/P_r (bar)</i>	<i>Conversion (%)</i> *	<i>Yield (%)</i>	<i>Selectivity (%)</i>
1	60	250	60/170	87	40	46
2	50	250	60/230	91	41	45
3	60	250	60/240	91	50	55
4	60	230	60/230	65	34	52
5	60	238 [#]	60/130	91	55	61

*determined by GC peak area, [#]hot plate temperature set at 250 °C but temperature probe read 238 °C

6.4.1 Product mass recovery and isolation

Mass recovery was investigated for the large scale synthesis and initially found to be a little above 50% of the mass of starting material. Attempts were made to collect resulting crude product mixture by washing reactor thoroughly with solvents (acetone, ethyl acetate and ethanol). The reactor was vented into a vial containing solvent (ethyl acetate, acetone, ethanol) to dissolve any possible organics being carried over by the vented ethene so as to account for this mass loss. Sonication time for resulting crude product mixture was also increased to 2 hours prior to filtration. Additionally by carefully controlling temperature and pressure on rotary evaporator to just be enough to distil only wash solvents, escape of volatile products such as toluene was averted. Fortunately enough these attempts yielded a mass recovery of about 75%.

Recovered catalyst from filtration was equally weighed and had an increase of 14%. Thermogravimetry-Infrared (TG-IR) analysis of recovered catalyst indicated loss of organic materials which suggests that FDEE and DET, in particular, were still trapped in the catalyst pores even after sonication. At this point, some reactions without prior adsorption of FDEE onto catalyst were considered and it was noticed

that higher mass recovery compared to the pre-adsorbed system was obtained though with lower conversion and yield.

Reaction crude product mixture was purified on Isolera Four automated flash chromatography (Biotage) with method developed from TLC plate measurement and using a UV-detector coupled with the instrument. The detection limit was set between 236 nm and 242 nm using λ max for FDEE and DET respectively. Cyclohexane-ethylacetate solvent mixture in ratio 6:1 was used and major R_f values obtained were 0.43 (DET), 0.25 (FDEE), and 0.69. Roughly 25 wt% DET and 10 wt% FDEE was recovered from the loaded sample, the remaining being unresolved mixtures of FDEE, DET and other side products including terephthalic acid. The isolated DET was brownish viscous liquid crystallizing out thereafter (Figure 6-17).



Figure 6- 17 Isolated DET crystallizes as soon as it cools down

6.4.2 Reuse of catalyst

Reuse of Al-P-MC in the reaction was investigated in three cycles. Results showed that conversion was approximately halved in the second and third cycles of reuse (Figure 6-18) possibly as a result of catalyst poisoning. DET yield followed the same trend as FDEE conversion in the three cycles. However, while selectivity increased

in the second cycle, it reduced in the third cycle as there was a trace of polyalkylated aromatics in the product. This could be as a result of possible collapse of the catalyst wall which made it behave like a normal Al-mont. It should be noted that the catalyst was reused as recovered without activation or drying in an oven.

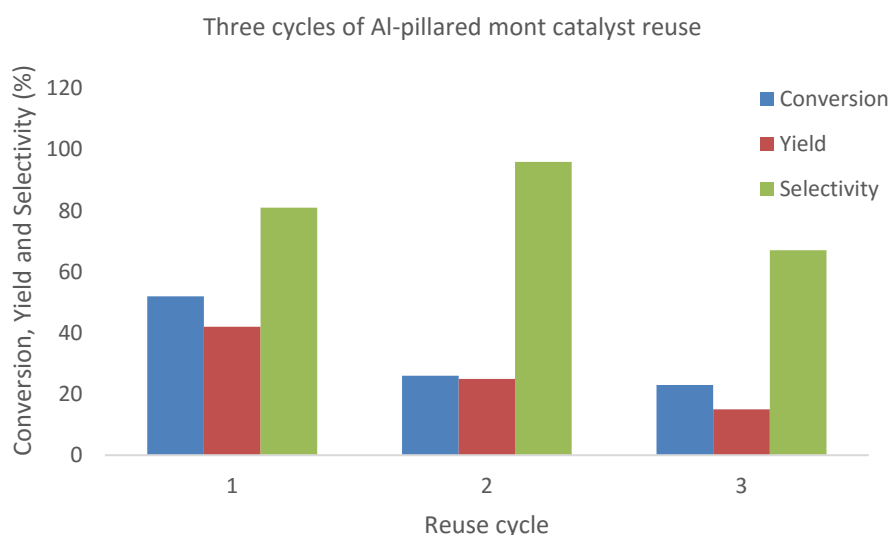


Figure 6- 18 Conversion, yield and selectivity of three reuse cycles of Al-pillared montmorillonite for scaled-up Diels-Alder addition of FDEE and ethene. Temperature (250 °C), filling pressure (60 bar), time (24 hr), 50% catalyst loading and pre-adsorbed system

6.4.3 Characterisation of isolated products

Recovered DET and FDEE were quantified by GC-FID and identified by FT-IR spectroscopy, GC-MS, ESI-MS, DSC and NMR spectroscopy. GC chromatograms showed the isolated product was ~95% DET and still contained trace impurities ~1% each of furan dibutyl esters, dibutyl terephthalate, ethyl benzoate, 2-ethyl furoate while the recovered starting material was 100% FDEE (Figure 6-19). Isolated DET was identified on GC-MS with fragmentation pattern matching suggestion from NIST library (Figure 6-20). Accurate mass determination for DET was performed on microTOF ESI-MS and mass to charge ration was measured as 245.0791 for $C_{12}H_{14}NaO_4$.

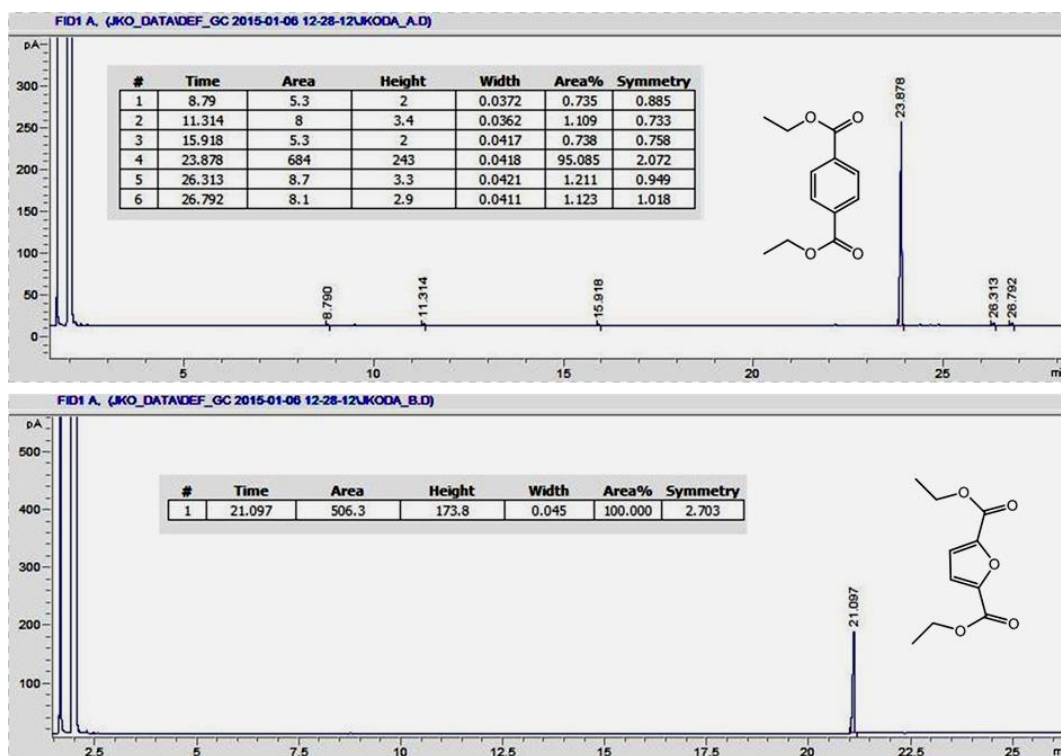


Figure 6- 19 GC-FID chromatograms of isolated DET and recovered FDEE

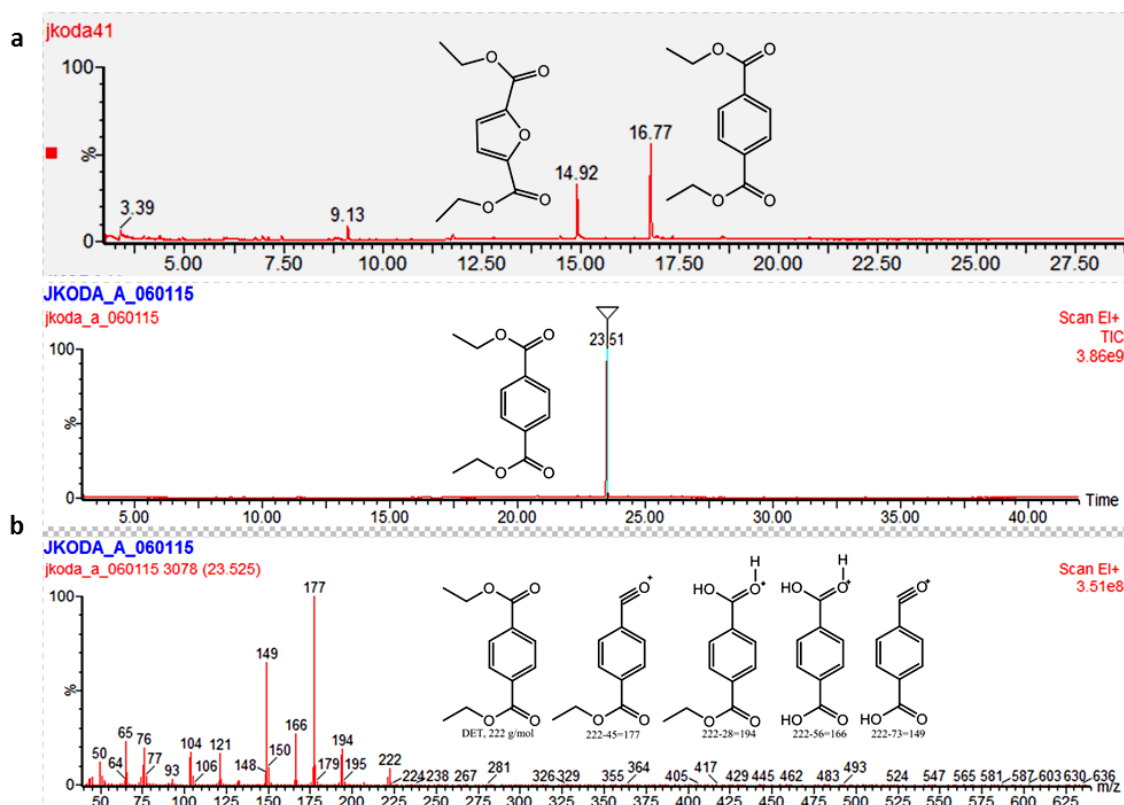


Figure 6- 20 GC-EI-MS chromatograms of DET (a) before isolation (b) after isolation with spectrum showing fragmentation pattern.

FT-IR spectroscopy showed the successful transformation from FDCA to FDEE and isolated DET along with standard DET. The carboxylic O-H ($3152\text{-}2560\text{ cm}^{-1}$) and C=O (1665 cm^{-1}) stretching disappeared as the C-H ($3113, 2990\text{ cm}^{-1}$) and C=O stretching in the furan esters appeared. A significant shift in the C-H aromatic stretching ($2980, 2935\text{ cm}^{-1}$) was observed as FDEE transformed to DET (Figure 6-21).

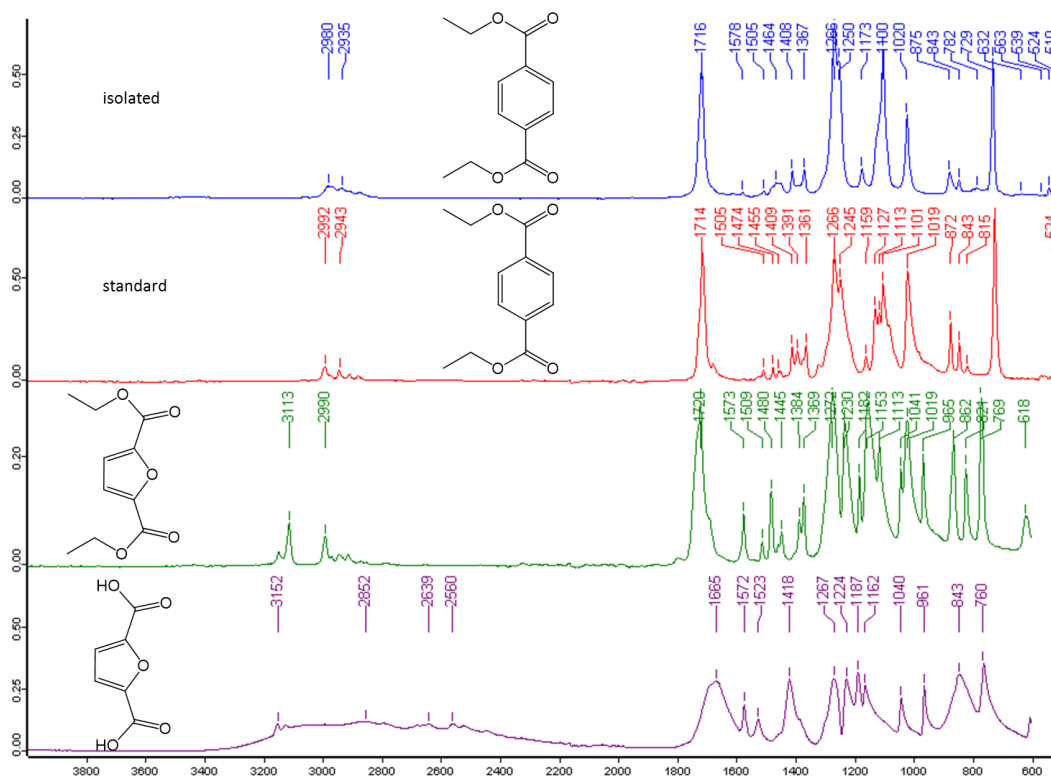


Figure 6- 21 FT-IR spectra showing transformation from FDCA to FDEE and then to isolated DET which is compared with a standard DET.

^1H NMR spectrum showed four aromatic protons at 8.06 ppm, six methyl protons and four methylene protons on the diester at 1.38 ppm and 4.38 ppm respectively (Figure 6-22). The spectrum confirmed there were trace impurities in the DET as signals from alkylated DET and FDEE were observed though very weak. ^{13}C NMR spectrum showed four signals at 14.34 ppm, 61.68 ppm, 129.5 ppm, 134.29 ppm, and 166.17 ppm. This is consistent with the literature.⁴¹⁹

Melting point determination for DET was performed on DSC by comparison with a commercial >99% DET from TCI chemicals. Commercial DET gave a sharp melting point range of 40-45 °C while isolated DET gave a broad melting range of 24-35 °C. The impurities in the latter likely the cause of its lowered melting point range.

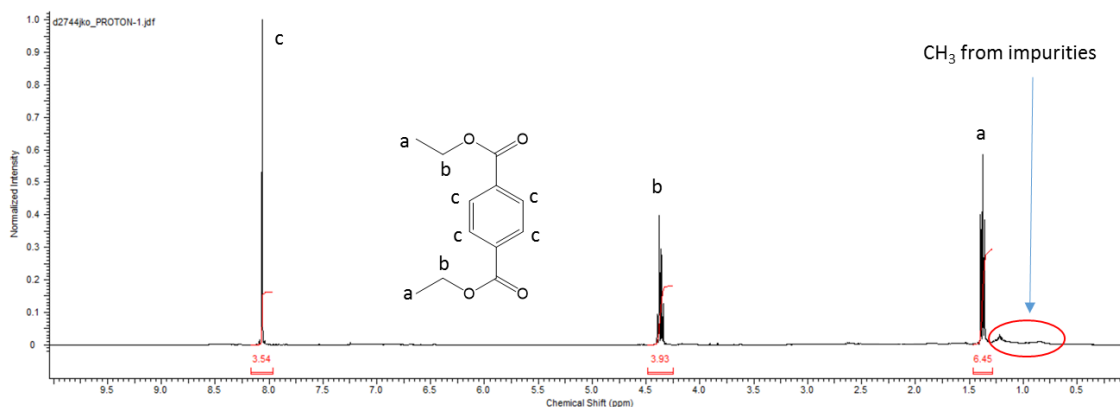


Figure 6- 22 ¹H NMR of isolated DET with trace impurity

6.5 Comparison of routes to bio-PET

For multi-step chemical processes, it is strongly recommended to use cumulative metrics of reactions from the starting material to the final product in order to have a fair assessment of how green the process is. Cumulative metrics of different routes from biomass-derived platform molecules to PET *via* TA to diethyl terephthalate (DET) is presented in Table 6-5. The evaluation is based on yield, conversion, selectivity, AE, RME, OE, PMI (reagents, catalyst and reactants), critical elements used and number of reaction steps. Detailed calculations can be found in the CD attached to this thesis. Most of the reported routes have been from bio-based chemicals (but not from the source biomass) to para-xylene or TA. To have an assessment of a 100% bio-based PET, transformations have been calculated from the biomass source (cellulose or hemicellulose) and extended to DET for uniformity with our process. All transformations originally reported by authors are drawn in black colour while extended transformations from biomass source are indicated in blue colour. Transformation step from TA to DET is based on the esterification conditions used for FDCE synthesis from FDCA in this study since both TA and FDCA

are diacids. For each route 5 mol of DET was targeted as the bio-based monomer. The limonene route (chapter 1 section 1.4) has not been included on the basis that limonene global production will be inadequate to meet the demand for PET production. As of now, little is known about the Virent route to TA (chapter 1 section 1.4) and as such are limited to include it in the metrics.

Table 6- 5 Cumulative Metrics Result for synthesis of 5 mol bio-derived DET from glucose/pentose

Process Entry	Yield (%)	Conversion (%)	Selectivity (%)	AE _T (%)	AE _P (%)	Critical Element used	Reaction step from glucose/pentose
1	7.6	70.3	10.8	38.9	4.2	Cu, Ni, Zn, P	8
2	20.8	92.2	22.5	41.6	9.4	Zn, Ni, P	5
3	9.4	31.0	30.4	34.9	10.6	Al, Zn, Cu, P	6
4	16.5	92.2	17.9	34.9	6.2	Al, Pt, P	8
5	5.5	96.0	5.7	26.4	1.5	Al, Pt, V, I, Cd	8
<i>This study</i>	25.5	63.2	40.4	44.8	18.1	Zn, Au, Al, P	4

Abundance code⁷⁹ 100-1000 years, 50-100 years, 5-50 years

Results showed that cumulative yield and selectivity for all the routes is less than 50%, the highest yield (25.5%) and selectivity (40.4%) being obtained *via* the route reported in this study. The HMF routes *via* DMF have cumulative theoretical atom economy (AE_T) of 38.9% (Table 6-5, entry 1, Figure 6-23) and 41.6% (Table 6-5, entry 2, Figure 6-24). This shows that it is atom uneconomic and environmentally damaging to first reduce HMF to DMF (removing two oxygens) before Diels-Alder addition to ethene or acrolein, only to later add these oxygens back.^{120, 124} The third example in the HMF route that uses oxidation product of HMF (Figure 6-25) was not included as there were no existing experiments of the oxidation of the final product reported by the author to TA in the literature.

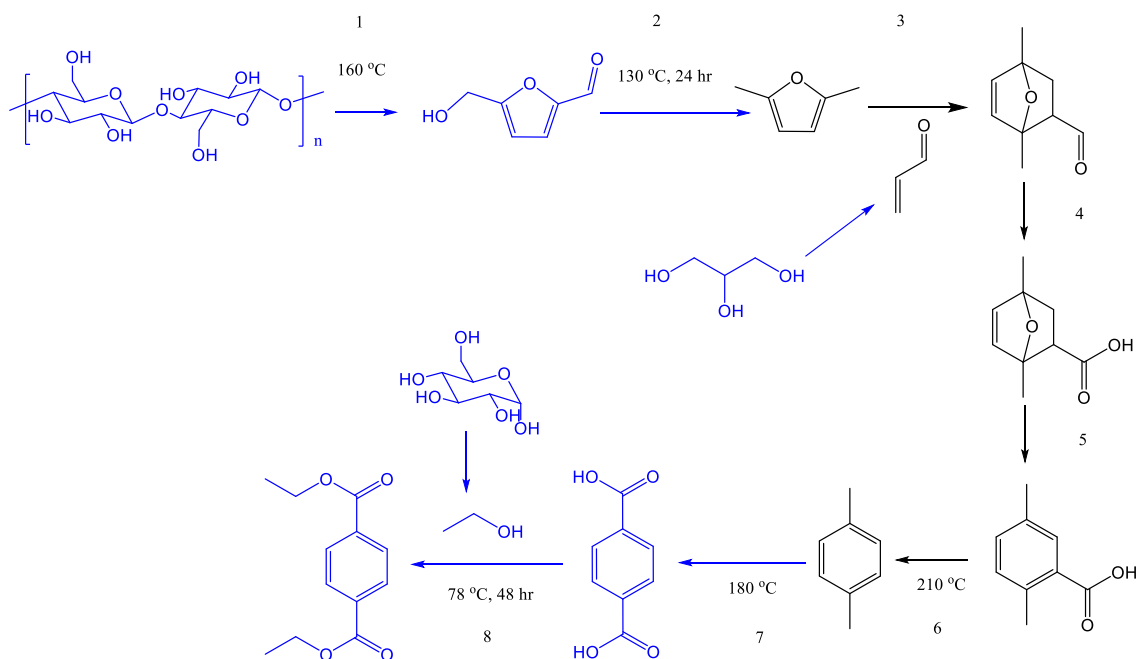


Figure 6-23 Transformations from cellulose to bio-based DET via Diels-Alder addition of DMF to acrolein.^{120, 387, 420, 421}

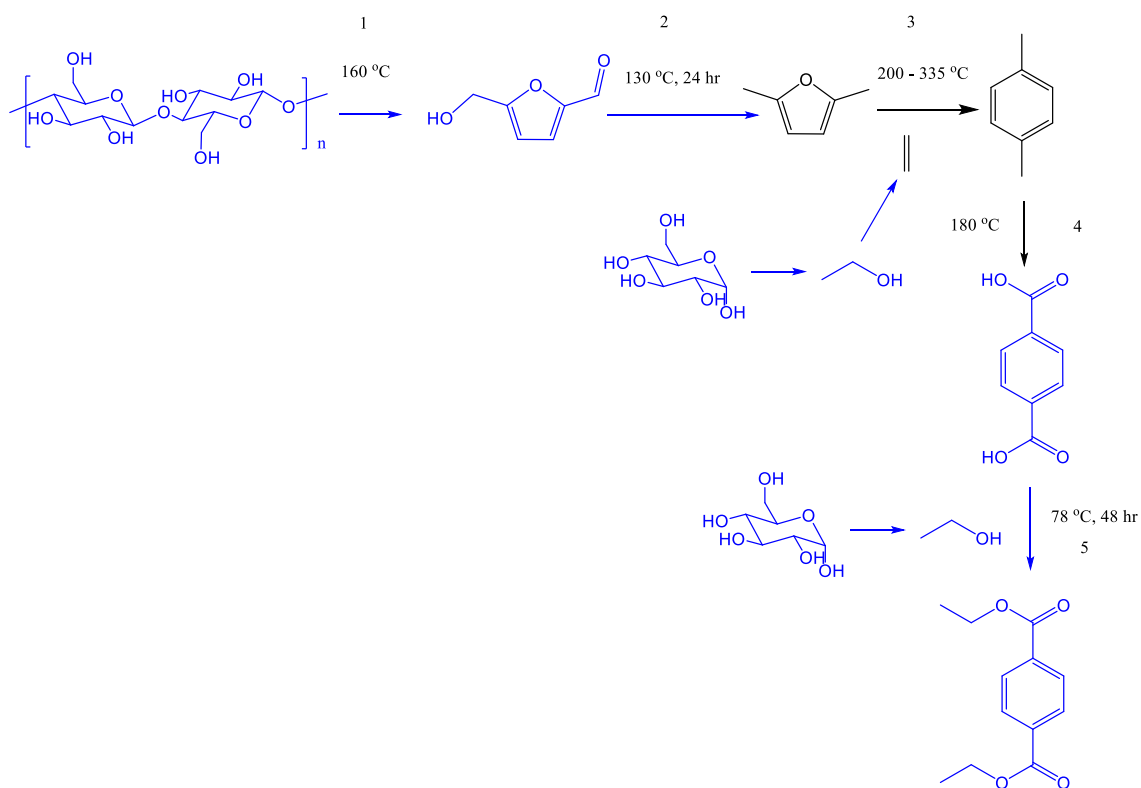


Figure 6-24 Transformations from cellulose to bio-based DET via Diels-Alder addition of DMF to ethene.^{124, 387, 420, 422}

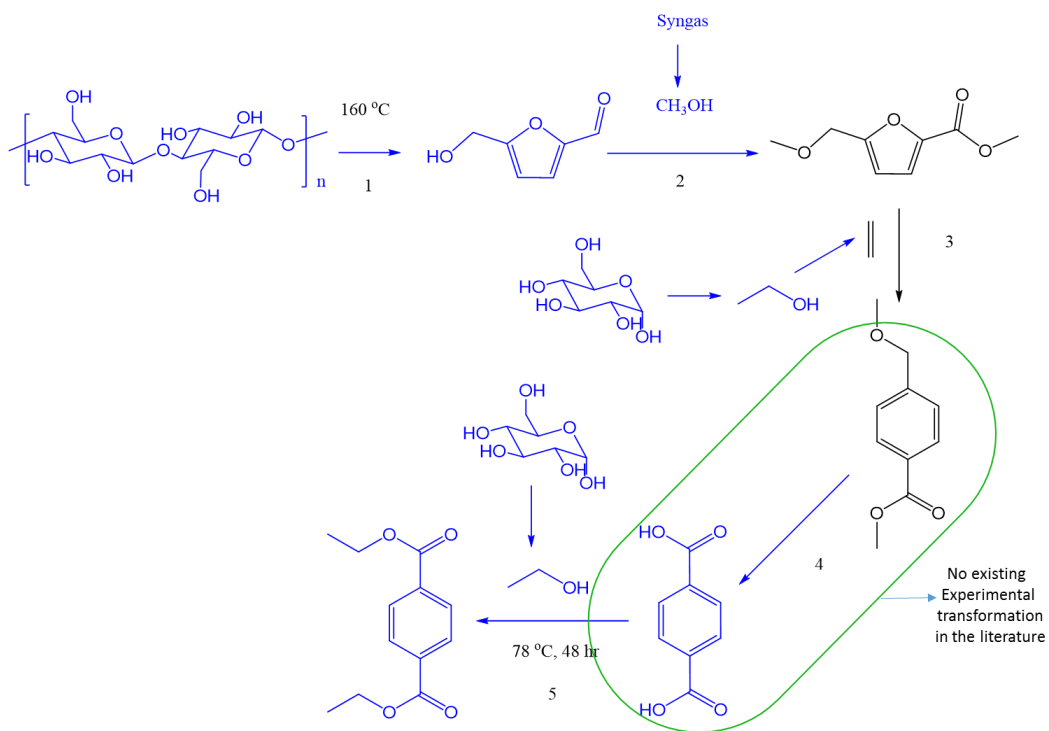


Figure 6- 25 Transformations from cellulose to bio-based DET via Diels-Alder addition of HMF oxidation derivatives to ethene.⁴²²

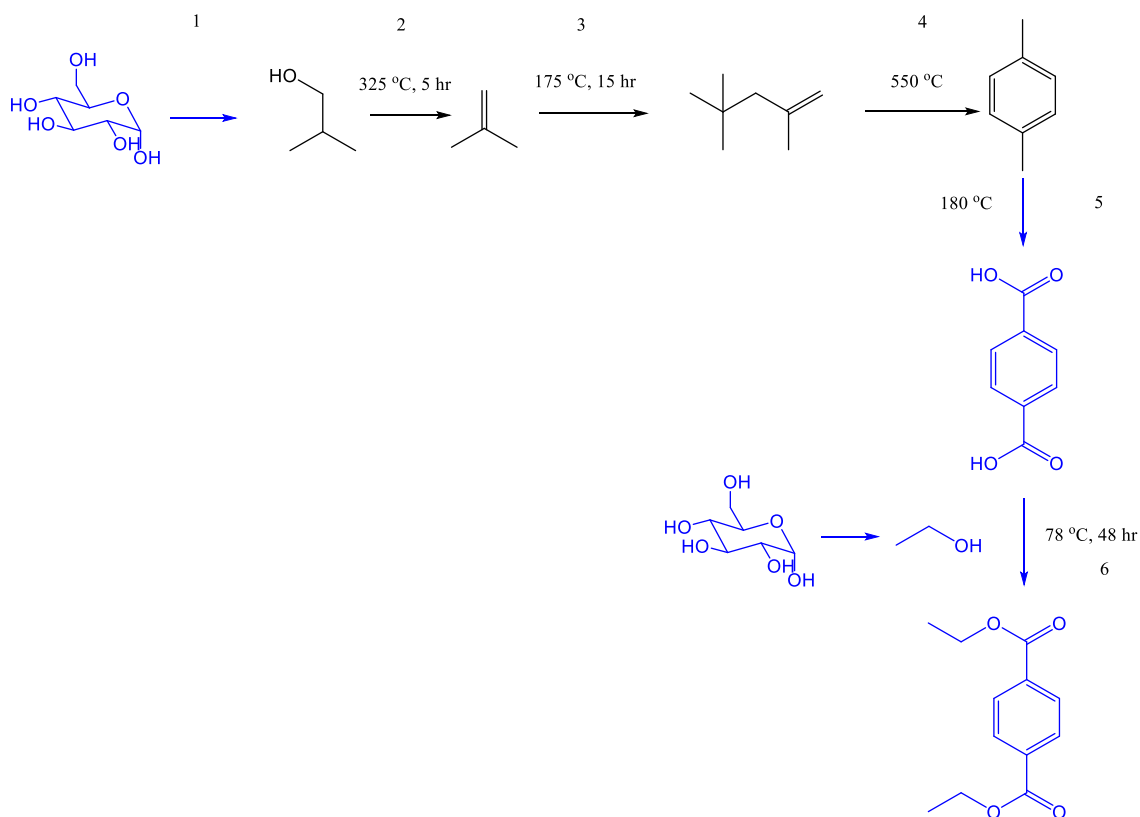


Figure 6- 26 Transformations from glucose to bio-based DET isobutanol- Gevo process.¹²⁸

The isobutanol (Gevo)¹²⁸ route having 6 reaction steps to DET but with 34.9% AE_T is also poorly atom economic as the C6 atoms in glucose were first reduced to C4 and all the six oxygen atoms removed to obtain isobutene (Table 6-5, entry 3, Figure 6-26). The isobutene was later dimerized to a C8 atom isooctene. AE_T for the “absolute ethene route” is also very low (34.9%) with 8 reaction steps to DET.¹²⁷ The route goes from C6 atoms in glucose to C2 atoms to obtain ethene and then back to C6 atoms to obtain hexene and finally to C8 atoms to obtain TA (Table 6-5, entry 4, Figure 6-27).

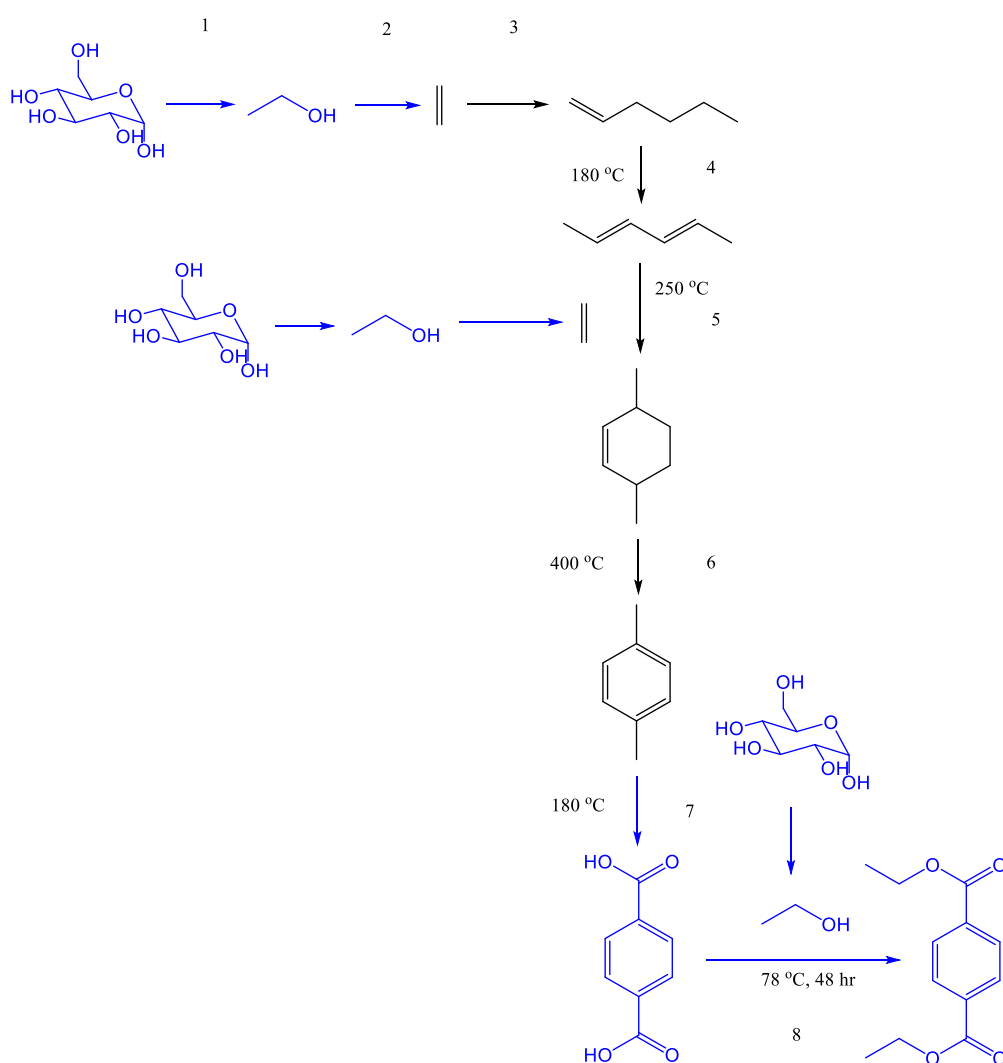


Figure 6-27 Transformations from glucose to bio-based DET via “absolute ethene” process.^{127, 391, 422, 423}

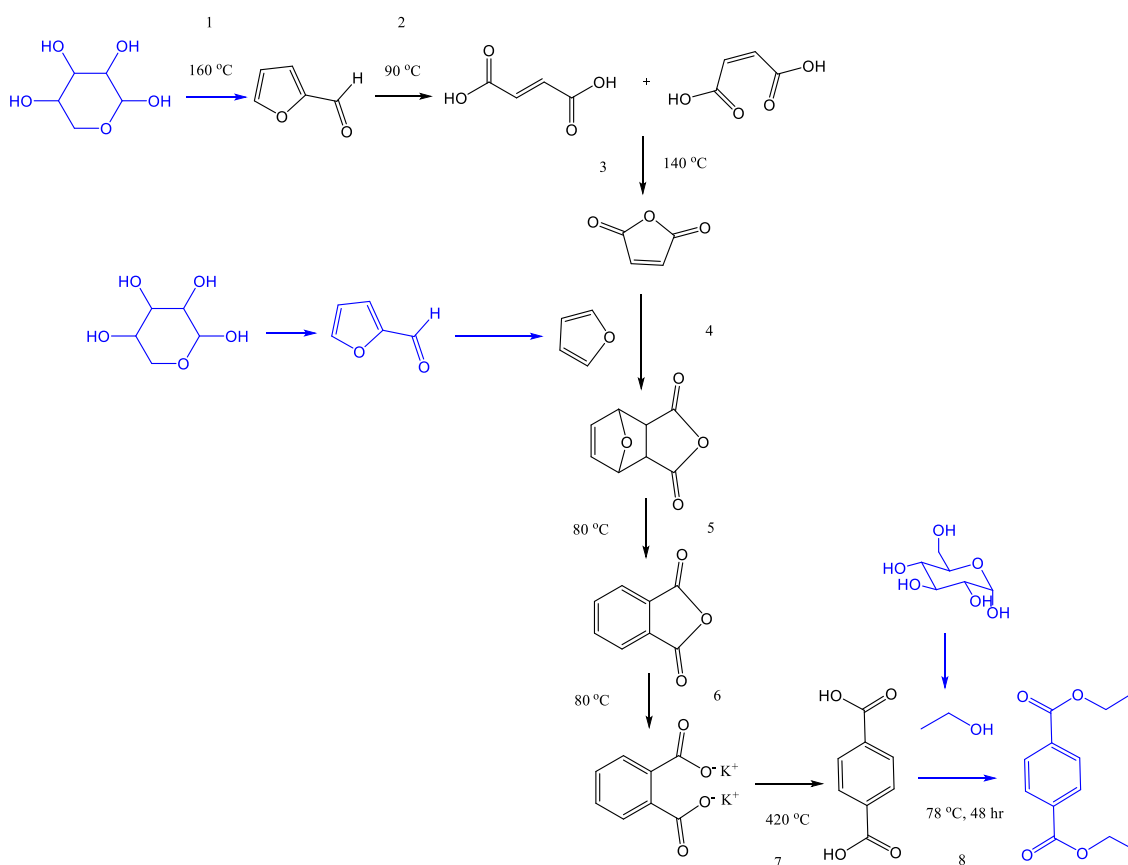


Figure 6- 28 Transformations from hemicellulose (xylose) to bio-based DET via “absolute furfural” process. ^{133, 134, 391, 423, 424}

The “absolute furfural route” has AE_T of 26.4% with 8 reaction steps to DET. Cumulative selectivity and yield of this route is very poor; less than 6% resulting from poor yields in reaction steps 1, 2, 7 and cumulative yield from the synthesis of furan used in step 4 (Table 6-5, entry 5, Figure 6-28). The HMF route *via* 2,5-furandicarboxylic acid (FDCA) recorded the highest AE_T , 44.8% (Table 6-5, this study, Figure 6-29). Although this route also has a low AE_T value it appears greener compared to others as it does not involve the harsh oxidation of *para*-xylene to TA in order to obtain PET. In a four-reaction step, the route goes from C6 atoms in glucose to a C8 atom to obtain DET, and keeps two of three oxygen atoms in HMF in the final terephthalate monomer.

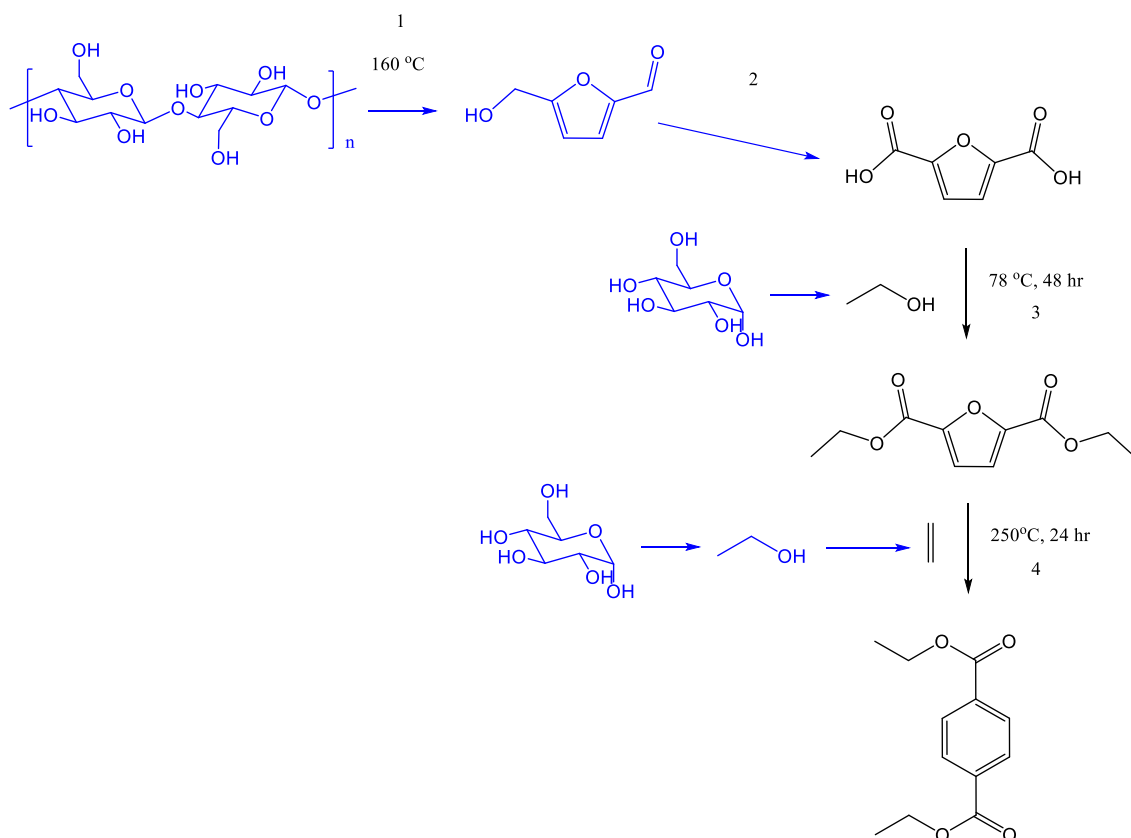


Figure 6-29 Transformations from cellulose to bio-based DET via Diels-Alder addition of FDEE to ethene.^{387, 422}

In a practical sense, information from a process selectivity and AE_T can give us the actual idea of AE called practical atom economy (AE_P). Selectivity of a reaction is defined as the number of moles of desired product per the number of moles of undesired product,⁴²⁵ and is not theoretical. AE_P is the product of selectivity and AE_T .²⁰ Using this information AE_P were calculated for all the routes to evaluate the degree of waste generated. The route herein reported has the highest AE_P which approximately doubles that of entry 2 route (the third highest AE_P and second shortest reaction step). By implication our route will generate the least amount of waste to produce bio-PET.

All the routes employed critical elements in their syntheses. Based on the abundance of critical elements used, the “absolute ethene” and “absolute furfural” routes (entries 4 and 5) are greener compared to other routes. They use elements whose abundance and supply put the least concern to the EU among the critical elements.⁸⁰,

⁴²⁶ Considering energy requirement all the routes at some point in the synthesis operated above 140 °C and thus received a red flag (shown in the metric sheet in the CD attached to this thesis), though these temperatures are often used for bulk chemical manufacturing. Additionally, some routes operated above 300 °C even up to 550 °C in a few transformations (Figure 6-23, Figure 6-26, Figure 6-27 and Figure 6-28). This means the routes are less energy efficient than route (Figure 6-24) and this study (Figure 6-29). Full reaction steps and process energy information are shown in the metrics available in the attached CD.

A full metric evaluation including process mass intensity (PMI), RME and OE are not presented in this report but were generated alongside the metrics (available in the CD). We chose to omit these calculations as we could not gather enough experimental data in the literature to use for a fair comparison of all the routes.

6.6 Conclusions

Our studies have shown that DET can be synthesised *via* Diels-Alder addition of FDEE and ethene under a solventless system catalysed by in-expensive heterogeneous Lewis acid catalysts. FDEE conversions, DET yields and DET selectivity were affected by pressure, temperature, catalyst loading, nature of catalyst and reaction time. It has been shown that temperature has a greater impact on yield than pressure and by varying these factors the optimum DET yield from FDEE was 59% for small scale (0.22 mmol) and 55% for large scale (0.65 mmol) at 250 °C with respect to selectivity and reaction time. This is a step change improvement compared to yields for the same or similar reaction of FDCA and its esters reported elsewhere.⁴²⁷ Although side reactions were observed, namely: oligomerisation of ethene leading to the formation of alkanes, alkenes and poly alkenes; formation of butanol and then transesterification or hydrolysis of FDEE, decarboxylation of diethyl terephthalate, the use of Al-pillared montmorillonite

catalyst allowed reactions to be carried out at higher temperature with higher DET yield achieved without any observed ethene oligomerisation products formed. While acidity has little or no effect on ethene oligomerisation, it (ethene oligomerisation) was seen to increase with higher catalyst loading at the expense of DET yield. Comparison of the route herein reported with other published routes to bio-PET using green metrics shows that our route is the most preferred in terms of yield, selectivity, atom economy and has the shortest reaction step to bio-based DET monomer from the common starting feedstock glucose.

Concluding Remarks and Future Work

Chapter 7

7.0 Concluding remarks and future work

Green chemistry is at the forefront of enlightening the world on the pathway to a “waste-free” and low carbon economy. Biomass has been identified as crucial resources that can be harnessed to save the chemical industry from current over-dependence on petrochemical feedstock. Biomass is renewable and inherently endowed with functionalities such as oxygen, nitrogen, sulphur present in many of today’s chemicals that are derived from petrochemical feedstock through expensive and sometimes harsh chemical transformations. Thus their use will reduce production cost, improve overall atom economy, and in the long term save the chemical industry a lot on transformation processes.

Unilever PLC, aims at generating more bio-based and readily degradable surfactants for incorporation into their home and personal care (HPC) products. This study intended to synthesise a range of diverse surfactants from oleic acid *via* clean synthetic routes, assess their properties and potential applications and incorporate them into Unilever’s formulations. It was also desired to obtain a bio-based aromatic monomer for the production of 100% bio-based PET, as plastic used widely by Unilever for the packaging of their formulations.

The use of biomass feedstock alone is not enough to deliver a clean chemical process unless accompanied with clean technologies, and this ethos has been demonstrated in this study. Over sixty non-ionic surfactants have been generated from renewable resources (oleic acid from rapeseed; linseed oil and lactonic sophorolipid). Chapter 2 shows that successful esterification of oleic acid with methanol gave methyl oleate which was subsequently transesterified with alcohols of varying chain length into corresponding alkyl oleates. Epoxides of the alkyl oleates were prepared and ring-opened with PEGs of varying EO number (PEG chain length). The synthetic routes to alkyl oleate-based surfactants are outlined in Figure 7-1.

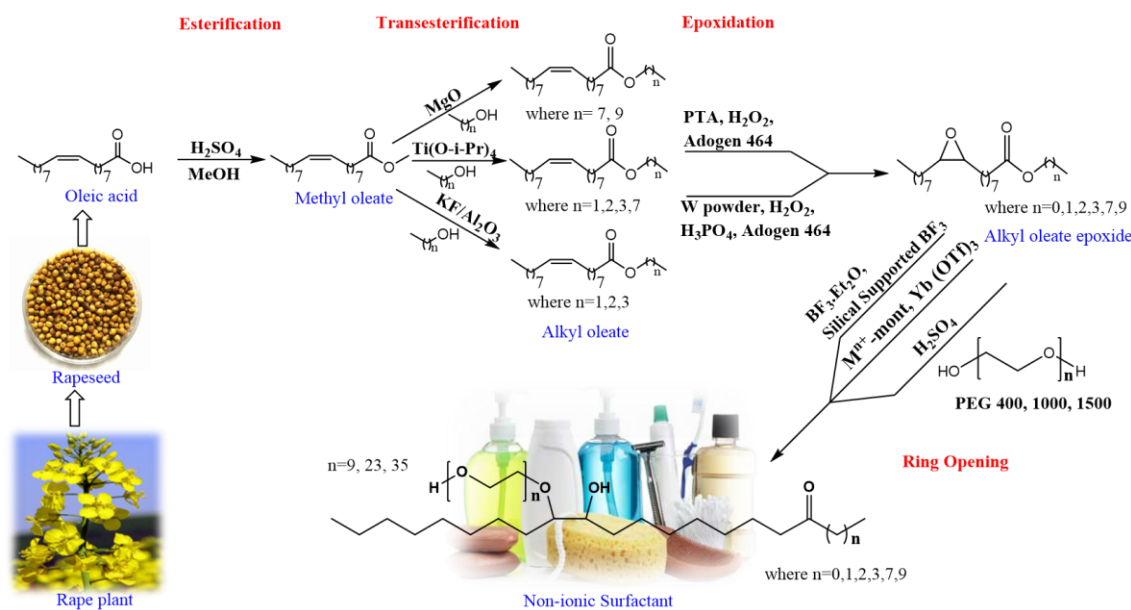


Figure 7- 1 Transformation from rapeseed oil to non-ionic surfactants via esterification of oleic acid to methyl oleate, transesterification to alkyl oleate and epoxidation to alkyl oleate epoxides and ring opening with PEGs.

Heterogeneous catalysts are sometimes more disadvantaged than homogeneous catalysts as they can require considerably higher temperature and catalyst loading as well as longer reaction time to effectively compete in performance with the latter. However, their advantages can far outweigh these shortcomings, with considerably improved recovery and reuse possible. However, leaching is sometimes known to occur in metal-supported catalysts, which often hampers their reuse prospects. KF/Al_2O_3 and $MgO-T600$ were found to be effective heterogeneous catalysts for the transesterification of methyl oleate to alkyl oleates. KF/Al_2O_3 proved more robust than MgO across all the chain lengths of alcohols screened for transesterification. However, reuse of the KF/Al_2O_3 catalyst was not as reliable as with MgO catalyst due to the former leaching into solution. Reactivation of KF/Al_2O_3 in the oven before reuse could possibly improve its performance, though this would require reoptimisation of the catalyst synthesis to mitigate leaching. The MgO catalyst was very stable after four cycles of reuse without significant reduction in conversion and selectivity. Higher alkyl oleates were obtained alongside their oxidation side reaction products (diols and ketones) though the latter were found in trace

quantities. It would be worth investigating if carrying out transesterification in an inert atmosphere could prevent the occurrence of these side products.

Obtaining high epoxide yield from the epoxidation of fatty acid esters is usually challenging because significant amounts of side reaction products such as aldehydes, ketones, epoxy acids and diols are formed. High acidity of the reaction medium, solvent nature, reaction time as well as high reaction temperature are factors that could contribute to the formation of these products. In chapter 3, the use of a PTC shortened the residence time of the epoxide in the acidic aqueous phase which could have initiated significant hydrolysis of both the epoxy ring and the ester end as it was being formed. Most of the heterogeneous catalysts that previously proved effective in the epoxidation of lower molecular olefins were not so effective with fatty acid esters.²³⁶ For silica-supported catalysts, hydrophobicity of the support is key to effective catalysis.⁴²⁸ It has been shown that the size of the support and the substrate matters in order to achieve a high conversion. It was demonstrated in chapter 3 that the supported PTA which was very effective for epoxidation of cyclohexene was not as effective for methyl oleate and completely ineffective for larger alkyl oleates even with prolonged reaction time and increased catalyst loading, this likely due to mass transfer limitations. Conversions with heterogeneously catalysed epoxidations of fatty acid esters and triglycerides were still low even with a combination of ultrasound techniques and mechanical agitation.⁴²⁹ There are still needs to develop heterogeneous epoxidation catalysts that will effectively and selectively transform the substrate having above C19 carbon atoms into their epoxides. As regards the formation of the side products the observed products are consistent with the mechanism provided in the literature. However, it is not obvious how 10-oxo-octadecenoic acid methyl ester was formed in the system as questioned in Figure 3-20 in chapter 3. It will also be interesting to investigate the formation of 2, 5-hexanedione, suberic acid monomethyl ester, methyl-8-oxo-octanoate and octanoic acid-8-hydroxymethyl ester formed as side products *via* UAE.

Another key development of this study was the use of heterogeneous catalysts (Fe-mont, and Al-mont) to effectively and selectively ring-open fatty acid ester epoxides for the first time. This provides a greener alternative to homogeneous boron-trifluoride which is currently the main reagent used for this purpose. Model reactions was instrumental to providing a clearer picture of the ring opening reactions and the structural elucidation of the polymeric surfactants. During the study NMR assignments showed the carbons and protons to which PEGs and hydroxyl groups are attached to the fatty acid epoxide chain are distinct contrary to what was earlier reported in a similar study.³³² Use of fructose, inulin and D-sorbitol as hydrophiles in this study did not yield success due to their insolubility in the reaction mixture and limited choice of solvents that will not complex with the carbohydrates or the product. Development of effective methods to ring-open fatty acid epoxides with these hydrophiles will deliver novel surfactants that are highly degradable and wholly bio-derived. Of particular interest in this study was the successful synthesis of novel lactonic sophorolipid epoxide and the five surfactants based on this exciting emerging platform chemical. Future work on this should look into a heterogeneous catalysis of the epoxidation process, based on developments made elsewhere in this study.

Efforts were made to have the synthesised surfactants tested at Unilever PLC but measurements were not concluded in time for inclusion in this thesis. However, some initial results were generated for the surfactants earlier tested in the company. Potential applications for surfactants based on the theoretical HLB concept are; O/W emulsification, detergency, wetting and solubilisation. The HLB values generated for surfactants in this study may not be totally accurate since the ECL method is based on surfactants in which polyethylene oxide is the main hydrophilic group, whilst we prepared a wider range of surfactants with differing hydrophilic groups. Currently HLB values were calculated for sophorolipid-based surfactants using Griffin's equations as there were no available methods that specifically considered this family of materials in the literature. As sophorolipids demonstrate biological

activities,^{430,431} it would be interesting to assess these novel compounds for possible microbial activities in addition to their surfactancy applications. The CPP concept discussed for surfactants in this study was based on the assumption that the hydrophilic head and hydrophobic tail are located in distinct positions; these using PEG as the main polar head. This, however is not completely true for all our surfactants as some have more than one hydrophilic groups scattered round the compound.

A bio-based aromatic monomer, diethyl terephthalate (DET), for the delivery of 100% bio-derived PET has also been developed in this study. Results obtained from comparing metrics of published main routes to bio-PET with our route show that our solventless pathway to DET which employs in-expensive heterogeneous Lewis acid catalysts shows prospects as the most convenient and “greenest” route to bio-based PET. Although oligomerisation of ethene leading to the formation of alkanes, alkenes and poly alkenes is perceived as an undesired side-reaction to this study, it is possible that these may serve as alternative routes to other useful bio-derived aromatics. In fact, there is already an established process that converts poly-alkylated aromatics to lighter mono-alkylated aromatics which have greater prospects.⁴³² Temperature and pressure were key parameters that needed to be controlled to achieve a high FDEE conversion. While we were able to vary temperature to a great extent not much variation was investigated for pressure (fill pressure) as we could not exceed the maximum pressure limit of the ethylene cylinder. In the current study, furan:ethene ratios used for small scale and large scale reactions were 1:82 and 1:5 moles respectively. Therefore, it will be worth carrying out more studies on the effects of furan:ethene and ethene/furan:catalyst ratio on both scales to optimise DET yield. Another major area that needs consideration is the possibility to use a flow system for DET synthesis. This will eliminate high catalyst loading required in this study and also likely prevent issues arising from FDEE sublimation. Studies on the reuse of the pillared catalysts suggest a possibility that the catalyst pillars started to collapse after the first cycle. Therefore, further

study should be carried out to improve on the current catalyst with a particular emphasis on improving its stability. Therefore it is worth considering zeolites and micelle templated aluminosilicates which are known to have significantly higher temperatures tolerance in comparison to clays. Product mass recovery for this current DET study is around 75 wt% of the starting materials. While sonication has been applied to facilitate product desorption from the catalyst pores, unreacted ethene vented into a solvent and the reactor thoroughly washed off, TG-IR study of the “washed” catalyst showed that the furans are still trapped in the catalyst pores, and this too may be responsible for issues for catalyst recycling a reuse. Real time analysis of the unreacted gas as it is being vented could also provide further information about this loss of mass during the reaction. Nevertheless, significant improvements in the yield of terephthalate from bio-derived furans has been made, showing great promise for a route to 100% bio-derived PET.

7.1 *Outcomes of this work*

7.1.1 Conferences

- 4th Northern Sustainable Chemistry (NORSC) Postgraduate Symposium, Huddersfield University, 23rd October, 2014.
- Building Sustainability into your Business: The case for Bio-based Chemicals, Green Chemistry Centre of Excellence (GCCE), Department of Chemistry, University of York, 6th October, 2014.
- Bio-based Polymer Day, Green Chemistry Centre of Excellence (GCCE), Department of Chemistry, University of York, 17th July, 2014.
- Natural Cosmetics Seminar organised by BEACON, WISE Network and BBSRC High Value Chemicals from Plants Network (HVCfP), University of Bangor, United Kingdom, 12th January 2015.

7.1.2 Presentations

- **Clean Synthetic Routes to Bio-based Products:** presented at the 4th Northern Sustainable Chemistry (NORSC) Postgraduate Symposium, Huddersfield University, 23rd October, 2014.
- **Bio-based Surfactants for a Greener Environment:** a poster presentation at the KMS Award Seminar, Department of Chemistry, University of York, 8th October, 2014.
- **Bio-based Surfactants for a Greener Environment:** presented at the Building Sustainability into your Business: The case for Bio-based Chemicals, Green Chemistry Centre of Excellence (GCCE), Department of Chemistry, University of York, 6th October, 2014.
- **Surfactants and Polymers from Biomass:** a poster presentation at the Bruker PhD Poster Competition, Department of Chemistry, University of York, United Kingdom, 18th March, 2015.

7.1.3 Publications

- Synthesis of Bio-derived Diethyl Terephthalate *via* Diels-Alder Addition of ethene to 2, 5-Furan dicarboxylic acid Diethyl Ester: a comparison of routes to bio-PET - a drafted publication due to be submitted shortly.

7.1.4 Awards

- Year 2 PhD Poster Session Winner, at the KMS Award Seminar, Department of Chemistry, University of York, 8th October, 2014.

Experimental

Chapter 8

8.0 Experimental

8.1 *Material and reagents*

Reagents used for this study were sourced as follows: oleic acid (~90%, Aldrich), silica-supported boron trifluoride (Sigma-Aldrich), K30 montmorillonite, iron (III) nitrate nonahydrate and iron (III) chloride (Sigma-Aldrich), PEG 400 (Sigma-Aldrich), MePEG 400 (Alfa-Aesar), MePEG 750 (Alfa-Aesar), PEG av. Mn 950-1050 (Aldrich), PEG 1500 (Sigma-Aldrich), N-methyl-2-pyrrolidone, fructose, inulin from Dahlia, triethyl amine, 2,5-furandicarboxylic acid (Sigma-Aldrich, TCI), Aluminium pillared montmorillonite (Sigma-Aldrich), montmorillonite (Fulmont), aluminium nitrate hexahydrate (Sigma-Aldrich), ammonium-Y-zeolite (Sigma-Aldrich), ethene (BOC gas), titanium silicon oxide (nanopowder <50 nm particle size, Aldrich), titanium dioxide (nanopowder ~21 nm particle size, Aldrich), phosphotungstic acid hydrate (PTA) (Aldrich), tungsten powder (Aldrich), >30% H₂O hydrogen peroxide solution (Sigma-Aldrich), adogen 464 (Sigma-Aldrich), orthophosphoric acid (Fischer Scientific), Celite 545 coarse molecular sieve (Sigma Aldrich), epoxidised linseed oil (Lanroflex chemical), cyclohexene oxide (Aldrich), ethanediol (Fischer scientific), 2-methoxyethanol (Sigma), triethylene glycol (Acros organics) and lactonic sophorolipid (Ecover).

8.2 *Analytical instruments and equipment*

8.2.1 Gas chromatography (GC)

Synthesised compounds were analysed on an Agilent Technologies 6890N Network GC System coupled with a flame ionisation detector. GC methods were developed to give adequate separation of the key reaction components in each reaction. The capillary column was ZB5HT inferno (5%-phenyl 95%-dimethyl polysiloxane). 1 µL automated sample injection (Agilent Technologies 7683B Series Injector) was used throughout analysis.

For the fatty acid-based compounds, the oven was first heated to 50 °C for 4 minutes, ramped at 10 °C/min to 290 °C and held for 10 minutes. Split ratio was 50:1.

For furan-based compounds, the oven heated to 50 °C for 1 minute, ramped at 5 °C/min to 250 °C and held for 1 minute.

8.2.2 GC-MS, SFC, IR and NMR

GC-EI-MS data was obtained using a Perkin Elmer Clarus 500 gas chromatograph interfaced with a Clarus 500 S mass spectrometer in positive ion mode. Accurate mass values were obtained using a Bruker MicrOTOF ESI-TOF, and compared to theoretical 4 decimal places relative molecular masses for assessment of product purity and elemental composition confirmation. SFC was performed on Thar SFC coupled with Waters 2424 ELS detector. IR spectra were obtained by running crude or purified samples neat on a Bruker Vertex 70 fitted with Specac Golden Gate ATR. NMR spectra were obtained on a Jeol 400 and Bruker Avance 700 NMR spectrometers in various solvents (CDCl₃, D₂O, CH₃OD, DMSO-d₆).

8.2.3 ICP-MS and CHN

Inductively coupled plasma mass spectroscopy (ICP-MS) was measured on Agilent 7700x fitted with standard Ni sample and skimmer cones and coupled to a mass spectrometer (MS). The samples were run in He and no-gas mode. CHN analysis was measured Exeter Analytical CE-440-Elemental Analyzer with samples weighed on a Sartorius SE2 balance.

8.2.4 TGA, DSC and porosimetry

Thermo-gravimetric analysis (TGA) was performed on a Netzsch STA 409c thermal analyzer. ~20 mg of accurately weighed sample in a ceramic sample cup was placed into the Netzsch STA 409c furnace with a N₂ flow of 100 ml/min and heated from room temperature to 900 °C and a heating rate of 10 °C/min. For TG-IR the off-gas from the furnace was passed through a 10 cm path-length IR gas-cell in a Bruker

Equinox 55 IR. Both the gas-cell and transfer line were held at 200 °C for the duration of the analysis.

Differential scanning calorimetry (DSC) was performed on a Q2000 TA Instruments DSC. Heat-cool-heat and modulated heat programmes were used and stated as follows:

Heat and cool method

*equilibrate at -80 °C
ramp 10 °C/min to 200 °C
mark end of cycle 0
ramp 10 °C/min to -80 °C
mark end of cycle 0
ramp 10 °C/min to 200 °C
mark end of cycle 0
end of method*

Modulated DSC method

*data storage: off
equilibrate at 100 °C
modulate +/- 0.32 °C every 60 sec
isothermal for 5 min
data storage: on
ramp 2 °C/min to -90 °C
mark end of cycle 0
ramp 2 °C/min to 100 °C
mark end of cycle 0
end of method*

Typically a sample (~9 mg) was weighed into a low mass aluminium pan and sealed with a Hemetic lid. The same reference cell, also sealed with a Hemetic lid, was used for all samples.

Surface analysis of catalysts (MgO-T600, MgO-600 and PTA-SBA-15-NH₂) was measured on a micromeritics TriStar porosimeter. 0.0588 g sample was weighed in a weighted porosimetry tube and degassed in a degassing chamber under an inert atmosphere at 60 °C for 4 hours. The sample tube was reweighed, new sample weight recorded and inserted in a porosimeter for analysis. Reweighted MgO-T600: 0.0583 g; MgO-600: 0.0556 g; PTA-SBA-15-NH₂: 0.0542 g.

8.2.5 Ultrasound and microwave

CEM Discover microwave was used at preset conditions for synthesis of surfactants. A 130 W and 20 kHz ultrasound was used to affect epoxidation and surfactant synthesis at some points in this research.

8.2.6 Tensiometry and dynamics of surfactants

Dynamics studies on synthesised surfactants including surface tension and critical micelle concentration (CMC) measurements among others, were recorded on Sinterface maximum bubble pressure tensiometer and Kruss K100 tensiometer coupled with Metrohm 700 dosino. The extended surfactant characteristic method was used to measure CMC. Dynamic light scattering (DLS) studies to determine cloud point, micelle particle size and micelle aggregation for synthesised surfactants were measured.

8.3 Catalyst preparation

8.3.1 Potassium fluoride on alumina (KF/Al₂O₃)

KF/Alumina was prepared following a procedure reported by Clark *et al.* with minor modifications.¹⁸² ~50 g neutral alumina was activated by drying in a vacuum oven at 150 °C for 15 hours. Catalyst was prepared by using a loading of 1.0 mmol, 2.5 mmol, 5.0 mmol, 7.5 mmol, and 10 mmol of potassium fluoride (KF) per gram of alumina. The appropriate amount of KF was dissolved in 50 mL methanol, and 20 g alumina was added to this KF/methanol solution and stirred at 50 °C for 30 minutes. The methanol was removed using a rotary evaporator; the resulting solid was thereafter dried in a vacuum oven at 150 °C for 18 hours.

8.3.2 Treated magnesium oxide catalyst

250 mL distilled water was slowly added to 25 g freshly opened MgO and stirred at room temperature following a procedure in the literature.²⁰⁸ Temperature was

raised to 80 °C while stirring continuously for 4 hours. Excess water was removed by drying in the oven at 85 °C overnight. The resulting Mg(OH)₂ was heated in nitrogen (30 mL/min) at 600 °C for 18 hours; the MgO obtained was crushed in a mortar and labelled MgO-T600.

8.3.3 Activated MgO catalyst

25 g freshly opened MgO was activated in a furnace by heating to 600 °C in nitrogen (30 mL/min) for 18 hours (hold) and labelled MgO-600. The furnace heating was programmed to ramp at 10 °C/min.

8.3.4 Fe-K30 montmorillonite catalyst

1 M solution iron (III) nitrate nonahydrate was prepared by dissolving 40.4 g of the salt in 100 mL distilled water. To this, 80 g K30 montmorillonite was added and stirred continuously for 24 hours at 50 °C, centrifuged at 3600 rpm at 25 °C for 7 minutes and the supernatant discarded. Resulting clay was washed repeatedly five times with distilled water while centrifuging each time, and dried in the oven at 120 °C for 24 hours and ground in a mortar and stored.^{433, 434}

8.3.5 Al-montmorillonite catalyst

2.8 g (10 mmol) aluminium nitrate was dissolved in 180 mL distilled water. To this solution, 7 g neutral montmorillonite (Fulmont) was added and the suspension heated at 60 °C for 18 hours. The resulting suspension was allowed to settle and the solution decanted to leave the exchanged clay. The catalyst was washed several times by re-suspending in distilled water, centrifuging, and the solution discarded. Finally, the collected solid was dried in a vacuum oven at 80 °C for 5 hours and ground into a powder and stored.

8.3.6 Acid free Al-montmorillonite catalyst

This was prepared as described in section 8.3.5 except that the exchange stage (i.e. contact with aluminium nitrate solution) was repeated two more times to ensure full replacement with Al^{3+} in the montmorillonite, thereby reducing possible acidity. The resulting suspension was allowed to settle and the solution decanted to leave the exchanged clay. The catalyst was washed several times by re-suspending in distilled water, centrifuging, and the solution discarded. Finally, the collected solid was dried in a vacuum oven at 80 °C for 5 hours and ground into a powder and stored.

8.3.7 Fe-montmorillonite catalyst

1.62 g (10 mmol) iron (III) chloride was dissolved in 180 mL distilled water. To this solution, 7 g neutral montmorillonite (Fulmont) was added and the suspension heated at 60 °C for 22 hours. The resulting suspension was allowed to settle and the solution decanted to leave the exchanged clay. The catalyst was washed several times by re-suspending in distilled water, centrifuging, and the solution discarded. Finally, the collected solid was dried in a vacuum oven at 90 °C for 5 hours and ground into a powder and stored.

8.3.8 Al-Y zeolite catalyst

1.86 mmol, 0.4 g, aluminium nitrate was dissolved in 60 mL distilled water and to this solution, 1 g of ammonium-Y-zeolite was added and the suspension heated to 60 °C for 18 hours. The resulting suspension was allowed to settle and the solution decanted to leave the exchanged clay. The catalyst was washed several times by re-suspending in distilled water, centrifuging, and the solution discarded. Finally, the collected solid was dried in a vacuum oven at 80 °C for 5 hours and ground into a powder and stored.

8.3.9 Mesoporous silica catalyst support

24 g Pluronic 123 TCP surfactant was dissolved in 624 mL de-ionised water and 120 mL 37% fuming HCl. This was heated to 35 °C with stirring, to this 51.2 g tetraethyl ortho silicate (TEOS) was added dropwise. The resulting gel was kept at 35 °C for 24 hours, filtered and washed four times with copious amount of de-ionised water. The filtered gel was dried at room temperature under vacuum and calcined in an oven to remove TCP by heating at 2 °C/min to 500 °C in air and holding for 15 hours as earlier reported.^{277, 278} The calcined catalyst was crushed in a mortar and weighed.

8.3.10 Amino-propyl functionalised mesoporous silica catalyst support

1 g pure calcined mesoporous silica prepared in section 8.3.9 was reacted with 50 mL 0.01 M solution 3-aminopropyl triethoxy silane (APTES) in dried toluene under reflux for 8 hours. The resultant white solid was filtered off, washed with dried toluene, filtered and dried under vacuum.

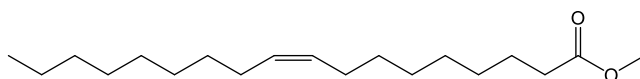
8.3.11 Phosphotungstic acid impregnated on mesoporous silica support

Impregnation of phosphotungstic acid (PTA) on the prepared mesoporous silica was performed as reported in the literature by suspending 0.25 g mesoporous silica in 2.5 mL PTA solution (0.7 M) in 1:1 mixture of acetonitrile and ethanol.²³⁶ The resulting mixture was gently stirred at 70 °C until equilibrium was reached in 24 hours. The solid product was centrifuged and washed several times with ethanol. The precipitate was dried at room temperature and labelled.

8.3.12 Phosphotungstic acid immobilized on amino propyl functionalised mesoporous silica support

20.2 g PTA was dissolved in 10 mL 1:1 acetonitrile and ethanol solvent mixture to obtain a 0.7 M solution. To this 1 g of functionalised mesoporous silica was suspended and the mixture heated to 70 °C and allowed to stay for 24 hours while stirring gently.²³⁶

8.4 Synthesis of methyl oleate



20 g oleic acid and 22.7 g methanol (mole ratio of 1: 10) and 0.2 g sulphuric acid were weighed into a 250 mL round bottom flask and heated under reflux with continuous stirrers for 18 hours. The reaction mixture was allowed to cool to room temperature and washed with water-2-methyl tetrahydrofuran solvent mixture (volume ratio of 1:2). The organic fraction was collected and washed with a further 15 mL distilled water, 25 mL 5% sodium bicarbonate, 15 mL brine solution, solution, dried over anhydrous magnesium sulphate, filtered and the solvent removed *in vacuo* to yield an amber oil (20.56 g, 98% yield by mass recovery, >99% purity). Purity and product identification confirmed by GC-FID, GC-MS, IR spectroscopy, ESI-MS and NMR spectroscopy. ¹H NMR (400 MHz, CDCl₃, δ ppm): 0.83 (3H, t, $J=7.0$ Hz, CH₃CH₂-), 1.24 (18H, overlapped, -(CH₂)₅CH₂CH=CHCH₂(CH₂)₄-), 1.57 (2H, quin, $J=7.0$ Hz, -CH₂CH₂COOCH₃), 1.95 (4H, m, -CH₂CH=CHCH₂-), 2.25 (2H, t, $J=7.3$ Hz, -CH₂COOCH₃), 3.61 (3H, s, -COOCH₃), 5.29 (2H, m, -CH=CH-); ¹³C NMR (100 MHz, CDCl₃, δ ppm): 14.12 (CH₃CH₂-), 22.73 (CH₃CH₂-), 24.98 (-CH₂CH₂COOCH₃), 27.19-27.25 (-CH₂CH=CHCH₂-), 29.13-29.82 (-(CH₂)₅CH₂CH=CHCH₂(CH₂)₄-), 31.96 (-CH₂CH₂CH₂COO-), 34.09 (-CH₂COOCH₃), 51.37 (-COOCH₃), 129.73-129.97 (-CH=CH-), 173.98 (-COO-); EI-MS, 296 (74), 296, 264, 222, 180, 152, 124, 110, 97, 74, 54, 43; ESI-MS accurate mass, 319.2604 (MNa⁺, 319.2608 calc. for C₁₉H₃₆NaO₂); IR (ATR, ν , cm⁻¹), 3004 (=C-H str.), 2924 (a. CH₂ str.), 2854 (s. CH₂ str.), 1742 (C=O str.), 1459 (a. CH₃ bend), 1363 (s. CH₃ bend), 1244, 1196 and 1170 (C-O- str.). NMR and IR spectroscopic assignments are within the range of values reported in the literature.^{150, 171-173}

8.5 Synthesis of alkyl oleates via transesterification of methyl oleate

8.5.1 Transesterification with KF/Al₂O₃ catalyst

5 g (16.8 mmol) methyl oleate was weighed into a 100 mL round bottom flask and calculated amount of desired alcohol was added at a molar ratio of 1:6 (methyl oleate to alcohol). KF/Al₂O₃ (10% wt with respect to methyl oleate) was added and the reaction agitated under reflux while fitted with a Dean-Stark trap. Reaction progression was monitored by GC-FID. 2 mL of the corresponding alcohol was added at 1 hour interval for at least the first 3 hours into the reaction to replenish the alcohol in the flask and force the reaction in favour of the product. After 24 hours, the resulting product was suction filtered to recover catalyst and a rotary evaporator used to remove the solvent to yield an amber oil. Purity and product identification confirmed by GC-FID, GC-MS, IR spectroscopy and ¹H and proton decoupled ¹³C NMR spectroscopy.

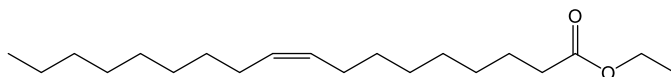
8.5.2 Transesterification with MgO catalyst

5 g (16.8 mmol) methyl oleate was weighed into a 100 mL round bottom flask and calculated amount of desired alcohol was added at a molar ratio of 1:6 (methyl oleate to alcohol). MgO (10% wt with respect to methyl oleate) was added and the reaction agitated under reflux while fitted with a Dean-Stark trap. Reaction progression was monitored by GC-FID. 2 mL of the corresponding alcohol was added at 1 hour interval for at least the first 3 hours into the reaction to replenish the alcohol in the flask and force the reaction in favour of the product. After 24 hours, the resulting product was allowed to cool down and centrifuged on a Thermo Scientific Megafuge 40R centrifuge at 3500 rpm at 20 °C for 20 minutes. The supernatant was transferred into a round bottomed flask and a rotary evaporator used to remove the solvent to yield an amber oil. Purity and product identification confirmed by GC-FID, GC-MS, IR spectroscopy and ¹H and proton decoupled ¹³C NMR spectroscopy.

8.5.3 Transesterification with Ti(O-*i*-Pr)₄ catalyst

5 g (16.8 mmol) methyl oleate was weighed into a 100 mL round bottom flask and calculated amount of desired alcohol was added at a molar ratio of 1:6 (methyl oleate to alcohol). Ti(O-*i*-Pr)₄ (10% wt with respect to methyl oleate) was added and the reaction agitated under reflux while fitted with a Dean-Stark trap. Reaction progression was monitored by GC-FID. 2 mL of the corresponding alcohol was added at 1 hour interval for at least the first 3 hours into the reaction to replenish the alcohol in the flask and force the reaction in favour of the product. After 24 hours of reaction, 25 mL distilled water was added to the reaction product to liberate titanium (IV) oxide and isopropanol, transferred into a separating funnel and shaken with dichloromethane. The organic phase was collected, dried over anhydrous magnesium sulphate, filtered and solvent removed *in vacuo* to yield an amber oil. Purity and product identification confirmed by GC-FID, GC-MS, IR spectroscopy and ¹H and proton decoupled ¹³C NMR spectroscopy.

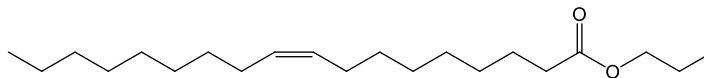
Ethyl oleate



19.73 g total product mass recovered. ¹H NMR (400 MHz, CDCl₃, δ ppm): 0.85 (3H, t, $J=7.0$ Hz, CH₃CH₂-), 1.24 (21H, overlapped, -(CH₂)₅CH₂CH=CHCH₂(CH₂)₄CH₂CH₂-, -COOCH₂CH₃), 1.59 (2H, quint, $J=7.3$ Hz, -CH₂CH₂COOCH₂CH₃), 1.97 (4H, sxt, $J=6.5$ Hz, -CH₂CH=CHCH₂-), 2.26 (2H, t, $J=7.5$ Hz, -CH₂COOCH₃), 4.09 (2H, q, $J=7.3$ Hz, -COOCH₂CH₃), 5.31 (2H, m, -CH=CH-); ¹³C NMR (100 MHz, CDCl₃, δ ppm): 14.16 (CH₃CH₂-), 14.31 (-COOCH₂CH₃), 22.75 (CH₃CH₂-), 25.04 (-CH₂CH₂COOCH₂CH₃), 27.22-27.28 (-CH₂CH=CHCH₂-), 29.16-29.83 (-(CH₂)₅CH₂CH=CHCH₂(CH₂)₄-), 31.98 (-CH₂CH₂CH₂COO-), 34.43 (-CH₂COOCH₃), 60.18 (-COOCH₂CH₃), 129.82-130.06 (-CH=CH-), 173.48 (-COO-); EI-MS, 310 (96), 264, 244, 222, 180, 110, 96, 88, 84, 67, 54, 43; ESI-MS accurate mass, 333.2749 (MNa⁺, 333.2764 calc. for C₂₀H₃₈NaO₂); IR

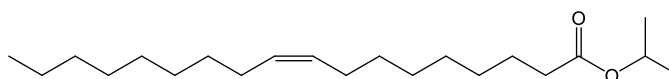
(ATR, ν , cm^{-1}), 3002 (=C-H str.), 2923 (a. CH_2 str.), 2854 (s. CH_2 str.), 1738 (C=O str.), 1464 (a. CH_3 bend), 1373 (s. CH_3 bend), 1244 and 1179 (C-O- str.).

1-propyl oleate



21.16 g total product mass recovered. ^1H NMR (400 MHz, CDCl_3 , δ ppm): 0.86 (3H, t, $J=7.0$ Hz, CH_3CH_2-), 0.92 (3H, t, $J=7.5$ Hz, $-\text{COOCH}_2\text{CH}_2\text{CH}_3$), 1.26 (18H, $J=14.6$ Hz, $-(\text{CH}_2)_5\text{CH}_2\text{CH}=\text{CHCH}_2(\text{CH}_2)_4-$), 1.62 (4H, overlapped, $-\text{CH}_2\text{CH}_2\text{COOCH}_2\text{CH}_2\text{CH}_3$), 1.99 (4H, q, $J=6.5$ Hz, $-\text{CH}_2\text{CH}=\text{CHCH}_2-$), 2.27 (2H, t, $J=7.5$ Hz, $-\text{CH}_2\text{COO}-$), 4.01 (2H, t, $J=6.6$ Hz, $-\text{COOCH}_2\text{CH}_2\text{CH}_3$), 5.32 (2H, m, $-\text{CH}=\text{CH}-$); ^{13}C NMR (100 MHz, CDCl_3 , δ ppm): 10.46 ($-\text{COOCH}_2\text{CH}_2\text{CH}_3$), 14.18 (CH_3CH_2-), 22.08 ($-\text{COOCH}_2\text{CH}_2-$), 22.76 (CH_3CH_2-), 25.09 ($-\text{CH}_2\text{CH}_2\text{COO}-$), 27.23-27.28 ($-\text{CH}_2\text{CH}=\text{CHCH}_2-$), 29.18-29.84 ($-(\text{CH}_2)_5\text{CH}_2\text{CH}=\text{CHCH}_2(\text{CH}_2)_3-$), 31.98 ($-\text{CH}_2\text{CH}_2\text{CH}_2\text{COO}-$), 34.45 ($-\text{CH}_2\text{COO}-$), 66.88 ($-\text{COOCH}_2\text{CH}_2\text{CH}_3$), 129.82-130.06 ($-\text{CH}=\text{CH}-$), 174.07 ($-\text{COO}-$); EI-MS, 324 (97), 264, 222, 180, 123, 111, 97, 83, 68, 54, 43; ESI-MS accurate mass, 347.2922 (MNa^+ , 347.2921 calc. for $\text{C}_{21}\text{H}_{40}\text{NaO}_2$); IR (ATR, ν , cm^{-1}), 3004 (=C-H str.), 2924 (a. CH_2 str.), 2854 (s. CH_2 str.), 1738 (C=O str.), 1464 (a. CH_3 bend), 1378 (s. CH_3 bend), 1242 and 1176 (C-O- str.).

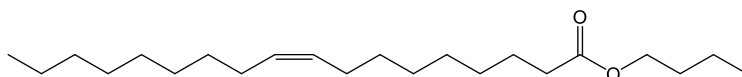
2-propyl oleate



20.06 g total product mass recovered. ^1H NMR (400 MHz, CDCl_3 , δ ppm): 0.86 (3H, t, $J=6.8$ Hz, CH_3CH_2-), 1.22 (26H, overlapped, $-(\text{CH}_2)_6\text{CH}_2\text{CH}=\text{CHCH}_2(\text{CH}_2)_4\text{CH}_2\text{CH}_2-$, $-\text{COOCH}(\text{CH}_3)_2$), 1.58 (2H, m, $-\text{CH}_2\text{CH}_2\text{COO}-$), 1.98 (4H, m, $-\text{CH}_2\text{CH}=\text{CHCH}_2-$), 2.23 (2H, t, $J=7.5$ Hz, $-\text{CH}_2\text{COO}-$), 4.98 (1H, spt, $J=6.2$ Hz, $-\text{COOCH}(\text{CH}_3)_2$), 5.31 (2H, m, $-\text{CH}=\text{CH}-$); ^{13}C NMR (100 MHz, CDCl_3 , δ ppm): 14.18 (CH_3CH_2-), 21.92 ($-\text{COOCH}(\text{CH}_3)_2$), 22.76 (CH_3CH_2-), 25.10 ($-\text{CH}_2\text{CH}_2\text{COO}-$), 27.23-27.28 ($-\text{CH}_2\text{CH}=\text{CHCH}_2-$), 29.18-29.84 ($-(\text{CH}_2)_5\text{CH}_2\text{CH}=\text{CHCH}_2(\text{CH}_2)_3-$), 31.98 ($-\text{CH}_2\text{CH}_2\text{CH}_2\text{COO}-$), 34.79 ($-\text{CH}_2\text{COO}-$), 67.36 ($-\text{COOCH}(\text{CH}_3)_2$).

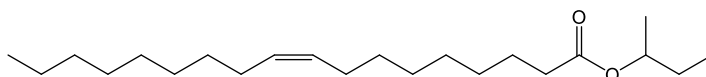
COOCH(CH₃)₂), 129.82, 130.05 (-CH=CH-), 173.48 (-COO-); EI-MS, 324 (55), 264, 222, 179, 125, 111, 97, 83, 69, 55, 43; ESI-MS accurate mass, 347.2919 (MNa⁺, 347.2921 calc. for C₂₁H₄₀NaO₂); IR (ATR, ν, cm⁻¹), 3006 (=C-H str.), 2980 (a. CH₃ str.), 2926 (a. CH₂ str.), 2856 (s. CH₂ str.), 1735 (C=O str.), 1468 (a. CH₃ bend), 1376 (s. CH₃ bend), 1249 and 1181 (C-O- str.).

1-butyl oleate



19.80 g total product mass recovered. ¹H NMR (400 MHz, CDCl₃, δ ppm): 0.85 (3H, t, *J*=7.0 Hz, CH₃CH₂-), 0.90 (3H, t, *J*=7.3 Hz, -COO(CH₂)₃CH₃), 1.28 (20H, overlapped, -(CH₂)₅CH₂CH=CHCH₂(CH₂)₄COOCH₂CH₂CH₂CH₃), 1.58 (4H, overlapped, -CH₂CH₂COOCH₂CH₂CH₂CH₃), 1.98 (4H, m, -CH₂CH=CHCH₂-), 2.26 (2H, t, *J*=7.5 Hz, -CH₂COO-), 4.04 (2H, t, *J*=6.8 Hz, -COOCH₂CH₂CH₂CH₃), 5.31 (2H, m, -CH=CH-); ¹³C NMR (100 MHz, CDCl₃, δ ppm): 13.75 (-COOCH₂CH₂CH₂CH₃), 14.15 (CH₃CH₂-), 19.21 (-COOCH₂CH₂CH₂CH₃), 22.74 (CH₃CH₂-), 25.06 (-CH₂CH₂COO-), 27.21, 27.27 (-CH₂CH=CHCH₂-), 29.16-29.83 (-(CH₂)₅CH₂CH=CHCH₂(CH₂)₃-), 30.77 (-COOCH₂CH₂CH₂CH₃), 31.97 (-CH₂CH₂CH₂COO-), 34.43 (-CH₂COO-), 64.14 (-COOCH₂CH₂CH₂CH₃), 129.82, 130.06 (-CH=CH-), 174.01 (-COO-); EI-MS, 338 (56), 264, 222, 180, 111, 96, 83, 68, 56; ESI-MS accurate mass, 361.3070 (MNa⁺, 361.3077 calc. for C₂₂H₄₂NaO₂); IR (ATR, ν, cm⁻¹), 3005 (=C-H str.), 2957 (a. CH₃ str.), 2924 (a. CH₂ str.), 2854 (s. CH₂ str.), 1737 (C=O str.), 1464 (a. CH₃ bend), 1379 (s. CH₃ bend), 1243 and 1174 (C-O- str.).

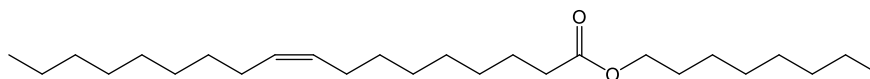
2-butyl oleate



21.27 g total product mass recovered. ¹H NMR (400 MHz, CDCl₃, δ ppm): 0.87 (6H, t, overlapped, CH₃(CH₂)₇CH=CH(CH₂)₇COOCH(CH₃)CH₂CH₃), 1.17 (3H, d, *J*=6.2 Hz, -COOCH(CH₃)CH₂CH₃), 1.26 (20H, d, -(CH₂)₆CH₂CH=CHCH₂(CH₂)₄-), 1.54 (4H, m,

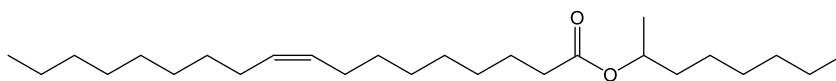
overlapped, $-CH_2CH_2COOCH(CH_3)CH_2CH_3$), 1.98 (4H, m, $-CH_2CH=CHCH_2-$), 2.25 (2H, t, $J=7.7$ Hz, $-CH_2COO-$), 4.82 (1H, sxt, $-COOCH(CH_3)CH_2CH_3$), 5.31 (2H, m, $-CH=CH-$); ^{13}C NMR (100 MHz, $CDCl_3$, δ ppm): 9.77 ($-COOCH(CH_3)CH_2CH_3$), 14.17 (CH_3CH_2-), 19.75 ($-COOCH(CH_3)CH_2CH_3$), 22.75 (CH_3CH_2-), 25.17 ($-CH_2CH_2COO-$), 27.23, 27.28 ($-CH_2CH=CHCH_2-$), 28.89 ($-COOCH(CH_3)CH_2CH_3$), 29.19-29.84 ($(CH_2)_5CH_2CH=CHCH_2(CH_2)_3-$), 31.98 ($-CH_2CH_2CH_2COO-$), 34.79 ($-CH_2COO-$), 71.93 ($-COOCH(CH_3)CH_2CH_3$), 129.81, 130.03 ($-CH=CH-$), 173.62 ($-COO-$); EI-MS, 338 (55), 265, 222, 179, 123, 111, 97, 83, 69, 55, 43; ESI-MS accurate mass, 361.3073 (MNa^+ , 361.3077 calc. for $C_{22}H_{42}NaO_2$); IR (ATR, ν , cm^{-1}), 3003 ($=C-H$ str.), 2924 (a. CH_2 str.), 2854 (s. CH_2 str.), 1733 ($C=O$ str.), 1460 (a. CH_3 bend), 1377 (s. CH_3 bend), 1246 and 1177 ($C-O$ str.).

1-octyl oleate



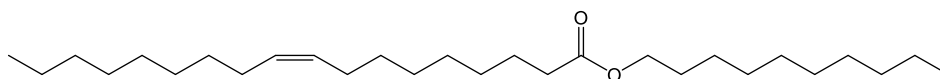
26.63 g total product mass recovered. 1H NMR (400 MHz, $CDCl_3$, δ ppm): 0.85 (6H, t, $J=6.6$ Hz, $CH_3(CH_2)_7CH=CH(CH_2)_7COO(CH_2)_7CH_3$), 1.26 (30H, d, $J=13.5$ Hz, $(CH_2)_6CH_2CH=CHCH_2(CH_2)_4CH_2CH_2COOCH_2CH_2(CH_2)_5CH_3$), 1.58 (4H, m, overlapped, $-CH_2CH_2COOCH_2CH_2-$), 1.98 (4H, m, $-CH_2CH=CHCH_2-$), 2.26 (2H, t, $J=7.5$ Hz, $-CH_2COO-$), 4.03 (2H, t, $J=6.8$ Hz, $-COOCH_2-$), 5.32 (2H, m, $-CH=CH-$); ^{13}C NMR (100 MHz, $CDCl_3$, δ ppm): 14.14, 14.17 ($CH_3(CH_2)_7CH=CH(CH_2)_7COO(CH_2)_7CH_3$), 22.70 ($-COO(CH_2)_6CH_2CH_3$), 22.75 (CH_3CH_2-), 25.09 ($-CH_2CH_2COO-$), 26.01 ($-COO(CH_2)_5CH_2-$), 27.23, 27.28 ($-CH_2CH=CHCH_2-$), 28.73 ($-COO(CH_2)_4CH_2-$), 29.18-29.83 ($(CH_2)_5CH_2CH=CHCH_2(CH_2)_3CH_2CH_2COOCH_2CH_2(CH_2)_2-$), 31.85 ($-COOCH_2CH_2-$), 31.98 ($-CH_2CH_2CH_2COO-$), 34.46 ($-CH_2COO-$), 64.46 ($-COOCH_2(CH_2)_6CH_3$), 129.80, 130.04 ($-CH=CH-$), 174.03 ($-COO-$); EI-MS, 394 (55), 264, 222, 180, 123, 111, 83, 69, 55, 43; ESI-MS accurate mass, 417.3685 (MNa^+ , 417.3703 calc. for $C_{26}H_{50}NaO_2$); IR (ATR, ν , cm^{-1}), 3004 ($=C-H$ str.), 2954 (a. CH_3 str.), 2923 (a. CH_2 str.), 2854 (s. CH_2 str.), 1738 ($C=O$ str.), 1588 ($C=C$ str.), 1465 (a. CH_3 bend), 1378 (s. CH_3 bend), 1243 and 1172 ($C-O$ str.).

2-octyl oleate



23.84 g total product mass recovered. ^1H NMR (400 MHz, CDCl_3 , δ ppm): 0.84 (6H, t, $J=6.6$ Hz, CH_3CH_2- , $-\text{COOCH}(\text{CH}_3)(\text{CH}_2)_5\text{CH}_3$), 1.16 (3H, d, $-\text{COOCH}(\text{CH}_3)(\text{CH}_2)_5\text{CH}_3$), 1.25 (28H, d, $J=13.5$ Hz, $-(\text{CH}_2)_6\text{CH}_2\text{CH}=\text{CHCH}_2(\text{CH}_2)_4\text{CH}_2\text{CH}_2\text{COO}-$, $-\text{CH}(\text{CH}_3)\text{CH}_2(\text{CH}_2)_4\text{CH}_3$), 1.43 (1H, m, $-\text{COOCH}(\text{CH}_3)\text{HCH}(\text{CH}_2)_4\text{CH}_3$), 1.55 (3H, m, overlapped, $-\text{CH}_2\text{CH}_2\text{COOCH}(\text{CH}_3)\text{HCH}(\text{CH}_2)_4\text{CH}_3$), 1.97 (4H, m, $-\text{CH}_2\text{CH}=\text{CHCH}_2-$), 2.23 (2H, t, $J=7.1$ Hz, $-\text{CH}_2\text{COO}-$), 4.86 (1H, m, $-\text{COOCH}-$), 5.30 (2H, m, $-\text{CH}=\text{CH}-$); ^{13}C NMR (100 MHz, CDCl_3 , δ ppm): 14.13, 14.18 ($\text{CH}_3(\text{CH}_2)_7\text{CH}=\text{CH}(\text{CH}_2)_7\text{COO}-$, $-\text{CH}(\text{CH}_3)(\text{CH}_2)_5\text{CH}_3$), 20.09 ($-\text{COOCH}(\text{CH}_3)(\text{CH}_2)_5\text{CH}_3$), 22.65 ($-\text{COOCH}(\text{CH}_3)(\text{CH}_2)_4\text{CH}_2\text{CH}_3$), 22.76 (CH_3CH_2-), 25.18 ($-\text{CH}_2\text{CH}_2\text{COO}-$), 25.45 ($-\text{COOCH}(\text{CH}_3)(\text{CH}_2)_3\text{CH}_2\text{CH}_2\text{CH}_3$), 27.24, 27.29 ($-\text{CH}_2\text{CH}=\text{CHCH}_2-$), 29.20-29.85 ($-(\text{CH}_2)_5\text{CH}_2\text{CH}=\text{CHCH}_2(\text{CH}_2)_3\text{CH}_2\text{CH}_2\text{COOCH}(\text{CH}_3)\text{CH}_2(\text{CH}_2)_2\text{CH}_2\text{CH}_2\text{CH}_3$), 31.83 ($-\text{COOCH}(\text{CH}_3)(\text{CH}_2)_2\text{CH}_2(\text{CH}_2)_2\text{CH}_3$), 31.98 ($-\text{CH}_2\text{CH}_2\text{CH}_2\text{COO}-$), 34.82 ($-\text{CH}_2\text{COO}-$), 36.04 ($-\text{COOCH}(\text{CH}_3)\text{CH}_2(\text{CH}_2)_4\text{CH}_3$), 70.79 ($-\text{COOCH}-$), 129.82, 130.05 ($-\text{CH}=\text{CH}-$), 173.61 ($-\text{COO}-$); EI-MS, 394 (55), 264, 220, 179, 123, 111, 97, 83, 69, 55, 43; ESI-MS accurate mass, 417.3698 (MNa^+ , 417.3703 calc. for $\text{C}_{26}\text{H}_{50}\text{NaO}_2$); IR (ATR, ν , cm^{-1}), 3003 ($=\text{C}-\text{H}$ str.), 2954 (a. CH_3 str.), 2924 (a. CH_2 str.), 2854 (s. CH_2 str.), 1733 ($\text{C}=\text{O}$ str.), 1462 (a. CH_3 bend), 1377 (s. CH_3 bend), 1246 and 1180 ($\text{C}-\text{O}$ str.).

1-decyl oleate



20.39 g total product mass recovered. ^1H NMR (400 MHz, CDCl_3 , δ ppm): 0.86 (6H, t, $J=6.8$ Hz, $\text{CH}_3(\text{CH}_2)_7\text{CH}=\text{CH}(\text{CH}_2)_7\text{COO}(\text{CH}_2)_9\text{CH}_3$), 1.26 (34H, d, $J=15.1$ Hz, $-(\text{CH}_2)_6\text{CH}_2\text{CH}=\text{CHCH}_2(\text{CH}_2)_4\text{CH}_2\text{CH}_2\text{COOCH}_2\text{CH}_2(\text{CH}_2)_7\text{CH}_3$), 1.58 (4H, quin, $-\text{CH}_2\text{CH}_2\text{COOCH}_2\text{CH}_2-$), 1.98 (4H, sxt, $J=6.4$ Hz, $-\text{CH}_2\text{CH}=\text{CHCH}_2-$), 2.26 (2H, t, $J=7.6$ Hz, $-\text{CH}_2\text{COO}-$), 4.03 (2H, t, $J=6.8$ Hz, $-\text{COOCH}_2-$), 5.32 (2H, dt, $J=5.6, 3.1$ Hz, $-\text{CH}=\text{CH}-$); ^{13}C

NMR (100 MHz, CDCl₃, δ ppm): 14.18 (CH₃CH₂-, -COO(CH₂)₉CH₃), 22.76 (CH₃CH₂-), 25.09 (-CH₂CH₂COO-), 26.01 (-COO(CH₂)₈CH₂-), 27.24, 27.29 (-CH₂CH=CHCH₂-), 28.73 (-COO(CH₂)₇CH₂-), 29.19-29.85 (-(CH₂)₅CH₂CH=CHCH₂(CH₂)₃CH₂CH₂COO-, -CH₂CH₂(CH₂)₅-), 31.97 (-COOCH₂CH₂-), 31.99 (-CH₂CH₂CH₂COO-), 34.47 (-CH₂COO-), 64.48 (-COOCH₂(CH₂)₈CH₃), 129.81, 130.05 (-CH=CH-), 174.06 (-COO-); EI-MS, 420 (55), 264, 222, 180, 123, 111, 97, 83, 69, 55, 43; ESI-MS accurate mass, 445.3993 (MNa⁺, 445.4016 calc. for C₂₈H₅₄NaO₂); IR (ATR, ν , cm⁻¹), 3005 (=C-H str.), 2923 (a. CH₂ str.), 2854 (s. CH₂ str.), 1738 (C=O str.), 1465 (a. CH₃ bend), 1354 (s. CH₂ bend), 1243 and 1170 (C-O- str.)

8.5.4 Reuse of KF/Al₂O₃ for transesterification

6.0 g (20.3 mmol) methyl oleate was weighed into a 100 mL round bottom flask and 5.6 g (121.5 mmol) ethanol was added. 0.6 g KF/Al₂O₃ was added and the reaction agitated under reflux while fitted with a Dean-Stark trap. Reaction progression was monitored by GC-FID. 2 mL of ethanol was added at 1 hour interval for at least the first 3 hours into the reaction to replenish ethanol in the flask and force the reaction in favour of the product. After 24 hours, the resulting product was suction filtered to recover catalyst and a rotary evaporator used to remove the solvent to yield an amber oil. The recovered catalyst was washed repeatedly (5x each) with cyclohexane and thereafter acetone, dried in the air and recirculated as a catalyst three more times. Purity and product identification confirmed by GC-FID, GC-MS, IR spectroscopy and ¹H and ¹³C NMR spectroscopy.

8.5.5 Reuse of MgO for transesterification

6.0 g (20.3 mmol) methyl oleate was weighed into a 100 mL round bottom flask and 27 g (207.3 mmol) octanol was added. 0.6 g MgO-T600 was added and the reaction agitated under reflux while fitted with a Dean-Stark trap. Reaction progression was monitored by GC-FID. 2 mL of octanol was added at 1 hour interval for at least the first 3 hours into the reaction to replenish octanol and force the reaction in favour of the product. After 24 hours, the resulting product was allowed to cool down and

centrifuged on a Thermo Scientific Megafuge 40R centrifuge at 3500 rpm at 20 °C for 20 minutes. The supernatant was transferred into a round bottomed flask connected to a vacuum pump to remove octanol to yield an amber oil. The recovered catalyst was washed repeatedly (5x each) with cyclohexane and thereafter acetone, dried in the air and recirculated as a catalyst three more times. Purity and product identification confirmed by GC-FID, GC-MS, IR spectroscopy and ¹H and ¹³C NMR spectroscopy.

8.6 Syntheses of alkyl oleate epoxides (octadecanoic acid-9, 10-epoxy alkyl esters)

8.6.1 Syntheses of alkyl oleate epoxides *via in situ* phosphotungstic acid

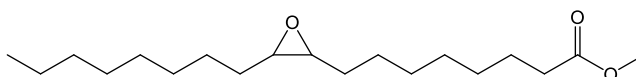
A known amount of tungsten powder (1% wt with respect to oleate), 0.7 mL hydrogen peroxide solution (>30% w/w water) and 0.7 mL water were added into a 250 mL round bottom flask and heated at 50 °C with serious agitation for 30 minutes. Ortho phosphoric acid (0.5% wt of oleate) pre-diluted in 0.5 mL water was added in drops over 15 minutes while heating continuously. 10 mmol alkyl oleate oil, 7 mL water, 2 mL hydrogen peroxide solution and Adogen 464 (1% wt of oleate oil) were added and heated at 50 °C for typically 3 hours. The resulting product was shaken with 100 mL ethylacetate in a separating funnel, the ethylacetate layer collected, dried over anhydrous magnesium sulphate, filtered and the solvent removed *in vacuo* to yield a light amber oil. The product was analysed by IR spectroscopy, GC-MS and ¹H and proton decoupled ¹³C NMR spectroscopy and quantified by GC-FID.

8.6.2 Syntheses of alkyl oleate epoxides *via* phosphotungstic acid

Typically 100.15 mmol alkyl oleate, phosphotungstic acid (6% wt with respect to alkyl oleate), 40 mL hydrogen peroxide solution, 30 mL water and Adogen 464 (3% wt with respect to alkyl oleate) were added into a 250 mL round bottom flask and was heated at 50 °C with vigorous stirring for typically 3 hours. Resulting product

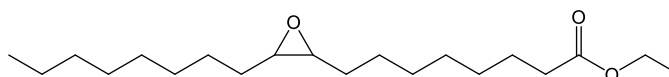
was transferred into a separating funnel and washed with water-ethylacetate mixture. The ethylacetate layer was dried over anhydrous magnesium sulphate, filtered and the filtrate passed down a column of neutral alumina. Ethyl acetate was removed *in vacuo* to yield a very light amber oil. The product was analysed by IR spectroscopy, GC-MS, ESI-MS, CHN elemental analysis (for a few), ¹H and proton decoupled ¹³C NMR spectroscopy and quantified by GC-FID.

Methyl oleate epoxide



29.84 g total product mass recovered. ¹H NMR (400 MHz, CDCl₃, δ ppm): 0.73 (3H, t, $J=6.8$ Hz, CH₃CH₂-), 1.22 (24H, overlapped, -(CH₂)₇HC(O)CH(CH₂)₅-), 1.47 (2H, m, -CH₂CH₂COOCH₃), 2.15 (2H, t, $J=7.3$ Hz, -CH₂COOCH₃), 2.74 (~2H, m, -HC(O)CH-), , 3.61 (3H, s, -COOCH₃); ¹³C NMR (100 MHz, CDCl₃, δ ppm): 14.01 (CH₃CH₂-), 22.61 (CH₃CH₂-), 24.83 (-CH₂CH₂COOCH₃), 26.52, 26.58 (-CH₂CH₂HC(O)CHCH₂CH₂-), 27.74, 27.78 (-CH₂HC(O)CHCH₂-), 28.97-29.50 (- (CH₂)₄CH₂CH₂HC(O)CHCH₂CH₂(CH₂)₂-), 31.82 (-CH₂CH₂CH₂COO-), 33.92 (-CH₂COOCH₃), 51.25 (-COOCH₃), 57.02, 57.06 (-HC(O)CH-), 174.00 (-COO-); EI-MS, 312 (55), 254, 223, 199, 185, 155, 109, 97, 83, 74, 55, 43; ESI-MS accurate mass, 335.2543 (MNa⁺, 335.2557 calc. for C₁₉H₃₆NaO₃); IR (ATR, ν , cm⁻¹), 2924 (a. CH₂ str.), 2855 (s. CH₂ str.), 1740 (C=O str.), 1463 (a. CH₃ bend), 1363 (s. CH₃ bend), 1247, 1197 and 1170 (C-O- str.), 979 (epoxy asym. def.), 823 (epoxy sym. def.). The epoxy bands assignment are in line with values reported in the literature.^{212, 245}

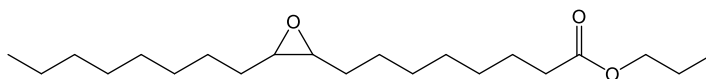
Ethyl oleate epoxide



33.10 g total product mass recovered. ¹H NMR (400 MHz, CDCl₃, δ ppm): 0.80 (3H, t, $J=6.8$ Hz, CH₃CH₂-), 1.26 (27H, overlapped, -(CH₂)₇HC(O)CH(CH₂)₅CH₂CH₂COO-, -CH₂CH₃), 1.54 (2H, quin, -CH₂CH₂COO-), 2.20 (2H, t, $J=7.3$ Hz, -CH₂COO-), 2.82 (2H,

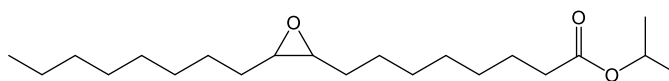
m, $-HC(O)CH-$), 4.04 (2H, q, $J=14.2, 7.3$ Hz, $-COOCH_2CH_3$); ^{13}C -NMR (100 MHz, $CDCl_3$, δ ppm): 14.11 (CH_3CH_2-), 14.26 ($-COOCH_2CH_3$), 22.69 (CH_3CH_2-), 24.94 ($-CH_2CH_2COO-$), 26.59, 26.63 ($-CH_2CH_2HC(O)CHCH_2CH_2-$), 27.82, 27.85 ($-CH_2HC(O)CHCH_2-$), 29.05-29.57 ($-(CH_2)_4CH_2HC(O)CHCH_2(CH_2)_3-$), 31.88 ($-CH_2CH_2CH_2COO-$), 34.33 ($-CH_2COO-$), 57.16, 57.21 ($-HC(O)CH-$), 60.14 ($-COOCH_2CH_3$), 173.78 ($-COO-$); EI-MS, 325 (69), 281, 213, 185, 155, 121, 109, 95, 81, 69, 54, 43; ESI-MS accurate mass, 349.2707 (MNa^+ , 349.2713 calc. for $C_{20}H_{38}NaO_3$); IR (ATR, ν , cm^{-1}), 2924 (a. CH_2 str.), 2855 (s. CH_2 str.), 1736 ($C=O$ str.), 1464 (a. CH_3 bend), 1373 (s. CH_3 bend), 1246 and 1178 ($C-O$ str.), 823 (epoxy sym. def.).

1-propyl oleate epoxide



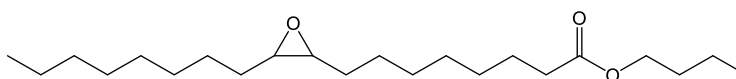
34.39 g total product mass recovered. 1H NMR (400 MHz, $CDCl_3$, δ ppm): 0.83 (3H, t, $J=6.8$ Hz, CH_3CH_2-), 0.89 (3H, t, $J=7.3$ Hz, $-COOCH_2CH_2CH_3$), 1.34 (24H, overlapped $-(CH_2)_7HC(O)CH(CH_2)_5-$), 1.59 (4H, overlapped, $-CH_2CH_2COOCH_2CH_2CH_3$), 2.25 (2H, t, $J=7.6$ Hz, $-CH_2COO-$), 2.85 ($\sim 2H$, m, $-HC(O)CH-$), 3.97 (2H, t, $J=6.8$ Hz, $-COOCH_2CH_2CH_3$); ^{13}C NMR (100 MHz, $CDCl_3$, δ ppm): 10.44 ($-COOCH_2CH_2CH_3$), 14.14 (CH_3CH_2-), 22.06 ($-COOCH_2CH_2CH_3$), 22.72 (CH_3CH_2-), 25.01 ($-CH_2CH_2COO-$), 26.61, 26.65 ($-CH_2CH_2HC(O)CHCH_2CH_2-$), 27.84, 27.87 ($-CH_2HC(O)CHCH_2-$), 29.09-29.60 ($(CH_2)_5CH_2HC(O)CHCH_2(CH_2)_3-$), 31.91 ($-CH_2CH_2CH_2COO-$), 34.38 ($-CH_2COO-$), 57.24, 57.29 ($-HC(O)CH-$), 65.87 ($-COOCH_2CH_2CH_3$), 173.98 ($-COO-$); EI-MS, 340 (97), 281, 227, 199, 167, 154, 139, 109, 97, 83, 67, 54, 43; ESI-MS accurate mass, 363.2871 (MNa^+ , 363.2870 calc. for $C_{21}H_{40}NaO_3$); IR (ATR, ν , cm^{-1}), 2925 (a. CH_2 str.), 2855 (s. CH_2 str.), 1736 ($C=O$ str.), 1464 (a. CH_3 bend), 1390 (s. CH_3 bend), 1245 and 1175 ($C-O$ str.), 968 (epoxy asym. def.), 823 (epoxy sym. def.).

2-propyl oleate epoxide



2-propyl oleate, 21.71 g (67 mmol), 25 mL H₂O₂ and 15 mL H₂O used. 24.67 g total product mass recovered. ¹H NMR (400 MHz, CDCl₃, δ ppm): 0.79 (3H, t, CH₃CH₂-), 1.13 (6H, d, *J*=6.4 Hz, -COOCH(CH₃)₂), 1.25 (24H, overlapped, -(CH₂)₇HC(O)CH(CH₂)₅-), 1.51 (2H, quin, *J*=6.8 Hz -CH₂CH₂COO-), 2.16 (2H, t, *J*=7.6 Hz, -CH₂COO-), 2.80 (~2H, m, -HC(O)CH-), 4.91 (1H, spt, *J*=6.3 Hz, -COOCH(CH₃)₂); ¹³C NMR (100 MHz, CDCl₃, δ ppm): 14.09 (CH₃CH₂-), 21.83 (-COOCH(CH₃)₂), 22.67 (CH₃CH₂-), 24.97 (-CH₂CH₂COO-), 26.57, 26.62 (-CH₂CH₂HC(O)CHCH₂CH₂-), 27.81, 27.84 (-CH₂HC(O)CHCH₂-), 29.01-29.55 (-(CH₂)₅CH₂HC(O)CHCH₂(CH₂)₃-), 31.86 (-CH₂CH₂CH₂COO-), 34.63 (-CH₂COO-), 57.13, 57.16 (-HC(O)CH-), 67.28 (-COOCH(CH₃)₂), 173.28 (-COO-); EI-MS, 340 (43), 281, 227, 185, 171, 155, 139, 109, 97, 83, 69, 55, 43; ESI-MS accurate mass, 363.2865 (MNa⁺, 363.2870 calc. for C₂₁H₄₀NaO₃); IR (ATR, v, cm⁻¹), 2957 (a. CH₃ str.), 2925 (a. CH₂ str.), 2855 (s. CH₂ str.), 1732 (C=O str.), 1466 (a. CH₃ bend), 1374 (s. CH₃ bend), 1248 and 1179 (C-O- str.), 961 (epoxy asym. def.), 823 (epoxy sym. def.).

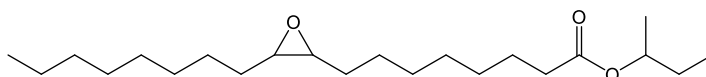
1-butyl oleate epoxide



1-butyl oleate, 21.72 g (64.2 mmol), 25 mL H₂O₂ and 15 mL H₂O used. 28.02 g total product mass recovered. ¹H NMR (400 MHz, CDCl₃, δ ppm): 0.86 (6H, t, overlapped, CH₃CH₂-, -COO(CH₂)₃CH₃), 1.39 (30H, overlapped, -(CH₂)₇HC(O)CH(CH₂)₆CH₂COO-, -CH₂(CH₂)₂CH₃), 2.23 (2H, t, -CH₂COO-), 2.84 (~2H, m, -HC(O)CH-), 4.00 (2H, t, -COOCH₂-); ¹³C NMR (100 MHz, CDCl₃, δ ppm): 13.74 (-COO(CH₂)₃CH₃), 14.12 (CH₃CH₂-), 19.19 (-COOCH₂CH₂CH₂CH₃), 22.71 (CH₃CH₂-), 24.99 (-CH₂CH₂COO-), 26.60, 26.64 (-CH₂CH₂HC(O)CHCH₂CH₂-), 27.84, 27.86 (-CH₂HC(O)CHCH₂-), 29.07-29.59 (-(CH₂)₅CH₂HC(O)CHCH₂(CH₂)₃-), 30.74 (-COOCH₂CH₂CH₂CH₃), 31.90 (-

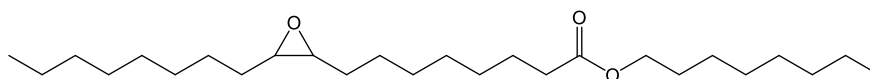
CH₂CH₂CH₂COO-), 34.37 (-CH₂COO-), 57.22, 57.27 (-HC(O)CH-), 64.13 (-COOCH₂-), 173.96 (-COO-); EI-MS, 354 (56), 241, 229, 167, 155, 139, 129, 109, 97, 83, 69, 56, 43; ESI-MS accurate mass, 377.3023 (MNa⁺, 377.3026 calc. for C₂₂H₄₂NaO₃); IR (ATR, ν, cm⁻¹), 2956 (a. CH₃ str.), 2855 (s. CH₂ str.), 1736 (C=O str.), 1464 (a. CH₃ bend), 1388 (s. CH₃ bend), 1245 and 1174 (C-O- str.), 977 (epoxy asym. def.), 823 (epoxy sym. def.).

2-butyl oleate epoxide



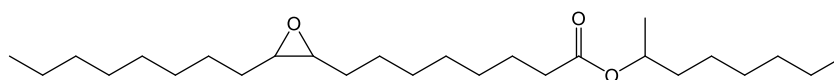
38.12 g total product mass recovered. ¹H NMR (400 MHz, CDCl₃, δ ppm): 0.71 (6H, t, overlapped, CH₃(CH₂)₇HC(O)CH(CH₂)₇COOCH(CH₃)CH₂CH₃), 1.02 (3H, d, J=6.4 Hz, -COOCH(CH₃)CH₂CH₃), 1.30 (28H, overlapped, -(CH₂)₇HC(O)CH(CH₂)₆-, -COOCH(CH₃)CH₂CH₃), 2.09 (2H, t, J=7.3 Hz, -CH₂COO-), 2.70 (~2H, m, -HC(O)CH-), 4.66 (1H, sxt, J=6.4 Hz, -COOCH(CH₃)CH₂CH₃); ¹³C NMR (100 MHz, CDCl₃, δ ppm): 9.60 (-COOCH(CH₃)CH₂CH₃), 13.98 (CH₃CH₂-), 19.38 (-COOCH(CH₃)CH₂CH₃), 22.59 (CH₃CH₂-), 24.94 (-CH₂CH₂COO-), 26.51, 26.57 (-CH₂CH₂HC(O)CHCH₂CH₂-), 27.74, 27.78 (-CH₂HC(O)CHCH₂-), 28.74 (-COOCH(CH₃)CH₂CH₃), 28.94-29.48 (-CH₂)₅CH₂HC(O)CHCH₂(CH₂)₃-, 31.79 (-CH₂CH₂CH₂COO-), 34.49 (-CH₂COO-), 56.90, 56.94 (-HC(O)CH-), 71.65 (-COOCH(CH₃)CH₂CH₃), 173.13 (-COO-); EI-MS, 354 (56), 281, 185, 171, 153, 139, 120, 109, 96, 81, 69, 56, 43; ESI-MS accurate mass, 377.3036 (MNa⁺, 377.3026 calc. for C₂₂H₄₂NaO₃); CHN: % C (70.712 found, 74.576 calc.), % H (11.329 found, 11.864 calc.), % N (0.148 found, nil calc.); IR (ATR, ν, cm⁻¹), 2923 (a. CH₂ str.), 2855 (s. CH₂ str.), 1731 (C=O str.), 1463 (a. CH₃ bend), 1377 (s. CH₃ bend), 1247 and 1176 (C-O- str.), 976 (epoxy asym. def.), 822 (epoxy sym. def.).

1-octyl oleate epoxide



1-octyl oleate, 18.03 g (46 mmol), 20 mL H₂O₂ and 15 mL H₂O used. 19.00 g total product mass recovered. ¹H NMR (400 MHz, CDCl₃, δ ppm): 0.64 (6H, t, overlapped, CH₃(CH₂)₇HC(O)CH(CH₂)₇COO(CH₂)₇CH₃), 1.20 (38H, overlapped, (CH₂)₇HC(O)CH(CH₂)₆CH₂COOCH₂(CH₂)₆CH₃), 2.04 (2H, t, -CH₂COO-), 2.63 (~2H, m, -HC(O)CH-), 3.81 (2H, t, *J*=6.6 Hz, -COOCH₂-); ¹³C NMR (100 MHz, CDCl₃, δ ppm): 13.90 (CH₃(CH₂)₇HC(O)CH(CH₂)₇COO(CH₂)₇CH₃), 22.51 (CH₃CH₂-), 24.79 (-CH₂CH₂COO-), 25.84 (-COO(CH₂)₆CH₂CH₃), 26.47, 26.54 (-CH₂CH₂HC(O)CHCH₂CH₂-), 27.68, 27.72 (-CH₂HC(O)CHCH₂-), 28.57 (-COOCH₂CH₂CH₂-), 28.91 (-COOCH₂CH₂CH₂-), 29.10-29.44 (-(CH₂)₅CH₂HC(O)CHCH₂(CH₂)₃-, -COOCH₂CH₂CH₂(CH₂)₃-), 31.69 (-COOCH₂CH₂-), 31.76 (-CH₂CH₂CH₂COO-), 34.03 (-CH₂COO-), 56.72, 56.78 (-HC(O)CH-), 64.03 (-COOCH₂(CH₂)₆CH₃), 173.28 (-COO-); EI-MS, 410 (56), 297, 263, 225, 185, 171, 154, 139, 109, 95, 83, 70, 56, 43; ESI-MS accurate mass, 433.3642 (MNa⁺, 433.3652 calc. for C₂₆H₅₀NaO₃); IR (ATR, ν , cm⁻¹), 2924 (a. CH₂ str.), 2855 (s. CH₂ str.), 1736 (C=O str.), 1465 (a. CH₃ bend), 1378 (s. CH₃ bend), 1246 and 1172 (C-O- str.), 962 (epoxy asym. def.), 825 (epoxy sym. def.).

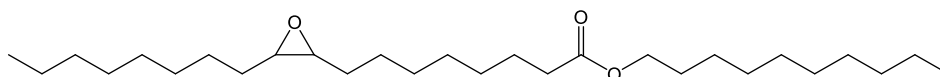
2-octyl oleate epoxide



2-octyl oleate, 17.72 g (45 mmol), 20 mL H₂O₂ and 15 mL H₂O used. 21.61 g total product mass recovered. ¹H NMR (400 MHz, CDCl₃, δ ppm): 0.82 (6H, t, *J*=6.4 Hz, CH₃CH₂-, -COOCH(CH₃)(CH₂)₅CH₃), 1.14 (3H, d, *J*=6.4 Hz -COOCH(CH₃)(CH₂)₅CH₃), 1.41 (36H, overlapped, -(CH₂)₇HC(O)CH(CH₂)₆CH₂COOCH(CH₃)(CH₂)₅CH₃), 2.21 (2H, t, *J*=7.3 Hz, -CH₂COO-), 2.84 (~2H, m, -HC(O)CH-), 4.84 (1H, sxt, *J*=6.4 Hz, -COOCH-); ¹³C NMR (100 MHz, CDCl₃, δ ppm): 14.11 (-COOCH(CH₃)(CH₂)₅CH₃), 14.13 (CH₃CH₂-), 20.05 (-COOCH(CH₃)(CH₂)₅CH₃), 22.62 (-COOCH(CH₃)(CH₂)₄CH₂CH₃),

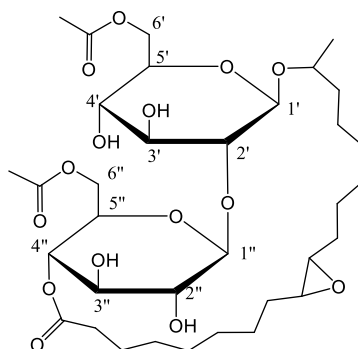
22.71 (CH₃CH₂-), 25.09 (-CH₂CH₂COO-), 25.42 (-COOCH(CH₃)(CH₂)₃CH₂CH₂CH₃), 26.61, 26.65 (-CH₂CH₂HC(O)CHCH₂CH₂-), 27.84, 27.87 (-CH₂CH=CHCH₂-), 29.07-29.60 (-(CH₂)₄CH₂CH₂HC(O)CHCH₂CH₂(CH₂)₂-, -COOCH(CH₃)CH₂(CH₂)₂-), 31.80 (-COOCH(CH₃)(CH₂)₂CH₂(CH₂)₂CH₃), 31.91 (-CH₂CH₂CH₂COO-), 34.73 (-CH₂COO-), 36.01 (-COOCH(CH₃)CH₂(CH₂)₄CH₃), 57.20, 57.24 (-HC(O)CH-), 70.76 (-COOCH-), 173.50 (-COO-); EI-MS, 410 (281), 263, 197, 169, 155, 129, 111, 97, 83, 69, 57, 43; ESI-MS accurate mass, 433.3644 (MNa⁺, 433.3652 calc. for C₂₆H₅₀NaO₃); IR (ATR, ν, cm⁻¹), 2955 (a. CH₃ str.), 2928 (a. CH₂ str.), 2857 (s. CH₂ str.), 1732 (C=O str.), 1464 (a. CH₃ bend), 1378 (s. CH₃ bend), 1248 and 1178 (C-O- str.), 953 (epoxy asym. def.), 837 (epoxy sym. def.).

1-decyl oleate epoxide



1-decyl oleate, 21.05 g (50 mmol), 20 mL H₂O₂ and 30 mL H₂O used. 24.06 g total product mass recovered. ¹H NMR (400 MHz, CDCl₃, δ ppm): 0.81 (6H, t, *J*=6.8 Hz, CH₃(CH₂)₇HC(O)CH(CH₂)₇COO(CH₂)₉CH₃), 1.32 (38H, overlapped, -(CH₂)₇HC(O)CH(CH₂)₅CH₂CH₂COOCH₂CH₂(CH₂)₇CH₃), 1.55 (4H, m, -CH₂CH₂COOCH₂CH₂-), 2.22 (2H, t, *J*=7.6 Hz, -CH₂COO-), 2.82 (~2H, m, -HC(O)CH-), 3.99 (2H, t, *J*=6.6 Hz, -COOCH₂-); ¹³C NMR (100 MHz, CDCl₃, δ ppm): 14.12 (CH₃CH₂-), 14.15 (-COO(CH₂)₉CH₃), 22.70, 22.72 (CH₃CH₂-, -COO(CH₂)₈CH₂CH₃), 24.99 (-CH₂CH₂COO-), 25.98 (-COO(CH₂)₇CH₂-), 26.61, 26.65 (-CH₂CH₂HC(O)CHCH₂CH₂-), 27.84, 27.87 (-CH₂HC(O)CHCH₂-), 28.69 (-COO(CH₂)₆CH₂-), 29.07-29.59 (-(CH₂)₄CH₂CH₂HC(O)CHCH₂CH₂(CH₂)₃CH₂CH₂COOCH₂CH₂(CH₂)₄-), 31.90 (-COOCH₂CH₂-), 31.94 (-CH₂CH₂CH₂COO-), 34.36 (-CH₂COO-), 57.16, 57.20 (-HC(O)CH-), 64.40 (-COOCH₂(CH₂)₈CH₃), 173.86 (-COO-); ESI-MS accurate mass, 461.3954 (MNa⁺, 461.3965 calc. for C₂₈H₅₄NaO₃); IR (ATR, ν, cm⁻¹), 2956 (a. CH₃ str.), 2925 (a. CH₂ str.), 2856 (s. CH₂ str.), 1739 (C=O str.), 1467 (a. CH₃ bend), 1380 (s. CH₂ bend), 1247 and 1173 (C-O- str.), 823 (epoxy sym. def.).

8.7 Synthesis of lactonic sophorolipid epoxide



0.75 g (4.10 mmol) tungsten powder (10% wt with respect to sophorolipid), 3.5 mL hydrogen peroxide solution (>30% w/w water) and 3.5 mL water were added into a 250 mL round bottom flask and heated at 50 °C with serious agitation for 30 minutes. 0.62 g (6.36 mmol) ortho phosphoric acid (~9% wt with respect to sophorolipid) pre-diluted in 3.5 mL water was added in drops over 15 minutes while stirring continuously. 7.38 g (10.72 mmol) lactonic sophorolipid pre-dissolved in 30 mL ethyl acetate, 20 mL hydrogen peroxide solution and 0.43 g Adogen 464 (~5% wt with respect to sophorolipid) were added and heated to 50 °C for 90 minutes. The resulting product was shaken with 250 mL ethyl acetate in a separating funnel, the ethyl acetate layer collected, dried over anhydrous magnesium sulphate, filtered and the solvent removed *in vacuo* to yield a sticky puffy product (7.49 g total product mass recovered, 99.2% yield). The product was ground into powder and analysed by IR spectroscopy, ESI-MS, CHN elemental analysis and ¹H and proton-decoupled ¹³C NMR spectroscopy. ¹H NMR (700 MHz, CDCl₃, δ ppm): 0.9 (~3H, t, -CH(CH₃)-), 1.40 (24H, overlapped, -(CH₂)₆CH(O)CH(CH₂)₆-), 2.08 (6H, s, (-CH₂COOCH₃)₂), 2.38 (2H, t, -CH₂COO-), 2.93 (~2H, m, -HC(O)CH-), 3.50 (4H, m, overlapped, H4', H2', H2'', H5''), 3.72 (4H, m, overlapped, -CH(CH₃)-, H3', H3'', H5'), 4.17 (1H, m br, H6'), 4.40 (3H, m br, overlapped, H6'', H6'', H6'), 4.59 (2H, d, H1', H1''), 4.98 (1H, H4''); ¹³C NMR (175 MHz, CDCl₃, δ ppm): 14.11, 20.81, 20.93, 22.26, 22.61, 22.67, 24.46, 25.59, 26.33, 27.20, 27.34, 27.79, 27.90, 28.51, 29.07, 29.12, 29.31, 29.50, 29.92, 30.09, 31.69, 31.87, 34.01, 37.54, 57.67, 57.91, 61.64, 62.28, 63.72, 69.80, 70.46, 72.37, 73.33, 74.01, 79.30, 102.29, 170.55, 171.48, 173.11; ESI-MS accurate mass,

727.3499 (MNa⁺, 727.3511 calc. for C₃₄H₅₆NaO₁₅); CHN: % C (56.040 found, 57.940 calc.), % H (7.826 found, 8.010 calc.), % N (0.105 found); IR (ATR, ν, cm⁻¹), 3386 (O-H str.), 2929 (a. CH₂ str.), 2858 (s. CH₂ str.), 1740 (C=O str.), 1451 (a. CH₃ bend), 1368 (s. CH₂ bend), 1236 (C-O- str.), 825 (epoxy sym. def.).

8.8 Epoxidation with PTA-SBA-15-NH₂

0.6 g (2.0 mmol) methyl oleate, 0.1 g PTA-SBA-15-NH₂ (20 wt% with respect to methyl oleate), 2 mL hydrogen peroxide solution and 2 mL solvent (any of acetonitrile, cyclohexane or dichloromethane) were added into a 25 mL round bottom flask and was heated to 60 °C with vigorous stirring. 1 mL hydrogen peroxide solution was added every hour in the first 3 hours of the reaction. Resulting product was dried over anhydrous magnesium sulphate, filtered and the filtrate passed down a column of neutral alumina. The product was analysed by IR spectroscopy, GC-MS, ¹H and ¹³C NMR spectroscopy and quantified by GC-FID.

8.9 Ultrasound-Assisted Epoxidation (UAE)

8.9.1 UAE epoxidation with phosphotungstic acid (PTA)

0.6 g (2.0 mmol) methyl oleate, 0.1 g phosphotungstic acid (20% wt with respect to methyl oleate) and 2 mL hydrogen peroxide solution were added into a 25 mL round bottom flask and placed in an ultrasound with a probe lightly immersed in the solution. The ultrasound amplitude was set at either 60% or 100% and the reaction heated and left for 2 hours. Resulting product was dried over anhydrous magnesium sulphate and passed down a bed of neutral alumina to deliver an amber oil. The product was analysed by IR spectroscopy, GC-MS, ¹H and ¹³C NMR spectroscopy and quantified by GC-FID.

8.9.2 UAE epoxidation with PTA-SBA-15-NH₂

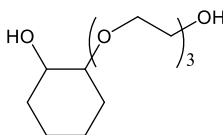
0.6 g (2.0 mmol) methyl oleate, 0.1 g PTA-SBA-15-NH₂ (20% wt with respect to methyl oleate) and 3 mL hydrogen peroxide solution were added into a 25 mL round

bottom flask and placed in an ultrasound with a probe lightly immersed in the solution. The ultrasound amplitude was set at 100% and the reaction was left running. 2 mL hydrogen peroxide solution each was added at the fourth and fifth hours and the resulting product was dried over anhydrous magnesium sulphate and passed through a bed of neutral alumina to deliver an amber oil. The product was analysed by IR spectroscopy, GC-MS, ^1H and ^{13}C NMR spectroscopy and quantified by GC-FID.

8.10 Ring opening of alkyl oleate, lactonic sophorolipid and linseed oil epoxides

8.10.1 Model reactions

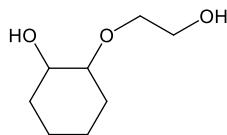
8.10.1.1 Cyclohexene oxide (CHexO) ring-opened with triethylene glycol (TEG)



1.5 g (10 mmol) TEG was heated to 80 °C in a glass vial and a catalyst (5% wt with respect to TEG) added and stirred rigorously on a multipoint reactor. ~1.0 g (10 mmol) CHexO was added in drops through a dropping funnel after which temperature was raised to 100 °C while stirring rigorously. Progress of reaction was monitored for 1 hour by taking portions at intervals for GC-FID and NMR spectroscopy analyses. ^1H NMR (400 MHz, CDCl_3 , δ ppm): 1.16 (4H, m, $-(\text{HCH})_4-$ eq.), 1.63 (2H, m, $-(\text{HCH})_2-$ ax.), 1.93 (2H, m, $-(\text{HCH}-\text{CH})_2-\text{O}-$ ax.), 3.01 (1H, m, $-\text{HC}(\text{OH})\text{CH}((\text{OCH}_2\text{CH}_2)_3-\text{OH})-$), 3.39 (1H, m, $-\text{HC}(\text{OH})\text{CH}((\text{OCH}_2\text{CH}_2)_3-\text{OH})-$); ^{13}C NMR (100 MHz, CDCl_3 , δ ppm): 24.01 ($-\text{CH}_2-$), 24.55 ($-\text{CH}_2-$), 30.42 ($-\text{CH}_2\text{CH}_2-$), 32.17 ($-\text{CH}_2\text{CH}_2-$), 61.63 ($-(\text{OCH}_2\text{CH}_2)_3\text{OH}$), 69.03 ($-(\text{OCH}_2\text{CH}_2)_3\text{OH}$), 69.94 ($-(\text{OCH}_2\text{CH}_2)_3\text{OH}$), 70.37 ($-(\text{OCH}_2\text{CH}_2)_3\text{OH}$), 70.71 ($-(\text{OCH}_2\text{CH}_2)_3\text{OH}$), 72.74 ($-(\text{OCH}_2\text{CH}_2)_3\text{OH}$), 73.29 ($-(\text{OCH}_2\text{CH}_2)_3\text{OH}$), 74.07 ($-\text{HC}(\text{OH})\text{CH}((\text{OCH}_2\text{CH}_2)_3\text{OH})-$),

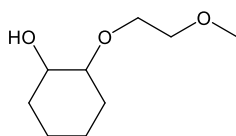
85.42 (-HC(OH)CH((OCH₂CH₂)₃OH-); IR (ATR, ν , cm⁻¹), 3452 (O-H str.), 2931 (a. CH₂ str.), 2859 (s. CH₂ str.), 1451 (a. CH₂ bend), 1243 (C-O- str.), 1083 (a. C-O-C str.).

8.10.1.2 Cyclohexene oxide (CHexO) ring-opened with ethylene glycol (EG)



0.6 g (10 mmol) EG was heated to 80 °C in a glass vial and a catalyst (5% wt with respect to EG) added and stirred rigorously on a multipoint reactor. ~1.0 g (10 mmol) CHexO was added in drops through a dropping funnel after which temperature was raised to 100 °C while stirring rigorously. Progress of reaction was monitored for 1 hour by taking portions at intervals for GC-FID and NMR spectroscopy analyses. ¹H NMR (400 MHz, CDCl₃, δ ppm): 1.17 (4H, m, -(HCH)₄- eq.), 1.62 (2H, m, -(HCH)₂- ax.), 1.99 (2H, m, -(HCH-CH)₂-O- ax.), 3.03 (1H, m, -HC(OH)CH(OCH₂CH₂OH)-), 3.37 (1H, m, -HC(OH)CH(OCH₂CH₂OH)-), 3.76 (5H, m, -OCH₂CH₂OH); ¹³C NMR (100 MHz, CDCl₃, δ ppm): 24.14 (-CH₂-), 24.16 (-CH₂-), 29.61 (-CH₂CH₂-), 32.73 (-CH₂CH₂-), 61.92 (-OCH₂CH₂OH), 63.70 (-OCH₂CH₂OH), 70.18 (-OCH₂CH₂OH), 73.77 (-HC(OH)CH(OCH₂CH₂OH)-), 84.17 (-HC(OH)CH(OCH₂CH₂OH)-); IR (ATR, ν , cm⁻¹), 3397 (O-H str.), 2931 (a. CH₂ str.), 2858 (s. CH₂ str.), 1451 (a. CH₂ bend), 1236 (C-O- str.), 1117 (a. C-O-C str.).

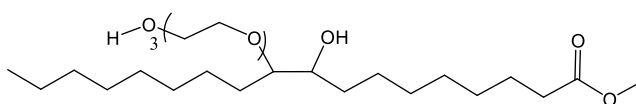
8.10.1.3 Cyclohexene oxide (CHexO) ring-opened with 2-methoxy ethanol (MeEG)



Typically 0.8 g (10 mmol) MeEG was heated to 80 °C in a glass vial and a catalyst (5% wt with respect to MeEG) added and stirred rigorously on a multipoint reactor. ~1.0 g (10 mmol) CHexO was added in drops through a dropping funnel after which temperature was raised to 100 °C while stirring rigorously. Progress of reaction was

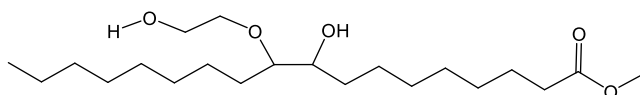
monitored for 1 hour by taking portions at intervals for GC-FID and NMR spectroscopy analyses. ^1H NMR (400 MHz, CDCl_3 , δ ppm): 1.11 (4H, m, $-(\text{HCH})_4-$ eq.), 1.56 (2H, m, $-(\text{HCH})_2-$ ax.), 1.88 (2H, m, $-(\text{HCH}-\text{CH})_2-\text{O}-$ ax.), 2.96 (1H, m, $-\text{HC}(\text{OH})\text{CH}(\text{OCH}_2\text{CH}_2\text{OCH}_3)-$), 3.51 (8H, m, overlapped $-\text{HC}(\text{OH})\text{CH}(\text{OCH}_2\text{CH}_2\text{OCH}_3)-$); ^{13}C NMR (100 MHz, CDCl_3 , δ ppm): 23.97 ($-\text{CH}_2-$), 24.00 ($-\text{CH}_2-$), 29.76 ($-\text{CH}_2\text{CH}_2-$), 32.20 ($-\text{CH}_2\text{CH}_2-$), 58.88 ($-\text{OCH}_2\text{CH}_2\text{OCH}_3$), 61.55 ($-\text{OCH}_2\text{CH}_2\text{OCH}_3$), 68.46 ($-\text{OCH}_2\text{CH}_2\text{OCH}_3$), 72.28 ($-\text{OCH}_2\text{CH}_2\text{OCH}_3$), 73.92 ($-\text{HC}(\text{OH})-$), 84.74 ($-\text{CH}(\text{OCH}_2\text{CH}_2\text{OCH}_3)-$).

8.10.1.4 Methyl oleate epoxide ring-opened with triethylene glycol (TEG)



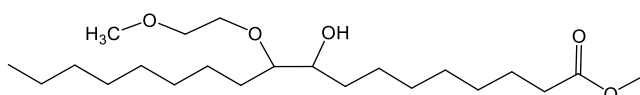
Typically 0.6 g (4 mmol) TEG was heated to 80 °C in a glass vial and a catalyst (10% wt with respect to methyl oleate) added and stirred rigorously on a multipoint reactor. 1.2 g (4 mmol) methyl oleate was added in drops through a dropping funnel after which temperature was raised to 100 °C while stirring rigorously. Progress of reaction was monitored for 1 hour by taking portions at intervals for GC-FID and NMR spectroscopy analyses. ^1H NMR (400 MHz, CDCl_3 , δ ppm): 0.81 (3H, t, CH_3CH_2-), 1.22 (26H, overlapped, $-(\text{CH}_2)_7\text{HC}(\text{OH})\text{CH}((\text{OCH}_2\text{CH}_2)_3-\text{OH})(\text{CH}_2)_6\text{CH}_2\text{COOCH}_3$), 2.24 (2H, t, $-\text{CH}_2\text{COOCH}_3$), 3.06 (1H, m, $-\text{HC}(\text{OH})\text{CH}(\text{OCH}_2\text{CH}_2)_3-\text{OH}-$), 3.42 (1H, m, $-\text{HC}(\text{OH})-$), 3.63 (20H, m, overlapped, $-\text{HC}(\text{OH})\text{CH}(\text{OCH}_2\text{CH}_2)_3-\text{OH}-$); ^{13}C NMR (100 MHz, CDCl_3 , δ ppm): 14.16, 22.71, 24.97, 25.18, 25.24, 25.38, 25.46, 28.97, 29.07, 29.11, 29.17, 29.26, 29.31, 29.38, 29.48, 29.55, 29.60, 29.71, 29.87, 29.91, 31.46, 31.91, 31.94, 32.72, 32.76, 34.10, 34.14, 51.51, 51.48, 61.54, 61.59, 69.94, 70.37, 70.57, 72.73, 73.15, 73.91, 85.27, 174.36; IR (ATR, ν , cm^{-1}), 3446 (O-H str.), 2924 (s. CH_3 str.), 2856 (s. CH_2 str.), 1737 (C=O str.), 1457 (a. CH_3 bend), 1350 (s. CH_2 bend), 1248 (C-O- str.), 1101 (a. C-O-C str.).

8.10.1.5 Methyl oleate epoxide ring-opened with ethylene glycol (EG)



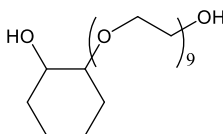
~0.1 g (2 mmol) EG was heated to 80 °C in a glass vial and a catalyst (10% wt with respect to EG) added and stirred rigorously on a multipoint reactor. ~0.6 g (2 mmol) methyl oleate was added in drops through a dropping funnel after which temperature was raised to 100 °C while stirring rigorously. Progress of reaction was monitored for 1 hour by taking portions at intervals for GC-FID and NMR spectroscopy analyses.

8.10.1.6 Methyl oleate epoxide ring-opened with 2-methoxy ethanol (MeEG)



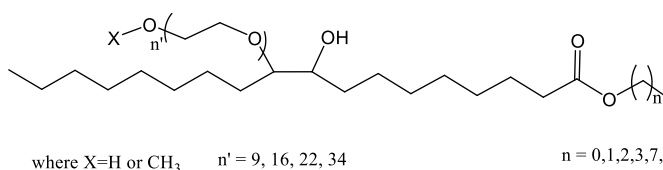
0.2 g (2 mmol) MeEG was heated to 80 °C in a glass vial and a catalyst (10% wt with respect to MeEG) added and stirred rigorously on a multipoint reactor. 0.6 g (2 mmol) methyl oleate was added in drops through a dropping funnel after which temperature was raised to 100 °C while stirring rigorously. Progress of reaction was monitored for 1 hour by taking portions at intervals for GC-FID and NMR spectroscopy analyses. ¹H NMR (400 MHz, CDCl₃, δ ppm): 0.80 (3H, t, CH₃CH₂-), 1.37 (26H, overlapped, -(CH₂)₇HC(OH)-, -(CH₂)₆CH₂COOCH₃), 2.22 (2H, t, -CH₂COOCH₃), 3.02 (1H, m, -HC(OH)CH(OCH₂CH₂OCH₃)-), 3.32 (3H, s, -CH(OCH₂CH₂OCH₃)-), 3.45 (1H, m, -HC(OH)-), 3.48 (2H, m, -HC(OH)CH(OCH₂CH₂OCH₃)-), 3.52 (1H, m, -HC(OH)CH(OHCH₂OCH₃)-), 3.59 (3H, s, -COOCH₃), 3.77 (1H, m, -HC(OH)CH(OHCH₂OCH₃)-); ¹³C NMR (100 MHz, CDCl₃, δ ppm): 14.12, 22.68, 23.90, 24.87, 24.92, 25.63, 28.95-29.29, 29.57, 29.90, 31.25, 31.89, 33.12, 34.08, 34.45, 51.43, 58.95, 70.49, 72.30, 73.57, 76.85, 77.16, 77.48, 84.93, 174.30; ESI-MS accurate mass, 411.3081 (MNa⁺, 411.3100 calc. for C₂₂H₄₄NaO₅).

8.10.1.7 Cyclohexene oxide (CHexO) ring-opened with polyethylene glycol 400 (PEG400)



6.00 g (15 mmol) PEG400 and 2 mL toluene were heated to 80 °C in a glass vial for 30 minutes and 0.03 g ytterbium (III) trifluoromethane sulfonate, Yb(OTf)₃, (0.5% wt with respect to PEG) added and stirred rigorously on a multipoint reactor. 0.51 g (5 mmol) CHexO was added in drops through a dropping funnel after which temperature was raised to 100 °C while stirring rigorously. The reaction was stopped after 20 hours and resulting product diluted with 50 mL ethyl acetate and suction filtered to recover the catalyst. The filtrate was shaken with 10 mL distilled water in a separating funnel followed by addition of brine. The organic phase was collected and dried over anhydrous MgSO₄ and product recovered on the rotary evaporator and characterised with GC-FID and NMR spectroscopy. ¹H NMR (400 MHz, CDCl₃, δ ppm): 1.13 (4H, m, -(HCH)₄- eq.), 1.56 (2H, m, -(HCH)₂- ax.), 1.92 (2H, m, -(HCH-CH)₂-O- ax.), 2.93 (1H, m, -HC(OH)CH((OCH₂CH₂)₉-OH)-), 3.30 (1H, m, -HC(OH)CH((OCH₂CH₂)₉-OH)-), 3.51 (30H, m, -CH((OCH₂CH₂)₉-OH)-); ¹³C NMR (100 MHz, CDCl₃, δ ppm): 24.01 (-CH₂-), 24.39 (-CH₂-), 29.84 (-CH₂CH₂-), 32.25 (-CH₂CH₂-), 61.56 (-(OCH₂CH₂)₉OH), 68.54 (-(OCH₂CH₂)₉OH), 70.29 (-(OCH₂CH₂)₉OH), 70.52 (-(OCH₂CH₂)₉OH), 70.78 (-(OCH₂CH₂)₉OH), 72.60 (-(OCH₂CH₂)₉OH), 73.79 (-HC(OH)CH((OCH₂CH₂)₉OH)-), 84.64 (-HC(OH)CH((OCH₂CH₂)₉OH)-).

8.10.2 Synthesis of alkyl oleate-based surfactant via PEGylation



Typically 10 mmol PEG or MePEG was heated to 80 °C in a 50 mL round bottom flask followed by addition of catalyst (5% wt of PEG or MePEG) and allowed to mix

thoroughly for 2 minutes. 5 mmol epoxide was added in drops through a dropping funnel for over 5 to 10 minutes and temperature raised to 100 °C while stirring rigorously with a stopper lightly placed on the flask. Progress of reaction was monitored with ¹H NMR spectroscopy with portions taken for analysis. The reaction was stopped after 50 minutes and resulting product transferred into a 250 mL beaker, diluted with 50 mL ethyl acetate and suction filtered to recover the catalyst. The filtrate was shaken with 25 mL distilled water in a separating funnel followed by addition of brine. The organic phase was collected and dried over anhydrous MgSO₄ and product recovered on the rotary evaporator. The product was run through a narrow column packed with Amberlyst 15 ion exchange resin and resulting solution concentrated on the rotary evaporator. Product identification was by IR spectroscopy, ESI mass spectrometry, CHN elemental analysis, DSC, SFC and ¹H and proton-decoupled ¹³C NMR spectroscopy.

Epoxidised methyl oleate ring opened with PEG 400 (PEMO400)

4.91 g total product mass recovered. ¹H NMR (400 MHz, CDCl₃, δ ppm): 0.77 (3H, t, *J*=6.3 Hz, CH₃CH₂-), 1.33 (26H, overlapped, -(CH₂)₇HC(OH)CH((OCH₂CH₂)₉-OH)(CH₂)₆CH₂COOCH₃), 2.19 (2H, t, -CH₂COOCH₃), 2.99 (1H, m, -HC(OH)CH((OCH₂CH₂)₉-OH)-), 3.61 (36H, overlapped, -HC(OH)CH((OCH₂CH₂)₉-OH)(CH₂)₇COOCH₃); ¹³C NMR (100 MHz, CDCl₃, δ ppm): 14.12, 22.61, 24.90, 25.38, 25.65, 29.04-299.90, 31.08, 31.89, 33.09, 34.04, 51.45, 61.47, 70.14-70.81, 72.73, 73.33, 84.53, 174.32; ESI-MS accurate mass, 749.5022 (MNa⁺, 749.5010 calc. for C₃₇H₇₄NaO₁₃); CHN: % C (60.673 found, 60.820 calc.), % H (10.089 found, 9.920 calc.), % N (nd); IR (ATR, ν, cm⁻¹), 3468 (O-H str.), 2925 (a. CH₂ str.), 2858 (s. CH₂ str.), 1739 (C=O str.), 1462 (a. CH₃ bend), 1352 (s. CH₂ bend), 1250 (C-O- str.), 1102 (a. C-O-C str.).

Epoxidised ethyl oleate ring opened with PEG 400 (PEEO400)

5.59 g total product mass recovered. ¹H NMR (400 MHz, CDCl₃, δ ppm): 0.78 (3H, t, *J*=6.4 Hz, CH₃CH₂-), 1.33 (29H, overlapped, -(CH₂)₇HC(OH)CH((OCH₂CH₂)₉-OH)(CH₂)₆CH₂COOCH₂CH₃), 2.18 (2H, t, *J*=7.1 Hz -CH₂COOCH₂CH₃), 2.99 (~1H, m, -

HC(OH)CH((OCH₂CH₂)₉-OH)-), 3.56 (37H, overlapped, -HC(OH)CH((OCH₂CH₂)₉-OH)(CH₂)₇COOCH₂CH₃), 4.02 (2H, q, *J*=7.3 Hz, -COOCH₂CH₃); ¹³C NMR (100 MHz, CDCl₃, δ ppm): 14.14, 14.28, 22.67, 24.94, 24.97, 25.59, 29.08-29.80, 31.10, 33.08, 31.90, 34.36, 60.16, 61.62, 70.29-72.64, 73.38, 84.57, 173.88; IR (ATR, ν , cm⁻¹), 3474 (O-H str.), 2926 (a. CH₂ str.), 2858 (s. CH₂ str.), 1736 (C=O str.), 1464 (a. CH₃ bend), 1351 (s. CH₂ bend), 1250 (C-O- str.), 1101 (a. C-O-C str.).

Epoxidised 1-propyl oleate ring opened with PEG 400 (PEPO400)

5.38 g total product mass recovered. ¹H NMR (400 MHz, CDCl₃, δ ppm): 0.84 (6H, t, overlapped, CH₃CH₂-, -COOCH₂CH₂CH₃), 1.21 (28H, overlapped, -(CH₂)₇HC(OH)CH((OCH₂CH₂)₉-OH)(CH₂)₆CH₂COOCH₂CH₂CH₃), 2.21 (2H, t, -CH₂COO-), 3.01 (~1H, m, -HC(OH)CH((OCH₂CH₂)₉-OH)-), 3.36 (~1H, m, -HC(OH)CH-), 3.61 (26H, m, -HC(OH)CH((OCH₂CH₂)₉-OH)-), 3.94 (2H, m, -COOCH₂-); ¹³C NMR (100 MHz, CDCl₃, δ ppm): 10.43, 14.14, 22.01, 22.05, 22.70, 22.72, 24.97, 25.00, 25.40, 25.66, 29.05, 29.28, 29.61, 29.90, 31.14, 31.18, 31.90, 31.92, 33.08, 34.36, 34.39, 61.64, 65.81, 70.34-70.83, 70.87, 72.58, 73.41, 84.61, 173.92; IR (ATR, ν , cm⁻¹), 3463 (O-H str.), 2924 (a. CH₂ str.), 2856 (s. CH₂ str.), 1734 (C=O str.), 1462 (a. CH₃ bend), 1350 (s. CH₂ bend), 1247 (C-O- str.), 1100 (a. C-O-C str.).

Epoxidised 2-propyl oleate ring opened with PEG 400 (PE2PO400)

6.39 g total product mass recovered. ¹H NMR (400 MHz, CDCl₃, δ ppm): 0.71 (3H, t, CH₃CH₂-), 1.21 (32H, overlapped, -(CH₂)₇HC(OH)CH((OCH₂CH₂)₉-OH)(CH₂)₆CH₂COOCH(CH₃)₂), 2.10 (2H, t, -CH₂COO-), 2.94 (~1H, m, -HC(OH)CH((OCH₂CH₂)₉-OH)-), 3.50 (40H, overlapped, -HC(OH)CH((OCH₂CH₂)₉-OH)(CH₂)₇COOCH(CH₃)₂), 4.83 (1H, spt, *J*=6.3 Hz, -COOCH(CH₃)₂); ¹³C NMR (100 MHz, CDCl₃, δ ppm): 14.09, 21.61, 22.60, 24.96, 28.96-29.85, 31.81, 31.84, 32.29, 33.00, 34.61, 34.59, 61.50, 67.25, 70.26-70.77, 72.62, 73.27, 73.29, 84.43, 84.46, 173.27, 173.30; IR (ATR, ν , cm⁻¹), 3481 (O-H str.), 2924 (a. CH₂ str.), 2857 (s. CH₂ str.), 1730 (C=O str.), 1465 (a. CH₃ bend), 1374 (s. CH₃ bend), 1350 (s. CH₂ bend), 1297 (end group C-O- str.), 1249 (C-O- str.), 1105 (a. C-O-C str.).

Epoxidised 1-butyl oleate ring opened with PEG 400 (PEBO400)

5.77 g total product mass recovered. ^1H NMR (400 MHz, CDCl_3 , δ ppm): 0.75 (6H, t, overlapped, CH_3CH_2- , $-\text{COO}(\text{CH}_2)_3\text{CH}_3$), 1.31 (31H, overlapped, $-(\text{CH}_2)_7\text{HC}(\text{OH})\text{CH}((\text{OCH}_2\text{CH}_2)_9\text{-OH})(\text{CH}_2)_6\text{CH}_2\text{COOCH}_2(\text{CH}_2)_2\text{CH}_3$), 2.11 (2H, t, $J=6.8$ Hz, $-\text{CH}_2\text{COO}-$), 2.93 ($\sim 1\text{H}$, m, $-\text{HC}(\text{OH})\text{CH}((\text{OCH}_2\text{CH}_2)_9\text{-OH})-$), 3.46 (43H, m, overlapped, $-\text{HC}(\text{OH})\text{CH}((\text{OCH}_2\text{CH}_2)_9\text{-OH})-$), 3.90 (2H, m, $-\text{COOCH}_2-$); ^{13}C NMR (100 MHz, CDCl_3 , δ ppm): 13.68, 14.08, 19.08, 22.60, 24.90, 24.93, 25.34, 25.59, 28.97-29.15, 29.18-29.25, 29.49-29.53, 29.71, 29.84, 30.64, 31.01, 31.60, 31.80, 32.98, 34.24, 61.48, 63.98, 70.28-70.58, 70.76, 72.59, 73.27, 84.42, 173.82; IR (ATR, ν , cm^{-1}), 3464 (O-H str.), 2926 (s. CH_3 str.), 2859 (s. CH_2 str.), 1736 (C=O str.), 1462 (a. CH_3 bend), 1352 (s. CH_2 bend), 1299 (end group C-O- str.), 1249 (C-O- str.), 1102 (a. C-O-C str.).

Epoxidised 2-butyl oleate ring opened with PEG 400 (PE2BO400)

5.42 g total product mass recovered. ^1H NMR (400 MHz, CDCl_3 , δ ppm): 0.70 (6H, t, overlapped, CH_3CH_2- , $-\text{COOCH}(\text{CH}_3)\text{CH}_2\text{CH}_3$), 1.26 (31H, overlapped, $-(\text{CH}_2)_7\text{HC}(\text{OH})\text{CH}((\text{OCH}_2\text{CH}_2)_9\text{OH})(\text{CH}_2)_6\text{CH}_2\text{COOCH}(\text{CH}_3)\text{CH}_2\text{CH}_3$), 2.07 (2H, t, $-\text{CH}_2\text{COO}-$), 2.90 ($\sim 1\text{H}$, m, $-\text{HC}(\text{OH})\text{CH}((\text{OCH}_2\text{CH}_2)_9\text{-OH})-$), 3.42 (34H, overlapped, $-\text{HC}(\text{OH})\text{CH}((\text{OCH}_2\text{CH}_2)_9\text{-OH})-$), 4.63 (1H, sxt, $-\text{COOCH}-$); ^{13}C NMR (100 MHz, CDCl_3 , δ ppm): 9.64, 14.06, 19.44, 22.57, 24.97, 25.28, 25.58, 28.73, 28.94, 28.98, 29.02, 29.14, 29.17, 29.19, 29.23, 29.48, 29.50, 29.63, 29.61, 29.69, 30.96, 31.78, 31.81, 32.91, 34.55, 61.45, 70.24, 70.48, 70.51, 70.74, 71.72, 72.57, 73.21, 84.38, 173.34; CHN: % C (63.418 found, 62.630 calc.), % H (10.395 found, 10.250 calc.), % N (nd); IR (ATR, ν , cm^{-1}), 3483 (O-H str.), 2924 (s. CH_3 str.), 2857 (s. CH_2 str.), 1730 (C=O str.), 1459 (a. CH_3 bend), 1377 (s. CH_3 bend), 1350 (s. CH_2 bend), 1249 (C-O- str.), 1097 (a. C-O-C str.).

Epoxidised 1-octyl oleate ring opened with PEG 400 (PEO0400)

3.87 g total product mass recovered. ^1H NMR (400 MHz, CDCl_3 , δ ppm): 0.66 (6H, t, overlapped, CH_3CH_2- , $-\text{COO}(\text{CH}_2)_7\text{CH}_3$), 1.07 (38H, overlapped, $-(\text{CH}_2)_7\text{HC}(\text{OH})\text{CH}((\text{OCH}_2\text{CH}_2)_9\text{-OH})(\text{CH}_2)_6\text{CH}_2\text{COO}(\text{CH}_2)_7\text{CH}_3$), 2.07 (2H, t, $J=6.8$ Hz, $-\text{CH}_2\text{COO}-$), 2.90 ($\sim 1\text{H}$, m, $-\text{HC}(\text{OH})\text{CH}((\text{OCH}_2\text{CH}_2)_9\text{-OH})-$), 3.42 (34H, overlapped, $-\text{HC}(\text{OH})\text{CH}((\text{OCH}_2\text{CH}_2)_9\text{-OH})-$), 4.63 (1H, sxt, $-\text{COOCH}-$); ^{13}C NMR (100 MHz, CDCl_3 , δ ppm): 9.64, 14.06, 19.44, 22.57, 24.97, 25.28, 25.58, 28.73, 28.94, 28.98, 29.02, 29.14, 29.17, 29.19, 29.23, 29.48, 29.50, 29.63, 29.61, 29.69, 30.96, 31.78, 31.81, 32.91, 34.55, 61.45, 70.24, 70.48, 70.51, 70.74, 71.72, 72.57, 73.21, 84.38, 173.34; CHN: % C (63.418 found, 62.630 calc.), % H (10.395 found, 10.250 calc.), % N (nd); IR (ATR, ν , cm^{-1}), 3483 (O-H str.), 2924 (s. CH_3 str.), 2857 (s. CH_2 str.), 1730 (C=O str.), 1459 (a. CH_3 bend), 1377 (s. CH_3 bend), 1350 (s. CH_2 bend), 1249 (C-O- str.), 1097 (a. C-O-C str.).

$(CH_2)_7HC(OH)CH((OCH_2CH_2)_9-OH)(CH_2)_6CH_2COOCH_2(CH_2)_6CH_3$, 2.06 (2H, t, - CH_2COO -), 2.88 (~1H, m, - $HC(OH)CH((OCH_2CH_2)_9-OH)$ -), 3.43 (41H, m, overlapped, - $HC(OH)CH((OCH_2CH_2)_9-OH)$ -), 3.83 (2H, m, - $COOCH_2$ -); ^{13}C NMR (100 MHz, $CDCl_3$, δ ppm): 14.01, 22.52, 24.85, 25.30, 25.56, 25.82, 25.88, 25.93, 28.54, 28.91-29.08, 29.16-29.68, 30.92, 31.67, 31.75, 32.91, 34.19, 61.39, 64.20, 70.16-70.48, 70.71, 72.57, 73.17, 84.34, 173.68; ESI-MS accurate mass, 825.6298 (MH^+ , 825.6300 calc. for $C_{44}H_{88}O_{13}$); IR (ATR, ν , cm^{-1}), 3457 (O-H str.), 2926 (s. CH_3 str.), 2856 (s. CH_2 str.), 1737 (C=O str.), 1466 (a. CH_3 bend), 1352 (s. CH_2 bend), 1297 (end group C-O- str.), 1250 (C-O- str.), 1104 (a. C-O-C str.).

Epoxidised 2-octyl oleate ring opened with PEG 400 (PE200400)

3.22 g total product mass recovered. 1H NMR (400 MHz, $CDCl_3$, δ ppm): 0.73 (6H, t, overlapped, CH_3CH_2 -, - $COOCH(CH_3)(CH_2)_5CH_3$), 1.05 (3H, dd, $J=1.7, 6.1$ Hz, - $COOCH(CH_3)(CH_2)_5CH_3$), 1.32 (36H, m, overlapped, - $(CH_2)_7HC(OH)CH((OCH_2CH_2)_9OH)(CH_2)_6CH_2COOCH(CH_3)(CH_2)_5CH_3$), 2.12 (2H, t, $J=7.6$ Hz, - CH_2COO -), 2.95 (~1H, m, - $HC(OH)CH((OCH_2CH_2)_9-OH)$ -), 3.48 (36H, overlapped, - $HC(OH)CH((OCH_2CH_2)_9-OH)$ -), 4.75 (1H, sxt, - $COOCH$ -); ^{13}C NMR (100 MHz, $CDCl_3$, δ ppm): 14.05, 20.10, 22.53, 22.62, 25.01, 25.04, 25.33, 25.36, 25.61, 29.06-29.87, 31.06, 31.71, 31.83, 31.86, 32.98, 33.02, 34.64, 34.67, 35.90, 61.51, 70.25, 70.48-70.55, 70.66, 70.79, 72.65, 73.31, 84.48, 173.45; IR (ATR, ν , cm^{-1}), 3488 (O-H str.), 2925 (s. CH_3 str.), 2856 (s. CH_2 str.), 1731 (C=O str.), 1460 (a. CH_3 bend), 1377 (s. CH_3 bend), 1350 (s. CH_2 bend), 1298 (end group C-O- str.), 1249 (C-O- str.), 1102 (a. C-O-C str.).

Epoxidised 1-decyl oleate ring opened with PEG 400 (PEDO400)

3.03 g total product mass recovered. 1H NMR (400 MHz, $CDCl_3$, δ ppm): 0.73 (6H, t, overlapped, CH_3CH_2 -, - $COO(CH_2)_9CH_3$), 1.25 (38H, overlapped, - $(CH_2)_7HC(OH)CH((OCH_2CH_2)_9-OH)(CH_2)_6CH_2COOCH_2CH_2(CH_2)_7CH_3$), 1.46 (4H, m, overlapped, - $CH_2CH_2COOCH_2CH_2$ -), 2.13 (2H, t, $J=7.3$ Hz, - CH_2COO -), 2.95 (~1H, m, - $HC(OH)CH((OCH_2CH_2)_9-OH)$ -), 3.28 (2H, m, - $HC(OH)CH((OCH_2CH_2)_9-OH)$ -), 3.52 (30H, m, overlapped, - $HC(OH)CH((OCH_2CH_2)_9-OH)$ -), 3.90 (2H, t, $J=6.8$ Hz, - $COOCH_2$ -

); ^{13}C NMR (100 MHz, CDCl_3 , δ ppm): 14.09, 22.63, 24.93, 24.95, 25.32, 25.37, 25.55, 25.61, 25.89, 28.61, 29.06-29.09, 29.20, 29.26, 29.48-24.56, 29.75, 29.87, 31.03, 31.05, 31.84, 31.88, 32.97, 33.61, 34.27, 34.29, 61.51, 64.30, 70.27, 70.48-70.56, 70.78, 72.63, 73.30, 84.48, 173.80; IR (ATR, ν , cm^{-1}), 3468 (O-H str.), 2923 (s. CH_3 str.), 2855 (s. CH_2 str.), 1735 (C=O str.), 1464 (a. CH_3 bend), 1350 (s. CH_2 bend), 1297 (end group C-O- str.), 1248 (C-O- str.), 1102 (a. C-O-C str.).

Epoxidised methyl oleate ring opened with MePEG 400 (MPEMO400)

3.37 g total product mass recovered. ^1H NMR (400 MHz, CDCl_3 , δ ppm): 0.83 (3H, t, CH_3CH_2 -), 1.24 (26H, overlapped, $-(\text{CH}_2)_7\text{HC}(\text{OH})\text{CH}((\text{OCH}_2\text{CH}_2)_9\text{OCH}_3)(\text{CH}_2)_6\text{CH}_2$ -, $-\text{COOCH}_3$), 2.25 (2H, t, $J=7.6$ Hz, $-\text{CH}_2\text{COOCH}_3$), 3.05 (~1H, m, $-\text{HC}(\text{OH})\text{CH}((\text{OCH}_2\text{CH}_2)_9\text{OCH}_3)$ -), 3.33 (3H, s, $-\text{CH}((\text{OCH}_2\text{CH}_2)_9\text{OCH}_3)$), 3.42 (~1H, m, $-\text{HC}(\text{OH})$ -), 3.60 (23H, m, $-\text{HC}(\text{OH})\text{CH}((\text{OCH}_2\text{CH}_2)_9\text{OCH}_3)(\text{CH}_2)_7\text{COOCH}_3$); ^{13}C NMR (100 MHz, CDCl_3 , δ ppm): 14.17, 22.73, 24.97, 25.68, 29.20-29.68, 31.21, 31.93, 33.11, 34.12, 51.51, 59.08, 69.25, 70.41-70.61, 71.98, 73.56, 84.64, 174.38; IR (ATR, ν , cm^{-1}), 3479 (O-H str.), 2928 (a. CH_2 str.), 2859 (s. CH_2 str.), 1740 (C=O str.), 1464 (a. CH_3 bend), 1352 (s. CH_2 bend), 1250 (C-O- str.), 1108 (a. C-O-C str.).

Epoxidised ethyl oleate ring opened with MePEG 400 (MPEEO400)

3.54 g total product mass recovered. ^1H NMR (400 MHz, CDCl_3 , δ ppm): 0.82 (3H, t, CH_3CH_2 -), 1.29 (29H, overlapped, $-(\text{CH}_2)_7\text{HC}(\text{OH})\text{CH}((\text{OCH}_2\text{CH}_2)_9\text{OCH}_3)(\text{CH}_2)_6\text{CH}_2\text{COOCH}_2\text{CH}_3$), 2.23 (2H, t, $-\text{CH}_2\text{COO}$ -), 3.04 (~1H, m, $-\text{HC}(\text{OH})\text{CH}((\text{OCH}_2\text{CH}_2)_9\text{OCH}_3)$ -), 3.33 (3H, s, $-\text{CH}((\text{OCH}_2\text{CH}_2)_9\text{OCH}_3)$), 3.41 (~1H, m, $-\text{HC}(\text{OH})$ -), 3.60 (34H, m, $-\text{HC}(\text{OH})\text{CH}((\text{OCH}_2\text{CH}_2)_9\text{OCH}_3)$), 4.06 (2H, q, $-\text{COOCH}_2$ -); ^{13}C NMR (100 MHz, CDCl_3 , δ ppm): 14.17, 14.31, 22.71, 24.95, 24.97, 25.01, 29.09-29.30, 29.62, 31.18, 31.92, 31.94, 33.03, 34.39, 34.41, 59.09, 60.21, 61.76, 70.38-70.87, 71.98, 72.59, 73.51, 84.67, 174.00; IR (ATR, ν , cm^{-1}), 3491 (O-H str.), 2926 (a. CH_2 str.), 2858 (s. CH_2 str.), 1735 (C=O str.), 1463 (a. CH_3 bend), 1350 (s. CH_2 bend), 1248 (C-O- str.), 1106 (a. C-O-C str.).

Epoxidised 1-propyl oleate ring opened with MePEG 400 (MPEPO400)

3.69 g total product mass recovered. ^1H NMR (400 MHz, CDCl_3 , δ ppm): 0.85 (6H, t, overlapped, CH_3CH_2- , $-\text{COOCH}_2\text{CH}_2\text{CH}_3$), 1.46 (28H, overlapped, $-(\text{CH}_2)_7\text{HC}(\text{OH})\text{CH}((\text{OCH}_2\text{CH}_2)_9-\text{OCH}_3)(\text{CH}_2)_6\text{CH}_2\text{COOCH}_2\text{CH}_2\text{CH}_3$), 2.21 (2H, t, $-\text{CH}_2\text{COO}-$), 3.02 ($\sim 1\text{H}$, m, $-\text{HC}(\text{OH})\text{CH}((\text{OCH}_2\text{CH}_2)_9-\text{OCH}_3)$), 3.31 (3H, s, $-\text{HC}(\text{OH})\text{CH}((\text{OCH}_2\text{CH}_2)_9-\text{OCH}_3)-$), 3.37 ($\sim 1\text{H}$, m, $-\text{HC}(\text{OH})-$), 3.60 (40H, m, $-\text{HC}(\text{OH})\text{CH}((\text{OCH}_2\text{CH}_2)_9-\text{OCH}_3)-$), 3.95 (2H, t, $-\text{COOCH}_2\text{CH}_2\text{CH}_3$); ^{13}C NMR (100 MHz, CDCl_3 , δ ppm): 10.45, 14.16, 22.02, 22.04, 22.70, 25.02, 25.42, 25.62, 25.68, 29.11-29.29, 29.62, 29.76, 31.18, 31.20, 31.89, 31.91, 34.38, 59.07, 61.72, 65.85, 70.38-70.86, 70.89, 71.97, 72.58, 73.47, 84.62, 173.99; IR (ATR, ν , cm^{-1}), 3506 (O-H str.), 2925 (s. CH_3 str.), 2858 (s. CH_2 str.), 1734 (C=O str.), 1460 (a. CH_3 bend), 1351 (s. CH_2 bend), 1290 (end group C-O- str.), 1248 (C-O- str.), 1106 (a. C-O-C str.).

Epoxidised 2-propyl oleate ring opened with MePEG 400 (MPE2PO400)

3.57 g total product mass recovered. ^1H NMR (400 MHz, CDCl_3 , δ ppm): 0.82 (3H, t, CH_3CH_2-), 1.26 (32H, overlapped, $-(\text{CH}_2)_7\text{HC}(\text{OH})\text{CH}((\text{OCH}_2\text{CH}_2)_9-\text{OCH}_3)(\text{CH}_2)_6\text{CH}_2\text{COOCH}(\text{CH}_3)_2$), 2.18 (2H, t, $-\text{CH}_2\text{COO}-$), 3.03 ($\sim 1\text{H}$, m, $-\text{HC}(\text{OH})\text{CH}((\text{OCH}_2\text{CH}_2)_9-\text{OCH}_3)-$), 3.31 (3H, s, $-\text{HC}(\text{OH})\text{CH}((\text{OCH}_2\text{CH}_2)_9-\text{OCH}_3)-$), 3.40 ($\sim 1\text{H}$, m, $-\text{HC}(\text{OH})-$), 3.62 (40H, m, $-\text{HC}(\text{OH})\text{CH}((\text{OCH}_2\text{CH}_2)_9-\text{OCH}_3)-$), 4.94 (1H, spt, $-\text{COOCH}-$); ^{13}C NMR (100 MHz, CDCl_3 , δ ppm): 14.17, 21.90, 22.72, 25.04, 25.44, 25.62, 27.38, 29.04-29.30, 29.65, 29.84, 29.95, 31.20, 31.92, 31.94, 33.13, 34.72, 59.08, 61.76, 67.37, 70.38-70.87, 71.97, 72.57, 73.50, 84.64, 173.45; IR (ATR, ν , cm^{-1}), 3502 (O-H str.), 2926 (s. CH_3 str.), 2859 (s. CH_2 str.), 1731 (C=O str.), 1465 (a. CH_3 bend), 1374 (s. CH_3 bend), 1350 (s. CH_2 bend), 1298 (end group C-O- str.), 1249 (C-O- str.), 1108 (a. C-O-C str.).

Epoxidised 1-butyl oleate ring opened with MePEG 400 (MPEBO400)

3.55 g total product mass recovered. ^1H NMR (400 MHz, CDCl_3 , δ ppm): 0.85 (6H, t, overlapped, CH_3CH_2- , $-\text{COO}(\text{CH}_2)_3\text{CH}_3$), 1.38 (31H, overlapped, $-(\text{CH}_2)_7\text{HC}(\text{OH})\text{CH}((\text{OCH}_2\text{CH}_2)_9-\text{OCH}_3)(\text{CH}_2)_6\text{CH}_2\text{COOCH}_2(\text{CH}_2)_2\text{CH}_3$), 2.21 (2H, t, $-\text{CH}_2\text{COO}-$), 3.02 ($\sim 1\text{H}$, m, $-\text{HC}(\text{OH})\text{CH}((\text{OCH}_2\text{CH}_2)_9-\text{OCH}_3)-$), 3.31 (3H, s, $-\text{HC}(\text{OH})\text{CH}((\text{OCH}_2\text{CH}_2)_9-\text{OCH}_3)-$), 3.37 ($\sim 1\text{H}$, m, $-\text{HC}(\text{OH})-$), 3.60 (40H, m, $-\text{HC}(\text{OH})\text{CH}((\text{OCH}_2\text{CH}_2)_9-\text{OCH}_3)-$), 3.95 (2H, t, $-\text{COO}(\text{CH}_2)_3\text{CH}_3$); ^{13}C NMR (100 MHz, CDCl_3 , δ ppm): 10.45, 14.16, 22.02, 22.04, 22.70, 25.02, 25.42, 25.62, 25.68, 29.11-29.29, 29.62, 29.76, 31.18, 31.20, 31.89, 31.91, 34.38, 59.07, 61.72, 65.85, 70.38-70.86, 70.89, 71.97, 72.58, 73.47, 84.62, 173.99; IR (ATR, ν , cm^{-1}), 3506 (O-H str.), 2925 (s. CH_3 str.), 2858 (s. CH_2 str.), 1734 (C=O str.), 1460 (a. CH_3 bend), 1351 (s. CH_2 bend), 1290 (end group C-O- str.), 1248 (C-O- str.), 1106 (a. C-O-C str.).

HC(OH)CH((OCH₂CH₂)₉-OCH₃-), 3.39 (~1H, m, -HC(OH)-), 3.54 (42H, m, -HC(OH)CH((OCH₂CH₂)₉-OCH₃-), 3.99 (2H, t, -COOCH₂-); ¹³C NMR (100 MHz, CDCl₃, δ ppm): 13.77, 14.16, 19.18, 22.71, 25.00, 25.40, 25.67, 29.09-29.18, 29.29, 29.35, 29.64-29.94, 30.73, 31.18, 31.67, 31.91, 31.94, 33.10, 33.13, 34.39, 59.05, 61.73, 64.13, 70.37-70.64, 70.86, 71.95, 72.59, 73.47, 84.63, 173.98; IR (ATR, ν , cm⁻¹), 3488 (O-H str.), 2926 (s. CH₃ str.), 2859 (s. CH₂ str.), 1734 (C=O str.), 1459 (a. CH₃ bend), 1350 (s. CH₂ bend), 1299 (end group C-O- str.), 1248 (C-O- str.), 1106 (a. C-O-C str.).

Epoxidised 2-butyl oleate ring opened with MePEG 400 (MPE2B0400)

3.48 g total product mass recovered. ¹H NMR (400 MHz, CDCl₃, δ ppm): 0.82 (6H, t, overlapped, CH₃CH₂-, -COOCH(CH₃)CH₂CH₃), 1.35 (31H, overlapped, -(CH₂)₇HC(OH)-, -(CH₂)₆CH₂COOCH(CH₃)CH₂CH₃), 2.18 (2H, t, -CH₂COO-), 3.02 (~1H, m, -HC(OH)CH((OCH₂CH₂)₉-OCH₃-), 3.31 (3H, s, -HC(OH)CH((OCH₂CH₂)₉-OCH₃-), 3.38 (~1H, m, -HC(OH)-), 3.54 (26H, m, -HC(OH)CH((OCH₂CH₂)₉-OCH₃)(CH₂)₇COO-), 4.76 (1H, spt, -COOCH-); ¹³C NMR (100 MHz, CDCl₃, δ ppm): 9.74, 14.14, 19.55, 22.69, 25.09, 25.40, 25.59, 25.66, 28.79-28.85, 29.13, 29.29, 29.61-29.82, 31.15, 31.90, 22.06, 34.71, 59.05, 70.33, 70.38, 70.52-70.59, 70.85, 71.94, 73.52, 84.60, 173.59; IR (ATR, ν , cm⁻¹), 3485 (O-H str.), 2928 (s. CH₃ str.), 2860 (s. CH₂ str.), 1733 (C=O str.), 1460 (a. CH₃ bend), 1379 (s. CH₃ bend), 1353 (s. CH₂ bend), 1250 (C-O- str.), 1112 (a. C-O-C str.).

Epoxidised 1-octyl oleate ring opened with MePEG 400 (MPEO0400)

3.69 g total product mass recovered. ¹H NMR (400 MHz, CDCl₃, δ ppm): 0.81 (6H, t, overlapped, CH₃CH₂-, -COO(CH₂)₇CH₃), 1.43 (38H, overlapped, -(CH₂)₇HC(OH)CH((OCH₂CH₂)₉-OCH₃)(CH₂)₆CH₂COOCH₂(CH₂)₆CH₃), 2.21 (2H, t, -CH₂COO-), 3.04 (~1H, m, -HC(OH)CH((OCH₂CH₂)₉-OCH₃-), 3.33 (3H, s, -HC(OH)CH((OCH₂CH₂)₉-OCH₃-), 3.41 (~1H, m, -HC(OH)-), 3.56 (14H, m, -HC(OH)CH((OCH₂CH₂)₉-OCH₃-), 3.99 (2H, t, -COOCH₂-); ¹³C NMR (100 MHz, CDCl₃, δ ppm): 14.14, 22.67, 25.00, 25.40, 25.98, 28.68, 29.14-29.30, 29.65-29.83, 31.17, 31.81, 31.91, 33.04, 34.38, 59.03, 64.44, 70.39, 70.52-70.59, 70.85, 71.95, 73.59,

84.59, 174.01; IR (ATR, ν , cm^{-1}), 3467 (O-H str.), 2926 (s. CH_3 str.), 2856 (s. CH_2 str.), 1736 (C=O str.), 1465 (a. CH_3 bend), 1351 (s. CH_2 bend), 1247 (C-O- str.), 1107 (a. C-O-C str.).

Epoxidised 2-octyl oleate ring opened with MePEG 400 (MPE200400)

3.85 g total product mass recovered. ^1H NMR (400 MHz, CDCl_3 , δ ppm): 0.83 (6H, t, overlapped, CH_3CH_2 -, $-\text{COOCH}(\text{CH}_3)(\text{CH}_2)_5\text{CH}_3$), 1.34 (39H, overlapped, $-(\text{CH}_2)_7\text{HC}(\text{OH})$ -, $-(\text{CH}_2)_6\text{CH}_2\text{COOCH}(\text{CH}_3)(\text{CH}_2)_5\text{CH}_3$), 2.20 (2H, t, $-\text{CH}_2\text{COO}$ -), 3.05 (~1H, m, $-\text{HC}(\text{OH})\text{CH}((\text{OCH}_2\text{CH}_2)_9-\text{OCH}_3)$ -), 3.34 (3H, s, $-\text{HC}(\text{OH})\text{CH}((\text{OCH}_2\text{CH}_2)_9-\text{OCH}_3)$ -), 3.42 (~1H, m, $-\text{HC}(\text{OH})$ -), 3.62 (22H, m, $-\text{HC}(\text{OH})\text{CH}((\text{OCH}_2\text{CH}_2)_9-\text{OCH}_3)$ -), 4.85 (1H, sxt, $-\text{COOCH}$ -); ^{13}C NMR (100 MHz, CDCl_3 , δ ppm): 14.13, 14.17, 20.08, 22.64, 22.72, 25.09, 25.14, 25.43, 28.69, 29.07-29.17, 29.33, 29.62-29.86, 31.22, 31.81, 31.95, 34.77, 36.01, 59.09, 70.44-70.62, 71.98, 73.55, 84.68, 173.60; IR (ATR, ν , cm^{-1}), 3492 (O-H str.), 2927 (s. CH_3 str.), 2857 (s. CH_2 str.), 1732 (C=O str.), 1464 (a. CH_3 bend), 1377 (s. CH_3 bend), 1350 (s. CH_2 bend), 1249 (C-O- str.), 1111 (a. C-O-C str.).

Epoxidised 1-decyl oleate ring opened with MePEG 400 (MPEDO400)

3.86 g total product mass recovered. ^1H NMR (400 MHz, CDCl_3 , δ ppm): 0.80 (6H, t, overlapped, CH_3CH_2 -, $-\text{COO}(\text{CH}_2)_9\text{CH}_3$), 1.38 (42H, overlapped, $-(\text{CH}_2)_7\text{HC}(\text{OH})\text{CH}((\text{OCH}_2\text{CH}_2)_9-\text{OCH}_3)(\text{CH}_2)_6\text{CH}_2\text{COOCH}_2(\text{CH}_2)_8\text{CH}_3$), 2.20 (2H, t, $J=7.6$ Hz, $-\text{CH}_2\text{COO}$ -), 3.01 (~1H, m, $-\text{HC}(\text{OH})\text{CH}((\text{OCH}_2\text{CH}_2)_9-\text{OCH}_3)$ -), 3.30 (3H, s, $-\text{HC}(\text{OH})\text{CH}((\text{OCH}_2\text{CH}_2)_9-\text{OCH}_3)$ -), 3.55 (45H, m, $-\text{HC}(\text{OH})\text{CH}((\text{OCH}_2\text{CH}_2)_9-\text{OCH}_3)$ -), 3.96 (2H, t, $-\text{COOCH}_2$ -); ^{13}C NMR (100 MHz, CDCl_3 , δ ppm): 14.14, 22.69, 24.99, 25.02, 25.42, 25.66, 25.95, 27.35, 28.66, 29.13-29.31, 29.54, 29.63, 29.82, 29.92, 31.17, 31.91, 33.12, 34.37, 59.03, 61.69, 64.41, 70.37, 70.53-70.64, 70.85, 71.95, 72.58, 73.45, 84.61, 173.92; IR (ATR, ν , cm^{-1}), 3490 (O-H str.), 2927 (s. CH_3 str.), 2859 (s. CH_2 str.), 1737 (C=O str.), 1467 (a. CH_3 bend), 1352 (s. CH_2 bend), 1300 (end group C-O- str.), 1250 (C-O- str.), 1108 (a. C-O-C str.).

Epoxidised methyl oleate ring opened with MePEG 750 (MPEMO750)

5.04 g total product mass recovered. ^1H NMR (400 MHz, CDCl_3 , δ ppm): 0.82 (3H, t, CH_3CH_2 -), 1.38 (26H, overlapped, $-(\text{CH}_2)_7\text{HC}(\text{OH})\text{CH}((\text{OCH}_2\text{CH}_2)_{16}\text{OCH}_3)(\text{CH}_2)_6\text{CH}_2$ -, $-\text{COOCH}_3$), 2.24 (2H, t, $J=7.6$ Hz, $-\text{CH}_2\text{COOCH}_3$), 3.03 ($\sim 1\text{H}$, m, $-\text{HC}(\text{OH})\text{CH}((\text{OCH}_2\text{CH}_2)_{16}\text{OCH}_3)$ -), 3.32 (3H, s, $-\text{CH}((\text{OCH}_2\text{CH}_2)_{16}\text{OCH}_3)$ -), 3.59 (84H, m, overlapped, $-\text{HC}(\text{OH})\text{CH}((\text{OCH}_2\text{CH}_2)_{16}\text{OCH}_3)(\text{CH}_2)_7\text{COOCH}_3$); ^{13}C NMR (100 MHz, CDCl_3 , δ ppm): 14.17, 22.71, 24.93, 24.96, 25.38, 27.38, 29.09-29.95, 30.99, 31.94, 34.11, 51.50, 59.08, 61.74, 70.37-70.75, 71.97, 72.57, 73.50, 84.62, 174.33; CHN: % C (57.262 found, 58.760 calc.), % H (9.637 found, 9.790 calc.), % N (nil found, nil calc.); IR (ATR, ν , cm^{-1}), 3467 (O-H str.), 2923 (a. CH_2 str.), 2862 (s. CH_2 str.), 1737 (C=O str.), 1465 (a. CH_3 bend), 1346 (s. CH_2 bend), 1245 (C-O- str.), 1108 (a. C-O-C str.).

Epoxidised ethyl oleate ring opened with MePEG 750 (MPEEO750)

5.13 g total product mass recovered. ^1H NMR (400 MHz, CDCl_3 , δ ppm): 0.72 (3H, t, $J=6.6$ Hz, CH_3CH_2 -), 1.21 (29H, overlapped, $-(\text{CH}_2)_7\text{HC}(\text{OH})\text{CH}((\text{OCH}_2\text{CH}_2)_{16}\text{OCH}_3)(\text{CH}_2)_6\text{CH}_2\text{COOCH}_2\text{CH}_3$), 2.12 (2H, t, $J=7.3$ Hz $-\text{CH}_2\text{COOCH}_2\text{CH}_3$), 2.94 ($\sim 1\text{H}$, m, $-\text{HC}(\text{OH})\text{CH}((\text{OCH}_2\text{CH}_2)_{16}\text{OCH}_3)$ -), 3.22 (3H, s, $-\text{HC}(\text{OH})\text{CH}((\text{OCH}_2\text{CH}_2)_{16}\text{OCH}_3)$ -), 3.49 (79H, overlapped, $-\text{HC}(\text{OH})\text{CH}((\text{OCH}_2\text{CH}_2)_{16}\text{OCH}_3)(\text{CH}_2)_7\text{COOCH}_2\text{CH}_3$), 3.96 (2H, q, $J=7.3$ Hz, $-\text{COOCH}_2\text{CH}_3$); ^{13}C NMR (100 MHz, CDCl_3 , δ ppm): 14.09, 14.23, 22.60, 24.87, 24.90, 26.17, 27.29, 28.87-29.72, 31.02, 31.59, 31.80, 32.95, 34.25, 58.94, 60.08, 61.48, 70.19-70.77, 71.86, 72.66, 73.29, 80.92, 84.46, 107.62, 173.77; IR (ATR, ν , cm^{-1}), 3484 (O-H str.), 2925 (a. CH_2 str.), 2861 (s. CH_2 str.), 1734 (C=O str.), 1486 (a. CH_3 bend), 1345 (s. CH_2 bend), 1243 (C-O- str.), 1110 (a. C-O-C str.).

Epoxidised 1-propyl oleate ring opened with MePEG 750 (MPEPO750)

5.15 g total product mass recovered. ^1H NMR (400 MHz, CDCl_3 , δ ppm): 0.87 (6H, t, overlapped, CH_3CH_2 -, $-\text{COOCH}_2\text{CH}_2\text{CH}_3$), 1.44 (28H, overlapped, $-(\text{CH}_2)_7\text{HC}(\text{OH})\text{CH}((\text{OCH}_2\text{CH}_2)_{16}\text{OCH}_3)(\text{CH}_2)_6\text{CH}_2\text{COOCH}_2\text{CH}_2\text{CH}_3$), 2.26 (2H, t, $J=7.3$ Hz, $-\text{CH}_2\text{COOCH}_2\text{CH}_2\text{CH}_3$), 3.05 ($\sim 1\text{H}$, m, $-\text{HC}(\text{OH})\text{CH}((\text{OCH}_2\text{CH}_2)_{16}\text{OCH}_3)$ -), 3.34

(3H, s, -HC(OH)CH((OCH₂CH₂)₁₆-OCH₃-), 3.59 (72H, m, overlapped, -HC(OH)CH((OCH₂CH₂)₁₆-OCH₃)(CH₂)₇COO-), 3.99 (2H, t, *J*=6.8 Hz, -COOCH₂CH₂CH₃); ¹³C NMR (100 MHz, CDCl₃, δ ppm): 10.48, 14.20, 22.01, 25.04, 27.40, 29.10-29.67, 31.94, 34.41, 59.11, 61.80, 65.90, 70.42-70.68, 72.00, 72.57, 73.54, 84.69, 174.08; IR (ATR, ν, cm⁻¹), 3477 (O-H str.), 2924 (a. CH₂ str.), 2871 (s. CH₂ str.), 1734 (C=O str.), 1465 (a. CH₃ bend), 1344 (s. CH₂ bend), 1242 (C-O- str.), 1109 (a. C-O-C str.).

Epoxidised 2-propyl oleate ring opened with MePEG 750 (MPE2P0750)

5.00 g total product mass recovered. ¹H NMR (400 MHz, CDCl₃, δ ppm): 0.76 (3H, t, CH₃CH₂-), 1.11 (32H, overlapped, -(CH₂)₇HC(OH)CH((OCH₂CH₂)₁₆-OCH₃)(CH₂)₆CH₂COOCH(CH₃)₂), 2.14 (2H, t, -CH₂COO-), 2.97 (~1H, m, -HC(OH)CH((OCH₂CH₂)₁₆-OCH₃-), 3.26 (3H, s, -HC(OH)CH((OCH₂CH₂)₁₆-OCH₃-), 3.53 (77H, m, overlapped, -HC(OH)CH((OCH₂CH₂)₁₆-OCH₃)(CH₂)₇COO-), 4.89 (1H, spt, -COOCH(CH₃)₂); ¹³C NMR (100 MHz, CDCl₃, δ ppm): 14.07, 14.11, 21.86, 22.64, 24.99, 25.56, 26.08, 28.88-29.77, 31.09, 31.85, 32.99, 34.64, 59.00, 61.58, 67.30, 70.25-71.91, 72.63, 73.38, 80.96, 84.53, 100.00, 173.37; IR (ATR, ν, cm⁻¹), 3471 (O-H str.), 2923 (a. CH₂ str.), 2862 (s. CH₂ str.), 1730 (C=O str.), 1466 (a. CH₃ bend), 1346 (s. CH₂ bend), 1281 (end group C-O-str.), 1246 (C-O- str.), 1108 (a. C-O-C str.).

Epoxidised 1-butyl oleate ring opened with MePEG 750 (MPEB0750)

5.24 g total product mass recovered. ¹H NMR (400 MHz, CDCl₃, δ ppm): 0.79 (3H, t, CH₃CH₂-), 0.84 (3H, t, *J*=7.3 Hz, -COO(CH₂)₃CH₃), 1.35 (31H, overlapped, -(CH₂)₇HC(OH)CH((OCH₂CH₂)₁₆-OCH₃)(CH₂)₆CH₂COOCH₂(CH₂)₂CH₃), 2.20 (2H, t, *J*=7.6 Hz, -CH₂COO-), 3.01 (~1H, m, -HC(OH)CH((OCH₂CH₂)₁₆-OCH₃-), 3.29 (3H, s, -HC(OH)CH((OCH₂CH₂)₁₆-OCH₃-), 3.56 (83H, m, -HC(OH)CH((OCH₂CH₂)₁₆-OCH₃-), 3.97 (2H, t, *J*=6.6 Hz, -COOCH₂-); ¹³C NMR (100 MHz, CDCl₃, δ ppm): 13.74, 14.14, 19.16, 22.59, 22.67, 24.92-25.00, 25.37, 25.65, 26.23, 27.35, 29.01-29.32, 29.61, 29.80, 29.91, 30.71, 31.14, 31.64, 31.88, 33.10, 34.36, 59.03, 61.64, 64.11, 70.28, 70.50-70.60, 70.84, 71.93, 72.67, 73.42, 84.59, 173.98; IR (ATR, ν, cm⁻¹), 3492 (O-H str.), 2925 (s. CH₃ str.), 2863 (s. CH₂ str.), 1734 (C=O str.), 1465 (a. CH₃ bend), 1346 (s. CH₂ bend), 1281 (end group C-O- str.), 1244 (C-O- str.), 1109 (a. C-O-C str.).

Epoxidised 2-butyl oleate ring opened with MePEG 750 (MPE2B0750)

5.26 g total product mass recovered. ^1H NMR (400 MHz, CDCl_3 , δ ppm): 0.85 (6H, t, overlapped, CH_3CH_2 -, $-\text{COOCH}(\text{CH}_3)\text{CH}_2\text{CH}_3$), 1.16 (3H, dd, $-\text{COOCH}(\text{CH}_3)$ -), 1.43 (28H, overlapped, $-(\text{CH}_2)_7\text{HC}(\text{OH})$ -, $-(\text{CH}_2)_6\text{CH}_2\text{COOCH}(\text{CH}_3)\text{CH}_2\text{CH}_3$), 2.24 (2H, t, $J=7.3$ Hz, $-\text{CH}_2\text{COO}$ -), 3.06 (~1H, m, $-\text{HC}(\text{OH})\text{CH}((\text{OCH}_2\text{CH}_2)_{16}-\text{OCH}_3)$ -), 3.35 (3H, s, $-\text{HC}(\text{OH})\text{CH}((\text{OCH}_2\text{CH}_2)_{16}-\text{OCH}_3)$ -), 3.61 (73H, m, overlapped, $-\text{HC}(\text{OH})\text{CH}((\text{OCH}_2\text{CH}_2)_{16}-\text{OCH}_3)(\text{CH}_2)_7\text{COO}$ -), 4.81 (1H, sxt, $J=6.0$ Hz, $-\text{COOCH}$ -); ^{13}C NMR (100 MHz, CDCl_3 , δ ppm): 9.80, 14.18, 19.59, 22.73, 25.14, 25.65, 27.40, 28.88, 29.21-29.39, 29.81, 31.23, 31.94, 31.96, 34.77, 59.12, 61.80, 70.42, 70.59-70.68, 72.01, 72.58, 72.89, 73.63, 84.68, 173.61; IR (ATR, ν , cm^{-1}), 3481 (O-H str.), 2927 (s. CH_3 str.), 2862 (s. CH_2 str.), 1730 (C=O str.), 1464 (a. CH_3 bend), 1345 (s. CH_2 bend), 1281 (end group C-O- str.), 1244 (C-O- str.), 1110 (a. C-O-C str.).

Epoxidised 1-octyl oleate ring opened with MePEG 750 (MPE00750)

5.41 g total product mass recovered. ^1H NMR (400 MHz, CDCl_3 , δ ppm): 0.77 (6H, t, overlapped, CH_3CH_2 -, $-\text{COO}(\text{CH}_2)_7\text{CH}_3$), 1.36 (38H, overlapped, $-(\text{CH}_2)_7\text{HC}(\text{OH})\text{CH}((\text{OCH}_2\text{CH}_2)_{16}-\text{OCH}_3)(\text{CH}_2)_6\text{CH}_2\text{COOCH}_2(\text{CH}_2)_6\text{CH}_3$), 2.17 (2H, t, $-\text{CH}_2\text{COO}$ -), 2.98 (~1H, m, $-\text{HC}(\text{OH})\text{CH}((\text{OCH}_2\text{CH}_2)_{16}-\text{OCH}_3)$ -), 3.27 (3H, s, $-\text{HC}(\text{OH})\text{CH}((\text{OCH}_2\text{CH}_2)_{16}-\text{OCH}_3)$ -), 3.36 (~1H, m, $-\text{HC}(\text{OH})$ -), 3.58 (79H, m, $-\text{HC}(\text{OH})\text{CH}((\text{OCH}_2\text{CH}_2)_{16}-\text{OCH}_3)$ -), 3.94 (2H, t, $J=6.8$ Hz, $-\text{COOCH}_2$ -); ^{13}C NMR (100 MHz, CDCl_3 , δ ppm): 14.11, 22.65, 24.97, 25.36, 25.63, 25.92, 27.33, 28.64, 29.09-29.25, 29.30, 29.59-29.71, 29.78, 29.89, 29.96, 31.11, 31.76, 31.86, 33.03, 34.34, 59.00, 61.61, 64.37, 70.28, 70.48-70.81, 71.92, 72.60, 73.40, 84.53, 173.89; IR (ATR, ν , cm^{-1}), 3464 (O-H str.), 2924 (s. CH_3 str.), 2867 (s. CH_2 str.), 1736 (C=O str.), 1467 (a. CH_3 bend), 1348 (s. CH_2 bend), 1283 (end group C-O- str.), 1248 (C-O- str.), 1111 (a. C-O-C str.).

Epoxidised 2-octyl oleate ring opened with MePEG 750 (MPE200750)

5.41 g total product mass recovered. ^1H NMR (400 MHz, CDCl_3 , δ ppm): 0.74 (6H, t, overlapped, CH_3CH_2 -, $-\text{COOCH}(\text{CH}_3)(\text{CH}_2)_5\text{CH}_3$), 1.34 (39H, overlapped, -

$(CH_2)_7HC(OH)-$, $-(CH_2)_6CH_2COOCH(CH_3)(CH_2)_5CH_3$, 2.15 (2H, t, $-CH_2COO-$), 2.98 (~1H, m, $-HC(OH)CH((OCH_2CH_2)_{16}-OCH_3)-$), 3.26 (3H, s, $-HC(OH)CH((OCH_2CH_2)_{16}-OCH_3)-$), 3.34 (~1H, m, $-HC(OH)-$), 3.58 (80H, m, $-HC(OH)CH((OCH_2CH_2)_{16}-OCH_3)-$), 4.77 (1H, sxt, $J=6.3$ Hz, $-COOCH-$); ^{13}C NMR (100 MHz, $CDCl_3$, δ ppm): 14.08, 20.03, 22.55, 22.64, 25.01, 25.04, 25.35, 25.62, 26.14, 28.98, 29.03-29.07, 29.26, 29.29, 29.58, 29.77, 29.89, 31.11, 31.60, 31.73, 31.85, 31.88, 32.99, 33.02, 34.68, 35.93, 58.99, 61.58, 70.25, 70.47, 70.50, 70.53, 70.57, 70.69, 70.81, 71.91, 72.64, 73.37, 84.52, 173.46; IR (ATR, ν , cm^{-1}), 3464 (O-H str.), 2925 (s. CH_3 str.), 2862 (s. CH_2 str.), 1731 (C=O str.), 1466 (a. CH_3 bend), 1345 (s. CH_2 bend), 1281 (end group C-O-str.), 1243 (C-O-str.), 1110 (a. C-O-C str.).

Epoxidised 1-decyl oleate ring opened with MePEG 750 (MPEDO750)

5.45 g total product mass recovered. 1H NMR (400 MHz, $CDCl_3$, δ ppm): 0.85 (6H, t, overlapped, CH_3CH_2- , $-COO(CH_2)_9CH_3$), 1.41 (42H, overlapped, $(CH_2)_7HC(OH)CH((OCH_2CH_2)_{16}-OCH_3)(CH_2)_6CH_2COOCH_2(CH_2)_8CH_3$), 2.26 (2H, t, $-CH_2COO-$), 3.06 (~1H, m, $-HC(OH)CH((OCH_2CH_2)_{16}-OCH_3)-$), 3.36 (3H, s, $-HC(OH)CH((OCH_2CH_2)_{16}-OCH_3)-$), 3.43 (~1H, m, $-HC(OH)-$), 3.62 (42H, m, $-HC(OH)CH((OCH_2CH_2)_{16}-OCH_3)-$), 4.02 (2H, t, $J=6.8$ Hz, $-COOCH_2-$); ^{13}C NMR (100 MHz, $CDCl_3$, δ ppm): 14.19, 22.75, 25.05, 26.00, 28.72, 29.32, 29.37, 29.60-29.87, 31.96, 33.10, 34.44, 59.12, 61.80, 64.50, 70.42-70.89, 72.01, 72.59, 73.52, 84.70, 174.07; IR (ATR, ν , cm^{-1}), 3482 (O-H str.), 2924 (s. CH_3 str.), 2862 (s. CH_2 str.), 1736 (C=O str.), 1467 (a. CH_3 bend), 1347 (s. CH_2 bend), 1283 (end group C-O-str.), 1245 (C-O-str.), 1112 (a. C-O-C str.).

Epoxidised methyl oleate ring opened with PEG 1000 (PEMO1000)

6.32 g total product mass recovered. 1H NMR (400 MHz, $CDCl_3$, δ ppm): 0.85 (3H, t, $J=6.4$ Hz, CH_3CH_2-), 1.40 (26H, overlapped, $-(CH_2)_7HC(OH)CH((OCH_2CH_2)_{22}-OH)(CH_2)_6CH_2COOCH_3$), 2.27 (2H, t, $J=6.4$ Hz, $-CH_2COOCH_3$), 3.06 (1H, m, $-HC(OH)CH((OCH_2CH_2)_9-OH)-$), 3.61 (104H, overlapped, $-HC(OH)CH((OCH_2CH_2)_{22}-OH)(CH_2)_7COOCH_3$); ^{13}C NMR (100 MHz, $CDCl_3$, δ ppm): 14.18, 22.73, 24.98, 25.41, 26.27, 26.34, 26.54, 27.50, 29.09-29.98, 31.94, 33.17, 34.14, 51.53, 61.80, 70.41-

70.64, 72.59, 73.54, 84.76, 174.34; IR (ATR, ν , cm^{-1}), 3450 (O-H str.), 2924 (a. CH_2 str.), 2867 (s. CH_2 str.), 1738 (C=O str.), 1467 (a. CH_3 bend), 1343 (s. CH_2 bend), 1242 (C-O- str.), 1109 (a. C-O-C str.).

Epoxidised ethyl oleate ring opened with PEG 1000 (PEEO1000)

6.28 g total product mass recovered. ^1H NMR (400 MHz, CDCl_3 , δ ppm): 0.73 (3H, t, $J=6.4$ Hz, CH_3CH_2-), 1.29 (29H, overlapped, $-(\text{CH}_2)_7\text{HC}(\text{OH})\text{CH}((\text{OCH}_2\text{CH}_2)_{22}\text{-OH})(\text{CH}_2)_6\text{CH}_2\text{COOCH}_2\text{CH}_3$), 2.14 (2H, t, $J=7.6$ Hz $-\text{CH}_2\text{COOCH}_2\text{CH}_3$), 2.95 (~1H, m, $-\text{HC}(\text{OH})\text{CH}((\text{OCH}_2\text{CH}_2)_{22}\text{-OH})-$), 3.52 (97H, overlapped, $-\text{HC}(\text{OH})\text{CH}((\text{OCH}_2\text{CH}_2)_{22}\text{-OH})(\text{CH}_2)_7\text{COOCH}_2\text{CH}_3$), 3.97 (2H, q, $J=7.2$ Hz, $-\text{COOCH}_2\text{CH}_3$); ^{13}C NMR (100 MHz, CDCl_3 , δ ppm): 14.11, 14.25, 22.63, 24.89, 24.92, 27.31, 28.89-29.86, 31.07, 31.58, 31.85, 32.98, 34.28, 60.10, 61.55, 70.26-70.79, 72.58, 73.34, 84.48, 173.80; IR (ATR, ν , cm^{-1}), 3455 (O-H str.), 2922 (a. CH_2 str.), 2888 (s. CH_2 str.), 1736 (C=O str.), 1467 (a. CH_3 bend), 1343 (s. CH_2 bend), 1242 (C-O- str.), 1109 (a. C-O-C str.).

Epoxidised 1-propyl oleate ring opened with PEG 1000 (PEPO1000)

6.47 g total product mass recovered. ^1H NMR (400 MHz, CDCl_3 , δ ppm): 0.78 (3H, t, $J=6.1$ Hz, CH_3CH_2-), 0.85 (3H, t, $-\text{COOCH}_2\text{CH}_2\text{CH}_3$), 1.37 (28H, overlapped, $-(\text{CH}_2)_7\text{HC}(\text{OH})\text{CH}((\text{OCH}_2\text{CH}_2)_{22}\text{-OH})(\text{CH}_2)_6\text{CH}_2\text{COOCH}_2\text{CH}_2\text{CH}_3$), 2.20 (2H, t, $J=6.8$ Hz, $-\text{CH}_2\text{COOCH}_2\text{CH}_2\text{CH}_3$), 2.99 (~1H, m, $-\text{HC}(\text{OH})\text{CH}((\text{OCH}_2\text{CH}_2)_{22}\text{-OH})-$), 3.56 (109H, m, overlapped, $-\text{HC}(\text{OH})\text{CH}((\text{OCH}_2\text{CH}_2)_{22}\text{-OH})(\text{CH}_2)_7\text{COO}-$), 3.92 (2H, t, $-\text{COOCH}_2\text{CH}_2\text{CH}_3$); ^{13}C NMR (100 MHz, CDCl_3 , δ ppm): 10.43, 14.14, 22.01, 22.67, 24.98, 25.35, 25.59, 29.05-29.91, 31.11, 31.62, 31.90, 33.09, 34.35, 61.60, 65.84, 70.23-70.83, 72.69, 73.41, 84.56, 174.00; IR (ATR, ν , cm^{-1}), 3482 (O-H str.), 2923 (a. CH_2 str.), 2886 (s. CH_2 str.), 1735 (C=O str.), 1467 (a. CH_3 bend), 1360 (s. CH_3 bend), 1343 (s. CH_2 bend), 1280 (end group C-O-str.), 1242 (C-O- str.), 1109 (a. C-O-C str.).

Epoxidised 2-propyl oleate ring opened with PEG 1000 (PE2PO1000)

6.37 g total product mass recovered. ^1H NMR (400 MHz, CDCl_3 , δ ppm): 0.85 (3H, t, $J=6.6$ Hz, CH_3CH_2-), 1.39 (32H, overlapped, $-(\text{CH}_2)_7\text{HC}(\text{OH})\text{CH}((\text{OCH}_2\text{CH}_2)_{22}\text{-OH})(\text{CH}_2)_6\text{CH}_2\text{COOCH}(\text{CH}_3)_2$), 2.23 (2H, t, $J=7.6$ Hz, $-\text{CH}_2\text{COO}-$), 3.05 (~1H, m, -

HC(OH)CH((OCH₂CH₂)₂₂-OH)-), 3.64 (80H, m, overlapped, - HC(OH)CH((OCH₂CH₂)₂₂-OH)(CH₂)₇COO-), 4.86 (1H, spt, -COOCH(CH₃)₂); ¹³C NMR (100 MHz, CDCl₃, δ ppm): 14.15, 14.20, 20.10, 22.65, 22.73, 25.44, 29.18-29.39, 31.82, 31.94, 34.80, 36.03, 61.80, 70.42-70.69, 72.59, 73.54, 84.69, 173.54; IR (ATR, ν , cm⁻¹), 3449 (O-H str.), 2886 (s. CH₂ str.), 1732 (C=O str.), 1467 (a. CH₃ bend), 1360 (s. CH₃ bend), 1343 (s. CH₂ bend), 1280 (end group C-O-str.), 1242, 1146 (C-O- str.), 1109 (a. C-O-C str.).

Epoxidised 1-butyl oleate ring opened with PEG 1000 (PEBO1000)

6.40 g total product mass recovered. ¹H NMR (400 MHz, CDCl₃, δ ppm): 0.82 (3H, t, CH₃CH₂-), 0.87 (3H, t, $J=7.3$ Hz, -COO(CH₂)₃CH₃), 1.41 (31H, overlapped, - (CH₂)₇HC(OH)CH((OCH₂CH₂)₂₂-OH)(CH₂)₆CH₂COOCH₂(CH₂)₂CH₃), 2.23 (2H, t, $J=7.6$ Hz, -CH₂COO-), 3.03 (~1H, m, -HC(OH)CH((OCH₂CH₂)₂₂-OH)-), 3.58 (108H, m, overlapped, -HC(OH)CH((OCH₂CH₂)₂₂-OH)-), 4.01 (2H, m, $J=6.6$ Hz, -COOCH₂-); ¹³C NMR (100 MHz, CDCl₃, δ ppm): 13.78, 14.19, 19.20, 22.72, 25.02, 29.09, 29.11, 29.19, 29.28, 29.30, 29.36, 29.65, 29.85, 30.73, 31.00, 31.92, 34.40, 61.74, 64.15, 70.37-70.66, 70.87, 72.58, 73.49, 84.63, 174.00; IR (ATR, ν , cm⁻¹), 3481 (O-H str.), 2925 (s. CH₃ str.), 2888 (s. CH₂ str.), 1737 (C=O str.), 1469 (a. CH₃ bend), 1361 (s. CH₃ bend), 1345 (s. CH₂ bend), 1282 (end group C-O- str.), 1243 (C-O- str.), 1111 (a. C-O-C str.).

Epoxidised 2-butyl oleate ring opened with PEG 1000 (PE2BO1000)

6.51 g total product mass recovered. ¹H NMR (400 MHz, CDCl₃, δ ppm): 0.83 (6H, t, overlapped, CH₃CH₂-, -COOCH(CH₃)CH₂CH₃), 1.41 (31H, overlapped, - (CH₂)₇HC(OH)CH((OCH₂CH₂)₂₂OH)(CH₂)₆CH₂COOCH(CH₃)CH₂CH₃), 2.22 (2H, t, - CH₂COO-), 3.03 (~1H, m, -HC(OH)CH((OCH₂CH₂)₂₂-OH)-), 3.60 (103H, overlapped, - HC(OH)CH((OCH₂CH₂)₂₂-OH)-), 4.78 (1H, sxt, $J=6.2$ Hz, -COOCH-); ¹³C NMR (100 MHz, CDCl₃, δ ppm): 9.76, 14.18, 19.57, 22.72, 25.11, 25.14, 25.62, 25.68, 28.87, 29.10, 29.14, 29.18, 29.29-29.36, 29.52, 29.61, 29.65, 29.76, 29.95, 31.00, 31.19, 31.92, 33.10, 34.74, 61.71, 70.32, 70.53-70.70, 70.87, 71.95, 72.64, 73.51, 84.64, 173.64; IR (ATR, ν , cm⁻¹), 3467 (O-H str.), 2877 (s. CH₂ str. PEG), 1731 (C=O str.),

1467 (a. CH₃ bend), 1343 (s. CH₂ bend), 1280 (end group C-O- str.), 1242 (C-O- str.), 1110 (a. C-O-C str.).

Epoxidised 1-octyl oleate ring opened with PEG 1000 (PEOO1000)

6.74 g total product mass recovered. ¹H NMR (400 MHz, CDCl₃, δ ppm): 0.83 (6H, t, overlapped, CH₃CH₂-, -COO(CH₂)₇CH₃), 1.41 (38H, overlapped, -(CH₂)₇HC(OH)CH((OCH₂CH₂)₂₂-OH)(CH₂)₆CH₂COOCH₂(CH₂)₆CH₃), 2.23 (2H, t, *J*=7.3 Hz, -CH₂COO-), 3.04 (~1H, m, -HC(OH)CH((OCH₂CH₂)₂₂-OH)-), 3.60 (88H, m, overlapped, -HC(OH)CH((OCH₂CH₂)₂₂-OH)-), 4.00 (2H, m, *J*=6.6 Hz, -COOCH₂-); ¹³C NMR (100 MHz, CDCl₃, δ ppm): 14.16, 22.69, 25.03, 25.42, 25.98, 28.69, 29.21-29.37, 29.62, 29.66, 29.74, 29.79, 29.96, 31.83, 31.92, 31.97, 34.41, 61.75, 64.47, 70.38, 70.44-70.67, 70.87, 72.58, 73.50, 84.65, 174.00; IR (ATR, ν , cm⁻¹), 3452 (O-H str.), 2926 (s. CH₃ str.), 2889 (s. CH₂ str. PEG), 2862 (s. CH₂ str.), 1738 (C=O str.), 1469 (a. CH₃ bend), 1361 (s. CH₃ bend), 1345 (s. CH₂ bend), 1282 (end group C-O- str.), 1243 (C-O- str.), 1112 (a. C-O-C str.).

Epoxidised 2-octyl oleate ring opened with PEG 1000 (PE20O1000)

6.52 g total product mass recovered. ¹H NMR (400 MHz, CDCl₃, δ ppm): 0.81 (6H, t, overlapped, CH₃CH₂-, -COOCH(CH₃)(CH₂)₅CH₃), 1.39 (39H, overlapped, -(CH₂)₇HC(OH)CH((OCH₂CH₂)₂₂-OH)(CH₂)₆CH₂COOCH(CH₃)(CH₂)₅CH₃), 2.20 (2H, t, -CH₂COO-), 3.03 (~1H, m, -HC(OH)CH((OCH₂CH₂)₂₂-OH)-), 3.59 (98H, m, overlapped, -HC(OH)CH((OCH₂CH₂)₂₂-OH)-), 4.83 (1H, sxt, *J*=6.2 Hz, -COOCH-); ¹³C NMR (100 MHz, CDCl₃, δ ppm): 14.13, 14.17, 20.08, 22.61, 22.71, 25.11, 25.13, 25.41, 25.43, 25.67, 26.25, 27.73, 29.02-29.14, 29.32, 29.29.35, 29.52-29.84, 31.19, 31.78, 31.91, 31.94, 33.10, 34.76, 34.78, 35.99, 61.73, 68.89, 70.37, 70.51-70.66, 70.75, 70.78, 70.86, 72.57, 73.48, 84.64, 173.56; IR (ATR, ν , cm⁻¹), 3458 (O-H str.), 2926 (s. CH₃ str.), 2888 (s. CH₂ str. PEG), 1734 (C=O str.), 1469 (a. CH₃ bend), 1361 (s. CH₃ bend), 1345 (s. CH₂ bend), 1282 (end group C-O- str.), 1244 (C-O- str.), 1111 (a. C-O-C str.).

Epoxidised 1-decyl oleate ring opened with PEG 1000 (PEDO1000)

6.61 g total product mass recovered. ^1H NMR (400 MHz, CDCl_3 , δ ppm): 0.74 (6H, t, overlapped, CH_3CH_2- , $-\text{COO}(\text{CH}_2)_9\text{CH}_3$), 1.33 (42H, overlapped, $-(\text{CH}_2)_7\text{HC}(\text{OH})\text{CH}((\text{OCH}_2\text{CH}_2)_{22}-\text{OH})(\text{CH}_2)_6\text{CH}_2\text{COOCH}_2(\text{CH}_2)_8\text{CH}_3$), 2.15 (2H, t, $J=7.3$ Hz, $-\text{CH}_2\text{COO}-$), 2.96 (~1H, m, $-\text{HC}(\text{OH})\text{CH}((\text{OCH}_2\text{CH}_2)_{22}-\text{OH})-$), 3.33 (1H, m, $-\text{HC}(\text{OH})-$), 3.53 (126H, m, overlapped, $-\text{HC}(\text{OH})\text{CH}((\text{OCH}_2\text{CH}_2)_{22}-\text{OH})-$), 3.92 (2H, m, $J=6.8$ Hz, $-\text{COOCH}_2-$); ^{13}C NMR (100 MHz, CDCl_3 , δ ppm): 14.11, 22.64, 24.95, 24.97, 25.36, 25.56, 25.61, 25.90, 27.31, 28.61, 29.01-29.26, 29.48-29.57, 29.60, 29.75, 29.87, 31.08, 31.85, 33.00, 34.31, 61.53, 64.35, 70.16-70.55, 70.79, 72.65, 73.34, 84.47, 173.88; IR (ATR, ν , cm^{-1}), 3469 (O-H str.), 2925 (s. CH_3 str.), 2890 (s. CH_2 str. PEG), 2861 (s. CH_2 str.), 1739 (C=O str.), 1469 (a. CH_3 bend), 1362 (s. CH_3 bend), 1345 (s. CH_2 bend), 1282 (end group C-O- str.), 1243 (C-O- str.), 1111 (a. C-O-C str.).

Epoxidised methyl oleate ring opened with PEG 1500 (PEMO1500)

8.45 g total product mass recovered. ^1H NMR (400 MHz, CDCl_3 , δ ppm): 0.76 (3H, t, CH_3CH_2-), 1.31 (26H, overlapped, $-(\text{CH}_2)_7\text{HC}(\text{OH})\text{CH}((\text{OCH}_2\text{CH}_2)_{34}-\text{OH})(\text{CH}_2)_6\text{CH}_2\text{COOCH}_3$), 2.18 (2H, t, $-\text{CH}_2\text{COOCH}_3$), 2.98 (~1H, m, $-\text{HC}(\text{OH})\text{CH}((\text{OCH}_2\text{CH}_2)_9-\text{OH})-$), 3.52 (146H, overlapped, $-\text{HC}(\text{OH})\text{CH}((\text{OCH}_2\text{CH}_2)_{34}-\text{OH})(\text{CH}_2)_7\text{COOCH}_3$); ^{13}C NMR (100 MHz, CDCl_3 , δ ppm): 14.13, 22.64, 24.89, 25.55, 27.34, 29.03-29.89, 31.12, 31.85, 31.88, 33.02, 34.03, 51.43, 61.64, 70.34-70.81, 72.53, 73.38, 84.54, 174.21; CHN: % C (55.236 found, 56.93 calc.), % H (8.782 found, 9.560 calc.), % N (nd); IR (ATR, ν , cm^{-1}), 3446 (O-H str.), 2889 (s. CH_2 str.), 1741 (C=O str.), 1469 (a. CH_3 bend), 1362 (s. CH_2 bend), 1243 (C-O- str.), 1109 (a. C-O-C str.).

Epoxidised ethyl oleate ring opened with PEG 1500 (PEEO1500)

7.53 g total product mass recovered. ^1H NMR (400 MHz, CDCl_3 , δ ppm): 0.75 (3H, t, CH_3CH_2-), 1.28 (29H, overlapped, $-(\text{CH}_2)_7\text{HC}(\text{OH})\text{CH}((\text{OCH}_2\text{CH}_2)_{34}-\text{OH})(\text{CH}_2)_6\text{CH}_2\text{COOCH}_2\text{CH}_3$), 2.16 (2H, t, $-\text{CH}_2\text{COOCH}_2\text{CH}_3$), 2.96 (~1H, m, $-\text{HC}(\text{OH})\text{CH}((\text{OCH}_2\text{CH}_2)_{34}-\text{OH})-$), 3.63 (130H, overlapped, $-\text{HC}(\text{OH})\text{CH}((\text{OCH}_2\text{CH}_2)_{34}-\text{OH})(\text{CH}_2)_7\text{COOCH}_2\text{CH}_3$), 3.97 (2H, q, $-\text{COOCH}_2\text{CH}_3$); ^{13}C NMR (100 MHz, CDCl_3 , δ ppm): 14.11, 14.28, 22.61, 24.87, 28.73-29.20, 31.86, 34.35, 60.11, 61.61, 70.27-

70.79, 72.56, 73.39, 84.52, 173.82; IR (ATR, ν , cm^{-1}), 3405 (O-H str.), 2888 (s. CH_2 str.), 1737 (C=O str.), 1467 (a. CH_3 bend), 1360 (s. CH_2 bend), 1241 (C-O- str.), 1107 (a. C-O-C str.).

Epoxidised 1-propyl oleate ring opened with PEG 1500 (PEPO1500)

7.97 g total product mass recovered. ^1H NMR (400 MHz, CDCl_3 , δ ppm): 0.68 (6H, t, overlapped, CH_3CH_2 -), - $\text{COOCH}_2\text{CH}_2\text{CH}_3$), 1.26 (28H, overlapped, - $(\text{CH}_2)_7\text{HC}(\text{OH})\text{CH}((\text{OCH}_2\text{CH}_2)_{34}\text{-OH})(\text{CH}_2)_6\text{CH}_2\text{COOCH}_2\text{CH}_2\text{CH}_3$), 2.06 (2H, t, - $\text{CH}_2\text{COOCH}_2\text{CH}_2\text{CH}_3$), 2.86 (~1H, m, - $\text{HC}(\text{OH})\text{CH}((\text{OCH}_2\text{CH}_2)_{34}\text{-OH})$ -), 3.39 (136H, m, overlapped, - $\text{HC}(\text{OH})\text{CH}((\text{OCH}_2\text{CH}_2)_{34}\text{-OH})(\text{CH}_2)_7\text{COO}$ -), 3.78 (2H, t, - $\text{COOCH}_2\text{CH}_2\text{CH}_3$); ^{13}C NMR (100 MHz, CDCl_3 , δ ppm): 10.35, 14.04, 21.89, 22.51, 24.82, 25.27, 28.88-29.62, 31.72, 32.84, 34.14, 61.41, 65.61, 70.20-70.44, 70.69, 72.48, 73.12, 80.82, 100.00, 107.51, 173.60; IR (ATR, ν , cm^{-1}), 3416 (O-H str.), 2887 (s. CH_2 str.), 1737 (C=O str.), 1467 (a. CH_3 bend), 1360 (s. CH_3 bend), 1342 (s. CH_2 bend), 1280 (end group C-O-str.), 1241 (C-O- str.), 1107 (a. C-O-C str.).

Epoxidised 2-propyl oleate ring opened with PEG 1500 (PE2PO1500)

7.99 g total product mass recovered. ^1H NMR (400 MHz, CDCl_3 , δ ppm): 0.75 (3H, t, $J=6.4$ Hz, CH_3CH_2 -), 1.27 (32H, overlapped, - $(\text{CH}_2)_7\text{HC}(\text{OH})\text{CH}((\text{OCH}_2\text{CH}_2)_{34}\text{-OH})(\text{CH}_2)_6\text{CH}_2\text{COOCH}(\text{CH}_3)_2$), 2.12 (2H, t, $J=7.6$ Hz, - CH_2COO -), 2.97 (~1H, m, - $\text{HC}(\text{OH})\text{CH}((\text{OCH}_2\text{CH}_2)_{34}\text{-OH})$ -), 3.53 (138H, m, overlapped, - $\text{HC}(\text{OH})\text{CH}((\text{OCH}_2\text{CH}_2)_{34}\text{-OH})(\text{CH}_2)_7\text{COO}$ -), 4.87 (1H, spt, - $\text{COOCH}(\text{CH}_3)_2$); ^{13}C NMR (100 MHz, CDCl_3 , δ ppm): 14.07, 14.11, 22.63, 24.96, 24.98, 26.07, 26.12, 28.99-29.87, 31.08, 31.10, 31.83, 32.98, 34.63, 61.60, 67.28, 70.28-70.58, 70.80, 72.58, 73.35, 80.95, 84.49, 173.34; IR (ATR, ν , cm^{-1}), 3409 (O-H str.), 2888 (s. CH_2 str.), 1732 (C=O str.), 1467 (a. CH_3 bend), 1360 (s. CH_3 bend), 1342 (s. CH_2 bend), 1280 (end group C-O-str.), 1241 (C-O- str.), 1107 (a. C-O-C str.).

Epoxidised 1-butyl oleate ring opened with PEG 1500 (PEBO1500)

8.57 g total product mass recovered. ^1H NMR (400 MHz, CDCl_3 , δ ppm): 0.68 (3H, t, CH_3CH_2 -), 0.74 (3H, t, $J=7.3$ Hz, - $\text{COO}(\text{CH}_2)_3\text{CH}_3$), 1.24 (31H, overlapped, -

$(CH_2)_7HC(OH)CH((OCH_2CH_2)_{34}-OH)(CH_2)_6CH_2COOCH_2(CH_2)_2CH_3$), 2.09 (2H, t, $J=7.6$ Hz, $-CH_2COO-$), 2.90 (~1H, m, $-HC(OH)CH((OCH_2CH_2)_{34}-OH)-$), 3.44 (148H, m, overlapped, $-HC(OH)CH((OCH_2CH_2)_{34}-OH)-$), 3.86 (2H, t, $J=6.6$ Hz $-COOCH_2-$); ^{13}C NMR (100 MHz, $CDCl_3$, δ ppm): 13.67, 14.06, 19.05, 22.49, 22.55, 24.86, 26.04, 26.15, 27.27, 28.91-29.14, 29.37-29.79, 30.61, 31.54, 31.76, 32.91, 34.20, 61.48, 63.92, 70.27, 70.48, 70.73, 72.49, 73.22, 84.36, 173.71; IR (ATR, v , cm^{-1}), 3432 (O-H str.), 2889 (s. CH_2 str.), 1737 (C=O str.), 1467 (a. CH_3 bend), 1360 (s. CH_3 bend), 1342 (s. CH_2 bend), 1280 (end group C-O-str.), 1241 (C-O- str.), 1107 (a. C-O-C str.).

Epoxidised 2-butyl oleate ring opened with PEG 1500 (PE2B01500)

8.26 g total product mass recovered. 1H NMR (400 MHz, $CDCl_3$, δ ppm): 0.79 (6H, t, overlapped, CH_3CH_2- , $-COOCH(CH_3)CH_2CH_3$), 1.35 (31H, overlapped, $(CH_2)_7HC(OH)CH((OCH_2CH_2)_{34}OH)(CH_2)_6CH_2COOCH(CH_3)CH_2CH_3$), 2.17 (2H, t, $J=7.3$ Hz, $-CH_2COO-$), 3.00 (~1H, m, $-HC(OH)CH((OCH_2CH_2)_{34}OH)-$), 3.57 (136H, overlapped, $-HC(OH)CH((OCH_2CH_2)_{34}OH)-$), 4.74 (1H, sxt, $J=6.3$ Hz, $-COOCH-$); ^{13}C NMR (100 MHz, $CDCl_3$, δ ppm): 9.74, 14.13, 19.54, 22.66, 25.06, 25.11, 25.37, 25.58, 26.16, 27.35, 28.83, 29.14, 29.24-29.31, 29.48, 29.60, 29.68, 29.78, 29.90, 31.14, 31.87, 32.98, 33.02, 34.69, 61.67, 70.33-70.62, 70.83, 71.89, 72.58, 73.41, 84.55, 173.53; IR (ATR, v , cm^{-1}), 3389 (O-H str.), 2887 (s. CH_2 str.), 1732 (C=O str.), 1467 (a. CH_3 bend), 1360 (s. CH_3 bend), 1342 (s. CH_2 bend), 1280 (end group C-O-str.), 1241 (C-O- str.), 1107 (a. C-O-C str.).

Epoxidised 1-octyl oleate ring opened with PEG 1500 (PEO01500)

8.12 g total product mass recovered. 1H NMR (400 MHz, $CDCl_3$, δ ppm): 0.62 (6H, t, overlapped, CH_3CH_2- , $-COO(CH_2)_7CH_3$), 1.18 (38H, overlapped, $(CH_2)_7HC(OH)CH((OCH_2CH_2)_{34}-OH)(CH_2)_6CH_2COOCH_2(CH_2)_6CH_3$), 2.03 (2H, t, $J=7.6$ Hz, $-CH_2COO-$), 2.83 (~1H, m, $-HC(OH)CH((OCH_2CH_2)_{34}-OH)-$), 3.39 (130H, m, overlapped, $-HC(OH)CH((OCH_2CH_2)_{34}-OH)-$), 3.79 (2H, m, $J=6.6$ Hz, $-COOCH_2-$); ^{13}C NMR (100 MHz, $CDCl_3$, δ ppm): 14.00, 22.48, 24.80, 25.44, 25.79, 26.00, 27.22, 28.50, 28.83-29.05, 29.08, 29.11, 29.32-29.45, 29.74, 31.62, 31.71, 32.81, 34.13, 61.36, 64.13, 70.18, 70.42, 70.68, 72.48, 73.11, 84.28, 173.56; IR (ATR, v , cm^{-1}), 3464 (O-H

str.), 2925 (s. CH₃ str.), 2888 (s. CH₂ str. PEG), 2860 (s. CH₂ str. oleate), 1737 (C=O str.), 1467 (a. CH₃ bend), 1360 (s. CH₃ bend), 1342 (s. CH₂ bend), 1280 (end group C-O-str.), 1241 (C-O- str.), 1108 (a. C-O-C str.).

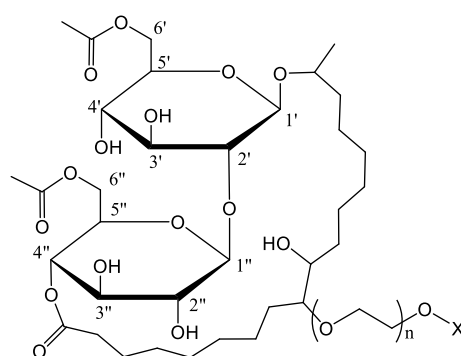
Epoxidised 2-octyl oleate ring opened with PEG 1500 (PE2001500)

8.43 g total product mass recovered. ¹H NMR (400 MHz, CDCl₃, δ ppm): 0.62 (6H, t, $J=6.6$ Hz, CH₃CH₂-, -COOCH(CH₃)(CH₂)₅CH₃), 1.18 (39H, m, overlapped, -(CH₂)₇HC(OH)-, -(CH₂)₆CH₂COOCH(CH₃)(CH₂)₅CH₃), 2.01 (2H, t, $J=7.3$ Hz, -CH₂COO-), 2.82 (~1H, m, -HC(OH)CH((OCH₂CH₂)₃₄-OH)-), 3.37 (141H, m, overlapped, -HC(OH)CH((OCH₂CH₂)₃₄-OH)-), 4.63 (1H, sxt, $J=6.3$ Hz, -COOCH-); ¹³C NMR (100 MHz, CDCl₃, δ ppm): 13.97, 14.02, 19.92, 22.41, 22.50, 23.69, 24.89, 25.21, 25.50, 25.94, 26.00, 26.07, 27.23, 28.87, 28.93, 29.08, 29.39-29.74, 30.90, 31.59, 31.71, 31.74, 32.85, 34.48, 35.80, 61.39, 70.20, 70.43, 70.68, 70.70, 72.44, 73.13, 84.30, 173.17; IR (ATR, ν , cm⁻¹), 3493 (O-H str.), 2925 (s. CH₃ str.), 2888 (s. CH₂ str. PEG), 2860 (s. CH₂ str. oleate), 1733 (C=O str.), 1467 (a. CH₃ bend), 1360 (s. CH₃ bend), 1342 (s. CH₂ bend), 1280 (end group C-O-str.), 1242 (C-O- str.), 1108 (a. C-O-C str.).

Epoxidised 1-decyl oleate ring opened with PEG 1500 (PEDO1500)

8.39 g total product mass recovered. ¹H NMR (400 MHz, CDCl₃, δ ppm): 0.57 (6H, t, $J=6.1$ Hz, CH₃CH₂-, -COO(CH₂)₉CH₃), 1.12 (42H, m, overlapped, -(CH₂)₇HC(OH)CH((OCH₂CH₂)₃₄-OH)(CH₂)₆CH₂COOCH₂(CH₂)₈CH₃), 1.97 (2H, t, $J=7.3$ Hz, -CH₂COO-), 2.79 (~1H, m, -HC(OH)CH((OCH₂CH₂)₃₄-OH)-), 3.34 (172H, m, overlapped, -HC(OH)CH((OCH₂CH₂)₃₄-OH)-), 3.74 (2H, t, $J=6.6$ Hz, -COOCH₂-); ¹³C NMR (100 MHz, CDCl₃, δ ppm): 13.98, 22.47, 24.77, 25.75, 27.18, 28.46-29.40, 31.68, 32.79, 34.05, 61.28, 64.03, 70.04-70.37, 72.43, 72.99, 84.19, 173.39; IR (ATR, ν , cm⁻¹), 3480 (O-H str.), 2925 (s. CH₃ str.), 2890 (s. CH₂ str. PEG), 2859 (s. CH₂ str. oleate), 1737 (C=O str.), 1467 (a. CH₃ bend), 1360 (s. CH₃ bend), 1343 (s. CH₂ bend), 1280 (end group C-O-str.), 1242 (C-O- str.), 1108 (a. C-O-C str.).

8.10.3 Synthesis of lactonic sophorolipid-based surfactant *via* PEGylation



where X=H or CH₃
n = 9, 16, 22, 34

0.765 mmol PEG or MePEG was heated at 80 °C in a 50 mL round bottom flask followed by addition of 5% (wt of PEG or MePEG) catalyst and allowed to mix thoroughly for 2 minutes. 0.766 mmol epoxide was dissolved in ethyl acetate and added in drops through a dropping funnel over 10 minutes and the temperature raised to 100 °C while stirring rigorously with the flask stoppered. Progress of reaction was monitored with ¹H NMR spectroscopy with portions taken for analysis. The reaction was stopped after 50 minutes and resulting product transferred into a 250 mL beaker, diluted with 50 mL ethyl acetate and suction filtered to recover the catalyst. The filtrate was shaken with 25 mL distilled water in a separating funnel followed by addition of brine. The organic phase was collected and dried over anhydrous MgSO₄ and product recovered on the rotary evaporator. The product was purified by re-dissolution in ethyl acetate and passing it through a narrow column packed with Amberlyst 15 ion exchange resin. The product was concentrated on the rotary evaporator. Product identification was by IR spectroscopy, ESI mass spectrometry, CHN elemental analysis and ¹H and ¹³C NMR spectroscopy.

Epoxidised lactonic sophorolipid ring opened with PEG 400 (PELSL400)

0.49 g total product mass recovered. ¹H NMR (700 MHz, CDCl₃, δ ppm): 0.88 (0.87H, t, -CH(CH₃-), 1.42 (31H, overlapped, -(CH₂)₆HC(OH)CH((OCH₂CH₂)₉OH)(CH₂)₆-), 2.07 (6H, s, (-CH₂COOCH₃)₂), 2.36 (2H, t, -CH₂COO-), 3.22 (~1H, m, -HC(OH)CH((OCH₂CH₂)₉OH)(CH₂)₆-), 3.56 (72H, m, overlapped, -

$HC(OH)CH((OCH_2CH_2)_9OH)(CH_2)_6$ -, H4', H2', H2'', H5'', -CH(CH₃)-, H3', H3'', H5'), 4.14 (1H, m, H6'), 4.27 (1H, m, H6''), 4.40 (2H, m, overlapped, H6'', H6'), 4.57 (2H, d, H1', H1''), 4.98 (1H, H4''); ¹³C NMR (175 MHz, CDCl₃, δ ppm): 14.10, 20.82, 20.89, 22.58, 22.70, 24.47, 26.22, 28.98, 29.03, 29.23, 31.61, 31.82, 61.55, 63.77, 70.02-70.47, 72.77, 73.88, 79.12, 83.75, 170.55, 171.29, 173.11; CHN: % C (53.249 found, 55.520 calc.), % H (8.610 found, 8.220 calc.), % N (nd); IR (ATR, ν , cm⁻¹), 3418 (O-H str.), 2926 (s. CH₃ str.), 2864 (s. CH₂ str.), 1741, 1647 (C=O str.), 1456 (a. CH₃ bend), 1367 (s. CH₂ bend), 1242 (C-O- str.), 1095 (a. C-O-C str.).

Epoxidised lactonic sophorolipid ring opened with MePEG 400 (MPELSL400)

0.79 g total product mass recovered. ¹H NMR (700 MHz, CDCl₃, δ ppm): 0.89 (1.22H, t, -CH(CH₃)-), 1.30 (31H, overlapped, -(CH₂)₆HC(OH)CH((OCH₂CH₂)₉OCH₃)(CH₂)₆-), 2.07 (6H, s, (-CH₂COOCH₃)₂), 2.37 (2H, t, -CH₂COO-), 2.92 (2H, m, -HC(O)CH-), 3.22 (~1H, m, -HC(OH)CH((OCH₂CH₂)₉OCH₃)-), 3.38 (3H, s, -HC(OH)CH((OCH₂CH₂)₉OCH₃)-), 3.68 (44H, m, overlapped, -HC(OH)CH((OCH₂CH₂)₉OCH₃)(CH₂)₆-, H4', H2', H2'', H5'', -CH(CH₃)-, H3', H3'', H5'), 4.12 (1H, m, H6'), 4.37 (3H, m, overlapped, H6'', H6'', H6'), 4.59 (2H, d, H1', H1''), 4.99 (1H, H4''); ¹³C NMR (175 MHz, CDCl₃, δ ppm): 14.10, 20.80, 20.90, 21.32, 22.29, 22.57, 22.65, 24.47, 25.29, 25.62, 26.24, 27.16, 27.35, 27.57, 27.82, 27.90, 28.50, 28.98, 29.24, 29.34, 29.42, 29.89, 30.08, 31.62, 34.02, 37.53, 57.62, 57.85, 59.02, 61.66, 63.67, 69.72, 70.24-70.57, 71.91, 72.57, 73.29, 74.06, 74.99, 76.18, 79.30, 170.54, 171.39, 173.02; CHN: % C (55.155 found, 55.910 calc.), % H (8.515 found, 8.244 calc.), % N (nd); IR (ATR, ν , cm⁻¹), 3438 (O-H str.), 2926 (s. CH₃ str.), 2860 (s. CH₂ str.), 1741 (C=O str.), 1455 (a. CH₃ bend), 1367 (s. CH₂ bend), 1240 (C-O- str.), 1109 (a. C-O-C str.).

Epoxidised lactonic sophorolipid ring opened with MePEG 750 (MPELSL750)

1.04 g total product mass recovered. ¹H NMR (700 MHz, CDCl₃, δ ppm): 0.87 (0.74H, t, -CH(CH₃)-), 1.39 (26H, overlapped, -(CH₂)₆HC(OH)CH((OCH₂CH₂)₁₆OCH₃)(CH₂)₆-), 2.07 (6H, s, (-CH₂COOCH₃)₂), 2.32 (2H, t, -CH₂COO-), 3.09 (~1H, m, -

HC(OH)CH((OCH₂CH₂)₁₆OCH₃)-, 3.37 (3H, s, -HC(OH)CH((OCH₂CH₂)₁₆OCH₃)-), 3.64 (74H, m, overlapped, -HC(OH)CH((OCH₂CH₂)₁₆OCH₃)(CH₂)₆-, H4', H2', H2'', H5'', -CH(CH₃)-, H3', H3'', H5'), 4.14 (1H, m, H6'), 4.36 (3H, m br, overlapped, H6'', H6', H6''), 4.54 (2H, d, H1', H1''), 4.98 (1H, H4''); ¹³C NMR (175 MHz, CDCl₃, δ ppm): 14.09, 20.89, 22.58, 22.63, 26.21, 28.97, 29.39, 31.81, 50.47, 52.33, 59.01, 61.65, 63.60, 70.26-70.56, 71.90, 72.54, 74.07, 76.04, 171.04, 171.63, 173.57; CHN: % C (54.852 found, 55.833 calc.), % H (8.581 found, 8.611 calc.), % N (nd); IR (ATR, ν , cm⁻¹), 3424 (O-H str.), 2863 (s. CH₂ str.), 1741 (C=O str.), 1455 (a. CH₃ bend), 1350 (s. CH₂ bend), 1242 (C-O- str.), 1107 (a. C-O-C str.).

Epoxidised lactonic sophorolipid ring opened with PEG 1000 (PELSL1000)

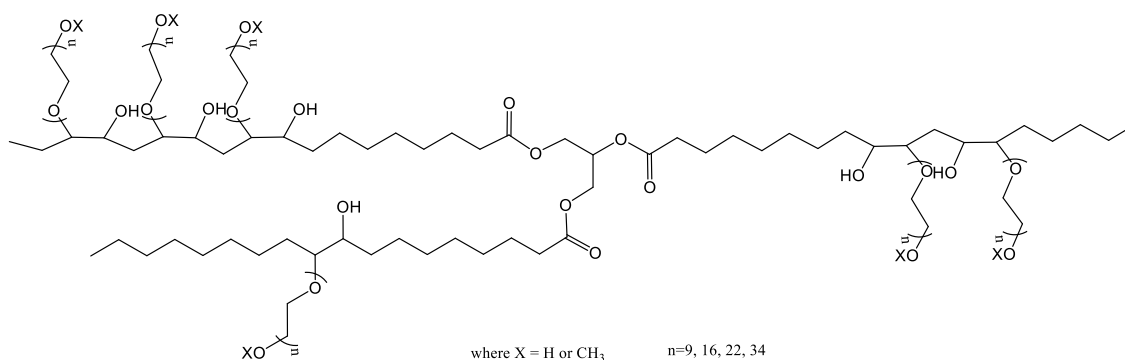
1.55 g total product mass recovered. ¹H NMR (700 MHz, CDCl₃, δ ppm): 0.87 (0.91H, t, -CH(CH₃)-), 1.38 (26H, overlapped, -(CH₂)₆HC(OH)CH((OCH₂CH₂)₂₂OH)(CH₂)₆-), 2.06 (6H, s, (-CH₂COOCH₃)₂), 2.34 (2H, t, -CH₂COO-), 3.22 (~1H, m, -HC(OH)CH((OCH₂CH₂)₂₂OH)(CH₂)₆-), 3.59 (150H, m, overlapped, -HC(OH)CH((OCH₂CH₂)₂₂OH)(CH₂)₆-, H4', H2', H2'', H5'', -CH(CH₃)-, H3', H3'', H5'), 4.11 (1H, m, H6'), 4.35 (3H, m, overlapped, H6'', H6', H6''), 4.52 (2H, d, H1', H1''), 4.99 (1H, H4''); ¹³C NMR (175 MHz, CDCl₃, δ ppm): 14.10, 20.89, 22.56, 26.20, 28.96, 29.02, 29.31, 29.39, 61.64, 63.02, 68.63, 70.10-70.54, 72.54, 72.63, 171.20; CHN: % C (53.724 found, 53.658 calc.), % H (8.702 found, 9.175 calc.), % N (nd); IR (ATR, ν , cm⁻¹), 3448 (O-H str.), 2888 (s. CH₂ str. PEG), 1741 (C=O str.), 1465 (a. CH₃ bend), 1344 (s. CH₂ bend), 1280 (end group C-O- str.), 1241 (C-O- str.), 1108 (a. C-O-C str.).

Epoxidised lactonic sophorolipid ring opened with PEG 1500 (PELSL1500)

1.53 g total product mass recovered. ¹H NMR (700 MHz, CDCl₃, δ ppm): 0.88 (0.91H, t, -CH(CH₃)-), 1.41 (29H, overlapped, -(CH₂)₆HC(OH)CH((OCH₂CH₂)₃₄OH)(CH₂)₆-), 2.07 (6H, s, (-CH₂COOCH₃)₂), 2.35 (2H, t, -CH₂COO-), 3.22 (~1H, m, -HC(OH)CH((OCH₂CH₂)₃₄OH)(CH₂)₆-), 3.61 (168H, m, overlapped, -HC(OH)CH((OCH₂CH₂)₃₄OH)(CH₂)₆-, H4', H2', H2'', H5'', -CH(CH₃)-, H3', H3'', H5'), 4.14 (1H, m, H6'), 4.33 (3H, m, overlapped, H6'', H6', H6''), 4.50 (2H, d, H1', H1''),

4.99 (1H, H^α); ¹³C NMR (175 MHz, CDCl₃, δ ppm): 14.10, 20.89, 22.30, 25.12, 26.21, 28.96, 29.02, 29.22, 29.39, 31.60, 31.81, 61.66, 63.63, 70.28-70.58, 72.54; CHN: % C (54.393 found, 55.190 calc.), % H (8.269 found, 8.760 calc.), % N (0.048 found); IR (ATR, ν, cm⁻¹), 3408 (O-H str.), 2888 (s. CH₂ str. PEG), 1741 (C=O str.), 1466 (a. CH₃ bend), 1360, 1341 (s. CH₂ bend), 1279 (end group C-O- str.), 1240 (C-O- str.), 1108 (a. C-O-C str.).

8.10.4 Synthesis of linseed oil-based surfactant *via* PEGylation



5 mmol PEG or MePEG was heated at 80 °C in a 50 mL round bottom flask followed by addition of catalyst (5% wt of PEG or MePEG) and stirred for 2 minutes. 0.167 mmol epoxide was added in drops through a dropping funnel for over 5 to 10 minutes after which temperature was raised to 100 °C while stirring rigorously and the vessel covered. Progress of reaction was monitored with proton NMR spectroscopy with portions taken for analysis. The reaction was stopped after 50 minutes and resulting product transferred into a 250 mL beaker, diluted with 50 mL DCM and suction filtered to recover the catalyst. The filtrate was shaken with 25 mL distilled water in a separating funnel followed by addition of brine. The organic phase was collected and dried over anhydrous MgSO₄ and product recovered on the rotary evaporator. Product identification was by IR spectroscopy, size exclusion chromatography and ¹H and proton-decoupled ¹³C NMR spectroscopy.

Epoxidised linseed oil ring opened with PEG 400 (PELO400)

2.33 g total product mass recovered. ^1H NMR (700 MHz, CDCl_3 , δ ppm): 0.85 (~6H, 2x CH_3CH_2 -), 0.96 (3H, $\text{CH}_3\text{CH}_2\text{CH}(\text{OH})$ -), 1.26 (56H, overlapped, $-(\text{CH}_2)_{34}$ -), 2.29 (6H, t, overlapped, 3x $-\text{CH}_2\text{COO}$ -), 3.07 (~1H, m, $-\text{CH}((\text{OCH}_2\text{CH}_2)_9\text{OH})$ -), 3.64 (226H, m, 6x $-\text{HC}(\text{OH})\text{CH}((\text{OCH}_2\text{CH}_2)_9\text{OH})$ -), 4.12 (2H, m, $-\text{COOCH}(\text{CH}_2\text{OOC}-)\text{CH}_2\text{OOC}-$), 4.27 (2H, m, $-\text{COOCH}(\text{CH}_2\text{OOC}-)\text{CH}_2\text{OOC}-$), 5.23 (1H, quint, $-\text{COOCH}(\text{CH}_2\text{OOC}-)\text{CH}_2\text{OOC}-$); ^{13}C NMR (175 MHz, CDCl_3 , δ ppm): 14.11, 22.66, 24.82, 25.62, 29.08, 29.24, 29.32, 29.44, 29.58, 29.62, 29.66, 29.88, 31.11, 31.84, 31.86, 31.88, 33.04, 34.01, 61.52, 61.59, 61.63, 62.05, 63.01, 63.34, 68.82, 69.16, 69.96, 70.13, 70.19, 70.24, 70.27, 70.40, 70.43, 70.49-70.57, 70.78, 72.36, 72.54, 72.56, 72.63, 72.88, 73.40, 78.53, 84.55, 172.82, 173.21; IR (ATR, ν , cm^{-1}), 3454 (O-H str.), 2922 (s. CH_3 str.), 2867 (s. CH_2 str.), 1739 (C=O str.), 1460 (a. CH_3 bend), 1350 (s. CH_2 bend), 1296 (end group C-O- str.), 1249 (C-O- str.), 1102 (a. C-O-C str.).

Epoxidised linseed oil ring opened with MePEG 400 (MPELO400)

2.27 g total product mass recovered. ^1H NMR (700 MHz, CDCl_3 , δ ppm): 0.91 (~8H, 2x CH_3CH_2 -, $\text{CH}_3\text{CH}_2\text{CH}(\text{OH})$ -), 1.25 (54H, overlapped, $-(\text{CH}_2)_{34}$ -), 2.28 (6H, t, overlapped, 3x $-\text{CH}_2\text{COO}$ -), 3.06 (~1H, m, $-\text{CH}((\text{OCH}_2\text{CH}_2)_9\text{OCH}_3)$ -), 3.35 (21H, s, 6x $-\text{CH}((\text{OCH}_2\text{CH}_2)_9\text{OCH}_3)$ -), 3.61 (222H, m, 6x $-\text{HC}(\text{OH})\text{CH}((\text{OCH}_2\text{CH}_2)_9\text{OCH}_3)$ -), 4.12 (2H, m, $-\text{COOCH}(\text{CH}_2\text{OOC}-)\text{CH}_2\text{OOC}-$), 4.26 (2H, m, $-\text{COOCH}(\text{CH}_2\text{OOC}-)\text{CH}_2\text{OOC}-$), 5.23 (1H, quint, $-\text{COOCH}(\text{CH}_2\text{OOC}-)\text{CH}_2\text{OOC}-$); ^{13}C NMR (175 MHz, CDCl_3 , δ ppm): 14.11, 22.65, 24.82, 29.07, 29.23, 29.32, 29.66, 31.10, 31.88, 33.95, 58.99, 61.63, 63.00, 68.82, 69.76, 70.24-70.56, 71.88, 72.55, 84.58; IR (ATR, ν , cm^{-1}), 3446 (O-H str.), 2868 (s. CH_2 str.), 1741 (C=O str.), 1457 (a. CH_3 bend), 1350 (s. CH_2 bend), 1297 (end group C-O- str.), 1248 (C-O- str.), 1104 (a. C-O-C str.).

Epoxidised linseed oil ring opened with MePEG 750 (MPELO750)

4.15 g total product mass recovered. ^1H NMR (700 MHz, CDCl_3 , δ ppm): 0.89 (~7H, 2x CH_3CH_2 -, $\text{CH}_3\text{CH}_2\text{CH}(\text{OH})$ -), 1.42 (52H, overlapped, $-(\text{CH}_2)_{34}$ -), 2.28 (6H, t, overlapped, 3x $-\text{CH}_2\text{COO}$ -), 3.07 (~1H, m, $-\text{CH}((\text{OCH}_2\text{CH}_2)_{16}\text{OCH}_3)$ -), 3.35 (19H, s, 6x

-CH((OCH₂CH₂)₁₆OCH₃)-, 3.55 (376H, m, 6x -HC(OH)CH((OCH₂CH₂)₁₆OCH₃)-), 4.11 (2H, m, -COOCH(CH₂OOC-)CH₂OOC-), 4.27 (2H, m, -COOCH(CH₂OOC-)CH₂OOC-), 5.22 (1H, quint, -COOCH(CH₂OOC-)CH₂OOC-); ¹³C NMR (175 MHz, CDCl₃, δ ppm): 14.11, 22.65, 24.81, 29.07- 29.32, 29.61, 29.65, 31.88, 34.00, 58.99, 61.63, 62.03, 62.99, 68.81, 69.77, 70.28-70.55, 71.88, 72.48; IR (ATR, v, cm⁻¹), 3481 (O-H str.), 2870 (s. CH₂ str.), 1740 (C=O str.), 1465 (a. CH₃ bend), 1345 (s. CH₂ bend), 1281 (end group C-O- str.), 1243 (C-O- str.), 1110 (a. C-O-C str.).

Epoxidised linseed oil ring opened with PEG 1000 (PELO1000)

5.32 g total product mass recovered. ¹H NMR (700 MHz, CDCl₃, δ ppm): 0.92 (~8H, 2x CH₃CH₂-, CH₃CH₂CH(OH)-), 1.43 (57H, overlapped, -(CH₂)₃₄-), 2.30 (6H, t, overlapped, 3x -CH₂COO-), 3.08 (~1H, m, -CH((OCH₂CH₂)₂₂OH)-), 3.63 (593H, m, 6x -HC(OH)CH((OCH₂CH₂)₂₂OH)-), 4.13 (2H, m, -COOCH(CH₂OOC-)CH₂OOC-), 4.28 (2H, m, -COOCH(CH₂OOC-)CH₂OOC-), 5.24 (1H, quint, -COOCH(CH₂OOC-)CH₂OOC-); ¹³C NMR (175 MHz, CDCl₃, δ ppm): 14.13, 22.67, 24.83, 29.24-29.67, 31.89, 34.14, 61.66, 63.00, 68.83, 69.17, 70.30-70.58, 70.78, 72.49; IR (ATR, v, cm⁻¹), 3451 (O-H str.), 2886 (s. CH₂ str.), 1739 (C=O str.), 1467 (a. CH₃ bend), 1360, 1343 (s. CH₂ bend), 1280 (end group C-O- str.), 1241 (C-O- str.), 1108 (a. C-O-C str.).

Epoxidised linseed oil ring opened with PEG 1500 (PELO1500)

6.71 g total product mass recovered. ¹H NMR (700 MHz, CDCl₃, δ ppm): 0.90 (~8H, 2x CH₃CH₂-, CH₃CH₂CH(OH)-), 1.42 (56H, overlapped, -(CH₂)₃₄-), 2.30 (6H, t, overlapped, 3x -CH₂COO-), 3.07 (~1H, m, -CH((OCH₂CH₂)₃₄OH)-), 3.60 (783H, m, 6x -HC(OH)CH((OCH₂CH₂)₃₄OH)-), 4.12 (2H, m, -COOCH(CH₂OOC-)CH₂OOC-), 4.29 (2H, m, -COOCH(CH₂OOC-)CH₂OOC-), 5.23 (1H, quint, -COOCH(CH₂OOC-)CH₂OOC-); ¹³C NMR (175 MHz, CDCl₃, δ ppm): 14.13, 22.63, 24.79, 29.25, 29.66, 31.89, 34.13, 61.66, 69.77, 70.30-70.58, 72.50; IR (ATR, v, cm⁻¹), 3442 (O-H str.), 2886 (s. CH₂ str.), 1741 (C=O str.), 1467 (a. CH₃ bend), 1360, 1342 (s. CH₂ bend), 1280 (end group C-O- str.), 1241 (C-O- str.), 1107 (a. C-O-C str.).

8.10.5 Synthesis of alkyl oleate-based surfactant *via* ring-opening with carbohydrates

8.10.5.1 Ring opening of alkyl oleate epoxides with fructose

Synthesis was carried out following methods reported for inulin etherification with minor modifications.^{351, 435} 1.64 g methyl oleate epoxide (2.0 equivalent of fructose) and 0.48 g finely ground fructose were dissolved in 2 mL N-methyl-2-pyrrolidone (NMP) in a 25 mL round bottom flask with 0.1 mL triethylamine (TEA) added as catalyst. Temperature was raised to 60 °C while stirring at 240 rpm to completely dissolve the fructose under nitrogen. The reaction was left to stand overnight for 18 hours. The reaction product was poured into thoroughly stirred dichloromethane contained in a beaker. The solution was filtered and the sticky solid obtained at the bottom of the beaker washed severally with dichloromethane. The product obtained was amber-like viscous material and was analysed with Supercritical fluid chromatography (SFC). The filtrate was also analysed with ¹H and proton-decoupled ¹³C NMR spectroscopy.

8.10.5.2 Ring opening of alkyl oleate epoxides with inulin

Synthesis was carried out following methods reported for inulin etherification with minor modifications.^{351, 435} 0.6 g inulin (0.12 mmol; 3.70 mmol of fructose equivalent) was first dissolved in 2 g N-methyl-2-pyrrolidone (NMP) in a 25 mL round bottom flask at 50 °C under a nitrogen atmosphere with stirring. 0.123 g triethylamine (TEA) was added and the temperature raised to 60 °C while stirring at 240 rpm for 30 min. 0.19 g methyl oleate epoxide (0.6 mmol equivalent of inulin) was added to the dissolved inulin and the reaction was left to stand overnight for 24 hours under nitrogen at 60 °C. The reaction mixture was poured into a beaker containing dichloromethane with vigorous stirring as the crystals emerge from the solution. The dichloromethane solution was sinter filtered and the residue washed severally with acetone. A crystalline white powder obtained was analysed with FT-IR spectroscopy, ¹H and proton-decoupled ¹³C NMR spectroscopy and SEM and DSC techniques.

8.10.5.3 Ring opening of alkyl oleate epoxide with D-sorbitol

0.91 g (5.00 mmol) D-sorbitol was heated to 80 °C in a 25 mL round bottom flask and a catalyst (5% wt with respect to D-sorbitol) and stirred for 2 minutes. 1.56 g (5.00 mmol) epoxide was added in drops through a dropping funnel for over 5 minutes and temperature raised to 100 °C while stirring rigorously. The reaction was stopped after 4 hours and the product characterised by IR spectroscopy and ¹H and proton-decoupled ¹³C NMR spectroscopy.

8.11 Microwave-Assisted PEGylation: ring opening of epoxide

0.65 g (2.08 mmol) methyl oleate epoxide), 2.45 g (6.13 mmol) PEG400 and a catalyst (0.50% wt with respect to PEG400) were added in a microwave vial and placed in a CEM Discover microwave under preset conditions (pressure: 300 psi, mode: dynamic, power: 200 W). Reaction temperature was set at 140 °C, 180 °C, 200 °C, 220 °C and 250 °C, stopped after 2 hours and the product characterised by IR spectroscopy and ¹H and proton-decoupled ¹³C NMR spectroscopy.

8.12 One-pot PEGylation of methyl oleate

0.59 g (2 mmol) methyl oleate, 2 mL hydrogen peroxide solution, a catalyst (6% wt with respect to PEG400) and 0.80 g (2 mmol) PEG400 were added into a 30 mL glass vial. This was placed in an ultrasound with a probe slightly touching the solution in the vial and was heated under preset conditions (130 W, 20 kHz, 60% amplitude) for 3 hours. The resulting solution was dried over anhydrous magnesium sulphate and passed through a bed of neutral alumina and was analysed with ¹H and proton-decoupled ¹³C NMR spectroscopy.

8.13. Reuse of iron-exchanged montmorillonite catalyst for PEGylation reaction

2.00 g (5 mmol) PEG was heated to 80 °C in a 25 mL round bottom flask for 15 minutes and 0.40 g (20% wt with respect to PEG) iron-exchanged montmorillonite (prepared from iron (III) chloride) added and stirred thoroughly for 2 minutes. 1.63

g (5 mmol) ethyl oleate epoxide was added in drops through a dropping funnel for over 5 minutes and temperature raised to 120 °C while stirring rigorously with a stopper lightly placed on the flask. The reaction was stopped after 60 minutes and resulting product diluted with 15 mL ethyl acetate and suction filtered to recover the catalyst. The filtrate was run through a bed of Amberlyst 15 ion exchange resin and resulting solution concentrated on the rotary evaporator to afford an amber viscous liquid. Product identification was by IR spectroscopy, and ^1H and proton-decoupled ^{13}C NMR spectroscopy. The procedure was repeated two more times using the recovered catalyst without reactivation in an oven.

8.14 Surfactant properties testing

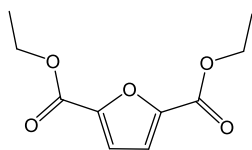
8.14.1 Dynamic surface tension measurement

99.9 g 10 mmol/L sodium chloride solution was added to 0.1 g surfactant in a 100 mL sample bottle to give a 1 g/L surfactant solution. 5 mL of the solution was measured in a beaker and placed under a maximum bubble pressure tensiometer. The tensiometer was operated under preset conditions according to standard procedures to obtain a set of data.

8.14.2 Equilibrium surface tension measurement

A Wilhelmy plate method was used for this measurement. 1 g/L surfactant solution was prepared as described in section 8.14.1 and about 30 mL measured in a clean beaker and placed under a Kruss K100 tensiometer. A bottle on the Dosino unit coupled to the tensiometer was filled with 10 mmol/L sodium chloride solution for sample multiple dilutions and the instrument ran under preset conditions. The extended surfactant programme was used and sets of measurements were taken until the change in surface tension was less than 0.1 mN/m. The plate and the beaker were thoroughly cleaned each time measurement was made.

8.15 Synthesis of 2,5-furandicarboxylic diethyl ester (FDEE)



5.23 g (33.5 mmol) 2, 5-furandicarboxylic acid (FDCA) was dissolved in 150 mL ethanol and heated to reflux. To this 0.4 mL concentrated H₂SO₄ was added and the reaction left under reflux for 24 hours. The excess ethanol was removed under reduced pressure and another 150 mL ethanol and 0.4 mL H₂SO₄ added and the reaction returned to reflux. After 24 hours the ethanol was removed under reduced pressure and an ethyl acetate-water wash applied, with this repeated twice more for the organic layer. The ethylate acetate layer was dried over anhydrous magnesium sulphate, filtered and the solvent removed *in vacuo* to yield a colourless oil that crystallised upon cooling to give the product (5.98 g, 83% yield by mass recovery, >99% purity). The product was analysed by IR spectroscopy, GC-MS, ESI-MS, ¹H and proton-decoupled ¹³C NMR spectroscopy and quantified by GC-FID. ¹H-NMR (400 MHz, CDCl₃, δ ppm): 1.41-1.43 (6H, t, $J=7.3$ Hz, 2CH₃-CH₂-), 4.41-4.44 (4H, q, $J=7.3$ Hz, 2CH₃-CH₂-), 7.24 (2H, s, =CH-C=C-C=OOR); ¹³C-NMR (100 MHz, CDCl₃, δ ppm): 14.34, 61.68, 118.34, 146.99, 158.17; IR (ATR, ν , cm⁻¹), 3148, 3113, 2990, 2945 (s. CH₃ str.), 1720 (C=O str.), 1573, 1480, 1445 (a. CH₃ bend), 1384, 1369 (s. CH₂ bend), 1272, 1230, 1182 (C-O- str.)

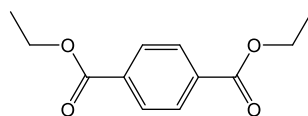
8.16 Synthesis of acid-free 2, 5-furandicarboxylic diethyl ester (FDEE)

Synthesis was as described for FDEE in section 8.15 but with a different method of purification. For this synthesis, ethanol was removed under reduced pressure after 24 hours and a dichloromethane-water wash was applied, with this repeated twice more for the organic layer. The organic layer was further washed with 5% sodium bicarbonate solution and brine solution, dried over anhydrous magnesium sulphate, filtered and the solvent removed *in vacuo* to yield a colourless oil that crystallised upon cooling to give the product (5.98 g, 84% yield by mass recovery, >99% purity).

8.17 Pre-adsorption of FDEE onto catalyst

A known amount of metal exchanged catalyst was added to 100 mL ethanol. An equal amount (or a calculated percentage of the amount of the catalyst depending on the intended catalyst loading in the reaction) by mass of the furan was added to the mixture on the rotary evaporator and the temperature raised to 60 °C. After 30 minutes, the solvent was removed and the resulting mixture cooled to solidify, this subsequently crushed in pestle and mortar to give a powder.

8.18 Synthesis of diethyl terephthalate (DET)



8.18.1 Small scale synthesis of diethyl terephthalate (DET)

A known amount (typically 200 mg) of pre-adsorbed FDEE-catalyst mixture (i.e. 100 mg of FDEE and 100 mg of catalyst) was loaded into a 16 mL HEL high pressure reactor equipped with a suspended magnetic stirrer. The reactor was sealed and the system purged with nitrogen followed by ethene (with each gas being purged at least three times). The reactor was filled with ethene to the desired pressure (at room temperature). The reactor was then inserted into a metal block seated on a hot plate. The reaction was set at a specific temperature (probe inserted into the heating block) and consistently stirred at 240 rpm. After a set time, the reaction was rapidly cooled under running water and excess ethene carefully vented. The reactor was opened and the product removed with ethyl acetate-ethanol-acetone wash. The resulting solution was sonicated for 20 minutes (to ensure desorption of product retained in the catalyst pores), filtered and the solvent removed *in vacuo* to give the product.

8.18.2 Large scale synthesis of diethyl terephthalate (DET)

Typically 1.35 g pre-adsorbed FDEE-catalyst mixture (i.e. 0.62 g of FDEE and 0.62 g of catalyst) was charged with a specific amount of pressurised ethene in a 50 mL HEL high pressure reactor equipped with a suspended magnetic stirrer set at 1100 rpm. Synthesis and work-up were carried out as described for small scale above. Reaction product was purified on Isolera Four flash chromatography (Biotage) with method developed from TLC plate measurement (cyclohexane-ethyl acetate solvent mixture, 6:1, R_f: 0.43, 0.25, 0.69). The product was analysed by IR spectroscopy, GC-MS, ESI-MS, ¹H and proton-decoupled ¹³C NMR spectroscopy and quantified by GC-FID. ¹H-NMR (400 MHz, CDCl₃, δ ppm): 1.39-1.43 (6H, t, $J=7.3$ Hz, 2CH₃-CH₂-), 4.37-4.41 (4H, q, $J=7.3$ Hz, 2CH₃-CH₂-), 8.10 (4H, s, =CH-C=C-C=OOR); ¹³C NMR (100 MHz, CDCl₃, δ ppm): 14.34, 61.68, 129.5, 134.29, 166.17; GC-MS (M⁺ =222); ESI-MS accurate mass, 245.0791 (MNa⁺, 245.0784 calc. for C₁₂H₁₄NaO₄); IR (ATR, ν , cm⁻¹): 2980, 2931 (s. CH₃ str.), 1761 (C=O str.), 1578, 1505, 1448 (a. CH₃ bend), 1404, 1367 (s. CH₂ bend), 1266, 1250, 1173 (C-O- str.), 1101 (a. C-O-C str.).

8.19 Effect of acidity on side reactions products from DET synthesis

Two different systems containing a known amount of pre-adsorbed FDEE on catalyst mixture (60% wt catalyst loading) and another equal amount of the same mixture already doped with three drops of concentrated sulphuric acid at pre-adsorption stage (also 60% wt catalyst loading) were used for this study. The systems were purged with ethene, charged with 60 bar pressurised ethane and heated at 200 °C while stirring at 240 rpm for 72 hours. The reactor vessels were rapidly cooled under running water and excess ethene vented. The reactors were opened and the resulting products removed with ethanol, sonicated for 20 minutes, and filtered. The filtrates were concentrated under vacuum and analysed using GC-FID and GC-MS.

8.20 Effect of Al-pillared montmorillonite on side reaction products from DET synthesis

0.258 g aluminium-pillared montmorillonite was charged into a 16 mL high pressure reactor, purged three times and filled with 60 bar ethene. The reactor was heated up to a temperature of 250 °C with stirring rate of 240 rpm for 48 hours. The reaction was cooled rapidly to room temperature under running water and excess ethene vented. The reactor was opened and the resulting content washed with ethanol, sonicated for 20 minutes, and filtered. The filtrate was concentrated under vacuum and analysed using GC-FID and GC-MS.

8.21 Reuse of aluminium-pillared montmorillonite for DET synthesis

Typically 1.35 g pre-adsorbed FDEE-catalyst mixture (i.e. 0.62 g of FDEE and 0.62 g of catalyst) was charged with a 60 bar pressurised ethene in a 50 mL HEL high pressure reactor equipped with a suspended magnetic stirrer set at 240 rpm. Synthesis and work-up were carried out as described for small scale above. After 24 hours, the reaction was rapidly cooled under running water and excess ethene carefully vented. The reactor was opened and the product removed with acetone wash. The resulting solution was sonicated for 20 minutes, filtered and the solvent removed *in vacuo* to give the product. The recovered catalyst was dried under air and recirculated for another reaction. The process was repeated two more times.

8.22 Measurement of titanium in aluminium-pillared montmorillonite

Aluminium pillared montmorillonite clay sample was digested in the Milestone ETHOS UP SK-15 microwave following the methodology to dissolve red clay described by milestone: 0.0744 g sample, 9 mL HCl and 3 mL HNO₃ were added in a microwave vial and heated under a preset programme (temperature programme was: 20 minutes ramped up to 220 °C and held for 15 minutes). Digested sample was diluted up to 100 mL with ultrapure water in a trace clean volumetric flask. The

sample introduction line was rinsed for 60 seconds between samples with 0.5% HNO₃ followed by 40 seconds of stabilisation.

8.23 Measurement of residual metal catalyst in surfactant

Ringed-opened ethyl oleate epoxide catalysed by Fe-mont (PEEO400_Fe-mont) was digested in the Milestone ETHOS UP SK-15 microwave following the methodology to dissolve polyester described by milestone: 0.058 g sample, 10 mL HNO₃ (trace SELECT, 69%) was added in a microwave vial and digested in the microwave and heated under a preset programme (temperature programme was: 40 minutes ramped up to 200 °C and held for 15 minutes). Digested sample was diluted up to 100 mL with ultrapure water in a trace clean volumetric flask. The sample introduction line was rinsed for 60 seconds between samples with 0.5% HNO₃ followed by 40 seconds of stabilisation.

8.24 Measurement of residual metal catalyst in oleate

2-octyl oleate was digested in the Milestone ETHOS UP SK-15 microwave following the methodology to dissolve stearic acid described by milestone: 0.161 g sample, 9 mL HNO₃ (trace SELECT, 69%) and 1 mL H₂O₂ (trace SELECT, ≥30%) were added in a microwave vial and digested in the microwave and heated under a preset programme (temperature programme was: 15 minutes ramped up to 200 °C and held for 15 minutes). Digested sample was diluted up to 100 mL with ultrapure water in a trace clean volumetric flask. The sample introduction line was rinsed for 60 seconds between samples with 0.5% HNO₃ followed by 40 seconds of stabilisation.

8.25 Measurement of residual metal catalyst in oleate epoxide

Methyl oleate epoxide was digested in the Milestone ETHOS UP SK-15 microwave following the methodology to dissolve soya oil described by milestone: 0.1376 g sample, 9 mL HNO₃ (trace SELECT, 69%) and 1 mL H₂O₂ (trace SELECT, ≥30%) were added in a microwave vial and digested in the microwave and heated under a preset

programme (temperature programme was: 15 minutes ramped up to 200 °C and held for 15 minutes). Digested sample was diluted up to 100 mL with ultrapure water in a trace clean volumetric flask. The sample introduction line was rinsed for 60 seconds between samples with 0.5% HNO₃ followed by 40 seconds of stabilisation.

Abbreviations

AE	Atom economy
Al-P-MC	Aluminium pillared montmorillonite clay
ATR	Attenuated total reflection
CDCl ₃	Deuterated chloroform
CHexO	Cyclohexene oxide
CHN	Carbon Hydrogen Nitrogen
CMC	Critical micelle concentration
COSY	Correlation spectroscopy
CPP	Critical packing parameter
d	doublet
DA	Diels-Alder
dd	double doublet
DEPT	Distortionless enhancement through polarisation transfer
DET	Diethyl terephthalate
DMF	2, 5-dimethyl furan
DMSO _{d6}	Deuterated dimethyl sulfoxide
DSC	Differential scanning calorimetry
E2BO	Epoxidised 2-butyl oleate
E2OO	Epoxidised 2-octyl oleate
E2PO	Epoxidised 2-propyl oleate
EBO	Epoxidised 1-butyl oleate

ECL	Effective chain length
EDG	Electron donating group
EDO	Epoxidised 1-decyl oleate
EEO	Epoxidised ethyl oleate
EG	Ethylene glycol
ELO	Epoxidised linseed oil
ELSL	Epoxidised lactonic sophorolipid
EMO	Epoxidised methyl oleate
EOO	Epoxidised 1-octyl oleate
EPO	Epoxidised 1-propyl oleate
ESI-MS	Electrospray ionisation mass spectrometry
EWG	Electron withdrawing group
FAAE	Fatty acid alkyl ester
FAME	Fatty acid methyl ester
FDCA	2, 5 furandicarboxylic acid
FDEE	2, 5 furandicarboxylic acid diester
FDME	2,5 furan dicarboxylic dimethyl ester
FID	Free induction decay
FMO	Frontier molecular orbital
FT-IR	Fourier transform-Infrared
GC-EI-MS	Gas chromatography electron ionisation mass spectrometry
GC-FID	Gas chromatography-flame ionisation detector

GC-FI-MS	Gas chromatography fast ionisation mass spectrometry
GC-MS	Gas chromatography-mass spectrometry
HMBC	Heteronuclear multiple bond correlation
HMF	5-hydroxymethyl furfural
HOMO	Highest occupied molecular orbital
HSQC	Heteronuclear single quantum correlation
ICP-MS	Inductively coupled plasma mass spectrometry
LSL	Lactonic sophorolipid
LUMO	Lowest unoccupied molecular orbital
m	multiplet
MeEG	2-methoxyethanol
MePEG	Monomethyl poly(ethylene glycol)
MPE2BO	monomethyl-PEGylated epoxidised 2-butyl oleate
MPE2OO	monomethyl-PEGylated epoxidised 2-octyl oleate
MPE2PO	monomethyl-PEGylated epoxidised 2-propyl oleate
MPEBO	monomethyl-PEGylated epoxidised 1-butyl oleate
MPEDO	monomethyl-PEGylated epoxidised 1-decyl oleate
MPEEO	monomethyl-PEGylated epoxidised ethyl oleate
MPELO	monomethyl-PEGylated epoxidised linseed oil
MPEMO	monomethyl-PEGylated epoxidised methyl oleate
MPEOO	monomethyl-PEGylated epoxidised 1-octyl oleate
MPEPO	monomethyl-PEGylated epoxidised 1-propyl oleate

NMR	Nuclear magnetic resonance
OE	Optimum efficiency
PE2BO	PEGylated epoxidised 2-butyl oleate
PE2OO	PEGylated epoxidised 2-octyl oleate
PE2PO	PEGylated epoxidised 2-propyl oleate
PEBO	PEGylated epoxidised 1-butyl oleate
PEDO	PEGylated epoxidised 1-decyl oleate
PEEO	PEGylated epoxidised ethyl oleate
PEG	Poly(ethylene glycol)
PELO	PEGylated epoxidised linseed oil
PEMO	PEGylated epoxidised methyl oleate
PEOO	PEGylated epoxidised 1-octyl oleate
PEPO	PEGylated epoxidised 1-propyl oleate
PET	Poly(ethylene terephthalate)
PMI	Process mass intensity
POM	Polyoxometalate
PTA	Phosphotungstic acid
PTC	Phase transfer catalyst
QNS	Quaternary nitrogen surfactants
quint	quintet
RME	Reaction mass efficiency
RP	Renewable percentage

s	singlet
SBA-15	Santa Barbara Amorphous-15
SFC	Super-critical fluid chromatography
sxt	sextet
t	triplet
T1	Titanium (IV) oxide
TA	Terephthalic acid
TCP	Triblock copolymer
TEG	Triethylene glycol
TFA	Trifluoromethane sulfonate
TGA	Thermogravimetry analysis
TOSCY	Total correlation spectroscopy
TS1	Titanium silicate
UAE	Ultrasound-Assisted Epoxidation

References

1. J. H. Clark, *Green Chemistry*, 2006, **8**, 17-21.
2. http://ec.europa.eu/environment/chemicals/reach/reach_en.htm, (accessed 08/04, 2016).
3. <https://www.chem21.eu/>, (accessed 09/04/2016, 2016).
4. M. Deleu and M. Paquot, *Comptes Rendus Chimie*, 2004, **7**, 641-646.
5. C. J. Campbell, *Oil & Gas Journal*, 2003, **101**, 38-45.
6. P. Foley, E. S. Beach and J. B. Zimmerman, *Chemical Society Reviews*, 2012, **41**, 1499-1518.
7. R. W. Bentley, *Energy policy*, 2002, **30**, 189-205.
8. K. Holmberg, D. O. Shah and M. J. Schwuger, *Handbook of applied surface and colloid chemistry*, Wiley New York, 2002.
9. A. Lavergne, Y. Zhu, A. Pizzino, V. Molinier and J.-M. Aubry, *Journal of Colloid and Interface Science*, 2011, **360**, 645-653.
10. S. Pilla, *Handbook of bioplastics and biocomposites engineering applications*, John Wiley & Sons, 2011.
11. R. Boethling, E. Sommer and D. DiFiore, *Chemical reviews*, 2007, **107**, 2207-2227.
12. I. Johansson and M. Svensson, *Current Opinion in Colloid & Interface Science*, 2001, **6**, 178-188.
13. A. Corma, S. Iborra and A. Velty, *Chemical reviews*, 2007, **107**, 2411-2502.
14. X. Domingo, ed. E. G. Lomax, Marcel Dekker, New York, Second edn., 1996, vol. 59.
15. T.-S. Kim, T. Tatsumi, T. Kida, Y. Nakatsuji and I. Ikeda, *Nihon yukagaku kaishi*, 1997, **46**, 747-753.
16. M. Braithwaite, in *Chemistry of Waste Minimization*, Springer, 1995, pp. 17-65.
17. P. T. Anastas, L. G. Heine and T. C. Williamson, *Green engineering*, American Chemical Society, 2000.

18. P. T. Anastas and J. C. Warner, *Green chemistry: theory and practice*, Oxford university press, 2000.
19. M. Lancaster, in *Handbook of green chemistry and technology*, eds. J. Clark and D. Macquarrie, Blackwell Publishing, London, UK, 2002, ch. 10-27, p. 562.
20. M. Lancaster, *Green chemistry: An Introductory Text*, Royal Society of Chemistry, Cambridge, UK, 2002.
21. J. A. Moulijn, M. Makkee and A. E. Van Diepen, *Chemical process technology*, John Wiley & Sons, New York, USA, 2013.
22. F. Rodriguez-Reinoso, *Carbon*, 1998, **36**, 159-175.
23. I. Chorkendorff and J. W. Niemantsverdriet, *Concepts of modern catalysis and kinetics*, John Wiley & Sons, 2006.
24. K. Martin, in *Handbook of Green Chemistry and Technology*, eds. J. H. Clark and D. J. Macquarrie, Blackwell Science Ltd, Great Britain, 2002, ch. 13, p. 540.
25. X. Zhang, J. Liu, Y. Jing and Y. Xie, *Applied Catalysis A: General*, 2003, **240**, 143-150.
26. S. He, C. Sun, Z. Bai, X. Dai and B. Wang, *Applied Catalysis A: General*, 2009, **356**, 88-98.
27. M. Saito, H. Kimura, N. Mimura, J. Wu and K. Murata, *Applied Catalysis A: General*, 2003, **239**, 71-77.
28. H. Dai, A. T. Bell and E. Iglesia, *Journal of Catalysis*, 2004, **221**, 491-499.
29. M. D. Argyle, K. Chen, A. T. Bell and E. Iglesia, *Journal of Catalysis*, 2002, **208**, 139-149.
30. A. Ayame, Y. Uchida, H. Ono, M. Miyamoto, T. Sato and H. Hayasaka, *Applied Catalysis A: General*, 2003, **244**, 59-70.
31. D. Yin, L. Qin, J. Liu, C. Li and Y. Jin, *Journal of Molecular Catalysis A: Chemical*, 2005, **240**, 40-48.
32. G. B. Hoflund and D. M. Minahan, *Journal of Catalysis*, 1996, **162**, 48-53.
33. D. M. Minahan, G. B. Hoflund, W. S. Epling and D. W. Schoenfeld, *Journal of catalysis*, 1997, **168**, 393-399.

34. D. M. Minahan and G. B. Hoflund, *Journal of Catalysis*, 1996, **158**, 109-115.
35. F. Haga, T. Nakajima, K. Yamashita and S. Mishima, *React Kinet Catal Lett*, 1998, **63**, 253-259.
36. S. Adhikari, S. Fernando and A. Haryanto, *Catalysis Today*, 2007, **129**, 355-364.
37. A. Iriondo, V. Barrio, J. Cambra, P. Arias, M. Guemez, M. Sanchez-Sanchez, R. Navarro and J. Fierro, *international journal of hydrogen energy*, 2010, **35**, 11622-11633.
38. M. Sánchez-Sánchez, R. Navarro and J. Fierro, *International Journal of Hydrogen Energy*, 2007, **32**, 1462-1471.
39. M. Verziu, M. Florea, S. Simon, V. Simon, P. Filip, V. I. Parvulescu and C. Hardacre, *Journal of catalysis*, 2009, **263**, 56-66.
40. N. Boz, N. Degirmenbasi and D. M. Kalyon, *Applied Catalysis B: Environmental*, 2009, **89**, 590-596.
41. E. Leclercq, A. Finiels and C. Moreau, *Journal of the American Oil Chemists' Society*, 2001, **78**, 1161-1165.
42. G. Arzamendi, I. Campo, E. Arguinarena, M. Sánchez, M. Montes and L. Gandia, *Chemical Engineering Journal*, 2007, **134**, 123-130.
43. E. S. Umdu, M. Tuncer and E. Seker, *Bioresource Technology*, 2009, **100**, 2828-2831.
44. W. Xie, H. Peng and L. Chen, *Applied Catalysis A: General*, 2006, **300**, 67-74.
45. T. Farmer, R. Castle, J. Clark and D. Macquarrie, *International Journal of Molecular Sciences*, 2015, **16**, 14912.
46. T. J. Farmer, J. H. Clark, D. J. Macquarrie, J. K. Ogunjobi and R. L. Castle, *Polymer Chemistry*, 2016, **7**, 1650-1658.
47. D. E. Keller, T. Visser, F. Soulimani, D. C. Koningsberger and B. M. Weckhuysen, *Vibrational spectroscopy*, 2007, **43**, 140-151.
48. A. J. Sandee, J. N. Reek, P. C. Kamer and P. W. van Leeuwen, *Journal of the American Chemical Society*, 2001, **123**, 8468-8476.

49. S. G. Shore, E. Ding, C. Park and M. A. Keane, *Catalysis Communications*, 2002, **3**, 77-84.
50. Y. Chen, J. Qiu, X. Wang and J. Xiu, *Journal of Catalysis*, 2006, **242**, 227-230.
51. B. M. Weckhuysen and R. A. Schoonheydt, *Catalysis Today*, 1999, **51**, 215-221.
52. G. Fink, B. Steinmetz, J. Zechlin, C. Przybyla and B. Tesche, *Chemical reviews*, 2000, **100**, 1377-1390.
53. T. Fey, H. Fischer, S. Bachmann, K. Albert and C. Bolm, *The Journal of organic chemistry*, 2001, **66**, 8154-8159.
54. T. Xue, S. Jiang, Y. Qu, Q. Su, R. Cheng, S. Dubin, C. Y. Chiu, R. Kaner, Y. Huang and X. Duan, *Angewandte Chemie International Edition*, 2012, **51**, 3822-3825.
55. H. Zhu, C. Liang, W. Yan, S. H. Overbury and S. Dai, *The Journal of Physical Chemistry B*, 2006, **110**, 10842-10848.
56. S. Ikeda, S. Ishino, T. Harada, N. Okamoto, T. Sakata, H. Mori, S. Kuwabata, T. Torimoto and M. Matsumura, *Angewandte Chemie*, 2006, **118**, 7221-7224.
57. M. L. Toebes, Y. Zhang, J. Hájek, T. A. Nijhuis, J. H. Bitter, A. J. Van Dillen, D. Y. Murzin, D. C. Koningsberger and K. P. de Jong, *Journal of catalysis*, 2004, **226**, 215-225.
58. J. Planeix, N. Coustel, B. Coq, V. Brotons, P. Kumbhar, R. Dutartre, P. Geneste, P. Bernier and P. Ajayan, *Journal of the American Chemical Society*, 1994, **116**, 7935-7936.
59. V. Lordi, N. Yao and J. Wei, *Chemistry of Materials*, 2001, **13**, 733-737.
60. J. Clark, *Chemical Communications*, 1998, 2135-2136.
61. K. Ding and Y. Uozumi, *Handbook of asymmetric heterogeneous catalysis*, Wiley Online Library, 2008.
62. D. Zhao, J. Feng, Q. Huo, N. Melosh, G. H. Fredrickson, B. F. Chmelka and G. D. Stucky, *science*, 1998, **279**, 548-552.
63. X. Zhao, G. Lu, A. Whittaker, G. Millar and H. Zhu, *The Journal of Physical Chemistry B*, 1997, **101**, 6525-6531.

64. J. M. Thomas, B. F. Johnson, R. Raja, G. Sankar and P. A. Midgley, *Accounts of chemical research*, 2003, **36**, 20-30.
65. X. Zhao, M. G. Lu and C. Song, *Journal of Molecular Catalysis A: Chemical*, 2003, **191**, 67-74.
66. Y. Hu, S. Tang, L. Jiang, B. Zou, J. Yang and H. Huang, *Process Biochemistry*, 2012, **47**, 2291-2299.
67. S. B. Hartono, S. Z. Qiao, J. Liu, K. Jack, B. P. Ladewig, Z. Hao and G. Q. M. Lu, *The Journal of Physical Chemistry C*, 2010, **114**, 8353-8362.
68. J. H. Clark and D. J. Macquarrie, *Handbook of green chemistry and technology*, John Wiley & Sons, 2008.
69. A. D. Curzons, D. J. C. Constable, D. N. Mortimer and V. L. Cunningham, *Green Chemistry*, 2001, **3**, 1-6.
70. C. R. McElroy, A. Constantinou, L. C. Jones, L. Summerton and J. H. Clark, *Green Chemistry*, 2015, **17**, 3111-3121.
71. R. A. Sheldon, *Fine chemicals*, 1996, **102**, 104.
72. R. A. Sheldon, *Pure and applied chemistry*, 2000, **72**, 1233-1246.
73. R. A. Sheldon, in *Industrial Environmental Chemistry*, eds. D. T. Sawyer and A. E. Martell, Plenum, New York, 1992.
74. B. M. Trost, *Science*, 1991, **254**, 1471-1477.
75. B. M. Trost, *Angewandte Chemie International Edition in English*, 1995, **34**, 259-281.
76. R. A. Sheldon, *Green Chemistry*, 2007, **9**, 1273-1283.
77. R. Sheldon, in *Methods and reagents for green chemistry*, eds. P. Tundo, A. Perosa and F. Zecchini, Wiley Hoboken, NJ, 2007, ch. 9, pp. 190-199.
78. D. Kramer, *Physics today*, 2010, **63**, 22.
79. Report on critical raw materials for the EU, http://mima.geus.dk/report-on-critical-raw-materials_en.pdf, (accessed April 13th, 2016).
80. A. J. Hunt, T. J. Farmer and J. H. Clark, in *Element Recovery and Sustainability*, ed. A. J. Hunt, RSC, Cambridge, UK 2013, ch. 1, p. 1.
81. T. J. Mason, *Chemical Society Reviews*, 1997, **26**, 443-451.

82. C. R. Hickenboth, J. S. Moore, S. R. White, N. R. Sottos, J. Baudry and S. R. Wilson, *Nature*, 2007, **446**, 423-427.
83. F. Chemat, M. Lucchesi, J. Smadja, L. Favretto, G. Colnaghi and F. Visinoni, *Analytica Chimica Acta*, 2006, **555**, 157-160.
84. T. M. Attard, B. Watterson, V. L. Budarin, J. H. Clark and A. J. Hunt, *New Journal of Chemistry*, 2014, **38**, 2278-2283.
85. W. Routray and V. Orsat, *Food and Bioprocess Technology*, 2012, **5**, 409-424.
86. T. J. Farmer and M. Mascal, in *Introduction to Chemicals from Biomass*, eds. J. Clark and F. Deswarte, Wiley, Singapore, Second edn., 2015, pp. 89-155.
87. T. Werpy and G. Petersen, *Top Value Added Chemicals from Biomass: Volume I - Results of Screening for Potential Candidates from Sugars and Synthesis Gas*, Report DOE/GO-102004-1992 United States, 2004.
88. H. Choudhary, S. Nishimura and K. Ebitani, *Applied Catalysis A: General*, 2013, **458**, 55-62.
89. Italy claims world's first facility to produce bio-plastic from glycerol., <http://www.biobasedworldnews.com/italy-claims-worlds-first-facility-to-produce-bio-plastic-from-glycerol>, (accessed April 15th, 2016).
90. X. Fan, R. Burton and Y. Zhou, *The Open Fuels & Energy Science Journal*, 2010, **3**.
91. W. De Jong and G. Marcotullio, *International journal of chemical reactor engineering*, 2010, **8**.
92. N. Jacquél, R. Saint-Loup, J.-P. Pascault, A. Rousseau and F. Fenouillot, *Polymer*, 2015, **59**, 234-242.
93. C. Vilela, A. F. Sousa, A. C. Fonseca, A. C. Serra, J. F. J. Coelho, C. S. R. Freire and A. J. D. Silvestre, *Polymer Chemistry*, 2014, **5**, 3119-3141.
94. E. Gubbels, L. Jasinska-Walc and C. Koning, *Journal of Polymer Science Part A: Polymer Chemistry*, 2013, **51**, 890-898.
95. R. J. Knoop, W. Vogelzang, J. Haveren and D. S. Es, *Journal of Polymer Science Part A: Polymer Chemistry*, 2013, **51**, 4191-4199.

96. S. Thiyagarajan, W. Vogelzang, R. J. Knoop, A. E. Frissen, J. van Haveren and D. S. van Es, *Green Chemistry*, 2014, **16**, 1957-1966.
97. ALPLA joins The Coca-Cola Company and Danone in Avantium's PEF bottle development <http://avantium.com/news/ALPLA-joins-The-Coca-Cola-Company-and-Danone-in-Avantium-s-PEF-bottle-development.html>, (accessed 19-05-2014, 2014).
98. Avantium and Mitsui aim to deliver PEF bottles for 2020 Olympics, <http://www.biobasedworldnews.com/avantium-and-mitsui-aim-to-deliver-pef-bottles-for-2020-olympics>, (accessed April 15th, 2016).
99. P. Harrison, C. Malins, S. Searle, A. Baral, D. Turley and L. Hopwood, *Wasted: Europe's untapped resource*, International Council on Clean Transportation, 2014.
100. H. Kobayashi, T. Komanoya, S. K. Guha, K. Hara and A. Fukuoka, *Applied Catalysis A: General*, 2011, **409**, 13-20.
101. D. B. Wilson, *Current opinion in microbiology*, 2011, **14**, 259-263.
102. J. Ogunjobi and L. Lajide, *International Journal of Green Energy*, **12**, 440-445.
103. J. K. Ogunjobi and L. Lajide, *Journal of Sustainable Energy & Environment*, 2013, **4**, 77-84.
104. S. Dutta and S. Pal, *biomass and bioenergy*, 2014, **62**, 182-197.
105. J. K. Ogunjobi, L. Lajide and B. J. Owolabi, *Int. J. Environment and Waste Management*, 2016, **17**, 91-102.
106. E. Ricca, V. Calabrò, S. Curcio and G. Iorio, *Process biochemistry*, 2009, **44**, 466-470.
107. S. Breeden, J. Clark, T. Farmer, D. Macquarrie, J. Meimoun, Y. Nonne and J. Reid, *Green Chemistry*, 2013, **15**, 72-75.
108. K. Anastasakis, A. Ross and J. Jones, *Fuel*, 2011, **90**, 598-607.
109. H. A. Ruiz, R. M. Rodríguez-Jasso, B. D. Fernandes, A. A. Vicente and J. A. Teixeira, *Renewable and Sustainable Energy Reviews*, 2013, **21**, 35-51.
110. F. J. Ruiz-Dueñas and Á. T. Martínez, *Microbial Biotechnology*, 2009, **2**, 164-177.

111. J.-M. Lavoie, W. Baré and M. Bilodeau, *Bioresource technology*, 2011, **102**, 4917-4920.
112. P. Azadi, O. R. Inderwildi, R. Farnood and D. A. King, *Renewable and Sustainable Energy Reviews*, 2013, **21**, 506-523.
113. S. Kang, X. Li, J. Fan and J. Chang, *Renewable and Sustainable Energy Reviews*, 2013, **27**, 546-558.
114. X. Zhang, M. Tu and M. G. Paice, *Bioenerg. Res.*, 2011, **4**, 246-257.
115. E. de Jong, *IEA Bioenergy, Task42 Biorefinery*, 2012.
116. J. H. Schut, The Race to 100% Bio PET, <http://plasticsengineeringblog.com/2012/08/13/the-race-to-100-bio-pet/>, (accessed 13-08-2013, 2014).
117. D. Komula, *Bioplastics MAGAZINE*, 2011, **6**, 14-17.
118. J. Holladay, J. Bozell, J. White and D. Johnson, *Volume II-Results of Screening for Potential Candidates from Biorefinery Lignin, Report prepared by members of NREL, PNNL and University of Tennessee*, 2007.
119. J. A. Brydson, *Plastics materials*, Butterworth-Heinemann, 1999.
120. M. Shiramizu and F. D. Toste, *Chemistry-A European Journal*, 2011, **17**, 12452-12457.
121. C. L. Williams, C.-C. Chang, P. Do, N. Nikbin, S. Caratzoulas, D. G. Vlachos, R. F. Lobo, W. Fan and P. J. Dauenhauer, *ACS Catalysis*, 2012, **2**, 935-939.
122. D. Wang, C. M. Osmundsen, E. Taarning and J. A. Dumesic, *ChemCatChem*, 2013, **5**, 2044-2050.
123. P. T. M. Do, J. R. McAtee, D. A. Watson and R. F. Lobo, *ACS catalysis*, 2012, **3**, 41-46.
124. T. A. Brandvold, *US Patent*, 2010, **331568**, A1.
125. J. J. Pacheco, J. A. Labinger, A. L. Sessions and M. E. Davis, *ACS Catalysis*, 2015, **5**, 5904-5913.
126. J. J. Pacheco and M. E. Davis, *Proceedings of the National Academy of Sciences of the United States of America*, 2014, **111**, 8363-8367.

127. T. W. Lyons, D. Guironnet, M. Findlater and M. Brookhart, *Journal of the American Chemical Society*, 2012, **134**, 15708-15711.
128. M. W. Peters, J. D. Taylor, M. Jenni, L. E. Manzer and D. E. Henton, 2011, **US20110087000 A1**.
129. Coca-Cola Debuts First 100% Biobased PET Bottle, [http://www.ptonline.com/articles/coca-cola-debuts-first-100-biobased-pet-bottle\(2\)](http://www.ptonline.com/articles/coca-cola-debuts-first-100-biobased-pet-bottle(2)), (accessed 24-09-2015, 2015).
130. Coca-Cola Introduced World's First 100% Biobased PET Bottle, <http://www.ptonline.com/articles/coca-cola-joins-race-for-100-biobased-pet-bottle>, (accessed 12th October, 2015).
131. R. A. Sheldon, *Green Chemistry*, 2014, **16**, 950-963.
132. C. Berti, E. Binassi, M. Colonna, M. Fiorini, G. Kannan, S. Karanam, M. Mazzacurati, I. Odeh and M. Vanninl, *US Patent*, 2008, **US 2010/0168373 A1**, 1-15.
133. Y. Tachibana, S. Kimura and K.-i. Kasuya, *Scientific Reports*, 2015, **5**, 8249.
134. L. Wambach, M. Irgang and M. Fischer, *US Patent*, 1988, **US4780552 A**.
135. F. M. Kerton and R. Marriott, *Alternative solvents for green chemistry*, Royal Society of chemistry, 2013.
136. T. Hargreaves, *Chemical Formulation- An overview of surfactant-based preparations used in everyday life*, RSC Paperbacks, 2003.
137. T. Dwars, E. Paetzold and G. Oehme, *Angewandte Chemie International Edition*, 2005, **44**, 7174-7199.
138. E. Soussan, S. Cassel, M. Blanzat and I. Rico-Lattes, *Angewandte Chemie International Edition*, 2009, **48**, 274-288.
139. H. Hosseinzadeh, F. Atyabi, R. Dinarvand and S. N. Ostad, *International Journal of Nanomedicine*, 2012, **7**, 1851-1863.
140. M. I. Levinson, *Handbook of detergents*, Taylor & Francis Group, Boca Raton, 2009.

141. *Surfactants Market by Product type [Anionic, Non-Ionic, Cationic, Amphoteric] Substrates [Synthetic/Petrochemical based and Natural/Bio-based/Green] and Applications - Global Trends & Forecast to 2019*, 2014.
142. B. Kronberg, K. Holmberg and B. Lindman, *Surface chemistry of surfactants and polymers*, John Wiley & Sons, 2014.
143. M. J. Rosen and J. T. Kunjappu, *Surfactants and interfacial phenomena*, John Wiley & Sons, 2012.
144. K. L. Mittal, ed., *Micellization, Solubilization and Microemulsions*, Plenum Press, New York, 1977.
145. T. J. Farmer and M. Mascall, in *Introduction to chemicals from biomass*, eds. J. H. Clark and F. Deswarte, John Wiley & Sons, Singapore, First edn., 2015, ch. 4, pp. 89-155.
146. *OECD-FAO Agricultural Outlook 2011-2020*, OECD-FAO, 2011.
147. Vegetable oils: global consumption by oil type 1995-2014, <http://www.statista.com/statistics/263937/vegetable-oils-global-consumption/>, (accessed September 2, 2014).
148. K. Hill, *Pure and applied chemistry*, 2000, **72**, 1255-1264.
149. J. M. Dyer, S. Stymne, A. G. Green and A. S. Carlsson, *The Plant Journal*, 2008, **54**, 640-655.
150. F. D. Gunstone, *The chemistry of oils and fats: Sources, Composition, Properties and Uses*, Blackwell and CRC Press, Oxford, UK, 2004.
151. F. D. Gunstone, Alander, J., Erhan, S.Z., Sharma, B.K., McKeon, T.A. and Lin, J.-T., in *The Lipid Handbook*, ed. F. D. Gunstone, Harwood, J.L. and Dijkstra, A.J., Taylor & Francis Group, Boca Raton, FL: , 3rd edn., 2006, p. 59.
152. U. Biermann, W. Friedt, S. Lang, W. Lühs, G. Machmüller, J. O. Metzger, M. Ruesch gen Klaas, H. J. Schaefer and M. P. Schneider, *Angewandte Chemie International Edition*, 2000, **39**, 2206-2224.
153. J. W. Veldsink, M. J. Bouma, N. H. Schön and A. A. Beenackers, *Catalysis Reviews*, 1997, **39**, 253-318.

154. U. R. Kreutzer, *Journal of the American Oil Chemists' Society*, 1984, **61**, 343-348.
155. K. Hill, in *Surfactants from renewable resources*, eds. M. Kjellin and I. Johansson, Wiley & Sons Ltd., Chichester, UK, 2010.
156. Z.-C. Zhou, X.-Q. Yang, Q.-L. Yang, Y.-J. Zhang and Y.-M. Cheng, *Tenside Surfactants Detergents*, 2008, **45**, 330-333.
157. H. Luders, in *Nonionic surfactants: alkyl polyglucosides*, eds. D. Balzer and H. Luders, Marcel Dekker, New York, 2000, vol. 91.
158. S. Nandi, H.-J. Altenbach, B. Jakob, K. Lange, R. Ihizane and M. P. Schneider, *Organic letters*, 2011, **13**, 1980-1983.
159. H. G. Bazin and R. J. Linhardt, *Synthesis*, 1999, 621-624.
160. J. Aburto, I. Alric, S. Thiebaud, E. Borredon, D. Bikiaris, J. Prinós and C. Panayiotou, *Journal of Applied Polymer Science*, 1999, **74**, 1440-1451.
161. I. J. Baker, B. Matthews, H. Soares, I. Krodkiewska, D. N. Furlong, F. Grieser and C. I. Drummond, *J Surfact Deterg*, 2000, **3**, 1-11.
162. K. Holmberg, in *Interfaces, Surfactants and Colloids in Engineering*, Springer, 1996, pp. 69-74.
163. J. Clayden, N. Greeves and S. Warren, *Organic chemistry*, Oxford University Press Inc., New York, USA, Second edition edn., 2012.
164. *USA Pat.*, 4,601,856, 1986.
165. S. S. Lin, Y. Murase, D. B. S. Min, O. A. L. Hsieh and S. S. Chang, *Journal of the American Oil Chemists' Society*, 1982, **59**, 42-46.
166. S. S. Lin, Y. Murase, D. B. S. Min, O. A. L. Hsieh and S. S. Chang, *Journal of the American Oil Chemists' Society*, 1982, **59**, 50-51.
167. Y. Murase, S. S. Lin, D. B. S. Min, O. A. L. Hsieh and S. S. Chang, *Journal of the American Oil Chemists' Society*, 1982, **59**, 47-50.
168. *USA Pat.*, US 6,498,261 B1, 2002.
169. G. Diechelmann and H. J. Heinz, *The basics of industrial oleochemistry*, Peter Pomp GmbH.

170. R. L. Arudi, M. W. Sutherland and B. H. Bielski, *Journal of Lipid Research*, 1983, **24**, 485-488.
171. R. G. Sinclair, A. F. McKay, G. S. Myers and R. N. Jones, *Journal of the American Chemical Society*, 1952, **74**, 2578-2585.
172. M. a. D. Guillén and A. Ruiz, *Trends in Food Science & Technology*, 2001, **12**, 328-338.
173. A. Spyros and P. Dais, *NMR spectroscopy in food analysis*, RSC publishing, Cambridge, UK, 2013.
174. G. Nawaratna, S. D. Fernando and S. Adhikari, *Energy & Fuels*, 2010, **24**, 4123-4129.
175. D. P. Birnie Iii, *J Mater Sci*, 2000, **35**, 367-374.
176. M. I. i. Siling and T. N. Laricheva, *Russian chemical reviews*, 1996, **65**, 279-286.
177. G. Shapiro and M. Marzi, *The Journal of organic chemistry*, 1997, **62**, 7096-7097.
178. N. Boz and M. Kara, *Chemical Engineering Communications*, 2008, **196**, 80-92.
179. X. Bo, X. Guomin, C. Lingfeng, W. Ruiping and G. Lijing, *Energy & Fuels*, 2007, **21**, 3109-3112.
180. S. Gryglewicz, *Bioresource Technology*, 1999, **70**, 249-253.
181. M. Di Serio, M. Ledda, M. Cozzolino, G. Minutillo, R. Tesser and E. Santacesaria, *Industrial & engineering chemistry research*, 2006, **45**, 3009-3014.
182. J. H. Clark, T. J. Farmer and D. J. Macquarrie, *ChemSusChem*, 2009, **2**, 1025-1027.
183. H. Kabashima, H. Tsuji, T. Shibuya and H. Hattori, *Journal of Molecular Catalysis A: Chemical*, 2000, **155**, 23-29.
184. V. K. Yadav and K. K. Kapoor, *Tetrahedron*, 1996, **52**, 3659-3668.
185. J. M. Fraile, J. García, J. Mayoral and F. Figueras, *Tetrahedron letters*, 1996, **37**, 5995-5996.
186. Y. Nakano, W.-Y. Shi, Y. Nishii and M. Igarashi, *Journal of Heterocyclic Chemistry*, 1999, **36**, 33-40.

187. J. Yamawaki, T. Ando and T. Hanafusa, *Chemistry Letters*, 1981, **10**, 1143-1146.
188. G. W. Kabalka, R. M. Pagni and C. M. Hair, *Organic Letters*, 1999, **1**, 1423-1425.
189. B. E. Blass, *Tetrahedron*, 2002, **58**, 9301-9320.
190. H.-J. Kim, B.-S. Kang, M.-J. Kim, Y. M. Park, D.-K. Kim, J.-S. Lee and K.-Y. Lee, *Catalysis today*, 2004, **93**, 315-320.
191. B. C. Smith, *Infrared spectral interpretation: a systematic approach*, CRC press, 1998.
192. R. M. Silverstein, F. X. Webster, D. Kiemle and D. L. Bryce, *Spectrometric identification of organic compounds*, John Wiley & Sons, 2014.
193. H. W. Thompson and P. Torkington, *Journal of the Chemical Society (Resumed)*, 1945, 640-645.
194. B. Stuart, *Infrared spectroscopy: fundamentals and applications*, Wiley Publishers, UK, 2004.
195. R. A. Nyquist, *Interpreting Infrared, Raman, and Nuclear Magnetic Resonance spectra*, Academic Press, USA, 2001.
196. D. Swern, H. B. Knight, J. T. Scanlan and W. C. Ault, *Journal of the American Chemical Society*, 1945, **67**, 1132-1135.
197. E. Selke, W. K. Rohwedder and H. J. Dutton, *Journal of the American Oil Chemists' Society*, 1977, **54**, 62-67.
198. H. B. Knight, C. R. Eddy and D. Swern, *The Journal of the American Oil Chemists' Society*, 1951, **28**, 188-192.
199. N. Jacquel, F. Freyermouth, F. Fenouillot, A. Rousseau, J. P. Pascault, P. Fuertes and R. Saint-Loup, *Journal of Polymer Science Part A: Polymer Chemistry*, 2011, **49**, 5301-5312.
200. T. A. Foglia, L. A. Nelson, R. O. Dunn and W. N. Marmer, *Journal of the American Oil Chemists' Society*, 1997, **74**, 951-955.
201. A. Röttig, L. Wenning, D. Bröker and A. Steinbüchel, *Appl Microbiol Biotechnol*, 2010, **85**, 1713-1733.
202. J. H. Clark, D. G. Cork and M. S. Robertson, *Chemistry Letters*, 1983, 1145-1148.

203. J. Yamawaki and T. Ando, *Chemistry Letters*, 1979, **8**, 755-758.
204. W. Xie and X. Huang, *Catal Lett*, 2006, **107**, 53-59.
205. W. Xie and H. Li, *Journal of Molecular Catalysis A: Chemical*, 2006, **255**, 1-9.
206. J. H. Clark and D. J. Macquarrie, *Chemical Society Reviews*, 1996, **25**, 303-310.
207. J.-M. Clacens, D. Genuit, L. Delmotte, A. Garcia-Ruiz, G. Bergeret, R. Montiel, J. Lopez and F. Figueras, *Journal of Catalysis*, 2004, **221**, 483-490.
208. V. Díez, C. Ferretti, P. Torresi, C. Apesteguía and J. Di Cosimo, *Catalysis Today*, 2011, **173**, 21-27.
209. A. Corma, S. Iborra, S. Miquel and J. Primo, *Journal of catalysis*, 1998, **173**, 315-321.
210. M. Bartok and K. L. Lang, ed. A. Hassner, Wiley, New York, USA, 1985, vol. 42, p. 1.
211. M. Bartok and K. L. Lang, ed. S. Patai, Wiley, Chichester, 1980, vol. 2, p. 609.
212. R. Mungroo, V. V. Goud, S. N. Naik and A. K. Dalai, *European Journal of Lipid Science and Technology*, 2011, **113**, 768-774.
213. W. R. Schmitz and J. G. Wallace, *Journal of the American Oil Chemists' Society*, 1954, **31**, 363-365.
214. T. W. Findley, D. Swern and J. T. Scanlan, *Journal of the American Chemical Society*, 1945, **67**, 412-414.
215. E. Milchert, A. Smagowicz and G. Lewandowski, *Organic Process Research & Development*, 2010, **14**, 1094-1101.
216. K. Kamata, K. Yonehara, Y. Sumida, K. Yamaguchi, S. Hikichi and N. Mizuno, *Science*, 2003, **300**, 964-966.
217. A. Campanella, C. Fontanini and M. A. Baltanás, *Chemical Engineering Journal*, 2008, **144**, 466-475.
218. P. S. Deshpande, PhD, North Maharashtra University, Jalgaon 425001, India, 2013.

219. N. Mizuno, K. Kamata, S. Uchida and K. Yamaguchi, in *Modern heterogeneous oxidation catalysis*, ed. N. Mizuno, Wiley-VCH Verlag GmbH & Co., Weinheim, Germany, 2009, ch. 6, pp. 185-216.
220. M. Borsanyiova, A. Patil, R. Mukherji, A. Prabhune and S. Bopegamage, *Folia Microbiologica*, 2016, **61**, 85-89.
221. A. d. J. Cortés-Sánchez, H. Hernández-Sánchez and M. E. Jaramillo-Flores, *Microbiological Research*, 2013, **168**, 22-32.
222. T. Laue and A. Plagens, *Named organic reactions*, John Wiley & Sons Ltd, Chichester, England, Second edn., 2005.
223. G. Berti, *Topics in Stereochemistry*, 1973, **7**, 93-251.
224. V. G. Dryuk, *Russian Chemical Reviews*, 1985, **54**, 986.
225. T. Okuhara, N. Mizuno and M. Misono, *Catalytic chemistry of heteropoly compounds*, 1996.
226. C. L. Hill and C. M. Prosser-McCarthy, *Coordination Chemistry Reviews*, 1995, **143**, 407-455.
227. C. L. Hill, *Journal of Molecular Catalysis A: Chemical*, 2007, **262**, 2-6.
228. N. Mizuno and M. Misono, *Chemical Reviews*, 1998, **98**, 199-218.
229. I. V. Kozhevnikov, *Chemical Reviews*, 1998, **98**, 171-198.
230. Y. Izumi, K. Urabe and M. Onaka, *Zeolite, clay, and heteropoly acid in organic reactions*, VCH, 1992.
231. R. Neumann, in *Modern Oxidation Methods*, ed. J.-E. Bäckvall, Wiley-VCH Verlag & Co., Weinheim, Germany, 2010, ch. 9, pp. 315-352.
232. J. Keggin, *Proceedings of the Royal Society of London A: Mathematical, Physical and Engineering Sciences*, 1934, **144**, 75-100.
233. J. F. Keggin, *Nature*, 1933, **132**, 351.
234. N. Dubey, S. S. Rayalu, N. K. Labhsetwar and S. Devotta, *international journal of hydrogen energy*, 2008, **33**, 5958-5966.
235. J. Yang, M. J. Janik, D. Ma, A. Zheng, M. Zhang, M. Neurock, R. J. Davis, C. Ye and F. Deng, *Journal of the American Chemical Society*, 2005, **127**, 18274-18280.
236. Z. Karimi, A. Mahjoub and S. Harati, *Inorganica Chimica Acta*, 2011, **376**, 1-9.

237. T. He and J. Yao, *Progress in Materials Science*, 2006, **51**, 810-879.
238. B. B. Bardin, S. V. Bordawekar, M. Neurock and R. J. Davis, *The Journal of Physical Chemistry B*, 1998, **102**, 10817-10825.
239. T. Okuhara, N. Mizuno and M. Misono, *Applied Catalysis A: General*, 2001, **222**, 63-77.
240. R. S. Drago, J. A. Dias and T. O. Maier, *Journal of the American Chemical Society*, 1997, **119**, 7702-7710.
241. D. Farcasiu and J. Q. Li, *Journal of Catalysis*, 1995, **152**, 198-203.
242. M.-L. Wang and T.-H. Huang, *Industrial & engineering chemistry research*, 2004, **43**, 675-681.
243. D. Swern, T. W. Findley and J. T. Scanlan, *Journal of the American Chemical Society*, 1944, **66**, 1925-1927.
244. J. H. Simpson, *Organic Structure Determination Using 2-D NMR Spectroscopy- A problem-Based Approach*, Academic Press, United States of America, Second edn., 2012.
245. T. Vlček and Z. S. Petrović, *Journal of the American Oil Chemists' Society*, 2006, **83**, 247-252.
246. M. Rozenberg, E. Vaganova and S. Yitzchaik, *New Journal of Chemistry*, 2000, **24**, 109-111.
247. B. Gao, Y. Lv and H. Jiu, *Polymer international*, 2003, **52**, 1468-1473.
248. D. Jordan, E. Tan and D. Hegh, *J Surfact Deterg*, 2012, **15**, 587-592.
249. H. NordbÖ, *European Journal of Oral Sciences*, 1971, **79**, 356-361.
250. L. M. Peters, *US Patent*, 1947, **US2429484 A**, 1-4.
251. F. Franks and B. Roberts, *Journal of Applied Chemistry*, 1965, **15**, 109-117.
252. V. V. Goud, S. Dinda, A. V. Patwardhan and N. C. Pradhan, *Asia-Pacific Journal of Chemical Engineering*, 2010, **5**, 346-354.
253. S. T. Oyama, ed., *Mechanisms in Homogeneous and Heterogeneous Epoxidation Catalysis*, Elsevier, United Kingdom, 2008.
254. C. Pazé, S. Bordiga and A. Zecchina, *Langmuir*, 2000, **16**, 8139-8144.

255. M. J. Janik, K. A. Campbell, B. B. Bardin, R. J. Davis and M. Neurock, *Applied Catalysis A: General*, 2003, **256**, 51-68.
256. E. Santacesaria, A. Sorrentino, F. Rainone, M. Di Serio and F. Speranza, *Industrial & Engineering Chemistry Research*, 2000, **39**, 2766-2771.
257. E. Santacesaria, M. Ambrosio, A. Sorrentino, R. Tesser and M. Di Serio, *Catalysis Today*, 2003, **79-80**, 59-65.
258. T. M. Luong, H. Schriftman and D. Swern, *Journal of the American Oil Chemists Society*, 1967, **44**, 316-320.
259. Y. Ishii, K. Yamawaki, T. Ura, H. Yamada, T. Yoshida and M. Ogawa, *The Journal of Organic Chemistry*, 1988, **53**, 3587-3593.
260. M. A. Oakley, S. Woodward, K. Coupland, D. Parker and C. Temple-Heald, *Journal of Molecular Catalysis A: Chemical*, 1999, **150**, 105-111.
261. C. Venturello and M. Gambaro, *Synthesis*, 1989, 295-297.
262. K. Fujitani, T. Mizutani, T. Oida and T. Kawase, *Journal of Oleo Science*, 2009, **58**, 37-42.
263. M. Shimizu, H. Orita, K. Suzuki, T. Hayakawa, S. Hamakawa and K. Takehira, *Journal of Molecular Catalysis A: Chemical*, 1996, **114**, 217-220.
264. J. Tsuji, *Palladium Reagents and Catalysts*, Wiley, First Edition edn., 2004.
265. B. M. Devassy, G. V. Shanbhag, F. Lefebvre, W. Böhringer, J. Fletcher and S. B. Halligudi, *Journal of Molecular Catalysis A: Chemical*, 2005, **230**, 113-119.
266. X.-M. Yan, J.-H. Lei, D. Liu, Y.-C. Wu and W. Liu, *Materials Research Bulletin*, 2007, **42**, 1905-1913.
267. P. Sharma, S. Vyas and A. Patel, *Journal of Molecular Catalysis A: Chemical*, 2004, **214**, 281-286.
268. E. Rafiee, H. Mahdavi, S. Eavani, M. Joshaghani and F. Shiri, *Applied Catalysis A: General*, 2009, **352**, 202-207.
269. A. V. Ivanov, T. V. Vasina, V. D. Nissenbaum, L. M. Kustov, M. N. Timofeeva and J. I. Houzvicka, *Applied Catalysis A: General*, 2004, **259**, 65-72.
270. J. A. Dias, E. Caliman, S. I. C. L. Dias, M. Paulo and A. T. C. P. de Souza, *Catalysis today*, 2003, **85**, 39-48.

271. E. Tsukuda, S. Sato, R. Takahashi and T. Sodesawa, *Catalysis Communications*, 2007, **8**, 1349-1353.
272. L. T. A. Sofia, A. Krishnan, M. Sankar, N. K. Kala Raj, P. Manikandan, P. R. Rajamohanam and T. G. Ajithkumar, *The Journal of Physical Chemistry C*, 2009, **113**, 21114-21122.
273. P. G. Vázquez, M. N. Blanco and C. V. Cáceres, *Catal Lett*, 1999, **60**, 205-215.
274. F. Omota, A. C. Dimian and A. Bliiek, *Applied Catalysis A: General*, 2005, **294**, 121-130.
275. A. Z. Abdullah, N. Razali and K. T. Lee, *Journal of Physical Science*, 2010, **21**, 13-27.
276. W. Zhao, J. Gu, L. Zhang, H. Chen and J. Shi, *Journal of the American Chemical Society*, 2005, **127**, 8916-8917.
277. T. P. B. Nguyen, J.-W. Lee, W. G. Shim and H. Moon, *Microporous and Mesoporous Materials*, 2008, **110**, 560-569.
278. Y. Wang, M. Noguchi, Y. Takahashi and Y. Ohtsuka, *Catalysis Today*, 2001, **68**, 3-9.
279. W. Xie and L. Zhao, *Fuel*, 2013, **103**, 1106-1110.
280. J. A. Bae, K.-C. Song, J.-K. Jeon, Y. S. Ko, Y.-K. Park and J.-H. Yim, *Microporous and Mesoporous Materials*, 2009, **123**, 289-297.
281. L. A. Rios, D. A. Echeverri and A. Franco, *Applied Catalysis A: General*, 2011, **394**, 132-137.
282. L. Rios, D. Echeverri and F. Cardeño, *Industrial Crops and Products*, 2013, **43**, 183-187.
283. M. Guidotti, N. Ravasio, R. Psaro, E. Gianotti, L. Marchese and S. Coluccia, *Green Chemistry*, 2003, **5**, 421-424.
284. M. Guidotti, E. Gavrilova, A. Galarneau, B. Coq, R. Psaro and N. Ravasio, *Green Chemistry*, 2011, **13**, 1806-1811.
285. L. A. Rios, P. Weckes, H. Schuster and W. F. Hoelderich, *Journal of Catalysis*, 2005, **232**, 19-26.

286. J. Sepulveda, S. Teixeira and U. Schuchardt, *Applied Catalysis A: General*, 2007, **318**, 213-217.
287. P. A. Z. Suarez, M. S. C. Pereira, K. M. Doll, B. K. Sharma and S. Z. Erhan, *Industrial & Engineering Chemistry Research*, 2009, **48**, 3268-3270.
288. M.-L. Wang and V. Rajendran, *Ultrasonics sonochemistry*, 2007, **14**, 46-54.
289. N. Azizi, E. Gholibeglo, M. Maryami, S. D. Nayeri and S. M. Bolourtchian, *Comptes Rendus Chimie*, 2013, **16**, 412-418.
290. N. Ben hamadi and M. Msaddek, *Comptes Rendus Chimie*, 2012, **15**, 409-413.
291. A. N. Dadhania, V. K. Patel and D. K. Raval, *Comptes Rendus Chimie*, 2012, **15**, 378-383.
292. P. Gorin, J. Spencer and A. Tulloch, *Canadian Journal of Chemistry*, 1961, **39**, 846-855.
293. D. Jones and R. Howe, *Journal of the Chemical Society C: Organic*, 1968, 2801-2808.
294. A. Tulloch and J. Spencer, *Canadian Journal of Chemistry*, 1968, **46**, 1523-1528.
295. D. W. G. Develter and S. J. J. Fleurackers, in *Surfactants from renewable resources*, eds. M. Kjellin and I. Johansson, John Wiley & Sons, United Kingdom, 2010, ch. 11, pp. 211-238.
296. H.-J. Asmer, S. Lang, F. Wagner and V. Wray, *Journal of the American Oil Chemists' Society*, 1988, **65**, 1460-1466.
297. C. N. Mulligan, R. N. Yong and B. F. Gibbs, *Journal of Hazardous Materials*, 2001, **85**, 111-125.
298. C. Schippers, K. Gessner, T. Müller and T. Scheper, *Journal of Biotechnology*, 2000, **83**, 189-198.
299. M. Baviere, D. Degouy and J. Lecourtier, *French Patent*, 1994, **37,382**, 1-8.
300. S. Ito, M. Kinta and S. Inoue, *Agricultural and Biological Chemistry*, 1980, **44**, 2221-2223.
301. R. A. Gross and V. Shah, *US Patent*, 2014, **US 12/360,486**, 1-12.

302. Y. Hirata, M. Ryu, Y. Oda, K. Igarashi, A. Nagatsuka, T. Furuta and M. Sugiura, *Journal of Bioscience and Bioengineering*, 2009, **108**, 142-146.
303. D. W. Develter and L. M. Laurysen, *European journal of lipid science and technology*, 2010, **112**, 628-638.
304. E. Delbeke, M. Movsisyan, K. Van Geem and C. Stevens, *Green Chemistry*, 2016, **18**, 76-104.
305. S. J. J. Fleurackers, *European journal of lipid science and technology*, 2006, **108**, 5-12.
306. W. Gao, R. Hagver, V. Shah, W. Xie, R. A. Gross, M. F. Ilker, C. Bell, K. A. Burke and E. B. Coughlin, *Macromolecules*, 2007, **40**, 145-147.
307. K. S. Bisht, W. Gao and R. A. Gross, *Macromolecules*, 2000, **33**, 6208.
308. Y. Peng, J. Decatur, M. A. R. Meier and R. A. Gross, *Macromolecules*, 2013, **46**, 3293-3300.
309. Y.-H. Liu, Q.-S. Liu and Z.-H. Zhang, *Journal of Molecular Catalysis A: Chemical*, 2008, **296**, 42-46.
310. H. Firouzabadi, N. Iranpoor and A. Khoshnood, *Journal of Molecular Catalysis A: Chemical*, 2007, **274**, 109-115.
311. B. Sreedhar, P. Radhika, B. Neelima and N. Hebalkar, *Journal of Molecular Catalysis A: Chemical*, 2007, **272**, 159-163.
312. B. Das, V. S. Reddy, M. Krishnaiah and Y. K. Rao, *Journal of Molecular Catalysis A: Chemical*, 2007, **270**, 89-92.
313. S. R. Kumar and P. Leelavathi, *Journal of Molecular Catalysis A: Chemical*, 2007, **266**, 65-68.
314. A. Kiasat and M. Fallah-Mehrjardi, *Journal of the Iranian Chemical Society*, 2009, **6**, 542-546.
315. O. D. Dailey Jr, N. T. Prevost and G. D. Strahan, *Journal of the American Oil Chemists' Society*, 2009, **86**, 1101-1114.
316. N. Supanchaiyamat, P. S. Shuttleworth, A. J. Hunt, J. H. Clark and A. S. Matharu, *Green Chemistry*, 2012, **14**, 1759-1765.

317. B. R. Moser and S. Z. Erhan, *European Journal of Lipid Science and Technology*, 2007, **109**, 206-213.
318. P. C. Smith, B. K. O'Neill, Y. Ngothai and Q. D. Nguyen, *Energy & Fuels*, 2009, **23**, 3798-3803.
319. P. Smith, Y. Ngothai, Q. Nguyen and B. O'Neill, *Fuel*, 2009, **88**, 605-612.
320. K. M. Doll, B. K. Sharma and S. Z. Erhan, *Industrial & Engineering Chemistry Research*, 2007, **46**, 3513-3519.
321. K. M. Doll, B. R. Moser and S. Z. Erhan, *Energy & Fuels*, 2007, **21**, 3044-3048.
322. P. Saenz Méndez, R. E. Cachau, G. Seoane and O. N. Ventura, *Journal of Molecular Structure: THEOCHEM*, 2009, **904**, 21-27.
323. R. O. Hutchins, I. M. Taffer and W. Burgoyne, *The Journal of Organic Chemistry*, 1981, **46**, 5214-5215.
324. P. N. Guivisdalsky and R. Bittman, *The Journal of Organic Chemistry*, 1989, **54**, 4637-4642.
325. P. N. Guivisdalsky and R. Bittman, *Journal of the American Chemical Society*, 1989, **111**, 3077-3079.
326. M. K. Ghorai, A. Kumar and D. P. Tiwari, *The Journal of organic chemistry*, 2009, **75**, 137-151.
327. L. Lattuada, E. Licandro, S. Maiorana, H. Molinari and A. Papagni, *Organometallics*, 1991, **10**, 807-812.
328. Z. Liu, K. M. Doll and R. A. Holser, *Green Chemistry*, 2009, **11**, 1774-1780.
329. A. Alexakis and D. Jachiet, *Tetrahedron*, 1989, **45**, 6197-6202.
330. I. Pastor and M. Yus, *Current Organic Chemistry*, 2005, **9**, 1-29.
331. X. Deng and N. S. Mani, *Tetrahedron: Asymmetry*, 2005, **16**, 661-664.
332. B. Hedman, P. Piispanen, E.-O. Alami and T. Norin, *J Surfact Deterg*, 2003, **6**, 47-53.
333. P. Saenz, R. E. Cachau, G. Seoane, M. Kieninger and O. N. Ventura, *The Journal of Physical Chemistry A*, 2006, **110**, 11734-11751.
334. M. Mushtaq, I. M. Tan, L. Ismail, S. Y. Lee, M. Nadeem and M. Sagir, *Journal of Dispersion Science and Technology*, 2014, **35**, 322-328.

335. M. Meguro, N. Asao and Y. Yamamoto, *Journal of the Chemical Society, Perkin Transactions 1*, 1994, DOI: 10.1039/P19940002597, 2597-2601.
336. A. T. Placzek, J. L. Donelson, R. Trivedi, R. A. Gibbs and S. K. De, *Tetrahedron letters*, 2005, **46**, 9029-9034.
337. P. R. Likhar, M. PraveenKumar and A. K. Bandyopadhyay, *Synlett*, 2001, **2001**, 836-838.
338. A. K. Chakraborti, A. Kondaskar and S. Rudrawar, *Tetrahedron*, 2004, **60**, 9085-9091.
339. T. S. Coope, U. F. Mayer, D. F. Wass, R. S. Trask and I. P. Bond, *Advanced Functional Materials*, 2011, **21**, 4624-4631.
340. M. Chini, P. Crotti, L. Favero, F. Macchia and M. Pineschi, *Tetrahedron letters*, 1994, **35**, 433-436.
341. M. M. Mojtahedi, M. R. Saidi and M. Bolourtchian, *Journal of Chemical Research, Synopses*, 1999, 128-129.
342. M. M. Mojtahedi, M. H. Ghasemi, M. S. Abaee and M. Bolourtchian, *Arkivoc*, 2005, **15**, 68-73.
343. P. J. Flory, *Journal of the American Chemical Society*, 1940, **62**, 1561-1565.
344. R. I. Mahato, *Biomaterials for delivery and targeting of proteins and nucleic acids*, CRC Press, 2004.
345. P. K. Working, M. S. Newman, J. Johnson and J. B. Cornacoff, *Poly (ethylene glycol)*, 1997, **680**, 45-57.
346. F. Fuertges and A. Abuchowski, *Journal of controlled release*, 1990, **11**, 139-148.
347. E. d. Hoffmann and V. Stroobant, *Mass spectrometry: principles and applications*, Wiley & Sons publishers, Chichester, England, Third edn., 2007.
348. T. J. Watson and D. O. Sparkman, *Introduction to mass spectrometry: instrumentation, applications and strategies for data interpretations*, Wiley & Sons, Ltd, Chichester, England, Fourth edn., 2008.

349. T. Inoue, Y. Higuchi and T. Misono, *Journal of Colloid and Interface Science*, 2009, **338**, 308-311.
350. G. Buckton, B. Z. Chowdhry, J. K. Armstrong, S. A. Leharne, J. A. Bouwstra and H. E. J. Hofland, *International Journal of Pharmaceutics*, 1992, **83**, 115-121.
351. T. M. Rogge, C. V. Stevens, K. Booten, B. Levecke, A. Vandamme, C. Vercauteren, B. Haelterman, J. Corthouts and C. D'Hooge, *Topics in Catalysis*, 2004, **27**, 39-47.
352. T. M. Rogge, C. V. Stevens, A. Colpaert, B. Levecke and K. Booten, *Biomacromolecules*, 2006, **8**, 485-489.
353. T. M. Rogge and C. V. Stevens, *Biomacromolecules*, 2004, **5**, 1799.
354. J. A. S. Howell, C. R. McElroy, R. Heathcote and D. P. Taylor, *WO Patent*, 2007, **WO2007015057 A1**.
355. J. Traube, *Justus Liebigs Annalen der Chemie*, 1891, **265**, 27-55.
356. K. G. Pepper, C. Bahrim and R. Tadmor, *Journal of Adhesion Science and Technology*, 2011, **25**, 1379-1391.
357. M. J. Rosen and X. Y. Hua, *Journal of Colloid and Interface Science*, 1990, **139**, 397-407.
358. P. Elworthy and C. Macfarlane, *Journal of Pharmacy and Pharmacology*, 1962, **14**, 100T-102T.
359. J. Corkill, J. Goodman and R. Ottewill, *Transactions of the Faraday Society*, 1961, **57**, 1627-1636.
360. J. N. Israelachvili, *Intermolecular and surface forces: revised third edition*, Academic press, 2011.
361. W. D. Bancroft, *The Journal of Physical Chemistry*, 1913, **17**, 501-519.
362. M. J. Rosen, *Surfactants and Interfacial Phenomena, Third Edition*, 2004, 105-177.
363. G. M. Kontogeorgis and S. Kiil, *Introduction to Applied Colloid and Surface Chemistry*, John Wiley & Sons, 2016.
364. W. C. Griffin, *J Soc Cosmetic Chemists*, 1946, **1**, 311-326.

365. K. P. Ananthapadmanabhan, *Surfactants Solutions: Adsorption and Aggregation Properties*, CRC Press Inc., Florida, USA, 1993.
366. W. C. Griffin, *J. Soc. Cosmet. Chem*, 1954, **5**, 249-256.
367. I. Lin, J. Friend and Y. Zimmels, *Journal of Colloid and Interface Science*, 1973, **45**, 378-385.
368. J. Davies, presented in part at the Gas/Liquid and Liquid/Liquid Interface. Proceedings of the International Congress of Surface Activity, 1957.
369. J. McGowan, *Tenside, surfactants, detergents*, 1990, **27**, 229-230.
370. R. Sowada and J. C. McGowan, *Tenside Surf. Det.*, 1992, **29**, 109-113.
371. R. C. Pasquali, M. P. Taurozzi and C. Bregni, *International Journal of Pharmaceutics*, 2008, **356**, 44-51.
372. R. C. Pasquali, N. Sacco and C. Bregni, *Lat Am J Pharm*, 2009, **28**, 313-317.
373. H. Schott, *Journal of Colloid and Interface Science*, 1989, **133**, 527-529.
374. X. Guo, Z. Rong and X. Ying, *Journal of Colloid and Interface Science*, 2006, **298**, 441-450.
375. S. Gerald, *Polymers and the Environment*, Royal Society of Chemistry, The Royal Society of Chemistry, Thomas Graham House, Science Park, Milton Road, Cambridge CB4 0WF, UK, 1999.
376. F. Welle, *Resources, Conservation and Recycling*, 2011, **55**, 865-875.
377. D. Paszun and T. Szychaj, *Industrial & Engineering Chemistry Research*, 1997, **36**, 1373-1383.
378. A. J. Peacock and A. Calhoun, *Polymer Chemistry: Properties and Applications*, Hanser Publisher, Munich, 2006.
379. A. Eerhart, A. P. C. Faaij and M. K. Patel, *Energy & Environmental Science*, 2012, **5**, 6407-6422.
380. G. P. Karayannidis and D. S. Achilias, *Macromolecular Materials and Engineering*, 2007, **292**, 128-146.
381. N. George and T. Kurian, *Industrial & Engineering Chemistry Research*, 2014, **53**, 14185-14198.

382. M. Kozlowski, *Anglais*, 2003, **48**, 4.
383. F. Awaja and D. Pavel, *European Polymer Journal*, 2005, **41**, 1453-1477.
384. C. Lorenzetti, P. Manaresi, C. Berti and G. Barbiroli, *Journal of Polymers and the Environment*, 2006, **14**, 89-101.
385. S. D. Mancini and M. Zanin, *Journal of applied polymer science*, 2000, **76**, 266-275.
386. N. K. Gupta, S. Nishimura, A. Takagaki and K. Ebitani, *Green Chemistry*, 2011, **13**, 824-827.
387. N. Shi, Q. Liu, Q. Zhang, T. Wang and L. Ma, *Green Chemistry*, 2013, **15**, 1967-1974.
388. R. J. Sheehan, *Ullmann's Encyclopedia of Industrial Chemistry*, 2011.
389. R. J. Sheehan, *Terephthalic Acid, Dimethyl Terephthalate, and Isophthalic Acid*, 1995.
390. J. A. Kent, ed., *Kent and Riegel's Handbook of Industrial Chemistry and Biotechnology*, Springer Science, New York, US, 2007.
391. D. Yuan, K. Rao, P. Relue and S. Varanasi, *Bioresource Technology*, 2011, **102**, 3246-3253.
392. K. Fukui, *Accounts of Chemical Research*, 1971, **4**, 57-64.
393. K. Fukui and S. Inagaki, *Journal of the American Chemical Society*, 1975, **97**, 4445-4452.
394. K. Fukui, H. Fujimoto and S. Yamabe, *The Journal of Physical Chemistry*, 1972, **76**, 232-237.
395. K. Houk and R. Strozier, *Journal of the American Chemical Society*, 1973, **95**, 4094-4096.
396. R. Woodward and T. J. Katz, *Tetrahedron*, 1959, **5**, 70-89.
397. R. B. Woodward and R. Hoffmann, *Angewandte Chemie International Edition in English*, 1969, **8**, 781-853.
398. J. E. Baldwin and V. P. Reddy, *The Journal of Organic Chemistry*, 1989, **54**, 5264-5267.

399. M. Imade, H. Hirao, K. Omoto and H. Fujimoto, *The Journal of organic chemistry*, 1999, **64**, 6697-6701.
400. K. N. Houk, *Tetrahedron Letters*, 1970, **11**, 2621-2624.
401. V. Mark, *The Journal of Organic Chemistry*, 1974, **39**, 3181-3183.
402. J. M. Mellor and C. F. Webb, *Journal of the Chemical Society, Perkin Transactions 2*, 1974, 17-22.
403. J. Mattay, J. Mertes and G. Maas, *Chemische Berichte*, 1989, **122**, 327-330.
404. R. Sustmann and W. Sicking, *Tetrahedron*, 1992, **48**, 10293-10300.
405. J. A. Berson, Z. Hamlet and W. A. Mueller, *Journal of the American Chemical Society*, 1962, **84**, 297-304.
406. G. Cainelli, P. Galletti, D. Giacomini and A. Quintavalla, *Tetrahedron letters*, 2003, **44**, 93-96.
407. T. Inukai and T. Kojima, *The Journal of Organic Chemistry*, 1966, **31**, 1121-1123.
408. T. Inukai and T. Kojima, *Journal of organic chemistry*, 1967, **32**, 869-872.
409. J. Sauer and J. Kredel, *Tetrahedron Letters*, 1966, **7**, 6359-6364.
410. H. Pellissier, *Tetrahedron*, 2009, **65**, 2839-2877.
411. T. L. Gresham and T. R. Steadman, *Journal of the American Chemical Society*, 1949, **71**, 737-738.
412. D. B. Todd and J. C. Elgin, *AIChE Journal*, 1955, **1**, 20-27.
413. F. Lochner and H. Reuther, *US Patent*, 1974, **US3808188 A**, 1-3.
414. J. Melsheimer and D. Ziegler, *Journal of the Chemical Society, Faraday Transactions*, 1992, **88**, 2101-2108.
415. A. Gil, L. M. Gandia and M. A. Vicente, *Catalysis Reviews*, 2000, **42**, 145-212.
416. M. J. Hernando, C. Pesquera, C. Blanco and F. González, *Langmuir*, 2002, **18**, 5633-5636.
417. D. E. W. Vaughan, R. Lussie and J. S. Magee, *Patent*, 1979, **4**, 176.
418. M. Sergio, M. Musso, J. Medina and W. Diano, *Advances in Technology of Materials and Materials Processing*, 2006, **8**, 5-12.

419. Diethyl terephthalate, http://www.chemicalbook.com/SpectrumEN_636-09-9_1HNMR.htm, (accessed May 1st, 2016).
420. L. Hu, X. Tang, J. Xu, Z. Wu, L. Lin and S. Liu, *Industrial & Engineering Chemistry Research*, 2014, **53**, 3056-3064.
421. T.-L. Chan, T. C. Mak, C.-D. Poon, H. N. Wong, J. H. Jia and L. L. Wang, *Tetrahedron*, 1986, **42**, 655-661.
422. J. Bi, X. Guo, M. Liu and X. Wang, *Catalysis Today*, 2010, **149**, 143-147.
423. Y. Suzuki, S. Kinoshita, A. Shibahara, S. Ishii, K. Kawamura, Y. Inoue and T. Fujita, *Organometallics*, 2010, **29**, 2394-2396.
424. H. D. Mansilla, J. Baeza, S. Urzúa, G. Maturana, J. Villaseñor and N. Durán, *Bioresource Technology*, 1998, **66**, 189-193.
425. S. H. Fogler, *Elements of Chemical Reaction Engineering (Prentice-Hall International Series in the Physical and Chemical Engineering Sciences)*, Prentice Hall, 1992.
426. J. R. Dodson, A. J. Hunt, H. L. Parker, Y. Yang and J. H. Clark, *Chemical Engineering and Processing: Process Intensification*, 2012, **51**, 69-78.
427. W. H. Gong, *US Patent*, 2008, **US7385081 B1**.
428. T. Kovalchuk, H. Sfihi, V. Zaitsev and J. Fraissard, *Journal of Catalysis*, 2007, **249**, 1-14.
429. J. Jiang, Y. Zhang, L. Yan and P. Jiang, *Applied Surface Science*, 2012, **258**, 6637-6642.
430. N. Lourith and M. Kanlayavattanakul, *International Journal of Cosmetic Science*, 2009, **31**, 255-261.
431. K. Joshi-Navare and A. Prabhune, *BioMed Research International*, 2013, **2013**, 8.
432. J. Chen and C. Y. Yeh, *US Patent*, 2000, **US6013848 A**.
433. B. Choudary, M. Sateesh, M. L. Kantam, K. Ranganath and K. Raghavan, *Catal Lett*, 2001, **76**, 231-233.
434. T. Kawabata, M. Kato, T. Mizugaki, K. Ebitani and K. Kaneda, *Chemistry-A European Journal*, 2005, **11**, 288-297.

435. J. Morros, B. Levecké and M. R. Infante, *Carbohydrate Polymers*, 2010, **81**, 681-686.